CORA Cork Open Research Archive
Cartlann Taighde Oscailte Chorcaí

Title	Regulation of insulin-like growth factor receptor activity and its therapeutic targeting in cancer
Authors	Rieger, Leonie
Publication date	2020-04-08
Original Citation	Rieger, L. 2020. Regulation of insulin-like growth factor receptor activity and its therapeutic targeting in cancer. PhD Thesis, University College Cork.
Type of publication	Doctoral thesis
Rights	© 2020, Leonie Rieger. - https://creativecommons.org/licenses/by-nc-nd/4.0/
Download date	2026-11-13 13:50:25
Item downloaded from	https://hdl.handle.net/10468/10440

UCC
University College Cork, Ireland
Coláiste na hOllscoile Corcaigh

Ollscoil na hÉireann, Corcaigh

National University of Ireland, Cork



Regulation of Insulin-like Growth Factor Receptor activity and its therapeutic targeting in cancer

Thesis presented by
Leonie Rieger, B.Sc., M.Sc.
for the degree of
Doctor of Philosophy

University College Cork

Cell Biology Laboratory
School of Biochemistry and Cell Biology
Head of School/Department: Prof. Rosemary O'Connor
Supervisor: Prof. Rosemary O'Connor

April 2020

TABLE OF CONTENT

DECLARATION I

ACKNOWLEDGMENT II

ABSTRACT IV

ABBREVIATIONS VI

1 CHAPTER 1: INTRODUCTION 1

1.1 The Insulin and Insulin-Like Growth Factor Family 2

1.1.1 Insulin, Insulin-like Growth factors and IGF binding proteins 3

1.1.2 Receptor Evolution and Structure 7

1.2 The physiological function of the IGF-1R system 10

1.2.1 IGF-1R promotes cell, organ and animal growth 10

1.2.2 IGF-1R mediates cell survival and differentiation 11

1.2.3 IGF-1R axis in aging and longevity 14

1.2.4 IGF-1R in metabolism and mitochondrial function 15

1.3 IGF-1 induced mechanisms and signalling pathways 18

1.3.1 How the IGF-1R kinase is activated 18

1.3.2 The autophosphorylation site Tyr^{950} IGF-1R 23

1.3.3 The function of the C-terminal tail in the IGF-1R 23

1.3.3.1 Point mutations in the C-terminal tail impair IGF-1R functions 23

1.3.3.2 The regulation of IGF-1R kinase activity 24
1.3.4 IGF-1R signal transduction 28
1.3.4.1 IRS and SHC as IGF-1R Adaptor Proteins 28
1.3.4.1.1 Insulin Receptor Substrate Family 28
1.3.4.1.2 The Src homology and Collagen (SHC) family of adaptor proteins 30
1.3.5 IGF-1R and adhesion signalling 31
1.3.6 IGF-1 mediated activation of PI3K pathway 32
1.3.7 IGF-1-mediated activation of the Ras/MAPK pathway 36

1.4 Endocytosis and trafficking of the IGF-1R 40
1.4.1 Ubiquitination of the receptor 42
1.4.2 Modulation of IGF-1R signalling by endocytosis 47
1.4.3 The IGF-1R translocates to the nucleus 50

1.5 IGF-1R activity in Cellular transformation and Cancer 54
1.5.1 IGF-1R facilitates cellular transformation 54
1.5.2 The IR-A and cancer 56
1.5.3 Cell Migration, Invasion and EMT 57
1.5.4 IGF-1R mediates chemoresistance 59
1.5.5 IGF-1 system as target for cancer therapy 61
1.5.5.1 Epidemiological data 61
1.5.5.2 IGF-1R targeting strategies 63
1.5.5.3 Therapy resistance and failures 66

1.6 Aim of the study 68

2 CHAPTER 2: MATERIAL AND METHODS 69

2.1 Material 70

2.1.1 General chemicals and reagents 70

2.1.2 Cell Culture reagents 70

2.1.3 Antibodies 71

2.1.4 Chemical Inhibitors 72

2.1.5 Mammalian Cell lines 73

2.1.6 Mammalian Expression Vectors 73

2.2 Methods 73

2.2.1 Cell culture, ligand stimulation and pharmacological inhibitors 73

2.2.2 Generation and transfection of IGF-1R mutants 75

2.2.2.1 General plasmid transfection 75

2.2.2.2 Plasmid transfection for CRISPR-mediated mutation in *igf-1r* 76

2.2.3 Genomic DNA extraction and genomic DNA PCR 77

2.2.4 SDS PAGE and western blotting 79

2.2.5 Phospho-Tyr$^{1250/1251}$-antibody adsorption 80

2.2.6 Immunoprecipitation and in-vitro kinase assays 80

2.2.7 Ubiquitination assay 81

2.2.8 Subcellular fractionation 82

2.2.9 Quantitative PCR 83

2.2.10 Immunofluorescence 84

2.2.11 In-Cell Western Assays for IGF-1 receptor 86

2.2.12 Proliferation, Colony formation, adhesion, clonogenic growth and migration 87

2.2.12.1 Cell proliferation 87

2.2.12.2 Colony formation 87

2.2.12.3 Adhesion assay 88
2.2.12.4 Clonogenic growth; soft agar assay 88
2.2.12.5 Migration; wound-healing assay 88
2.2.13 Statistical analysis 90

3 CHAPTER 3: NON-RECEPTOR TYROSINE KINASE FER ACTIVATES IGF-1R IN POINTS OF FOCAL CELL ADHESION 91

3.1 Abstract 92

3.2 Introduction 93

3.3 Results 98

3.3.1 FER kinase enhances IGF-1R phosphorylation and IGF-1 mediated signalling 98
3.3.2 FER is an IGF-1- and adhesion-activated kinase 105
3.3.3 FER, IGF-1R and β1-Integrin localise in points of focal adhesion of cancer cells 111
3.3.4 FER kinase activity can be inhibited by an ALK-inhibitor 116

3.4 Discussion 124

4 CHAPTER 4: SELECTION AND CHARACTERIZATION OF MCF-7 CELL CLONES WITH CRISPR-MEDIATED KNOCK-IN OF TYROSINE AND SERINE MUTATIONS IN THE *IGF-1R* AND CRISPR-MEDIATED *IGF-1R* KNOCK-OUT IN THREE CANCER CELL LINES 130

4.1 Abstract 131

4.2 Introduction 133

4.3 Results 137

4.3.1 CRISPR/Cas9 system introduced specific point-mutations in the SFYYS motif of *igf-1r* 137

4.3.2 Cell cloning and genomic DNA PCR-based selection of MCF-7 cells expressing IGF-1R knock-in mutations 139

4.3.3 MCF-7 cells expressing the IGF-1R FF knock-in mutation exhibit similar signalling responses to parental MCF-7 cells 143

4.3.4 CRISPR/Cas9 mediated knock-out of IGF-1R protein leads to impaired IGF-1 signalling in three cancer cell lines 147

4.3.5 Cancer cell lines respond differently to knock-out of the IGF-1R protein 156

4.4 Discussion 165

4.5 Supplementary Data 170

5 CHAPTER 5: IGF-1 RECEPTOR ACTIVITY IN THE GOLGI OF MIGRATORY CANCER CELLS REQUIRES ADHESION-DEPENDENT PHOSPHORYLATION ON TYROSINES 1250 AND 1251 174

5.1 Abstract 175

5.2 Introduction 176

5.3 Results 179

5.3.1 Phosphorylation of Tyr^{1250} and Tyr^{1251} occurs in cells 179

5.3.2 Adhesion signals and IGF-1R kinase activity are required for Tyr$^{1250/1251}$ phosphorylation 186

5.3.3 A Tyr$^{1250/1251}$ phosphomimetic mutant IGF-1R is fully active, but rapidly turned over 192

5.3.4 Tyr$^{1250/1251}$ phosphorylation promotes IGF-1R translocation to the Golgi apparatus 204

5.3.5 Tyr$^{1250/1251}$ phosphorylation and adhesion signals promote IGF-1R presence in and signalling from the Golgi 217

5.4 Discussion 229

6 CHAPTER 6: GENERAL DISCUSSION 235

6.1 Summary 235

6.2 Association of FER and IGF-1R in points of Focal Adhesion 239

6.2.1 FER enhances Tyr$^{1250/1251}$ IGF-1R phosphorylation to destabilize focal adhesions and induce IGF-1R endocytosis 239

6.2.2 The interplay of FER, β1-Integrin and the IGF-1R signalling in focal adhesion dynamics 241

6.2.3 FER overexpression in MCF-7 cells may enhance migratory potential 244

6.3 The Golgi apparatus as a signalling compartment 245

6.3.1 Golgi-derived signalling facilitates cell migration 245

6.3.2 Mechanism of anchoring and releasing IGF-1R from the Golgi apparatus 249

6.3.3 IGF-1R as a cargo protein in exocytosis and endocytosis 250

6.3.4 IGF-1R localisation in the Golgi as a potential biomarker 253

6.3.5 The insulin receptor and the Golgi apparatus 255

6.4 Conclusion 256

7 REFERENCES 257

8 APPENDIX 297

8.1 FES-related tyrosine kinase activates the insulin-like growth factor-1 receptor at sites of cell adhesion .....

8.2 IGF-1 receptor activity in the Golgi of migratory cancer cells depends on adhesion-dependent phosphorylation of Tyr^{1250} and Tyr^{1251}

TABLE OF FIGURES

Figure 1.1: Overview of the Insulin and Insulin-like Growth factor family. 6

Figure 1.2: Biosynthesis pathway and important domains within the IGF-1R. 9

Figure 1.3: Stages of IGF-1R tyrosine kinase activation. 19

Figure 1.4: Conformational changes in the IGF-1R upon IGF-1 binding. 22

Figure 1.5: Mutation of $Tyr^{1250/1251}$ to phenylalanine impairs the IGF-1R function. 27

Figure 1.6: IGF-1-mediated activation of the PI3K/AKT pathway. 35

Figure 1.7: IGF-1-mediated activation of the Ras/ERK1/2 pathway. 38

Figure 1.8: Interacting E3 ligases mediate IGF-1R ubiquitination. 46

Figure 1.9: Regulation of IGF-1R signalling by receptor endocytosis. 49

Figure 1.10: IGF-1R translocates to the nucleus in response to IGF-1. 53

Figure 3.1: Z-Scores distribution from the tumour suppressor and oncogene siRNA screen. 95

Figure 3.2: FER kinase enhances IGF-1R phosphorylation. 100

Figure 3.3: FER induced signalling in a kinase-dependent manner. 102

Figure 3.4: FER kinase enhances IGF-1R signalling. 104

Figure 3.5: IGF-1-induced FER activation is IGF-1R kinase dependent. ... 106

Figure 3.6: FER is an adhesion-activated kinase. 108

Figure 3.7: Adhesion signalling is required of FER-mediated IGF-1R activation. 110

Figure 3.8: FER is highly expressed in migratory breast cancer cell lines. 113

Figure 3.9: FER is located in points of focal adhesion where it co-localises with IGF-1R and β1-integrin. 115

Figure 3.10: Structural similarities between TAE684 and AP26113 and c-FES and FER kinase domains. 117
Figure 3.11: The ALK inhibitor, AP26113 inhibits FER activity and FER-mediated IGF-1R activation. 119
Figure 3.12: AP26113 inhibits endogenous FER. 121
Figure 3.13: FER inhibition caused reduced migration of HS-578T. 123
Figure 3.14: Proposed model of how FER enhances phosphorylation on catalytically active and inactive IGF-1R. 129
Figure 4.1: Overview of experimental plan for CRISPR-mediated knock-in *igf-1r* point mutations in MCF-7 cells. 138
Figure 4.2: Isolation and identification of group-clones containing cells carrying the mutated region of the *igf-1r*. 140
Figure 4.3: Isolation and identification of MCF-7 cell clones uniquely expressing the *igf-1r* mutants. 142
Figure 4.4: MCF-7 cells expressing the knock-in IGF-1R FF mutant display normal IGF-1-mediated signalling. 144
Figure 4.5: MCF-7 cells expressing knock-in Y1250F/Y1251F mutation do not display impaired cell growth. 146
Figure 4.6: Overview of approach used to generate CRISPR-mediated *igf-1r* knock-out in three cancer cell lines. 149
Figure 4.7: CRIPSR-mediated *igf-1r* deletion leads to reduced IGF-1R protein levels. 151
Figure 4.8: MCF-7 *igf-1r* knock-out cell lines display lack of IGF-1R and IGF-1-mediated signalling. 153
Figure 4.9: IGF-1R protein depletion and impaired IGF-1 signalling in *igf-1r* knock-out cell lines. 155

Figure 4.10: MCF-7 IGF-1R knock-out cell lines are defective in proliferation, adhesion and anchorage-independent growth. 158
Figure 4.11: MDA-MB-231 IGF-1R KO cells are not impaired in monolayer cell proliferation, but exhibit enhanced anchorage-independent growth and cell migration. 161
Figure 4.12: DU-145 IGF-1R knock-out cells are impaired in anchorage-independent growth but not in cell migration. 164
Figure 5.1: $Tyr^{1250/1251}$ IGF-1R phosphorylation occurs in R^- cells. 181
Figure 5.2: IGF-1 induce $Tyr^{1250/1251}$ IGF-1R phosphorylation in a dose dependent manner. 183
Figure 5.3: IGF-1 induces $Tyr^{1250/1251}$ IGF-1R phosphorylation in cancer cells. 185
Figure 5.4: $Tyr^{1250/1251}$ IGF-1R phosphorylation is an IGF-1R autophosphorylation site. 187
Figure 5.5: Adhesion kinases FER and FAK contribute to $Tyr^{1250/1251}$ IGF-1R phosphorylation 189
Figure 5.6: Adhesion signalling is required for $Tyr^{1250/1251}$ IGF-1R phosphorylation 191
Figure 5.7: Double or single mutations of IGF-1R $Tyr^{1250/1251}$ to glutamic acid cause lower IGF-1R protein expression, but do not affect mRNA levels. 193
Figure 5.8: The EE mutant exhibits similar IGF-1R and downstream activation to WT receptor. 195
Figure 5.9: IGF-1R EE mutant exhibits a similar kinase activity to the WT IGF-1R. 197
Figure 5.10: IGF-1R mutants are synthesized at a similar rate to the WT receptor 199

Figure 5.11: Phosphorylation of Tyr$^{1250/1251}$ IGF-1R targets the receptor for proteasomal degradation. 201
Figure 5.12: Tyr$^{1250/1251}$ phosphorylation facilitates IGF-1R protein turnover. 203
Figure 5.13: Tyr$^{1250/1251}$ phosphorylation promotes IGF-1R translocation to the perinuclear region. 206
Figure 5.14: IGF-1 induces surface depletion in the IGF-1R WT and the EE. 208
Figure 5.15: Receptor activation induces internalisation of IGF-1R WT and EE into large vesicles. 210
Figure 5.16: Tyr$^{1250/1251}$ phosphorylation mediates IGF-1R translocation to the Golgi-apparatus. 212
Figure 5.17: Disruption of the Golgi apparatus causes decreased levels of IGF-1R WT and EE, but not FF mutant. 214
Figure 5.18: Tyr$^{1250/1251}$ phosphorylation is not required for nuclear translocation of the IGF-1R. 216
Figure 5.19: IGF-1R localises in the Golgi of migratory cancer cells. 218
Figure 5.20: Disruption of the Golgi reduces IGF-1R levels in migratory cell lines. 220
Figure 5.21: Disruption of the Golgi impairs IGF-1-induced SHC activation in HS-578T. 222
Figure 5.22: Formation of nascent focal adhesion points recruits IGF-1R to the membrane. 224
Figure 5.23: Formation of adhesion points during migration releases IGF-1R from the Golgi and disruption of the Golgi inhibits migration. 226

Figure 5.24: Cell-ECM contact regulates phosphorylation on $Tyr^{1250/1251}$ IGF-1R in migratory cells. 228
Figure 5.25: Model for function of $Tyr^{1250/1251}$ phosphorylation in determining IGF-1R location and signalling in the Golgi apparatus. 234
Figure 6.1: Model for function of adhesion-activated FER and $Tyr^{1250/1251}$ phosphorylation in promoting focal adhesion turnover and in determining IGF-1R location and signalling in the Golgi apparatus. 238

TABLE OF SUPPLEMENTAL FIGURES

Figure S 4.1: PCR-based identification of cell clones with exclusive amplification of *igf-1r* with the S1248A mutation. 170

Figure S 4.2: PCR-based identification of cell clones with exclusive amplification of *igf-1r* with the Y1250F/Y1251F mutation. 171

Figure S 4.3: Identification of cell clones deficient in IGF-1R protein expression..... 172

Figure S 4.4: Cell morphology is not affected by IGF-1R knock-out in MCF-7 and MDA-MB-231, but in DU-145. 173

TABLE OF TABLES

Table 1.1: IGF-1R TKI used in clinical trials. 66

Table 2.1: List of antibodies. 71

Table 2.2: Designed ssOND (full length) for DNA repair. 77

Table 2.3: Primer sequences used for PCR to verify the mutation in the *igf-1r.* 78

Table 2.4: Designed primer pair used to verify the *igf-1r* knock-out. 79

Table 2.5: Primers used to detect the IGF-1R in qRT-PCR. 84

Table 2.6: Primary antibody dilution for immunofluorescence. 85

Table 2.7: Secondary antibodies and dyes used for immunofluorescence. . 85

Table 4.1: Summary of phenotypic behaviour of cell lines with an *igf-1r* knock-out. 167

DECLARATION

This thesis has not been previously submitted, in whole or in part, to this or any other University for any degree, and is, unless otherwise stated the original work of the author.

Signed 

Leonie Rieger

ACKNOWLEDGMENT

It would have not been possible to conduct my PhD research without the help of Professor Rosemary O'Connor and the financial support of the Science Foundation Ireland. I would like to thank Rosemary for her guidance, her scientific input, the endless scientific discussions and her critical revision on data. I am very grateful for all the opportunities throughout my training, to develop and expand my skills and competencies as a Scientist.

It was a great pleasure to work together with the past and present members of the Roclab family: Joanna Stanicka, Mike Coleman, Janina Berghoff, Orla Cox, Grant Godsmark, Sarah Riis, Stephanie Ward and Joss Murray. Thank you all for your help, scientific discussions, the chitchat and the fabulous and so desperately needed coffee breaks.

Throughout my PhD, I had the chance to meet great people and I would like to thank the lunch group for the regular get-togethers (12 o'clock on the spot). Thanks to Patrycja, Sarah O'D, Julia and Kevin for always giving your support and for your motivating words and thanks to my Tag teams and the Quiz group for the daily distractions and for making me leave the lab on time. Thanks to my friends Susi and Stella back home in Germany for hours of phone chats, for the visits and for always cheering me up.

To Mum, Dad and my family; thank you for all of your support over the last years, for helping me reach my goals, financially and emotionally, and for always believing in me and my craziness. Thank you for your constant patience, love and support.

Start by doing what's necessary;
Then do what's possible;
and suddenly you are doing the impossible.
Franz of Assisi

ABSTRACT

Insulin-like Growth Factor-1 Receptor signalling is essential for cell growth, and also promotes migration, survival and cellular transformation, thus, linking it to cancer progression. IGF-1R activity and signalling in cancer cells is regulated by the C-terminal tail of the receptor. In particular the $Tyr^{1250/1251}$, as their mutation to phenylalanine (FF) profoundly impairs IGF-1 signalling and the crosstalk between Integrin and IGF-1R signalling that facilitates a migratory phenotype in cancer cells. This thesis investigated the mechanisms of adhesion-modulated IGF-1R signalling, the function of $Tyr^{1250/1251}$, and whether these mechanisms might influence the efficacy of IGF-1R-targeted drugs.

Following the identification of FER kinase as a mediator of sensitivity to IGF-1R kinase inhibition, we found that ectopic expression of FER enhanced IGF-1R and SHC/MAPK pathway activation in an IGF-1R kinase-independent manner. FER also specifically phosphorylated the IGF-1R on $Tyr^{1250/1251}$. FER activity was cell adhesion-dependent and FER expression correlated with a migratory cancer phenotype. FER inhibition profoundly decreased IGF-1R and SHC signalling and reduced cell migration in breast cancer cells.

The mechanisms and consequences of IGF-1R phosphorylation on $Tyr^{1250/1251}$ phosphorylation were investigated for their contribution to IGF-1R function. It was established that IGF-1R, FER and FAK kinase activity may all contribute to $Tyr^{1250/1251}$ phosphorylation and that cell adhesion is required for this phosphorylation. The consequence of $Tyr^{1250/1251}$ phosphorylation was further investigated using a phosphomimetic Y1250E/Y1251E (EE) and the non-phosphorylatable FF IGF-1R mutant. These studies determined that IGF-1R phosphorylation on $Tyr^{1250/1251}$ IGF-1R enhanced IGF-1R

internalisation and proteasomal degradation. Moreover, the WT and EE receptors became rapidly internalised in response to IGF-1 ligation and accumulated in the Golgi apparatus, while the FF mutant remained at the plasma membrane or sites of cell adhesion. Importantly, Golgi-associated IGF-1R signalling correlated with a migratory cancer cell phenotype, and disruption of the Golgi apparatus impaired IGF-1-promoted SHC phosphorylation and cell migration. In migratory cells, the formation of new focal adhesion points caused a transient release of the IGF-1R from the Golgi-apparatus to the membrane and lower IGF-1R $Tyr^{1250/1251}$ phosphorylation. Thus, phosphorylation on $Tyr^{1250/1251}$ enables IGF-1R signalling from the Golgi-apparatus, and Golgi-derived IGF-1R signalling can support an aggressive cancer phenotype.

Overall, this study identifies FER kinase and $Tyr^{1250/1251}$ phosphorylation as adhesion-dependent mechanisms that modulate IGF-1R signalling and localisation in migratory cancer cells. The fact that the IGF-1R may be activated by other kinases and is predominantly located in the Golgi in migratory cells may explain the poor clinical efficacy of monoclonal antibodies and kinase inhibitors that specifically target the surface IGF-1R.

ABBREVIATIONS

32D	IL 3 dependent murine 32D myeloid cell line
4EBP1	Eukaryotic translation initiation factor 4E-binding protein 1
Ab	Antibody
ABL	Abelson murine leukaemia viral oncogene homolog 1
Adam12	Metalloprotease domain 12
Adam9	Metalloprotease domain 9
adh	Adhesion
ADP	Adenosine diphosphate
ALS	Acid Labile Subunit
AP-2	Adapter Protein 2
ARF	ADP-ribosylation factor
Arg	Arginine
ATP	Adenosine triphosphate
AurA/B	Aurora kinase A/B
Bad	Bcl-2 antagonist of cell death
BCL-2	B-Cell Lymphoma-2
BCL-XL	B-cell lymphoma-extra large
BFA	Brefeldin A
BNIP3	BCL2-interacting protein 3
BP	Base Pairs
BPV	Bovine papillomaviruses
BSA	Bovine Serum Albumin
C	Celsius
$CaCl_2$	Calcium chloride
c-Cbl	Casitas B-lineage Lymphoma
CCP	Clathrin-coated pits
Cdc42	Cell division control protein 42 homolog
cm	Centimetre
CO_2	carbon dioxide
CQ	Chloroquine
CRA	Colorectal adenoma
CREB	cAMP response element-binding protein
CRISPR	Clustered Regularly Interspaced Short Palindromic Repeats
CRMP2	Collapsin Response Mediator Protein-2
CT	cycle threshold
CTL/Ctl	Control
CV	Crystal Violet
Daf-2	abnormal dauer formation protein 2
DDR1	Discoidin domain receptor family
DMEM	Dulbecco's Modified Eagles Medium
DMSO	Dimethyl sulfoxide
DNA	Deoxyribonucleic acid

DR	aspartate on position 743 FER mutated to arginine
DTT	Dithiothreitol
ECM	Extracellular Matrix
EDTA	Ethylene diamine tetra-acetic acid
EE	tyrosines position 1250/1251 IGF-1R mutated to glutamic acid
EEA	Early Endosome Antigen
EEA1	Early Endosome Antigen 1
EGFR	Epidermal growth factor
EGTA	Ethylene glycol tetra-acetic acid
eLF4E	Eukaryotic translation initiation factor 4E
EMT	Epithelial-to-Mesenchymal
ER	Endoplasmic reticulum
ERAD	Endoplasmic-reticulum-associated protein degradation
ERK5	Extracellular-signal-regulated kinase 5
Esp15	Epidermal growth factor receptor substrate 15
EtOH	Ethanol
Ets	E26 transformation-specific
EV	Empty Vector control
FACS	Fluorescence-Activated Cell Sorting
FAK	Focal Adhesion kinase
FASL	Fas-ligand
FBS	Foetal Bovine Serum
FER	Feline Sarcoma-Related Protein
FES	Feline sarcoma oncogene
FF	tyrosines position 1250/1251 IGF-1R mutated to phenylalanine
FGFR	Fibroblast Growth Factor Receptor
FKHR	Forkhead transcription factor
FOXO	Forkhead box protein O1
Fwd	forward Primer
g	Gramm
GAP-DH	Glyceraldehyde 3-phosphate dehydrogenase
GDP	Guanine diphosphate
GEF	Guanine nucleotide exchange factor
GFP	Green fluorescent protein
GH	Growth Hormone
GLOM1	Golgi Membrane Protein 1
GPCR	G-Protein Coupled Receptor
Grb10	Growth factor receptor-bound protein 10
Grb2	Growth Receptor Binding protein-2
GRK	G-protein coupled receptor kinase
gRNA	guide RNA
GSK3ß	Glycogen synthase kinase 3 beta
GTP	Guanine triphosphate
HBSS	Hank's Balanced Salt Solution
HCl	Hydrochloric acid

HDR	Homology directed repair
HDR-1	3-hydroxy-3-methylglutaryl reductase degradation 1
HER 2	Human Epidermal Growth Factor Receptor 2
HIS	Histidine
Hr	Hour
IB	Immunoblotted
IC_{50}	Inhibitory concentration
IF	Immunofluorescence
IGF	Insulin-like Growth Factor
IGF-1	Insulin-like Growth Factor-1
IGF-1R	Type-1 Insulin-like Growth Factor Receptor
IGF-2	Insulin-like Growth Factor-2
IGF-2R	Type-2 Insulin-like Growth Factor Receptor
IGFBP	Insulin-Like Growth Factor-Binding Protein
IL-3	Interleukin-3
Indels	Insertion–deletion mutations
Ins	Insulin
IP	Immunoprecipitation
IR	Insulin Receptor
IR-A	Insulin Receptor Isoform A
IR-B	Insulin Receptor Isoform B
IRS-1	Insulin Receptor Substrate-1
JNK	c-Jun-N-Terminal kinase
K	Lysine
KCl	Potassium chloride
Kd	Dissociation constant
kDa	Kilo Dalton
KDEL	Endoplasmic Reticulum Protein Retention Receptor 3
KI	Knock-in
KO	Knock-out
KR	Lysine 1003 IGF-1R to Arginine mutant
LC3	Microtubule-associated protein 1A/1B-light chain 3
LIR	LC3-interacting region
m	Mouse
mAB	Monoclonal antibody
MAPK	Mitogen Activated Protein kinase
MDM2	Transformed 3T3 cell double minute 2. P53 binding protein
MEK	MAPKK
MeOH	Methanol
MET	mesenchymal–epithelial transition
MET	Hepatocyte growth factor receptor
Mg	Magnesium
mg	Milligram
$MgCl_2$	Magnesium chloride
min	Minute

ml	Millilitre
mm	Millimetre
mM	Millimolar
$MnCl_2$	Manganese chloride
mRNA	messenger RNA
mTOR	Mammalian Target of Rapamycin
N/A	not available
NaCl	Sodium chloride
NaF	Sodium fluoride
NaOH	Sodium hydroxide
Nedd4	neural precursor cell-expressed developmentally downregulated gene 4
NEM	*N*-Ethylmaleinimid
ng	Nanogram
NHEJ	Non-homologues end joining
NLS	Nuclear location sequence
nM	Nanomolar
NP-40	Tergitol NP-40 (Non-Phenoxy poly ethoxy ethanol)
ON	Over night
OXPHOS	Oxidative phosphorylation
PBS	Phosphate Buffered Saline
PCR	Polymerase chain reaction
PDGFRβ	Platelet-derived growth factor receptor
PDK-1	3'-phosphatidylinositide Dependent kinase 1
PFA	Paraformaldehyde
PH	Pleckstrin Homology
PI3K/AKT	Phosphoinostid-3-Kinase/Protein kinase B
PIP2	Phosphatidyl Inositol (3,4)-bis Phosphate (PtdIns(3,4)P2)
PIP3	Phosphatidyl Inositol (3,4,5)-tris Phosphate (PtdIns(3,4,5)P3)
PKC	Protein kinase C
PNC1	Mitochondrial pyrimidine nucleotide carrier
PP2A	Protein Phosphatase 2A
PTB	Phosphotyrosine-binding domain
Ptdins	Phosphatidylinositol
PTEN	Phosphatase and Tensin Homolog
PTPa	PTP Protein tyrosine Phosphatase
PyMT	Polyoma middle T
qRT-PCR	quantitative reverse transcriptase PCR
R cells	3T3-like mouse embryonic fibroblast cell line derived from the IGF 1R knock-out mouse
R	Arginine
RACK1	Receptor for Activated C kinase 1
RAF	Rapidly Accelerated Fibrosarcoma
Rev	Reverse Primer
RGB	Red/Green/Blue

RNA	Ribonucleic Acid
RNAi	interference RNA
ROS	Reactive oxygen species
Rpm	round per minute
RPMI	Roswell Park Memorial Institute
RT	Room temperature
RTK	Receptor tyrosine kinase
SAPK	Stress Activated Protein kinase
SDS	Sodium Dodecyl Sulphate
sec	Seconds
SH2	Src homology 2 domain
SH3	Src homology 3 domain
SHC	The Src homology and Collagen adaptor protein
SHIP	SH2-containing inositol polyphosphate 5-phosphatase 1
Shp-2	SH2-containing protein tyrosine phosphatase 2
SOS	Sons of Sevenless
ssOND	single strand oligo nucleotide donor
STAT-3	Signal transducer and activator of transcription 3
SUS	Suspension
SV 40	Simian virus 40
TBS-T	TBS containing 0.5% Tween-20
Thr	Threonine
Tk	Tyrosine Kinase domain
TNF-α	Tumour necrosis factor α
TRIS	Tris(hydroxymethyl)aminomethane
TrkA/B	Tropomyosin receptor kinase A/B
TWISTS1/2	Twist Family BHLH Transcription Factor 1/2
Tyr	Tyrosine
UBI	Ubiquitin
UTP	Uridine Triphosphate
UV	Ultraviolet radiation
v/v	volume/volume percent
VGFR	Vascular endothelial growth factor receptor
WB	Western blotting
WCL	Whole cell lysates
WT	IGF-1R wildtype
ZEB	Zinc finger E-box-binding-homeobox
µl	Microliter
µM	Micromolar

1 CHAPTER 1: INTRODUCTION

1.1 THE INSULIN AND INSULIN-LIKE GROWTH FACTOR FAMILY

Receptor tyrosine kinases (RTKs) transmit extracellular stimuli from their ligands into specific intracellular signals to activate and regulate various cellular functions, including growth and survival signals for cell proliferation.

Insulin (Ins) and Insulin-like Growth Factors (IGFs) are a highly conserved family of hormone peptides. Upon binding to their cell surface receptors (illustrated in Figure 1.1), they activate a signalling system that is conserved from simple organisms to mammals (Barbieri et al., 2003, Eivers et al., 2004). The cell surface receptors are the Insulin Receptors (IR-A and IR-B), type I Insulin-like Growth Factor Receptor (IGF-1R), and the Insulin-Receptor-Related Receptor (IRR) (Figure 1.1). The type II Insulin-like Growth Factor Receptor (IGF-2R), in mammals also known as cation-independent mannose 6-phosphate receptor, exhibits no intrinsic kinase activity (Liu et al., 1993) and is not officially a member of the Insulin Receptor family (Hernández-Sánchez et al., 2008). However, the receptor is important for the IGF signalling axis as it has role in IGF-2 turnover (Liu et al., 1993). The two IR receptors are the product of alternative splicing and while the IR-B is mainly expressed in muscle, liver and adipose tissue, the IR-A is predominantly expressed in foetal and cancer cells (Belfiore et al., 2009). Members of the IR family are all expressed in the same cells, which allows the formation of hybrid receptors (Soos et al., 1993, Bailyes et al., 1997, Belfiore et al., 2009). In addition to the receptors and ligands, the Insulin and IGF signalling axis contains IGF binding proteins (IGFBPs) (Figure 1.1).

1.1.1 Insulin, Insulin-like Growth factors and IGF binding proteins

Three ligands have been shown to activate members of the Insulin Receptor family by binding to their extracellular domain. Insulin (Ins), Insulin-like growth factor 1 (IGF-1) and Insulin-like growth factor 2 (IGF-2) (Figure 1.1). Exclusively produced by the pancreas, the main function of Ins is the regulation of the carbohydrate metabolism (Sussenbach et al., 1992). While Ins preferentially binds to IR-B, IGF-1 and IGF-2 bind to the IGF-1R with high affinity and a dissociation constant (Kd) of 1 nM and 3 nM respectively (Steele-Perkins et al., 1988, Denley et al., 2005) (Figure 1.1). However, although IGF-1 and Ins display a higher affinity for their respective receptors, they can also activate the other receptors when the ligand concentration is supra-physiological levels (Sepp-Lorenzino, 1998). The lower affinity of Ins to the IGF-1R (a Kd 100-fold less) is due to the lack of the C-domain in Ins (Bayne et al., 1989). While IGFs are single polypeptides containing A, B, C, and D domains, Insulin contains separate A and B domains joined by disulfide bonds (Sussenbach et al., 1992).

IGFs have a primary function in promoting growth, proliferation and differentiation of cells, organs and organisms. The concentration of circulating IGFs in plasma is normally in the ng/ml range and it is produced mainly by the liver in response to Growth Hormones (GH) produced in the pituitary. However, as it was demonstrated with liver IGF-1-deficient (LID) mice, liver-derived IGF-1 is not essential for most tissues (Yakar et al., 1999). IGFs are also produced locally in most tissues by fibroblasts, epithelial cells and macrophages (Ferber et al., 1993, Chand et al., 2012, Barrett et al., 2015). Systemic macrophage-derived IGF-1 is essential for the adoption of the M2 phenotype of macrophages (Barrett et al., 2015), and local production of IGF-1 by

macrophages in response to muscle injury is required for muscle regeneration through myoblast proliferation and myoblast growth (Tonkin et al., 2015, Yu et al., 2015). Macrophages may also be an important source of locally acting IGFs in tumour environments and linked to tumour growth and recurrence (Ireland et al., 2016, Quail et al., 2016, Liu et al., 2018a). In these microenvironments, IGF-1 mediates anti-apoptotic signalling and promote resistance to chemotherapeutics (Chapuis et al., 2010, Fox et al., 2013, Ireland et al., 2016).

Only a small amount of IGFs are biologically active. In the bloodstream and in local tissue most circulating IGF molecules (90%) are bound to one of the six members of the IGFBP family (Allard and Duan, 2018) (Figure 1.1). Binding IGF molecules with a higher affinity than the IGF-1R, the IGFBPs have the distinct function of regulating ligand accessibility for the receptor and thereby, modulating IGF-1R activity in cells locally. The most represented IGFBP in human adult serum is IGFBP-3 with a concentration that is approximately 5-fold higher than the other family members (Jones and Clemmons, 1995, Rajaram et al., 1997).

About 75-80% of all IGF forms a complex with IGFBP-3 and the glycoprotein acid labile subunit (ALS), whereas the remaining 20-25% are bound to other IGFBP members. The formation of a binary complex of IGFBP/IGF prolongs the half-time of circulating IGF molecules from 10 min to approximately 25 min. The double complex can rapidly leave the capillaries (Guler et al., 1989), but the addition of ALS to the complex increases the IGF half-life time to about 16 hours maintaining a long-lasting reservoir of IGF molecules in circulation (Rajaram et al., 1997). Proteases are needed to release IGF molecules from the complex. Specific IGFBP proteases have been

described including the pregnancy-associated plasma protein 1 (PAPP-A1) and PAPP-A2 (Lawrence et al., 1999, Conover and Bale, 2007, Ning et al., 2008), Adam 9 (Mohan et al., 2002), Adam 12 (Shi et al., 2000) as well as Pappalysin-1 (Monget and Oxvig, 2016).

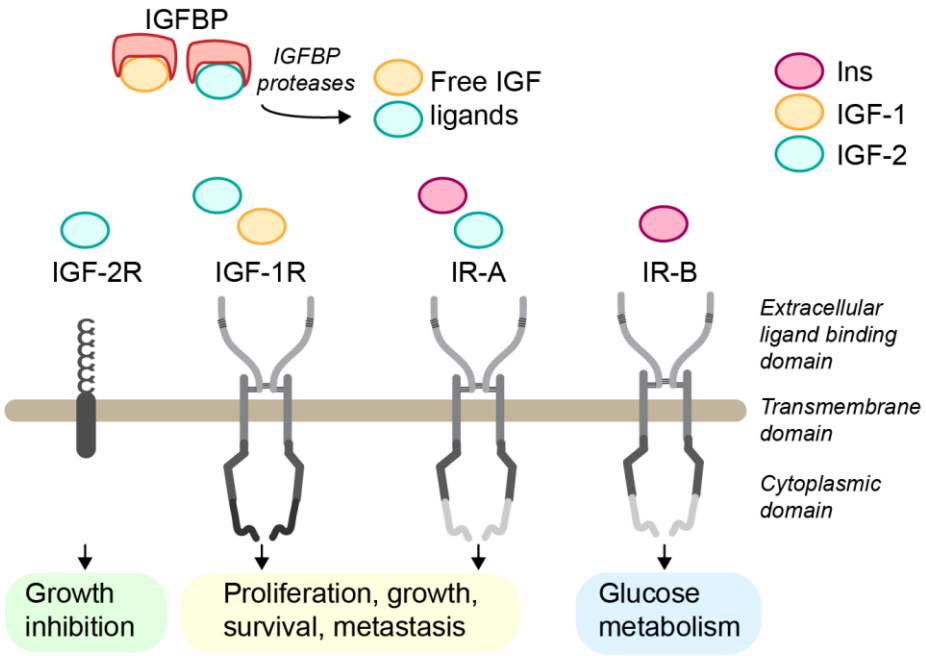


Figure 1.1: Overview of the Insulin and Insulin-like Growth factor family.

Insulin and IGF hormone peptides bind to the members of the Insulin Receptor family with different affinities. IGF-1R and both IRs contain an intrinsic kinase domain, which is activated upon ligand binding to regulate cellular processes. The IGF-2R is a single-chain polypeptide devoid of tyrosine kinase activity with an apparent role in IGF-2 degradation. To prolong their half-time circulating IGFs are bound to IGFBP. Specific proteases release the IGFs from the complex allowing them to bind to the cell surface receptors.

1.1.2 Receptor Evolution and Structure

The common Insulin/IGF-1R orthologue called decay accelerating factor-2 (Daf-2) receptor in *Caenorhabditis elegans* shares 35% similarity to IGF-1R and 36% similarity to the IR (Kimura et al., 1997, Sepp-Lorenzino, 1998). Daf-2 controls development, growth, aging and resistance to stress (Kimura et al., 1997).

Both the IR and the IGF-1R are tetrameric glycoproteins consisting of two extracellular α-subunits and two intracellular β-subunits connected though disulphide bonds (illustrated in Figure 1.2). Translated as a single-chain precursor (1.367 amino acids), the IGF-1R protein undergoes various modifications during maturation in the endoplasmic reticulum (ER) and Golgi-apparatus (Baserga et al., 1997, Sepp-Lorenzino, 1998, Adams et al., 2000) (Figure 1.2). Upon translocation of the nascent protein into the ER the first 30 amino acid signal peptide is cleaved leaving a 1337 amino acid long αβ-proreceptor. To generate the mature $\alpha_2\beta_2$ heterodimer, the proreceptor undergoes further processes including N-linked glycosylations, proteolytic cleavage on its R-K-R-R sequence and dimerization (Ullrich et al., 1986, Marino-Buslje et al., 1999, Adams et al., 2000, Denley et al., 2005).

The α-subunit, responsible for ligand-binding, contains a cysteine rich region and is located extracellular. The ligand-binding site of the IR and the IGF-1R share 45-65% homology (Ullrich et al., 1986, Whittaker et al., 2001) and are most similar in the cysteine-rich regions, which are involved in ligand recognition and binding (Belfiore et al., 2009). The region between amino acid 223 and 274 of the IGF-1R ensures specificity of IGF-1 as its ligand (Gustafson and Rutter, 1990, Keyhanfar et al., 2007). However, in conditions of excessive ligand amounts, both IGF-1 and Insulin can activate the other receptor.

The β-chain, consisting of an intracellular juxtamembrane domain, tyrosine kinase domain (TK) and the C-terminal tail (Figure 1.2), is 627 amino acids long. The IGF-1R transmembrane domain extends from residues 906-929. The TK of the IR and the IGF-1R share 84% homology, while the juxtamembrane domain exhibits 61% homology (Ullrich et al., 1986, Hubbard et al., 1994, Prager et al., 1994). The TK domain contains a cluster of three tyrosines Tyr^{1131}, Tyr^{1135} and Tyr^{1136} ($Tyr^{1135/1136}$), an ATP binding motif (976-GQGSFG-981) and on position 1003 an ATP binding lysine (K), essential for the Mg-ATP binding (Ullrich et al., 1986). Mutation of the ATP binding site K1003 to alanine (A) or arginine (R) abolishes the tyrosine kinase activity and the biological function of the IGF-1R (Tennagels et al., 1999, Scotlandi et al., 2002). The C-terminal of the IGF-1R (amino acids 1225-1337) is 44% homologous to the corresponding IR region making it the least similar domain in the IGF-1R and IR (Ullrich et al., 1986). Hence it is proposed that this domain regulates key differences in the function of IR and IGF-1R (Miura et al., 1995b, Miura and Baserga, 1997, Leahy et al., 2004, Kiely et al., 2005, Kelly et al., 2012, Zheng et al., 2012).

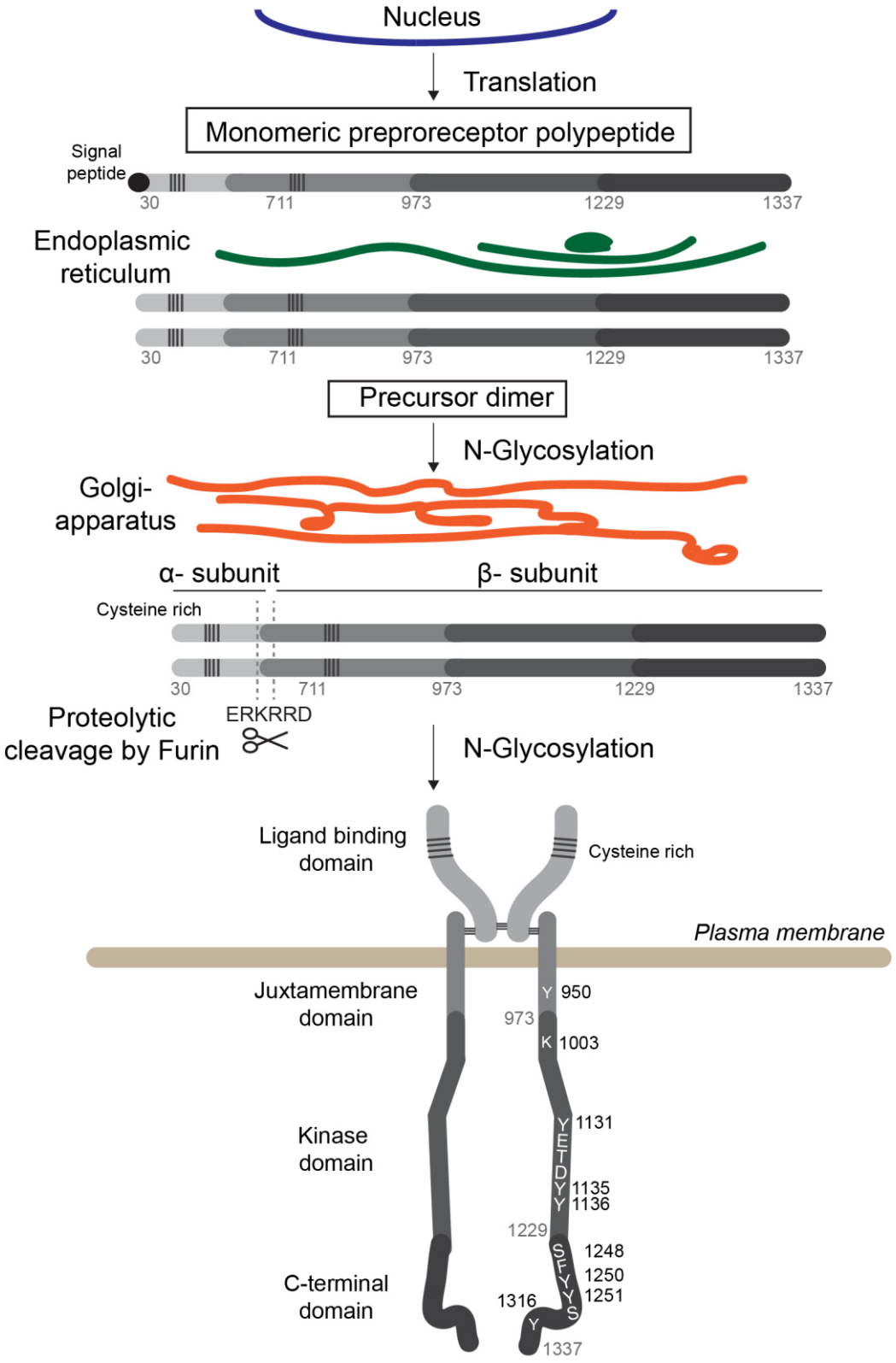


Figure 1.2: Biosynthesis pathway and important domains within the IGF-1R.

The momomeric proreceptor polypeptide is processed to the mature plasma membrane receptor by proteolysis and glycosylations in different compartments of the cell. Domains that have been identified to be essential for the IGF-1R function are indicated with amino acid residues that are important for this study.

1.2 THE PHYSIOLOGICAL FUNCTION OF THE IGF-1R SYSTEM

In response of IGF-1 binding to the receptor, the IGF-1R induces various signalling pathways and thereby regulating the cellular processes, including cellular growth, survival and differentiation, aging and longevity and metabolism. The two most well-characterized pathways activated by the IGF-1R are the Phosphoinositide 3 kinase (PI3K) pathway (Figure 1.6) and the Mitogen-Activated Protein Kinase-1 (MAPK) pathway (Figure 1.7) (Pollak, 2012).

1.2.1 IGF-1R promotes cell, organ and animal growth

It is believed that IGF-1 together with its receptor accounts for up to 70% of embryonic growth and is therefore essential for the normal development of the embryo and growth of animals (Baker et al., 1993). While in the early embryonic phase foetal growth is mainly dependent on IGF-2 acting through the IGF-1R and IR receptor, growth in the later foetal and postnatal phase is predominantly regulated by IGF-1 (Baker et al., 1993). As children and adults age, levels of plasma IGF-1 can be used as an indicator for body growth, with high levels of IGF-1 generally correlating with greater size (Gourmelen et al., 1984, LeRoith et al., 1991).

The endocrine disorder called Acromegaly is caused by the elevation of GH levels which leads to an increase in IGF-1 secretion. Acromegaly is characterised by the abnormal growth of hands, feet and head (Melmed, 2006). Pathological Acromegaly also results in the enlargement of visceral organs and patients are at higher risk of morbidity and mortality due to cardiovascular diseases (Dekkers et al., 2008, Holdaway et al., 2008). In contrast, in pygmies and Laron dwarfs, disorders characterized by the small

stature of humans are caused by a genetic defect in the growth hormone receptor and these individuals display low levels of plasma IGF-1 (Amselem et al., 1989, LeRoith et al., 1991, Baserga et al., 1997).

The essential function of IGF-1 in growth is not limited to humans, but is also present in animals including dogs and mice. In mice, targeted disruption of the IGF-1 or IGF-2 gene causes a 60% reduction in weight at birth and IGF-1R null mice display 45% decrease in body weight compared to controls and die at birth due to respiratory failure. These mice also exhibit organ hypoplasia in muscle, development delays in ossification and abnormalities in the central nervous system and the epidermis (Liu et al., 1993). Abnormalities found in IGF-1R null mice are primarily caused by the elongation of the cell cycle (Sell et al., 1994). Furthermore, fibroblasts derived from IGF-1R null mice (R^- cells) show a reduction in growth rates compared to fibroblasts, where the *igf-1r* gene was reintroduced (R^+ cells, (Sell et al., 1994). In contrast, the over-expression of GH or IGF-1 in mice results in larger organs compared to controls (Palmiter et al., 1982, Holdaway et al., 2008, Dekkers et al., 2008).

1.2.2 IGF-1R mediates cell survival and differentiation

Apoptosis is an innate process of programmed cell death that is triggered by cellular damage, while also required for normal cell growth and mammalian development. Dysregulation of apoptosis or cell death is implicated in the development and abnormal growth of cancer cells. IGF-1 acting through the IGF-1R promotes potent cell survival in response to many apoptotic stimuli including hypoxia (Stoeltzing et al., 2003), overexpression of c-Myc (Harrington et al., 1994), 1994), chemotherapeutic agents (Sell et al., 1995), TNF-α (Wu et al., 1996), IL-3 withdrawal (O'Connor et al., 1997), p53 (Prisco

et al., 1997) and UV radiation (McMahon et al., 2010). IGF-1-mediated cell survival is also important for the recovery of cardiomyocytes after myocardial infarction (O'Sullivan et al., 2011) as well as neuronal cells following ischemic brain injury (Guan et al., 2003, Brywe et al., 2005).

IGF-1R-mediated cell survival is induced by the activation of downstream signalling pathways including the PI3K/AKT, Ras/MAPK, p38 and JNK (O'Connor, 2003). PI3K activation causes phosphorylation of Bad, a member of the pro-apoptotic BCL-2 family. This IGF-1R-facilitated serine phosphorylation inhibits Bad heterodimerization with BCL-XL. Heterodimerization of Bad and BCL-XL triggers the release of Cytochrome C from the mitochondria leading to induction of a caspase cascade and apoptosis (Datta et al., 1997). IGF-1 stimulates the phosphorylation of Bad which prevents its interaction with BCL-XL and thereby mediates an anti-apoptotic effect (Datta et al., 1997). The activation of PI3K also prevents the translocation of FKHR into the nucleus. As a transcriptional enhancer, FKHR is responsible for the transcription of multiple pro-apoptotic genes (Biggs et al., 1999). Furthermore the PI3K-mediated activation of AKT results in translocation of MDM2, a major inhibitor of the p53. Thus IGF-1 induced signalling negatively regulates p53 targets (Carter et al., 2007). In addition to IGF-1R-mediated activation of PI3K/AKT signalling to promote cell-survival, it was recently reported that the translocation of the IGF-1R to the nucleus induces the transcription of the pro-survival gene JUN (Aleksic et al., 2018).

Anti-apoptotic signalling from the IGF-1R requires the presence of distinct residues located in the C-terminal tail including $Tyr^{1250/1251}$ and His^{1293}/Lys^{1294}. Point mutations of these amino acids abolish the IGF-1 anti-apoptotic effects (O'Connor et al., 1997), and ectopic expression of this domain

induced apoptosis in cancer cells *in vivo* and inhibited tumorigenesis in nude mice (Liu et al., 1998, Hongo et al., 1998).

Cell proliferation and differentiation are processes that are mutually exclusive in most cell types. Growth-factors can inhibit differentiation to stimulate cell proliferation. During development though, it is believed that the balance between cell differentiation and cell proliferation can be regulated by the activity of growth factors like IGF-1. Under certain conditions, IGFs may induce both proliferation and differentiation in a wide range of cells including osteoblasts (Wang et al., 2015), adipocytes (Boucher et al., 2016), oligodendrocytes (Hsieh et al., 2004), neuronal cells (Ziegler et al., 2015) and hematopoietic cells (Petley et al., 1999).

In hematopoietic cells, ectopic expression of IGF-1R allows the normally IL-3-dependent murine 32D myeloid cell line, to grow independently of IL-3. The additional expression of IRS-1 leads to cell proliferation, whereas the addition of SHC results in cell differentiation (Valentinis et al., 1999). This indicates that IGF-1 signals through different adapter proteins and signalling pathways.

During bone fracture healing, IGF-1 is also involved in cell proliferation and differentiation of mesenchymal cells, periosteal cells, osteoblasts, osteoclasts and chondrocytes. Moreover, loss of IGF-1R from osteoblasts highly effects the process of fracture healing (Wang et al., 2015).

The IGF-1R plays an essential role in the growth of skeletal muscle as IGF-1 induces both myoblast proliferation and differentiation (Florini et al., 1996). The same effect is observed, when IGF-1R is constitutively overexpressed in myogenic cells. *In-vivo* studies demonstrated that injury- and exercise-induced muscle regeneration is accompanied by increased IGF-1

expression (DeVol et al., 1990) and that IGF-1 expression in muscle can reduce age-related muscle-atrophy (Barton-Davis et al., 1998).

The IGF-1R system contributes to the development of the central nervous system and is also involved in recovery post-injury (Dyer et al., 2016). IGF-1 promotes proliferation and survival of progenitor cells, neurons and oligodendrocyte and is therefore crucial to the post-injury neuroprotection and regeneration (Isgaard et al., 2007, Dyer et al., 2016). Due to its neuroprotective role, IGF-1 may have potential to be used as therapeutic treatment for neurodevelopmental disorders as well as treatment after injuries to the central nervous system (Mangiola et al., 2015, Dyer et al., 2016, Costales and Kolevzon, 2016).

1.2.3 IGF-1R axis in aging and longevity

Aging and the environmental and genetic regulation of the lifespan of organisms are fundamental processes in life. There is evidence that IGF-1 signalling can accelerate aging mainly through the activation of the PI3K pathway. In *C. elegans*, the mutation of the *daf-2* (the IR/IGF-1R orthologue), was found to extend the life-span by 2-fold (Kenyon et al., 1993). Similar results were observed in *Drosophila melanogaster* (Tatar et al., 2001). Mouse studies have revealed that either a reduction of the IGF-1R or the levels of circulating IGF-1 are linked to an increase in life span (Brown-Borg et al., 1996, Flurkey et al., 2002, Holzenberger et al., 2003). Whilst the involvement of the IGF-1 system can be easily studied in model organisms including mice, *C. elegans* or *Drosophila melanogaster*, its role in human aging is more difficult to determine. However, emerging evidence indicates a correlation between low IGF-1 levels and human lifespan. A longer lifespan is associated with lower

levels of IGF-1 in an aging population that had a history of malignancy (Milman et al., 2014). In families of Ashkenazi Jewish centenarians, where two mutations in the IGF-1R (A37T and R407H) are enriched, reduced IGF-1R-mediated activation of the PI3K pathway is proposed to increase the lifespan of individuals (Tazearslan et al., 2011). A unique subgroup of Ecuadorian individuals, characterized by a mutation in the growth hormone receptor gene, have reduced levels of circulating IGF-1. This deficiency confers a profound reduction in pro-aging signalling on this population, and is associated with reduced occurrence of cancer and diabetes (Guevara-Aguirre et al., 2011).

1.2.4 IGF-1R in metabolism and mitochondrial function

The IR/IGF-1R system controls metabolic homeostasis and the dysregulation of this system is linked to metabolic disorders (Clemmons, 2012). Since IGF-1 stimulates growth of all cell types in foetal development as well in adolescence, its signalling through the IGF-1R has major impact on cellular protein, carbohydrate or fat metabolism. These processes are tightly coordinated with insulin and GH.

The major player in cellular metabolism and bioenergetics is the mitochondrion. Its general function is to convert metabolites such as glucose into Adenosine-tri-phosphate (ATP) to provide energy for cellular processes (Sádaba et al., 2016). This process is known as oxidative phosphorylation (OXPHOS). Reactive oxygen species (ROS) are a normal by-product of OXPHOS, which are neutralized by superoxide dismutase (SOD) and eventually converted into water and oxygen (Mailloux, 2015) to avoid the accumulation of cell damaging ROS (Zorov et al., 2014). As mitochondria hold

an essential function in cells, their synthesis (mitochondrial biogenesis) and regulation of their numbers and quality (mitochondrial fission and fusion) are well-orchestrated and controlled processes within every cell. The importance of mitochondrial quality control and mitochondrial homeostasis in the maintenance of healthy tissues is well documented (Rambold and Lippincott-Schwartz, 2011, Sádaba et al., 2016). Impaired mitophagy can lead to the accumulation of dysfunctional mitochondria and oxidative stress, which is associated with various diseases including neurodegeneration, diabetes, heart disease and cancer (Ritov et al., 2005, Pieczenik and Neustadt, 2007, Ren et al., 2010, Sheng et al., 2012, Sádaba et al., 2016, Macleod, 2020).

While the influence of IGF-1 signalling on carbohydrate metabolism/glycolysis is well studied (reviewed by (Clemmons, 2012)), the regulation of mitochondrial function by IGF-1 signalling is an emerging topic. IGF-1 promotes mitochondrial biogenesis (Lyons et al., 2017). The IGF-1R/PI3K axis was demonstrated to mediate biogenesis by inducing the expression of key regulators of the process, PGC1β and PRC. When IGF-1R signalling is supressed or the activation of PI3K pathway is inhibited, PGC1β and PRC expression are decreased, which leads to a reduction in mitochondrial mass and biogenesis (Lyons et al., 2017). Furthermore IGF-1R is reported to induce the expression of the mitophagy receptor BNIP-3 (Lyons et al., 2017). BNIP-3 is inserted into the mitochondrial membrane and acts through its LIR domain as adaptor protein for LC3 (Liu et al., 2014), which subsequently leads to lysosomal degradation of dysfunctional mitochondria. Inhibition or suppression of IGF-1R signalling causes reduced expression of PGC1β and PRC, and BNIP-3 protein, resulting in impaired mitophagy, an

accumulation of dysfunctional mitochondria and the increased production of ROS (Lyons et al., 2017).

Further evidence for essential IGF-1 signalling in maintaining healthy mitochondria comes from our identification of an IGF-1 inducible mitochondrial UTP importer, pyrimidine nucleotide carrier 1 (PNC1) that is required for maintaining mitochondrial RNA and DNA (Floyd et al., 2007, Favre et al., 2010). Suppression of PNC-1 correlates with high ROS production, and under normal oxygen conditions, PNC1 suppression mediates an increase in glycolysis for ATP production whilst also decreasing OXPHOS. Increased ROS as a result of PNC1 suppression causes a profound induction of EMT in MCF-7 and HeLa cells (Favre et al., 2010).

Taken together, there is strong evidence that IGF-1 signalling has a role in mitochondrial protection and in maintenance of mitochondrial homeostasis (also discussed in (Sádaba et al., 2016)).

1.3 IGF-1 INDUCED MECHANISMS AND SIGNALLING PATHWAYS

1.3.1 How the IGF-1R kinase is activated

The IGF-1R is activated in response to IGF-1 binding to the α-dimer. The first event induced by ligand binding is autophosphorylation on the tyrosine cluster at positions 1131, 1135, and 1136 in the proposed order of 1135>1131>1136 (Figure 1.3). The autophosphorylation on the A-loop tyrosines allows ATP, magnesium and the substrate to access the active site (Hubbard, 1997) (Figure 1.3). To restrain IGF-1R kinase activity when IGF-1 is not present, IGF-1R forms an auto-inhibitory conformation (Figure 1.3, Figure 1.4). IGF-1 binding and subsequent phosphorylation on Tyr^{1135} and Try^{1131} destabilizes this auto-inhibition, whereas Tyr^{1136} phosphorylation subsequently stabilizes the active conformation. Salt bridges between phosphorylated Tyr^{1135} and Arg^{1128} as well as phosphorylated Tyr^{1136} with Arg^{1128} and Lys^{1138} maintain the active kinase conformation of the IGF-1R (Favelyukis et al., 2001).

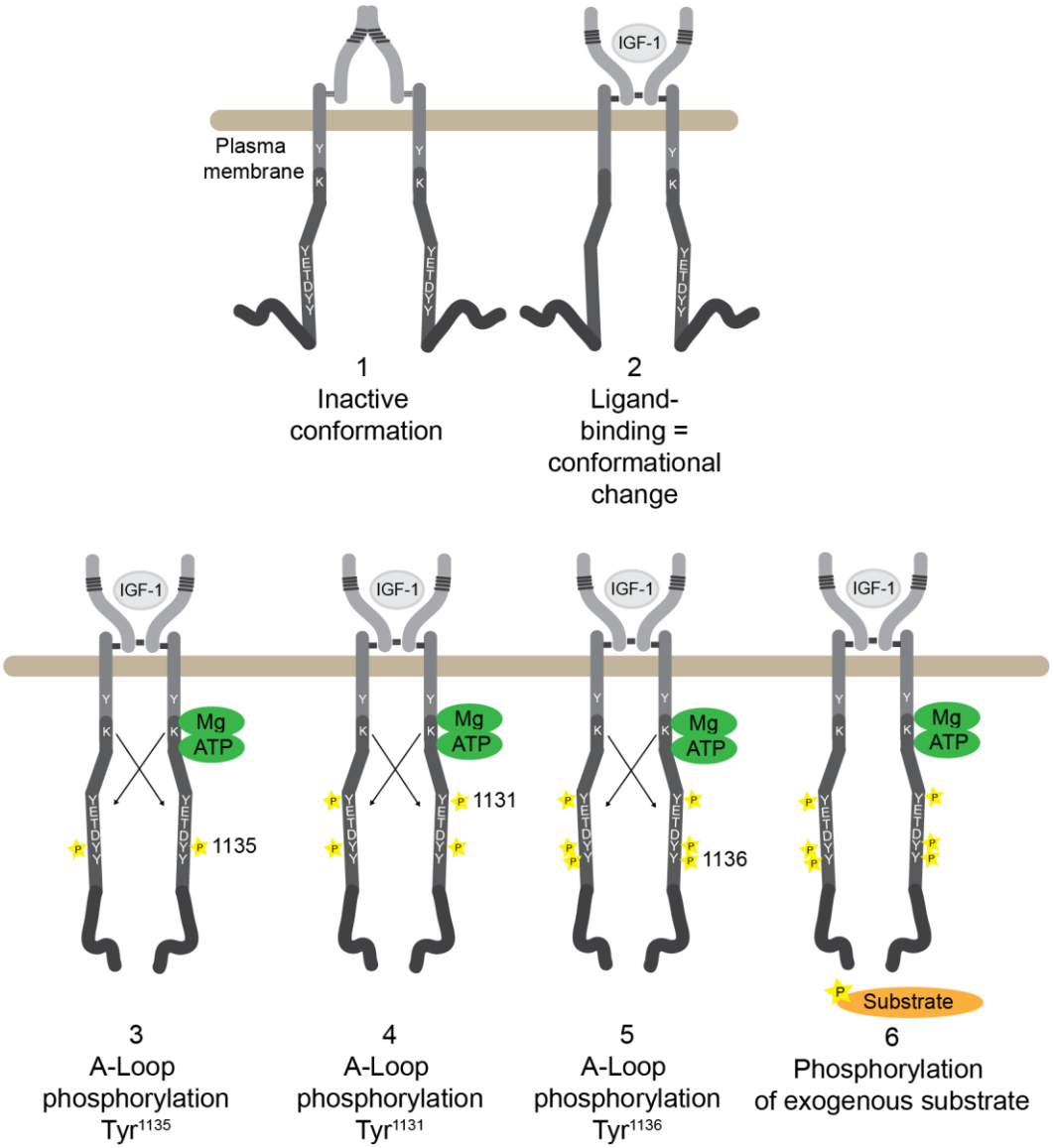


Figure 1.3: Stages of IGF-1R tyrosine kinase activation.

(1) The IGF-1R is present in dimeric form at the cell membrane prior to ligand binding. (2) IGF-1 binding induced a conformational change in the IGF-1R subunits, which allows the trans-autophosphorylation of (3) Tyr^{1135}, (4) Tyr^{1131}, (5) Tyr^{1136}. This leads to increased access of ATP and the (6) subsequent phosphorylation of exogenous substrate.

Whereas other RTKs are activated upon receptor dimerization the members of the Insulin receptor family are present as pre-formed dimers (Figure 1.3) and therefore require a different mechanism in activation and restraining the activation to prevent ligand independent receptor activity. Recent studies showed that once the IGF-1R is phosphorylated and the kinase is active, neither the ligand nor structures outside the kinase domain contribute to the kinase activity (Kavran et al., 2014, Xu et al., 2018). It was furthermore demonstrated that the two extracellular domains maintain an "inverted V-shape" (Figure 1.4), leading to the conformational separation of the transmembrane domain. Upon IGF-1 binding the transmembrane regions dimerize resolving the auto-inhibitory conformation allowing autophosphorylation (Kavran et al., 2014, Xu et al., 2018). This describes a mechanism in which ligand binding is responsible for disrupting an inhibitory structure rather than activating the receptor.

Each IGF-1R arm contains two ligand binding pockets and each binding pocket is composed of interacting residues either located on the same αβ- arm or the interacting arm. The binding pockets are composed of the L1, CR, L2, FnIII-1, -2, -3 (domains of first dimer^{1} domains of second dimer^{2}) (Figure 1.4) and are formed by the interaction of residues on the L1^{2} and CR^{2} domains and αCT^{1} and FNIII-1^{1} (Williams et al., 1995, Mynarcik et al., 1996, Whittaker et al., 2001, Whittaker et al., 2008, Smith et al., 2010, Li et al., 2019). Although IGF-1R contains two IGF-1 binding pockets, the stoichiometry of IGF-1:IGF-1R is 1:1. The binding of a ligand molecule to in pocket 1 decreases the affinity to pocket 2, a mechanism that has been described as negative cooperativity (De Meyts, 2004, Surinya et al., 2008). Li *et al.*, recently discovered the reason for the negative cooperativity, where liganded αCT interacts with unliganded αCT

preventing the conformational rearrangement needed for binding of a second IGF-1 molecule. In addition, the group described the interaction between unliganded L1 and unliganded FnIII-2 as stabilisation for the active IGF-1R dimer formation (Li et al., 2019). Truncation of the intracellular domain disrupts negative cooperativity indicating that the full length protein is needed for optimal IGF-1 binding and activation of the receptor (De Meyts, 1994). Whereas negative cooperativity for Insulin binding to the Insulin receptor is abolished with Insulin concentrations greater than 100 nM, negative cooperativity for IGF-1 binding to IGF-1R remains even with high concentrations. Hence the dissociation curve is sigmoidal (Christoffersen et al., 1994, De Meyts, 1994).

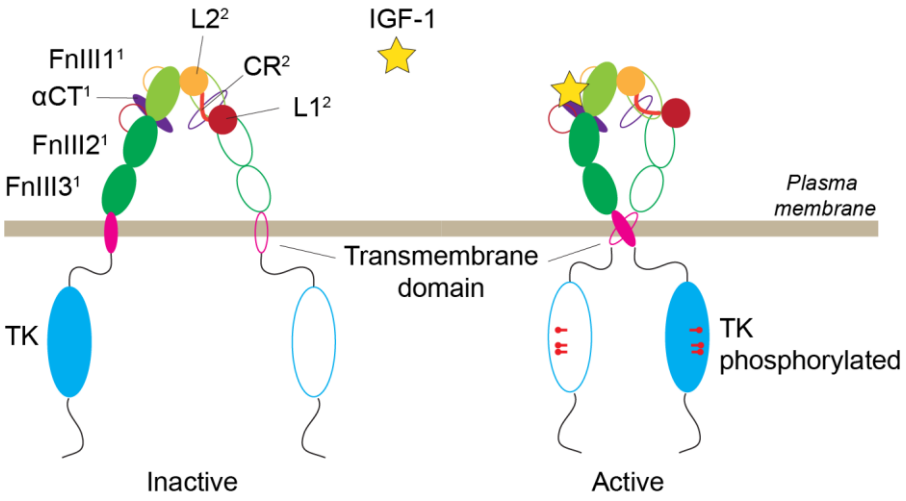


Figure 1.4: Conformational changes in the IGF-1R upon IGF-1 binding.

Cartoon illustrating the 'inverted V' shape restraining the IGF-1R activity upon IGF-1 ligand binding. Ligand binding to one of the two ligand pockets composed of $L1^2$, CR^2 and αCT^1 and $FNIII\text{-}1^1$ leads to the release of the autoinhibitory conformation allowing the IGF-1R autophosphorylation (red strokes).

1.3.2 The autophosphorylation site Tyr^{950} IGF-1R

In response to IGF-1 binding to the IGF-1R, the intrinsic tyrosine kinases activity autophosphorylates the tyrosine cluster in the kinase domain (Figure 1.3). However, tyrosines outside the A-loop are phosphorylated by the IGF-1R. Form the three tyrosines (Tyr^{943}, Tyr^{950} and Tyr^{957}) located in the juxtamembrane domain of the IGF-1R (Figure 1.2) (Prager et al., 1994), IGF-1R autophosphorylates Tyr^{950}, which is important for signal transmission as it critical for the recruitment of IGF-1R substrates. Although Tyr^{950} is not required for the IGF-1R kinases activity, the mutation of the Tyr^{950} to phenylalanine inhibits IGF-1-induced signalling and cellular transformation (Miura et al., 1995a).

1.3.3 The function of the C-terminal tail in the IGF-1R

The IGF-1R and the IR are most distinguishable in the C-terminal region, and it is proposed to be a regulatory domain that distinguishes features of IGF-1R-specific signalling from IR signalling in cells. However, how the contribution of the C-terminal tail to IGF-1R activity and function in normal cells or cancer cells is still not understood.

1.3.3.1 Point mutations in the C-terminal tail impair IGF-1R functions

The Tyr$^{1250/1251}$ in IGF-1R are not present in the corresponding region of the human IR (Ullrich et al., 1986). Mutation to phenylalanine Y1250F/Y1251F (FF) profoundly impairs IGF-1R activity in cells, but the exact role of these residues in regulating the IGF-1R activity is still unknown (Figure 1.5).

R$^-$ cells or other cells overexpressing the FF IGF-1R mutant are refractory to cellular transformation (Miura et al., 1995b), and exhibit impaired

cell survival (O'Connor et al., 1997) as well as the ability to support a metastatic and invasive phenotype, mainly displayed by anchorage-independent growth and reduced cell migration (Brodt et al., 2001, Kiely et al., 2005). The FF mutant does not associate with the scaffolding protein RACK1 (Figure 1.5) causing a loss of interaction with β1-Integrin which is required for IGF-1-promoted cell migration (Kiely et al., 2005). Several components of the migration machinery regulated by IGF-1, require RACK1 interaction with the IGF-1R, including SHC, Src and Shp-2 (Kiely et al., 2005, Kiely et al., 2002, Manes et al., 1999, Chang and Karin, 2001, Cox et al., 2015). Any modifications in the adhesion complexes generally causes impaired IGF-1-induced cell migration (Hermanto et al., 2002, Kiely et al., 2005, Taliaferro-Smith et al., 2015).

The IGF-1R FF mutant, and even a single mutation of Y1251F cannot mediate an anti-apoptotic signal when overexpressed in different cells (O'Connor et al., 1997, Brodt et al., 2001). However, truncation of the C-terminal tail at Δ1229 or Δ1245 does not abolish IGF-1R-mediated protection from apoptosis, suggesting that their ability to transmit an anti-apoptotic effect might be due to their modification such as phosphorylation (O'Connor et al., 1997). The single mutation of Y1250F was also proposed to be involved in IGF-1R internalisation. Truncation of the C-terminal tail Δ1229 IGF-1R and the Y1250F IGF-1R both reduced IGF-1R internalisation (Miura and Baserga, 1997).

1.3.3.2 The regulation of IGF-1R kinase activity

Once the IGF-1R kinase domain is activated, it is proposed that the extracellular domain, the transmembrane domain, and the C-terminal tail do

not contribute further to IGF-1R activity (Kavran et al., 2014, Xu et al., 2018). However, much evidence supports a function for the IGF-1R C-terminal tail in regulating kinase activity.

The double Y1250F/Y1251F mutation is sufficient to profoundly reduce SHC/Ras/MAPK activation (Leahy et al., 2004, Chen et al., 1998, Kiely et al., 2005), which may be due to less Grb-2 interaction with SHC. Interestingly, the mutation does not reduce IGF-1-induced PI3K/AKT activation, but rather increases it, suggesting that IRS-1 interaction with the IGF-1R does not require $Tyr^{1250/1251}$ (Leahy et al., 2004, Kiely et al., 2005).

The IGF-1R FF mutant also exhibits significantly impaired IGF-1R kinase activity in *in vitro* kinase assays. Immunoprecipitated IGF-1R FF mutant is significantly less autophosphorylated in both serum-free cell cultures or in the presence of exogenously added ATP compared to the IGF-1R WT. This again supports the involvement of $Tyr^{1250/1251}$ in IGF-1R kinase regulation (O'Connor et al., 1997).

Two serines flank $Tyr^{1250/1251}$ (Ser^{1248} and Ser^{1252}), and these are proposed to function in negative regulation of IGF-1R kinase activity by restraining the kinase activity upon ligand binding (Kelly et al., 2012). Ser^{1252} is proposed as a priming phosphorylation site for GSK-3β to phosphorylate Ser^{1248}, which phosphorylation would be inhibited by IGF-1 (through AKT-mediated phosphorylation on Ser^{9} and suppression of GSK-3β activity). Phosphorylated Ser^{1248} would allow the C-terminal tail to 'wrap' around the kinase domain, which blocks the activation of the receptor. Upon ligand binding, dephosphorylation of Ser^{1248} would release the C-terminal tail from the inhibitory position, thereby exposing the IGF-1R kinase domain for full activation (Kelly et al., 2012). Mutation of Ser^{1248} to alanine disrupts this

regulatory mechanism leading to a locked active IGF-1R kinase and an observed increase in cell growth and proliferation (Kelly et al., 2012).

Although substitution of Tyr^{1250} Tyr^{1251} with phenylalanines impairs IGF-1R kinase activity (Figure 1.5), the mechanism of phosphorylation on this phosphosite and its function in cell biology is still poorly understood. Indeed, evidence of this phosphorylation in cells is lacking and all the work on understanding their contribution to IGF-1R-mediated cellular transformation and migration are dependent on studies with the FF or single mutants. A better understanding of the function of these tyrosines and the IGF-1R C terminal tail might also reveal essential details distinguishing IGF-1R from the Insulin receptor function in cells. A major part of the work in this thesis was built on the finding that Tyr^{1250} and Tyr^{1251} are phosphorylated in cells and that IGF-1R activity enhances their phosphorylation (S. O'Shea PhD thesis, 2016). This opens up new avenues for investigating the mechanisms and importance of this phospho-site in the IGF-1R.

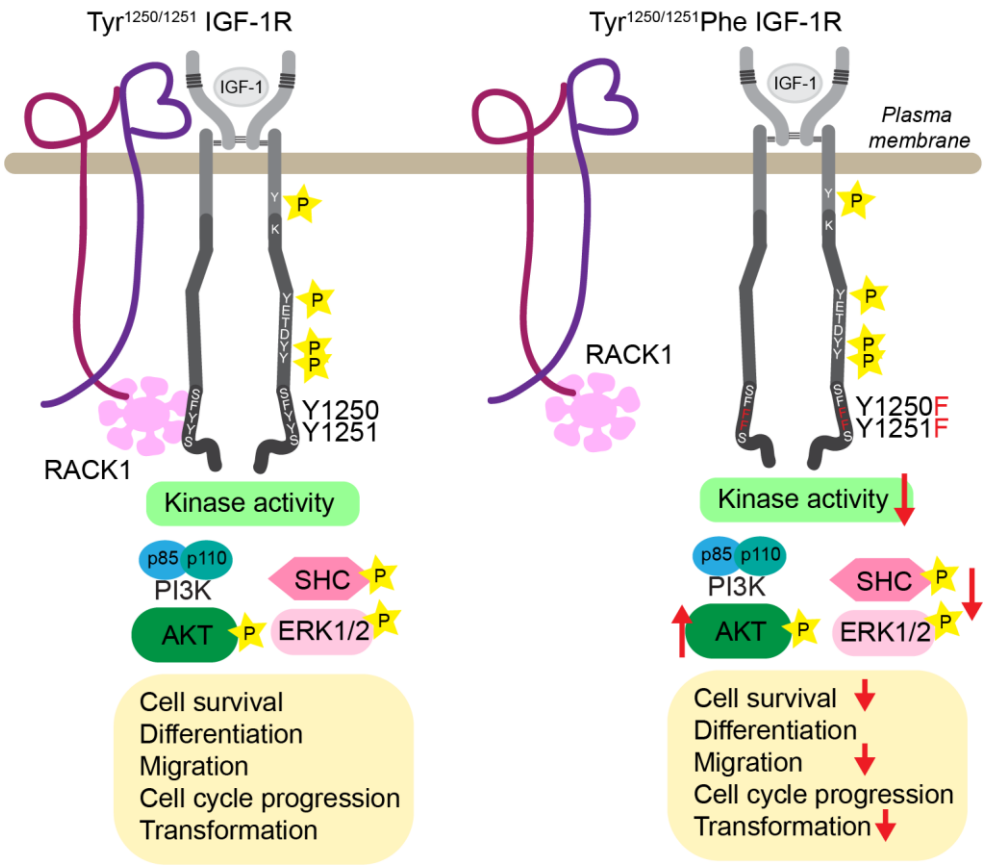


Figure 1.5: Mutation of Tyr$^{1250/1251}$ to phenylalanine impairs the IGF-1R function.

Ligand-activated IGF-1R, interacts with RACK1 and β1-Integrin. Upon autophosphorylation, it induces the PI3K/AKT and the SHC/Ras/MAPK pathway, facilitating different cellular processes. Mutation of Tyr$^{1250/1251}$ to phenylalanines abolishes the interaction with RACK1 and reduces the activation of SHC/Ras/MAPK signalling. Consequently, IGF-1R-mediated cellular functions are impaired.

1.3.4 IGF-1R signal transduction

Upon kinase activation the conformational changes and autophosphorylation of the IGF-1R introduces specific binding sites for proteins recruited to the IGF-1R upon ligand binding. These proteins interact with the IGF-1R either through their Src homology 2 (SH2) or the protein tyrosine binding (PTB) domain. The interaction with these specific adaptor proteins allows IGF-1R to activate a wide range of downstream signalling pathways. The two best characterized pathways induced by IGF-1R-mediated phosphorylation are the Phosphoinositide 3 kinase (PI3K) pathway and the Mitogen-Activated Protein Kinase-1 (MAPK) pathway (Myers et al., 1994, O'Connor, 2003). The interaction with recruited proteins can alter the activity of IGF-1R and modulate the signalling output (Buckley et al., 2002, Kiely et al., 2005, Taliaferro-Smith et al., 2015, Yoneyama et al., 2018).

1.3.4.1 IRS and SHC as IGF-1R Adaptor Proteins

1.3.4.1.1 Insulin Receptor Substrate Family

Insulin Receptor Substrate (IRS) proteins are a family of cytoplasmic adaptor proteins that are recruited to the autophosphorylated Tyr^{950}/Tyr^{960} site in the IGF-1R/IR and subsequently become phosphorylated on key tyrosines in their C-terminal tail by the IGF-1R/IR kinase. IRS proteins act as scaffolding proteins to recruit different signalling complexes (Sun et al., 1991). They contain a PTB domain that recognizes the NPEY motif in the IGF-1R when Try^{950} is phosphorylated and a pleckstrin homology (PH) sequence which is essential for IRS binding to the receptor (Voliovitch et al., 1995, Yenush et al., 1996). Tyrosine phosphorylated IRS proteins provide a docking site for downstream effector proteins containing a SH2 domain (Sun et al., 1993),

including the p85 domain of PI3K, Grb-2, SHP-2, Fyn, c-Crk, CrkII and Nck (Pollak, 2008). However, multiple studies have demonstrated that the main role of IRS proteins is to amplify IGF-1-mediated PI3K signalling (Figure 1.6).

The family consists of 6 members (IRS-1-6). Both IRS-1 and IRS-2 are ubiquitously expressed in most cell types (White, 2002) and although IRS-1 and IRS-2 proteins share significant homology, they each have non-redundant cellular functions. IRS-1 null mice exhibit a decrease (~70%) in size compared to WT mice and are not able to recover throughout their lives, demonstrating a main function of IRS-1 in organismal growth. Although they show hyper-insulinemia, IRS-1 null mice do not develop insulin resistance (Araki et al., 1994, Shaw, 2011). IRS-2 null mice show no significant reduction in size but rather exhibit tissue-specific defects such as a decrease in brain size, due to a reduction in neuronal proliferation, and infertility. They also develop insulin resistance and diabetes (Withers et al., 1998, Shaw, 2011).

IRS-1 and IRS-2 also play a role in facilitation of tumorigenesis. Their overexpression in the mouse mammary gland causes mammary hyperplasia and tumorigenesis, potentially due to the constitutive activation of AKT and ERK1/2 (Dearth et al., 2006). IRS-1 and IRS-2 are also distinguishable in facilitating different aspects of cancer progression. It has been demonstrated that the targeted deletion of IRS-2 leads to impaired metastasis of polyoma middle T (PyMT) tumours (Nagle et al., 2004, Ma et al., 2006, Shaw, 2011). In contrast, the loss of IRS-1 enhances metastasis caused by a compensatory mechanism of increasing IRS-2 levels and activity (Ma et al., 2006). Overexpression of IRS-1 cells in T47D-TA breast cancer cells that lack IRS expression leads to enhanced proliferation, whereas the overexpression of IRS-2 causes increased motility (Gibson et al., 2007, Shaw, 2011).

1.3.4.1.2 The Src homology and Collagen (SHC) family of adaptor proteins

The family of SHC adaptor proteins contains four members, which are encoded by four distinct genes (Ahmed and Prigent, 2017). The most studied SHC family member is SHCA (referred to as SHC) which is widely expressed in human tissue (Pelicci et al., 1992). SHC contains a PTB domain as well as a SH2 domain (Ahmed and Prigent, 2017) and is recruited, similar to IRS proteins, to the activated IGF-1R where it binds to the receptor at Tyr^{950} (Gustafson et al., 1995) via its PTB domain. In response to IGF-1, SHC is phosphorylated on its 3 tyrosine sites ($Try^{239/240}$, Tyr^{317}). SHC mediates activation of the Ras/MAPK pathway by binding the Grb-2-SOS complex (Figure 1.7) (Gotoh et al., 1997), but was also reported to mediate IR signalling through binding of SH2-containing-Inositol Phosphatase (SHIP2). SHIP2 competes with Grb-2 for binding to SHC (Liu et al., 1997), and may also activate the PI3K pathway (Gu et al., 2000).

Three isoforms of SHC are found in intracellular compartments; p46, p52 and p66 SHC, each of which is implicated in distinct intracellular pathways. The longest SHC isoform (p66 SHC) is linked to apoptosis in response to oxidative stress (Migliaccio et al., 1999), whereas the shorter isoforms (p46 and p52) are involved in cell cycle progression and differentiation (Wary et al., 1996, Stevenson et al., 1999). The isoforms p46 and p52 SHC are responsible for amplifying IGF-1R-mediated induction of Ras/MAPK (Luzi et al., 2000), whereas p66 SHC may inhibit the IGF-1R-meidated mitogenic response by also binding Grb-2 (Pellegrini et al., 2005).

SHC was originally characterized as a cytoplasmic adapter protein. However, recent studies have shown SHC is located in different intracellular

compartments where it may transmit signals. Translocation of p66 SHC to the mitochondria is proposed in the regulation of oxidative stress (Nemoto et al., 2006). Furthermore, nuclear localisation of p46 SHC was reported in both hepatocytes and hepatic carcinoma (Yukimasa et al., 2005), despite the fact that SHC isoforms lack a classical nuclear localisation (NLS) sequence. Subcellular fractionation demonstrates that SHC is also present in endosomes and the rough endoplasmic reticulum located within the perinuclear region (Di Guglielmo et al., 1994, Lotti et al., 1996).

1.3.5 IGF-1R and adhesion signalling

Cell migration is an essential process in normal cells to facilitate organ and tissue development as well as wound healing (Bitar, 1997, Emmerson et al., 2012, Millarte and Farhan, 2012). Cell migration requires the interaction of cells with the extra cellular matrix (ECM), which is mediated by the Integrin receptor family (Huttenlocher and Horwitz, 2011). IGF-1-induced cell migration, cancer cell growth as colonies and activation of the MAPK pathway all require cells to receive an adhesion signal via Integrins (Brodt et al., 2001, Hermanto et al., 2002, Kiely et al., 2005). The interaction of IGF-1R with β1-Integrin can be facilitated by the scaffolding protein Receptor for activated C kinase 1 (RACK1). This interaction enhances IGF-1R-mediated SHC and Ras/MAPK activation as well as IGF-1-induced cell migration (Kiely et al., 2002, Kiely et al., 2005). Although the interaction of RACK1 and IGF-1R does not require activation of IGF-1R, the recruitment of β1-Integrin to the complex does. In response to IGF-1R activation β1-Integrin displaces PP2A from Tyr^{302} RACK1 allowing β1-Integrin to join the complex (Kiely et al., 2006, Kiely et al., 2008) (Figure 1.7). The release of PP2A also allows SHC activation, as PP2A

has been described as a negative regulator of SHC (Ugi et al., 2002). Src also associates with RACK1, and IGF-1 mediates the dissociation of Src from RACK1 allowing Src become phosphorylated and activated (Adams et al., 2011). RACK1 and IGF-1R was recently shown to associate with PTPα and to promote its IGF-1-induced phosphorylation (Khanna et al., 2015). PTPα induces Src activation by dephosphorylating its inhibitory site and thereby enables Src to activate focal adhesion kinase (FAK) (Su et al., 1996, Zeng et al., 2003). In turn the Src-FAK complex activates the PTPα on Tyr^{789} to facilitate cytoskeleton remodelling, focal adhesion formation and consequently, cell migration (Chen et al., 2006).

1.3.6 IGF-1 mediated activation of PI3K pathway

The PI3K pathway is the canonical evolutionally conserved signalling pathway activated by both Insulin and IGF-1 to regulate metabolism, cell survival, differentiation and cell proliferation (Fukushima et al., 2012, Hakuno and Takahashi, 2018). From the three existing PI3K classes, designated I-III, the PI3K Ia class phosphorylates inositol-containing lipids known as phosphatidylinositols (PtdIns) in response to RTK activation including IGF-1R (Figure 1.6). PI3K consists of a heterodimer with a regulatory subunit (p85) and a catalytic subunit (p110) (Vivanco and Sawyers, 2002). Ins/IGF-1 generally activate the PI3K pathway through p85 recognition of phosphorylated tyrosine residues of IRS-1 via its SH2 domain (Myers et al., 1994, Metz and Houghton, 2011). Direct binding of p85 to phosphorylated Tyr^{1316} located in the C-terminal tail of the IGF-1R has also been described. P85 binding releases the inhibition of p110 by p85 which allows the activation

of PI3K (Franke et al., 2003). Prolonged interaction of IRS-1 with IGF-1R leads to sustained PI3K activation (Yoneyama et al., 2018).

Activation of PI3K coverts PtdIns (4, 5) P2 (PIP2) to PtdIns (3, 4, 5) P3 (PIP3) and is reversed by the PTEN phosphatase (Vivanco and Sawyers, 2002) (Figure 1.6). PIP2 conversion to PIP3 enables the recruitment of PH domain-containing serine/threonine kinases, phosphoinositide-dependent kinase-1 (PDK-1) and AKT, to the membrane. Activated by PI3K, PDK-1 phosphorylates AKT kinase on Thr^{308} (Chan et al., 1999, Hemmings and Restuccia, 2012). Although not yet fully activated, AKT phosphorylated on Thr^{308} is required for activation of the mammalian target of Rapamycin (mTOR) pathway.

mTOR is the catalytic subunit of mTORC1 (raptor) and mTORC2 (rictor), which are distinguishable by their unique accessory proteins and activity. While mTORC1, which is sensitive to rapamycin consists of mTOR, Raptor, mLST8, PRAS40 and Deptor, mTORC2 is rapamycin insensitive and composed of mTOR, Rictor, mSIN1, mLST8, Protor-1 and Deptor (Sengupta et al., 2010). The mTORC1 complex mediates phosphorylation of p70 ribosomal S6 kinase (p70S6K) and eukaryotic translation initiation factor 4E (eIF4E)-binding protein (4EBP1), both of which are regulators of mRNA translation, initiation and progression, subsequently leading to protein synthesis, growth and cell division (Mader et al., 1995, Mendoza et al., 2011, Fukushima et al., 2012). mTORC1 phosphorylates 4EBP1 which blocks its inhibitory effect on mRNA translation (Beretta et al., 1996, Gingras et al., 2001). Phosphorylated by mTORC1 on Thr^{389}, p70SK6K promotes progression through the G1 phase of the cell cycle. Activated p70S6K subsequently phosphorylates S6 protein of the 40S ribosomal subunit, eIF4B

and Bad to prevent apoptosis (Jefferies et al., 1994, Myers et al., 1994, Harada et al., 2001). mTORC2 regulates the cytoskeleton by stimulating F-actin stress fibers, paxillin, RhoA, Rac1, Cdc42 and PKCα (Jacinto et al., 2004). mTORC2 complex also mediates an additional phosphorylation on Ser^{473} in AKT, causing the full activation of AKT kinase (Sarbassov et al., 2005, Fruman et al., 2017) (Figure 1.6).

AKT is the primary mediator of PI3K-induced signalling and is both an activator of proteins like IκKα and CREB as well as an inhibitor of proteins such as Bad, procaspase-9, FOXO3a and GSK-3β. By modulating the activity of several components of the pro-apoptotic machinery, AKT can suppress cells built-in potential for apoptosis and thereby mediate an essential survival signal. AKT also phosphorylates FKHR, a member of the forkhead family of transcription factors. Phosphorylation of FKHR inhibits its nuclear translocation and thereby prevents the activation of FKHR downstream targets including pro-apoptotic genes such as BIM and FASL (Biggs et al., 1999). By inhibiting Glycogen Synthase kinase 3β (GSK-3β), AKT prevents Cyclin D1 degradation, leading to its accumulation and sustained IGF-1-induced cell proliferation (Franke et al., 2003, Fukushima et al., 2012).

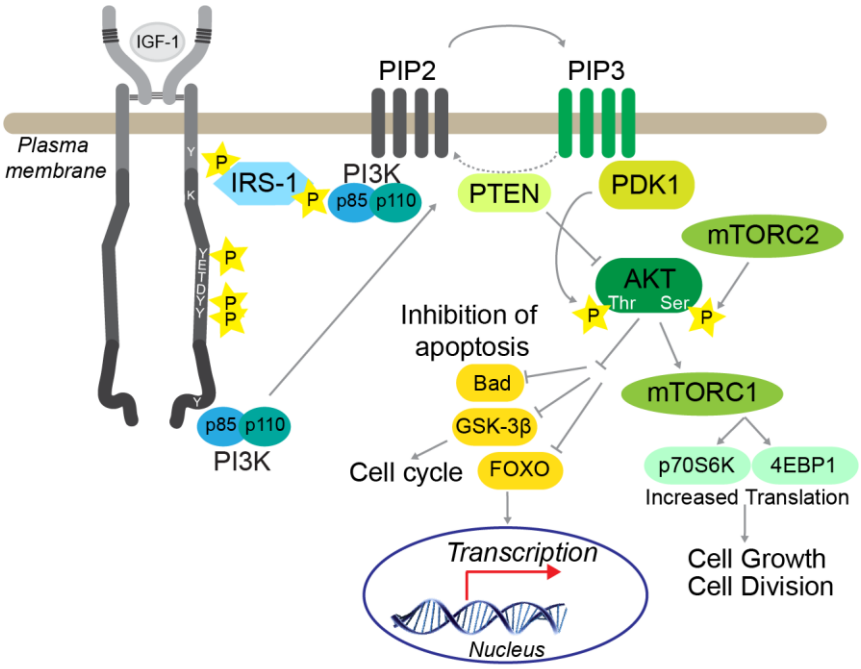


Figure 1.6: IGF-1-mediated activation of the PI3K/AKT pathway.

Ligand binding to the α-subunit of the IGF-1R leads to the autophosphorylation of the IGF-1R. Activation of the receptor triggers the activation of PI3K, which catalyses the conversion of PIP2 to PIP3. Following the recruitment of PDK1 and AKT to the membrane by PIP3, AKT is activated, which induces essential cellular processes including cell growth, survival and transcriptional regulation.

1.3.7 IGF-1-mediated activation of the Ras/MAPK pathway

Four MAPK cascades have been described in mammalian cells, each containing three kinases that act in signalling cascades. The cascade initiated by MAPK kinase kinase (MAP3K) includes a MAPK kinase (MAP2K) and a terminal MAPK that is one of the extracellular signal-related kinases (ERK1/2, ERK5), Stress Activated Protein Kinase/Jun N-Terminal Kinase (SAPK/JNK) or p38 α/β/γ/δ kinases (reviewed in (Baserga et al., 1997, O'Connor, 2003, Montagut and Settleman, 2009)). This cascade is commonly presented in simplified models as unidirectional signalling pathways. However, it should be noted that there is greater complexity to the pathway, such as signalling crosstalk and the association with other proteins (Chang and Karin, 2001, Montagut and Settleman, 2009).

An activated IGF-1R can mediate activation of the Ras pathway by inducing the exchange of GDP for GTP on the small GTPase Ras (Figure 1.7). This is mediated by the recruitment of Son of Sevenless (SOS) to the membrane, which allows the association of the guanine nucleotide exchange factor (GEF) with Grb-2 via its SH3 domain (Pronk et al., 1994). Grb-2 in turn contains a SH2 domain that can either recognise phosphorylated tyrosine residues of IRS-1 or the adaptor protein SHC. However, even though the Grb2-SOS complex can interact with both SHC and IRS-1, the interaction with SHC is preferred (five-fold higher) over IRS-1 and therefore appears to be more important for linking Grb2-SOS to the IGF-1R (Sasaoka et al., 1996). Once located at the plasma membrane, SOS can trigger the exchange of GTP for GDP on Ras (Chardin et al., 1993).

Upon Ras activation, Raf is recruited to the cell membrane triggering the release of the 14-3-3 dimer, which destabilizes the auto-inhibitory state of

Raf on both the N- and the C-terminus of Raf. Once released from its inhibitory state Raf can be phosphorylated, which leads to the activation of its serine-threonine kinase activity (Clark et al., 1997, Thorson et al., 1998, Avruch et al., 2001, Malumbres and Barbacid, 2003). The activation of Raf family members is followed by the phosphorylation of the MEK1/MEK2 dual-specificity protein kinases, which in turn activates ERK1/2 (McKay and Morrison, 2007). Subsequently ERK1/2 translocates to the nucleus and regulates the activity of several transcription factors that induce genes required for survival and proliferation and responsible for changing the phenotype of cells, including the Ets family, STAT-3, c-FOS and c-Myc (Roberts and Der, 2007).

IGF-1R-mediated phosphorylation of SHC and activation of ERK1/2 requires IGF-1R internalisation facilitated by β-arrestin, occurring independently of IRS-1 (Chow et al., 1998, Lin et al., 1998, Girnita et al., 2007, Yoneyama et al., 2018). Furthermore, cooperation of IGF-1R and adhesion signalling mediated by the scaffolding protein RACK1 promotes activation of the MAPK pathways (Kiely et al., 2002, Hermanto et al., 2002). Crosstalk between IGF-1R and adhesion complexes allows RACK1 to mediate IGF-1-induced phosphorylation of FAK, Src and SHC for ERK1/2 activation (Kiely et al., 2002, Kiely et al., 2005, Kiely et al., 2009).

While the Raf-MEK-ERK1/2 cascade is essential for normal physiological processes like cell proliferation and survival, the deregulation of this signalling pathway is frequently seen in several human cancers and contributes to oncogenic features including enhanced proliferation and survival (Montagut and Settleman, 2009).

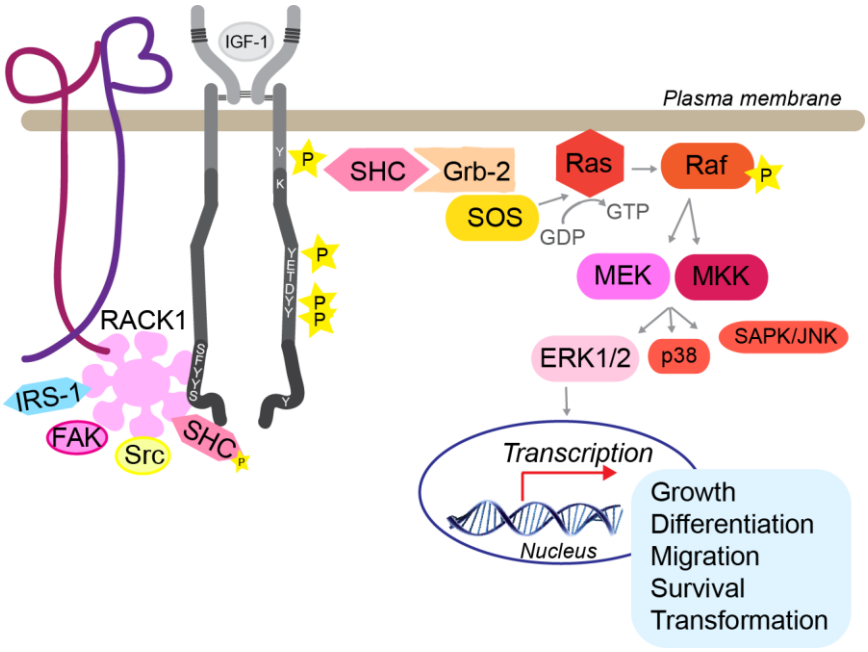


Figure 1.7: IGF-1-mediated activation of the Ras/ERK1/2 pathway.

Upon IGF-1R kinase activation, SHC is recruited to the receptor and activated. SHC then binds Grb-2-SOS complex, which mediates the exchange of GDP to GTP on Ras. Activated Ras recruits Raf kinase to the membrane. Following the translocation of Raf to the membrane, it becomes activated and phosphorylates MEK and MKKs. MEK activates ERK1/2 which translocates to the nucleus to regulate gene expression. IGF-1-mediated ERK1/2 activation requires the integration of IGF-1R into adhesion signalling, which is facilitated by RACK1.

There is also evidence of an interplay between Ras/ERK1/2 and PI3K/AKT pathway. The activation/inhibition of one of the pathways may lead to the inhibition/activation of the other pathway. In response to various stimuli including IGF-1, activation of AKT has a negative effect on MAPK activation by regulating phosphorylation on the auto-inhibitory site of Raf (Zimmermann and Moelling, 1999, Dhillon et al., 2002, Mendoza et al., 2011). Conversely, the inhibition of AKT activity up-regulates ERK1/2 phosphorylation in multiple myeloma cells (Ramakrishnan et al., 2012). Recently a direct interaction of MEK1/MEK2 of the MAPK cascade and AKT of the PI3K/AKT pathway has been also been reported. This interaction is regulated by specific serine phosphorylation of MEK1/2 and was linked to the phosphorylation of FOXO1, cellular migration and adhesion signalling in cells (Procaccia et al., 2017).

1.4 ENDOCYTOSIS AND TRAFFICKING OF THE IGF-1R

Ligand induced endocytosis is a major regulator of IGF-1R signalling (Lin et al., 1998, Chow et al., 1998, Sehat et al., 2007, Girnita et al., 2007, Romanelli et al., 2007, Yoneyama et al., 2018, Crudden et al., 2019). The availability of IGF-1R on the plasma membrane is regulated by synthesis and trafficking of the receptor as well as ligand-induced receptor endocytosis. Small amounts of basal IGF-1R internalise without ligand-binding. This ligand-independent endocytosis is a slow process and is thought to be important for homeostasis of RTKs (Goh and Sorkin, 2013, Crudden et al., 2019).

Ligand-induced endocytosis or retention on the membrane is regulated by the recruitment of interacting proteins to IGF-1R. It has been suggested that under patho-physiological conditions such as cancer, IGF-1R can recruit several different proteins (Goh and Sorkin, 2013, Crudden et al., 2019). In particular, adhesion-related proteins and kinases, shown to associate with the IGF-1R such as E-cadherin (Nagle et al., 2018), β1-Integrin (Kiely et al., 2005), FAK (Taliaferro-Smith et al., 2015), Src (Peterson et al., 1996) or the discoidin domain receptor 1 (DDR1) (Belfiore et al., 2018) are most likely involved in regulating IGF-1R endocytosis to modulate its signalling outcome.

IGF-1R endocytosis is initiated by vesicle formation on the membrane. Recent studies have shown that endocytosis via clathrin-coated-pits (CCP) is the fastest and predominate mode of IGF-1R internalisation. The formation of CCPs involves the recruitment of proteins that contain an ubiquitin-interacting motif, such as epsin, Eps15, or AP-2, to the activated receptor (Yoneyama et al., 2018, Crudden et al., 2019). It has been suggested that once clathrin-dependent endocytosis is saturated due to a large number of surface receptors being activated, alternative endocytosis mechanisms support the IGF-1R

internalisation (Backer et al., 1991, Prager et al., 1994, Sehat et al., 2008). A clathrin-independent mechanism of endocytosis has been described for the uptake of ligand-activated EGFR by micro- and macropinocytic vesicles. This involves the reorganization of the cytoskeleton and dynamic membrane ruffling (Haigler et al., 1979, Yamazaki et al., 2002, Sorkin and Goh, 2008). A similar process could be possible for endocytosis of the IGF-1R. However, clathrin-independent IGF-1R endocytosis could also involve the formation of lipid rafts/caveolae, which are typically described as surface plasma membrane invaginations. Indeed, IGF-1R has been shown to co-localise with the phosphorylated version of caveolin-1, the main component of these lipid rafts (Sehat et al., 2008).

By analysing IGF-1R mutants different domains of the receptor were proposed to be either required for, or involved in the process of IGF-1R internalisation. The kinase-inactive IGF-1R mutant (K1003R), and the truncated Δ1245 IGF-1R are impaired in ligand-induced internalisation (Marshall, 1985, Sehat et al., 2007). Tyr^{950}, located in the juxtamembrane domain of the IGF-1R has also been linked to IGF-1R internalisation. One study showed that mutation of the Tyr^{950} to phenylalanine did not modify IGF-1R ubiquitination suggesting that this tyrosine may not be essential in IGF-1R endocytosis (Sehat et al., 2007). However, in contrast Prager and colleagues demonstrated reduced IGF-1R internalisation when Tyr^{950} was mutated (Prager et al., 1994). It was also suggested that phenylalanine substitution of Tyr^{1250}, located in the C-terminus of the IGF-1R, caused a reduction in IGF-1R internalisation (Miura and Baserga, 1997).

1.4.1 Ubiquitination of the receptor

Ubiquitination on the β-subunit of the IGF-1R is an important signal to initiate IGF-1R endocytosis. Ubiquitination on the receptor is dependent on IGF-1R kinase activity and requires the presence of the C-terminal tail (Marshall, 1985, Sehat et al., 2007). While it is clear that the IGF-1R kinase activity is necessary for the recruitment of interacting proteins facilitating internalisation and ubiquitination, it is unknown whether the C-terminal is required for direct ubiquitination on one of the three lysines or offers a binding site for an adaptor protein/E3 ligase (Sehat et al., 2007).

Covalent binding of ubiquitin polypeptides to IGF-1R involves the sequential action of E1, E2, and E3 components of the Ubiquitin system. Since the E3 complex transfers the ubiquitin polypeptides to the IGF-1R, it confers substrate specificity. For the IGF-1R, four E3 ligases have been described to either directly or indirectly interact with IGF-1R to facilitate its ubiquitination. Little is known about the most recently identified E3 ligase HRD1 (Xu et al., 2015), whereas others are well studied. These include Nedd4 (Vecchione et al., 2003, Monami et al., 2008), MDM2 (Girnita et al., 2003, Girnita et al., 2007, Sehat et al., 2007, Worrall et al., 2017) and c-Cbl (Sehat et al., 2008) (Figure 1.8). Most studies report ubiquitination of the IGF-1R as a ligand-induced process resulting in IGF-1R endocytosis. In response to IGF-1, IGF-1R ubiquitination occurs within the first 5 min of stimulation, and K1138 and K1141 located within the kinase domain are believed to be the key lysine residues for ubiquitination (Mao et al., 2011).

HRD-1 (Figure 1.8A) was demonstrated to downregulate IGF-1R expression and may be an IGF-1R interacting protein, facilitating IGF-1R degradation through the proteasome (Xu et al., 2015, Yan et al., 2016).

Furthermore, low HRD-1 expression was associated with EMT and regulation of breast cancer cell growth, migration and invasion *in vivo* and *in vitro* (Xu et al., 2015). It was proposed that this downregulation of HRD-1 in cancer cells increases levels of IGF-1R expression and activity, and therefore promotes an IGF-1R-mediated EMT.

The E3 ligase MDM2 (Mouse double minute 2 homolog) (Figure 1.8B) is regulating the activity of tumour suppressor p53 protein in the nucleus by forming an inactivating complex. Different stress signals release p53 from the complex leading to its activation (Worrall et al., 2017). Activation of p53 by DNA damage causes cell cycle arrest, cell senescence or apoptosis (Jin and Levine, 2001). Restrained nuclear localisation of p53 is regulated by PI3K/AKT activity. Once released from the complex with p53 upon p53 activation, MDM2 translocates to the cytoplasm. However, MDM2 translocation to the cytoplasm is can also be mediated by lack of p53 expression, mutation of p53 or inhibition of complex formation (Girnita et al., 2003, Worrall et al., 2017). Located in the cytoplasm, MDM2 associates with the IGF-1R leading to its ubiquitination (Girnita et al., 2003, Girnita et al., 2007, Worrall et al., 2017). MDM2-mediated ubiquitination has been proposed to play a key role in IGF-1R internalisation and endosomal sorting (reviewed in (Crudden et al., 2019)). Even though MDM2 can facilitate ubiquitination on its own, its interaction with IGF-1R requires the adaptor protein β-arrestin. β-arrestin has a well-established function in G-Protein-Coupled Receptor (GPCR) trafficking (Lefkowitz and Shenoy, 2005), which suggests similar endocytosis mechanisms for IGF-1R and GPCR (reviewed in (Crudden et al., 2019)). The phosphorylation on GPCR is induced by GPCR kinases (GRK), facilitating and regulating the interaction of the transmembrane receptors with β-arrestin (Zheng et al.,

2012). GRK2 and GSK6, were proposed from *in silico* studies to be serine kinases for Ser^{1248} and Ser^{1291} in the IGF-1R. Phosphorylation of IGF-1R induced by GRK6 leads to the transient recruitment of β-arrestin, whilst increased GRK2/phosphorylation on Ser^{1248} protects the IGF-1R from degradation (Zheng et al., 2012).

Nedd4 mediated multi-ubiquitination (Figure 1.8C) of the IGF-1R requires formation of a complex with the adaptor protein Grb-10 (Vecchione et al., 2003, Monami et al., 2008). This complex multi-ubiquitinates the IGF-1R in a ligand-dependent way to initiate receptor internalisation via either clathrin-coated pits or caveolar compartments and causing downregulation of the IGF-1R. The Grb-10/Nedd4 complex remains associated with the IGF-1R in early endosomes (EE) and detaches from the receptor in order to be recycled and not degraded, like the IGF-1R itself (Monami et al., 2008).

c-Cbl (Figure 1.8D) is an E3 ligase for EGFR, PDGFR, the colony-stimulating factor-1 receptor and other RTKs (Lee et al., 1999, Levkowitz et al., 1999, Zeng et al., 2005, Huang and Sorkin, 2005), and the IGF-1R(Sehat et al., 2008). c-Cbl associates with the IGF-1R, mediates poly-ubiquitination of the receptor and initiates its internalisation via caveolin/lipid rafts, as was previously described (Sigismund et al., 2005). A model was presented where MDM2 recruitment to the receptor occurs with low amounts of IGF-1 availability (5 ng/ml) , leading to IGF-1R endocytosis via clathrin, while high concentrations (50-100 ng/ml) initiate c-Cbl-mediated ubiquitination of the receptor followed by endocytosis using the caveolin/lipid raft route (Sehat et al., 2008).

The complex of MDM2/β-arrestin links K63-conjugated ubiquitin polypeptide chains to the IGF-1R. This mode of ubiquitination is generally

more associated with cell signalling, DNA repair and protein trafficking (Spence et al., 1995, Hoege et al., 2002, Acconcia et al., 2009). c-Cbl attaches K48-conjugated ubiquitin polypeptide chains to the IGF-1R, which is suggested to initiate degradation of the receptor (Acconcia et al., 2009). Thus it is possible that depending on the IGF-1 stimulus, different E3 ligases are recruited to the receptor to initiate alternative trafficking routes for IGF-1R. This could ensure that IGF-1R-mediated signalling is aligned with the cell's requirements.

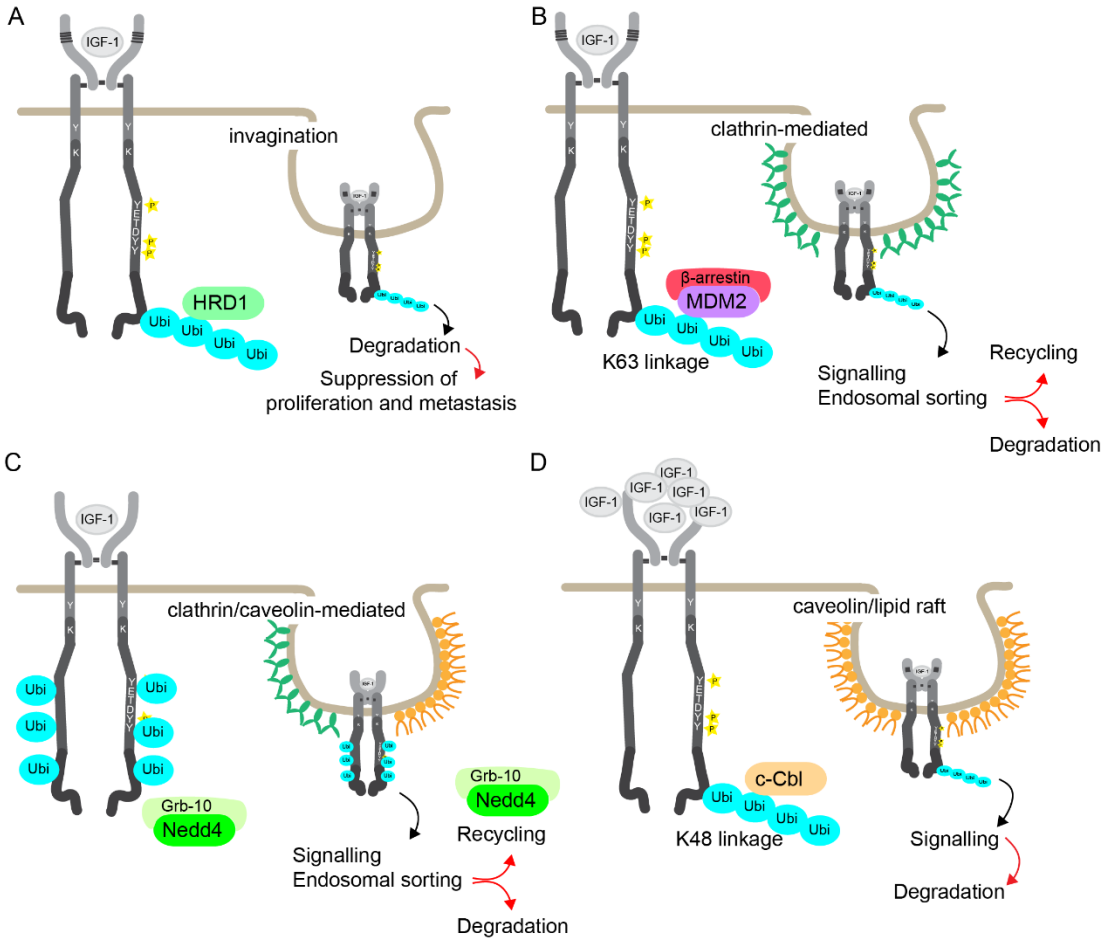


Figure 1.8: Interacting E3 ligases mediate IGF-1R ubiquitination.

(A) HRD1 is an IGF-1R-interacting E3 ligase, which initiates the ubiquitination and downregulation of IGF-1R, which is proposed to supress IGF-1-induced proliferation and metastasis. **(B)** The complex of MDM2/β-arrestin initiates K63-conjugated ubiquitination of the IGF-1R in presence of low amounts of IGF-1, causing its internalisation via clathrin-coated pits, signalling and endosomal sorting. **(C)** The complex of Grb-10/Nedd4 multi-ubiquitinates IGF-1R to induce its internalisation via clathrin-coated pits or caveolin/lipid rafts and thereby facilitates signalling. While Grb-10/Nedd4 is recycled, IGF-1R undergoes degradation. **(D)** High concentrations of IGF-1 recruit c-Cbl to the IGF-1R and addition of K48-linked ubiquitin polypeptides to the receptor. This induces IGF-1R internalisation via caveolin/lipid rafts and subsequent degradation.

1.4.2 Modulation of IGF-1R signalling by endocytosis

IGF-1R endocytosis, the level of receptor retention on the plasma membrane or induction of rapid recycling, may all modulate IGF-1R signalling. PI3K/AKT activation requires IGF-1R plasma membrane retention, whereas the phosphorylation of SHC and activation of Ras/MAPK require IGF-1R endocytosis (Chow et al., 1998, Girnita et al., 2003, Romanelli et al., 2007, Girnita et al., 2007, Sehat et al., 2007, Yoneyama et al., 2018) (Figure 1.9A).

Sustained AKT signalling can be induced from plasma membrane-located IGF-1R, or the rapid recycling of the receptor back to the membrane, and this is independent of newly synthesized receptor (Romanelli et al., 2007). The retention of IGF-1R on the plasma membrane was recently shown to be regulated by the recruitment of IRS-1 to the receptor (Yoneyama et al., 2018) (Figure 1.9B). IRS-1 inhibits the binding of the adaptor protein AP-2 to the receptor. As, AP-2 is an important adaptor for clathrin-mediated endocytosis, this prolongs retention of IGF-1R on the membrane leading to sustained activation of PI3K/AKT by IGF-1. Eventually a feedback signal from mTORC1 triggers the degradation of IRS-1, allowing AP-2 to interact with IGF-1R to initiate IGF-1R internalisation through CCP (Yoneyama et al., 2018). This persistent PI3K activation has also been linked to regulation of IGF-1-induced cell proliferation (Fukushima et al., 2012).

It has been reported that by blocking IGF-1R internalisation either pharmacologically or by a reduction in temperature, SHC phosphorylation is abolished (Chow et al., 1998). Consequently, Grb-2 is not recruited to SHC leading to impaired IGF-1-induced MAPK phosphorylation (Chow et al., 1998). This study and others also showed that IGF-1R internalisation does not reduce IRS-1 activation, but rather, increases it (Girnita et al., 2007, Sehat et al., 2007,

Sehat et al., 2008), causing the prolonged association of PI3K with the receptor and the activation of AKT.

The IGF-1R C-terminal tail has been associated with ERK1/2 activation (Yu et al., 2003, Girnita et al., 2003, Sehat et al., 2007, Girnita et al., 2007). As activation of ERK1/2 is linked to IGF-1R internalisation mediated by ubiquitination of the receptor (Girnita et al., 2007, Sehat et al., 2007), impaired IGF-1R endocytosis is proposed to cause a reduction in ERK1/2 activation in cells expressing a C-terminal tail mutant. Ubiquitination of the IGF-1R and the induction of ERK1/2 correlated with the recruitment of β-arrestin to the receptor (Lin et al., 1998, Girnita et al., 2007, Zheng et al., 2012, Worrall et al., 2017). It was demonstrated that enhanced interaction of β-arrestin/MDM2 to the IGF-1R in cells overexpressing either the adaptor protein or the E3 ligase display sustained ERK1/2 activation.

In summary (Figure 1.9A), in normal cells IGF-1R is expressed at basal levels with recruitment of IRS-1 and β-arrestin to the ligand-activated receptor. This leads to the induction of PI3K/AKT and IGF-1R ubiquitination and internalisation, followed by SHC/Ras/ERK1/2 induction. Overexpression of IRS-1 in cells (Figure 1.9B) causes a retention of IGF-1R on the plasma membrane and a sustained PI3K/AKT activation, while the overexpression of β-arrestin/MDM-2 (Figure 1.9C) sustains ERK1/2 signalling. Thus, IGF-1R association with distinct interacting proteins can modulate its endocytosis and signalling.

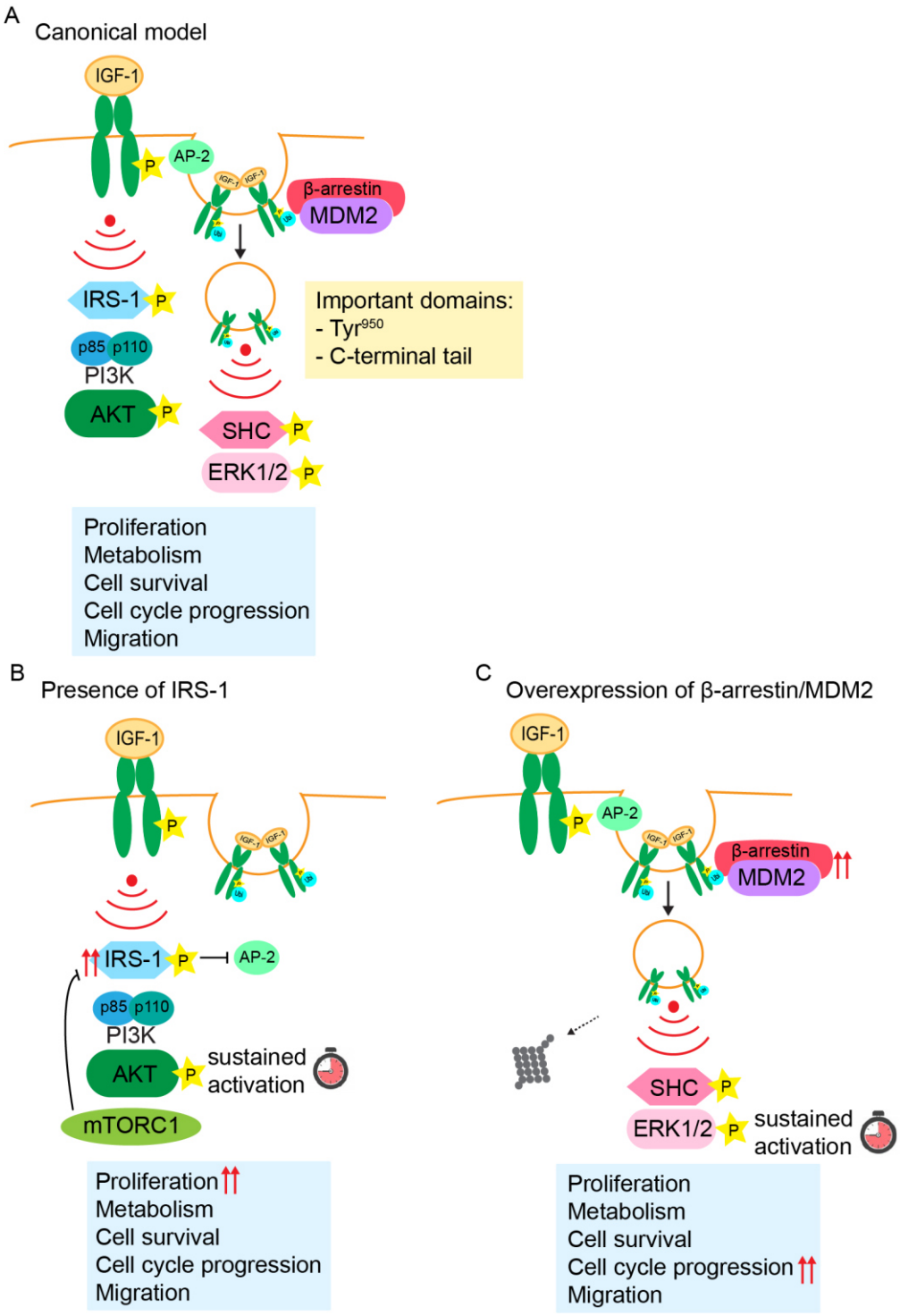


Figure 1.9: Regulation of IGF-1R signalling by receptor endocytosis.

(A) The canonical model in which IRS-1 functions as a signalling mediator to induce the PI3K/AKT pathway, and β-arrestin/MDM-2 initiate IGF-1R ubiquitination followed by internalisation and induction of SHC and ERK1/2. **(B)** The overexpression of IRS-1 prolongs the IGF-1R retention on the cell surface by inhibiting AP-2 interaction with the receptor, inducing sustained PI3K/AKT signalling. A feedback signal from mTORC1 eventually leads to the degradation of IRS-1, allowing AP-2 to initiate IGF-1R internalisation via CCP. **(C)** The overexpression of either β-arrestin or MDM2 initiates IGF-1R ubiquitination and internalisation leading to a sustained ERK1/2 activation upon receptor activation with IGF-1.

1.4.3 The IGF-1R translocates to the nucleus

Emerging evidence indicates the presence of different RTKs in the nucleus of cancer cells. These include family members of EGFR family (Lin et al., 2001, Offterdinger et al., 2002, Wang et al., 2004), FGFR1 and 3 (Johnston et al., 1995, Stachowiak et al., 2003), the IR (Kim and Kahn, 1993, Seol and Kim, 2003) and VEGFR (Feng et al., 1999, Mayo et al., 2001).These nuclear pools of receptors are proposed to promote transcription of specific target genes either as full or partially cleaved receptors. It was also reported that this might occur independently of their respective ligands. Translocation of the IGF-1R to the nucleus in cancer cells is induced by IGF-1/2 and insulin (Aleksic et al., 2010, Codony-Servat et al., 2017, Aleksic et al., 2018). Nuclear IGF-1R was shown to be more pronounced in various cancer cell lines, including breast cancer cells and sarcoma cells, compared to normal cells (Deng et al., 2011). Furthermore, nuclear IGF-1R has been linked to a poor outcome for cancer patients and suggested to promote a more advanced tumour stage (Aleksic et al., 2010, van Gaal et al., 2013, Codony-Servat et al., 2017, Aleksic et al., 2018).

The level of IGF-1R nuclear translocation was found to be proportional to the ligand-induced IGF-1R kinase activation, and the translocation was inhibited using pharmacological inhibitors blocking the IGF-1R activation or internalisation (Aleksic et al., 2010, Sehat et al., 2010, Aleksic et al., 2018).

Mechanisms of IGF-1R import into the nucleus are still unclear as IGF-1R itself has no nuclear localisation sequence (NLS) (Sehat et al., 2010, Aleksic et al., 2010). One proposal is that SUMOylation of the IGF-1R induced by IGF-1R internalisation is important for the translocation (Sehat et al., 2010). Packham *et al.* recently demonstrated that IGF-1R translocation is facilitated

by a specific subunit of dynactin p150^{Glued}. This study showed that IGF-1-activated and internalised IGF-1R is transported within early endosome antigen 1 (EEA1)-positive vesicles, and trafficked to the nucleus, where it is positioned in the nuclear pore complex by β-importin and is subsequently SUMOylated by RanBP2 for translocation into the nucleus (Packham et al., 2015). Suppression of any of the proteins involved in this import, leads to a significant decrease in nuclear IGF-1R. However, mutation of the SUMOylation lysine sites on IGF-1R did not abolish accumulation of IGF-1R in the nucleus (Sehat et al., 2010), suggesting that additional import mechanisms exist. IGF-1R association with other proteins containing an NLS like IRS-1, which was previously shown to translocate to the nucleus in response to IGF-1, could also promote the import (Prisco et al., 2002). In addition, it has been suggested that heterodimerization with the IR, which was shown to accumulate rapidly in response to Insulin stimulation in the nucleus (Kim and Kahn, 1993) could promote the import as well (Warsito et al., 2016) (Figure 1.10).

Nuclear IGF-1R was reported to bind to DNA to enhance transcription (Sehat et al., 2010), for example, by mediating the recruitment of RNAPol2 (Aleksic et al., 2018). Nuclear IGF-1R was demonstrated to regulate its own expression in breast cancer (Sarfstein et al., 2012) and to bind to LEF1 transcription factor, which subsequently leads to upregulated protein levels of cyclinD1 and axin 2, promoting cell proliferation (Warsito et al., 2012). In HeLa cells, nuclear IGF-1R can increase the expression of SNAI2, which is part of the SNAIL family and involved in EMT by suppressing E-cadherin expression (Rukstalis and Habener, 2007). In prostate cancer cells nuclear IGF-1R facilitates expression of JUN and FAM 21, which are linked promoting survival, anchorage independent growth and cell migration, features that have been

associated with advanced tumour stage (Aleksic et al., 2018). Nuclear IGF-1R was also demonstrated to enhance proliferation of alveolar rhabdomyosarcoma cells (Aslam et al., 2013) and contribute to chemoresistance in sarcomas and hepatocellular carcinoma (Asmane et al., 2012, Bodzin et al., 2012).

Overall the results from recent studies suggests that nuclear IGF-1R facilitates an aggressive cancer phenotype. However, Aleksic *et al.* suggest that the sites of IGF-1R binding to the DNA, and therefore the genes influenced by nuclear IGF-1R might be cell type specific and that this could be defined by nuclear structure and the chromatin organization (Aleksic et al., 2018).

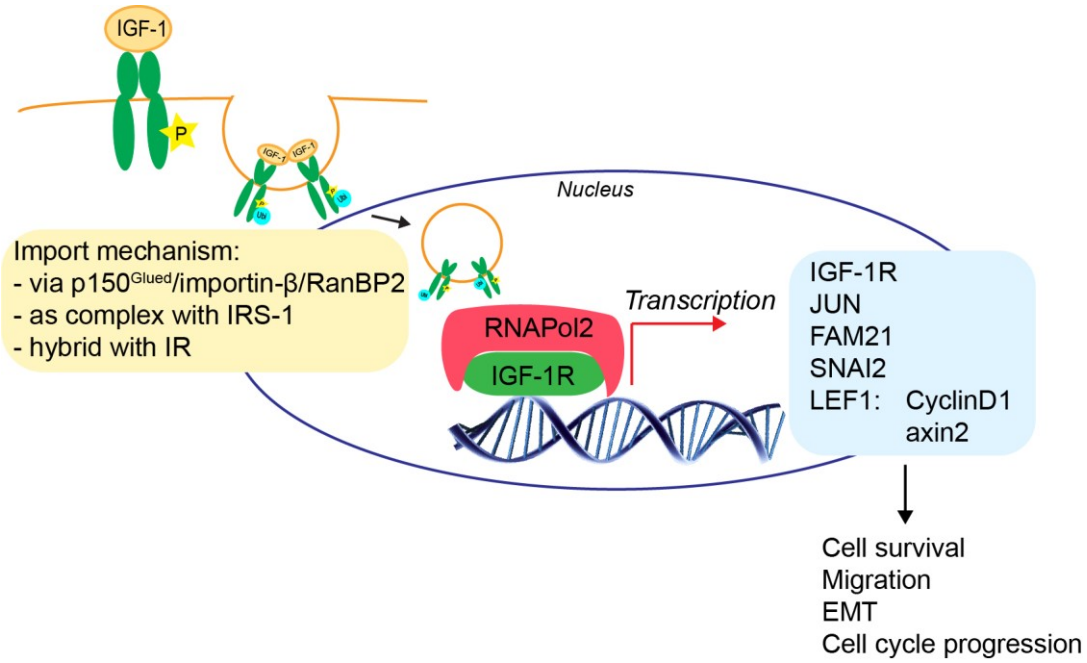


Figure 1.10: IGF-1R translocates to the nucleus in response to IGF-1.

Ligand binding to the IGF-1R induces the translocation of the membrane receptor to the nucleus. Various mechanisms have been proposed for the import of the IGF-1R to the nucleus. Nuclear IGF-1R can bind to DNA and enhance or initiate the transcription of various genes, leading to cell survival, migration, EMT and cell cycle progression.

1.5 IGF-1R ACTIVITY IN CELLULAR TRANSFORMATION AND CANCER

Although the IGF-1R does not act as an oncogene, its activity can enhance all the processes described as “Hallmarks of Cancer” (Hanahan and Weinberg, 2011), that define the progression of normal cells to a malignant state as a multistep event. For human tumours to arise, cells need to be capable of sustained proliferation signals, evading growth suppressors, resisting cell death, limitless replicative potential, inducing angiogenesis, tissue invasion and metastasis, reprogramming metabolism and evading the immune system.

1.5.1 IGF-1R facilitates cellular transformation

Cellular transformation is the profound change from normal cells into tumorigenic cells, through which cells gain the capability for uncontrolled survival and proliferation. Cells in the transformed stage can further undergo malignant transformation where they acquire invasiveness and metastatic potential. The process of cellular transformation requires oncogene activation or the suppression/inactivation of tumour suppressors. In cancer models, cellular transformation is indicated by the ability of cells to from colonies in soft agar (anchorage-independent growth) and/or the ability to form tumours when inoculated into mice.

IGF-1R was first reported to have an essential function in facilitating oncogenic transformation and maintenance of the transformed phenotype by the Baserga laboratory (Resnicoff et al., 1995, Baserga et al., 1997, Hongo et al., 1998). Surprisingly, only low levels of IGF-1R are required for cellular transformation, yet when expression levels of IGF-1R are decreased, or the IGF-1R gene is targeted for disruption, tumour cells undergo apoptosis (Resnicoff et al., 1995, Baserga et al., 1997, Hongo et al., 1998). Mouse

embryonic fibroblasts derived from IGF-1R null mice (R^- cells) are refractory to transformation by cellular and viral oncogenes (Sell et al., 1993) including SV40 Large T antigen (Sell et al., 1993), activated Ras (Sell et al., 1994), EGFR (Coppola et al., 1994) and PDGFR-β (DeAngelis et al., 1995). PDGFR-β was shown to interact with the E5 oncoprotein of the bovine papillomavirus (BPV) and the interaction is needed for the E5 capability to transform cells. Interestingly, R^- cells are also refractory to E5-BPV induced transformation, which suggests an important crosstalk between growth factors and viral oncogenes (Morrione et al., 1995). Conversely, transient overexpression of IGF-1R in fibroblasts results in a ligand-dependent, highly transformed phenotype, which includes the formation of tumours in nude mice (Kaleko et al., 1990, Liu et al., 1993, Sell et al., 1994, Coppola et al., 1994). The requirement for active IGF-1R to mediate cellular transformation is supported by the fact that overexpression of either a kinase-inactive IGF-1R (K1003R) or the related IR, do not result in transformation of R^- cells (Coppola et al., 1994, Sell et al., 1994, Miura et al., 1995b).

IGF-1R availability and activity in facilitating transformation may be regulated by many factors including subcellular localisation, degradation or activity of interacting kinases or phosphatases. Proteins that have been linked to regulation of IGF-1R-mediated transformation include AIRAPL, an ER-associated degradation (ERAD) protein (Osorio et al., 2016), the adhesion-related kinases FAK and Src (Peterson et al., 1996, Flossmann-Kast et al., 1998, Ucar et al., 2012, Taliaferro-Smith et al., 2015), as well as the phosphatases PTP1B (Buckley et al., 2002), PTPα (Khanna et al., 2015) and Shp-2 (Ivins Zito et al., 2004, Kiely et al., 2005, Carver et al., 2010).

1.5.2 The IR-A and cancer

While the insulin-activated IR-B mediates mainly metabolic effects, the IR-A, preferentially activated by IGF-2, mediates a mitogenic effect similar to IGF-1R signalling (Vella et al., 2018). Overexpression of the IR was previously associated with malignancies, with predominantly mitogenic, rather than metabolic effects on malignant cells (Sciacca et al., 2003, Pandini et al., 2003, Malaguarnera et al., 2011, Malaguarnera and Belfiore, 2014). Thus, it is believed that signalling in malignant cells is mediated by the IR-A and a higher IR-A:IR-B ratio (Vigneri et al., 2016). IR expression is associated with different cancer types including liver cancer (Wang et al., 2012), prostate cancer (Cox et al., 2009) and bladder cancer (Roudnicky et al., 2017). Interestingly, in a subset of small cell lung cancer (11%) the IR-A was the only IR receptor expressed (Jiang et al., 2014). Furthermore, IR expression has been linked to breast cancer (Rostoker et al., 2015). One study shows that secreted IGF-2 by both the epithelial as well as the stromal cells, activates both the IR-A and the IGF-1R (Sciacca et al., 1999) and the inhibition of either IGF-2 or IR reduces cell growth (Sciacca et al., 1999).

Activated IR-A/IGF-2 was recently associated with the stem cell like capabilities including self-renewal, promoting cancer cell survival and migration (Malaguarnera et al., 2011). Cancer stem cells (CSC) and stem-like features are believed to be responsible for the initiation of cancer (cancer-initiating cells, CIC), and the maintenance of uncontrolled growth, metastasis and recurrence (Vella et al., 2018, Afify and Seno, 2019).

Like the IGF-1R, the IR was shown to regulate EMT and pluripotency by activating several transcription factors (Zhao and Xu, 2010). The hybrid formation of IR-A and the IGF-1R also has the potential to drive a stem-like

phenotype, which causes resistance to cancer therapy. IR-A:IGF-1R hybrids regulate pluripotency and self-renewal (Ziegler et al., 2014), and it was further postulated that the hybrid receptors facilitate the resistance to anti-IGF-1R inhibitor (Vella et al., 2018).

1.5.3 Cell Migration, Invasion and EMT

IGF-1R activity is required for maintenance of the transformed state, and may further promote an aggressive cancer phenotype characterized by tumour cell invasion and metastasis (Samani et al., 2007).

The initiation of directed cell migration is a complex process and involves leading edge protrusion, adhesion to the ECM, and retraction of the trailing end of the cell. It also engages the actin cytoskeleton through the assembly and disassembly of actin filaments (Insall and Machesky, 2009, Millarte and Farhan, 2012). Actin polymerization is a key mechanism in cell migration and actin filament bundling on the plasma membrane (lamellipodia and filopodia) is responsible for the formation of cell protrusions. Adhesion to the ECM is mainly controlled by the Integrin adhesion receptor family (Seguin et al., 2015). Cooperative signalling between the IGF-1R, Integrins and other components of the adhesion machinery, including FAK and Src, has been shown to facilitate migration and the EMT of cells (Peterson et al., 1996, Flossmann-Kast et al., 1998, Kiely et al., 2002, Kiely et al., 2005, Ucar et al., 2012, Taliaferro-Smith et al., 2015). IGF-1R has also recently been shown to induce the transcription of FAM21 (Aleksic et al., 2018), which is reported to be essential for cell migration. Indeed, inhibition of IGF-1R signalling or internalisation causes a marked decrease in IGF-1-mediated induction of

FAM21A transcription and this suppression of FAM21A led to decreased cell migration (Aleksic et al., 2018).

EMT describes the process of cell transition from an epithelial to a more mesenchymal phenotype. Although this transition is needed during embryonic development, tissue regeneration and wound healing (Roche, 2018), it is used by cancer cells to escape the tumour during metastasis and to acquire stem-like features that render cells resistant to anoikis, the immune system and cancer therapies (Nieto et al., 2016, Lambert et al., 2017, Moustakas and de Herreros, 2017). EMT is reversible through the mesenchymal-to-epithelial transition (MET), and can occur when metastasised cancer cells form secondary tumours. Many characteristics of migration are involved in EMT, including the disruption of cell-cell adhesion and cell polarity, rearrangement of the cytoskeleton and dissociation of the cell-ECM adhesions (Roche, 2018). Various external stimuli, including hypoxia and growth factors can initiate the transcription of genes that induce EMT (EMT-markers). The expression of specific proteins such as cadherin family members (Thiery, 2002) is controlled by transcription factors which include SNAI1 and SNAI2, ZEB1 and ZEB2 and TWIST1/2 (Li et al., 2017b, Roche, 2018).

IGF-1R involvement in EMT-mediated tumour metastasis and drug resistance, is mainly linked to the overexpression of the receptor, increased downstream signalling, and cross-talk with other pathways. It has been reported that the combined actions of Src and IGF-1R induce Slug mediated EMT, which activates a feedback loop and enhances IGF-1 production (Sivakumar et al., 2009). Both downstream signalling pathways AKT and ERK1/2 have been linked to IGF-1 induced-EMT in gastric cancer and their suppression partially reverses IGF-1-induced EMT through the release of

ZEB2 as transcriptional repressor of E-cadherin (Li et al., 2014, Li et al., 2017a) The activation of ERK1/2 was shown to upregulate ZEB1 expression upon IGF-1 stimulation inducing EMT of prostate cancer (Graham et al., 2008). IGF-1-induced activation of AKT supresses GSK-3β through phosphorylation on Ser^{9}. GSK-3β can bind to Snail and Slug to meditate their degradation (Kim et al., 2007), and hence, AKT-mediated GSK-3β suppression stabilizes Snail (Zhou et al., 2004). It has also been reported that the translocation of IGF-1R to the nucleus in HeLa cells enhances the expression of SNAI2, which initiates EMT by suppressing E-cadherin expression (Rukstalis and Habener, 2007).

Taken together, these studies provide strong evidence for IGF-1-promoted EMT and tumour metastasis that is also modulated by IGF-1R signalling and trafficking.

1.5.4 IGF-1R mediates chemoresistance

One of the biggest challenges in the treatment of cancer is resistance to chemotherapy, which leads to disease progression and mortality. In recent years, IGF-1R has been associated with promotion of chemoresistance to a broad range of cancer therapies. IGF-1R is proposed to contribute to drug resistance through its crosstalk with other RTK signalling networks that promote proliferation and upregulation of anti-apoptotic proteins (Liu et al., 2014).

One significant example of this is the HER2-targeted drug, Trastuzumab. The anti-HER2 receptor monoclonal antibody is used to treat breast cancer with ErbB2-overexpression. However, development of drug resistance is common and caused by increased levels of IGF-1R signalling, which causes enhanced activation of the PI3K/AKT pathway. This was further

linked to increased degradation of p27Kip1, which under normal conditions induces cell cycle arrest (Lu et al., 2001, Lu et al., 2004). Moreover, under normal conditions, HER2 and IGF-1R do not interact and the basal phosphorylation of HER2 is not mediated by IGF-1R. However, HER2 and IGF-1R can form heterodimers in breast cancer cells during the initiation of drug resistance, which leads to IGF-1R-induced HER2 phosphorylation, thereby conferring resistance to Trastuzumab on the tumour cells (Nahta et al., 2005).

IGF-1R has also been shown to heterodimerize with EGFR. This crosstalk between the two receptors leads to the IGF-1R-mediated activation of mTOR, subsequently inducing EGFR protein synthesis. This mechanism allows small cell lung cancer cells to proliferate in the presence of the EGFR-inhibitor, Erlotinib (Jones et al., 2004, Morgillo et al., 2006, Kaulfuss et al., 2009). IGF-1R-mediated resistance to EGFR inhibitors was also demonstrated in primary human glioblastoma cells caused by sustained activation of the PI3K pathway (Chakravarti et al., 2002).

However, IGF-1R also facilitates the resistance to conventional chemotherapeutics. IGF-1R mediates resistance to cisplatin because inhibition of IGF-1R enhances the efficacy of cisplatin (Singh et al., 2014, O'Flanagan et al., 2016). O'Flanagan *et al* suggested, that IGF-1R kinase inhibition delays DNA damage repair, sensitizing cells to the DNA damaging and cytotoxic agents (O'Flanagan et al., 2016). Furthermore, inhibition of IGF-1R activity, normally acting as a potent survival factor in Ewing's sarcoma (ES) causes cell cycle arrest in the G_1-phase and sensitised ES cells to apoptosis induced by Doxorubicin and Vincristine, potentiating their cytotoxic actions in Ewing's sarcoma (Benini et al., 2001).

1.5.5 IGF-1 system as target for cancer therapy

The widespread expression of the IGF-1R in different tissues, combined with its actions in cellular transformation and facilitating aggressive cancer phenotypes, mark the IGF-1R, its ligands and signalling pathway as promising candidates for cancer therapy. Although preclinical studies targeting the IGF-1R showed promising anti-tumour effects, numerous clinical trials ended in disappointment (Osher and Macaulay, 2019). The disappointing efficacy of IGF-1R inhibitors in clinical trials is mainly due to incomplete knowledge of the complexity of IGF-1R kinase regulation, the crosstalk with other membrane and cellular kinases, and the identification of features within the receptor that may drive an aggressive phenotype.

1.5.5.1 Epidemiological data

It is well established that individuals in the general population who have elevated serum IGF-1 levels are at a higher risk of developing certain cancer types including prostate, breast, colon, lung and colorectal cancer (Hankinson et al., 1998, Chan et al., 1998, Ma et al., 1999, Renehan et al., 2004, Key et al., 2010, Travis et al., 2016). Levels of IGF-1 are regulated by GH and dietary intake and individuals who are challenged with metabolic diseases like diabetes are at higher risk of developing cancer (Clemmons, 2012).

Yoon *et al.*, conducted a meta-analysis to investigate the association of IGF-1, IGFBP-3 and their relative levels in colorectal cancer. Although their study showed that the ratio of levels of IGF-1:IGFBP-3 does not correlate with the occurrence of colorectal adenoma (CRA), high levels of IGF-1 were associated with increased risk of advanced CRA (Yoon et al., 2015).

Studies on prostate cancer also reported that circulating IGF-1 levels correlate with risk (Cohen et al., 1993, Kanety et al., 1993). An *in vivo* study showed that the proliferation of PC-3 cells is profoundly reduced in hosts with an IGF-1 deficiency (Pollak, 1998), and increased invasive potential was reported in DU-145 cells in response to exogenous IGF-1 (Saikali et al., 2008). Moreover, prostate cancer epithelial cells are capable of responding to autocrine IGF-1 (Grimberg and Cohen, 2000). One of the largest epidemiological studies on prostate cancer was conducted by Travis *et al.* (Travis et al., 2016). Again, this study showed that high levels of circulating IGF-1 is associated with prostate cancer risk. Moreover, they reported that this correlation is independent of cancer stage or grade (Travis et al., 2016).

An initial study on breast cancer conducted by Peyrat *et al.* (Peyrat et al., 1993) reported higher levels of circulating IGF-1 in patients with breast cancer compared to the control group. Several epidemiological studies conducted since then, however, only associated a high risk of breast cancer with circulating levels of plasma IGF-1 (Hankinson et al., 1998, Rinaldi et al., 2010, Kaaks et al., 2014). One of the largest studies showed a clear correlation between circulating IGF-1 and breast cancer risk in Estrogen Receptor positive (ER^+) tumours. Moreover, they demonstrated that the correlation was not dependent on levels of IGFBP-3 or the menopausal status (Key et al., 2010). These results were later also supported by Kaaks *et al.* (Kaaks et al., 2014).

Overall, epidemiological and experimental evidence to date suggest that high levels of IGF-1 facilitates the risk of various types of cancers.

1.5.5.2 IGF-1R targeting strategies

IGF-1R was the first RTK to be targeted with an inhibitory antibody in preclinical studies (Arteaga et al., 1989). Although the neutralizing antibody αIR3 was shown to inhibit growth in both breast cancer cells *in vitro* and as xenografts in immunodeficient mice, its potential for toxicity and to inhibit both the IGF-1R and IR in normal tissue rendered it unsuitable for clinical trials (Macaulay, 1992). Since then, multiple approaches have been investigated for targeting the IGF-1/IGF-1R system including molecular approaches, anti-IGF1R antibodies, small molecular tyrosine kinase inhibitors (TKIs), IGF-1/IGF-2 ligand TRAPs and ligand neutralizing antibodies.

Nucleic acid-based approaches were leading the way in preclinical experiments. Antisense-mediated downregulation of IGF-1 or IGF-1R was reported to inhibit growth of murine tumours *in vivo* and to inhibit growth of prostate cancer xenografts as drug (administered as the drug ATL1101), but it apparently never progressed further (Trojan et al., 1993, Resnicoff et al., 1994, Furukawa et al., 2010).

Following the discovery of RNA interference (RNAi) technology, this approach was used to supress IGF-1R in various settings. Influenced by secondary structures in the IGF-1R mRNA, suppression of IGF-1R using RNAi causes high sensitivity to chemotherapy, ionizing radiation and targeted agents in prostate, renal and oesophageal cancer *in vitro* and *in vivo* (Bohula et al., 2003, Niu et al., 2007, Yuen et al., 2009, Turney et al., 2012, Zhao and Gu, 2014). In clinical trials however, this approach, is challenged by the instability of RNAi and by finding a suitable delivery mechanism (Soutschek et al., 2004).

Another approach to inhibit IGF-1R is based on the fact that as a heterotetramer, the IGF-1R binds its ligands in a pocket formed by two subunits. This mechanism was exploited to generate dominant negative receptors that would dimerize with the wildtype IGF-1R to allow ligand binding but to inhibit kinase activation (D'Ambrosio et al., 1996, Dunn et al., 1998, Samani et al., 2004, Sachdev et al., 2004, Min et al., 2005). Although this approach was effective in inducing apoptosis, inhibiting tumorigenesis and metastasis *in vivo* the clinical application is limited by the regulation and the biological complexity of gene transfer (Husain et al., 2015).

Monoclonal antibodies (mAb) that compete for binding of IGF-1 to the α-subunit of IGF-1R were a logical approach. In addition to blocking IGF-1 binding and signalling, IGF-1R mAb also induce IGF-1R internalisation and degradation (Sachdev et al., 2003). However, because the IGF-1R and IR-A/IR-B form hybrids, targeting the IGF-1R signalling with this approach leads to hyperglycemia due to the hybrid internalisation and degradation. Another reason for hyperglycemia is that the blockage of IGF-1R causes an endocrine response, inducing secretion of GH and IGFBPs which can impair glucose tolerance (Pollak et al., 2004, Sachdev et al., 2006, Pandini et al., 2007). Although IGF-1R-targeting antibodies that do not cause downregulation of the IR have been tested, compensatory mechanisms have been reported including the activation of IR-A by insulin or IGF-2 (Ulanet et al., 2010, Buck et al., 2010, Bid et al., 2012, Feng and Dimitrov, 2012, Weinstein et al., 2014, Forest et al., 2015), or through the crosstalk with other RTK such as EGFR and MET (van der Veeken et al., 2009, Liu et al., 2018b). These approaches showed initial success (Lacy et al., 2008, Tolcher et al., 2009), but only two mAbs targeting the IGF-1R are still in testing. One of them, Ganutiumab shows

promising results in Ewing sarcoma and is currently being tested in dual therapy with the Src inhibitor dasatinib in patients with rhabdomyosarcoma, and in combination with chemotherapy in Ewing sarcoma (NCT03041701, NCT02306161).

Small molecules have also been generated to inhibit the IGF-1R kinase (TKIs). Only a few of these compounds have progressed to clinical trials after showing promising results during preclinical evaluation (Table 1.1). Despite this, the results from clinical trials were disappointing, mainly because of toxicity and because they targeted both the IGF-1R and IR. Blocking the IR system can lead to hyperinsulinemia and dose-limiting hyperglycemia (Weroha and Haluska, 2008). However, there are reports of some success in Ewing sarcoma patients and in cell models when the TKI were combined with other chemotherapy drugs (O'Flanagan et al., 2016, Macaulay et al., 2016, Leighl et al., 2017, Oza et al., 2018).

Table 1.1: IGF-1R TKI used in clinical trials.

Drug name	Mechanism of inhibition	Potency (IC50) IGF-1R	IR	Addi-tional targets	Clinical trial phase	References
Linsitinib (OSI-906)	ATP competitive	35 nM	75 nM	N/A	III	(Barata et al., 2018, Oza et al., 2018, Macaulay et al., 2016)
BMS-754807	ATP competitive	1.8 nM	1.7 nM	MET, RON, TrkA/B, AurA/B	II	(Carboni et al., 2009, Haluska et al., 2011)
XL-228	ATP competitive	1.6 nM	N/A	BCR-ABL, AurA, SRC, LYN	I	(Cortes et al., 2008, Toretsky et al., 2001)
AXL1717 (Picropodophyllin)	Non-ATP competitive	40 nM	N/A	Micro-tubules	II	(Girnita et al., 2004, Aiken et al., 2017, Waraky et al., 2014)
Masoprocol (INSM-18, nordihydroguaiaretic acid)	Non-ATP competitive natural product of *Larrea divaricata*	31 μM	N/A	HER2	II	(Youngren et al., 2005, Ryan et al., 2008, Friedlander et al., 2012)

1.5.5.3 Therapy resistance and failures

Despite all of the efforts and promising results in the preclinical evaluations, inhibition of the IGF-1R alone failed in patient clinical trials, with the possible exception of Ewing sarcoma (Tolcher et al., 2009, van Maldegem et al., 2016). In response to IGF-1R inhibition, compensatory activity of other receptors including the IR-A and IR-B as well as EGFR and MET can be activated (Qu et al., 2017, Buck et al., 2010, van der Veeken et al., 2009, Liu et al., 2018b). The complexity of IGF-1R signalling is another potential reason for the inefficacy of drugs targeting it. For example, the adhesion kinase Src was

reported to mediate resistance to IGF-1R kinase inhibitors. Src has been shown to phosphorylate the IGF-1R autophosphorylation sites directly and can therefore substitute for IGF-1R kinase activity (Peterson et al., 1996). Indeed, in an ongoing clinical trial, Ganutiumab is being used in combination with the Src inhibitor dasatinib, in patients with rhabdomyosarcoma (NCT03041701).

We recently identified components of the DNA damage response (DDR) including ATM and Ataxia Telangiectasia and RAD3-related kinase (ATR) as mediators of IGF-1R kinase inhibition. It was demonstrated that upon IGF-1R inhibition with Linsitinib or BMS-754807, the DDR was induced in MCF-7 cells. Hence, the combined inhibition of the IGF-1R kinase activity and ATR kinase with VE-821 leads to synergetic cytotoxicity in these cells (O'Flanagan et al., 2016).

Recently it was also proposed that influencing receptor endocytosis and translocation to the nucleus enhanced the effects of chemotherapy and targeted agent resistance (Codony-Servat et al., 2017, Aleksic et al., 2010, Aleksic et al., 2018). Codony *et al.*, observed that upon IGF-1R inhibition with Ganitumab or Src inhibition with Dasatinib, IGF-1R accumulation in the nucleus was increased (Codony-Servat et al., 2017). However, the inhibition of IGF-1R internalisation decreased the translocation to the nucleus (Aleksic et al., 2018).

Overall, although there is compelling evidence for the concept of IGF-1/IGF-1R targeting as cancer therapy, ongoing research is still required to understand the complexity of inhibiting the signalling pathways and the variability of responses in different tumours.

1.6 AIM OF THE STUDY

Although the IGF-1/IGF-1R system has been extensively investigated in cellular processes in normal cells and cancer, knowledge about the regulation of the receptor activity, the complexity of its induced signalling and its capability to avoid effective targeting in cancer therapy is still missing. Our research group and others established that crosstalk between IGF-1R and adhesion-signalling is a key to modulating IGF-1R activity and/or signalling. Furthermore, we established that $Tyr^{1250/1251}$ in the IGF-1R C-terminal tail are essential residues for receptor activity and cooperation with adhesion signalling. This thesis aims to investigate how adhesion-related signalling modulates IGF-1R activity and how $Tyr^{1250/1251}$ phosphorylation contributes to these mechanisms.

The aims of the study are:

1) To investigate how the non-receptor kinase, FER influences IGF-1R activation and whether it contributes to resistance to IGF-1R kinase inhibition.
2) To generate a series of cancer cell lines harbouring CRISPR-mediated knock-in of tyrosine and serine mutations in the *igf-1r* gene or CRISPR-mediated knock-out of the *igf-1r* to study the function of the C-terminal tail in IGF-1R function.
3) To establish how $Tyr^{1250/1251}$ phosphorylation is controlled and how they contribute to IGF-1R activity in cancer cells.

2 CHAPTER 2: MATERIAL AND METHODS

2.1 MATERIAL

2.1.1 General chemicals and reagents

Unless it is stated otherwise, chemicals including sodium chloride and other salts for the preparation of buffers were purchased from Sigma-Aldrich (Dublin, Ireland). Bradford protein estimation reagent was purchased from Bio-Rad Laboratories (Hercules, CA) and the pre-stained molecular weight markers (10-250 kDa) was purchased from Fisher Scientific (Dublin, Ireland). Amersham nitrocellulose membrane was also purchases from Fisher Scientific (Dublin, Ireland). Recombinant IGF-1 and IGF-2 were from Pepro Technology (Rocky Hill, NJ). For western blot detection of primary antibodies IRDYE-conjugated secondary antibodies were purchased from LI-COR Biosciences (Lincoln, NE). Paraformaldehyde (16%) and the 12 mm coverslips used for immunofluorescence microscopy was purchase from Fisher Scientific. The microscope slides were acquired from KB Scientific. Fluorophore conjugated secondary antibodies used in the immunofluorescence microscopy were purchased from Jackson Immuno Research (Cambridgeshire, UK). The QuickChange Lightning site-directed mutagenesis kit was purchased from Agilent Technologies (Santa Clara, CA). The IGF-1R Double Nickase Plasmid (h) (sc-400084-NIC) was obtained from Santa Cruz Biotechnologies, Inc (Dallas, Texas, USA).

2.1.2 Cell Culture reagents

Dulbecco's Modified Eagles Medium (DMEM), Hams Nutrient F12 medium, Roswell Park Memorial Institute media (RPMI)-1640 medium, foetal Bovine Serum (FBS), L-Glutamine, penicillin/streptomycin antibiotics and trypsin-EDTA were purchased from Sigma Aldrich (Dublin, Ireland). Zeocin,

Lipofectamine and Lipofectamine 2000 were purchased from Invitrogen (Paisley, UK). Puromycin was purchased from Calbiochem (La Jolla. CA). Cell culture plates were supplied by Sarstedt (Nümbrecht, Germany). Migration assay plates were purchased from Ibidi (Munich, Germany).

2.1.3 Antibodies

Table 2.1: List of antibodies.

Antibodies were used for immunofluorescence cytology (IF), immunoprecipitation (IP), in-cell western (IW) and western blotting (WB) and are either monoclonal (m) or polyclonal (p).

Antibody Target (Anti-)	IF/WB/ IP	p/ m Ab	Species	Company	Catalogue Number
IGF-1Rβ	WB	p	rabbit	Cell Signaling Technology (CST)	3027
IGF-1Rβ	IF	m	rabbit	CST	9750
IGF-1Rα (α-IR-3)	IW/IF/ IP	m	mouse	Callbiochem /Merk	GR11
IGF-1Rβ	WB	m	mouse	Santa-Cruz	sc-81464
p-Tyr$^{1135/1136}$ IGF-1R	WB	p	rabbit	CST	3024
p-Tyr^{1131} IGF-1R	WB	p	rabbit	CST	3021
p-Tyr^{950} IGF-1R	WB	p	rabbit	CST	4568
p-Tyr^{1250} IGF-1R	WB	p	rabbit	Santa Cruz	sc-293102
p-Tyr^{1250} IGF-1R	WB	p	rabbit	biorbyt	orb43345
FER	WB/ IF	m	mouse	CST	4268
FER	WB	p	rabbit	Santa Cruz	sc-28771
p-Tyr^{402} FER	WB	p	rabbit	abcam	ab79573
p-Tyr^{397} FAK	WB	p	rabbit	CST	3283
p-Tyr^{925} FAK	WB	p	rabbit	CST	3284

FAK	WB	m	mouse	Santa Cruz	sc-1688
FAK	WB	p	rabbit	Santa Cruz	sc-558
p-Tyr^{416} Src	WB	p	rabbit	CST	2101
Src	WB	m	mouse	CST	2110
p-Thr^{202}/Try^{204} ERK	WB	p	rabbit	CST	4377
ERK1/2 (p44/42 MAPK)	WB	p	rabbit	CST	4696
p-Ser^{473} AKT	WB	p	rabbit	CST	4060
AKT	WB	m	mouse	CST	2920
p-Tyr$^{239/240}$ SHC	WB	p	rabbit	CST	2434
SHC	WB		mouse	BD Transdution Labs	610879
snail	WB	m	mouse	CST	3895
LC-3	WB	m	rabbit	CST	3868
Ubiquitin	WB	m	mouse	Santa Cruz	sc-8017
GM130	IF	m	mouse	BD Transdution Labs	610822
β-actin	WB	m	mouse	Sigma-Aldrich	A5441
α-Tubulin	WB	m	mouse	Santa Cruz	sc-23948
GAP-DH	WB	m	rabbit	CST	2118

2.1.4 Chemical Inhibitors

BMS-754807 (cat# S1124-SEL) and AP26113 (cat# S7000-SEL) were purchased from Stratech/Selleckchem (Munich, Germany), PF-573228 (cat#3239-10) was purchased from Tocris Bioscience (Bristol, UK), and PP2 (cat#529573-5mg) was purchased from Sigma/Merck (Darmstadt, Germany).

MG-132 (cat#474790) was purchased from Calbiochem/Merck (Darmstadt, Germany). Brefeldin A (cat# B7651-5mg), Leupeptin (cat#L2884-

25 mg) and E64 (cat#E3132-5mg) were from Sigma/Merck (Darmstadt, Germany). Chloroquine (cat#14774s) was purchased from Cell Signalling (Danvers, MA, United States).

2.1.5 Mammalian Cell lines

MCF-7, MDA-MB-231 and DU-145 were originally obtained from American Type Culture Collection (ATCC, Rockville, MA, USA). HS-578T and Cal-51 cell lines were a kind gift from Almac Diagnostics, Craigavon (Northern Ireland). R^- cells (3T3-like mouse embryonic fibroblast cell line derived from the IGF-1R knock-out mouse) were obtained from Professor Rosemary O'Connor's laboratory stocks and were originally generated by Sell *et al.* (Sell et al., 1994).

2.1.6 Mammalian Expression Vectors

Expression vector plasmids pcDNA3/pcDNA4 encoding the IGF-1R wildtype, Y1250F/Y1251F and IGF-1R kinase inactive (K1003R, KR) were obtained from Professor Rosemary O'Connor's laboratory stocks. pSG5 plasmids encoding FER kinase was obtained from Addgene. Point mutations in the IGF-1R (Y1250E/Y1251E) or FER (D743R, DR) were introduced using QuickChange Lightning site-directed mutagenesis kit.

2.2 METHODS

2.2.1 Cell culture, ligand stimulation and pharmacological inhibitors

MCF-7, MDA-MB-231, HEK293T, HS-578T and R^- cells were maintained in DMEM. CAL-51 cells in a 50/50 mix of DMEM/Hams Nutrient F12 media. DU-145 were cultured in RPMI. All media were supplemented with 10% (v/v) heat inactivated Foetal Bovine Serum (FBS), 10 mM L-Glutamine, and 5 mg/ml

penicillin/streptomycin. Cells were cultured at 37 °C in a humidified atmosphere at 5% CO_2. All cells were determined to be free of mycoplasma following the laboratory protocol.

For the analysis of IGF-1 stimulation in western blotting, cells were seeded 20 hr prior to starvation and allowed to reach approximately 70% confluency. Following serum-starvation for 4 hr, cells were stimulated with the indicated concentration of IGF-1, IGF-2 and Insulin. In general, R^- cells and HEK293T cells transiently expressing the IGF-1R (see below), were stimulated with 10 ng/ml IGF-1 and cell lines with endogenous IGF-1R were stimulated with 50 ng/ml IGF-1.

For analyses of detached cells (suspension), cells seeded on 10 cm plates were cultured overnight (ON) in complete medium and then starved of serum for 4 hr in total. After 3 hr, cells were enzymatically detached using Trypsin/EDTA, and cultured in suspension (SUS) for 1 hr. Cells were then stimulated with IGF-1, collected by centrifugation at 1000 rpm for 5 minutes, washed with PBS and lysed.

For kinase inhibition experiments, BMS-754807, AP26113, PF-573228 and PP2 were added to cells for 1 hr, unless otherwise stated.

Cycloheximid was added to the cell cultures for 24 hr followed by a wash of cell cultures for 6 hr or 8 hr. The appropriate vehicle was added to the control sample (0 hr) The proteasomal or lysosomal inhibitors MG-132, Leupeptin, E64 and Chloroquine were added to cell cultures for 4 or 6 hr and the appropriate vehicle (DMSO, H_20, EtOH) was added to control samples (0 hr). Brefeldin A (BFA) was added to cells in either complete medium or serum-free media for 4 hr.

2.2.2 Generation and transfection of IGF-1R mutants

2.2.2.1 General plasmid transfection

Cells were transiently transfected with pcDNA3/pcDNA4 plasmid encoding the IGF-1R WT or KR mutant, pSG5 plasmids encoding FER WT or DR and pcDNA4 plasmid encoding IGF-1R WT, FF or EE mutants. For co-transfection of IGF-1R and FER in HEK293T cells; cells were transfected using Calcium Phosphate method: Cells were seeded 5 hr prior to transfection to give a confluency of 70%. Plasmid encoding for FER (3 μg), together with 1 μg of pcDNA3 IGF-1R expressing plasmids were added to $CaCl_2$. The DNA/$CaCl_2$ mixture was then added dropwise to 2x HBSS at a ratio of 1:1. Samples were allowed to stand for 1-2 min and the solution was then distributed to the pre-seeded cells in a dropwise manner. Cells were incubated ON to allow the transfection to proceed. Cells were re-seeded for experiments and lysed 24 hr later.

R^- cells were seeded 24 hr prior to transfection at a density of approximately $1.0x10^6$ cells/10 cm plate. Lipofectamine 2000 diluted in OptiMem was used to transfect cells with relevant DNA plasmid (12-16 μg). After 24 hr cells were re-seeded for experiments at 48 hr post transfection. For stable expression of pcDNA4 plasmids encoding the WT, FF or EE IGF-1R, transfected R^- cells pools were cultured in selection medium supplemented with 400 μg/ml Zeocin for 4 weeks to select cells expressing the plasmids only.

MDA-MB-231, MCF-7 and DU-145 cells were seeded 24 hr prior to transfection to approximately 70% confluency in 6-well or 10 cm plates for transfection with Lipofectamine 2000. All cell lines were transfected with 2 μg/6 well plate and 12 μg/10 cm plate of pcDNA4 plasmid. Cells were re-seeded 24 hr post transfection for experiments.

2.2.2.2 Plasmid transfection for CRISPR-mediated mutation in *igf-1r*

CRISPR induced mutation of the *igf-1r* gene in MCF-7 cells was conducted in Prof. Shin-Ichiro Takahashi (University of Tokyo) by Dr. Fujii, who also designed the gRNA sequences and the single-stranded oligo donor (ssOND) (Table 2.2). MCF-7 cells were transfected with either U6p cloning plasmid encoding for the Cas9 nuclease, the guide RNA, the GFP-tag and a second U6p plasmid encoding for the respective ssOND (S1248A mutation and Y1250F/Y1251F; Table 2.2) or, for control cells (CTL), with the U6p plasmid encoding for the Cas9 nuclease, a scrambled RNA and the GFP-tag using Lipofectamine LTX. According to the manufacturer's protocol of the transfection reagent, transfected cells were left for 48 hr following separation of transfected cells from non-transfected cells using the GFP-tag and fluorescence-activated cell sorting (FACS). Enriched cell pools were then shipped from Japan to Ireland. After recovery, the MCF-7 pools were cultured and separated into groups of ~10 cells/well of a 96-well plate to identify group clones encoding IGF-1R with the selected mutation. Cells were allowed to grow until confluent. DNA was extracted and a PCR was performed (Method 2.2.3) on ~50,000 cells while the remaining cells were frozen. Serial dilution was used on three group clones positive for the particular mutation/controls to obtain cells only encoding for the mutated IGF-1R or the wildtype IGF-1R. Cells were again allowed to reach confluency and a PCR was performed on DNA extracted from ~50,000 cells. Serial dilution followed by PCR was performed twice on cells. Single cell clones positive for the mutation of interest were recombined (MCF-7-KI: MCF-7-WT, MCF-7-FF).

Table 2.2: Designed ssOND (full length) for DNA repair.

ssODN_S1248A
CATGTGGGCGTAAGGCTGTCTCTCGTCGAAGCTGGCGCGGAGGACC AGCACCCCAGGGCCGGGGCCGTTCTCGGCCTTGTGTCCTGAGTGTC TGTCGGGCAGTGGCAGGGAGGACGAGGAGGCCGAGGGGTCCAGGG GGACGCTCTCCATGTTCTCTGGCTCCAGGTCCAGCTCCTCCGGCTCG GGCAGCTTGTTCTCCTCGCTGTAGTAGAAtGcGACCTCCCGGAAGCCA GGCTCCATCTCCTCTTTGATGCTGCTGATGATCTCCAGGAAGGAAGG CCTCATCTTGGGGTTATACTGCCAGCACATGCGCATCAGTTCAAACCT GCAGCCAAGACACACGGGAGGGGGTCC
ssODN2_Y1250F_Y1251F
CATGTGGGCGTAAGGCTGTCTCTCGTCGAAGCTGGCGCGGAGGACC AGCACCCCAGGGCCGGGGCCGTTCTCGGCCTTGTGTCCTGAGTGTC TGTCGGGCAGTGGCAGGGAGGACGAGGAGGCCGAGGGGTCCAGGG GGACGCTCTCCATGTTCTCTGGCTCCAGGTCCAGCTCCTCCGGCTCG GGCAGCTTGTTCTCCTCGCTGaAGaAGAAGctGACCTCCCGGAAGCCA GGCTCCATCTCCTCTTTGATGCTGCTGATGATCTCCAGGAAGGAAGG CCTCATCTTGGGGTTATACTGCCAGCACATGCGCATCAGTTCAAACCT GCAGCCAAGACACACGGGAGGGGGTCC

IGF-1R knock-out cells were generated using CRISPR technology as described in Chapter 4. The IGF-1R Double Nickase Plasmid (h) was obtained from Santa Cruz Biotechnologies, Inc. and transfections carried out as described in the manufacturer's protocol. Selection of transfected cells was achieved with Puromycin (0.5 μg/ml for MDA-MB-231 and MCF-7 cells, or 0.4 μg/ml for DU-145 cells). IGF-1R knock-out cell pools were selected by immunoblotting for IGF-1R and then cloned by serial dilution. IGF-1R knock-out (KO) clones were also subsequently pooled.

2.2.3 Genomic DNA extraction and genomic DNA PCR

CRISPR MCF-7 cells cultured in normal medium (~50.000 cells), were harvested and transferred into a 1.5 ml eppendorf tube and centrifuged at 14.000 x g for 10 sec. The pellet was washed with PBS and the centrifugation step was repeated. DNA was either extracted immediately following the Wizard

genomic DNA extraction Kit (Promega cat#A1125). PCR was performed using 20 ng of extracted DNA diluted in 8 μl of nuclease free water, 1 μl of each primer (Table 2.3) and 10 μl of the GoTaq G2 Green Master Mix (Promega cat# M7823). PCR was performed in 35 cycles (DNA denaturation 94˚C for 30 sec, annealing: 55˚C for 30 sec, extension: 72˚C for 1 min). Fragment amplification was assessed on 1.5 % Agarose gel and visualized under UV-light. The expected band size is 500 base pairs (BP).

Table 2.3: Primer sequences used for PCR to verify the mutation in the *igf-1r.*

IGF-1R	Forward primer sequence
WT	GCTTCCGGGAGGTCTCC
S1248A	GCTTCCGGGAGGTCGCA
Y1250F/Y1251F	CGGGAGGTCAGATTCTTCTT
Reverse primer sequence	
CTTAAAGGCCCATGTCAGTTAAGG	

To verify the knock-out of the *igf-1r* in MDA-MD-231 and DU-145 cells, DNA was extracted using the Wizard genomic DNA extraction Kit (Promega cat#A1125). Designed primers, binding before and after the gRNA targeted region were used to amplify the DNA via PCR. PCR was performed in 35 cycles (DNA denaturation 94˚C for 30 sec, annealing: 55˚C for 30 sec, extension: 72˚C for 1 min). Fragment amplification was assessed on 1.5 % agarose gel and visualized under UV-light. Fragments were separated from the rest of the agarose gel and DNA was extracted using the KeyPrep Spin Gel DNA Clean Up Kit (Anachem # AM-113163). Extracted DNA was sent for sequencing using the Eurofins genomics service (Ebersberg, Germany).

Table 2.4: Designed primer pair used to verify the *igf-1r* knock-out.

Primer Exon 1
5'- GGG AGC GAA GAC TGA GTT TG -3' (Fwd)
3'- GCG GGA CAA ACG CTT TGG -5' (Rev)
Primer Exon 2
5'- AACTGTCAGTCTGCAACCCACA -3' (Fwd)
3'- TGACCAGGGCGTAGTTGTAG -5' (Rev)

2.2.4 SDS PAGE and western blotting

Cells were washed with ice-cold PBS twice and lysed immediately with cold lysis buffer (20 mM Tris, pH 8, 50 mM NaCl, 50mM NaF, 1% NP40) containing protease and phosphatase inhibitors for 30 min on ice, followed by centrifugation at 14.000 rpm for 15 min at 4˚C. Protein concentration of samples was determined using a BSA standard curve in a Bradford assay. Samples were denatured by boiling for 5 min with 5x SDS PAGE loading buffer. Technical replicates of the same denatured samples (30 μg protein) were separated on 8-10% gels to enable analysis of distinct IGF-1R phospho-sites. Proteins were then transferred to nitrocellulose membranes that were blocked for 1 hr at room temperature in 5% BSA in Tris-buffered saline-T (20 mM Tris, 150 mM NaCl and 0.05% Tween 20, pH 7.6 (TBS-T). Primary antibodies were diluted at 1/1000 or 1/10000 dilution for β-actin in TBS-T containing 5% milk or 5% BSA and incubated with membranes at 4 °C ON. To detect distinct IGF-1R phospho-sites, each blot was incubated with rabbit phospho-IGF-1R or mouse/rabbit total IGF-1R antibodies and a mouse antibody detecting a protein input control (α-Tubulin, β-actin, GAP-DH). For detection of p-Thr^{202}/Tyr^{204}/ERK, p-Ser^{473}/AKT and p-Tyr$^{239/240}$/SHC, blots were probed with a combination of rabbit antibody detecting the

phosphorylated protein, and a mouse antibody detecting the total protein. Immunoblots were subsequently probed with mouse antibodies to detect the protein input control. IRDye-fluorophore-conjugated secondary antibodies (1/10,000) were used for detection with the Odyssey Image Scanner System and Image Studio™ quantification software was used for densitometry measurements (LI-COR Biosciences). Each phospho-IGF-1R protein was normalized to total IGF-1R, or first to the input control and then to total IGF-1R. Other phosphoproteins were normalized to their respective total protein.

2.2.5 Phospho-Tyr$^{1250/1251}$-antibody adsorption

The phospho-Tyr^{1250} IGF-1R antibody (biorbyt cat#orb43345) was adsorbed to nitrocellulose membrane that was coated with non-phosphorylated SFYYS peptide. Membranes dotted with peptide were allowed to dry completely and blocked with PBS containing 1% BSA for 1 hr at RT. These membranes were then incubated with the phospho-Tyr^{1250} antibody for 1 hr rotating at RT, and the antibody recovered for subsequent use in western blotting.

2.2.6 Immunoprecipitation and in-vitro kinase assays

Cells were lysed and 0.5-1 mg of protein lysate was incubated with antibodies detecting IGF-IR at 1/100 dilution, ON rotating at 4˚C. Immune complexes were obtained by adding 50 μl of pre-washed Protein G-Agarose beads to the antibody-lysate mix for 2 hr with rotation at 4˚C. Beads were washed three times using lysis buffer and loading dye was added to the washed beads (2x) before samples were boiled for 5 mins at 95˚C, centrifuged at 14,000 rpm for 2 min, followed by SDS PAGE and western blotting. To investigate multiple IGF-1R phospho-sites, denatured samples were split to load on separate gels. The antibody detecting the phospho-site was then removed using stripping

buffer (200 mM NaOH with 1% SDS) for 10 min at RT. Before incubation with total IGF-1R (1/1000), blots were re-blocked with 5% BSA in TBS-T, incubated with secondary antibody and re-scanned to ensure that stripping was successful.

The ADP-GloTM Kinase Assay kit (Promega) was used for in-vitro kinase assays. For these kinase assays, protein input for immunoprecipitations of IGF-1R WT and FF were adjusted to be equivalent to EE. Beads with immunoprecipitated IGF-1R were washed twice with kinase buffer (40 mM Tris (pH 7.5), 20 mM $MgCl_2$, 2 mM $MnCl_2$, 0.1 mg/ml BSA, 2 mM DTT, 100 μM Sodium Vanadate) and then incubated with kinase buffer containing 150 μM ATP (ADP-GloTM Kinase Assay) and 2 mg/ml poly(Glu, Tyr) (4:1) (P0275; Sigma) as an exogenous substrate for 30 min, with samples mixed every 10 min. Beads were centrifuged for 30 sec at 14,000 rpm and triplicates (5 μl) of supernatant were added to a white 384-well plate for incubation with ADP-Glo (5 μl per sample) for 60 min at room temperature. The ADP-Glo Kinase detection reagent (10 μl) was added to each reaction for 30 min at room temperature, and kinase activity measured with a luminometer (BioTek, Winooski, USA).

2.2.7 Ubiquitination assay

R^- cells overexpressing the IGF-1R WT, FF or EE mutants were harvested in 1 ml ice-cold PBS from a 15 cm plate and 900 μl of cell solution was added to a fresh eppendorf tube, leaving ~100 μl of cell solution for the whole cell lysate (WCL) input analysis. Tubes were centrifuged for 2 min at 1000 rpm at 4°C, and supernatants were discarded. The pellets of the WCL were lysed in NP40 lysis buffer as described earlier.

To determine the ubiquitination profile on IGF-1R using an IP, the cell pellets, were lysed in 80 μl of 1% SDS containing protease/phosphatase inhibitors and 150 mM *N*-Ethymaleimide (NEM). To enhance cell lysis, samples were resuspended with a 21 gauge needle attached to a 1 ml syringe at least 10 times before boiling for 5 min at 95°C. After samples cooled to RT, 125 μl of covalent buffer containing (50 nM Tris, pH 8.0, 150 mM NaCl, 1% Trition-X-100, 0.1% SDS plus protease/phosphatase inhibitors), and 150 mM NEM was added. Samples were vortexed for 20 sec and centrifuged for 30 min at 14,000 rpm at 4°C. The viscous pellet was removed with a wooden tooth pick. The Bradford assay was performed on WCL and IP samples before continuing with protocols for western blotting and immunoprecipitation.

2.2.8 Subcellular fractionation

Cytoplasmic and soluble nuclear extracts were prepared from R^- cells overexpressing the IGF-1R WT, FF or EE. For the extraction of cytoplasmic proteins (Lau et al., 2007), cells were first lysed on ice for 10 min with 80 μl buffer A [10 mM HEPES, pH 7.9, 10 mM KCl, 1.5 mM $MgCl_2$, 0.34 M Sucrose, 10% glycerol 1 mM DTT and 0.1% (v/v) Triton-X-100]. Protease/phosphatase inhibitors were added to buffer A. After centrifugation of samples at 4000 rpm at 4°C for 5 min, supernatants containing the cytoplasmic fractions were collected. Pellets containing the nuclear proteins were washed three times in the buffer A without Triton-X-100, followed by centrifugation at 4000 rpm at 4°C for 5 min. Pellets were lysed in 50 μL of buffer B (0.2 mM EGTA, pH 8.0, 3 mM EDTA, pH 8.0 and 1 mM DTT) plus protease/phosphatase inhibitors, ON in the cold-room on a vortex genie. After centrifugation of samples at 4000 rpm for 5 min at 4°C, supernatants containing nuclear fractions were collected.

Cytoplasmic, soluble, and insoluble nuclear extracts were prepared (Tanaka et al., 2007) from R^- cells overexpressing the IGF-1R WT, FF or EE. Cells lysed on ice for 10 min with 80 µl buffer A [10 mM Tris-HCl, pH 7.5, 1.5 mM $MgCl_2$, 140 mM NaCl, 0.05% (v/v) NP40] containing protease/phosphatase inhibitors. After incubation the solution was added to a fresh tube containing buffer A with 50% (v/v) sucrose, which causes the separation into two phases. Tubes were then centrifuged at 12,000g for 10 min at 4°C, to obtain nuclear and cytoplasmic fractions. Supernatants containing the cytoplasmic fractions were collected. Pellets were washed three times in buffer A and then lysed for 10 min on ice in 50 µl buffer B [10 mM Tris, 100 mM NaCl, 1 mM EGTA, 300 mM sucrose, 50 mM NaF, 0.5% (v/v) Trion-X-100] supplemented with protease/phosphatase inhibitors. Samples were centrifuged at 2,000 g at 4°C for 5 min and the supernatant (nuclear soluble fraction) and pellet (nuclear insoluble/chromatin fraction) were collected.

For both fractionation protocols described, protein concentration of the cytosolic fraction was determined using the Bradford assay. All samples were boiled in 5x SDS-PAGE sample buffer, and equal amounts for the cytosolic fraction as well as equal volumes of the nuclear fraction (soluble and insoluble) compared to the cytosolic fraction were subjected to electrophoresis on 10% SDS-polyacrylamide gels. The purity of the fractions was confirmed by western blotting α-tubulin as cytoplasm marker.

2.2.9 Quantitative PCR

R^- cells transiently expressing WT, FF or EE IGF-1R were prepared for RNA extraction 48 hr post-transfection. RNA was extracted using the PureLink RNA Mini Kit (Thermo Scientific) according to the manufacturer's protocol. To

synthesize cDNA, 1 μg of RNA and the QuantiTect reverse transcription kit (Qiagen) was used. Quantitative PCR was performed using the Roche FastStart essential DNA Green Master Kit and the Lightcycler® 96 Instrument (Roche Diagnostics). Actin was used as housekeeping control. The 2^-ΔΔCT method (Livak and Schmittgen, 2001) was used to analyse data and to determine relative mRNA expression levels. IGF-1R mRNA expression values were normalized to actin and expressed as fold-change relative to the WT IGF-1R (set to 1). Primers used for to detect IGF-1R are displayed in Table 2.5.

Table 2.5: Primers used to detect the IGF-1R in qRT-PCR.

Forward primer
5'- ATGTCCAGGCCAAACAGGAT -3'
Reverse primer
5'- CCTCCCACTCATCAGGAACG -'3.

2.2.10 Immunofluorescence

Transfected and un-transfected cells were plated on 12 mm glass coverslips 24 hr prior to the experiment. At the end of the experiment, cells were washed with phosphate-buffered saline and fixed with 4% paraformaldehyde in PHEM buffer for 60 min at RT. Aldehyde groups from PFA fixation were quenched with 50 mM Ammonium Chloride for 20 min, and cells were permeabilized using 0.1% Triton/PHEM for 5 min. PHEM buffer containing donkey serum (5%) was used for blocking and dilution of antibodies. Coverslips were incubated with primary antibodies at 4˚C ON, washed three times with PHEM followed by secondary antibody incubation. The primary antibodies (Material 2.1.3) were diluted as displayed in Table 2.6 and secondary antibodies or dyes

to detect actin filaments as displayed in Table 2.7. The nuclei was stained with Hoechst.

Table 2.6: Primary antibody dilution for immunofluorescence.

Detection	Details	Cell line	Dilution
IGF-1R	CST#9750	R^- cells	1/200
IGF-1R	CST#3027	MCF-7 cells	1/200
IGF-1R	CST#3027	HS-578T, MDA-MB-231 cells	1/100
GM-130	*cis*-Golgi:	R^- cells, MCF-7, HS-578T, MDA-MB-231 cells	1/200
biotinylated Vicia Villosa (VVA)	*cis*- and *trans*-Golgi network; Lectin Vector Laboratories cat#B-1235-2	R^- cells, MCF-7, HS-578T, MDA-MB-231 cells	1/400

Table 2.7: Secondary antibodies and dyes used for immunofluorescence.

Fluorophore/Cyanine Dyes	Dilution
Cy3-conjugated AffiniPure Anti-Mouse antibody	1/1000
Alexa Fluor 488-conjucated AffiniPure Anti-Rabbit antibody	1/200
Alexa Fluor 594-conjucated Streptavidin	1/1000
Alexa Fluor 488-conjucated Streptavidin	1/200
Phalloidin TRITC Sigma cat# P1951	1/1000
Phalloidin AlexaFluor 405 ThermoFisher cat# A30104	1/40 (66μM)

Images were acquired using a SPOT charge-coupled device camera mounted on a Nikon T600 fluorescent microscope or a Nikon DSFi1c camera attached to the Leica DM LB2 microscope. For confocal microscopy, images were acquired using an Olympus Fluoview FV1000 confocal laser scanning

microscope (numerical aperture: 1.4) with a 60x-immersion objective. Maximum intensity projections and z-stacks were processed using ImageJ software. Brightness and contrast were adjusted in Adobe Photoshop if required.

To determine fluorescent intensity within the cells, ImageJ software was used. A line plot was drawn using the RGB profiler from ImageJ to measure the signal intensity per pixel (Y-axis) along the line (X-axis). Acquired intensity was exported to GraphPad to generate the line plots.

2.2.11 In-Cell Western Assays for IGF-1 receptor

Cells were seeded at $5x10^4$ cells per well in 96-well tissue culture plates in complete medium for 24 hr, washed three times with PBS, serum-starved for 4 hr followed by stimulation with 10 ng/ml IGF-1 for 10 min or left in serum-free medium or complete medium. Cells were immediately fixed with 100 μl of a freshly prepared 4% PFA/PHEM and incubated at RT for 30 min followed by quenching with 50 mM Ammonium Chloride for 20 min and 1x washed with PHEM. Triton/PHEM (0.1%) was used to permeabilize cells in the wells used for total receptor detection and wells for p-Ser^{473}/AKT detection (stimulation control) and secondary antibody control for 5 min at RT followed by a wash with PHEM. All wells were then blocked for 1 hr with 50 μl of blocking buffer (5% goat serum/PHEM). Primary antibody (IGF-1R IR3 for surface and IGF-1Rβ cat#3027 for total receptor, or p-Ser^{473}/AKT) was added for 2 hr with gentle rocking followed by washing and incubation with secondary antibody. Goat anti-Mouse IRDye® 680 (1/1000) (LI-COR Biosciences; cat#926-32220), Goat anti-Mouse IRDye® 800 (1/1000) (LI-COR Biosciences; cat#926-32210) or Goat anti-Rabbit IRDye® 800 (1/1000) (LI-COR Biosciences; cat#926-

32211) were used to detect primary antibodies. Syto60 (Invitrogen) was also included (1:10,000) as a cell-permeable nucleic acid stain that fluoresces at 680 nm, and is detected using the Odyssey infrared scanner. Cells were washed five times with PHEM. Plates were dried, and intensity of IGF-1R signal (surface and total levels) was quantified using the Image Studio™ quantification software with normalization to Syto60 levels.

2.2.12 Proliferation, Colony formation, adhesion, clonogenic growth and migration

2.2.12.1 Cell proliferation

For measurement of cell proliferation MCF-7, MDA-MB-231 and DU-145 knock-out cell lines and control cell lines were seeded in triplicate at 3.0×10^4 cells/well in 24-well plates. Cells were collected every 24 hr up to 96 hr. Media was removed, cells were washed once with PBS and trypsinized. Cell numbers were determined by triplicate counts using a Haemocytometer.

2.2.12.2 Colony formation

Cells were seeded in triplicate at 1.0×10^4 cells/well in 6-well plates in complete media. After 14 days, cells were washed in PBS, fixed in 96% ethanol (EtOH) and stained with 0.05% crystal violet (CV) in 20% EtOH, before extensive washing in distilled H_2O. Colony formation was quantified using the Odyssey infrared imaging system (LI-COR Biosciences). For DU-145 cells, media was removed, cells were washed once with PBS and trypsinized. Cell numbers were determined by triplicate counts using a Haemocytometer.

2.2.12.3 Adhesion assay

The wells of a 96-well plate were coated with 100 μl of fibronectin (Sigma, UK; 5 μg/ml) for 2 h at 37°C.The plates were washed extensively with PBS and blocked with 100 μl of 2.5% bovine serum albumin/well for 1 hr before further washing with PBS. MCF-7 cells (100 μl containing 5×10^4 cells) were added to each coated well in triplicate and allowed to attach for the indicated times. The medium was removed, the wells were washed with PBS, and attached cells were fixed with methanol (MeOH) and stained with 0.05% CV, scanned and quantified using the Odyssey infrared imaging system (LI-COR Biosciences).

2.2.12.4 Clonogenic growth; soft agar assay

The wells of a 6-well plate were covered with 2 ml of 0.8% low-melting agarose per well (Sigma #A9414-25g), which was left to solidify. Next, a second layer of 0.4% agarose solution was slowly poured on top of this first one consisting of 1 ml of the 0.8% agarose solution mixed with 1 ml of media containing cells. Cell numbers were $2x10^5$ of MCF-7-WT or MCF-7-FF cells, $2x10^5$ MCF-7-CTL cells or KO, $3,5x10^5$ MDA-MB-231-CTL or KO cells or $2,5x10^5$ DU-145-CTL or KO cells. Cells are allowed to form colonies for 4-6 week and they were supplemented with fresh media every 3-5 days. After 4-6 weeks, the media was removed and cells are stained with 0.05% CV in 20% EtOH at 4˚C ON before being extensively washed with distilled H_2O at 4˚C for 3-4 weeks. Clonogenic growth was quantified using the Odyssey infrared scanner (LI-COR Biosciences, Cambridge, UK).

2.2.12.5 Migration; wound-healing assay

MDA-MB-231-CTL or KO and HS-578T cells were seeded in Culture-Insert 2 well 35 mm dish (70 μl per well) (ibidi Gmbh cat# 81176), at a concentration of

4.0x10^5 cells/ml. Cells were allowed to attach in the respective chambers for 24 hr. The wound was generated by removal of the insert, allowing cells to migrate. To assess migration of HS-578T cells in presence of the Golgi disruptor BFA, cells were serum-starved for 4 hr, and DMSO (vehicle) or BFA was added upon removal of the insert. The medium was then supplemented with IGF-1 (50 ng/ml).

DU-145 CTL or KO cells were seeded in 6-well plates at a concentration of 5×10^5 cells/ml 24 hr prior to wounding. The monolayer was scratched using a sterile P20 tip (Time 0 h). Cells were allowed to migrate for 20 hr.

To assess migration of HS-578T cells in presence of AP26113, HS-578T cells were seeded in 6-well plates at a concentration of ~3.5x10^5 cells/ml 24 hr prior to wounding. The monolayer was scratched using a sterile P10 tip (Time 0 hr). AP26113 was added to the cells, while DMSO at the appropriate volume was added to the control cells. Cells were allowed to migrate for 15 hr.

All wound areas were photographed at 10x magnification with a Nikon charge-coupled device camera connected to an inverted Nikon Eclipse TE 300 microscope at the indicated times. The drawing tool of ImageJ was used to assess the cell free area.

For immunofluorescence, HS-578T cells were seeded in Culture-Insert 2 well inserts placed on a coverslips (ibidi Gmbh cat# 80209) and allowed to attach for 24 hr. The wound area was photographed at 0 hr and 6 hr of migration. Subsequently, coverslips were recovered for immunofluorescence.

2.2.13 Statistical analysis

Western blot densitometry results were expressed as fold-change in the ratio of phospho/total protein relative to the control condition (set to 1), which is indicated as a white bar in each graph. Quantification of migration in a wound healing assay was expressed as fold change in cell free area relative to time 0 hr of migration (set to 1).

For calculations comparing fold-change of each group to the control, one-sample *t*-tests were used to test the null hypothesis that the expected ratio was 1. For calculations comparing fold change of groups (≠ control condition) independent two-sample *t*-tests were used. *P*-values were adjusted using Benjamini-Hochberg correction for multiple testing. A 3x3 ANOVA was conducted to examine the main effects of Group and Condition, and the interaction between Group and Condition. Statistical significance was determined as a *P*-value <0.05 and all tests were two-tailed.

3 CHAPTER 3: NON-RECEPTOR TYROSINE KINASE FER ACTIVATES IGF-1R IN POINTS OF FOCAL CELL ADHESION

Orla Cox generated the data presented in Fig. 3.8A. Joanna Stanicka generated data presented in Fig. 3.8B, 3.9A and 3.9C.

Results of this study were published in Oncogene in March 2018. The publication is attached to the thesis.

DOI: 10.1038/s41388-017-0113-z

3.1 ABSTRACT

In clinical trials several drugs were tested to suppress IGF-1R activity in cancer, but showed poor efficacy despite exhibiting promising results in cell and animal models. The complexity of IGF-1R signalling and compensatory mechanisms regulated by other cellular kinases is one possible explanation for the lack of sucess. In a functional siRNA screen we sought to identify cellular kinases that may influence IGF-1R activity in cells. From this screen, the non-receptor tyrosine kinase FER was identified as a candidate mediator of resistance to IGF-1R inhibition.

In this study we investigated the actions of FER in enhancing IGF-1R activation and signalling in cancer cells. It was first observed that FER enhances IGF 1R activation by phosphorylating it on the specific autophosphorylation sites (Tyr^{950}, Tyr^{1131}, $Tyr^{1250/1251}$). FER also enhances IGF-1-mediated activation of SHC ($Tyr^{239/240}$), ERK1/2 (Thr^{202}/Tyr^{204}) and the activity of FAK. FER-enhanced activation of the IGF-1R is IGF-1R kinase-independent, but is dependent on cell adhesion signals. In different cancer cell types, FER and the IGF-1R associated at points of focal cell adhesion where β1-Integrin is also located. FER (Tyr^{402}), SHC and MAPK phosphorylation and IGF-1R protein levels could all be reduced with the ALK inhibitor, AP26113 that shows high specificity for FER kinase. Overall the data demonstrate that FER enhances phosphorylation of catalytically active and inactive IGF-1R in an adhesion-dependent manner. We conclude that FER-mediated activation of IGF-1 signalling in cancer cells may facilitate cancer progression and enable resistance to IGF-1R inhibition.

3.2 INTRODUCTION

Various IGF-1R kinase inhibitors show poor efficiency in clinical trials (Osher and Macaulay, 2019). It is believed that the complexity of IGF-1R signals may mediate drug resistance and that the interplay with other cellular kinases may act as compensatory mechanisms for signalling upon IGF-1R inhibition (Osher and Macaulay, 2019). This compensatory signalling may come from activation of the IR-A and IR-B, as well as EGFR and MET (Qu et al., 2017, Buck et al., 2010, van der Veeken et al., 2009, Liu et al., 2018b).

Much effort is now focused on the identification of cellular kinases that may modulate the effects of IGF-1R inhibition. The combined inhibition of IGF-1R together with these modifying kinases has the potential to increase the success of anti-tumour therapy.

Several years ago, the adhesion-associated kinase Src was identified to directly phosphorylate IGF-1R autophosphorylation sites (Peterson et al., 1996). It was also demonstrated that R^- cells, lacking the IGF-1R are deficient in cellular transformation by *src*, indicating a close association between these two kinases. Combined targeting of the IGF-1R and Src (Ganutiumab and Dasatinib respectively) is currently in clinical trials treating patients with rhabdomyosarcoma (NCT03041701).

In order to identify potential mediators of sensitivity or resistance to IGF-1R kinase inhibition, we used a targeted RNAi screen and identified a number of genes that either sensitise or desensitise cells to IGF-1R inhibition (O'Flanagan et al., 2016). Among these was the non-receptor tyrosine Fes-related (FER) kinase which was identified as a mediator of resistance to the IGF-1R tyrosine kinase inhibitor, BMS-754807, in MCF-7 cells (Figure 3.1),

as cells with FER suppressed were more sensitive to BMS-754807, suggesting that FER may influence the IGF-1R kinase activity.

In addition, a previous study using peptide libraries identified FER as a kinase that has the potential to phosphorylate specific tyrosines in the Insulin and IGF-1 Receptors (Liu et al., 2012). Taken together these observations indicate that FER could modulate IGF-1R activity.

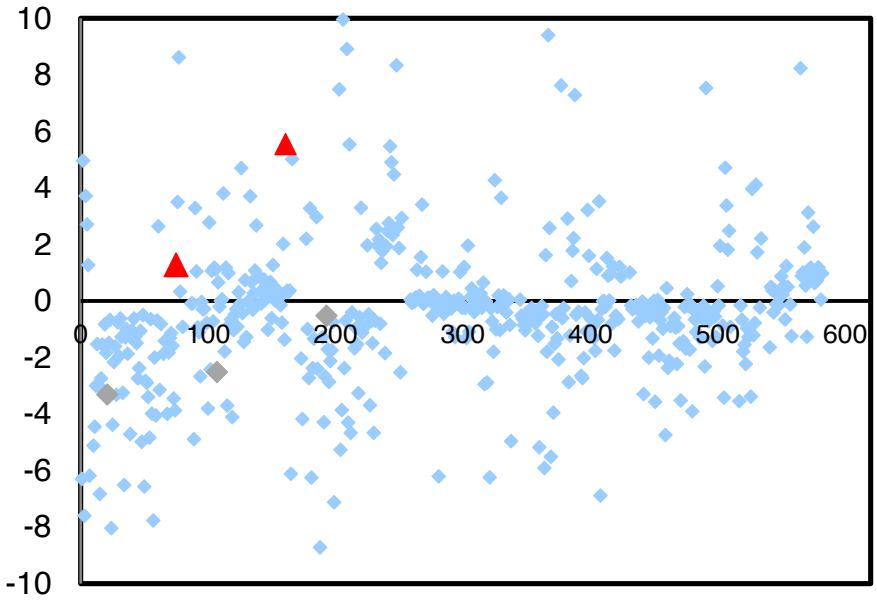


Figure 3.1: Z-Scores distribution from the tumour suppressor and oncogene siRNA screen.

Potential mediators of sensitivity to BMS-754807 showed negative scores, while positive scores indicate potential mediators of resistance. Scores for FER are indicated as red triangles. Graph is representative of two independent screens, and those Z-Scores which were robust across both screens were carried forward as potential targets (O'Flanagan et al., 2016).

FER, along with FES, belongs to a distinct subfamily of non-receptor tyrosine kinases that possess Fes/CIP4 homology Bin-Amphiphysin-Rvs (F-BAR) domains (Greer, 2002). FER activity has been described in several cancers, including ovarian, lung, hepatic, prostate and breast and is reported to facilitate tumorigenesis and chemoresistance by mediating microtubule instability and enhancing cell migration, invasion and proliferation (Zheng et al., 2018, Ivanova et al., 2013, Guo and Stark, 2011, Ahn et al., 2013, Fan et al., 2016, Sangrar et al., 2015). FER was also shown to facilitate crosstalk between growth factor receptors and cell-cell- or cell-matrix- adhesion complexes (Greer, 2002) and to regulate α6- and β1-Integrin-dependent adhesion (Ivanova et al., 2013). FER modulates the distribution of α6- and β1-Integrin in MDA-MB-231 cells, thereby regulating cell morphology and the actin cytoskeleton. Hence, FER can mediate an aggressive cancer phenotype characterized by cell migration and invasion (Ivanova et al., 2013)

The aim of this study was to investigate whether FER modulates IGF-1R signalling to promote an aggressive cancer phenotype. FER significantly increases IGF-1R phosphorylation on specific autophosphorylation sites to activate IGF-1-mediated SHC and MAPK pathways. Our data also showed that FER was activated by IGF-1 and cell adhesion and that cell adhesion is required for FER-mediated phosphorylation of the IGF-1R. In several cancer cells, FER localises in points of focal adhesion where it associated with IGF-1R and β1 Integrin. Pharmacological inhibition of FER activity led to reduced SHC and ERK1/2 activation, a reduction of FER and IGF-1R localisation in focal adhesion points and decrease in migration. We conclude that the adhesion associated FER kinase is an important modulator of IGF-1R activity in cancer

cells and propose that combined targeting of FER kinase activity may increase the effect of IGF-1R inhibition.

3.3 RESULTS

3.3.1 FER kinase enhances IGF-1R phosphorylation and IGF-1 mediated signalling

Suppression of FER by siRNA increased the responses to IGF-1R kinase inhibition, suggesting that FER may enhance IGF-1R activity (O'Flanagan et al., 2016). Therefore our first objective was to identify the mechanism through which FER could modulate IGF-1R kinase activity.

FER kinase was transiently co-expressed with a catalytically active IGF-1R (WT) or inactive (K1003R, KR) IGF-1R in HEK293T cells. The level of autophosphorylation on Tyr^{950}, Tyr^{1131} and $Tyr^{1135/1136}$ IGF-1R and phosphorylation on $Tyr^{1250/1251}$ in presence of FER was then assessed by western blotting of cell lysates. Increased levels of phosphorylation on Tyr^{950}, Tyr^{1131} and $Tyr^{1250/1251}$ but not on $Tyr^{1135/1136}$ sites were observed in cells transfected with either the IGF-1R WT or KR, when FER was present compared to vector- transfected control (EV) (Figure 3.2A). This observation with KR IGF-1R indicates that IGF-1R kinase activity is not required for FER-mediated phosphorylation of Tyr^{950}, Tyr^{1131} or $Tyr^{1250/1251}$. However, FER-enhanced phosphorylation of $Tyr^{1135/1136}$ IGF-1R was only observed with IGF 1R WT indicating that phosphorylation of this tyrosine requires IGF-1R kinase activity (Figure 3.2A).

Due to the endogenous levels of IGF-1R expressed by HEK293T cells which possibly contributes to the phosphorylation of IGF-1R KR, we further tested FER actions by co-expressing it with the IGF-1R WT or KR in R^- cells, which do not express the IGF-1R (Sell et al., 1994). Again, in R^- cells the co-expression of FER and IGF-1R WT or KR resulted in enhanced IGF-1R phosphorylation on Tyr^{950}, Tyr^{1131} and $Tyr^{1250/1251}$. Co-expression of FER did

not enhance phosphorylation of $Tyr^{1135/1136}$ in cells expressing the kinase-inactive IGF-1R KR (Figure 3.2B). Thus, FER activates the IGF-1R independent of its kinase activity in both HEK293T and R^- cell.

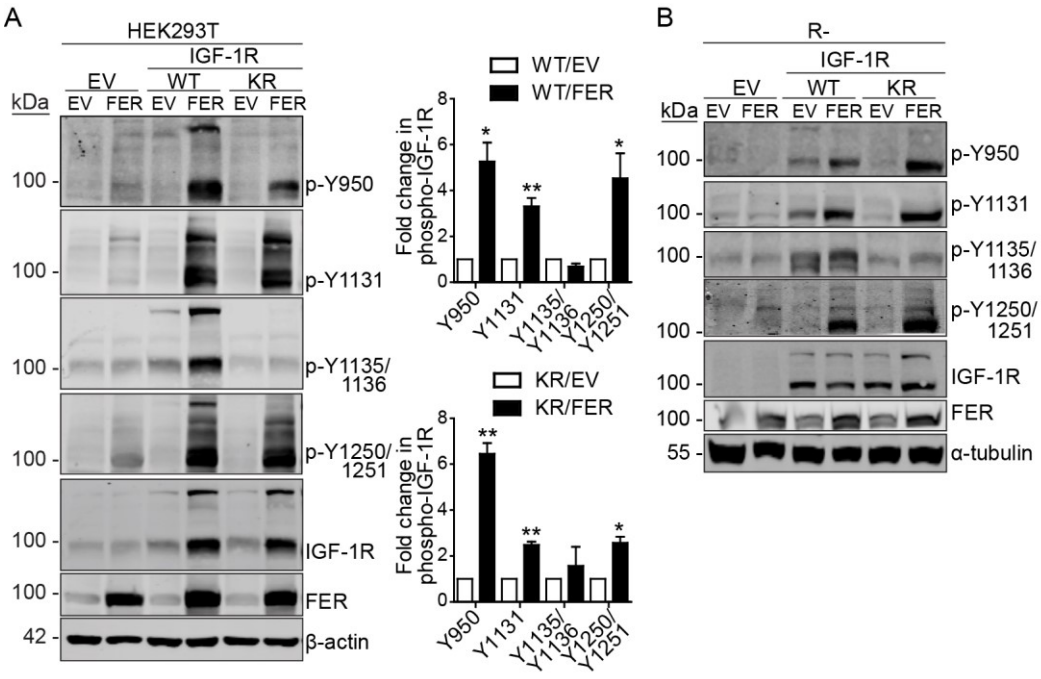


Figure 3.2: FER kinase enhances IGF-1R phosphorylation.

(A) Immunoblotting for, and quantification of the indicated phosphotyrosines (p-Y) and total IGF-1R in whole cell lysates (WCL) of HEK293T cells over-expressing: EV or FER with EV, IGF-1R WT or KR. Quantification of phospho/total IGF-1R is expressed as average fold-change ± SEM relative to the control condition (set to 1; white bar). Blots are representative of n≥3 independent experiments. Significance was calculated using a two-sided one-sample *t*-test. *P*-values are indicated by *<0.05, **<0.01, ***<0.001. **(B)** Immunoblotting for phosphotyrosines (p-Y) and total IGF-1R from WCL of R^- cells overexpressing: EV or FER with EV, IGF-1R WT or KR.

Due to FER-enhanced phosphorylation, independent of the IGF-1R kinase, we next investigated whether this is induced in response to IGF-1 and whether overexpression of FER also leads to enhanced signalling from ligand-activated endogenous IGF-1R. Moreover, we investigated whether the effect is dependent on the kinase activity of FER. First, we overexpressed both the FER WT and a FER mutant, where the aspartate on position 743 in the activation loop was mutated to an arginine (D743R; FER DR) in HEK293T cells. This mutation was previously shown to abolish FER kinase activity (Cole et al., 1999). We observed, that FER WT but not the kinase inactive DR mutant can increase FAK activation (Tyr^{397}), SHC phosphorylation on $Tyr^{239/240}$ and ERK1/2 phosphorylation (Thr^{202}/Try^{204}) (Figure 3.3). The phosphorylation on AKT (Ser^{473}) was not enhanced, indicating that FER dominantly activates the SHC/MAPK pathway (Figure 3.3).

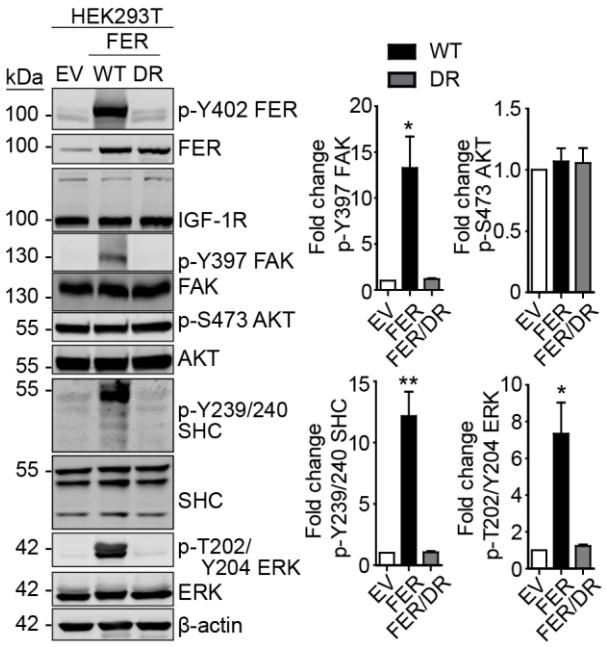


Figure 3.3: FER induced signalling in a kinase-dependent manner.

Immunoblotting for phosphorylation of FER on Tyr^{402} and total FER, IGF-1R, FAK phosphorylated on Tyr^{397} (p-Y397) and FAK, AKT phosphorylated on Ser^{473} (p-S473) and total AKT, SHC phosphorylated on Tyr$^{239/240}$ (p-Y239/240) and total SHC, ERK1/2 phosphorylated on Thr^{202} and Tyr^{204} (p-T202/Y204) and total ERK1/2 in WCL from HEK293T cells overexpressing: EV, FER WT (black bar) or FER DR (grey bar). Densitometry quantification is presented as the average fold-change ± SEM in ratio of phospho/total protein relative to the control condition (white bar). Blots are representative of n≥3 independent experiments. Significance was calculated using a two-sided one-sample or two-sample *t*-test. *P*-values are indicated by *<0.05, **<0.01, ***<0.001.

To investigate whether FER also increased IGF-1-induced signalling, we overexpressed EV, FER or FER DR mutant in HEK293T cells. The phosphorylation on Tyr^{950}, Tyr^{1131}, $Tyr^{1135/1136}$ and $Tyr^{1250/1251}$ on IGF-1R was significantly increased in response to IGF-1 (Figure 3.4A). The addition of FER WT did not enhance basal or IGF-1-induced phosphorylation on Tyr^{950} and $Tyr^{1135/1136}$ of endogenous IGF-1R. However, the basal phosphorylation on Tyr^{1131} and $Tyr^{1250/1251}$ was increased in presence of FER. In response to IGF-1, the ectopic overexpression of FER WT led to a significant increase in phosphorylation on $Tyr^{1250/1251}$ (Figure 3.4A). Phosphorylation on FAK (Tyr^{397} and Tyr^{925}) was also enhanced by FER WT overexpression in basal conditions as well as in response to IGF-1, but not by FER DR. Basal phosphorylation on $Tyr^{239/240}$ SHC in HEK293T cells was low and was not increased by stimulating the endogenous IGF-1R with IGF-1. However, the overexpression of FER WT but not the inactive FER DR significantly enhanced the basal phosphorylation on SHC and in response to IGF-1 (Figure 3.4A). Following SHC activation, ERK1/2 phosphorylation on Thr^{202}/Tyr^{204} was increased in both basal conditions and in response to IGF-1 by ectopic overexpression of FER WT. Similar to the phosphorylation on $Tyr^{1135/1136}$, IGF-1R signalling output of AKT (phosphorylation on Ser^{473}) was not enhanced by the overexpression of FER WT. Moreover, it was observed that IGF-1 stimulation of the cells increased the autophosphorylation on Tyr^{402} FER, which was not noticed with the FER DR mutant, indicating that IGF-1 can mediate FER activation.

We further found that FER overexpression also causes increased basal levels of $Tyr^{1250/1251}$ phosphorylation in R^- cells (Figure 3.4B).

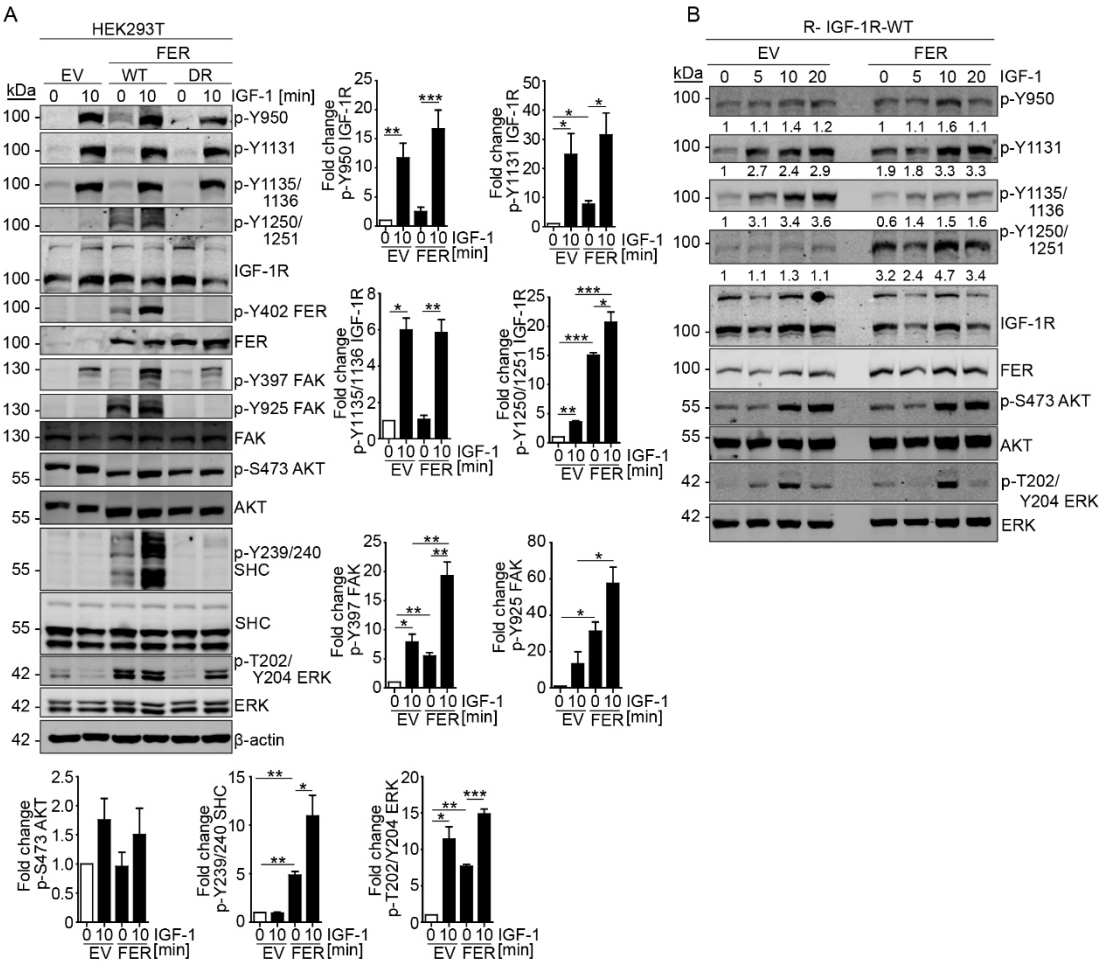


Figure 3.4: FER kinase enhances IGF-1R signalling.

(A) Immunoblotting for the indicated tyrosine-phosphorylated forms of IGF-1R (p-Y), total IGF-1R, FAK phosphorylated on Tyr^{397} (p-Y397) and Tyr^{925} (p-Y925), total FAK, AKT phosphorylated on Ser^{473} (p-S473) and total AKT, SHC phosphorylated on Tyr$^{239/240}$ (p-Y239/240) and total SHC and ERK1/2 phosphorylated on Thr^{202} and Tyr^{204} (p-T202/Y204) and total ERK1/2 in WCL from HEK293T cells overexpressing: EV, FER WT or FER DR, serum starved and stimulate with 10 ng/ml IGF-1 for the indicated times. Densitometry quantification is presented for EV and FER WT as the average fold-change ± SEM in ratio of phospho/total protein relative to the control condition (white bar). Blots are representative of n≥3 independent experiments. Significance was calculated using a two-sided one-sample or two-sample *t*-test. *P*-values are indicated by *<0.05, **<0.01, ***<0.001. **(B)** Immunoblotting for indicated phosphotyrosines (p-Y), total IGF-1R, AKT phosphorylated on Ser^{473} (p-S473), ERK1/2 phosphorylated on Thr^{202} and Tyr^{204} (p T202/Y204), and total AKT and ERK1/2 in WCL from R^{-} cells overexpressing: EV or FER with EV or IGF-1R WT, serum starved and stimulate with 10 ng/ml IGF-1 for the indicated times.

Overall we, conclude that FER enhances the phosphorylation on specific autophosphorylation sites of catalytically active and inactive IGF-1R. FER specifically enhances phosphorylation of IGF-1R on $Tyr^{1250/1251}$, SHC and MAPK in both basal and IGF-1-stimulation conditions in a FER kinase dependent manner.

3.3.2 FER is an IGF-1- and adhesion-activated kinase

FER is ubiquitously expressed in the cytoplasm (Zirngibl et al., 2001). However, in response to growth factor receptor activation, such as c-MET, EGFR, PDGFR and FLT3 (Guo and Stark, 2011, Zheng et al., 2018, Lennartsson et al., 2013, Voisset et al., 2010), FER was shown to be recruited to the plasma membrane. Located on the plasma membrane FER is activated FER by the growth factor stimulation and in turn associates and activates adhesion-related proteins including the actin-binding protein cortactin (Kim and Wong, 1998, Kim and Wong, 1995). Therefore we further investigated whether IGF-1R kinase is required for FER activation by IGF-1, and whether adhesion signalling is required for FER and FER enhanced IGF-1R activation.

It was apparent that IGF-1 stimulation of HEK293T cells resulted in phosphorylation of FER at its autophosphorylation site Tyr^{402} (Figure 3.5) in the vector control (EV) cells which only expresse endogenous IGF-1R. Overexpression of IGF-1R WT further increased phosphorylation on Tyr^{402}, while overexpression of IGF-1R KR mutant did not increase Tyr^{402} phosphorylation over endogenous IGF-1R (Figure 3.5). This indicates that IGF-1-induced FER activation required a kinase active IGF-1R.

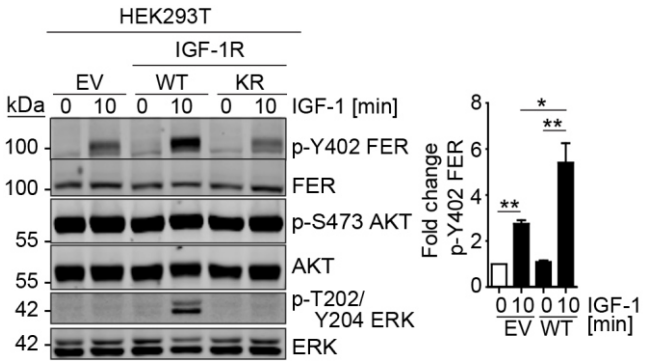


Figure 3.5: IGF-1-induced FER activation is IGF-1R kinase dependent.

Immunoblotting for p-Tyr^{402} and FER, AKT phosphorylated on Ser^{473} (p-S473), ERK1/2 phosphorylated on Thr^{202} and Tyr^{204} (p-T202/Y204), and total AKT and ERK1/2 in WCL from HEK293T cells overexpressing: EV, IGF-1R WT or IGF-1R KR, serum starved and stimulate with 10 ng/ml IGF-1 for the indicated times. Densitometry quantification is presented as the average fold-change ± SEM in ratio of phospho/total protein relative to the control condition (white bar). Blots are representative of n≥3 independent experiments. Significance was calculated using a two-sided one-sample or two-sample *t*-test. *P*-values are indicated by *<0.05, **<0.01, ***<0.001.

To investigate whether adhesion signalling is required for FER activation, we overexpressed EV, FER and FER DR mutant in HEK293T cells and examined FER activation in non-adherent compared with adherent cells. Cells detached from the substratum (suspension) displayed decreased phosphorylation of Tyr^{402} FER compared to attached cells (adhesion) (Figure 3.6A). We confirmed this result in R^- cells overexpressing IGF-1R WT as again, autophosphorylation of Tyr^{402} FER was decreased when cell adhesion was lost (Figure 3.6B).

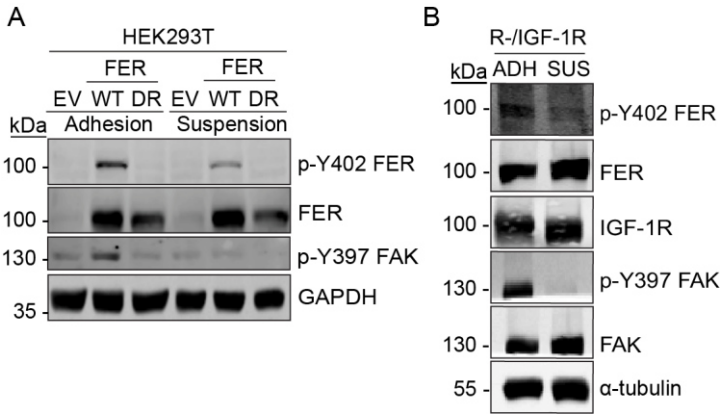


Figure 3.6: FER is an adhesion-activated kinase.

(A) Immunoblotting for FER phosphorylation on Tyr^{402} and total FER as well as FAK phosphorylated on Tyr^{397} in WCL of cell overexpressing EV, FER or FER DR. Cells for suspension were detached from the substratum 1 hr prior to lysis. **(B)** Immunoblotting for FER phosphorylation on Tyr^{402} and total FER, total IGF-1R, as well as FAK phosphorylated on Tyr^{397} and total FAK in WCL lysates of R^- cell overexpressing IGF-1R WT. ADH: Adherent, SUS: suspension cells were detached from the substratum 1 hr prior to lysis. n=1.

The data showed that IGF-1-induced IGF-1R activation can enhance FER activity and that FER is an adhesion- activated kinase. Therefore, we next investigated whether adhesion signalling is required for FER-mediated activation of the catalytically active and inactive IGF-1R and downstream signalling. IGF-1R WT or KR were overexpressed, together with EV, FER or FER DR mutant in HEK293T cells. As expected (Figure 3.2), in adherent cells, FER overexpression increased IGF-1R phosphorylation on Tyr^{1131} and $Tyr^{1250/1251}$ in both the kinase active and the kinase inactive IGF-1R, as well as both SHC and ERK1/2 phosphorylation (Figure 3.7), and phosphorylation on $Tyr^{1135/1136}$ was not enhanced by FER overexpression. This effect, was again dependent on FER kinase activity.

However, in the absence of adhesion signalling, FER-mediated phosphorylation of all of the IGF-1R tyrosine residues was reduced in cells expressing IGF-1R WT (quantification) or KR. SHC phosphorylation was also considerably less, however, decreased ERK1/2 phosphorylation was only observed with IGF-1R KR and the effect downstream from IGF-1R WT was minimal (Figure 3.7).

Overall, these data demonstrate that FER kinase is activated by IGF-1R and adhesion signals and that both the FER-enhanced phosphorylation of IGF-1R as well as IGF-1-induced SHC signalling are dependent on adhesion signalling.

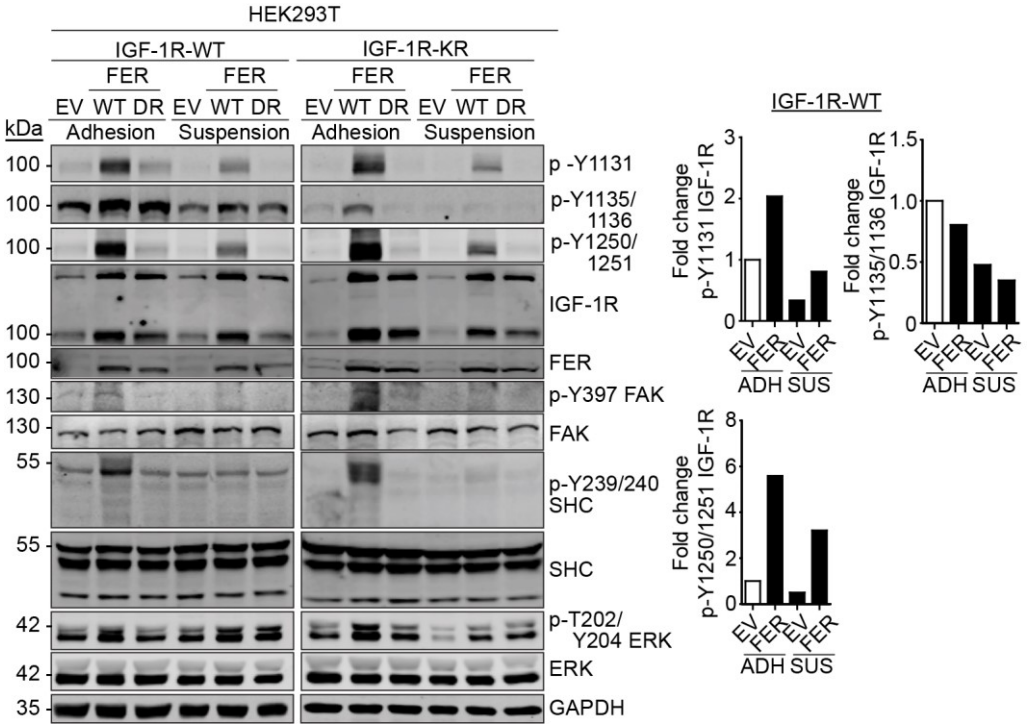


Figure 3.7: Adhesion signalling is required of FER-mediated IGF-1R activation.

Immunoblotting for the indicated tyrosine-phosphorylated forms of IGF-1R (p-Y), total IGF-1R and FER, FAK phosphorylated on Tyr^{397} (p-Y397), total FAK, SHC phosphorylated on $Tyr^{239/240}$ (p-Y239/240) and total SHC and ERK1/2 phosphorylated on Thr^{202} and Tyr^{204} (p-T202/Y204) and total ERK1/2 in WCL from HEK293T cells overexpressing: EV, FER WT or FER DR in either IGF-1R WT or IGF-1R KR conditions. Densitometry quantification for IGF-1R WT/EV or IGF-1R WT/FER in adhesion and suspension is presented as the average fold-change of phospho/total protein relative to the control condition (white bar). Blots are representative of n=2 independent experiments.

3.3.3 FER, IGF-1R and β1-Integrin localise in points of focal adhesion of cancer cells

Several studies indicate that FER promotes malignant progression and has been linked to various cancer types including lung, prostate and renal cancer (Zoubeidi et al., 2009, Wei et al., 2013, Ahn et al., 2013). FER is reported to promote cell cycle progression (Pasder et al., 2006) as well as migration and invasion in breast cancer through the regulation of α6- and β1-Integrin (Ivanova et al., 2013). Having established that FER significantly enhances IGF-1R activation (Figure 3.2) and its signalling (Figure 3.4) in an adhesion-dependent manner (Figure 3.7), we next investigated whether this is solely a signal transduction phenomenon, or if physical interactions are important using cancer cell lines expressing endogenous levels of IGF-1R and FER.

We first identified breast cancer cell lines with high FER expression levels which also express the IGF-1R (Figure 3.8A). The cell line panel includes representatives of epithelial-like and mesenchymal-like cell lines, and also MCF-10A as a normal epithelial breast cell line. We observed high FER expression in breast cancer cell lines which exhibit an migratory/aggressive phenotype, such as MDA-MB-231 and HS-578T cells, while ZR-751 and MCF-7 cells, which are low-migratory cell lines, show lower FER expression (Figure 3.8A). This was also observed in the analysis of RNA-Seq expression profiles of 78 breast cancer cell lines extracted from the study of Marcotte *et al.* (Marcotte et al., 2016), which demonstrated that breast cancer cell lines with high migratory capacity express FER at significantly higher levels than cell lines with low migratory capacity (Figure 3.8B).

We next analysed the low-migratory cell line MCF-7 cells and the highly invasive triple negative breast cancer cell lines MDA-MB-231 and HS-578T for their levels of β1-Integrin, in addition to FER and IGF-1R (Figure 3.8C). All three breast cancer cell lines expressed endogenous levels of IGF-1R, FER and β1-Integrin, with MDA-MB-231 cells expressing the highest and MCF-7 cells, the lowest levels of FER and β1-Integrin. It needs to be noted that MCF-7 cells express IGF-1R at higher levels compared to MDA-MB-231 and HS-578T cells which have rather low levels of IGF-1R (Figure 3.8A, C). To confirm that endogenous FER kinase activity is also adhesion dependent, HS-578T were detached from the substratum and phosphorylation of FER on Tyr^{402} was analysed (Figure 3.8D). Results showed that Tyr^{402} phosphorylation of endogenous FER is also reduced in non-adherent cells.

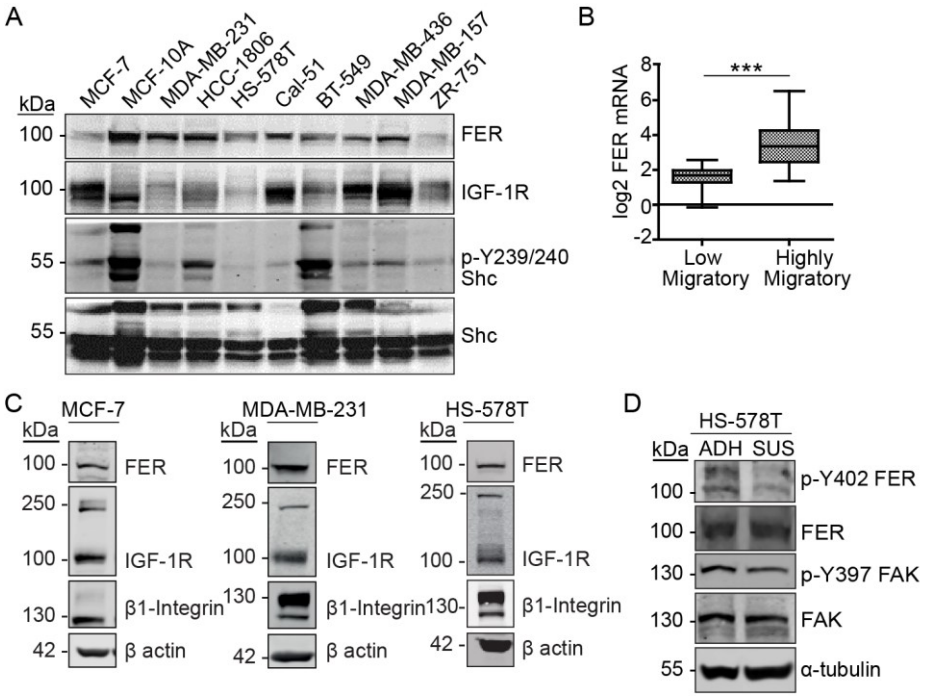


Figure 3.8: FER is highly expressed in migratory breast cancer cell lines.

(A) Immunoblotting for FER, IGF-1R, SHC phosphorylated on $Tyr^{239/240}$ and total SHC in WCL of different breast cancer cell lines. Equal amounts of protein (~60 μg) were loaded to compare the expression level. **(B)** RNA-Seq analysis of FER mRNA expression in low compared to highly migratory breast cancer cell lines (n = 78). FER mRNA expression is plotted on a log2 scale. Significance was calculated using a two-sided one-sample or *t*-test. *P*-values are indicated by *<0.05, **<0.01, ***<0.001. **(C)** Immunoblotting for FER, IGF-1R and β1-Integrin in WCL of MCF-7, MDA-MB-231 and HS-578T cells (~30 μg of protein). **(D)** Immunoblotting for FER phosphorylated on Tyr^{402} (p-Y402) as well as total FER, FAK phosphorylated on Tyr^{397} (p-Y397), total FAK in WCL of HS-578T cells. Suspension cells were detached from the substratum 1hr prior to lysis.

We next looked at the localisation of FER and IGF-1R in the cell lines using immunofluorescence co-staining and confocal microscopy. We found that both FER and IGF 1R were localised at focal adhesions in both the low-migratory MCF-7 breast cancer cells (Figure 3.9A) and the migratory cell lines MDA-MB-231 and HS-578T (Figure 3.9B).

To test the spatial localisation of FER, IGF-1R and β1-Integrin, cells were immunofluorescently stained for these proteins and analysed by microscopy (Figure 3.9C, D). The majority of IGF-1R in MCF-7 cells appeared to be located on the cell surface where it accumulated in large adhesion complexes, containing FER and β1-Integrin (Figure 3.9A, C). However, although the majority of IGF-1R in the two migratory TNBC cell lines exhibited a more intracellular staining pattern, IGF-1R was also clearly localised with FER in the lamellipodia (Figure 3.9B, D).

We conclude that cells exhibiting a high migratory phenotype express higher levels of FER, which is in agreement with previous studies (Ivanova et al., 2013). FER, IGF-1R and β1-Integrin all associate at points of focal cell adhesion, indicating FER-mediated enhanced IGF-1R signalling is likely the result of close physical proximity of these proteins. The localisation in close proximity possibly facilitates a direct phosphorylation of FER on IGF-1R or FER mediates another cellular kinase to phosphorylate IGF-1R.

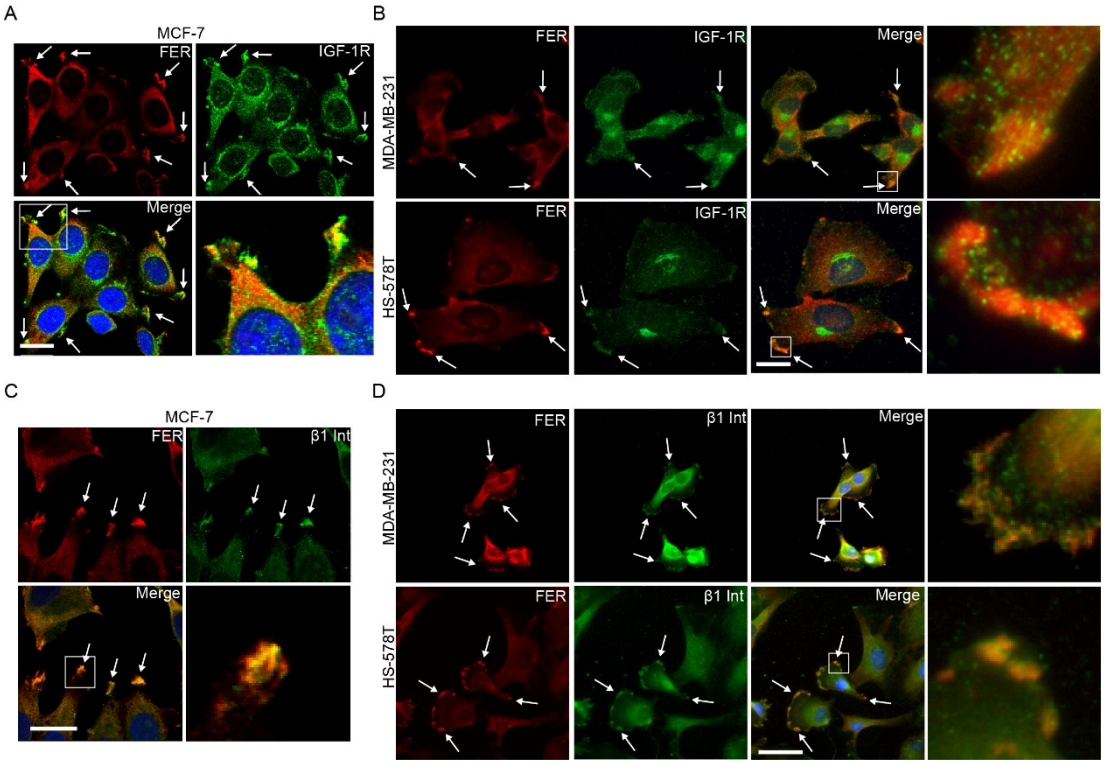


Figure 3.9: FER is located in points of focal adhesion where it co-localises with IGF-1R and β1-integrin.

(A) Immunofluorescence of MCF-7 stained for FER (red) and IGF-1R (green). Images were acquired using the Olympus Fluoview FV1000 confocal laser scanning microscope and are representatives of n>3 independent experiment with a 20 μm scale bar. **(B)** Immunofluorescence of MDA-MB-231 and HS-578T cells stained for FER (red) and IGF-1R (green). Images were acquired using a 100x oil objective and the Nikon DSFi1c camera attached to the Leica DM LB2 microscope and are representatives of n=2 independent experiment with a 20 μm scale bar. **(C)** Immunofluorescence of MCF-7 stained for FER (red) and β1-Integrin (green). Images were acquired using the Olympus Fluoview FV1000 confocal laser scanning microscope and are representative of n>3 independent experiments with a 20 μm scale bar. **(D)** Immunofluorescence of MDA-MB-231 and HS-578T cells stained for FER (red) and β1-Integrin (green). Images were acquired using the Nikon T600 fluorescent microscope using a 40× objective and are representatives of n=1 experiment are shown with 50 μm scale bar.

3.3.4 FER kinase activity can be inhibited by an ALK-inhibitor

Our data shows that ectopic expression of FER leads to hyperactivation of IGF-1R and its cooperative signalling with adhesion pathways (Figure 3.2, Figure 3.4 Figure 3.7). This may have significant implications for cancer progression and therapy resistance and could be a possible explanation for the lack of efficacy in targeting IGF-1R in cancer treatment. FER expression was recently suggested to facilitate resistance to the anti-tumour agent quinacrine, through an EGF-dependent activation of nuclear factor κB (Guo and Stark, 2011). Moreover Ivanova *et al.* demonstrated by immunohistochemistry that FER expression is associated with aggressive breast cancer in patients (n=485) and inversely correlates with progression-free survival of ovarian cancer patients (Ivanova et al., 2013, Fan et al., 2016).

Therefore, we next sought to test pharmacological inhibition of FER in breast cancer cells, and determine whether FER inhibition may also reduce IGF-1R activity. As there is no specific FER kinase inhibitor available, we used an inhibitor for the anaplastic lymphoma kinase (ALK) inhibitor, AP26113 (Brigatinib). AP26113 was shown to potently inhibit FER in *in vitro* kinase assays, and FER was described as its next most selective target following ALK (Zhang et al., 2016). A similar ALK inhibitor (TAE684) has been reported to inhibit FES kinase that is structurally close to FER (Figure 3.10A) (Hellwig et al., 2012).

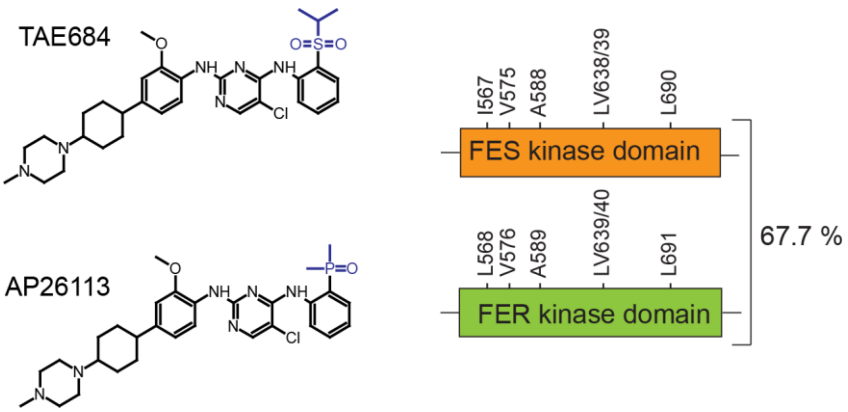


Figure 3.10: Structural similarities between TAE684 and AP26113 and c-FES and FER kinase domains.

The indicated residues (blue) were determined to be involved in FES interaction with TAE684 as reported by Hellwig *et al*. 2012. The kinase domains for FES and FER share 67.7% homology.

To determine the potency of AP26113 on FER inhibition, we first conducted a dose response over a range of concentrations of AP26113 (0.05-0.5 μM) in HEK293T cells overexpressing FER (Figure 3.11). Concentrations as low as 0.05 μM, decreased FER autophosphorylation on Tyr^{402} and also reduced FER-mediated phosphorylation of Tyr^{1131} or $Tyr^{1250/1251}$ IGF-1R in FER overexpression. However, consistent with previous results the phosphorylation of $Tyr^{1135/1136}$ IGF-1R was not increased with FER overexpression (Figure 3.2, Figure 3.4) and therefore the chemical inhibition of FER did not decrease the phosphorylation on this site (Figure 3.11), indicating that IGF-1R kinase is not affected by the AP26113. Moreover, FER kinase inhibitor potently suppressed phosphorylation of SHC ($Tyr^{239/240}$) and ERK (Thr^{202}/Tyr^{204}). We conclude that AP26113 inhibits FER kinase and FER enhanced IGF-1R signalling.

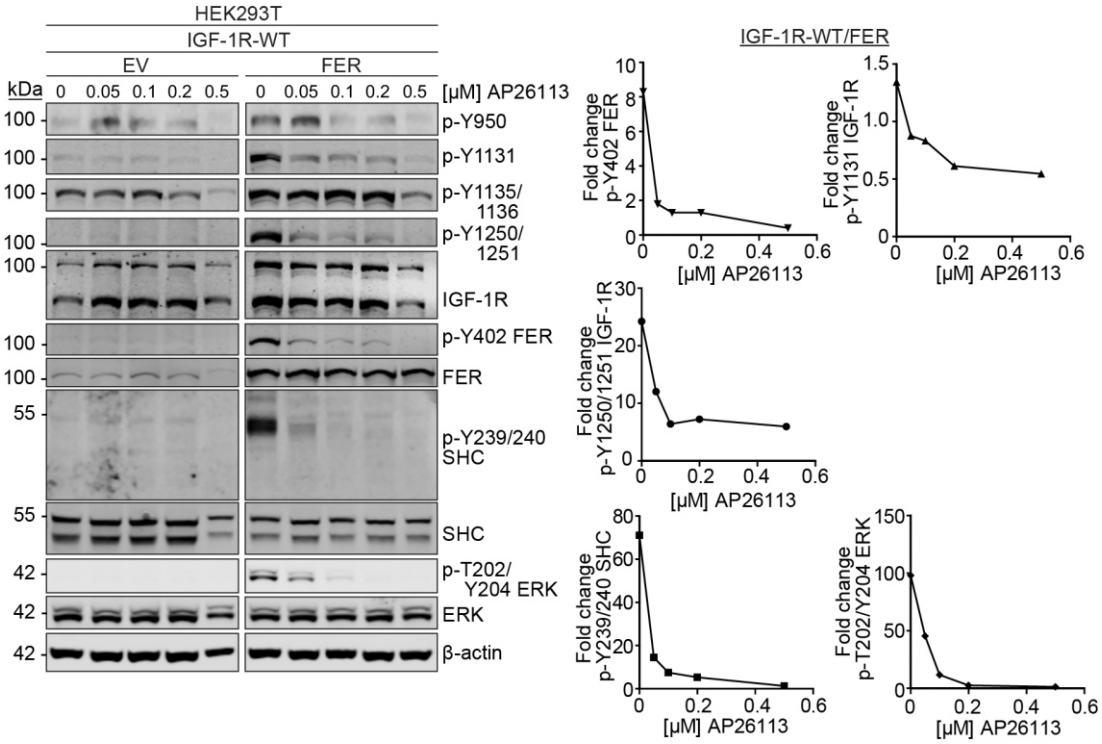


Figure 3.11: The ALK inhibitor, AP26113 inhibits FER activity and FER-mediated IGF-1R activation.

Immunoblotting for the indicated tyrosine-phosphorylated forms of IGF-1R (p-Y), total IGF-1R, FER phosphorylated on Tyr^{402} (p-Y402) as well as total FER, SHC phosphorylated on $Tyr^{239/240}$ (p-Tyr239/240) and total SHC, ERK1/2 phosphorylated on Thr^{202} and Tyr^{204} (p-Thr202/Tyr204) and total ERK1/2 in WCL of HEK293T cells overexpressing EV or FER together with IGF-1R WT. Cells were treated with 0-0.5 μM of AP26113 for 2 hr prior to lysis. Densitometry quantification for IGF-1R-WT/FER is presented as dose dependent fold change in ratio of phospho/total protein relative to the control condition IGF-1R/EV 0 μM from n=1 experiments.

We therefore next tested AP26113 on cells expressing endogenous levels of FER, to exclude the possibility that the overexpression of FER might increase the susceptibility of the cells to the drug. We used AP26113 in HS-578T cells that express FER at high levels (Figure 3.8A, C) (Marcotte et al., 2016) to inhibit FER kinase activity. Treatment of HS-578T cells with AP26113 (0.1-2 μM) resulted in inhibition of FER kinase autophosphorylation (Figure 3.12A), and decreased phosphorylation of SHC, Src and ERK1/2, without affecting AKT phosphorylation. Interestingly, total levels of FER and IGF-1R were also suppressed, following AP26113 treatment. In the case of FER, this may be due to destabilisation of inactive FER, which has been previously reported (Voisset et al., 2010).

We next wanted to test whether pharmacological inhibition of FER kinase changes the localisation of FER and IGF-1R in cell focal adhesion points (Figure 3.9) Therefore, we treated HS-578T cells with AP26113 and observed a retraction of FER and IGF-1R from the cell surface and from focal adhesion points (Figure 3.12B). This suggests that FER may be important in modulating the localisation and possibly the distribution of IGF-1R in points of focal adhesion along the lamellipodia, as it was suggested for α6- and β1-Integrins as well (Ivanova et al., 2013).

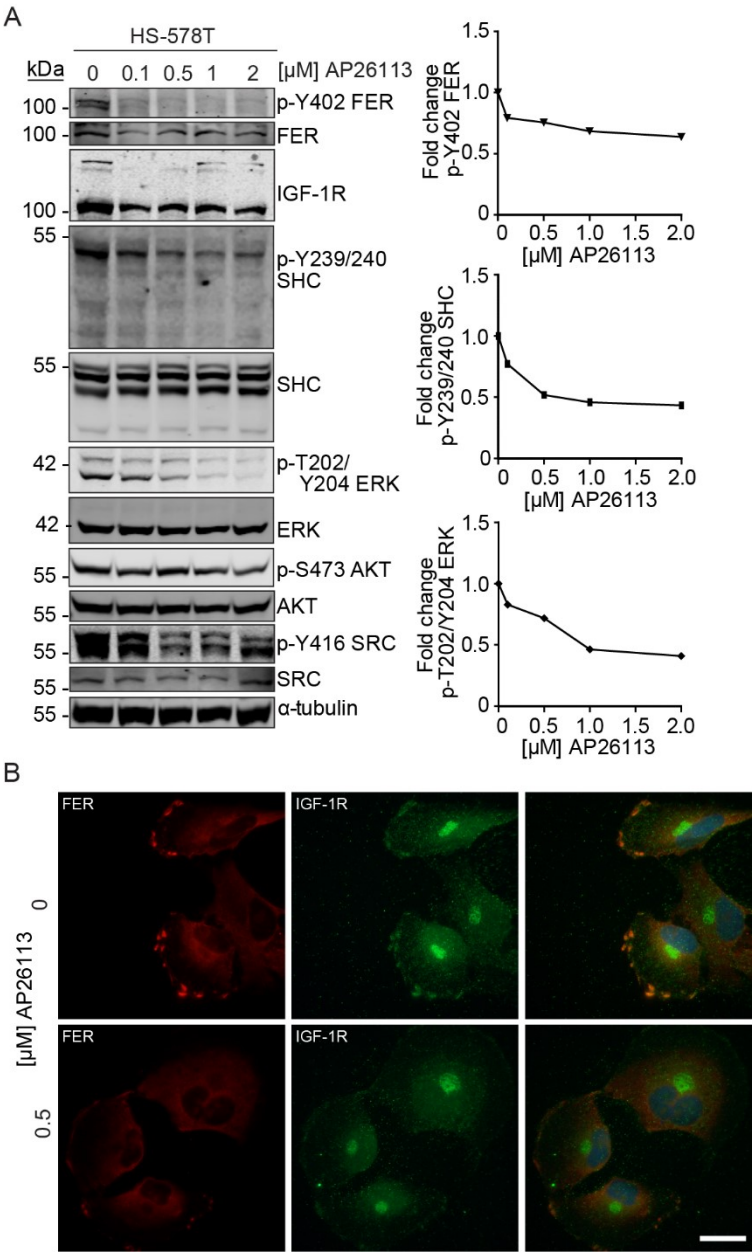


Figure 3.12: AP26113 inhibits endogenous FER.

(A) Immunoblotting for FER phosphorylated on Tyr^{402} (p-Y402) and total FER, total IGF-1R, SHC phosphorylated on $Tyr^{239/240}$ (p-Tyr239/240) and total SHC, ERK1/2 phosphorylated on Thr^{202} and Tyr^{204} (p-Thr202/Tyr204) and total ERK1/2, AKT phosphorylated on Ser^{473} (p-Ser473) and AKT, and Src phosphorylated on Tyr^{416} (p-Y416) and total Src in WCL from HS-578T cells treated with 0-2 μM of AP26113 for 2 hr. Densitometry quantification is presented as dose dependent fold change in ratio of phospho/total protein relative to the control condition (0 μM) from n=2 experiments **(B)** Immunofluorescence of HS-578T cells treated with 0 μM or 0.5 μM of AP26113 for 2 hr, stained for FER (red) and IGF-1R (green). Images were acquired using a 100x oil objective and the Nikon DSFi1c camera attached to the Leica DM LB2 microscope and are representatives of n=2 independent experiment with a 20 μm scale bar.

FER and IGF-1R were implicated in regulating migration of cells (Kiely et al., 2005, Itoh et al., 2009, Yoneyama et al., 2012, Ivanova et al., 2013), and the involvement of SHC in migration has also been well studied (Ahmed and Prigent, 2017). Here, we show that FER, SHC and MAPK pathway activation (phosphorylation on FER, ERK1/2 and SHC) was impaired in HS-578T after treatment with AP26113 (Figure 3.12A). Therefore, we next investigated whether FER inhibition could alter cell motility. As expected, treatment of HS-578T with AP26113, over the incubation time of 15 hr, caused reduced FER and IGF-1R levels and SHC phosphorylation (Figure 3.13A), and indeed, these cells exhibited reduced migration in a wound healing assay (Figure 3.13B).

Taken together, these data indicate that the pharmacological inhibition of FER kinase activity using the AP26113-ALK inhibitor, is sufficient to inhibit downstream signalling and disrupt FER and IGF-1R subcellular localisation and migratory capacity of cancer cells.

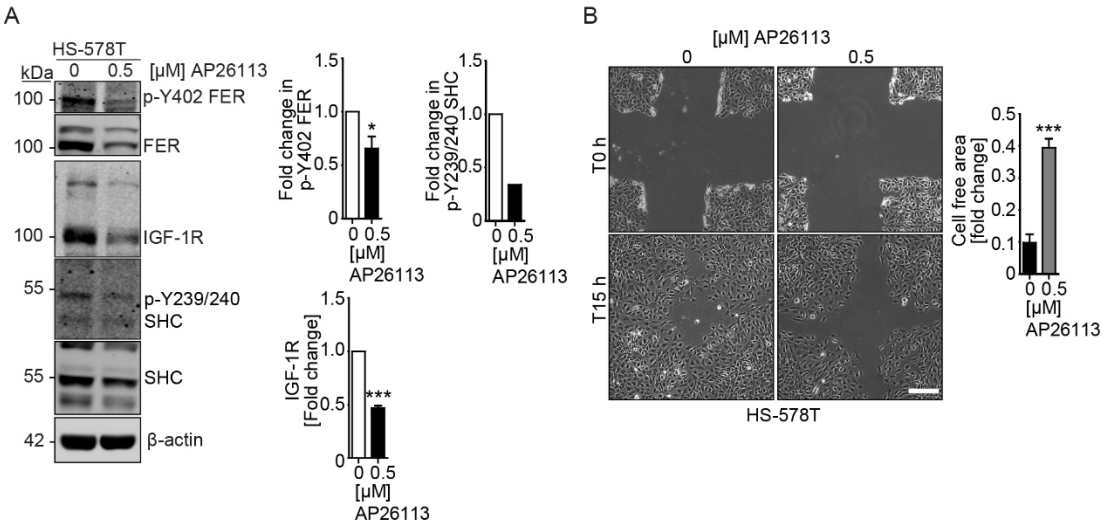


Figure 3.13: FER inhibition caused reduced migration of HS-578T.

(A) Immunoblotting for FER phosphorylated on Tyr^{402} (p-Y402) total FER and total IGF-1R, SHC phosphorylated on Tyr$^{239/240}$ (p-Tyr239/240) and total SHC in WCL of HS-578T cells untreated (0 μM) or treated with 0.5 μM AP26113 for 15 hr. Densitometry quantification is presented as the average fold-change ± SEM in ratio of phospho/total protein relative to the control condition (white bar). Blots are representative of n=3 independent experiments. Significance was calculated using a two-sided one-sample or *t*-test. **(B)** Phase contrast images of HS-578T cells in a wound healing assay cultured in control medium (0 μM) or with 0.5 μM AP26113, taken at 0 hr and 15 hr of migration at 10x magnification with Nikon Eclipse TE 300 microscope. Images are representatives of n=3 independent experiments with a scale bar of 250 μm. Image based assessment of the cell free area was determined using ImageJ and graphs present average fold change in the area relative to 1 at 0 hr of migration. *P*-values are indicated by *<0.05, **<0.01, ***<0.001.

3.4 DISCUSSION

The crosstalk of IGF-1R and adhesion signalling has previously been proposed to facilitate tumour development (Hermanto et al., 2002, Kiely et al., 2005, Cox et al., 2015). This work demonstrates that the non-receptor tyrosine kinase FER, as a component of focal adhesions, enhances IGF-1R activation and regulates adhesion-mediated signalling. FER enhanced phosphorylation of catalytically active and inactive IGF-1R in an adhesion-dependent manner. Our data also provides strong evidence that targeting FER pharmacologically may sensitize cancer cells to IGF-1R inhibitor treatments (Figure 3.14).

FER was previously shown to be activated by growth factors (Kim et al. 1995) and FER interaction with other growth factors such as EGFR, c-MET, PDGF and FLT3 (Guo and Stark, 2011, Fan et al., 2016, Voisset et al., 2010, Lennartsson et al., 2013, Zhang et al., 2018) has been reported to enhance their activity. The studies on EGFR and c-MET reported that FER overexpression led to their ligand-independent activation and induction of downstream signalling (Guo and Stark, 2011, Fan et al., 2016, Zhang et al., 2018). FER overexpression significantly increased phosphorylation on key sites of the IGF-1R in cells (Figure 3.2) and mediated ligand-independent phosphorylation on $Tyr^{1250/1251}$ IGF-1R, SHC ($Tyr^{239/240}$) and ERK1/2 (Thr^{202}/Tyr^{204}) (Figure 3.4), indicating that FER can modulate IGF-1R in conditions where either ligand binding or activation of the IGF-1R kinases is inhibited. This is an important observation, as targeting the IGF-1R with TKI (Table 1.1) as well as blocking the IGF-1 binding with mAb failed as anti-tumour agents (Introduction 1.5.5.2).

There are two different mechanisms of action through which FER could modulate the IGF-1R activation. As a cellular kinase recruited to the

membrane upon growth factor receptor activation and reported to activate the actin-binding protein cortactin (Kim and Wong, 1998, Kim and Wong, 1995), FER could facilitate IGF-1R phosphorylation through the activation of other adhesion-related kinase such as FAK and Src. Src has previously been shown to phosphorylate IGF-1R (Peterson et al., 1996). However, in his study the authors concluded that Src predominantly phosphorylates Tyr^{950}, Tyr^{1131} and $Tyr^{1135/1136}$ in IGF-1R which would not explain the significantly increased phosphorylation on $Tyr^{1250/1251}$ IGF-1R we observed. Another focal adhesion related kinase, which is clearly activated by FER, on both its tyrosine residues, is FAK (Figure 3.3, Figure 3.4). FAK has been demonstrated to promote IGF-1R function in cells and was linked to IGF-1R-mediated EMT, migration and invasion of cancer cells (Taliaferro-Smith et al., 2015). Indeed, FAK was shown to directly interact with IGF-1R in cancer cells (Andersson et al., 2009). Furthermore, down-regulation of FAK leads to the degradation of IGF-1R, and co-targeting FAK and IGF-1R increases the efficacy of anti-tumour agents (Watanabe et al., 2008, Liu et al., 2007). Although, FER and IGF-1R co-localise in points of focal adhesion (Figure 3.9), the fact that both FAK and Src are located there as well makes it not possible to state whether FER mediated IGF 1R activation is direct or indirect, through FAK or Src.

Association with IGF-1R can reciprocally activate FER kinase, as indicated by autophosphorylation on Tyr^{402} (Figure 3.5). A kinase impaired mutant of FER is incapable of mediating IGF-1R phosphorylation or IGF-1R signalling transduction (Figure 3.4). FER recruitment to points of focal adhesion was reported to enhance FER activation (Kim and Wong, 1998, Kim and Wong, 1995). Hence, FER-mediated phosphorylation of IGF-1R most likely occurs in these distinct points along the lamellipodia (Figure 3.9). It has

been shown that FER regulates cellular distribution of Integrins by downregulating surface expression of α6- and β1-Integrin (Ivanova et al., 2013). The interplay between Integrin heterodimers and growth factors can modulate the outcome for growth factor activation and signalling (Ivaska and Heino, 2011). Hence, modulations of surface expression of different Integrin subunits can alter the growth factor signal. Our data showing the association of FER, IGF-1R and β1 Integrin in points of focal adhesion suggests that their close subcellular proximity may enhance their reciprocal activation.

We noticed that FER profoundly enhanced $Tyr^{1250/1251}$ IGF-1R phosphorylation (Figure 3.2, Figure 3.4). Despite the fact that $Tyr^{1250/1251}$ were shown to be essential for the IGF-1R function in cells (Kiely et al., 2005, O'Connor et al., 1997, Miura et al., 1995b), the role of phosphorylated $Tyr^{1250/1251}$ IGF-1R still remains to be identified. Mutational studies on the C-terminal tail of IGF-1R suggested that flanking Ser^{1248} has an important function in conformational reorganization of the C-terminal (Kelly et al., 2012), and that $Tyr^{1250/1251}$ may be involved in regulating or enhancing the IGF-1R kinase activity (Kiely et al., 2005, O'Connor et al., 1997). In addition, $Tyr^{1250/1251}$ was shown to be required for the full activation of SHC and ERK1/2 in response to IGF-1 (Leahy et al., 2004, Kiely et al., 2005). Both pathways were also demonstrated to require IGF 1R endocytosis (Chow et al., 1998, Girnita et al., 2007, Sehat et al., 2007) and their activity has been linked to cell migration (Montagut and Settleman, 2009, Ahmed and Prigent, 2017). FER was reported to be involved in the dissociation of adherens junctions and focal adhesions and thereby promoting cell migration (Ivanova et al., 2013). This indicates that FER possibly enhances IGF-1R activation at points of focal adhesions to promote their turnover and thereby mediating SHC and ERK1/2

phosphorylation through IGF-1R endocytosis. However, whether $Tyr^{1250/1251}$ IGF-1R phosphorylation contributes to IGF-1R endocytosis and whether this contributes to the IGF-1R function remains to be investigated.

FER is commonly expressed in various tissues and cells (Greer, 2002) and was reported to be expressed at higher levels in malignant cells compared to corresponding normal cells (Guo and Stark, 2011). Additionally a recent study (Ivanova et al., 2013) demonstrated that FER expression correlates with aggressive breast cancer in patients (n=485). Considering, that FER is described, here and elsewhere, as a modulator for growth factor signalling facilitating an aggressive cancer phenotype, targeting FER may have a great potential for a new therapeutic strategy and may increase the efficiency of IGF-1R inhibitors. Although a FER-specific inhibitor had not yet been identified, a recent screen for inhibitors targeting other FES related family kinases, proposed putative candidates (Hellwig et al., 2012). Here, we introduce AP26116, as a novel FER inhibitor that inhibits the catalytic activity of FER kinase and signalling at nanomolar concentration. The inhibition of FER altered the expression of IGF-1R on the membrane (Figure 3.12B). However, this might be due to the alteration of focal adhesion complex formation containing FER/IGF-1R/β1 Integrin, as described previously (Ivaska and Heino, 2011, Ivanova et al., 2013). As an anaplastic lymphoma kinase (ALK) inhibitor, it is currently in phase 2 clinical trials for treating non-small cell lung cancer (Brigatinib; ID: NCT02706626). Hellwig *et al.* reported that TAE684, another ALK-inhibitor with high similarity to AP26113 (Figure 3.10) targets FES, which has a kinase domain highly homologous to FER (Figure 3.10). The interacting residues between TAE684 and FES kinase are conserved in FER kinase (Figure 3.10) (Hellwig et al., 2012).

In summary, this work presents a reciprocal positive regulation between the adhesion-associated kinase FER and IGF-1R. In this context, FER acts as a key signalling mediator of a crosstalk between adhesion and IGF-1R signals. High FER expression could lead to hyperactivation of both adhesion and IGF-1R complexes that, in turn, promote migration, invasion and potential chemoresistance, facilitating a more aggressive cancer phenotype. In conclusion, we propose that FER may be a potential biomarker of adhesion-enhanced IGF-1R activity. In addition, the FER kinase inhibitor presented in this work may target tumour cells addicted to IGF-1R/adhesion signalling cross-talk, which are often cells with a more aggressive tumour phenotype.

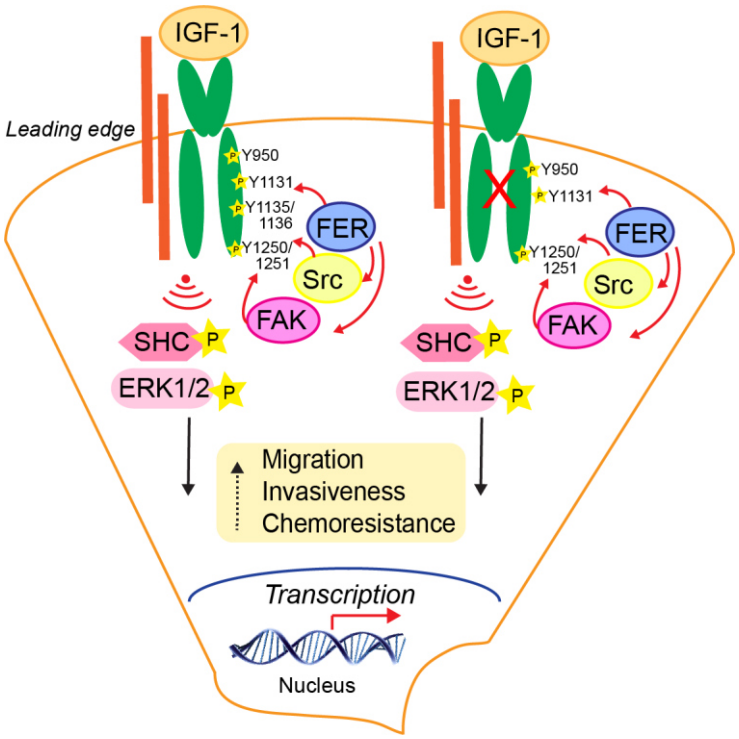


Figure 3.14: Proposed model of how FER enhances phosphorylation on catalytically active and inactive IGF-1R.

As a component of focal adhesion points, FER co-localises with IGF-1R and β1-Integrin. This interaction of FER and IGF-1R leads to hyperactivation of IGF-1R independently of the IGF-1R kinase. Additionally IGF-1 mediated signalling transduction from both the catalytically active and inactive IGF-1R is increased, in the presence of FER. The IGF-1R kinase independent hyperactivation and induction of signalling by FER causes increased IGF-1R signalling in cancer cells, leading to increased migration, invasiveness and chemoresistance.

4 CHAPTER 4: SELECTION AND CHARACTERIZATION OF MCF-7 CELL CLONES WITH CRISPR-MEDIATED KNOCK-IN OF TYROSINE AND SERINE MUTATIONS IN THE *IGF-1R* AND CRISPR-MEDIATED *IGF-1R* KNOCK-OUT IN THREE CANCER CELL LINES

Dr. Fujii and Prof. Shin-Ichiro Takahashi designed the targeting sequence and generated the original (uncloned) MCF-7 CRISPR knock-in cells.

Grant Godsmark and Stephanie Ward contributed to cell culture and genomic PCR of MCF-7 cell clones.

4.1 ABSTRACT

Although much information on IGF-1R function has been gained from overexpressing receptor mutants in R^- cells and HEK293T cells, these cell models are limited, mainly due to a potential interplay between IGF-1R and other cellular proteins overexpressed in human cancer cells. Analysis of IGF-1R mutants in human cancer cell lines could provide new insights into its function in different cancer cell phenotypes.

Here CRIPSR/Cas9 technology was used to generate MCF-7 cells expressing endogenous levels of IGF-1R carrying point mutations in the -SFYYS- motif of the C-terminal tail. Following several rounds of sub-cloning and identification of clones uniquely expressing the mutated IGF-1R protein by PCR using specific primers, MCF-7 cells expressing the Y1250F/Y1251F mutation were further tested to determine whether this mutation altered IGF-1R signalling and clonogenic growth. These studies demonstrated no significant signalling or growth difference between MCF-7 IGF-1R-WT cells and IGF-1R-FF mutant expressing cells, indicating that this mutation did not alter the phenotype of these cells.

As an alternative approach CRISPR gene editing was used to delete different regions of the *igf-1r* gene in MCF-7, MDA-MB-231 and DU-145 cells, causing a knock-out of IGF-1R protein. Upon IGF-1 stimulation, the *igf-1r* knock-out cells were deficient in the induction of downstream pathways. We demonstrated that MCF-7 and DU-145 require IGF-1R to maintain their clonogenic growth potential, while MDA-MB-231 IGF-1R knock-out cells still formed colonies in soft agarose and displayed a more aggressive phenotype. It was concluded that these *igf-1r* knock-out cell lines are useful models for

subsequent expression of different IGF-1R mutants and to investigate IGF-1R specific pathways in these cells.

4.2 INTRODUCTION

Investigating IGF-1R function, and understanding its reciprocal cross-talk with cellular kinases in human cancer cells is challenging. The main reason is that studies using ectopically expressed IGF-1R mutants, which are needed to study receptor function and signalling, are confounded by the already high levels of IGF-1R present in most cancer cell lines.

The CRISPR/Cas9 system revolutionized the ability of scientists to edit DNA in living cells (Cong et al., 2013). It is now commonly used to edit genetic information and facilitate the study of gene functions and the effects of their encoded products on biological processes (Pickar-Oliver and Gersbach, 2019). In nature, CRISPR/Cas9 is part of the prokaryotic adaptive immunity mechanism and is used to cleave invading nucleic acids. A broad spectrum of Cas endonucleases can be found in bacteria and archaea. The system uses cellular DNA repair mechanisms- non-homologous end-joining (NHEJ) and homology-directed repair (HDR) pathways. The CRISPR/Cas9 system relies on a guide RNA, which directs the Cas nuclease to the specific region of interest. Another key element is the Protospacer Adjacent Motif (PAM), which is a) specific for each Cas nuclease, for example, for Cas9 the motif is -NGG- and is b) limiting factor to induce the double strand breaks into the genome (Pickar-Oliver and Gersbach, 2019).

While NHEJ is normally used to introduce gene knock-outs, HDR serves to introduce point mutations into the gene of interest. Using NHEJ the double strand break is repaired by small fragment insertions and deletions (indel), which leads to indel-mediated frameshifts and therefore the loss of gene expression (Pickar-Oliver and Gersbach, 2019). However, it was shown that the Cas9 nuclease has significant off target effects (Fu et al., 2013, Pickar-

Oliver and Gersbach, 2019). To reduce these off target effects a mutation in the Cas9 nuclease was introduced (Cas9n), which leads to the introduction of single strand nicks, instead of the double strand breaks. When paired together, the single nickases introduce a double strand break again within a short distance of each other. Since these Cas9n are also directed by guide RNAs (two sequences), the off target effects are reduced (Gopalappa et al., 2018). To insert specific point mutations into the target gene, the system relies on HDR which is typically used with a lower efficiency in nature. In this instance, the cells repair the double strand break based on the homologous sequence, a single stranded oligo donor (ssOND) containing the point mutation (Gopalappa et al., 2018).

R^- cells have been extensively and successfully used for expressing and studying IGF-1R mutants in cell survival, clonogenic growth, cell migration, as well as for detailed signalling studies (Miura et al., 1995b, Brodt et al., 2001, O'Connor et al., 1997, Kiely et al., 2005, Blakesley et al., 1998). HEK293T cells have also been used in some studies due to ease of transfection and protein overexpression, but as shown in (Chapter 3), these cells express transfected plasmids and their encoded proteins at high levels but also express endogenous IGF-1R, which can confound signalling studies and protein-location studies. These cells are also not derived from human cancers and lack several of the phenotypic features of specific cancers, such as breast or prostate.

Therefore, to better understand IGF-1R activity and its regulation by other kinases and adhesion proteins in cancer cells, and in order to develop better ways to target the IGF-1R, it would be desirable to express and study certain IGF-1R mutants in cancer cells where the endogenous wildtype

receptor has been knocked-out. Therefore, we aimed to use CRISPR technology to generate knock-in *igf-1r* mutations in cancer cells and also to generate *igf-1r* knock-out cancer cells, in which we could subsequently express different IGF-1R mutants.

Most of the mutation studies investigating the IGF-1R function were conducted in R^- cells. Two tyrosines $Tyr^{1250/1251}$ located in the C-terminal tail of the IGF-1R are essential for the receptor function in transformed cells. When R^- cells overexpress an IGF-1R where $Tyr^{1250/1251}$ are mutated to phenylalanine (FF), cells are refractory of cellular transformation, migration and invasion (Miura et al., 1995b, Brodt et al., 2001, Blakesley et al., 1996, Kiely et al., 2005). Moreover, IGF-1-mediated anti-apoptotic protection is abolished in R^- cells with an IGF-1R FF mutant (O'Connor et al., 1997). Recent results from our group have shown that $Tyr^{1250/1251}$ can be phosphorylated in cells (S. O'Shea PhD thesis, 2016) and that the adhesion associated kinase FER can enhance this phosphorylation (Chapter 3). However, the specific contribution of these tryosines to IGF-1R function in cancer cells is still unknown. Expression of the $Tyr^{1250/1251}$ FF mutant in cancer cells may reveal new insights about the receptor function.

$Tyr^{1250/1251}$ are flanked by two serines (Ser^{1248} and Ser^{1252}). Mutation of Ser^{1248} to alanine (S1248A) was previously reported to enhance IGF-1R kinase activity, autophosphorylation and PI3K/AKT pathway activity leading to enhanced cell growth (Kelly et al., 2012). Crystallographic analysis of IGF-1R protein structure demonstrated that when Ser^{1248} is phosphorylated, the C-terminal tail is wrapped around the IGF-1R kinase domain and therefore restrains its activity. However, once Ser^{1248} is dephosphorylated (as mimicked by the S1248A mutation), the IGF-1R C-terminal tail is released from its

autoinhibitory state and can be fully activated. Although IGF-1R activity is elevated in R^- cells expressing the S1248A mutant these cells exhibit impaired cell migration and also exhibit a faster and higher adhesion rate than control cells (Kelly et al., 2012).

The aim of this study was to select and characterize MCF-7 cells expressing IGF-1R knocked-in with mutations that have been previously linked to altered IGF-1R activity (O'Connor et al., 1997, Leahy et al., 2004, Kiely et al., 2005, Kelly et al., 2012): Ser^{1248} IGF-1R was mutated to alanine and $Tyr^{1250/1251}$ IGF-1R were mutated to phenylalanine. A second aim was to induce targeted deletions in the *igf-1r* gene to generate knock-out MCF-7, MDA-MB-231 and DU-145 cell lines.

4.3 RESULTS

4.3.1 CRISPR/Cas9 system introduced specific point-mutations in the SFYYS motif of *igf-1r*

In order to introduce specific point mutations in the -SFYYS- motif a series of guide RNAs (gRNAs) were designed (Figure 4.1A), that recruit Cas9 endonuclease to the nucleotide sequence encoding the –SFYYS- region in the *igf-1r*. To introduce the mutation in the -SFYYS- domain, the components of homology-directed repair (HDR) mechanism were supplied with single stranded oligonucleotide (ssOND) as template to repair the double strand break generated by Cas9 (two single nicks). These ssOND shown in Figure 4.1A, C (full length Table 2.2) were designed to substitute the serine 1248 (S) with an alanine (A) and tyrosines 1250/1251 (YY) with phenylalanines (FF) (Figure 4.1C). The design of targeting sequences (gRNAs) and the ssOND for the DNA repair was carried out in Professor Shin-Ichiro Takahashi's laboratory at the University of Tokyo. In addition the transfection of MCF-7 cells with plasmids encoding a) the gRNAs/Cas9/GFP and b) the ssONDs to introduce the mutations in the *igf-1r* DNA was conducted in his laboratory (Figure 4.1). The cloning vector U6p encoding the $Cas9^{D10A}$ system to introduce two single DNA strand break that together cause a double strand break, also encoded a GFP-tag (Figure 4.1A), which was initially used to sort and select the transfected population of MCF-7 cells by flow cytometry (Figure 4.1E).

The second cloning vector encoded for the ssOND (Figure 4.1A), hence introducing the point mutation (Figure 4.1D). The GFP-sorted MCF-7 pools were then frozen and subsequently transferred to UCC for expansion, sub-cloning and selection of clones expressing each of the knock-in mutants.

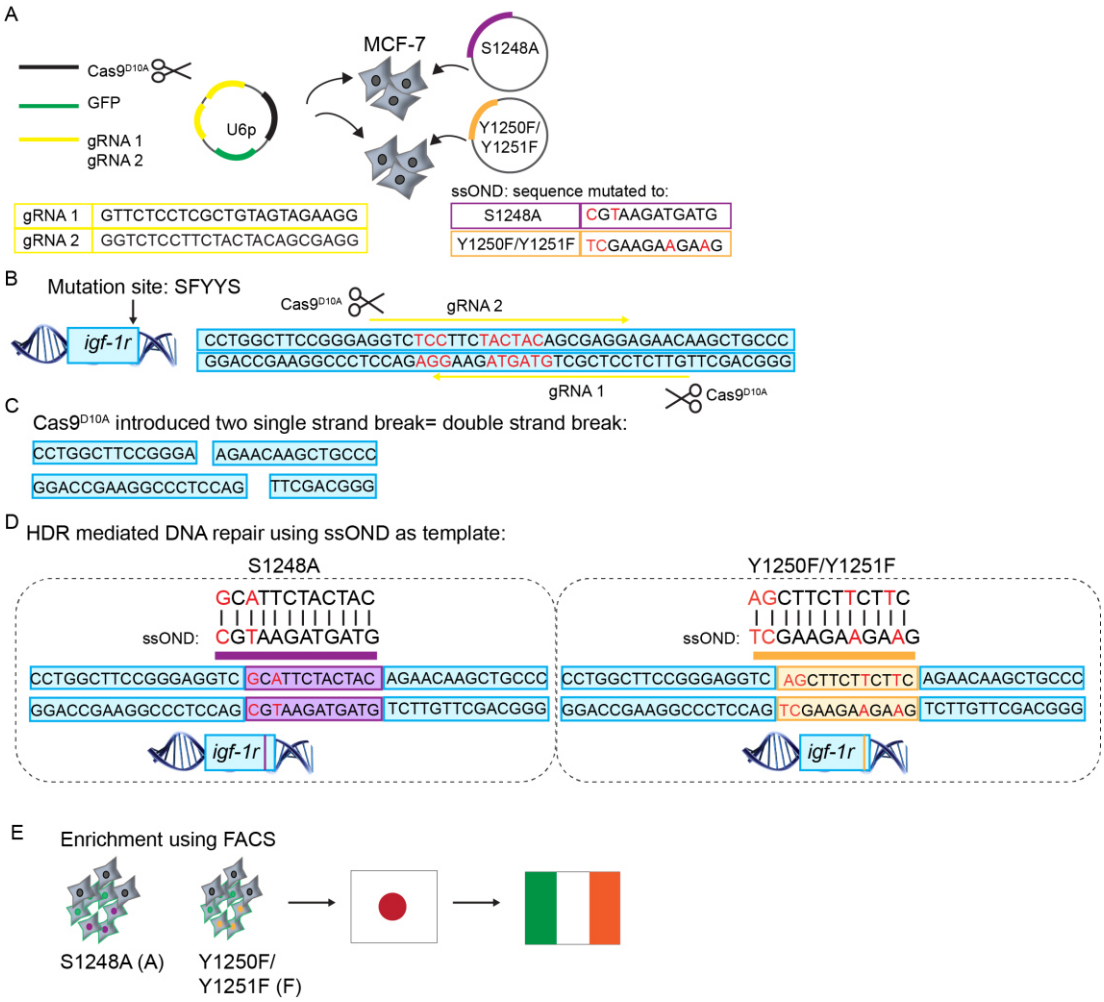


Figure 4.1: Overview of experimental plan for CRISPR-mediated knock-in *igf-1r* point mutations in MCF-7 cells.

(A) A combinations of plasmids encoding for a) the gRNAs, the Cas9 nuclease and the GFP and b) the ssOND, carrying the mutation S1248A and Y1250F/Y1251F were transfected into MCF-7 cells. **(B)** The guide RNAs (gRNA) directed the CAS9^{D10A} nuclease to the site of mutation, the SFYYS motif in the *igf-1r*. **(C)** The CAS9^{D10A} nuclease introduced a DNA double strand break. **(D)** The components of HDR DNA repair synthesised new DNA strands based on the ssONDs and thereby introduced the S1248A mutation and the Y1250F/Y1251F mutation into the *igf-1r* gene. **(E)** To enrich MCF-7 pools transfected with the plasmid combination, the cells were subjected to FACS analysis using the GFP tag on plasmid a). The MCF-7 pools were then send to Ireland.

4.3.2 Cell cloning and genomic DNA PCR-based selection of MCF-7 cells expressing IGF-1R knock-in mutations

To select MCF-7 cell clones that expressed only the edited *igf-1r* with the specific point mutation and not the wildtype *igf-1r*, primer sets were designed for PCR to exclusively bind to the target DNA sequence for each mutation (Figure 4.2A, Table 2.3Table 2.4). Primers for amplification of the wildtype (WT) *igf-1r* were also designed to monitor expression of the WT *igf-1r* in cells expressing the mutants and confirm its absence (Figure 4.3, Table 2.3). Although the GFP-expressing MCF-7 cell pools were already enriched for cells carrying the Cas9 plasmid, cell cloning was required to select those few cells that acquired the CRISPR-induced mutation (Figure 4.1). Cells were therefore cultured in 10 cm plates and group clones (cell colonies of approximately ~10 cells) were selected using ring cloning (Figure 4.2A). These cells were expanded in a 96 well plate, transferred to a 24 well plates, till they reached confluency. Approximately $0.5x10^5$ cells were used for genomic DNA extraction and PCR (Figure 4.2B) to identify clones, which showed a strong amplification of each of the mutated *igf-1r* sequence (Figure 4.2C, D). The rest of the cells ($1.5x10^5$) were collected as stocks (-80°C), ready to be expanded again after the PCR. More than half of the group of clones contained cells carrying the point mutations in the *igf-1r* (Figure 4.2C, D). Group clones S1248A #50, #51#, #52 and group clones Y1250F/Y1251F #7, #71, #72 were selected for further sub-cloning (Figure 4.3).

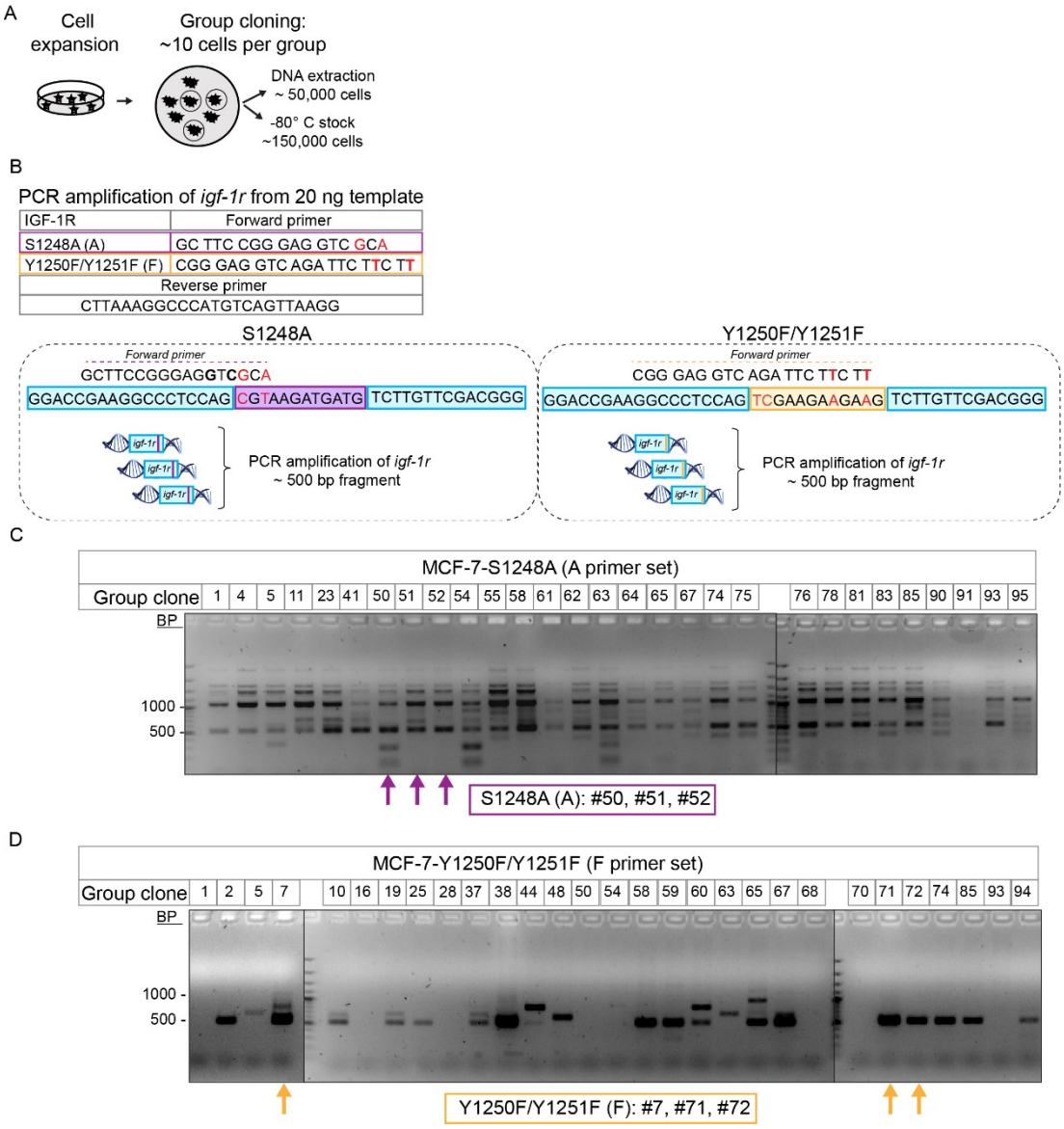
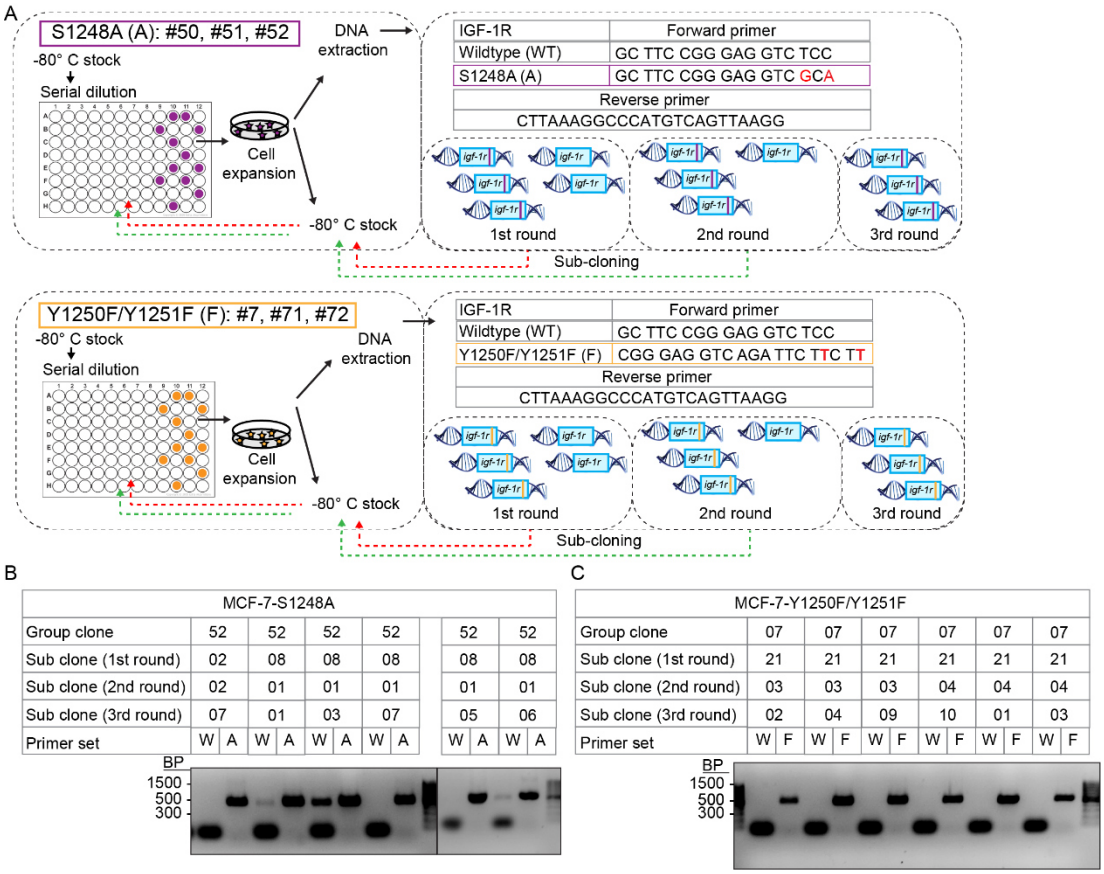


Figure 4.2: Isolation and identification of group-clones containing cells carrying the mutated region of the *igf-1r*.

(A) (B) Overview of experimental plan isolating and identifying group clones that contain cells with point mutations in the *igf-1r*. **(A)** MCF-7 clones from Japan were expanded and group clones were isolated using ring cloning. Genomic DNA of the group clones (~50,000 cells) was isolated and the rest of the cells (~ 150,000 cells) of each group clone was collected as stock. **(B)** The mutated region of the *igf-1r* was amplified using PCR, 20 ng of DNA template and designed primers that specifically bind to the mutated region. Expected DNA fragment at 500 BP. **(C)** Groups containing cells with the S1248A mutation were identified and several groups were picked (purple arrows) for further sub-cloning. **(C)** Groups containing cells with the Y1250F/Y1251F mutation were identified and several groups were picked (orange arrows) for further sub-cloning.

Group cell clones were recovered from -80°C stocks, expanded and further sub-cloned by serial dilution in 96 well plates. A second round of PCR analysis (Figure 4.3A), this time using both the WT primer set and the primer set amplifying the point mutation (Table 2.3), was performed. However, the PCR with the WT (W) primer revealed that these sub-clones still contained cells expressing *igf-1r-wt* (Figure S 4.1, Figure S 4.2.). Therefore the sub-cloning was repeated twice more (Figure 4.3A). The final round of sub-cloning followed by PCR analysis identified three MCF-7-knock-in clones (MCF-7-KI) (sub clones (3rd round)), that exclusively expressed the *igf-1r* with the S1248A mutation (band in lanes A), and where the *igf-1r wt* gene (band in lanes W) was not detected, (clones 52.02.02.07, 52.08.01.05, 52.08.01.07, Figure 4.3B). For the Y1250F/Y1251F mutation, six cell clones were identified after diluting the initial group clone (Figure 4.3C). Again, PCR analysis demonstrated that these cells express only the *igf-1r* FF mutant (band in lanes F) and no WT *igf-1r* (band in lanes W). Mutant-positive clones were expanded in culture and equal cell numbers of each clone were also subsequently pooled to minimise potential for selecting clones with unique phenotypes that may not reflect the original cell line. MCF-7-48A and MCF-7-FF cell pools were then used to further investigate the function of the SFYYS domain of the IGF-1R in MCF-7 cells.



MCF-7-S1248A											
Group clone	52	52	52	52	52	52					
Sub clone (1st round)	02	08	08	08	08	08					
Sub clone (2nd round)	02	01	01	01	01	01					
Sub clone (3rd round)	07	01	03	07	05	06					
Primer set	W	A	W	A	W	A	W	A	W	A	W	A

MCF-7-Y1250F/Y1251F												
Group clone	07	07	07	07	07	07						
Sub clone (1st round)	21	21	21	21	21	21						
Sub clone (2nd round)	03	03	03	04	04	04						
Sub clone (3rd round)	02	04	09	10	01	03						
Primer set	W	F	W	F	W	F	W	F	W	F	W	F

Figure 4.3: Isolation and identification of MCF-7 cell clones uniquely expressing the *igf-1r* mutants.

(A) Overview of experimental procedure to isolate and identify cell clones that consist of cells with point mutations in the *igf-1r*. MCF-7 group clones identified in Figure 4.2 were recovered from their -80°C stocks and separated in a 96-well plate using serial dilution. The cells were allowed to expand and ~50.000 cells were used for genomic DNA extraction, while the rest (~150.00 cells) was collected for stocks. The genomic DNA (20 ng) was used as templet for PCR with the designed primers (Band in A or F). A second PCR was performed to identify whether the sub-clones still contained cells with *igf-1r-wt* (band in W) (Figure S 4.1, Figure S 4.2). The sub-cloning procedure was repeated twice. **(B)** MCF-7-S1248A-clones and **(C)** MCF-7-1250F/Y1251F were isolated in three rounds of serial dilution and identified using PCR and the WT primer (W) or mutation specific primers (A or F). Expected DNA fragment at 500 BP. Cell clones uniquely expressing mutated *igf-1r* were expanded and combined.

4.3.3 MCF-7 cells expressing the IGF-1R FF knock-in mutation exhibit similar signalling responses to parental MCF-7 cells

R^- cells and MCF-7 cells overexpressing the Y1250F/Y1251F mutant IGF-1R were previously shown to exhibit impaired kinase activity, and to be deficient in integration of IGF-1 and adhesion signalling, anchorage-independent growth and cell migration (Miura et al., 1995b, O'Connor et al., 1997, Leahy et al., 2004, Kiely et al., 2005).

To test the function of the CRISPR-generated MCF-7 cell knock-in (MCF-7-KI) Y1250F/Y1251F mutant and WT control (CTL), we first investigated whether the mutation affects levels of IGF-1R protein expression. As shown in Figure 4.4A MCF-7-FF cells expressed the mutant IGF-1R at significantly lower levels than the wild type IGF-1R in MCF-7 parental cells (WT). Figure 4.4A also shows that the $Tyr^{1250/1251}$ phosphorylation was not detectable in MCF-7-FF cells using a commercially available antibody specific for this phospho-site. Although it was previously shown that the IGF-1R FF mutation impairs IGF-1R kinase activity in R- cells (O'Connor et al., 1997) and impairs downstream signalling in FL5.12 cells (Leahy et al., 2004), this was not seen in MCF 7-FF cells compared to the MCF-7-WT cells (Figure 4.4B). However, a general lower induction of autophosphorylation on Tyr^{950}, Tyr^{1131} and $Tyr^{1135/1136}$ was observed in MCF-7-FF cells, with significantly less IGF-1-induced phosphorylation Tyr^{950} IGF-1R in the MCF-7-FF cells compared to WT at 10 min. As expected, phosphorylation on $Tyr^{1250/1251}$ was abolished in MCF-7-FF cells (Figure 4.4B).

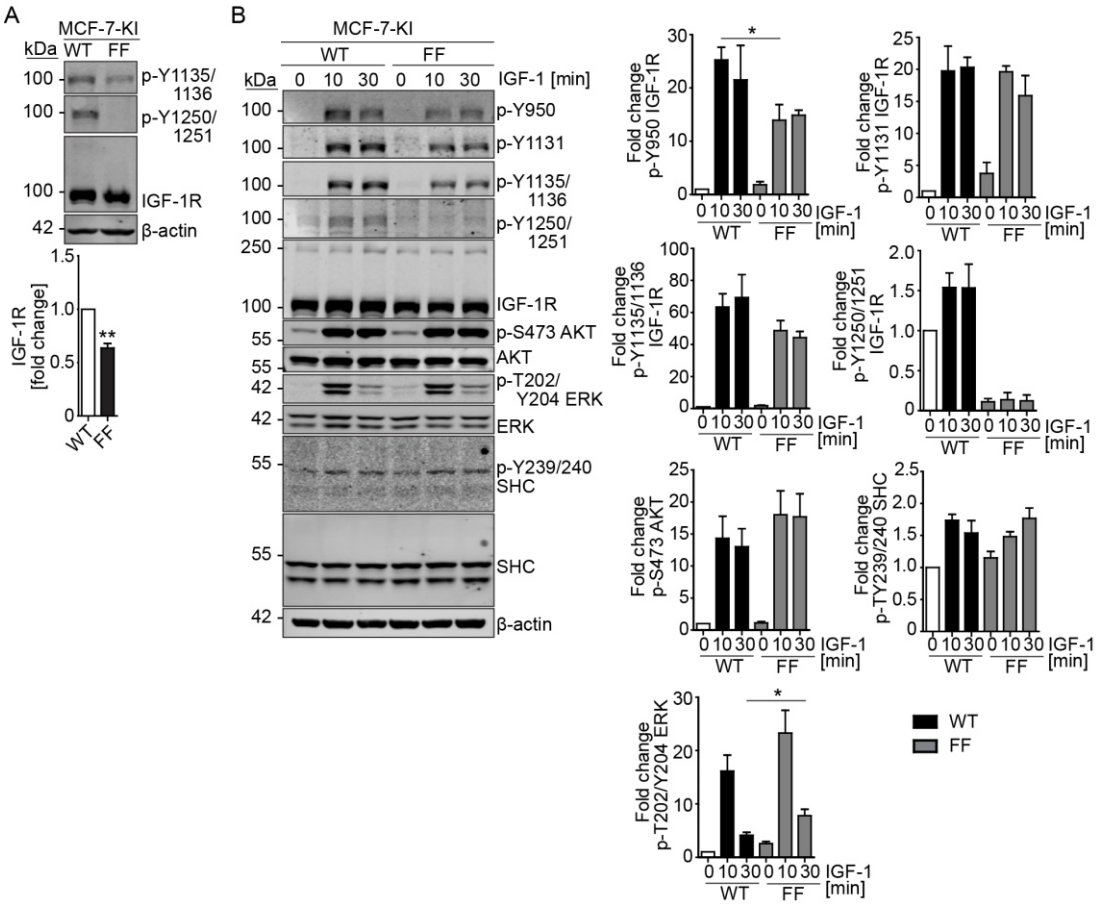


Figure 4.4: MCF-7 cells expressing the knock-in IGF-1R FF mutant display normal IGF-1-mediated signalling.

(A) Immunoblotting for IGF-1R phosphorylated on $Tyr^{1135/1136}$ (p-Y1135/1136) and $Tyr^{1250/1251}$ (p-Y1250/1251) in WCL from MCF-7-KI parental (WT) or FF cells. Densitometry quantification is presented as the average fold-change ± SEM of the ratio of total protein/β-actin relative to the control condition (white bar). Blots are representative of n≥3 independent experiments. Significance was calculated using a two-sided one sample *t*-test. **(B)** Immunoblotting for phosphotyrosines (p-Y) and total IGF-1R, AKT phosphorylated on Ser^{473} (p-S473) and total AKT, SHC phosphorylated on $Tyr^{239/240}$ and total SHC, ERK1/2 phosphorylated on Thr^{202} and Tyr^{204} (p-T202/Y204) and total ERK1/2 in total lysates from MCF-7-KI WT and FF cells serum-starved and stimulated with 50 ng/ml IGF-1 for the indicated times. Densitometry quantification is presented as the average fold-change ± SEM in ratio of phospho/total protein relative to the control condition (white bar). Blots are representative of n≥3 independent experiments. Significance was calculated using a two-sided one-sample or two-sample *t*-test. *P*-values are indicated by *<0.05, **<0.01, ***<0.001.

Previous studies also showed that R- cells expressing the IGF-1R FF mutation are impaired in anchorage-independent growth, which is an indicator of cellular transformation and/or tumourigenicity (Miura et al., 1995b). Furthermore, although lung cancer cell lines stably overexpressing the IGF-1R-FF mutant are impaired in colony formation in soft agar (Brodt et al., 2001), proliferation of cells in monolayer cultures is not affected by IGF-1R-FF mutation. We therefore tested both colony formation (plating efficiency) in monolayer cultures as well as anchorage-independent colony formation in soft agarose of MCF-7 cells with the IGF-1R-FF mutation. The results demonstrate that MCF-7-FF cells were not impaired in normal growth (Figure 4.5A) and were able to form colonies in soft agar (Figure 4.5B).

Thus mutation of $Tyr^{1250/1251}$ is not sufficient to impair either of these IGF-1R functions in MCF-7 cells.

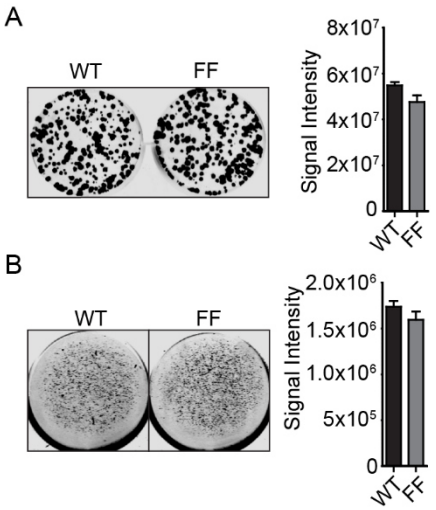


Figure 4.5: MCF-7 cells expressing knock-in Y1250F/Y1251F mutation do not display impaired cell growth.

(A) MCF-7 cell proliferation in monolayer cultures was determined by seeding cells at 1000 cells per plate and allowing colonies to form for 14 days. Densitometry measurements of crystal-violet-stained cells show the normalized mean± SEM fold-change of three replicate cultures. **(B)** Clonogenic growth in soft agar was used to determine anchorage-independent growth of cells. Densitometry measurements of crystal violet stained cells at 6 weeks is presented as normalized mean± SEM fold-change of 6 replicate cultures from n=2 independent experiments.

4.3.4 CRISPR/Cas9 mediated knock-out of IGF-1R protein leads to impaired IGF-1 signalling in three cancer cell lines

The CRISPR/Cas9 system was next used to generate *igf-1r* knock-out cancer cell lines. For this MCF-7, MDA-MB-231, and DU-145 cell lines were chosen. MCF-7 cells express IGF-1R abundantly, are highly responsive to IGF-1 and have been used to study IGF-1R signalling complexes. MCF-7 cells are also sensitive to IGF-1R suppression (O'Flanagan et al., 2016, Lyons et al., 2017), but are not migratory. MDA-MB-231 cells were chosen for their migratory capacity and the possibility to investigate IGF-1 signals in promoting cancer cell migration and invasion. DU-145 cells were also included as a prostate cancer cell line, which are also highly migratory (Bowe et al., 2014). DU-145 cells are highly responsive to IGF-1 and have also been used to study IGF1-R function in promoting prostate cancer progression (Aleksic et al., 2010, Aleksic et al., 2018).

Commercially available CRISPR plasmids that employ a double nickase system (Figure 4.6A) were used to introduce a deletion of a DNA fragment leading to a frame shift and therefore loss of IGF-1R protein expression. The double nickase system is a combination of two plasmids, both carrying the information for the Cas9 endonuclease. Each plasmid encoded a different guide RNA and contains a selection marker (Puromycin or GFP) (Figure 4.6A). Two different plasmid combinations were obtained, where the guide RNAs are targeting different regions in the *igf-1r* gene (Figure 4.6A). The guide RNAs of H0 target a region at the end of Exon 1 of the *igf-1r*, the guide RNAs of H1 target a region at the beginning of Exon 2 of the *igf-1r* (Figure 4.6B). MCF-7, MDA-MB-231 and DU-145 cells were transfected with a control vector that encodes for a non-targeting scrambled guide RNA, which does not recognize

any DNA sequence, the H0- or H1 plasmid combinations (control; CTL cells). Transfected cells, including the CTL cells, were split into two populations (Figure 4.6A), expanded under puromycin selection pressure for 4-6 weeks and screened for knock out of the IGF-1R by western blotting (Figure 4.6A).

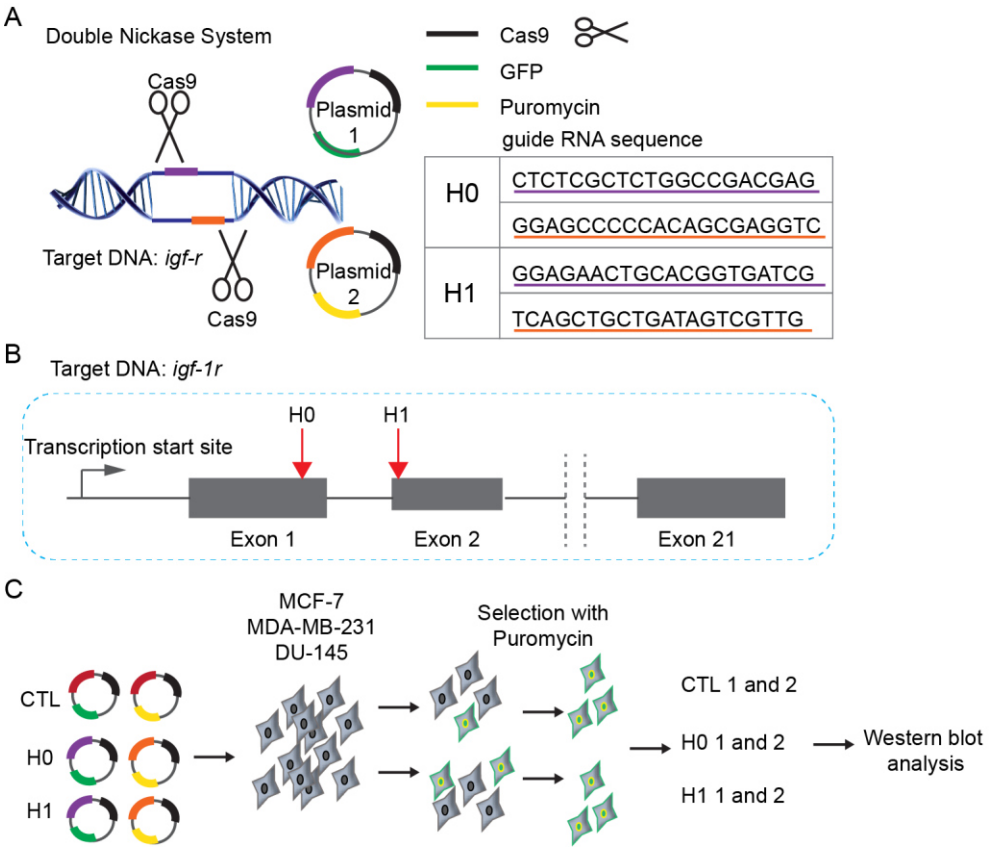


Figure 4.6: Overview of approach used to generate CRISPR-mediated *igf-1r* knock-out in three cancer cell lines.

(A) A double nickase system was used, which is based on two gRNA targeting sequences directing the Cas9 system to the *igf-1r* gene and inducing two fragment deletions. Two different sets of gRNAs were used H0 and H1. **(B)** H0 contains gRNAs targeting the end Exon 1 for the disruption of and H1 targeting the beginning of Exon of the *igf-1r* for the disruption. **(C)** MCF-7, MDA-MB-231 and DU-145 were transfected with a control plasmid (CTL), the H0 plasmids or the H1 plasmid. Cells were selected and analysed for IGF-1R protein expression.

As shown in Figure 4.7A MCF-7-H0 or H1 and DU-145- H0 or H1 cells retained expression of the IGF-1R protein, however at lower abundance than the IGF-1R in MCF 7 and DU-145 parental cells (CTL) (Figure 4.7A). In the H0 or H1 of the MDA MB 231 cells no IGF-1R protein was detectable (Figure 4.7A).

MCF-7, MDA-MB-231 and DU-145 H0, H1 and CTL cell lines were separated using serial dilution (Figure 4.7B) to isolate single cell clones, where the IGF-1R protein expression was completely abolished (Figure S 4.3). Reduction or suppression of the IGF-1R reduces cell growth and proliferation (Arteaga et al., 1989, Sell et al., 1994), therefore we tested the IGF-1R sub-clones for their capability to proliferate over two weeks (MCF-7, Figure S 4.3A MDA-MB-231 Figure S 4.3B, DU-145 Figure S 4.3C). Individual sub-clones of each group (CTL, H0 or H1) exhibited a similar proliferation rate with no major outliers (Figure S 4.3A). Due to implication of the adhesion machinery (Cox et al., 2015), images were taken of all sub-clones to visualise any changes in morphology (Figure S 4.4). No change in morphology was observed in H0 and H1 cells compared to CTL in the MCF-7 (Figure S 4.4A) and MDA-MB-231 (Figure S 4.4B) cells. Yet, DU-145 H0 cells displayed increased cell body size compared to the controls. In contrast, the DU-145 H1 cells were more elongated compared to the DU-145 CTL cells. The individual sub-clones within each group (CTL, H0 or H1), however, display no profound changes in morphology. We pooled the sub-clones (Figure S 4.4) of each cell line to reduce the potential selection for clones exhibiting an exceptional phenotype.

These combined IGF-1R knock-out cell clones were further analysed to identify IGF-1R functions in MCF-7, MDA-MB-231 and DU-145 cells.

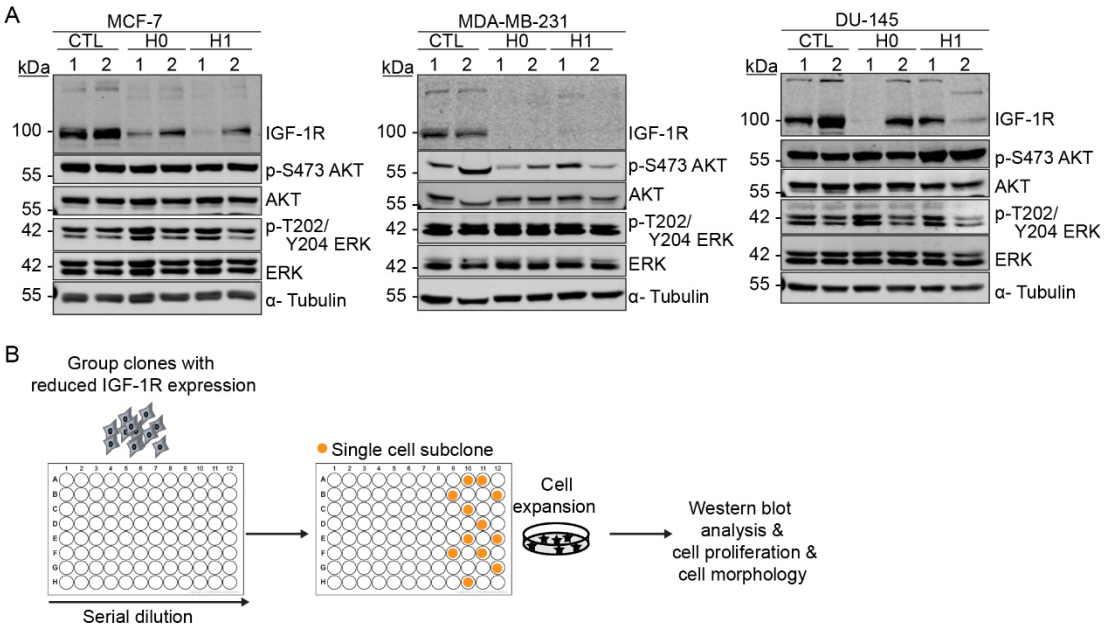


Figure 4.7: CRIPSR-mediated *igf-1r* deletion leads to reduced IGF-1R protein levels.

(A) Immunoblotting for total IGF-1R as well as AKT phosphorylated on Ser^{473} (p-S473), ERK1/2 phosphorylated on Thr^{202} and Tyr^{204} (p-T202/Y204), and total AKT and ERK1/2 from WCL of MCF-7, MDA-MB-231 and DU-145 cells transfected with CRISPR/Cas9 CTL, H0 or H1 plasmids. **(B)** Graphical explanation of cloning process to isolate single cell clones from MCF-7, MDA-MB-231 and DU-145 CRISPR/Cas9 CTL, H0 or H1 cell lines.

We next confirmed that the IGF-1R was knocked out in MCF-7 cells by using immunofluorescence. The IGF-1R can be observed in large focal cell adhesion points, as shown in Figure 4.8A and in Chapter 3 for MCF-7 CTL cells. MCF-7 H0 or H1, cells however showed no IGF-1R staining. Western blot analysis demonstrated that the expression of IGF-1R and the autophosphorylation on $Tyr^{1135/1136}$ IGF-1R was also abolished (Figure 4.8B). In addition, upon IGF-1 stimulation, AKT phosphorylation (Ser^{473}) and ERK1/2 phosphorylation ($Thr^{202/}Tyr^{204}$) were not induced in MCF-7 H0 or H1 cells (Figure 4.8B).

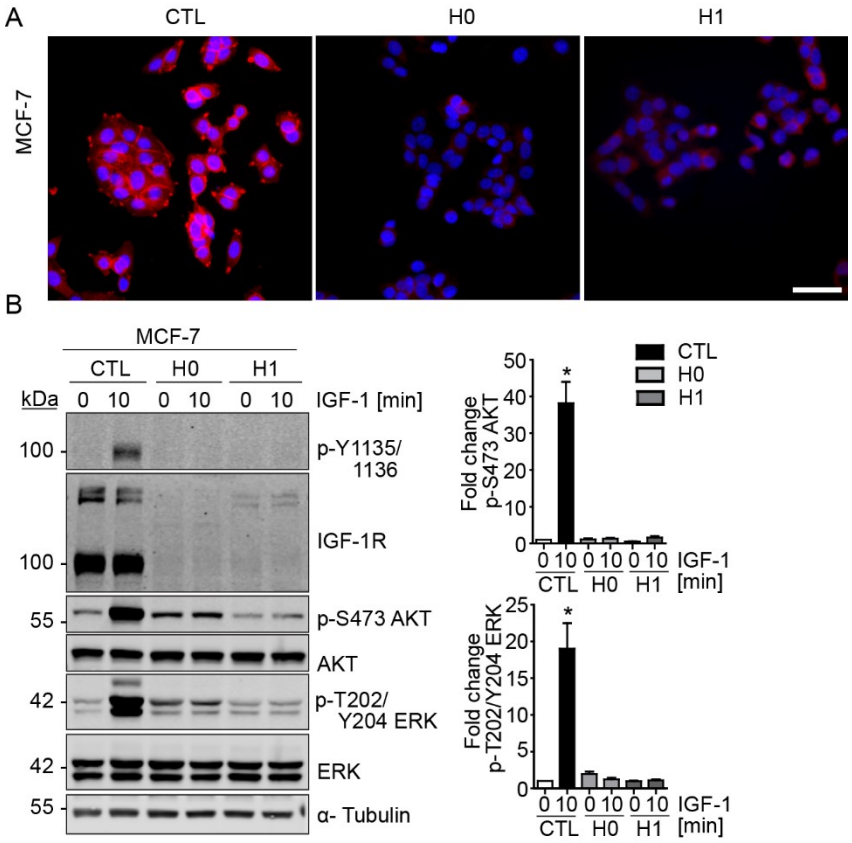


Figure 4.8: MCF-7 *igf-1r* knock-out cell lines display lack of IGF-1R and IGF-1-mediated signalling.

(A) Immunofluorescence of MCF-7 CTL, H0 or H1 cells cultured in complete medium and stained for IGF-1R. Images were acquired using Nikon T600 fluorescent microscope at 40x magnification. Scale bar is 50 µm. **(B)** Immunoblotting for IGF-1R phosphorylated on $Tyr^{1135/1136}$ (p-Y1135/1136) total IGF 1R, AKT phosphorylated on Ser^{473} (p-S473), ERK phosphorylated on Thr^{202} and Tyr^{204} (p-T202/Y204), and total AKT and ERK in WCL of MCF-7 CTL, H0 or H1 cells serum-starved and stimulated with 50 ng/ml IGF-1 for the indicated times. Densitometry quantification is presented as the average fold-change ± SEM in ratio of phospho/total protein relative to the control condition. Blots are representative of n=3 independent experiments. Significance was calculated using a two-sided one-sample or two-sample *t*-test.
P-values are indicated by *<0.05, **<0.01, ***<0.001.

We next examined MDA-MB-231 and DU-145 H0 and H1 cells which indeed demonstrated knock out of IGF-1R protein expression and impaired induction of AKT signalling (phosphorylation on Ser^{473} AKT) (Figure 4.9A, B). DU-145 H0 and H1 IGF-1R also lacked IGF-1-induced ERK1/2 signalling (Figure 4.9B).

Taken together, it is clear that CRIPSR-mediated fragment deletion in the *igf-1r* gene abolished IGF-1R protein expression in cancer cell lines and generation of IGF-1R knock-out cancer cells that are impaired in IGF-1-induced signalling was successful.

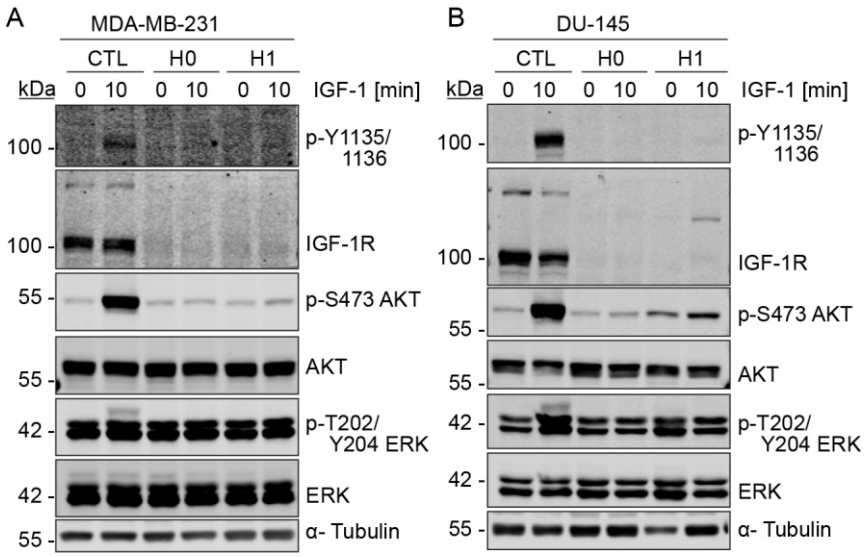


Figure 4.9: IGF-1R protein depletion and impaired IGF-1 signalling in *igf-1r* knock-out cell lines.

(A) Immunoblotting for IGF-1R phosphorylated on $Tyr^{1135/1136}$ (p-Y1135/1136) total IGF-1R, AKT phosphorylated on Ser^{473} (p-S473), ERK1/2 phosphorylated on Thr^{202} and Tyr^{204} (p-T202/Y204), and total AKT and ERK1/2 from WCL of MDA-MB-231 and **(B)** DU-145 CTL, H0 or H1 cells, serum-starved and stimulated with 50 ng/ml IGF-1 for the indicated times.

4.3.5 Cancer cell lines respond differently to knock-out of the IGF-1R protein

Igf-1r knock-out cells were deficient in IGF-1-mediated downstream signalling (Figure 4.8, Figure 4.9), so the next objective was to investigate whether the depletion of IGF-1R modifies IGF-1R-mediated cellular functions associated with transformation (Resnicoff et al., 1995, Baserga et al., 1997, Hongo et al., 1998, O'Connor, 2003, Kiely et al., 2005, Taliaferro-Smith et al., 2015, Cox et al., 2015). It was also interesting to test whether there may be differences in the three cells lines because it has previously been suggested that cellular kinases and their substrates or EMT markers can modulate IGF-1R (Cox et al., 2015, Osher and Macaulay, 2019).

We first investigated whether proliferation of MCF-7 H0 and H1 knock-out cell lines was altered compared to the parental cell line (CTL) by monitoring proliferation over a short time period of time (up to 96 hr in monolayer culture) (Figure 4.10A). Cell proliferation within this time was not significantly reduced in H0 or H1 cells compared to CTL. We next performed a colony formation assay, where cells are plated at a low density in monolayer culture. As can be seen in Figure 4.10B, H0 and H1 cells produced fewer colonies in these conditions, potentially due to impaired cell-cell contact mediated proliferation (Nelson and Chen, 2002, Nagle et al., 2018).

Cooperation of IGF-1 and adhesion signalling has been well reported (reviewed in Cox et al., 2015). We therefore next tested whether cell adhesion to plates coated with the ECM protein, Fibronectin, was impaired in IGF-1R knockout cells. Fewer IGF-1R H0 and H1 cells adhered to fibronectin compared to CTL cells (Figure 4.10C), indicating that MCF-7 cells require the presence of IGF-1R to enable adhesion to ECM. To assess anchorage-

independent growth in these cells, a feature that is essential for tumour cells, colony formation in a soft agarose assay was examined. As shown in Figure 4.10D, both *igf-1r* knock-out H0 and H1 cells lost their ability to form colonies, suggesting that the transformed phenotype has been reversed by knockout of the IGF-1R. This concurs with previous studies in MCF-7 cells using IGF-1R inhibitors and antisense strategies (Osher and Macaulay, 2019).

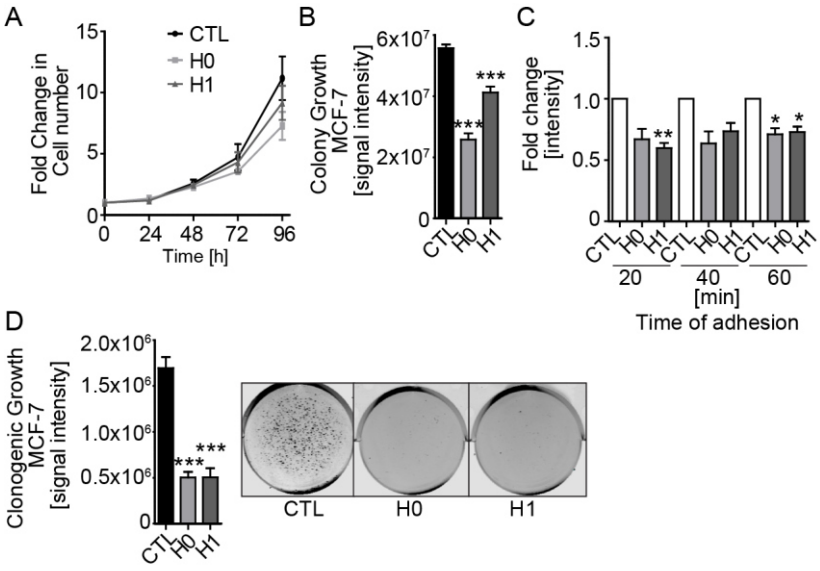


Figure 4.10: MCF-7 IGF-1R knock-out cell lines are defective in proliferation, adhesion and anchorage-independent growth.

(A) Cell proliferation of MCF-7 H0, H1 or CTL was assessed by counting three technical replicates of each cell line on a daily base over the indicated time period. Quantification is presented as the average fold-change ± SEM in ratio to the initial cell number (3.0×10^4). Graphs present the combined data of n≥3 independent experiments. **(B)** Colony formation of MCF-7 H0, H1 or CTL was measured after 14 days using crystal violet staining. Quantification is presented as the average fold-change ± SEM in signal intensity. Graphs show the combined data of 6 replicates. Significance was calculated using a two-sided two-sample *t*-test. **(C)** Capabilty of MCF-7 H0, H1 and CTL cells to adhere to fibronectin over the indicated time. Quantification was measured by crystal violet staining and is presented as the average fold-change ± SEM as ratio in signal intensity relative to control condition (CTL). Graphs show the combined data of 6 replicates. Significance was calculated using a two-sided one-sample *t*-test. **(D)** Anchorage-independent colony formation of MCF-7 H0, H1 and CTL cells was assesed using crystal violet staining after 6 weeks of growth. Quantification is presented as the average fold-change ± SEM in signal intensity. Graphs present the combined data of 6 replicates. Significance was calculated using a two-sided one-sample *t*-test.
P-values are indicated by *<0.05, **<0.01, ***<0.001.

A similar set of cell function assays were carried with MDA-MB-231 H0, H1 and CTL cells. Since MDA-MB-231 cells are highly migratory and IGF-1 is known to stimulate cell migration (Kiely et al., 2005, Taliaferro-Smith et al., 2015) we also performed wound healing assays.

Similar to observations with MCF-7 cells, there was no marked difference in the proliferation of MDA-MB-231 H0, H1 cells compared to CTL cells over 96 hr (Figure 4.11A). However, unlike MCF-7 cells, the MDA-MB-231 H0 and H1 IGF-1R knockout cells did not exhibit reduced proliferation in colony formation assays (Figure 4.11B). Furthermore, the number of colonies H0 and H1 MDA-MB-231 cells formed in soft-agarose was significantly higher than in MDA-MB-231-CTL cells, indicating that they retained a transformed phenotype in the absence of IGF-1R and that the knock-out of IGF-1R may have led to a gain of function. Supporting this, the H0 and H1 MDA-MB-231 cells also exhibited a higher migratory capacity compared to CTL cells (Figure 4.11D), suggesting that loss of IGF-1R may actually enhance the migration of MDA-MB-231 cells.

To rule out that IGF-1R knock-out mediated gain of function was not due to off target effects from the CRISPR/Cas9 system, we further validated that the mutation was introduced at the correct region in the *igf-1r*. This was achieved by designing specific primer sets (Table 2.4) that would bind before and after the region targeted by the guide RNAs (Figure 4.6A). Genomic DNA was extracted from the CTL, H0 and H1 MDA-MB-231 cells. The amplified fragments were extracted and analysed by sequencing. The gene analysis and comparison of the MDA-MB-231-H0 with the MDA-MB-231-CTL sequence displayed the deletion of a DNA fragment in the *igf-1r* resulted in a frame shift causing the loss of IGF-1R protein (Figure 4.7, Figure S 4.1). The gene

analysis and comparison of the MDA-MB-231-H1 with MDA-MB-231-CTL cells revealed that the depletion of IGF-1R was due to different small insertions and deletions (indels) causing a frameshift mutation in the region of the *igf-1r* compared to the CTL. This confirms that the mutations were introduced at the targeted region and that the increased colony formation and increased migration observed in the MDA-MB-231-H0 and H1 cells Figure 4.11C, D are due to the knock-out of IGF-1R expression.

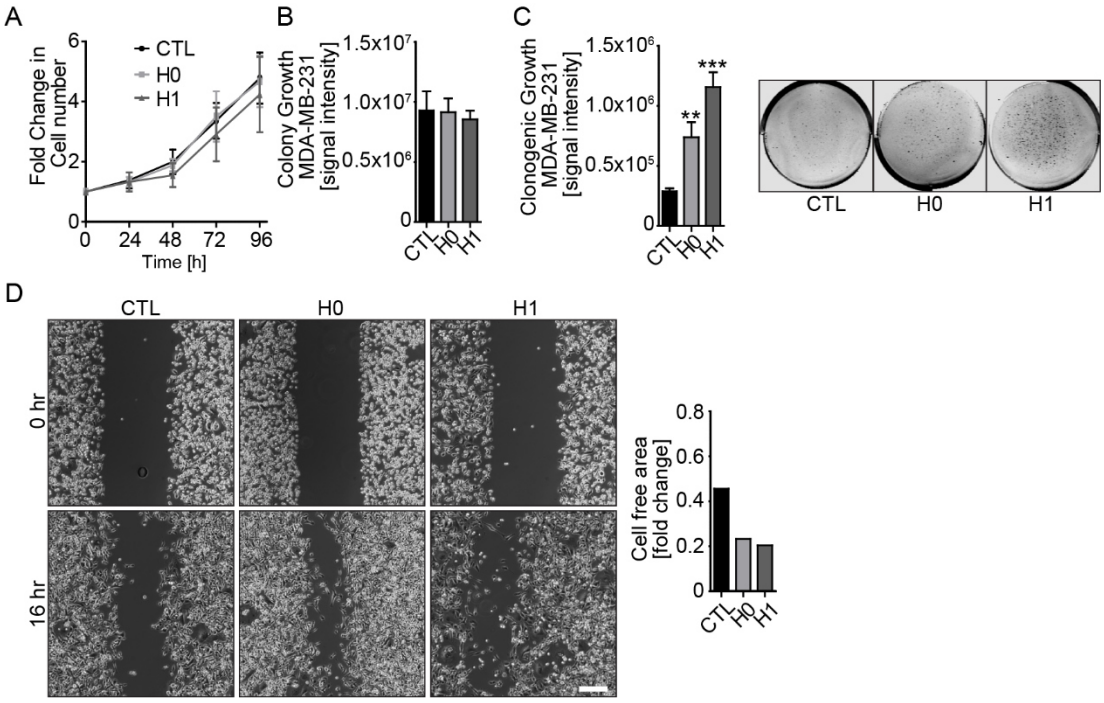


Figure 4.11: MDA-MB-231 IGF-1R KO cells are not impaired in monolayer cell proliferation, but exhibit enhanced anchorage-independent growth and cell migration.

(A) Cell proliferation of MDA-MB-231 H0, H1 or CTL was assessed by counting three technical replicates of each cell line daily for 96 hr. Quantification is presented as the average fold-change ± SEM in ratio to the initial cell number (3.0×10^4). Graphs present the combined data of n≥3 independent experiments. **(B)** Colony formation of MDA-MB-231 H0, H1 or CTL was assessed after 14 days using crystal violet. Quantification is presented as the average fold-change ± SEM in signal intensity. Graphs present the combined data of 6 replicates. Significance was calculated using a two-sided two-sample *t*-test. **(C)** Anchorage-independent colony formation of MDA-MB-231 H0, H1 and CTL cells was assessed using crystal violet staining after 6 weeks of growth. Quantification is presented as the average fold-change ± SEM in signal intensity. Graphs present the combined data of 6 replicates. Significance was calculated using a two-sided one-sample *t*-test. **(D)** Phase contrast images of wound healing assay to assess migration capability of MDA-MB-231 H0, H1 and CTL cells. Images were obtained with a Nikon Eclipse TE 300 microscope. Images are representatives of n=2 and the scale bar is 200 μm. Image based assessment of the cell free area was determined using ImageJ and graphs present average fold change in the area relative to 1 at 0 hr of migration.
P-values are indicated by *<0.05, **<0.01, ***<0.001.

DU-145 H0, H1 and CTL cells were also assessed for proliferation, colony formation, anchorage-independent colony formation and migration. Unlike MCF-7 and MDA-MB-231 cells, DU-145-H0 cells exhibited a profound reduction in cell proliferation over 96 hr. However, this impaired cell proliferation could be due to proliferation contact-inhibition after reaching confluency in the plate, because DU-145-H0 also exhibited an increase in cell size (Figure S 4.4C, Figure 4.12D). Proliferation potential was further assessed in colony formation assays in monolayer cultures. Here, DU-145-H0 cells exhibited no reduction in cell proliferation compared to the control cells (Figure 4.12B) and in contrast, DU-145-H1 grew significantly more than the DU-145 CTL cell line (Figure 4.12B). In the anchorage independent growth assays, DU145-H0 and H1 did not form colonies, indicating that IGF-1R knockout reversed their transformed state (Figure 4.12C). Surprisingly, loss of IGF-1R did not abolish the migratory feature of DU145 cells, in fact, DU-145-H1 displayed increased migration in a wound closure assays (Figure 4.12D).

As the DU-145-H1 cells displayed an increase proliferation rate and a higher migratory capacity than the DU-145-CTL cells, which was unexpected we validated the mutation again as described for the MDA-MB-231 cells. No deletion was to be found in the beginning of the Exon 2 of the *igf-1r* in the DU-145-H1 and the amplified sequence aligned perfectly with the respective sequence of the DU-145-CTL *igf-1r* cell line.

The results show that knock-out of the IGF-1R in MCF-7, MDA-MB-231 and DU-145 cells accompanied by reduced IGF-1 signalling results in cell type dependent effects on cell phenotype. Interestingly, IGF-1R knock-out in both MCF-7 and DU-145 reversed their transformed phenotype, whereas it did not in MDA-MB-231 cells. However, due to the fact that we could not confirm the

mutation causing the loss of IGF-1R protein of the DU-145-H1 cells and to keep the region of mutation consistent throughout the cell lines, we excluded all H1 groups of the MCF-7, MDA-MB-231 and DU-145.

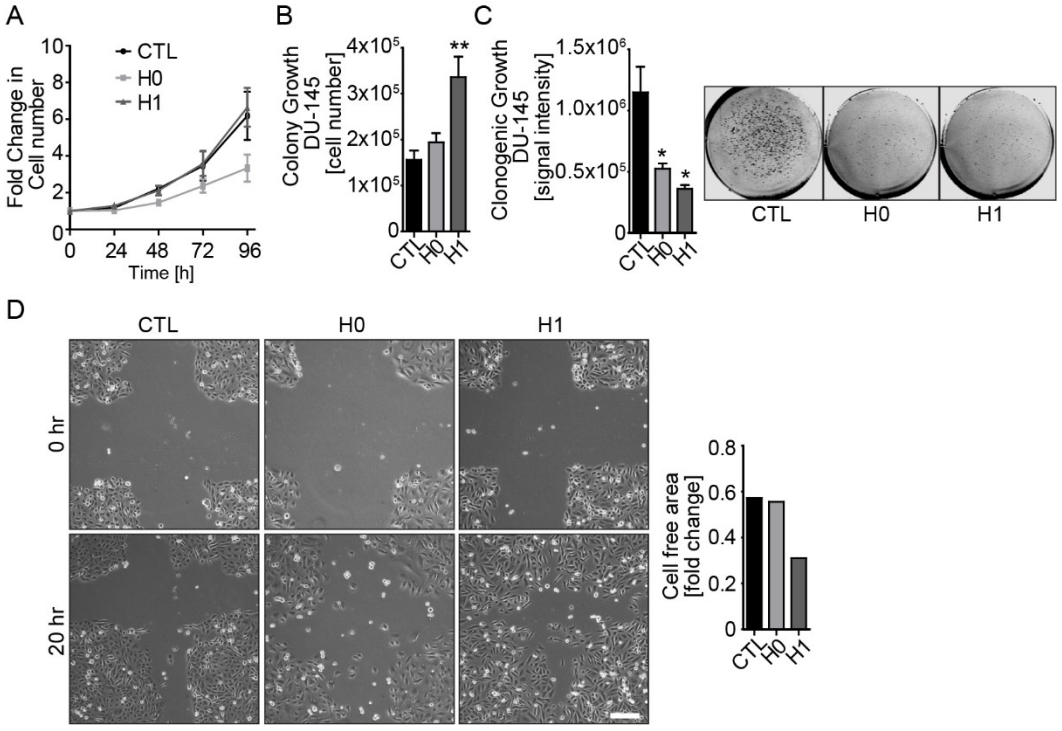


Figure 4.12: DU-145 IGF-1R knock-out cells are impaired in anchorage-independent growth but not in cell migration.

(A) Cell proliferation of DU-145 H0, H1 or CTL was assessed by counting three technical replicates of each cell line daily 96 hr. Quantification is presented as the average fold-change ± SEM in ratio to relative the initial cell number. Graphs present the combined data of n≥3 independent experiments. **(B)** Colony formation of DU-145 H0, H1 or CTL was assessed after 14 days using crystal violet. Quantification is presented as the average fold-change ± SEM in signal intensity. Graphs present the combined data of 6 replicates. Significance was calculated using a two-sided two-sample *t*-test. **(C)** Anchorage-independent colony formation of DU-145 H0, H1 and CTL cells was assessed using crystal violet staining. Quantification is presented as the average fold-change ± SEM in signal intensity. Graphs present the combined data of 6 replicates. Significance was calculated using a two-sided one-sample *t*-test. **(D)** Phase contrast images of wound healing assay to assess migration capability of DU-145 H0, H1 and CTL cells. Images were obtained with a Nikon Eclipse TE 300 microscope. Images are representatives of n=2 and the scale bar is 200 μm. Image based assessment of the cell free area was determined using ImageJ and graphs present the average fold change in the area relative to 1 at 0 hr of migration.
P-values are indicated by *<0.05, **<0.01, ***<0.001.

4.4 DISCUSSION

The results here demonstrate that genome editing of human cancer cells using CRISPR/Cas9 was successful in generating cell lines expressing IGF-1R point mutations and for generating *igf-1r* knock-out cell lines. Introducing point mutations into the IGF-1R sequence was possible and cells expressing IGF-1R containing these mutations were successfully cloned and expanded in culture.

Tyrosines 1250/1251 were previously shown to be important for the IGF-1R function in cancer cells, yet, the data from this study suggests that their function for MCF-7 cancer cells may be redundant. In line with previous studies with expression of the Y1250F/Y1251F mutant in R^- and other cells, it was anticipated that the knock-in mutant MCF-7 cells would display impaired IGF-1R activity, indicated by reduced activation and signalling, as well as loss of cellular transformation. However, there were no significant differences in the activity of the IGF-1R or in downstream signalling MCF-7-FF cells (Figure 4.4B). This suggests that $Tyr^{1250/1251}$ might be redundant for the IGF-1R activity in MCF-7 cells. However, it is also possible that other receptors or receptor hybrids could mask the expected reduction in IGF-1R activity, when $Tyr^{1250/1251}$ are mutated. Especially the expression of IR-A in MCF-7 cells could lead to an hybrid formation of IGF-1R-FF/IR-A hybrids in MCF-7-FF cells. Activation of the hybrid receptor and its derived signalling could compensate for the impaired IGF-1R-FF activity. IGF-1-FF/IR-A hybrid formation could also explain, the lack of an effect on the cellular functions that were attributed to the IGF-1R when cells express the IGF-1R FF mutation. However, here other receptors could compensate for the loss in IGF-1R function as well.

Additionally, it is possible that $Tyr^{1250/1251}$ mediates a function in cells that is not essential for MCF-7 cells.

Levels of IGF-1R-FF protein were significantly reduced compared to the IGF-1R in MCF-7-WT cells. It is likely that the MCF-7-FF cells adapted to the lack of $Tyr^{1250/1251}$ and deregulated other RTKs, as previously shown in MCF-7 cells (Lyons et al., 2017). The suppression of IGF-1R leads to lower levels of IGF-1R protein expression and to increased activation of the Epidermal Growth Factor Receptor (EGFR), which may compensate for the lack of IGF-1R function (Lyons et al., 2017). However, other compensatory mechanisms including signalling from the IR-A and IR-B as well as MET RTK could have similar effect (van der Veeken et al., 2009, Buck et al., 2010, Qu et al., 2017, Liu et al., 2018b). Further analysis, for example a total proteome profile for the MCF-7-FF cells and MCF-7-WT cells, would be one option to test this concept.

Phosphorylation on specific amino acids is commonly used by RTKs for signal transduction. This can lead to structural changes required for the full activity of the RTK, can serve as a binding domain for other proteins, or can be a signal for specific trafficking. Recently, it has been shown (S. O'Shea PhD thesis, 2016) and confirmed (Chapter 3) that $Tyr^{1250/1251}$ are phosphorylated in cells. However, it is possible that the MCF-7 cells do not require the presence of $Tyr^{1250/1251}$ phosphorylation for IGF-1R function. This requires further investigation under conditions where these tyrosines are phosphorylated to determine whether their function as phosphotyrosines is important for MCF-7 cells.

Although the disruption of the *igf-1r* gene was successful and the IGF-1R protein was depleted from MCF-7, MDA-MB-231 and DU-145 cells leading to impaired signalling transduction in response to IGF-1, observations on cell

phenotypes relevant to the IGF-1R were very different between these cell lines (Table 4.1). For MCF-7 and DU-145 loss of IGF-1R impaired cellular transformation (Figure 4.10, Figure 4.12, Table 4.1), whereas the MDA-MB-231 cells remained competent in forming colonies in soft-agar (Figure 4.11, Table 4.1). Furthermore, IGF-1R-deficient MDA-MB-231 cells retained their migratory capacity (Figure 4.11, Table 4.1). However, migration is linked to the activation of the Ras/MAPK pathway, and IGF-1R activation does not regulate ERK1/2 signalling in MDA-MB-231 (Figure 4.9) (Stanicka et al., 2018). The activation of this pathway may be regulated by other RTKs or the reduction in IGF-1R activity could lead to compensatory activation of other RTKs, as it has been previously suggested (van der Veeken et al., 2009, Buck et al., 2010, Qu et al., 2017, Liu et al., 2018b).

Table 4.1: Summary of phenotypic behaviour of cell lines with an *igf-1r* knock-out.

Phenotypical behaviour observed in MCF-7, MDA-MB-231 and DU-145 H0 and H1 cell lines with an *igf-1r* knock-out compared to parental cell lines (CTL): Increase compared to CTL indicated with ↑, decrease with ↓, unchanged with →, not available with N/A.

	MCF-7		**MDA-MB-231**		**DU-145**	
	H0	H1	H0	H1	H0	H1
Proliferation	→	→	→	→	↓	→
Colony growth	↓	↓	→	→	→	↑
Adhesion	↓	↓	N/A	N/A	N/A	N/A
Anchorage-independent growth	↓↓	↓↓	↑	↑↑	↓↓	↓
Migration	N/A	N/A	↑↑	↑↑	→	↑↑

Two different plasmids targeting different regions in the DNA of *igf-1r* were used to introduce deletions in the *igf-1r* sequence (Figure 4.6A). Although the MCF-7, MDA-MB-231 and DU-145 H0 and H1 cells were deficient in IGF-1R

protein expression, we noticed differences between cells targeted with the two plasmids in some of the functional assays performed (Table 4.1). This was particularly evident with MDA-MB-231, and especially with the DU-145 knock-out cell lines (Figure 4.11, Figure 4.12, Table 4.1). The gene analysis for the DU-145-H1 cells compared to the DU-145-CTL cells showed that the targeted region of the *igf-1r* was not mutated, and we were not able to identify the cause for the loss of IGF-1R protein in these cells.

Off-target effects are reported to be rare, especially using a paired Cas9 nickase system (Gopalappa et al., 2018). However, this possibility cannot be excluded. We designed specific primers to amplify the region in the DNA of the IGF-1R targeted by the guide RNA (Figure 4.6) and isolated the amplified region for sequencing. Using the Cas-OFFinder (Bae et al., 2014), we searched for potential off-targets of the guide RNAs used. However, besides the specific target region, no further off targets in the IGF-1R sequence were identified. Further sequencing analysis may be required to ensure that the Cas9 nuclease targeted the correct region.

We conclude that we successfully modified the IGF-1R -SFYYS- motif in the *igf-1r* gene using CRISPR technology. However, as the cells displayed no obvious phenotype, it is possible that these tyrosines are not essential for MCF-7 cell function. Importantly, we generated and characterized three cancer cell lines deficient in IGF-1R expression. The data from these cell lines indicates that IGF-1R function and its signalling outcome may be influenced by the pre-existing cell phenotype, rather than IGF-1R influencing the cells phenotype per se. The knock-out cell lines (in particular, H0 knock-out) we established here, will be useful tools for further investigation of the significance

of IGF-1R in promoting cancer progression, and also for analysis of how specific residues on IGF-1R influence its function in various types of cancer.

4.5 SUPPLEMENTARY DATA

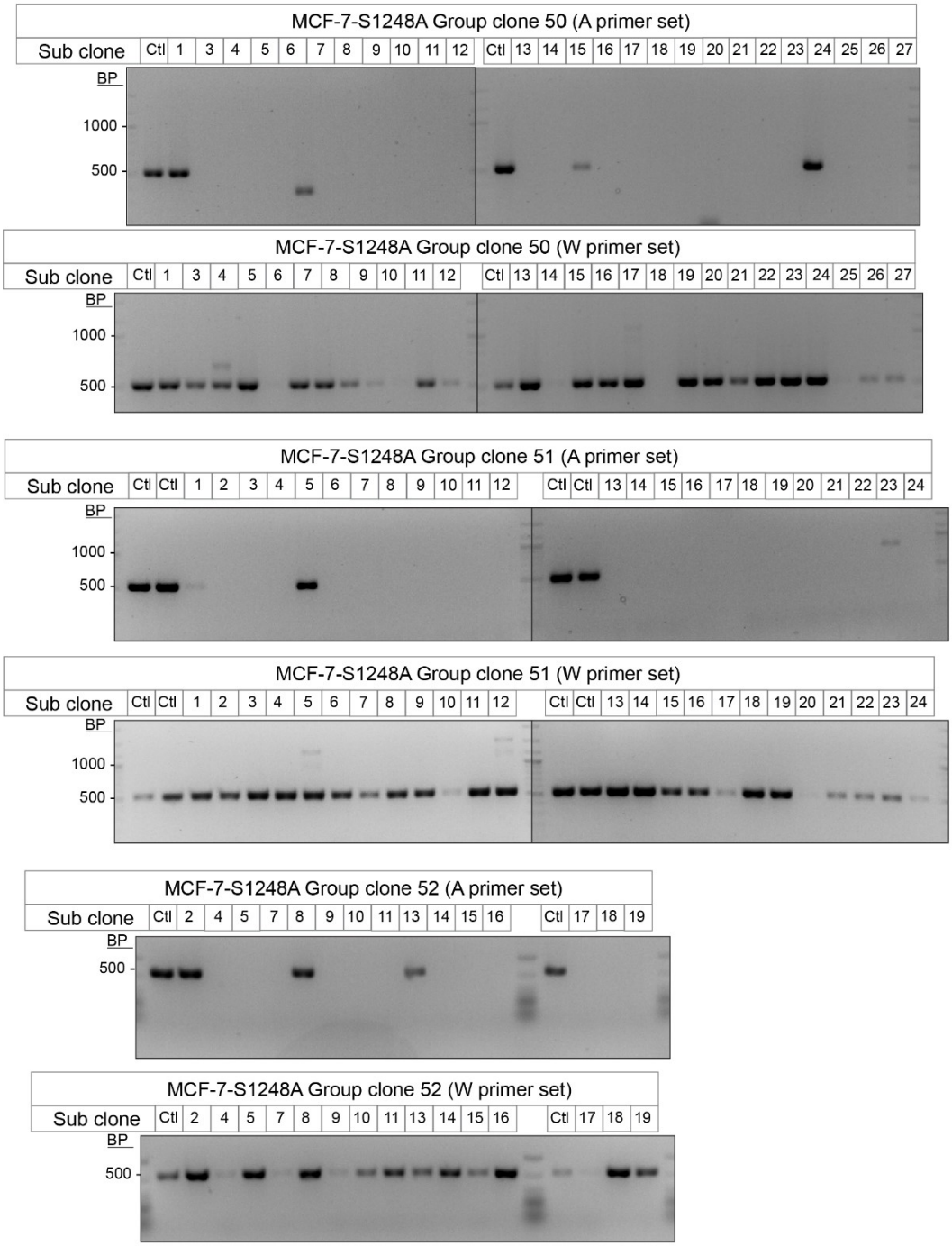


Figure S 4.1: PCR-based identification of cell clones with exclusive amplification of *igf-1r* with the S1248A mutation.

Group clones identified to contain cells encoding for the mutated IGF-1R were separated. DNA was extracted and PCR was performed with both the forward primer detecting the IGF-1R S1248A mutation as well as the WT IGF-1R in cells.

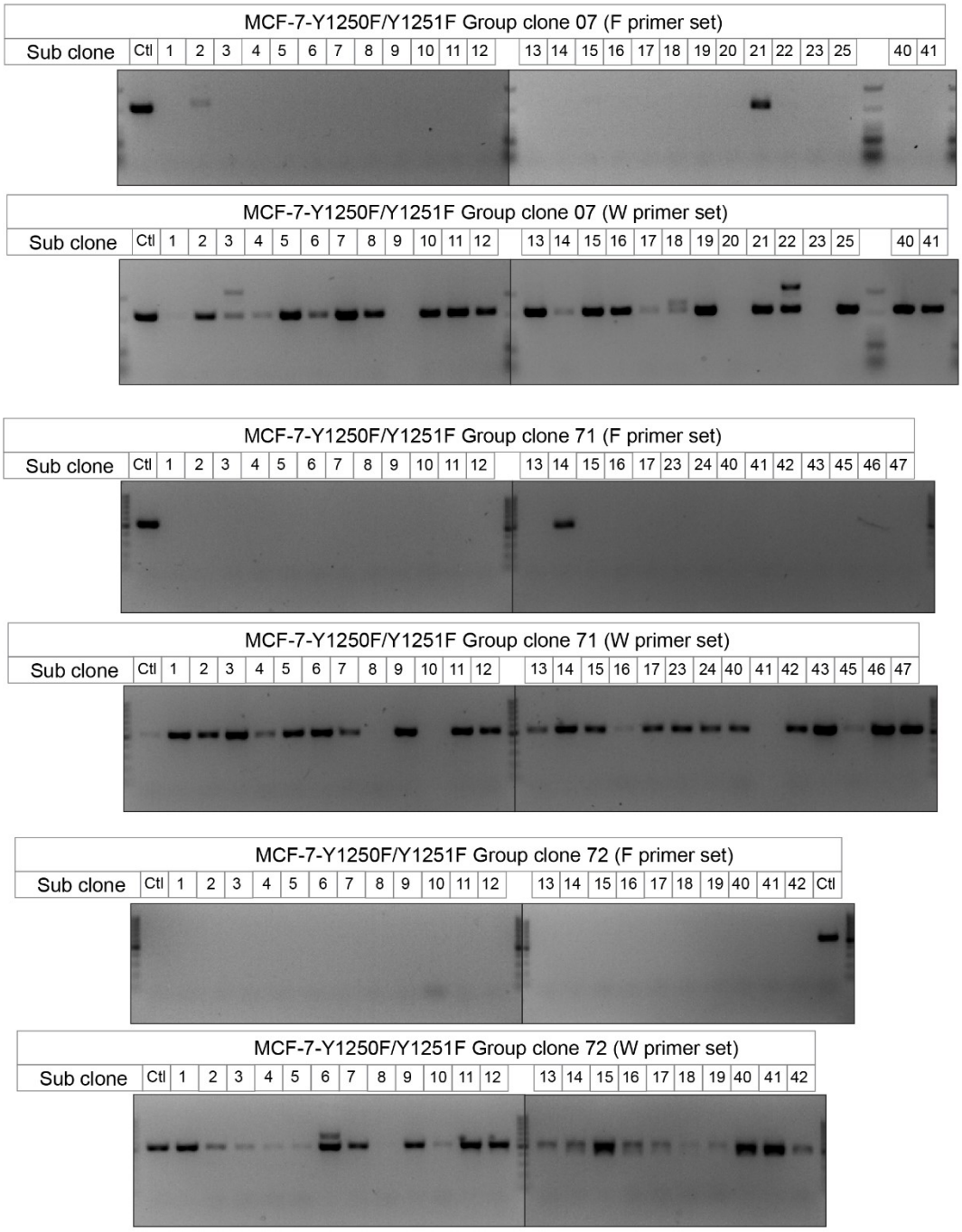
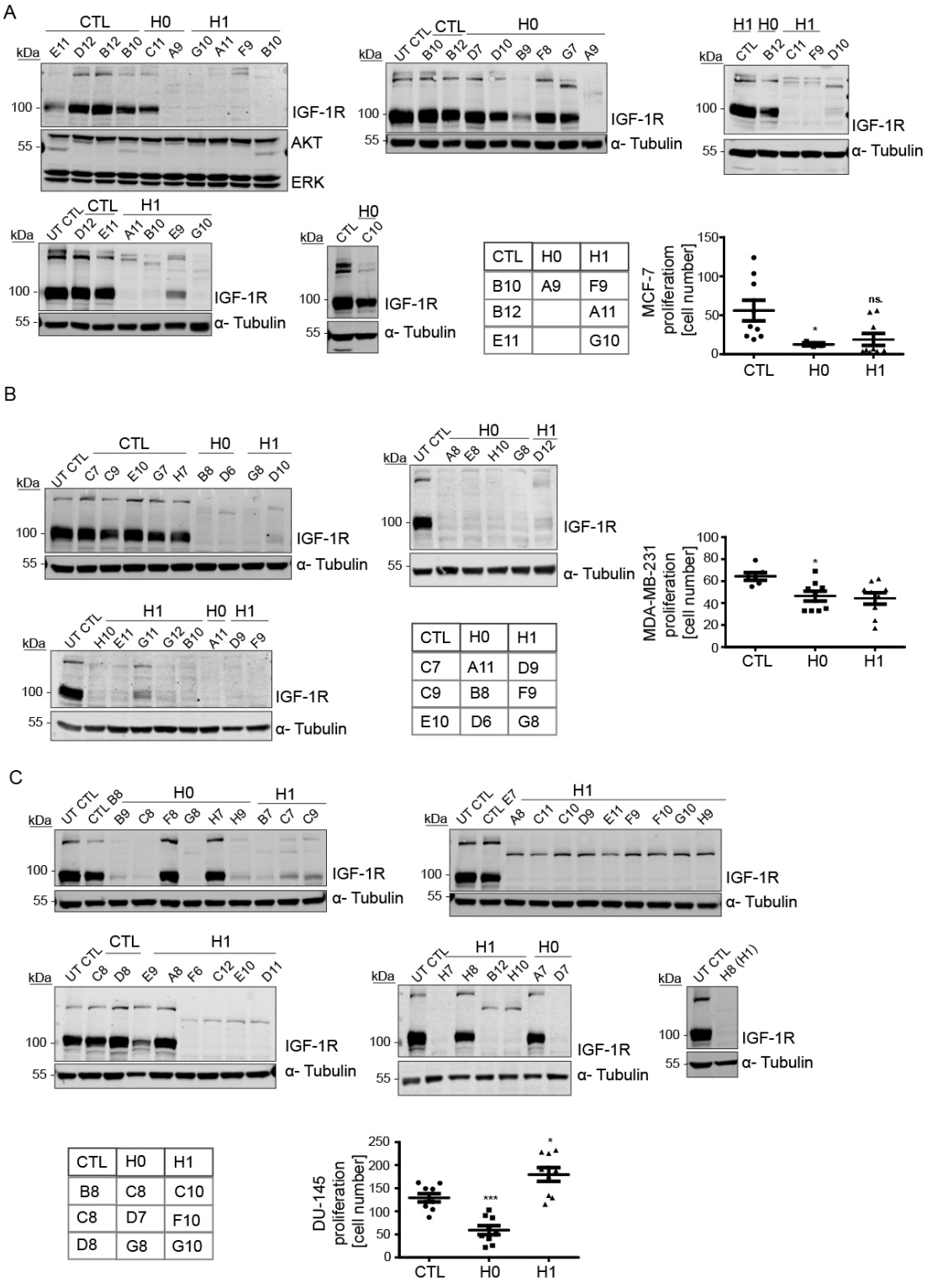


Figure S 4.2: PCR-based identification of cell clones with exclusive amplification of *igf-1r* with the Y1250F/Y1251F mutation.

DNA was extracted from diluted group clones of MCF-7 cells identified to contain cells encoding for FF point mutation. PCR was performed with both the forward primer for detection of the IGF-1R Y1250F/Y1251F mutations as well as the WT IGF-1R in cells.



CTL	H0	H1
B10	A9	F9
B12		A11
E11		G10

CTL	H0	H1
C7	A11	D9
C9	B8	F9
E10	D6	G8

CTL	H0	H1
B8	C8	C10
C8	D7	F10
D8	G8	G10

Figure S 4.3: Identification of cell clones deficient in IGF-1R protein expression.

Immunoblotting for IGF-1R in total cell lysates of **(A)** MCF-7 CTL, H0 or H1 cells **(B)** MDA-MB-231 CTL, H0 or H1 cells and **(C)** DU-145 CTL, H0 or H1 cells to assess IGF-1R expression in single cell clones. Proliferation of the identified knock-out clones of **(A)** MCF-7, **(B)** MDA-MB-231 and **(C)** DU-145 cells was assessed after 14 days. Quantification shows total cell number obtained from three technical replicates of n=3 independent experiments. Summary tables present sub clones that were recombined.

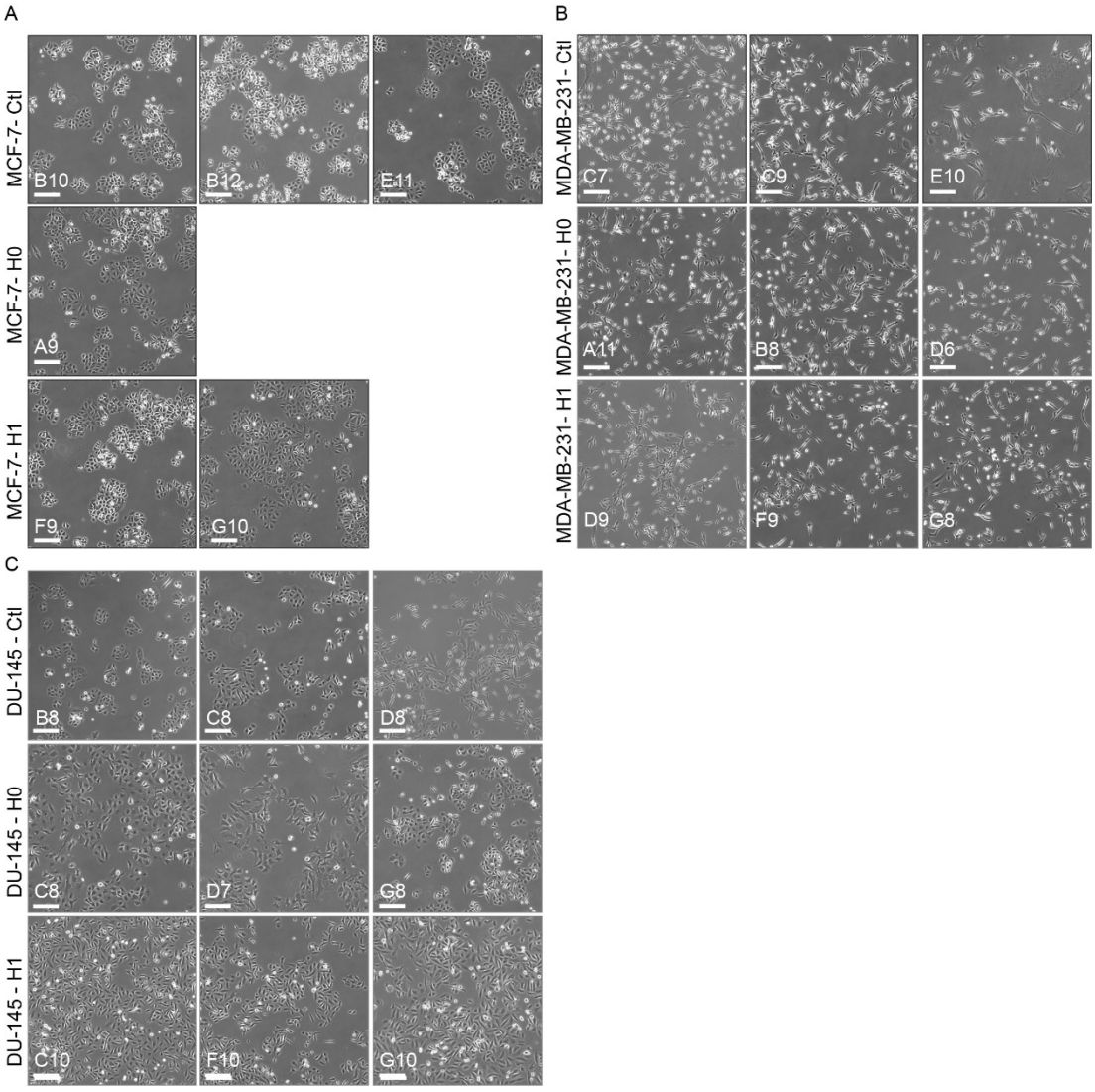


Figure S 4.4: Cell morphology is not affected by IGF-1R knock-out in MCF-7 and MDA-MB-231, but in DU-145.

Phase contrast images of **(A)** MCF-7 CTL, H0 and H1 clones **(B)** MDA-MB-231 CTL, H0 and H1 clones and **(C)** DU-145 CTL, H0 and H1 clones were acquired to assess cell morphology. Images were obtained with a Nikon Eclipse TE 300 microscope. The scale bar is 200 μm.

5 CHAPTER 5: IGF-1 RECEPTOR ACTIVITY IN THE GOLGI OF MIGRATORY CANCER CELLS REQUIRES ADHESION-DEPENDENT PHOSPHORYLATION ON TYROSINES 1250 AND 1251

Sandra O'Shea and Geraldine Kelly generated data presented in Figure 5.1A.

Sandra O'Shea contributed to Figure 5.1B, 5.2, 5.4 and 5.6A.

Results of this chapter were published in May 2020 in Science Signaling. The publication is attached to the thesis.

DOI: 10.1126/scisignal.aba3176

5.1 ABSTRACT

Although Insulin-like growth factor (IGF-1) signalling promotes tumour growth and cancer progression, therapies that target IGF-1 receptor (IGF-1R) have shown poor clinical efficacy. This study addresses IGF-1R activity in cancer cells and also how this differs from the closely related Insulin receptor (IR). The IGF-1R C-terminal tail contains two tyrosines that are not present in the IR, which have been shown to be essential for IGF-1–mediated cancer cell survival, migration and tumorigenic growth. Here, we found that Tyr^{1250} and Tyr^{1251} ($Tyr^{1250/1251}$) were autophosphorylated in a cell adhesion-dependent manner. We investigated the consequences of this phosphorylation using a phosphomimetic Y1250E/Y1251E (EE) and a non-phosphorylatable Y1250/Y1251F (FF) IGF-1R mutant. Although fully competent in kinase activity and signalling, the EE mutant was more rapidly internalised and degraded than either the wild-type (WT) or FF receptor. IGF-1 promoted accumulation of WT and EE IGF-1R within the Golgi apparatus, whereas the FF mutant remained at the plasma membrane or sites of cell adhesion. Golgi-associated IGF-1R signalling was found to be a feature of migratory cancer cells, and disruption of the Golgi impaired IGF-1–induced phosphorylation of the adaptor protein SHC and cell migration. Upon formation of new cell adhesions, IGF-1R transiently re-localised to the plasma membrane from the Golgi. Thus overall, phosphorylation at $Tyr^{1250/1251}$ promoted IGF-1R signalling from the Golgi to support an aggressive cancer phenotype. This could contribute to the poor clinical efficacy of antibodies that target IGF-1R on the cell surface and also distinguish IGF-1R from IR signalling potential.

5.2 INTRODUCTION

The Insulin-like Growth Factor–1 receptor (IGF-1R) and its ligands (IGF-1 and IGF-2) are widely present throughout different cell and tissue types and play essential roles in cell, organ, and organismal growth (Liu et al., 1993, Pollak, 2012). The IGF system is also linked to cancer risk, tumorigenesis, tumour growth and survival, and in promoting cell migration in both normal and transformed cells (Arcaro, 2013, Christopoulos et al., 2015, Brahmkhatri et al., 2015, Osher and Macaulay, 2019). Numerous pre-clinical studies have shown a clear effect of IGF-1R suppression or inhibition on limiting tumorigenesis, tumour growth and metastatic potential (Arcaro, 2013, Brahmkhatri et al., 2015, Osher and Macaulay, 2019). However, this has not been replicated in large-scale clinical trials, wherein IGF-1R blocking antibodies and kinase inhibitors show an overall poor efficacy (Brahmkhatri et al., 2015, Osher and Macaulay, 2019). There are no predictive biomarkers for IGF-1R activity, and there is limited understanding of the cellular signalling events that promote resistance to or evasion of IGF-1R inhibitors.

Although IGF-1 signalling in cancer cells has been extensively studied, it is still poorly understood how IGF-1R expression, abundance and signalling output are influenced by oncogenic and adhesion signals in different cancers. The amount of cell surface IGF-1R may not predict responses to ligand stimulation in terms of downstream signalling output, as this appears to be influenced by cell phenotype (Niepel et al., 2013). We and others previously demonstrated that adhesion signals enhance IGF-1R activation and signalling, and that Integrin signals are essential for IGF-1-promoted cancer cell proliferation and migration (reviewed in (Cox et al., 2015)). Moreover, IGF-1R association with E-cadherin and collagen DDR receptors can control receptor

stability and signalling output (Nagle et al., 2018, Bajrami et al., 2018, Belfiore et al., 2018).

Cooperation between β1-Integrin and IGF-1R signalling involves an adhesion-dependent signalling complex composed of scaffolding proteins, Focal adhesion kinase (FAK) and phosphatases that ultimately leads to activation of mitogen-activated protein kinase (MAPK) pathways (Blakesley et al., 1998, Hermanto et al., 2002, Kiely et al., 2002, Kiely et al., 2008). Mutation of two tyrosines (Tyr^{1250} and Tyr^{1251}) in the C-terminal tail is sufficient to abrogate IGF-1R function in facilitating cellular transformation, cell survival and migration (Miura et al., 1995b, O'Connor et al., 1997, Brodt et al., 2001). This $Tyr^{1250/1251}$ site was also found to be essential for integrating IGF-1R and adhesion signalling (Kiely et al., 2005). However, these tyrosines are not present in the human insulin receptor (IR), which has an almost identical kinase domain to the IGF-1R but shares less than 50% homology with the C-terminal tail. We previously hypothesized that the function of these tyrosines may distinguish IGF-1R and IR actions in cell growth and cancer. However, despite the clear loss of IGF-1R function observed upon mutation of Tyr^{1250} and Tyr^{1251} ($Tyr^{1250/1251}$) to phenylanines (Y1250F/Y1251F), and *in silico* predictions for phosphorylation in cells, evidence for actual phosphorylation *in vivo* has remained elusive, as has knowledge of how this phospho-site functions. This has hindered efforts to understand how these IGF-1R tyrosines facilitate tumorigenesis or may distinguish IGF-1R and IR signalling.

In this study, we established that the IGF-1R was autophosphorylated on $Tyr^{1250/1251}$ in cells at basal levels using mass spectroscopy and phospho-specific antibodies, and this was further induced by IGF-1 and adhesion signalling. The functions of $Tyr^{1250/1251}$ phosphorylation were determined by

using a phosphomimetic (EE mutant IGF-1R) which was found to be more rapidly internalised and less stable than the wild type (WT) IGF-1R or the Y1250F/Y1251F (FF) mutant. Upon IGF-1 stimulation both the WT and the EE IGF-1R rapidly accumulated within the Golgi-apparatus, whereas the FF mutant was retained on the plasma membrane. IGF-1R localisation in the Golgi-apparatus was associated with migratory potential, and an intact Golgi-apparatus was required for IGF-1R signalling in migrating cells. Overall, the data indicate that $Tyr^{1250/1251}$ phosphorylation drives translocation of the IGF-1R to the Golgi, where it contributes to a migratory phenotype. These results distinguish IGF-1R and IR function, and may also explain the inefficacy of targeting cell surface IGF-1R with monoclonal antibodies in several cancers.

5.3 RESULTS

5.3.1 Phosphorylation of Tyr^{1250} and Tyr^{1251} occurs in cells

First, to address the question whether the $Tyr^{1250/1251}$ site becomes phosphorylated in cells, we used mass spectroscopy and phosphopeptide analysis of IGF-1R immunoprecipitated from mouse embryonic fibroblasts derived from IGF-1R knockout mice (R^- cells) transiently expressing the receptor and either serum-starved or stimulated with IGF-1. The isolation of IGF-1R phosphopeptides including $Tyr^{1250/1251}$ was less efficient than isolation of other phosphopeptides from the receptor, which we attributed to the fact that these tyrosines reside with a sequence, SFYYS, that also includes phosphorylated serines (Zheng et al., 2012, Kelly et al., 2012), and would thus be highly charged and difficult to capture. Following peptide extraction and mass spectrometry analysis, a series of phosphopeptides was identified (ion score >19) containing tyrosines that are known to be phosphorylated in response to IGF-1, including Tyr^{950} and the kinase activation site tyrosines, Tyr^{1131}, Tyr^{1135}, and Tyr^{1136} (Figure 5.1A). In addition, phosphopeptides were captured from both serum-starved and IGF-1 stimulated cells demonstrating phosphorylation on the Tyr^{1250} site, with a higher score obtained from IGF-1 stimulated cells, indicating IGF-1 induced phosphorylation on this tyrosine (Figure 5.1A).

We next employed an antibody specific for the phosphorylated $Tyr^{1250/1251}$ site to further assess $Tyr^{1250/1251}$ phosphorylation over time in response to either serum starvation or IGF-1. In phosphopeptide arrays, an antibody postulated to recognize phosphorylated Tyr^{1250} also detected peptides containing either one of the single phosphorylated tyrosines

(phosphorylated Tyr^{1250} or phosphorylated Tyr^{1251}) or the doubly phosphorylated site (S. O'Shea PhD thesis, 2016). We therefore concluded that this antibody reacts with the $Tyr^{1250/1251}$ phosphosite. We next compared the profile of IGF-1-stimulated phosphorylation of the $Tyr^{1250/1251}$ with the IGF-1R autophosphorylation sites Tyr^{950}, Tyr^{1131} and $Tyr^{1135/1136}$. This analysis demonstrated that basal amounts of Tyr^{950}, Tyr^{1131} and $Tyr^{1135/1136}$ phosphorylation were low and then rapidly induced by IGF-1 at 1-5 min. In contrast, basal phosphorylation of $Tyr^{1250/1251}$ was evident in serum-starved cells, and IGF-1-induced phosphorylation accumulated more slowly than on the other sites (Figure 5.1B). This result is consistent with the mass spectrometry analysis indicating phosphorylation of $Tyr^{1250/1251}$ in serum-starved cells (Figure 5.1A).

A

Sample	Site	Sequence	Ion Score >19
Serum Starved	1248/1250/1251/1252	EVSFYYSEENK	27
IGF-1 10 min	943/945/950/952/957	LGNGVLYASVN PEYFSAADVYVP DEWEVAREK	39
	1131	DIYETDYYRK	28
	1131/1135/1136	DIYETDYYRK	26
	1248/1250/1251/1252	EVSFYYSEENK	49

B

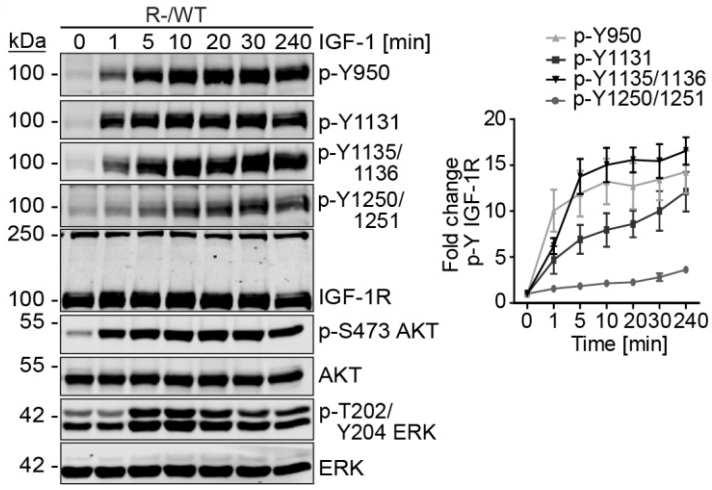


Figure 5.1: Tyr$^{1250/1251}$ IGF-1R phosphorylation occurs in R$^-$ cells.

(A) Phosphopeptides identified by mass spectroscopy from IGF-1R immunoprecipitated from R- cells stably expressing WT IGF-1R following serum starvation or 10 min exposure to IGF-1. Phosphorylated (p-) IGF-1R tyrosines are indicated in red. **(B)** Immunoblotting for the indicated phosphotyrosines (p-Y) and total IGF-1R, AKT phosphorylated on Ser^{473} (p-S473) and total AKT, ERK1/2 phosphorylated on Thr^{202} and Tyr^{204} and total ERK1/2 in WCL of R$^-$ cells stably expressing WT IGF-1R (R-/WT), serum-starved and stimulated with 10 ng/ml IGF-1 for the indicated times. Quantification of phospho/total IGF-1R is expressed as average fold-change ± SEM relative to 0 min of IGF-1 (set to 1). Blots are representative of n≥3 independent experiments.

Although IGF-1 and Insulin display a higher affinity for their respective receptors, they can activate the other receptor when the ligand concentration is high. Therefore, we investigated whether $Tyr^{1250/1251}$ phosphorylation was influenced by ligand concentration in serum-starved R- cells expressing WT IGF-1R stimulated with either 1, 10, 50, or 100 ng/ml IGF-1. From this it was observed that $Tyr^{1250/1251}$ phosphorylation was induced in a dose-responsive manner with highest amounts of phosphorylation achieved using 50 ng/mL (Figure 5.2).

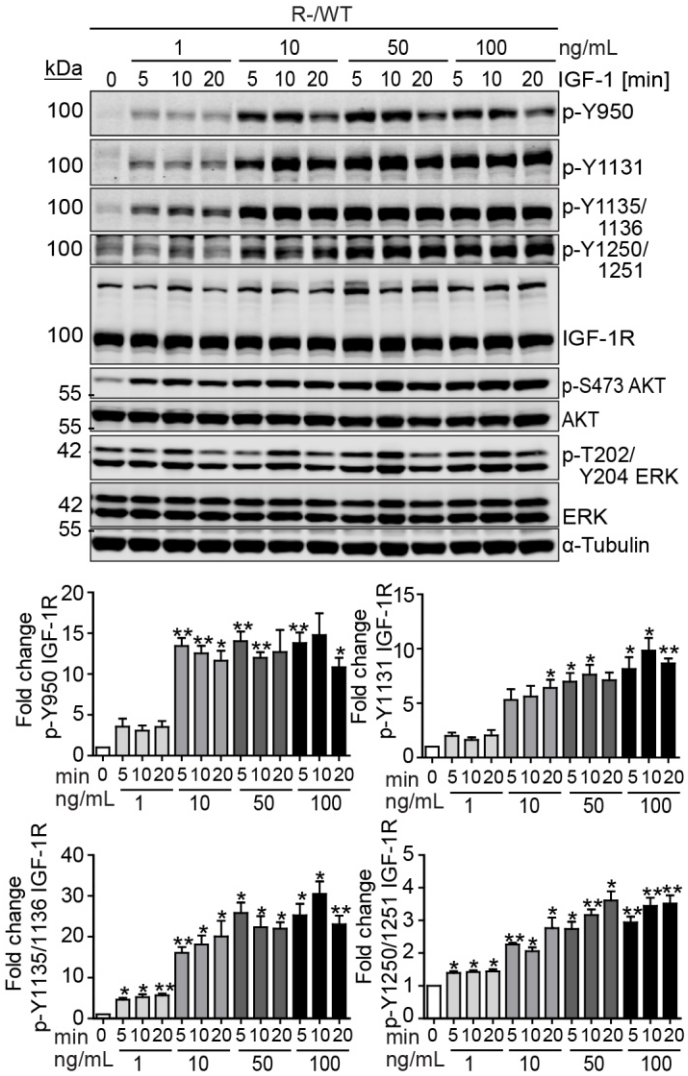


Figure 5.2: IGF-1 induce Tyr$^{1250/1251}$ IGF-1R phosphorylation in a dose dependent manner.

Immunoblotting for the indicated phosphorylated forms of IGF-1R, total IGF-1R, AKT phosphorylated on Ser^{473} (p-S473), total AKT, ERK1/2 phosphorylated on Thr^{202} and Tyr^{204} (p-T202/Y204), and total ERK1/2 in WCL of R^{-}/WT cells stimulated with IGF-1 at the indicated concentrations and times following serum starvation. Quantification of phospho/total IGF-1R is expressed as average fold-change ± SEM relative to the control condition (set to 1). Blots are representative of n=3 independent experiments. Significance was calculated using a two-sided one-sample *t*-test. *P*-values are indicated by *<0.05, **<0.01, ***<0.001.

We next examined phosphorylation of $Tyr^{1250/1251}$ on endogenous IGF-1R in several cancer cell lines (MDA-MB-231, Cal-51, HS-578T, and DU-145) (Figure 5.3). Results show that again, $Tyr^{1250/1251}$ are phosphorylated in serum-starved cells and this was increased upon IGF-1 stimulation.

Overall, these data demonstrate that $Tyr^{1250/1251}$ phosphorylation is present in cells at low basal amounts and is induced by IGF-1 in a concentration- and time-dependent manner.

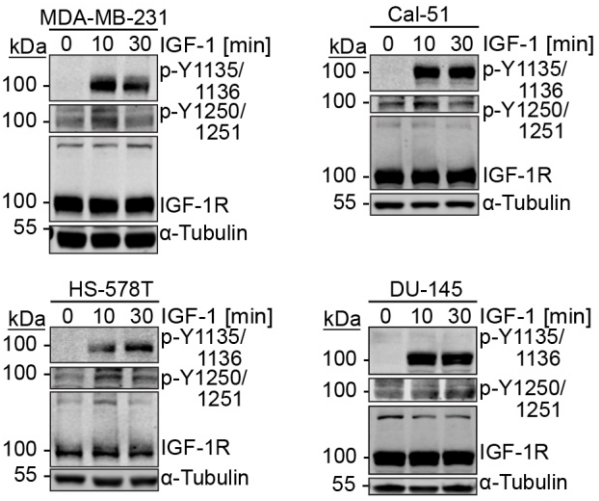


Figure 5.3: IGF-1 induces $Tyr^{1250/1251}$ IGF-1R phosphorylation in cancer cells.

Immunoblotting for IGF-1R phosphorylated on $Tyr^{1135/1136}$ (p-Y1135/1136), $Tyr^{1250/1251}$ (p-Y1250/1251) and total IGF-1R in WCL of cancer cells serum-starved and stimulated with 50 ng/ml IGF-1. Blots are representatives of n=3 independent experiments.

5.3.2 Adhesion signals and IGF-1R kinase activity are required for $Tyr^{1250/1251}$ phosphorylation

$Tyr^{1250/1251}$ phosphorylation was enhanced by IGF-1, and because this phosphorylation has not previously been demonstrated in cells, we next investigated whether it is a *bona fide* autophosphorylation site in the IGF-1R. The first approach was to determine whether $Tyr^{1250/1251}$ phosphorylation could be reduced in the presence of an IGF-1R kinase inhibitor. In serum-starved cells, $Tyr^{1250/1251}$ phosphorylation was not affected by the IGF-1R kinase inhibitor BMS-754807 (Figure 5.4A). However, IGF-1-induced $Tyr^{1250/1251}$ phosphorylation was abolished by the kinase inhibitor. To further test autophosphorylation, we examined WT IGF-1R and a kinase-inactive IGF-1R (K1003R, ATP-binding site mutant, KR), in the absence or presence of exogenously added ATP to stimulate kinase activity. Although phosphorylation on $Tyr^{1250/1251}$ was detectable on both the WT and KR receptors, this was increased by exogenously added ATP on the WT but not on the KR receptor (Figure 5.4B). This indicates that IGF-1R kinase activity was required for maximal phosphorylation on $Tyr^{1250/1251}$. The observation that phosphorylation was evident with the KR mutant also suggests that other cellular kinases may phosphorylate $Tyr^{1250/1251}$.

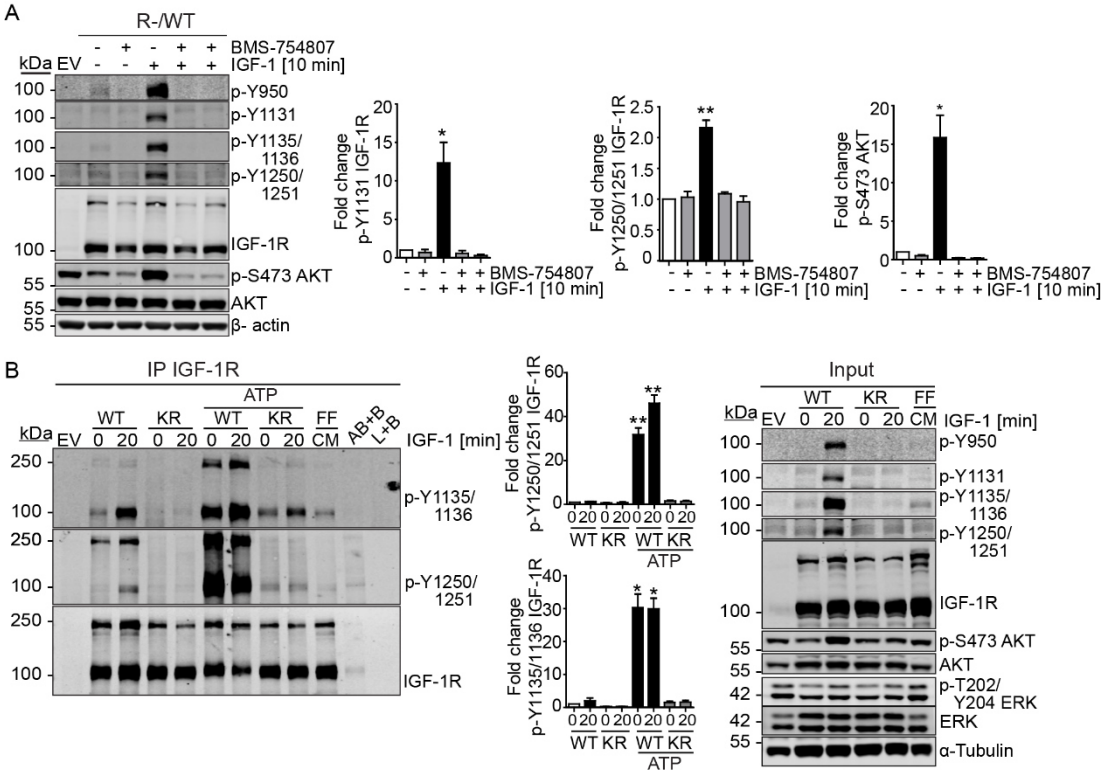


Figure 5.4: Tyr$^{1250/1251}$ IGF-1R phosphorylation is an IGF-1R autophosphorylation site.

(A) Immunoblotting for the indicated phosphorylated forms of IGF-1R, total IGF-1R, AKT phosphorylated on Ser^{473} (p-S473) and total AKT from WCL of R$^-$/WT cells that were serum-starved followed by stimulation with 10 ng/ml IGF-1 for the indicated times. Cells were incubated with 300 or 1000 nM of BMS-754807 for 1 hr prior to stimulation. Densitometry quantification is presented as average fold-change ± SEM in ratio of phospho/total protein relative to the control condition (white bar). Blots are representative of n≥3 independent experiments. Significance was calculated using a two-sided one-sample *t*-test. **(B)** Immunoblotting for phosphorylated Tyr$^{1135/1136}$ (p-Y1135/1136), Tyr$^{1250/1251}$ (p-Y1250/1251) on IGF-1R immunoprecipitated from WCL of R$^-$ cells expressing either IGF-1R WT or KR mutant that were serum-starved and stimulated with IGF-1. Immunoprecipitates were incubated with kinase buffer containing ATP or not. The ratio of phospho/total protein was quantified using densitometry and graphs present average fold-change ± SEM relative to the control condition (WT, 0 min IGF-1). Blots are representative of n=3 independent experiments. Significance was calculated using a two-sided one-sample *t*-test. Protein input is shown in immunoblots for each IGF-1R phosphotyrosine, total IGF-1R, phosphorylated Ser^{473} (p-S473) and total AKT, and ERK1/2 phosphorylated on Thr^{202}/Tyr^{204} (p-T202/Y204) and total ERK1/2. Blots are representative of n=3.
P-values are indicated by *<0.05, **<0.01, ***<0.001.

Previous studies have shown that the $Tyr^{1250/1251}$ site is required for cooperative IGF-1R and adhesion signalling (Kiely et al., 2005) and that IGF-1R kinase activity is influenced by adhesion signalling and adhesion-associated kinases (Stanicka et al., 2018, Taliaferro-Smith et al., 2015) (Chapter 3). Therefore, we asked whether adhesion-activated kinases (FER, FAK and Src) contribute to $Tyr^{1250/1251}$ phosphorylation. To test this, we used Cal-51 breast cancer cells in which IGF-1 and adhesion signalling are active (Mahauad-Fernandez and Okeoma, 2017, Bajrami et al., 2018), and measured IGF-1-induced phosphorylation on the $Tyr^{1250/1251}$ and also the $Tyr^{1135/1136}$ sites, which are required for full kinase activation, in the presence of either the IGF-1R kinase inhibitor BMS-754807, a FER kinase inhibitor (AP-26113, Chapter 3), a FAK kinase inhibitor (PF-573228), or a Src kinase inhibitor (PP2) (Figure 5.5). We observed that IGF-1-induced phosphorylation on both sites was decreased by BMS-754807, AP-26113 and PF-573228 but not by PP2 (Figure 5.5). Thus, IGF-1R, FER or FAK inhibition can all suppress IGF-1R autophosphorylation and full kinase activation.

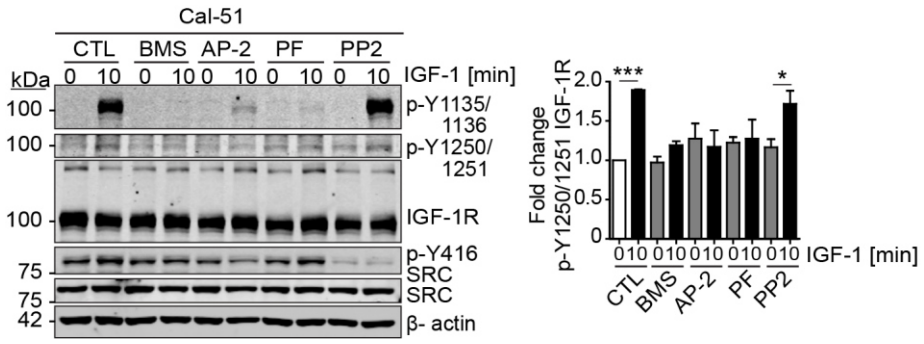


Figure 5.5: Adhesion kinases FER and FAK contribute to Tyr$^{1250/1251}$ IGF-1R phosphorylation.

Immunoblotting for phosphorylated Tyr$^{1135/1136}$ IGF-1R (p-Y1135/1136), phosphorylated Tyr$^{1250/1251}$ IGF-1R (p-Y1250/1251), total IGF-1R, Src phosphorylated on Tyr^{416} (p-Y416) and total Src in WCL of Cal-51 cells that were serum-starved, exposed to kinase inhibitors for 1hr BMS (IGF-1R inhibitor), AP-2 (FER inhibitor), PF (FAK inhibitor), PP2 (Src-inhibitor) as described in text, and stimulated with 50 ng/ml IGF-1. Densitometry quantification of phosphorylated Tyr$^{1250/1251}$ IGF-1R is presented as average fold-change ± SEM in ratio of phospho/total protein relative to the control condition (white bar). Blots are representative of n≥3 independent experiments. Significance was calculated using a two-sided one-sample or two-sample *t*-test. *P*-values are indicated by *<0.05, **<0.01, ***<0.001.

We furthermore investigated, whether IGF-1-induced phosphorylation on Tyr^{950}, Tyr^{1131}, $Tyr^{1135/1136}$ and $Tyr^{1250/1251}$ IGF-1R was dependent on adhesion signalling, as IGF-1R autophosphorylation was reduced in cells that were detached from the substratum (Chapter 3). IGF-1-stimulated phosphorylation of the Tyr^{950}, Tyr^{1131}, $Tyr^{1135/1136}$ and $Tyr^{1250/1251}$ sites were reduced by detachment of R^- cells expressing WT IGF-1R (Figure 5.6A), as well as of Cal-51 and DU-145 cancer cells (Figure 5.6B). IGF-1-induced activation of AKT and ERK1/2 was also reduced in detached cells compared to adherent cells (Figure 5.6).

We conclude that both IGF-1R and adhesion signalling are essential for maximal phosphorylation of the IGF-1R on $Tyr^{1250/1251}$, and confirm that overall IGF-1R autophosphorylation and activation are enhanced by cell adhesion.

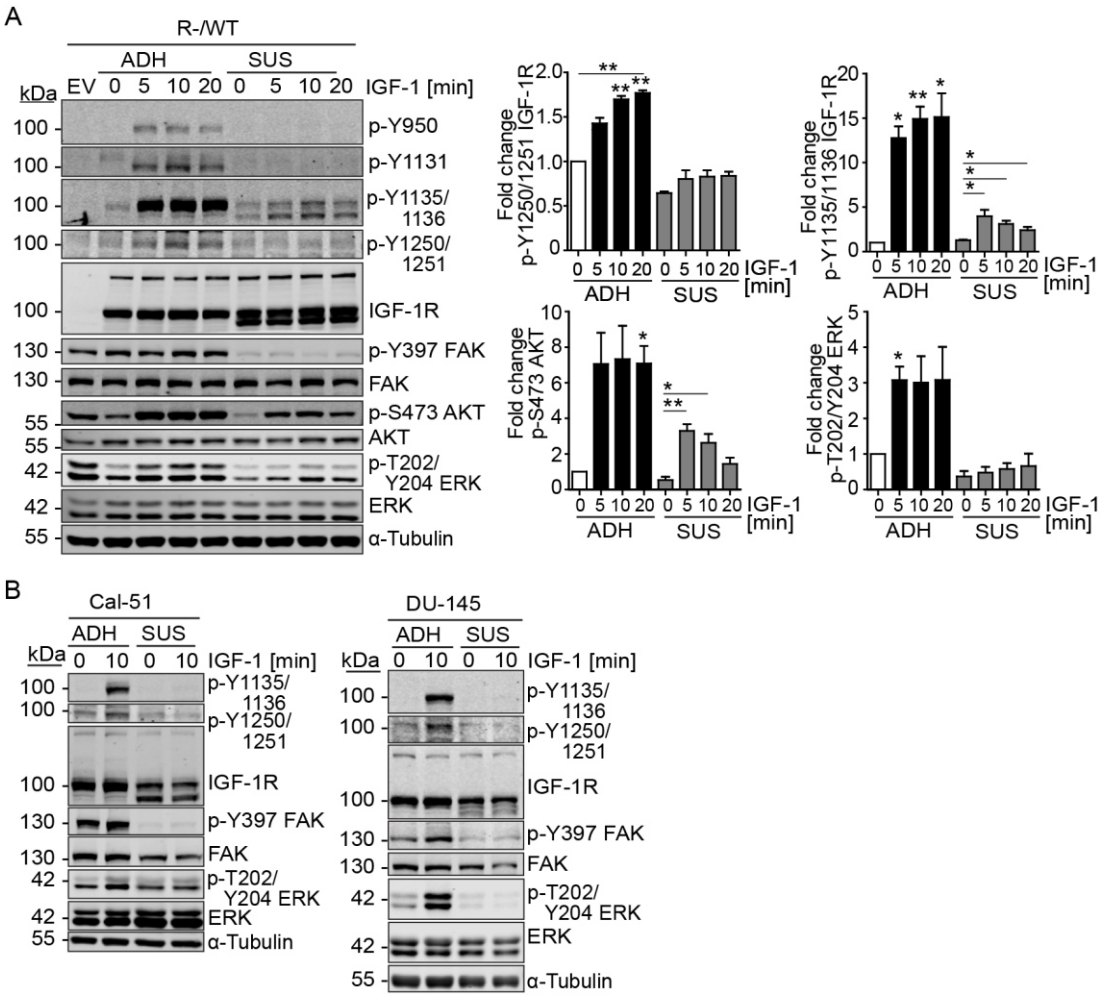


Figure 5.6: Adhesion signalling is required for Tyr$^{1250/1251}$ IGF-1R phosphorylation.

(A) Immunoblotting for the indicated phosphorylated forms of IGF-1R, total IGF-1R, FAK phosphorylated on Tyr^{397} (p-Y397), total FAK, AKT phosphorylated on Ser^{473} (p-S473), ERK1/2 phosphorylated on Thr^{202} and Tyr^{204} (p-T202/Y204), and total AKT and ERK1/2 in WCL of R^{-}/WT cells stimulated with 10 ng/ml IGF-1 for the indicated times following serum starvation. Suspension cells were detached after 3 hr and left in suspension for 1 hr. Densitometry quantification is presented as the average fold-change ± SEM in ratio of phospho/total protein relative to the control condition. Blots are representative of n=3 independent experiments. Significance was calculated using a two-sided one-sample or two-sample *t*-test. **(B)** Immunoblotting of phosphorylated Tyr$^{1135/1136}$ IGF-1R (p-Y1135/1136), Tyr$^{1250/1251}$ IGF-1R (p-Y1250/1251), total IGF-1R, FAK phosphorylated on Tyr^{397} (p-Y397), total FAK, ERK1/2 phosphorylated on Thr^{202}/Tyr^{204} (p-T202/Y204) and total ERK1/2 of cancer cells serum-starved and stimulated with 50 ng/ml IGF-1 for indicated times. The blots are representative of n=3 independent experiments.
P-values are indicated by *<0.05, **<0.01, ***<0.001.

5.3.3 A Tyr$^{1250/1251}$ phosphomimetic mutant IGF-1R is fully active, but rapidly turned over

The next question we asked was how the phosphorylation on the Tyr$^{1250/1251}$ site contributes to IGF-1R function and signalling. To address this, we generated a phosphomimetic for this site, a mutant IGF-1R with tyrosines Tyr$^{1250/1251}$ substituted by negatively charged glutamic acids (EE mutant). When transiently transfected into either R$^-$ cells or the three different cancer cell lines in which the IGF-1R was knocked-out by CRISPR technology (MCF-7, MDA-MB-231, DU-145 KO; Chapter 4), the EE mutant was consistently expressed at significantly lower levels than either the WT IGF-1R or FF mutant (Figure 5.7A). A similar pattern of lower expression was observed in R$^-$ cells stably expressing the EE mutant (Figure 5.7B), although mRNA expression for the transfected WT, FF and EE constructs were similar (Figure 5.7C). Single mutation of either Tyr^{1250} or Tyr^{1251} to glutamic acid was also sufficient to impair receptor protein expression compared to WT IGF-1R, as shown for MCF-7 in Figure 5.7D.

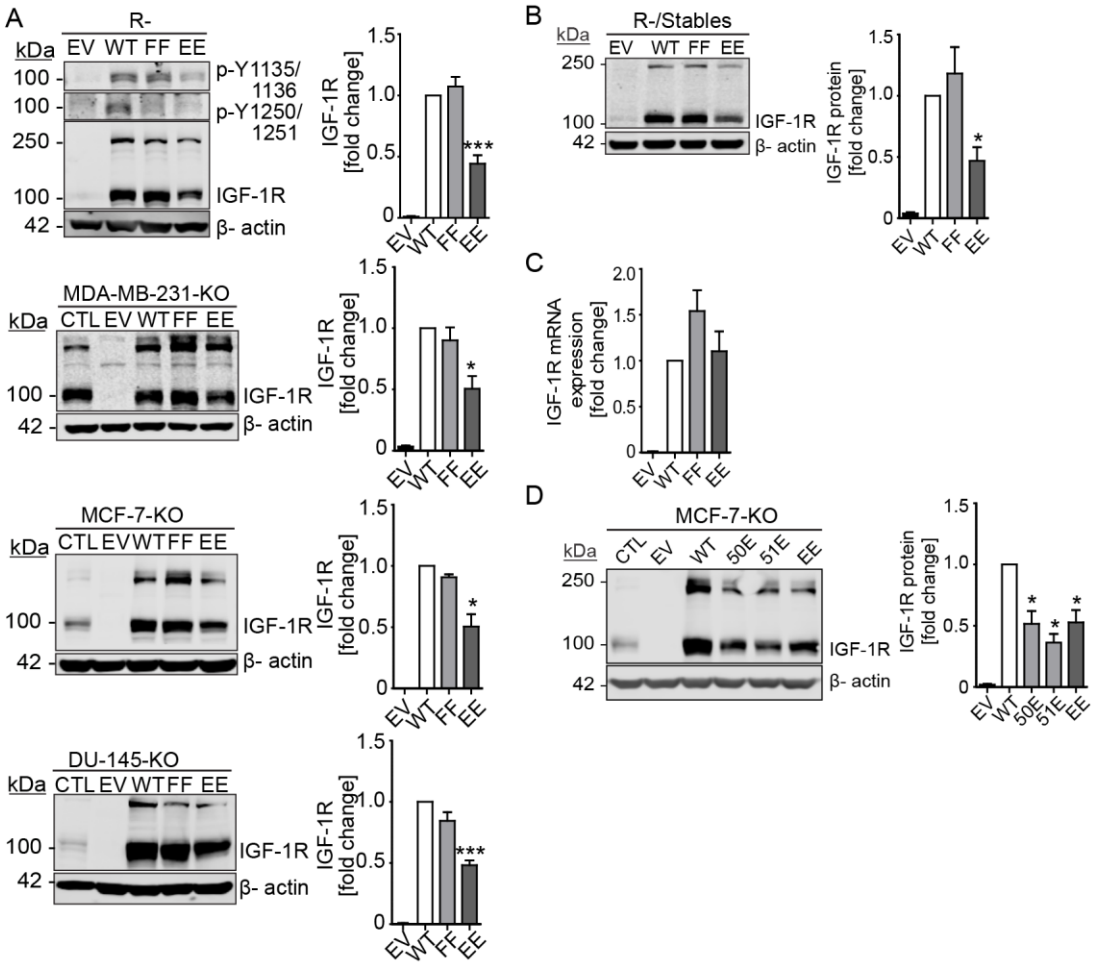


Figure 5.7: Double or single mutations of IGF-1R Tyr$^{1250/1251}$ to glutamic acid cause lower IGF-1R protein expression, but do not affect mRNA levels.

(A) Immunoblotting for phosphorylated Tyr$^{1135/1136}$ (p-Y1135/1136) and Tyr$^{1250/1251}$ (p-Y1250/1251) IGF-1R and total IGF-1R in WCL of R$^-$ cells and total IGF-1R in WCL of MCF-7-KO, MDA-MB-231-KO and DU-145-KO cells expressing the WT, FF or EE IGF-1R. Densitometry quantification is presented as the average fold-change ± SEM in IGF-1R protein relative to the control condition. Blots are representative of n≥3 independent experiments. Significance was calculated using a two-sided one-sample *t*-test. **(B)** Immunoblotting for IGF-1R in WCL of R- cells stably expressing IGF-1R WT, FF or EE. Fold change in IGF-1R protein were measured by densitometry and presented as mean± SEM fold change relative to control condition (white bare; set to 1); significance as calculated using a two sided single sample *t*-test Blots are representative of n=3. **(C)** IGF-1R mRNA expression in R$^-$ cells transiently expressing the IGF-1R WT, FF or EE was assessed by qRT-PCR. CT values were normalized to actin as housekeeping gene. Data is presented as mean± SEM fold change relative to control condition (set to 1; white bar). Significance was calculated from n=3 independent experiments using a single sample *t*-test **(D)** Immunoblotting for IGF-1R in whole cell lysates of MCF-7-KO cells transiently expressing IGF-1R WT, 1250E, 1251E or EE. Fold change in IGF-1R protein was measured by densitometry and presented as mean± SEM fold change relative to the control conditions (set to 1). Significance was calculated using a single sample *t*-test. Blots are representative of n=3 independent experiments. *P*-values are indicated by *<0.05, **<0.01, ***<0.001.

Although present at lower levels in cells, the EE mutant was functional and mediated IGF-1-stimulated kinase activation and downstream signalling. Cells expressing either the WT or EE IGF-1R exhibited similar IGF-1 stimulated AKT and ERK1/2 activation (Figure 5.8A). The Y12501F/Y1251F (FF) mutant exhibited lower IGF 1R and ERK1/2 activation than WT (Figure 5.8A), which is consistent with previous studies (Leahy et al., 2004). Transient overexpression of WT, FF or EE in MDA-MB-231-KO cells also demonstrated that the activation of EE was comparable to WT IGF-1R, whereas it was higher than FF (Figure 5.8B).

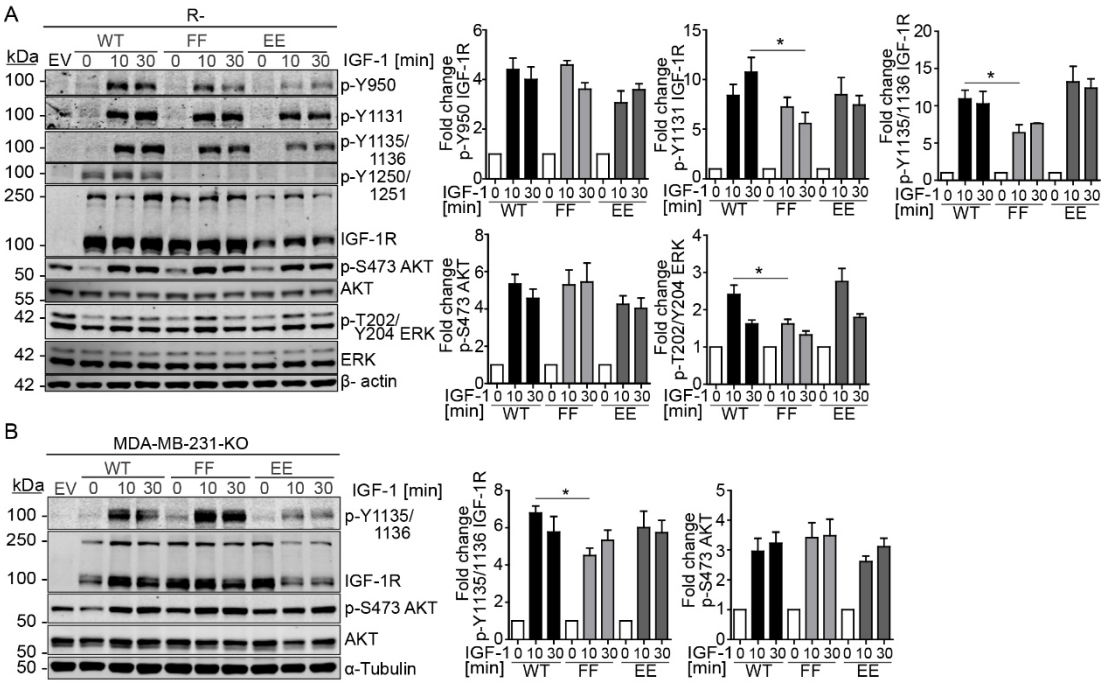


Figure 5.8: The EE mutant exhibits similar IGF-1R and downstream activation to WT receptor.

(**A**) Immunoblotting for the indicated phosphorylated forms of IGF-1R, total IGF-1R, AKT phosphorylated on Ser^{473} (p-S473), ERK1/2 phosphorylated on Thr^{202} and Tyr^{204} (p-T202/Y204) in WCL of R^- cell transiently overexpressing IGF-1R WT, FF or EE and stimulated with 10 ng/ml IGF-1 for the indicated times following serum starvation. Densitometry quantification is presented as the average fold-change ± SEM in ratio of phospho/total protein relative to the control condition (white bar). Blots are representative of n=3 independent experiments. Significance was calculated using a two-sided two-sample *t*-test. **(B)** Immunoblotting for phosphorylated $Tyr^{1135/1136}$ IGF-1R (p-Y1135/1136) and total IGF-1R, AKT phosphorylated on Ser^{473} (p-S473) and total AKT in WCL of MDA-MB-231-KO cells transiently overexpressing the IGF-1R WT, FF or EE and stimulated with 10 ng/ml IGF-1 for the indicated times following serum starvation. Densitometry quantification shows the average fold-change ± SEM in ratio of phospho/total protein relative to the control (white bar). Blots are representative of n≥3 independent experiments. Significance was calculated using a two-sided two-sample *t*-test. *P*-values are indicated by *<0.05, **<0.01, ***<0.001.

It was demonstrated before, that the IGF-1R FF displayed lower IGF-1R kinase activity than the WT IGF-1R (O'Connor et al., 1997). Thus we next used *in vitro* kinase assays to compare the IGF-1R kinase activity of EE with WT and the FF mutant. *In vitro* EE kinase activity was similar to WT, whereas FF kinase activity was lower than WT (Figure 5.9).

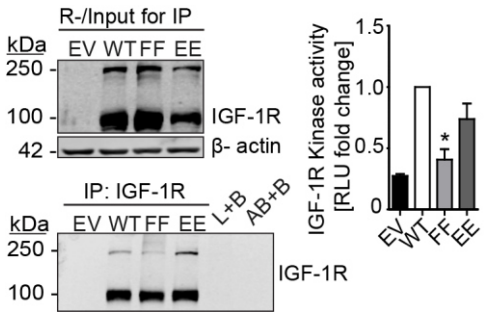


Figure 5.9: IGF-1R EE mutant exhibits a similar kinase activity to the WT IGF-1R.

Immunoblotting for total IGF-1R in WCL of R^- cells transiently overexpressing IGF-1R WT, FF or EE used to determine protein input to IP for *in vitro* kinase assays followed by immunoblotting of immunoprecipitated IGF-1R (all adjusted to EE protein level). Kinase assay data are presented as average fold-change ± SEM in kinase activity (measured in relative luciferase units: RLU) relative to IGF-1R WT (set to 1). Blots are representative of n=3 independent kinase preparations. Significance was calculated using two-sided one-sample *t*-test. *P*-values are indicated by *<0.05, **<0.01, ***<0.001.

The lower cellular abundance of the EE mutant compared to WT and FF suggested that $Tyr^{1250/1251}$ phosphorylation may influence the translation or stability of the IGF-1R protein. To rule out the possibility that low EE protein was due to impaired protein synthesis, we used cycloheximide (CHX) to suppress protein synthesis, and then assessed levels of newly synthesized protein over time (Figure 5.10). From these experiments, it was clear that levels of WT and both IGF-1R mutants were expressed at similar levels following CHX exposure (Figure 5.10), thereby indicating similar protein synthesis.

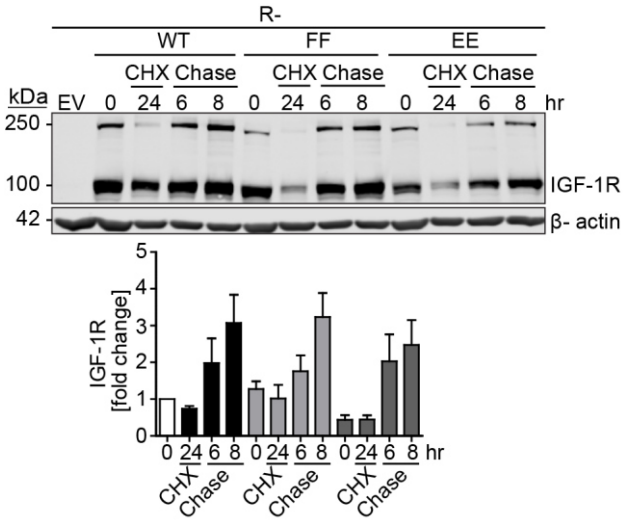


Figure 5.10: IGF-1R mutants are synthesized at a similar rate to the WT receptor.

Immunoblotting for IGF-1R in whole cell lysates of R- cells transiently expressing IGF-1R WT, FF and EE cultured in control medium (0 hr) or medium with Cycloheximide (50 μg/ml CHX) for 24 hr followed by culture in complete medium (chase) for 6 or 8 hr. Densitometry quantification is presented as the average fold-change ± SEM in IGF-1R protein relative to the control condition (white bar; WT IGF-1R UT). Blots are representative of n=3 independent experiments. Significance was calculated using one-way ANOVA.

Since the reduced levels of IGF-1R EE protein were not due to impaired IGF-1R synthesis, we next tested whether inhibition of proteasomal or lysosomal activity could restore IGF-1R EE protein in cells. We observed that inhibition of proteasomal activity with MG-132 for 6hr restored the EE β chain to protein levels that were similar to WT and FF IGF-1R in control cells (0 hr), and in addition, the pro-receptor was also recovered (Figure 5.11A). Lysosomal inhibition with E64D+Leupeptin or Chloroquine (CQ), while successfully inhibiting LC3 degradation, did not affect EE protein abundance (Figure 5.11B) indicating that the EE mutant is not more susceptible to lysosomal degradation than the WT receptor.

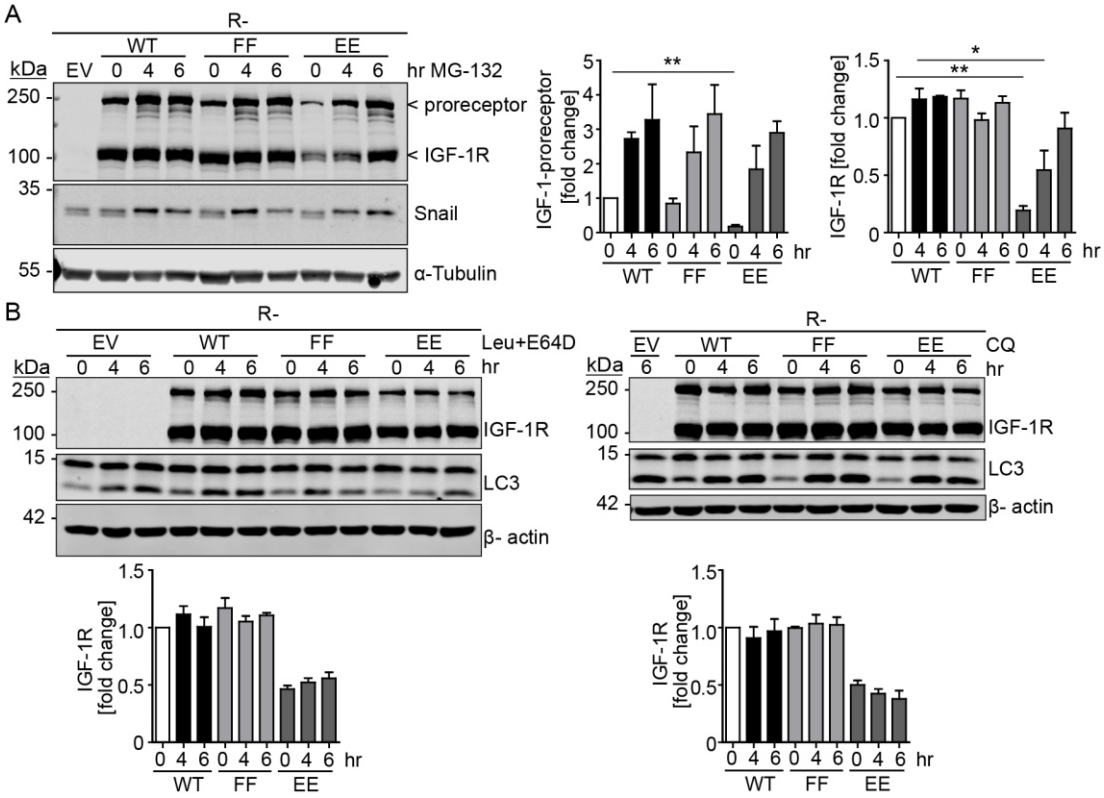


Figure 5.11: Phosphorylation of Tyr$^{1250/1251}$ IGF-1R targets the receptor for proteasomal degradation.

(A) Immunoblotting for total IGF-1R and SNAIL in WCL of R$^-$ cells transiently expressing IGF-1R WT, FF or EE cultured in control medium (0 hr) or medium containing 10 μM MG-132 for 4 or 6 hr. Densitometry quantification is presented as the average fold-change ± SEM in IGF-1R protein relative to the control condition (white bar; WT 0 hr). Blots are representative of n=3 independent experiments. Significance was calculated using a two-sided one-sample or two-sample *t*-test. **(B)** Immunoblotting for total IGF-1R and LC3 in WCL of R$^-$ cells transiently expressing IGF-1R WT, FF or EE cultured in control medium (0 hr), or medium containing either 2 μM Leupetin+ 2.6 μM E64D (Leu+E64D) or 50 μM Chloroquine (CQ) for 4 or 6 hr. Densitometry quantification is presented as average fold-change ± SEM in IGF-1R protein relative to the control condition (white bar; WT 0 hr). Blots are representative of n=3 independent experiments. Significance was calculated using a two-sided one-sample or two-sample *t*-test.
P-values are indicated by *<0.05, **<0.01, ***<0.001.

Since the inhibition of the proteasomal activity recovered the IGF-1R EE protein, it suggests that $Tyr^{1250/1251}$ IGF-1R phosphorylation enhances the receptor degradation. Protein degradation of the IGF-1R is tightly linked to ubiquitination (Sehat et al., 2007). We therefore tested whether phosphorylation of $Tyr^{1250/1251}$ IGF-1R increases IGF-1R ubiquitination. We observed that significantly more ubiquitin was immunoprecipitated with the IGF-1R EE mutant compared to the WT, and that the FF IGF-1R is less ubiquitinated than the WT IGF-1R (Figure 5.12A), indicating that the EE IGF-1R is degraded at higher rate than the WT or FF IGF-1R and that the FF is degraded less than the WT. We further investigated whether stimulation of R^- cells with high or low IGF-1 concentrations influenced the degradation of the EE compared to the WT IGF-1R and FF. This demonstrated that IGF-1 stimulation at either high or low IGF-1 concentrations resulted in a similar reduction in WT and EE receptor at 6 and 12 hours, whereas FF abundance was not significantly reduced after 6 hours and was comparable to unstimulated cells. Thus, the FF mutant appears to be protected from degradation (Figure 5.12B).

Taken together, these results demonstrate that the IGF-1R EE mutant is kinase active and responsive to IGF-1 but is less stable than WT. The data suggest that $Tyr^{1250/1251}$ phosphorylation accelerates IGF-1R protein turnover.

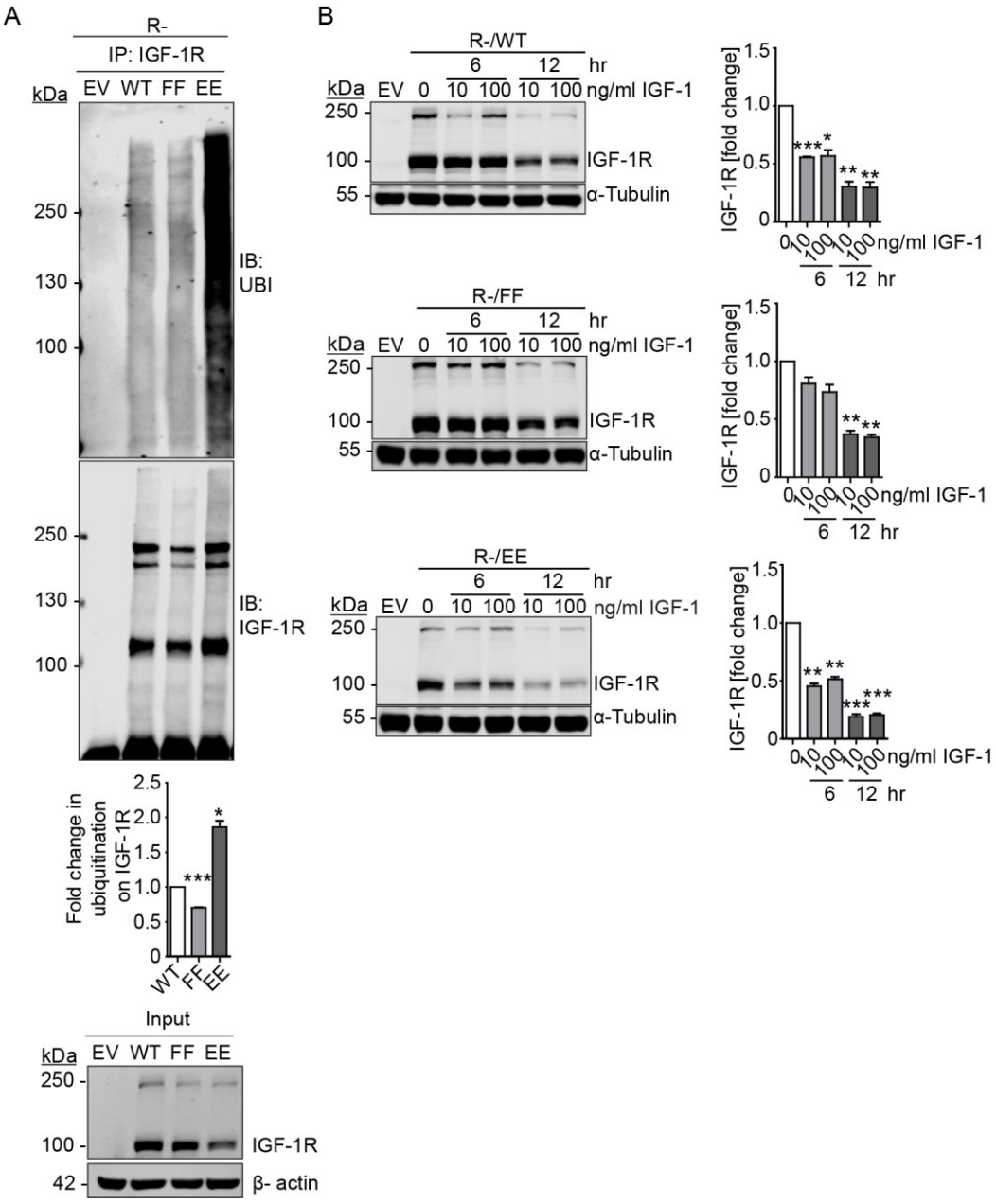


Figure 5.12: Tyr$^{1250/1251}$ phosphorylation facilitates IGF-1R protein turnover.

(A) Immunoblotting for ubiquitin on IGF-1R immunoprecipitated from WCL of R$^-$ cells transiently overexpressing WT, FF or EE IGF-1R followed by immunoblotting for IGF-1R. Immunoblotting for total IGF-1R in WCL of R$^-$ cells transiently overexpressing IGF-1R WT, FF or EE used to determine protein input to IP for ubiquitination assay (all adjusted to EE protein level). Densitometry quantification is presented as average fold change ± SEM in ratio of ubiquitin/IGF-1R protein relative to control condition (white bar, IGF-1R WT). Blots are representatives of from n=3 independent immunoprecipitations. **(B)** Immunoblotting for IGF-1R in WCL from R$^-$ cells transiently expressing IGF-1R WT, FF or EE stimulated with the indicated concentrations and times of IGF-1 stimulation. Densitometry quantification is presented as average fold change ± SEM in IGF-1R protein relative to control condition. Blots are representative of n=3 independent experiments. Significance was calculated using a two-sided one-sample or two sample *t*-test. *P*-values are indicated by *<0.05, **<0.01, ***<0.001.

5.3.4 Tyr$^{1250/1251}$ phosphorylation promotes IGF-1R translocation to the Golgi apparatus

The EE mutant IGF-1R was highly active in signalling even with low levels of protein (Figure 5.8, Figure 5.9), so we next investigated its sub-cellular localisation to gain further insights into the function of IGF-1R Tyr$^{1250/1251}$ phosphorylation. We also compared IGF-1-stimulated EE internalisation and trafficking with the WT and FF receptors.

As expected, WT was mainly located on the cell membrane in serum-deprived cells (Figure 5.13A; 0 min IGF-1; zoom b), however, we observed that a pool of IGF-1R was located at the perinuclear region (Figure 5.13A; 0 min IGF-1; zoom a) of these cells. In IGF-1-stimulated cells, both WT and EE receptors were visible in large vesicles. Over time these vesicles appeared to accumulate at the perinuclear region and were less evident at the plasma membrane (Figure 5.13A; 10 min IGF-1). These IGF-1R-containing vesicles were less evident in cells expressing the FF mutant, in which the receptor was predominantly located at the plasma membrane in both serum-deprived cells and in IGF-1 stimulated cells (Figure 5.13A; 0 and 10 min IGF-1). The relative translocation patterns of IGF-1R WT and EE from the membrane to perinuclear region of the cells observed in Figure 5.13A were illustrated by showing the intensity in fluorescence signal along a line that was drawn diagonally from cell membrane to cell membrane through the nucleus (Figure 5.13B). In the absence of IGF-1 (0 min), cells expressing the EE mutant exhibited a clear peak in green fluorescence signal close to the nucleus (blue line). This peak was less prominent in cells expressing WT and was not visible with the FF mutant. Over time cells expressing either WT or EE displayed a shift in green

signal towards the blue line and a reduction in green signal intensity at the beginning of the line (representing the plasma membrane) (Figure 5.13B).

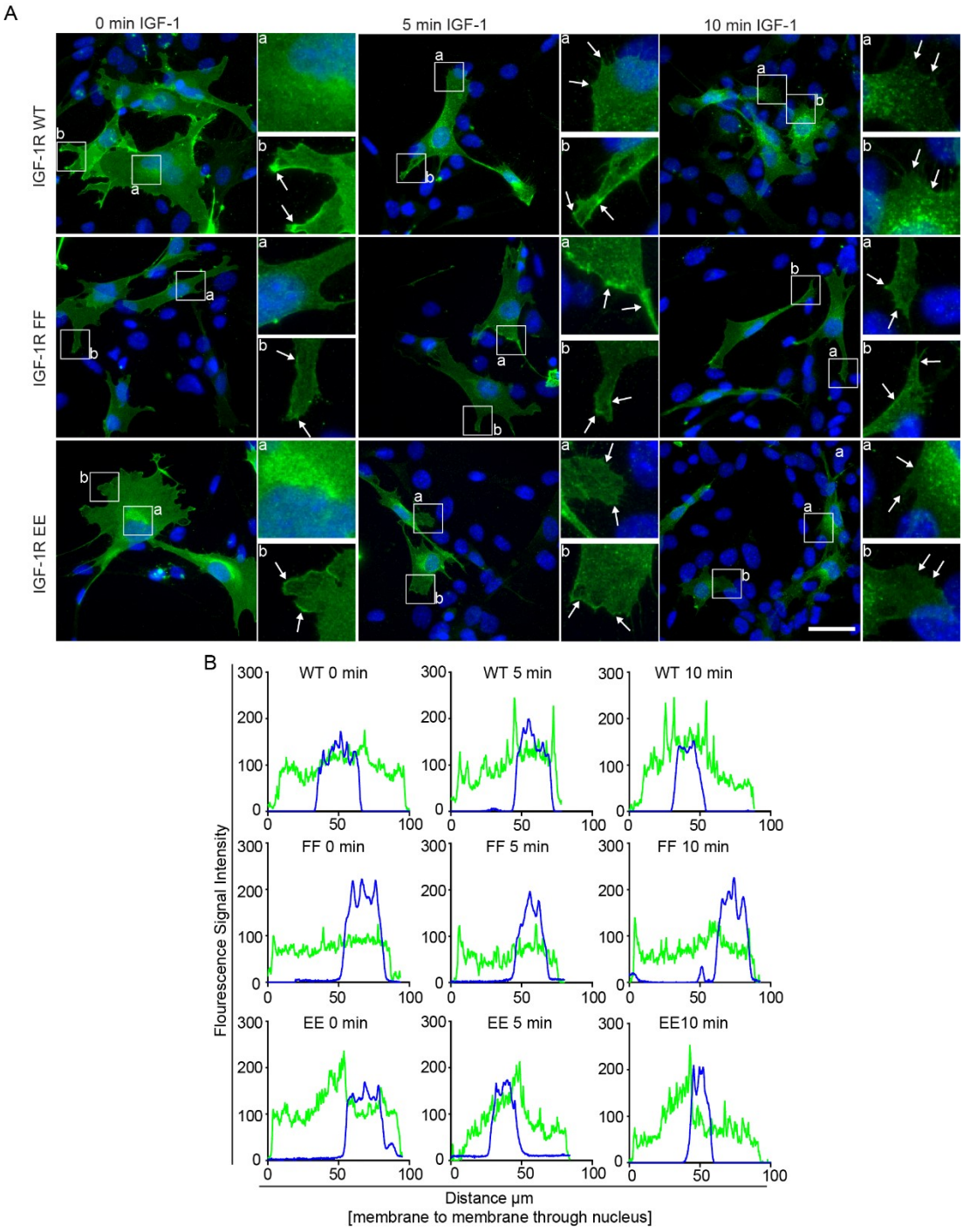


Figure 5.13: Tyr$^{1250/1251}$ phosphorylation promotes IGF-1R translocation to the perinuclear region.

(A) Immunofluorescence of R$^-$ cells transiently expressing WT, FF or EE IGF-1R showing IGF-1R (green) and nuclei (blue) following serum starvation (0 min IGF-1) or IGF-1 stimulation (5 and 10 min). Images are representative of n≥4 independent experiments with a 50 μm scale bar. **(B)** Staining intensity (Y-axis) of IGF-1R (green line) in relation to the nuclear area (blue line) measured using the RGB plot profiler from ImageJ software. Representative cells were used to draw a line (X-axis) from the cell membrane through the nucleus to the membrane.

Immunofluorescence analysis showed that both the IGF-1R WT and EE rapidly translocated from the plasma membrane to the perinuclear region in response to IGF-1. Therefore, we next assessed receptor internalisation using in-cell western assays to quantify the ratio of IGF-1R present at the plasma membrane relative to total receptor in cells stimulated with IGF-1. Whereas the amounts of the receptor on the cell surface declined in response to IGF-1 in cells expressing either the WT or EE receptors, the cell surface amounts of FF receptors were not altered (Figure 5.14).

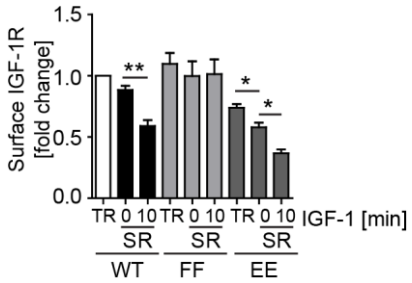


Figure 5.14: IGF-1 induces surface depletion in the IGF-1R WT and the EE.

In-cell-western from R^- cells transiently transfected with WT, FF or EE IGF-1R probed for total (TR) and surface (SR) IGF-1R. Densitometry quantification is presented as average fold- change ± SEM in IGF-1R surface protein relative to the control condition (white bar; TR in WT). Graphs were generated from n=3 independent experiments. Significance was calculated using a two-sided one-sample or two-sample *t*-test. *P*-values are indicated by *<0.05, **<0.01, ***<0.001.

To test whether WT and EE were being actively internalised into vesicles, we used an antibody detecting the α-chain-IGF-1R (α-IR-3) that competes with IGF-1 for binding to the α-subunit and is known to induce receptor internalisation (Arteaga et al., 1989). R^- cells expressing the WT, FF or EE IGF-1R were serum-starved for 4 hr and cultured with the α-IR-3 antibody for 30 min either at 37˚C or on ice, which inhibits cellular processes, including endocytosis (Figure 5.15). The cells were fixed and stained with a primary antibody to detect the β-chain IGF 1R and secondary antibody staining against α-IR-3 antibody and β-chain IGF 1R. Co-localisation of α-IR-3 with the β-chain was demonstrated for the α-IR-3 antibody that was internalised in vesicles after 30 min at 37°C, in cells expressing the IGF-1R WT or EE mutant. For cells expressing the FF mutant co-localisation of α-IR-3 with the β-chain was observed at the plasma membrane (Figure 5.15).

We conclude that activated WT IGF-1R and EE mutant were rapidly internalised into intracellular vesicles that accumulate at the perinuclear region over time. The observation that the FF mutant neither accumulated within vesicles nor underwent post-endocytotic trafficking suggests that phosphorylation on $Tyr^{1250/1251}$ is required for internalisation and accumulation of the IGF-1R at the perinuclear region.

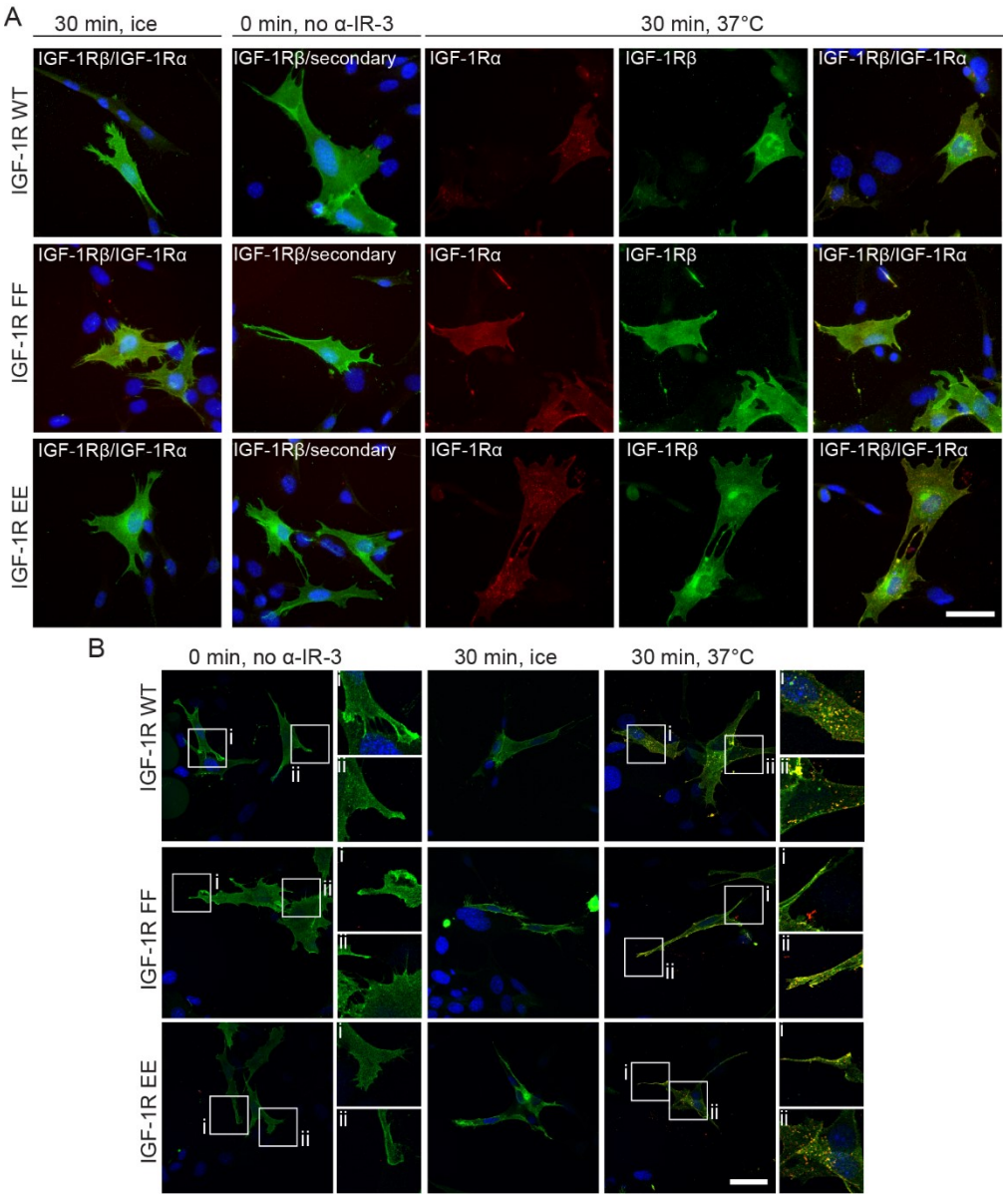


Figure 5.15: Receptor activation induces internalisation of IGF-1R WT and EE into large vesicles.

(A), (B): Immunofluorescence of R^- cells transiently expressing the WT, FF or EE IGF-1R that were serum for 4 hr or incubated with an antibody detecting the IGF-1R α-chain (α-IR-3 100 ng/ml) for 30 min either on ice or at 37˚C. Co-localisation of IGF-1R α-IR-3 antibody (red) and IGF-1Rβ (green) is indicated as a yellow signal. **(A)** Multiple images were acquired using the SPOT charge-coupled device camera mounted on a Nikon T600 fluorescent microscope. Representative images of n=2 independent experiments are shown with a 50 μM scale bar. **(B)** Multiple images (n≥3) of cells were acquired using the Fluoview FV1000 confocal laser scanning microscope. Representative images from n=2 independent experiments. Scale bar is 50 μm.

Post-endocytic trafficking of surface receptors and proteins to the Golgi-apparatus has been described as retrograde trafficking and a process that may be important for cell signalling (Johannes and Popoff, 2008, Ye et al., 2016). We therefore further investigated IGF-1R co-localisation with the *cis*-Golgi marker GM130 in cells expressing WT, FF or EE mutant. The WT and EE IGF-1R co-localised with GM130 at the *cis*-Golgi compartment over time (Figure 5.16A). In addition, we used a biotin-VVA lectin, which labels *N*-acetylgalactosamine and is a marker for both *trans*- and *cis*-Golgi (co-localisation with GM130; Figure 5.16B), and co-localisation of WT and EE IGF-1R was also evident (Figure 5.16C). The EE mutant was also observed at the Golgi apparatus in serum-starved cells, suggesting that phosphorylation on this site was sufficient in part, for IGF-1R translocation to the Golgi.

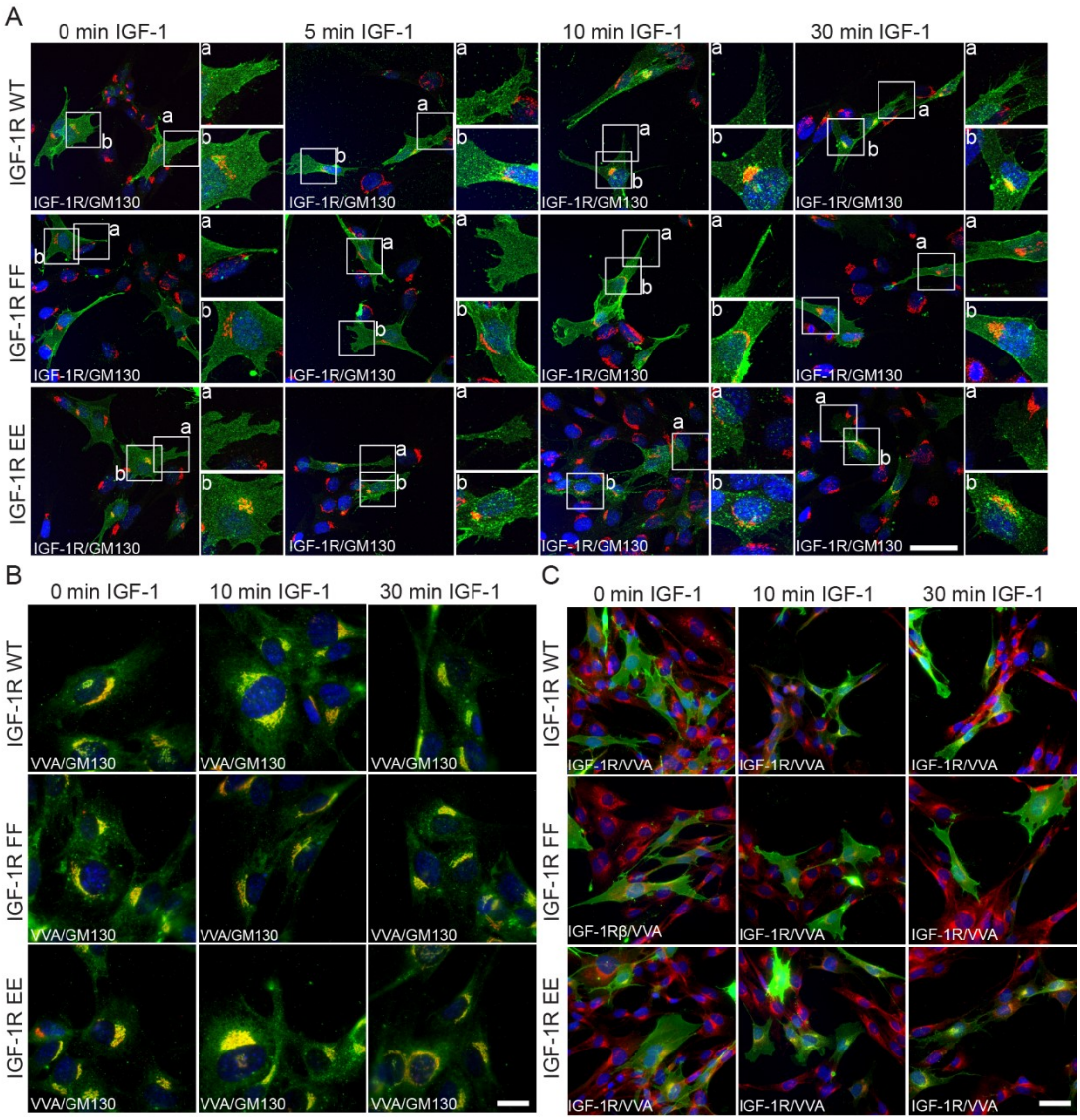


Figure 5.16: Tyr$^{1250/1251}$ phosphorylation mediates IGF-1R translocation to the Golgi-apparatus.

(A) Immunofluorescence of R$^-$ cells expressing WT, FF or EE IGF-1R that were either serum-starved (0 min IGF-1) or stimulated with IGF-1 (5, 10, 30 min IGF-1) showing IGF-1R in green, cis-Golgi (GM130) in red and the nucleus (Hoechst) in blue. Images were acquired as 0.5 μm z stacks using the Fluoview FV1000 confocal laser scanning microscope and are displayed as maximum intensity projection with a 50 μm scale bar. Images are representatives of n≥3 independent experiments. **(B), (C):** Immunofluorescence of R$^-$ cells expressing WT, FF or EE IGF-1R following IGF-1 stimulation for the indicated times showing **(B)** VVA (green), the Golgi apparatus (VVA/GM130: red) **(C)** IGF-1R (green), the Golgi apparatus (VVA/GM130: red) and the nucleus (blue). Multiple images (n≥3) were acquired using a Nikon T600 microscope. Representative images of n=2 are shown with and **(B)** a 20 μm scale bar and **(C)** a scale bar a 50 μm scale bar.

To further test whether WT and EE IGF-1R were present in the Golgi apparatus, we used Brefeldin A (BFA), to induce *cis*-Golgi fragmentation (Lippincott-Schwartz et al., 1989) in R^- cells expressing the WT, FF or EE receptors. Fragmentation of the *cis*-Golgi using BFA resulted in lower levels of WT and EE mutant expression (Figure 5.17), whereas the IGF 1R FF mutant was not affected.

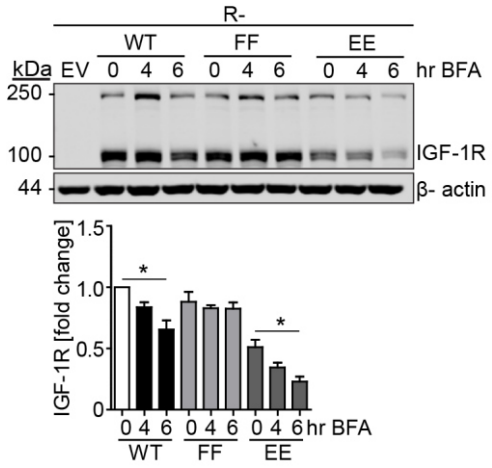


Figure 5.17: Disruption of the Golgi apparatus causes decreased levels of IGF-1R WT and EE, but not FF mutant.

Immunoblotting for total IGF-1R in WCL of R^- cells transiently expressing IGF-1R WT, FF or EE mutant cultured in control medium (0 hr) or medium containing 10 μg/ml Brefeldin A (BFA) for 4 and 6 hr. Densitometry quantification is presented as average fold- change ± SEM in IGF-1R protein relative to the control condition (white bar, WT 0 hr). Blots are representative of n=3 independent experiments. Significance was calculated using a two-sided one-sample or two-sample *t*-test. *P*-values are indicated by *<0.05, **<0.01, ***<0.001.

Recently it was demonstrated that the IGF-1R translocates to the nucleus in response to IGF-1 (Aleksic et al., 2010, Aleksic et al., 2018). The level of IGF-1R nuclear translocation was found to be proportional to the ligand-induced IGF-1R kinase activation. Furthermore the translocation was inhibited using pharmacological inhibitors blocking the IGF-1R activation or internalisation. We observed IGF-1 rapidly induced IGF-1R WT and EE translocation into the perinuclear region and thus, tested whether $Tyr^{1250/1251}$ phosphorylation may also be required for further translocation to the nucleus. However, IGF-1R WT, FF and EE were all found in both the cytosolic as well as the nuclear fraction, indicating that $Tyr^{1250/1251}$ phosphorylation is not required for nuclear translocation (Figure 5.18A). Furthermore, IGF-1R WT, FF and EE were observed in both the soluble phase as well as the insoluble phase of the nucleus, suggesting that $Tyr^{1250/1251}$ phosphorylation is not needed for binding to the chromatin (Figure 5.18B).

Taken together these results indicate that IGF-1-induced internalisation and accumulation of the IGF-1R in the Golgi apparatus requires phosphorylation on $Tyr^{1250/1251}$, however, translocation to the nucleus does not.

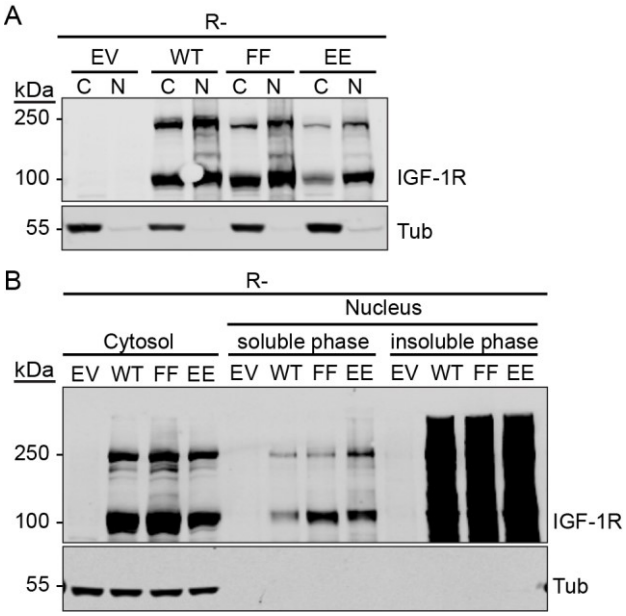


Figure 5.18: Tyr$^{1250/1251}$ phosphorylation is not required for nuclear translocation of the IGF-1R.

(A) Immunoblotting for IGF-1R in the cytosolic (C) and nuclear (N) fractions of R$^-$ cells overexpressing the IGF-1R WT, FF or EE mutant. Blots are representatives of n=2 independent experiment. **(B)** Immunoblotting for IGF-1R in the cytosolic fraction, as well as the soluble and insoluble nuclear fraction of R$^-$ cells overexpressing the IGF-1R WT, FF or EE mutant; n=1.

5.3.5 Tyr$^{1250/1251}$ phosphorylation and adhesion signals promote IGF-1R presence in and signalling from the Golgi

The Tyr$^{1250/1251}$ site is required to support a transformed phenotype, cancer cell survival, cell migration, tumour growth and metastasis *in vivo* (Brodt et al., 2001, Samani et al., 2007, Osher and Macaulay, 2019). Golgi-derived signalling is implicated in cell migration (Millarte and Farhan, 2012), so we hypothesized that Tyr$^{1250/1251}$ phosphorylation and IGF-1R Golgi location may be a feature of migratory cancer cells.

To test this, IGF-1R localisation in low-migratory MCF-7 cancer cells was compared with migratory MDA-MB-231 and HS-578T cells which also exhibited relatively high IGF-1R Tyr$^{1250/1251}$ phosphorylation levels (Figure 5.3). The IGF-1R was evident at sites of focal adhesion in MCF-7 cells (arrows) while in MDA-MB-231 and HS-578T cells it was also clearly located within the Golgi apparatus (Figure 5.19).

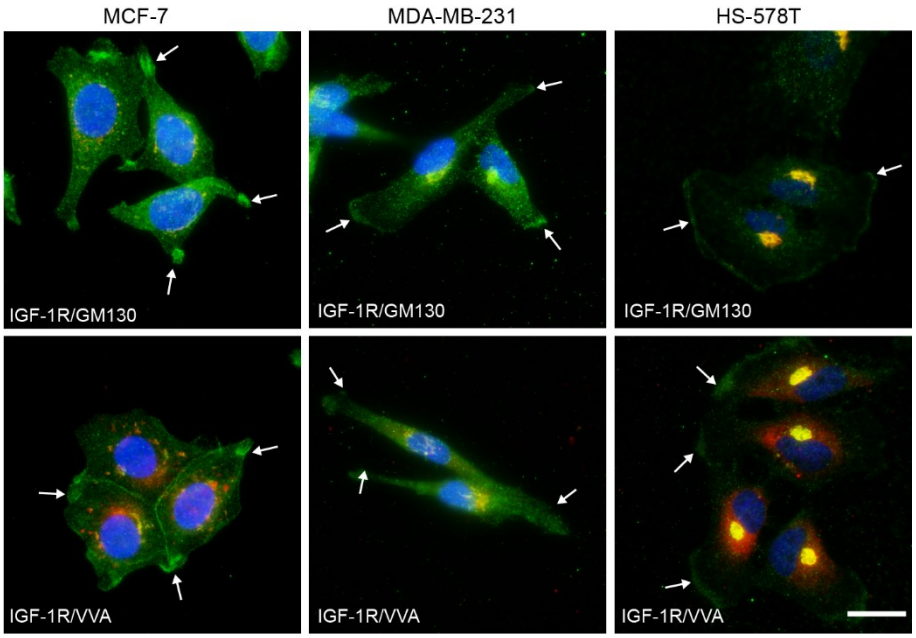


Figure 5.19: IGF-1R localises in the Golgi of migratory cancer cells.

Immunofluorescence of MCF-7, MDA-MB-231 and HS578T cells stained for IGF-1R (green) and the cis-Golgi (GM130; red) or IGF-1R (green) and the cis/trans-Golgi (VVA: red). Images were acquired using the Leica DM LB2 microscope. Images were acquired using the Leica DM LB2 microscope and are representatives of n≥3 experiments with a 20 μm scale bar.

To test, whether disruption of the Golgi-apparatus would decrease the levels of IGF-1R in these cells as well, as observed in (Figure 5.17), we fragmented the *cis*-Golgi compartment with Brefeldin A (BFA). IGF-1R levels were reduced by the Golgi fragmentation in MDA-MB-231 and HS-578T cells, whereas in MCF-7 cells IGF-1R levels were not affected (Figure 5.20A). Furthermore, while disruption of the Golgi with BFA did not alter the distribution of the IGF-1R from the plasma membrane in MCF-7 cells, BFA caused dispersal of the IGF-1R from the Golgi apparatus in MDA-MB-231 and HS-578T cells (Figure 5.20B). In these cells IGF-1R staining remained visible at the leading edge within lamellipodia.

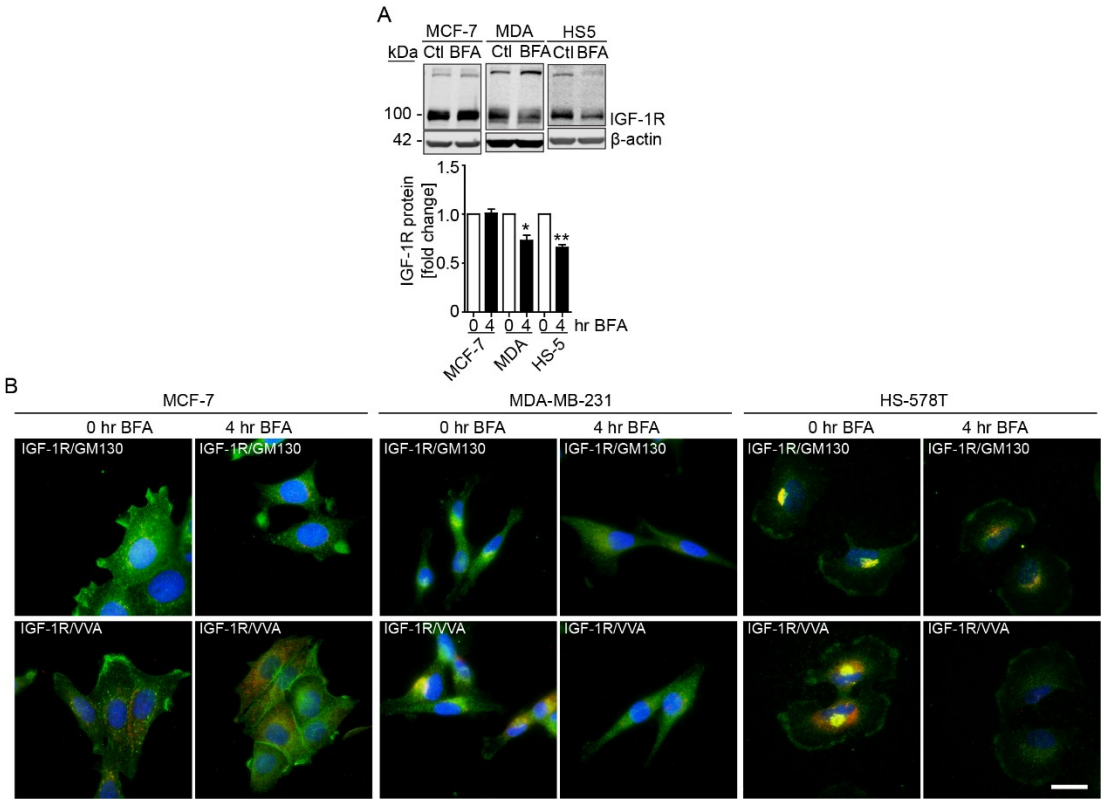


Figure 5.20: Disruption of the Golgi reduces IGF-1R levels in migratory cell lines.

(A) Immunoblotting for IGF-1R in whole cell lysates of MCF-7, MDA-MB-231 and HS 578T cells cultured in control medium (0 hr) or medium containing 10 μg/ml Brefeldin A (BFA) for 4 hr. Densitometry quantification is presented as average fold-change ± SEM in IGF-1R protein relative to the control condition (white bar; Ctl). Blots are representative of n≥3 independent experiments. Significance was calculated using a two-sided one-sample *t*-test. **(B)** Immunofluorescence of MCF-7, MDA-MB-231 and HS-578T cells cultured in control medium (0 hr) or 10 μg/ml Brefeldin A (BFA) for 4 hr and stained for top panels: IGF-1R (green) and the *cis*-Golgi (GM130: red) or bottom panels: IGF-1R (green) and the *cis*/*trans*-Golgi (VVA: red). Images were acquired using the Leica DM LB2 microscope. Images are representatives of n≥3 and with a 20 μm scale bar.
P-values are indicated by *<0.05, **<0.01, ***<0.001.

Golgi-localisation of the IGF-1R associated with a migratory phenotype and since we observed that levels of IGF-1R were profoundly decreased in these cell lines, we next investigated whether IGF-1R signalling can derive from the Golgi-compartment. While IGF-1-induced phosphorylation on $Tyr^{1250/1251}$ was detectable in both MCF-7 and HS 578T cells, the basal amounts of SHC ($Tyr^{239/240}$) phosphorylation and IGF-1 induced SHC phosphorylation ($Tyr^{239/240}$) were impaired by BFA in HS-578T cells, but not in MCF-7 cells (Figure 5.21).

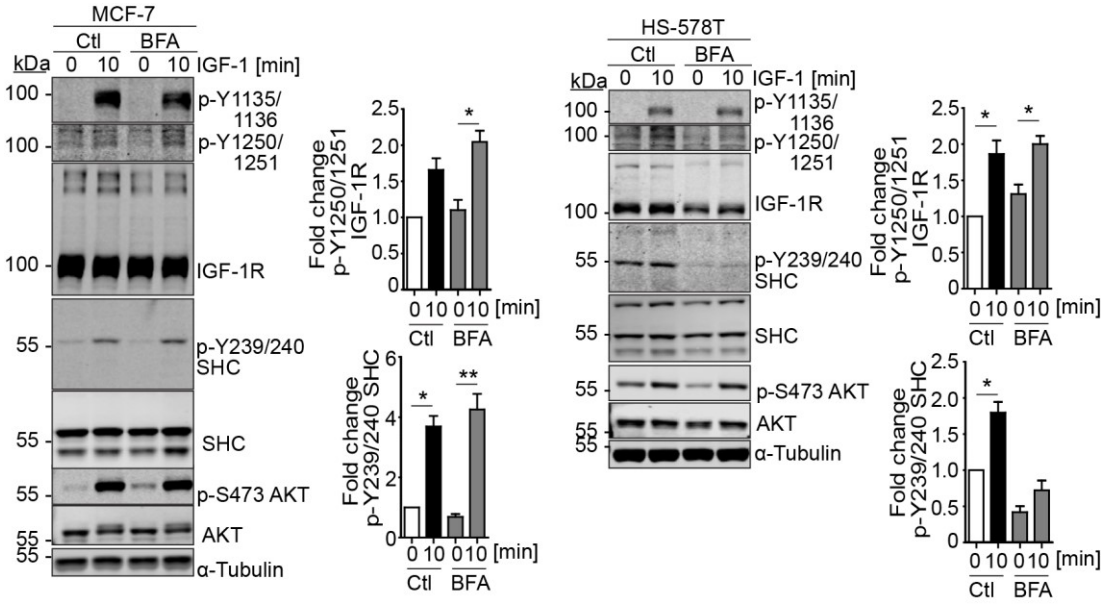


Figure 5.21: Disruption of the Golgi impairs IGF-1-induced SHC activation in HS-578T.

Immunoblotting for phosphorylated $Tyr^{1135/1136}$ (p-Y1135/1136), $Tyr^{1250/1251}$ IGF-1R (p-Y1250/1251), total IGF-1R, FAK phosphorylated on Tyr^{397} (p-Y397), total FAK, SHC phosphorylation on $Tyr^{239/240}$ and total SHC, AKT phosphorylated on Ser^{473} (p-S473), total AKT, ERK1/2 phosphorylated on Thr^{202}/Tyr^{204} (p-T202/Y204) and total ERK1/2 in WCL of MCF-7 and HS-578T cells stimulated with IGF-1 for the indicated time following 4 hr serum starvation. Densitometry quantification is presented as the average fold-change ± SEM in ratio of phospho/total protein relative to the control condition. Blots are representative of n≥3 independent experiments. Significance was calculated using a two-sided one-sample or two-sample *t*-test. *P*-values are indicated by *<0.05, **<0.01, ***<0.001.

We found that the IGF-1R was expressed at the lamellipodia of cells, even when the Golgi was disrupted (Figure 5.20), and that $Tyr^{1250/1251}$ phosphorylation required adhesion signalling (Chapter 3, Figure 5.5 and Figure 5.6). Therefore, we next investigated whether cell adhesion controls IGF-1R localisation at the plasma membrane or Golgi in MCF-7 and HS-578T cells. IGF-1R location and phosphorylation on $Tyr^{1250/1251}$ was monitored over time in response to the formation of nascent focal adhesion contacts in cells that were allowed to attach to fibronectin-coated plates and coverslips. Immunofluorescence showed that IGF-1R was present at the plasma membrane in both cell types at 15 min after cell seeding (Figure 5.22A). At this time phosphorylation on $Tyr^{1250/1251}$ was low (Figure 5.22B). In MCF-7 cells the IGF-1R was observed in focal adhesion points at 30 min post cell seeding and it remained there for up to 60 min (Figure 5.22A). In HS-578T cells at 30 min the IGF-1R appeared to have retracted from the plasma membrane to the Golgi and be exclusively Golgi-located by 60 min (Figure 5.22A). In MCF-7 cells phosphorylation on $Tyr^{1250/1251}$ remained low over time after cell adhesion, whereas in HS-578T cells $Tyr^{1250/1251}$ phosphorylation increased over time after adhesion (Figure 5.22B). These results indicate that IGF-1R becomes rapidly recruited to nascent focal adhesion points in HS-578T cells, and that IGF-1R and adhesion-dependent $Tyr^{1250/1251}$ phosphorylation promotes subsequent translocation of the receptor to the Golgi.

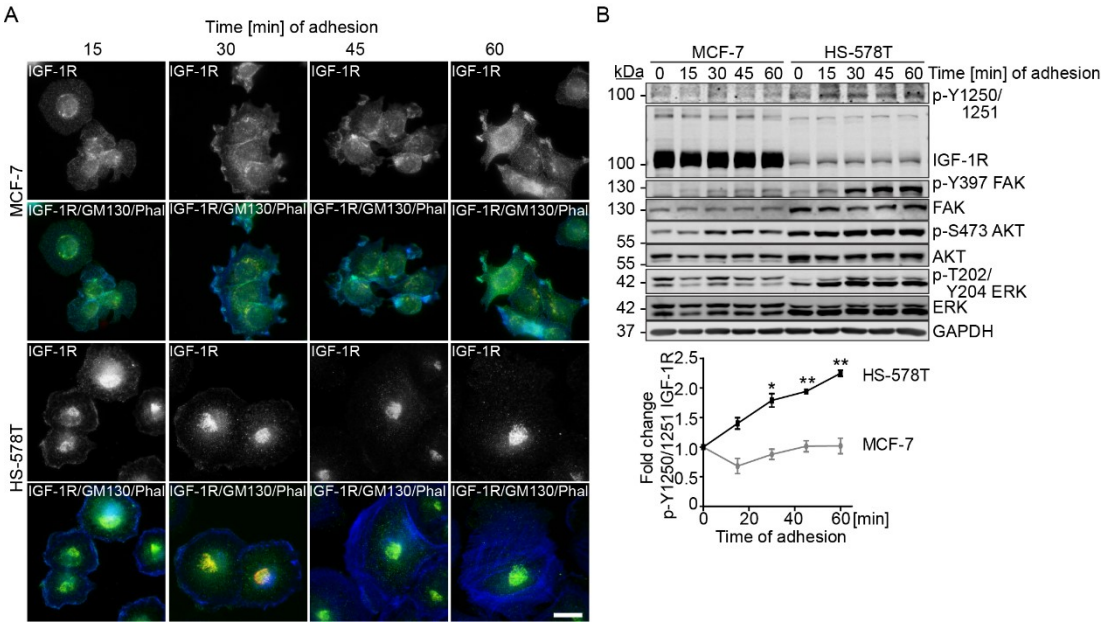


Figure 5.22: Formation of nascent focal adhesion points recruits IGF-1R to the membrane.

(A) Immunofluorescence of MCF-7 and HS-578T cells stained for IGF-1R (green), GM-130 (red) and actin (Phalloidin: blue), after adhesion to 5 μg/ml Fibronectin for the indicated times. Images were acquired using the Leica DM LB2 microscope and are representatives of n≥3 experiments with the scale bar at 20 μm. **(B)** Immunoblotting for $Tyr^{1250/1251}$ IGF-1R (p-Y1250/1251), total IGF-1R, FAK phosphorylated on Tyr^{397} (p-Y397), total FAK, AKT phosphorylated on Ser^{473} (p-S473), total AKT, ERK1/2 phosphorylated on Thr^{202}/Tyr^{204} (p-T202/Y204) and total ERK1/2 in WCL of MCF-7 and HS-578T cells cultured on fibronectin (5 μg/ml) for the indicated times. Densitometry quantification is presented as the average fold-change ± SEM in ratio of phospho-$Tyr^{1250/1251}$ IGF-1R/total IGF-1R relative to the control condition (0 min of adhesion) over time. Blots are representative of n≥3 independent experiments. Significance was calculated using a two-sided one-sample *t*-test. *P*-values are indicated by *<0.05, **<0.01, ***<0.001.

Directed migration of epithelial cells requires the formation of leading edge protrusions and repeated adhesion to the ECM, which involves the formation of new focal adhesion points (Millarte and Farhan, 2012). We therefore investigated whether the IGF-1R becomes recruited to focal adhesion points in migrating cells. In a wound healing assay using HS-578T cells, large focal adhesion points were visible at the leading edge of the migrating cells, 6 hr post-wounding (Figure 5.23A). In agreement with observations in Figure 5.19A immunofluorescence analysis showed that the IGF-1R was clearly located within the protrusions of moving cells (Figure 5.23A). In these cell cultures it was also clear that IGF-1R was predominantly located in the Golgi apparatus within cells that were part of the high confluency monolayer. To test whether Golgi apparatus is essential for IGF 1 promoted migration, cells were allowed to migrate for 6 hr post-wounding in the presence or absence of BFA for 4 hr. This demonstrated that IGF-1-stimulated HS-578T cell migration was abolished by disrupting the Golgi (Figure 5.23B).

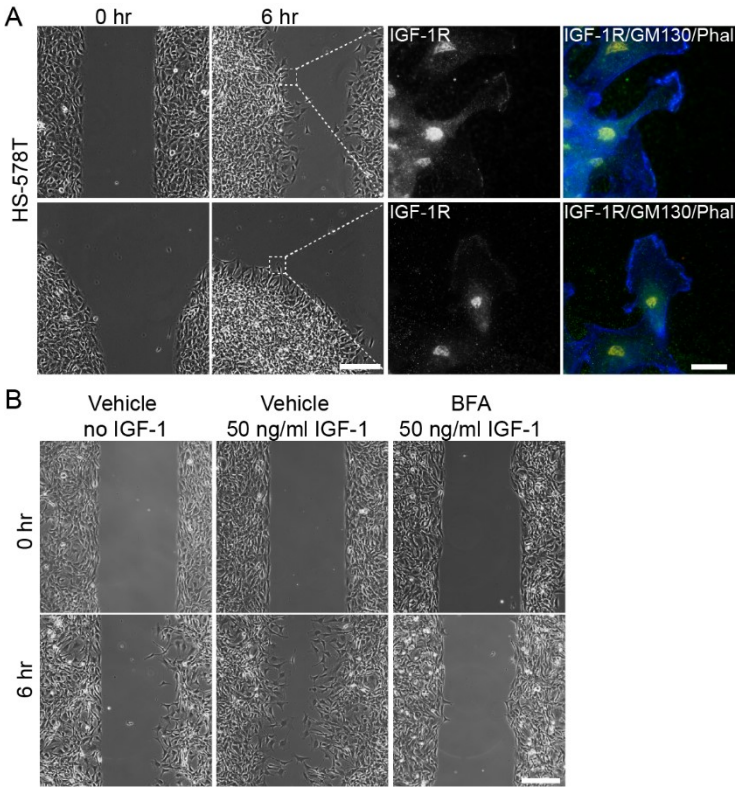


Figure 5.23: Formation of adhesion points during migration releases IGF-1R from the Golgi and disruption of the Golgi inhibits migration.

(A) Phase contrast images of HS-578T cells in a wound healing assay. Representative images (n=3) were acquired using the Nikon Eclipse TE 300 microscope at 0 hr and 6 hr of migration (scale bar 250 μm). Cells were then fixed and stained for IGF-1R (green), Golgi (GM-130: red) and actin (Phalloidin: blue). Immunofluorescence images were acquired using a Leica DM LB2 microscope and are representatives of n=3 with the scale bar at 20 μm. **(B)** Phase contrast images of HS-578T cells in a wound healing assay cultured in serum-free control medium or with BFA (10 μg/ml) added, or with IGF-1 (50 ng/ml) or with both BFA+IGF-1 added at 0 and 6 hr of migration. Images were obtained with a Nikon Eclipse TE 300 microscope and are representatives of n=3. Scale bar is 250 μm.

To better understand what promotes IGF-1R localisation to Golgi, we further assessed IGF-1R location in MCF-7 and HS-578T cells that were cultured to either sub-confluence (with potential for cell migration and cell/matrix contacts) or high confluence (favouring cell-cell adhesion). We observed that when cell-cell adherence was high in MCF-7 cells, the IGF-1R was located at the plasma membrane sites of cell-cell adhesion (Figure 5.24A) as has been previously described (Nagle et al., 2018), whereas it was located at sites of focal cell adhesion in sub-confluent cultures. In both MCF-7 cultures, basal phosphorylation on $Tyr^{1250/1251}$ was present and IGF-1 induced phosphorylation of SHC ($Tyr^{239/240}$) was evident (Figure 5.24B). In contrast, in sub-confluent HS-578T cells, the IGF-1R was located at the leading edge and in Golgi with significant IGF-1-induced phosphorylation of $Tyr^{1250/1251}$ evident, whereas in confluent cells, the IGF-1R was predominantly located in the Golgi (Figure 5.24A), where constitutive $Tyr^{1250/1251}$ phosphorylation was evident. HS-578T cells growing under high-confluency conditions exhibited little IGF-1-stimulated SHC phosphorylation (Figure 5.24B). However, induction of phosphorylation on $Tyr^{1135/1136}$ and activation of AKT and ERK1/2 was present, confirming that the IGF-1R is likely to be active within the Golgi in these cells.

Taken together, these data indicate that phosphorylation on $Tyr^{1250/1251}$ promotes accumulation of IGF-1R in the Golgi. Moreover, within the Golgi, the IGF-1R is active and induces downstream signalling. On the other hand, cell-ECM adhesion signals during cell migration enhance IGF-1-induced phosphorylation on $Tyr^{1250/1251}$ resulting in the IGF-1R being predominantly located both in Golgi and at the leading edge of migrating cells.

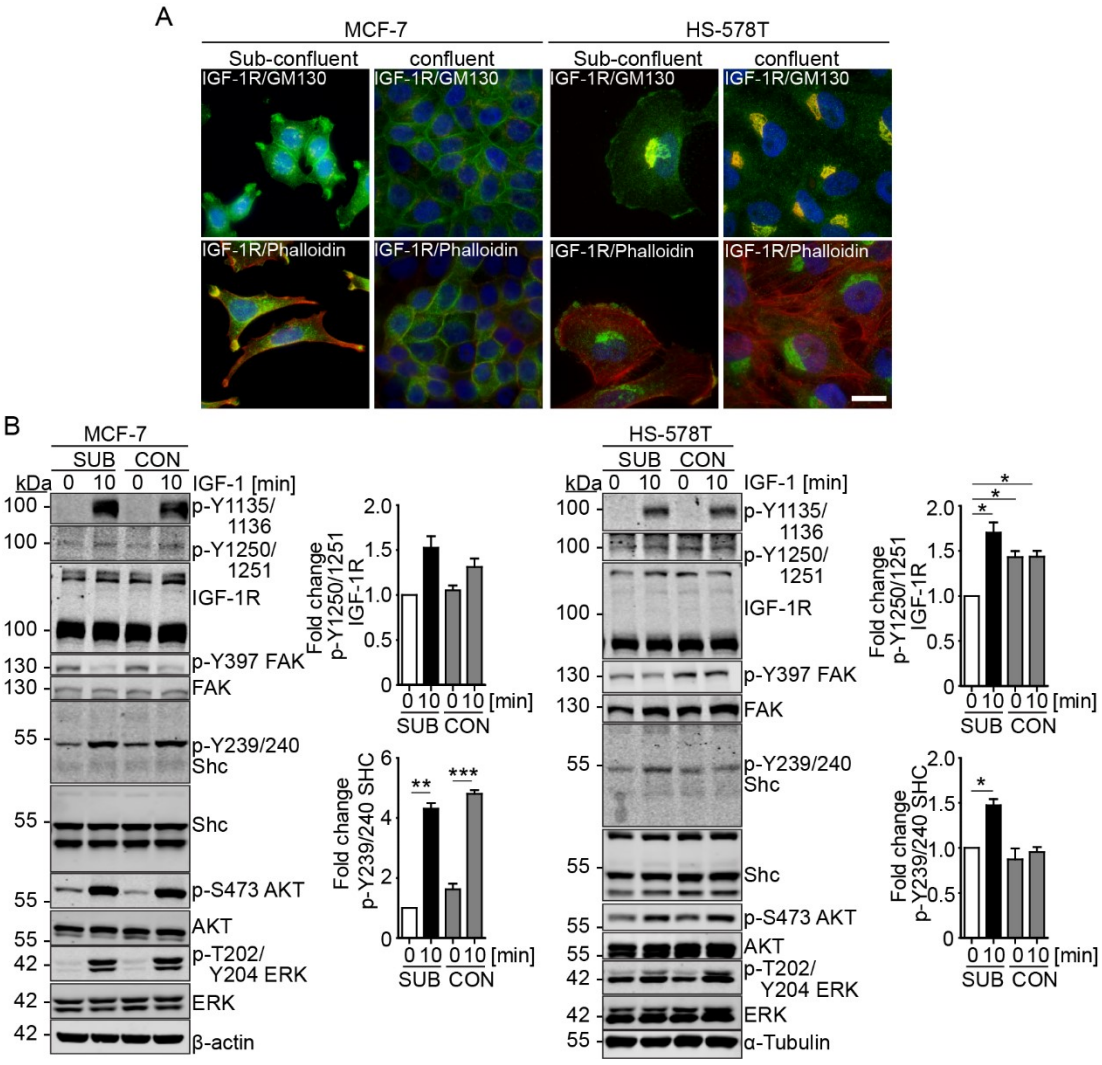


Figure 5.24: Cell-ECM contact regulates phosphorylation on Tyr$^{1250/1251}$ IGF-1R in migratory cells.

(A) Immunofluorescence of MCF-7 and HS-578T cells cultured at the indicated confluency and stained for IGF-1R (green)/Golgi (GM130: red), IGF-1R (green)/Actin (Phalloidin: red). Immunofluorescence images were acquired using a Leica DM LB2 microscope and are representatives of n=3 with a scale bar of 20 μm. **(B)** Immunoblotting for Tyr$^{1135/1136}$ IGF-1R (p-Y1135/1136), Tyr$^{1250/1251}$ IGF-1R (p-Y1250/1251), total IGF-1R, FAK phosphorylated on Tyr^{397} (p-Y397), total FAK, SHC phosphorylated in Tyr$^{239/240}$ (P-Y239/240), AKT phosphorylated on Ser^{473} (p-S473), total AKT, ERK1/2 phosphorylated on Thr^{202}/Tyr^{204} (p-T202/Y204) and total ERK1/2 from MCF-7 and HS 578T cells cultured to the same confluency as cells shown in images, and stimulated with IGF-1following serum starvation. Densitometry quantification is presented as the average fold-change ± SEM in ratio of phospho/total protein relative to the control condition (white bar). Blots are representative of n=3 independent experiments. Significance was calculated using a two-sided one-sample or two sample *t*-test. *P*-values are indicated by *<0.05, **<0.01, ***<0.001.

5.4 DISCUSSION

Although IGF-1 signalling has a well-described function in facilitating tumorigenesis and promoting tumour growth, it is unresolved why levels of IGF-1R expression do not correlate with activity in cancer cells, and why IGF-1R-targeting drugs have been largely ineffective. Our findings here (summarized in the model in Figure 5.25), explain a hidden activity of the IGF-1R in promoting an aggressive cancer phenotype and evading therapy. Adhesion-dependent phosphorylation of the IGF-1R on $Tyr^{1250/1251}$ promoted receptor internalisation, accelerates receptor turnover and translocation to Golgi from where it elicited signalling and was available for transport to and from new focal adhesion sites in migrating cells.

Previous studies have reported that IGF-1R activity and signalling can be modulated by cell adhesion signals (reviewed in (Cox et al., 2015)) and directly by adhesion-associated kinases including FAK, Src and FER (Peterson et al., 1996, Flossmann-Kast et al., 1998, Ucar et al., 2012, Taliaferro-Smith et al., 2015, Stanicka et al., 2018). The presence of $Tyr^{1250/1251}$ is necessary for the integration of IGF-1R and β1-Integrin signalling mediated by their co-recruitment into a scaffolding complex containing RACK1, SHC and other signalling mediators for activation of MAPK signalling (Hermanto et al., 2002, Kiely et al., 2005). Loss of this interaction with mutation of the tyrosines to phenylalanine results in impaired IGF-1-induced cell migration and tumour growth *in vivo* (Brodt et al., 2001, Kiely et al., 2005). Our observations here, that the phosphomimetic EE mutant (for $Tyr^{1250/1251}$ phosphorylation) became more rapidly internalised and trafficked from the Golgi apparatus to the leading edge of migrating cells, indicate that phosphorylation on this site is necessary for cooperation with adhesion signalling. We found that IGF-1 also stimulates

internalisation of WT IGF 1R to Golgi, demonstrating that this is an intrinsic component of IGF-1R signalling when it is phosphorylated on these residues. In migrating cells, the retraction of IGF-1R from focal adhesion (FA) points mediated by phosphorylation on $Tyr^{1250/1251}$, may facilitate disassembly of FA to promote migration of cells, and may also explain the impaired migratory capacity of cells expressing the FF mutant, where the IGF-1R is retained at the plasma membrane.

It is well documented that the outcome of RTK activation and signalling can vary depending on receptor location (Disanza et al., 2009, Warren et al., 2014, Yoneyama et al., 2018). Compartmentalization of RTK signalling may facilitate recruitment of different effector proteins that might be dictated by a specific cell phenotype. Emerging evidence suggests an important role for the Golgi in oncogenic RTK signalling (Obata et al., 2017, Obata et al., 2018, Frazier et al., 2019). Overexpressed or mutated MET causes ligand-independent activation and signalling from MET in the Golgi, including HER3/ERBB3 phosphorylation (Frazier et al., 2019). Similarly, mutated forms of the KIT receptor are retained in the Golgi where they are active and induce downstream signalling (Xiang et al., 2007, Tabone-Eglinger et al., 2008, Bougherara et al., 2009, Obata et al., 2018). VEGFR2, FGFR and EGFR are also reported to be located at and induce signalling from the Golgi (Citores et al., 2007, Warren et al., 2014, Ye et al., 2016). Our findings with the IGF-1R add important knowledge to the understanding of Golgi-derived RTK signalling, because we demonstrate that trafficking of this RTK to the Golgi-apparatus is promoted by a specific adhesion and ligand-dependent phosphorylation on $Tyr^{1250/1251}$. In migrating cells, IGF-1R was located at the leading edge of nascent focal adhesions and was subsequently rapidly

trafficked back to the Golgi. This suggests that a pool of $Tyr^{1250/1251}$ phosphorylated IGF-1R is stored in the Golgi for signalling and fast trafficking back to the membrane in migrating cells. Indeed, a similar trafficking route is proposed for GOLM-mediated trafficking of ligand-activated EGFR in hepatocellular carcinoma (Ye et al., 2016).

We have not however, established whether the IGF-1R is a cargo protein, or whether it might participate in regulating secretion of proteins from the Golgi, or what controls its trafficking out from the Golgi. Phosphorylation on $Tyr^{1250/1251}$ was low when the IGF-1R was recruited to the plasma membrane, which suggests that phosphatases may facilitate dephosphorylation of $Tyr^{1250/1251}$, leading to the release of IGF-1R from its Golgi location. Once located at points of nascent focal adhesions, the IGF-1R may promote the recruitment of other interacting partners and proteins leading to the stabilization of focal adhesions. It is likely that the IGF-1R is subsequently retracted from focal adhesions following IGF-1R phosphorylation on $Tyr^{1250/1251}$. An alternative possibility is that the IGF-1R trafficks to the Golgi compartment as part of a multi-protein complex that is stored there for signalling.

Golgi-derived oncogenic signalling may be especially active in cell migration (Millarte and Farhan, 2012). Here, we observed that fragmentation of the Golgi impaired cell migration in the presence of IGF-1. This was associated with impaired SHC phosphorylation in migratory HS-578T cells, but not in low-migratory MCF-7 cells. This is consistent with a previously described requirement for an intact Golgi apparatus in activating the RAS pathway and ERK signalling to establish cell polarity in migrating cells (Millarte and Farhan, 2012). The observation that impaired SHC phosphorylation was not observed

in low-migratory cells suggests that different signalling outcomes can be dictated by the same receptor dependent on its location and on cell phenotype, as previously suggested (Niepel et al., 2013). Our data suggest that distinct cell adhesion signals have an essential function in determining IGF-1R autophosphorylation and location. Mesenchymal cancer cells exhibiting high migratory capacity and aggressiveness are often deficient in E-cadherin, which interacts with the IGF-1R and may retain it at cell-cell junctions in low-migratory cells like MCF-7 cells (Nagle et al., 2018). Loss of E-cadherin would therefore be likely to alter IGF-1R location and potentially facilitate IGF-1R interactions with Integrins.

Activated intracellular and nuclear IGF-1R have previously been linked to an aggressive cancer phenotype. For example, intracellular IGF-1R is more abundant in malignant than benign epithelium in prostate cancer patient tissues (Aleksic et al., 2018), and nuclear IGF-1R has been proposed to facilitate breast, ovarian and prostate cancer (Aleksic et al., 2010, Deng et al., 2011). Moreover, although abundance of the IGF-1R itself is not associated with survival in breast cancer patients, high levels of IGF-1R phosphorylation are linked to poor outcomes (Law et al., 2008). Our finding of Golgi-derived IGF-1R signalling offers a mechanistic explanation for these effects, because although the EE IGF-1R was expressed at lower levels in cells it retained high activity.

In summary, phosphorylation-specific trafficking of the IGF-1R to the Golgi and the association of this with aggressive cancer phenotype has important consequences for IGF-1 signalling. Phosphorylated $Tyr^{1250/1251}$ could be a biomarker for identifying subsets of cancer that may not be targetable with

anti-receptor antibodies but may be amenable to other therapies that would target a signalling hub within the Golgi.

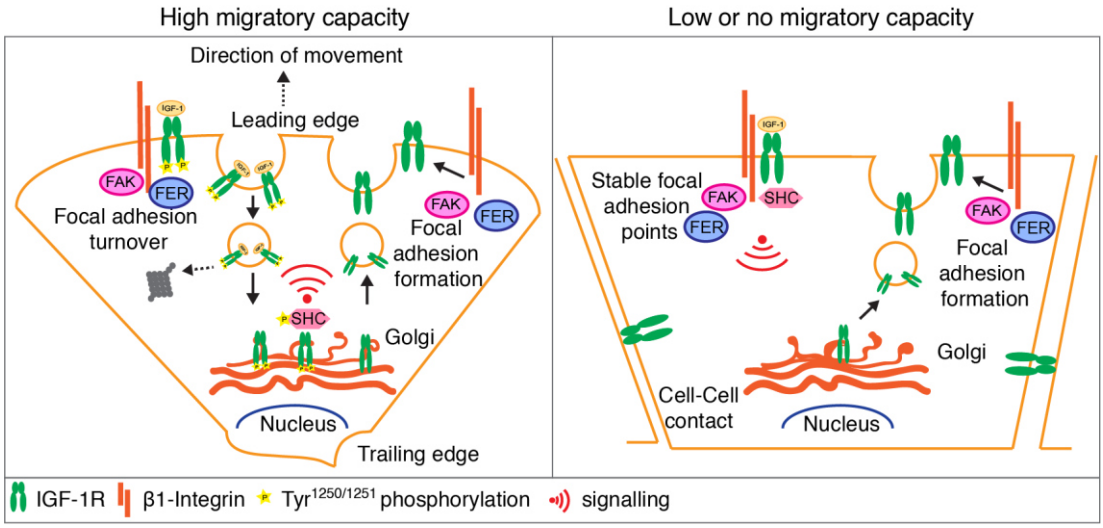


Figure 5.25: Model for function of Tyr$^{1250/1251}$ phosphorylation in determining IGF-1R location and signalling in the Golgi apparatus.

IGF-1 and adhesion signals promote Tyr$^{1250/1251}$ phosphorylation in both low or no-migratory and migratory cells. In low or non-migratory cells, IGF-1R is predominantly located at the plasma membrane or at stable focal adhesion points. However, in migratory cells IGF-1R is predominantly located in the Golgi apparatus, and upon induction of cell migration, translocates from the Golgi to the leading edge of cells. Here, mediated by FAK, FER and IGF-1R kinase activity, Tyr$^{1250/1251}$ subsequently becomes phosphorylated and returned to the Golgi where it mediates signalling including phosphorylation of SHC.

6 CHAPTER 6: GENERAL DISCUSSION

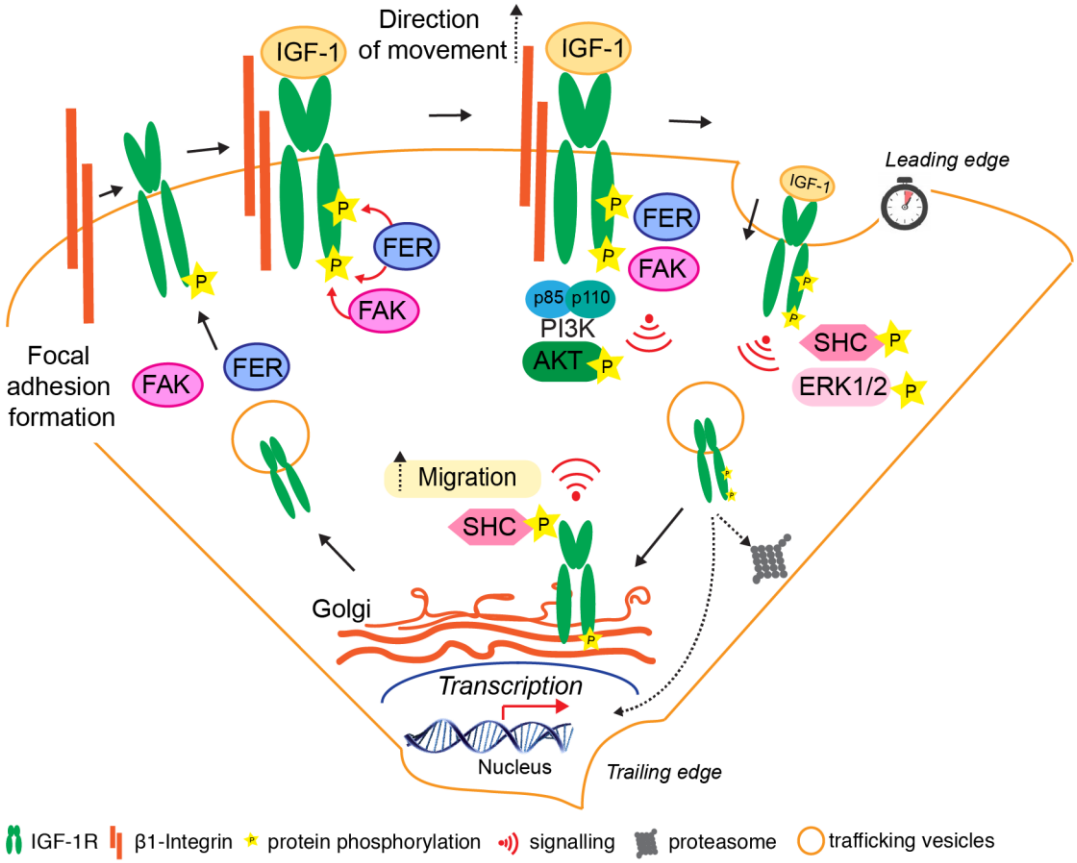
6.1 SUMMARY

Understanding IGF-1R kinase regulation and the complexity of its signalling pathways is required before revisiting the therapeutic targeting of the IGF-1R in cancer. IGF-1R signalling output may be influenced by cell-type and it can be modulated by environmental changes (Pollak, 2012). Targeting the system has been challenging because of compensatory signalling mechanisms and cancer cells adapting to the loss of IGF-1R function (Osher and Macaulay, 2019). This thesis work, summarized in Figure 6.1, identifies two adhesion-related mechanisms through which the IGF-1R activation and function can be modified. First, it establishes the non-receptor tyrosine-kinase FER as a novel cellular kinase for IGF-1R activation in cancer cells. Second, it identifies the Golgi apparatus as a novel compartment for IGF-1R localisation and signalling following rapid endocytosis that is dependent on phosphorylation of two key tyrosines in the IGF-1R C-terminal-tail ($Tyr^{1250/1251}$). These findings provide valuable new insights into IGF-1R regulation in cancer cells and also to our understanding of IGF-1R function in normal cells.

The Fes-related, F-BAR containing, cellular kinase FER enhanced IGF-1R and SHC/MAPK pathway activation, even in conditions where the IGF-1R is catalytically inactive. We observed that FER overexpression specifically enhanced $Tyr^{1250/1251}$ IGF-1R phosphorylation either directly or through protein complex formation with FAK. FER activation was facilitated by IGF-1 and FER associated with IGF-1R and β1-Integrin at focal points of cell adhesion. $Tyr^{1250/1251}$ in the IGF-1R was autophosphorylated in the presence of adhesion-signalling and it was determined that both FER and FAK can also

enhance this tyrosine phosphorylation in cancer cells. Using an IGF-1R phosphomimetic, we established that IGF-1-induced $Tyr^{1250/1251}$ autophosphorylation was associated with the rapid translocation of IGF-1R to the Golgi apparatus. $Tyr^{1250/1251}$ phosphorylation was also found to be high in migratory cancer cell lines. In these cell lines IGF-1R is predominantly located in the Golgi-apparatus and upon IGF-1 stimulation, this Golgi-localised receptor was activated and could induce downstream signalling. Upon formation of new focal adhesions and interaction with the ECM, either in the process of cell adherence on substrate or during cell migration, the IGF-1R was released from the Golgi to the plasma membrane. This coincided with low levels of $Tyr^{1250/1251}$ IGF-1R phosphorylation. Interestingly, in migratory cell lines, IGF-1-induced phosphorylation on $Tyr^{1250/1251}$ IGF-1R and subsequent accumulation of IGF-1R in the Golgi-apparatus is influenced by cell-cell and cell-ECM contacts, whereas in low or non-migratory cell lines, the IGF-1R is predominantly located at the plasma membrane and this is independent of cell-cell and cell-ECM contacts.

A Migrating cells (focal adhesion trunover):



B Non-migrating cells (stable focal adhesion points):

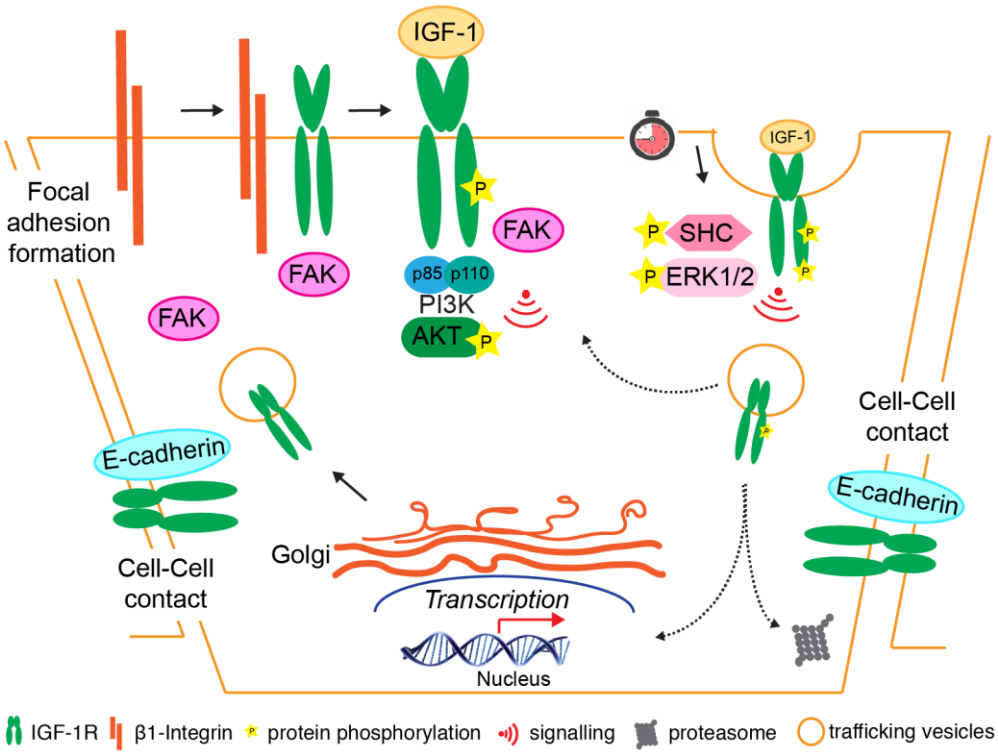


Figure 6.1: Model for function of adhesion-activated FER and Tyr$^{1250/1251}$ phosphorylation in promoting focal adhesion turnover and in determining IGF-1R location and signalling in the Golgi apparatus.

(A) In migratory cell lines, IGF-1R is recruited to formations of new focal adhesion points. It associates with β1-Integrin, FER and FAK, which in turn, mediate the phosphorylation on Tyr$^{1250/1251}$ IGF-1R. Rapid initiation of IGF-1R endocytosis leads to activation of the MAPK pathway and results in translocation of the IGF-1R to the Golgi which promotes sustained SHC activation to facilitate migration. **(B)** In cells with low or no migratory capacity, where levels of FER are low, IGF-1R remains on the surface inducing signalling from the membrane. The interaction with other proteins, including E-cadherin, stabilizes the adhesion points and internalisation rate of the IGF-1R is low.

6.2 ASSOCIATION OF FER AND IGF-1R IN POINTS OF FOCAL ADHESION

6.2.1 FER enhances Tyr$^{1250/1251}$ IGF-1R phosphorylation to destabilize focal adhesions and induce IGF-1R endocytosis

Recent studies have linked high FER expression to poor cancer patient outcome (Greer, 2002, Ivanova et al., 2013, Stanicka et al., 2018, Zheng et al., 2018). In our study, we investigated FER involvement in the regulation of IGF-1R activation. Our data demonstrate that FER overexpression increased IGF-1R activation, predominantly mediated by phosphorylation on Tyr$^{1250/1251}$ IGF-1R and the activation of SHC and the MAPK/ERK1/2 pathway (Figure 3.3, Figure 3.4). This adhesion-dependent autophosphorylation on IGF-1R was further linked to rapid endocytosis of the IGF-1R and subsequent localisation in the Golgi-apparatus (Chapter 5). Thus, the question arose whether FER enhances phosphorylation on Tyr$^{1250/1251}$ IGF-1R to promote IGF-1R endocytosis.

FER is a member of the F-BAR (Bin-Amohiphysin-RVS) domain family. Together with other family members, FER contains a single tyrosine kinase module (Zirngibl et al., 2001, Greer, 2002, Itoh et al., 2005). F-BAR domain proteins are most commonly reported to be involved in cytoskeleton organisation acting in close proximity to the plasma membrane. They are also linked to membrane-deformation and suggested to be involved in endocytosis (Itoh et al., 2005). With their SH3 domain they can bind to dynamin (Itoh et al., 2005), a small GTPase responsible for vesicle budding and scission of the lipid bilayer from intracellular membranes during clathrin-mediated endocytosis (Kamioka et al., 2004, Neumann and Schmid, 2013). IGF-1R endocytosis can be clathrin-mediated and this suggests that the rapid vesicle formation that

was observed in R^- cells stimulated with IGF-1 in Figure 5.13 may be enhanced by FER kinase activity. This proposes that FER may enhance IGF-1R phosphorylation on $Tyr^{1250/1251}$ (mimicked by the EE mutant) to enable rapid IGF-1R internalisation (Figure 5.13). It is, however, unlikely that FER itself internalises in the distinct vesicles observed to contain IGF-1R WT and EE mutant (Figure 5.13). FER was reported to be diffusely localised throughout the cytoplasm, whereas Fes is localised in distinct cytoplasmic vesicles and in the perinuclear region consistent with the Golgi (Zirngibl et al., 2001). Fes also co-localises with Rabs, which are key GTPase proteins involved in regulating endocytosis (Rab5B and Rab7) as well as exocytosis (Rab1A and Rab3A) (Zirngibl et al., 2001), suggesting its potential role in both pathways. However, while Fes may play a role in vesicular trafficking, this has not been suggested for FER. Our data is consistent with this study by Zirngibl *et al.*, because we observed that FER localised in the cytoplasm and focal adhesion points, but not in vesicles (Figure 3.9). The distinct localisation of IGF-1R in the perinuclear region, subsequently established to be the Golgi apparatus (Figure 3.9, Figure 5.19), also showed no co-localisation with FER, again confirming that FER does not localise in the Golgi compartment. This proposes, that FER-mediated IGF-1R activation exclusively occurs at focal adhesion points. When associated with IGF-1R in focal points of cell adhesion, FER specifically enhanced $Tyr^{1250/1251}$ IGF-1R phosphorylation to enable IGF-1R endocytosis and its subsequent trafficking to the Golgi.

FER-enhanced IGF-1R $Tyr^{1250/1251}$ phosphorylation and the initiation of IGF-1R endocytosis may also be associated with enhanced SHC and ERK1/2 activation upon FER overexpression (Figure 3.4). Blocking IGF-1-induced receptor internalisation using pharmacological compounds is known to inhibit

vesicle transport, which prevents the activation of SHC (Chow et al., 1998). As a consequence less Grb-2 is recruited to SHC which impairs MAPK activation. ERK1/2 activation is also linked to IGF-1R endocytosis (Sehat et al., 2007, Girnita et al., 2007), and is proposed to require the presence of the IGF-1R C-terminal tail. Ligand-independent activation of SHC and ERK1/2, seen in Figure 3.4A may be the result of increased ligand-independent $Tyr^{1250/1251}$ IGF-1R phosphorylation and therefore enhanced receptor endocytosis. Moreover, FER did not enhance PI3K/AKT activation, which can be activated by plasma membrane-located IGF-1R (Romanelli et al., 2007, Yoneyama et al., 2018). Thus, our data suggest, that FER-mediated $Tyr^{1250/1251}$ IGF-1R phosphorylation leads to IGF-1R endocytosis which activates SHC and MAPK pathways.

6.2.2 The interplay of FER, β1-Integrin and the IGF-1R signalling in focal adhesion dynamics

FER regulates actin cytoskeleton organisation by facilitating the phosphorylation of the actin-binding protein cortactin in a growth-factor dependent manner (Kim and Wong, 1998, Kim and Wong, 1995). FER is also linked to destabilizing microtubules by phosphorylating CRMP2 (Collapsin response mediator protein 2) on its C-terminal located tyrosine, which causes bundling of microtubules to form Filopodia, while inhibition of FER increases the stabilization of microtubules (Zheng et al., 2018). Furthermore, overexpression of FER causes destabilisation of focal adhesions and major changes in cell morphology (Rosato et al., 1998, Ivanova et al., 2013), again showing that an essential function of FER is as a facilitator of cytoskeleton remodelling.

Detachment of cells from the substratum and reattachment is required for migration and is regulated by an interplay between Integrin and cadherin signalling (Huttenlocher et al., 1998, Huttenlocher and Horwitz, 2011). FER regulates α6- and β1-Integrin distribution in breast cancer cell lines (Ivanova et al., 2013) and inhibition of FER activity increases levels of β1- and α6-Integrin on the cell surface, thereby promoting cell adhesion (Ivanova et al., 2013). Other studies have also reported FER regulation of focal adhesion destabilization and cell migration (Rosato et al., 1998).

Cooperative β1-Integrin and IGF-1R signalling is essential for IGF-1 mediated cell migration (Hermanto et al., 2002, Kiely et al., 2005). This interaction is mediated by RACK1 and requires the presence of $Tyr^{1250/1251}$ IGF-1R (Kiely et al., 2005). Here, it was found that the IGF-1R is located within protrusions of migrating cell at the leading edge of cells migrating into a wound (Figure 5.23A). Furthermore, IGF-1-induced migration required an intact Golgi-apparatus (Figure 5.23B), suggesting that the Golgi apparatus is important for IGF-1-induced migration. We also observed that during cell adherence, the IGF-1R is recruited to the plasma membrane, and that at this time phosphorylation on $Tyr^{1250/1251}$ IGF-1R is low (Figure 5.22). The attachment of cells to the substratum, either during cell adherence or migration, can be regulated by β1-Integrin, which connects the ECM with the actin cytoskeleton. Through this connection, Integrins can provide both a structural function for cell adhesions but also act as signal transducers (Huttenlocher et al., 1998, Hynes, 2002). β1-Integrin involvement in focal adhesion turnover normally facilitates adhesion and de-adhesion from the ECM to allow migration, however, in conditions of high cell-cell contact, β1-Integrin-mediated signalling inhibits motile activity (Huttenlocher et al.,

1998, Huttenlocher and Horwitz, 2011). Interestingly, we found that confluent HS-578T cells, which are unable to migrate due to cell-cell contact inhibition of migration, retain IGF-1R with high $Tyr^{1250/1251}$ phosphorylation in the Golgi apparatus (Figure 5.24). This suggests that membrane-derived β1-Integrin signalling may be involved in the mechanisms that regulates IGF-1R release and retention in the Golgi-apparatus.

The inhibition of Integrin-mediated migration can be accompanied by higher expression of cadherin (Huttenlocher et al., 1998). The differential expression of cadherins and Integrins are linked to the migratory phenotype of cells during cellular processes, including development, tumour invasion and metastasis (Hynes and Lander, 1992, Hamidi and Ivaska, 2018, Yu et al., 2019). Cadherins may modulate migration by increasing cell-cell adhesion and/or transmitting signals to inhibit cell motility (Chen and Obrink, 1991, Chen et al., 1997). Our data suggests that in mesenchymal cells exhibiting high migratory capacity, the IGF1-R is recruited by β1-Integrin to the leading edge of migrating cells. Upon IGF-1R and β1-Integrin interaction, or initiation of focal adhesion disassembly during migration, $Tyr^{1250/1251}$ IGF-1R is phosphorylated and the IGF-1R traffics to the Golgi (Figure 5.22, Figure 5.23). In cancer cells with no or low migratory capacity, such as MCF-7 cells, the expression of cadherins on the cell membrane and cell-cell contacts may retain IGF-1R at the cell-cell junctions (Figure 5.24) (Nagle et al., 2018), as rapid endocytosis of the IGF-1R from focal adhesion points is not required. Thus the signalling function of $Tyr^{1250/1251}$ phosphorylation is not essential for MCF-7 cells. This is reflected in a generally low $Tyr^{1250/1251}$ IGF-1R phosphorylation in MCF-7 compared to HS-587T cells (Figure 5.22) and the lack of a significant induction of phosphorylation in these cells upon IGF-1 stimulation (Figure 5.22, Figure

5.24). Furthermore, it also provides an explanation for why CRISPR-mediated knock-in mutation of $Tyr^{1250/1251}$ had minor effects on MCF-7 cells (Chapter 4).

6.2.3 FER overexpression in MCF-7 cells may enhance migratory potential

High FER expression is associated with migratory capacity in several cell models (Ivanova et al., 2013). Our results from Chapter 3 suggests, that FER might mediate the turnover of focal adhesion points by promoting IGF-1R endocytosis. Figure 3.8A shows, that MCF-7 cells have low expression levels of FER, which correlates with their low-migratory phenotype. MCF-7 cells also exhibit high amounts of E-cadherin (Nagle et al., 2018), which, our data suggests, may facilitate the retention of IGF-1R on the membrane. FER overexpression leads to dissolution of cell-cell-adherens junctions by decreasing the amount of β-catenin interacting with E-cadherin (Rosato et al., 1998). This has important implications for cancer cell phenotype, as the stabilization of the E-cadherin/β-catenin complex was suggested to suppress EMT in colorectal cancer cells (Chen et al., 2016). Stabilization of E-cadherin complexes on the membrane may supress β1- Integrin-mediated migration (Huttenlocher et al., 1998). FER regulates β1-Integrin distribution on the cell membrane and is thereby regulating adhesion and migration of cells (Ivanova et al., 2013). By influencing both β1-Integrin- and cadherin-mediated cell adhesions, FER kinase can facilitate the turnover of focal adhesions. This suggests, that FER overexpression in MCF-7 cells may have the potential to promote the turnover of cell adhesion complexes and to enhance their migratory capacity, as it has been observed with overexpression of RACK1 (Kiely et al., 2008). The common mechanism could be through enhancing the

phosphorylation on $Tyr^{1250/1251}$ IGF-1R. Moreover, FER overexpression could promote accumulation of the IGF-1R in the Golgi apparatus in MCF-7 cells. Although, the present study proposes a mechanism on how FER regulates IGF-1R activity and contributes to the migratory phenotype of cancer cells, it is limited and it could be of interest to further elucidate the interplay of FER, IGF-1R and adhesion in facilitating cell migration.

6.3 THE GOLGI APPARATUS AS A SIGNALLING COMPARTMENT

6.3.1 Golgi-derived signalling facilitates cell migration

The recruitment of effector proteins to RTKs is essential for their signalling outcome. Cell type-specific subcellular localisation of RTKs and their compartmentalization provides an important mechanism for the recruitment and activation of effector proteins, and therefore defines the outcome of signalling. Although other cellular organelles, including the nucleus may act as signalling compartments for the IGF-1R, our study identified the Golgi apparatus as a novel compartment. Until recently the role of the Golgi was limited to the secretion of newly synthesized proteins. However, emerging evidence links it to the regulation of cellular processes such as cell polarization (Kupfer et al., 1983), directional migration (Millarte and Farhan, 2012), stress (Sasaki and Yoshida, 2015) and DNA repair (Farber-Katz et al., 2014).

The possibility that the secretion of proteins could be regulated by plasma membrane receptors was first proposed after the observation that the recruitment of ADP-ribosylation factor (ARF) to the Golgi was mediated by receptor kinase activity (De Matteis et al., 2008). An associated signalling network was subsequently identified, including the KDEL receptor and the Src kinases (Bard et al., 2003). In a recent study, 159 signalling proteins were

determined to affect the morphology of the Golgi apparatus, including IGF-1R and other growth factor receptors (Chia et al., 2012). Several cytoplasmic kinases, including ROCK1 and PAK1 that are involved in regulating actin dynamics were also identified. Furthermore, the presence of a wide range of kinases and phosphatases in the Golgi apparatus indicate that the Golgi can receive and transmit signals that influence cellular processes (Farhan et al., 2010, Chia et al., 2012, Makhoul et al., 2018).

Previous reports suggest the Golgi apparatus as an important compartment for signalling, during cell migration (Millarte and Farhan, 2012). Directed migration of fibroblasts requires the relocation of the Golgi to the side of the nucleus facing the leading edge (Kupfer et al., 1983). This process enhances direct delivery of membrane components, such as Integrins to the leading edge, thereby supporting cell polarization and directional motility (Bisel et al., 2008, Millarte and Farhan, 2012, Saraste and Prydz, 2019). Suppression of Golgi-proteins, including golgin-160 and GMAP210 leads to inhibition of cell migration (Yadav et al., 2009), and proteins mediating cell migration including MAPK and YSK1 are also localised at the Golgi (Preisinger et al., 2004, Farhan et al., 2010).

Ras signalling is proposed to emanate from the Golgi apparatus (Farhan and Rabouille, 2011, Mor and Philips, 2006, Kholodenko et al., 2010). Chiu *et al.* showed that upon growth-factor stimulation (EGF and TGFα), Ras is activated on the plasma membrane as well as at the Golgi apparatus. The study also demonstrated that the kinetics of activation in the two compartments is different. While Ras activation on the plasma membrane was rapid and transient, Ras activation from the Golgi was sustained (Chiu et al., 2002). It was suggested that Ras traffics between compartments, perhaps bound to

another protein (Mor and Philips, 2006), and it was furthermore observed that activated Ras in various subcellular locations differentially regulates downstream signalling pathways (Chiu et al., 2002). MEK/Ras activity was also shown to be required for the breakdown of cell-cell adhesions in response to stimulus, including growth factor signalling (Khoury et al., 2001, Ahmed and Prigent, 2017), which leads to the initiation of cell migration.

The role of SHC, the main activator of Ras, in mediating cell migration has been well described (Ahmed and Prigent, 2017). SHC is crucial for TGF-β-induced cell migration, and mutation of the three activating tyrosine residues in p52-SHC ($Tyr^{239/240/317}$) is sufficient to inhibit TGF-β-mediated cell migration and invasion (Northey et al., 2008). Overexpression of SHC in low-migratory MCF-7 cells (MCF-7/SHC) revealed an increase in the association of SHC with β1-Integrin, but this was not sufficient to impact their ability to migrate. However, increased migration was induced in the MCF-7/SHC cells following stimulation with IGF-1 or EGF, demonstrating that input from growth factor signalling is required for SHC-mediated migration (Mauro et al., 1999).

There is emerging evidence that different RTKs, including MET, KIT, VGFR2, EGFR and FGFR (Citores et al., 2007, Warren et al., 2014, Obata et al., 2018, Frazier et al., 2019) also all use the Golgi apparatus as a signalling compartment. This could, as described for Ras, modify their signalling outcome. Various mechanisms have been described on regulation of RTK localisation in the Golgi. Mutated and overexpressed MET was demonstrated to signal from the Golgi, regulating transformation of cells and migration (Hongo et al., 1998, Joffre et al., 2011, Kon et al., 2014) and cause ligand-independent HER3/ERBB3 phosphorylation (Frazier et al., 2019). Upon

ligand stimulation, EGFR interacts with Golgi-membrane protein-1 (GOLM1) in Rab5-positive vesicles. This interaction of EGFR with GOLM1 anchors EGFR to the Golgi, although EGFR is eventually recycled back to the membrane in a Rab11-dependent manner (Ye et al., 2016).

Our study adds significantly to the current understanding of Golgi-derived signalling. Similar to what has been proposed for Ras (Chiu et al., 2002), a dynamic protein modification, in this case, the phosphorylation of IGF-1R on $Tyr^{1250/1251}$, regulates IGF-1R cellular location. This mechanism enables the IGF-1R to be active and to induce signalling from different cellular compartments, including the plasma membrane, endosomes, or the Golgi apparatus. High basal levels of $Tyr^{1250/1251}$ (Figure 5.16, Figure 5.19, Figure 5.22) as well as IGF-1-induced phosphorylation on IGF-1R promotes translocation to the Golgi This is also associated with cell migration and a more migratory cancer cell phenotype (Figure 5.19, Figure 5.23).

Our data together with reports from the literature propose that IGF-1R-induced SHC/Ras signalling may occur at the Golgi-apparatus to promote cell migration and perhaps other cellular processes. We observed that fragmentation of the Golgi apparatus abolishes IGF-1R mediated cell migration in HS-578T cells (Figure 5.23). This is accompanied by loss of IGF-1-induced SHC phosphorylation and reduced basal SHC phosphorylation (Figure 5.21), indicating that SHC/Ras signalling may emanate from the Golgi apparatus. Interestingly, this was not observed in MCF-7 cells (Figure 5.21, Figure 5.24), suggesting a different location for SHC/Ras in these cells.

IGF-1-mediated activation of Ras signalling in the Golgi may also mediate the release of vesicles from the Golgi to facilitate the rearrangement of the actin cytoskeleton permissive to migration, or the signals that lead to the

disassembly of focal adhesions, as has been proposed previously (Chiu et al., 2002). We also demonstrated that when migratory cells are grown in cultures with many cell-cell adhesions, IGF-1R is predominantly located at the Golgi apparatus and the activation of SHC is impaired (Figure 5.24). This might be caused, as described above, by β1-Integrin-mediated contact inhibition of migration. The high basal phosphorylation of SHC in HS-578T cells, indicates that IGF-1R localisation at the Golgi could also mediate sustained SHC activation, as it has been described for Golgi-derived Ras signalling.

Taken together, this work proposes a complex network between SHC/Ras and β1-integrin/IGF-1R. Together they regulate different cellular processes dependent on their subcellular location, which is influenced by the cellular phenotype and environmental conditions. This is the first study to describe the Golgi-apparatus as a novel compartment for IGF-1R signalling.

6.3.2 Mechanism of anchoring and releasing IGF-1R from the Golgi apparatus

This thesis work also opens up possibilities for new areas of investigation on the mechanisms of action of Golgi-derived IGF-1R in key cellular processes. The first question is how does $Tyr^{1250/1251}$ promote Golgi accumulation of the IGF-1R? IGF-1 enhances the already evident basal phosphorylation of $Tyr^{1250/1251}$ in cells (Figure 5.3, Figure 5.4 and Figure 5.8) leading to rapid internalisation and translocation of the receptor to the Golgi (Figure 5.13, Figure 5.16). This is also observed for the EGFR in hepatocellular carcinoma, where the EGFR interacts with GOLM1 in Rab5-positive vesicles shortly after EGF stimulation. This interaction anchors EGFR to the Golgi. $Tyr^{1250/1251}$ phosphorylation could enable IGF-1R interaction with a Golgi membrane

protein and thereby promote accumulation in the Golgi. Phosphorylation on $Tyr^{1250/1251}$ could be used as a docking site to recruit SH2 domain-containing proteins. In addition we show here that the dephosphorylation of IGF-1R on $Tyr^{1250/1251}$ is associated with release of the IGF-1R from its Golgi location. The question arises, whether one of the identified, Golgi-associated phosphatases (Farhan et al., 2010) is responsible for dephosphorylating the IGF-1R and thereby releasing it from the Golgi compartment. Although, known IGF-1R phosphatases including SHP2 (Ivins Zito et al., 2004, Kiely et al., 2005, Carver et al., 2010) and PTP-1B (Wälchli et al., 2000, Buckley et al., 2002) were not included in Golgi phosphatases identified in a functional siRNA screening (Farhan et al., 2010), a novel phosphatase may dephosphorylate $Tyr^{1250/1251}$ in the IGF-1R. Furthermore, Ye *et al*, showed that the release of the EGFR from the Golgi apparatus is dependent on Rab11 recruitment to the complex of EGFR and GOLM1 (Ye et al., 2016). Therefore, it is possible, that Rab proteins participate in IGF-1R dephosphorylation of $Tyr^{1250/1251}$ and subsequently release from the Golgi- compartment.

Since Golgi-derived IGF-1R signalling is proposed to associate with a migratory cancer cell phenotype, it would be of great interest to further investigate the mechanisms by which the IGF-1R is anchored to the Golgi and the mechanisms of its release.

6.3.3 IGF-1R as a cargo protein in exocytosis and endocytosis

Our model for IGF-1R release from the Golgi to the leading edge of migrating cells suggests that the IGF-1R could act as a cargo protein for other cell membrane or cell adhesion proteins such as Integrins. Other growth factor receptors have previously been demonstrated to modulate Integrin

internalisation (Roberts et al., 2001, Mai et al., 2014) or to internalise together with Integrin (Caswell and Norman, 2006, Muller et al., 2013). The internalisation of β1-Integrin with cell membrane components was proposed for the EGFR (Caswell et al., 2008). EGFR-mediated activation of the Ras/MAPK pathway requires receptor endocytosis (von Zastrow and Sorkin, 2007), whereas, like the IGF-1R, PI3K activation occurs near or at the plasma membrane (Haugh and Meyer, 2002). In lung cancer cells EGFR and β1-Integrin recycle rapidly back to the membrane in a Rab-coupling protein-dependent manner, which facilitates β1-Integrin-mediated migration. The translocation of the IGF-1R to the Golgi apparatus following endocytosis, however, suggests that IGF-1R and β1-Integrin are part of different endocytosis pathways, because Integrins are known to undergo fast recycling back to the membrane (Jones et al., 2006, Caswell and Norman, 2006, Caswell et al., 2008, Ivaska and Heino, 2011).

IGF-1R internalisation was recently shown to be regulated by an interaction with IRS-1 (Yoneyama et al., 2018). The prolonged interaction of these proteins causes the retention of IGF-1R on the plasma membrane. Overexpression of IRS-1 also partially inhibits β1-Integrin and EGFR endocytosis, however, although the function of IRS-1 in β1-Integrin and EGFR endocytosis has not been identified, it suggests that IRS-1 facilitates endocytosis of proteins that are in close proximity to the IGF-1R (Yoneyama et al., 2018). Thus it will be of interest to further investigate, whether the IGF-1R internalises as part of a complex, or whether its internalisation also leads to the endocytosis of other proteins.

The Golgi apparatus has a bidirectional trafficking function- anterograde and retrograde. It is involved in the secretory transport of cargo proteins to the

plasma membrane, but can also receive vesicles with cargo from the cell surface. Endocytosis and exocytosis of membrane proteins is associated with the Rab superfamily which contains 61 members (Pereira-Leal and Seabra, 2001). Rab proteins are small GTPases that regulate intracellular vesicular transport and protein trafficking between compartments of the endocytic and secretory pathway (Zerial and McBride, 2001). They mediate the formation and budding of vesicles from the donor compartment and transport to the acceptor compartment, where they facilitate the release of the vesicle cargo (Wennerberg et al., 2005). Little is known about the interaction of Rab proteins and IGF-1R. However, it is thought, that the endocytosis of IGF-1R, similar to other RTKs, may be mediated by Rab5. Therefore, although not addressed in this thesis, the involvement of Rab5 in the IGF-1R endocytosis is a clear research area for future investigation.

Interestingly, both Rab5-mediated EGFR endocytosis and Rab11-mediated EGFR recycling were proposed to be involved in the GOLM-mediated EGFR anchorage to the Golgi and its release to the membrane (Ye et al., 2016). Furthermore Rab6 has recently been described to regulate several anterograde and retrograde trafficking pathways to and from the Golgi apparatus (Fourriere et al., 2019). The latter study demonstrates that exocytosis of proteins did not occur randomly at the cell surface but is rather restricted to secretion hotspots in close proximity to focal adhesion points, and is directed by microtubules. Since we observed a fast recruitment of IGF-1R to nascent focal adhesion points which is associated with lower levels of IGF-1R phosphorylation on $Tyr^{1250/1251}$, IGF-1R could be a cargo protein for the secretory pathway initiating the assembly of focal adhesion points (Figure 5.22).

During cell adhesion, dephosphorylated $Tyr^{1250/1251}$ IGF-1R transiently relocated form the Golgi to the membrane, where phosphorylation on $Tyr^{1250/1251}$ was induced in a time-dependent manner and the active IGF-1R became anchored at the Golgi again (Figure 5.22). Furthermore, IGF-1R was recruited to the cell protrusions of migrating cells (Figure 5.23), indicating that the release of active IGF-1R from its Golgi anchorage is regulated by the dynamic formation of focal adhesion points. However, whether IGF-1R is involved in the process of cargo proteins leaving the Golgi, either directly or indirectly, needs to be further investigated.

Considering our results, that IGF-1R is released from the Golgi upon the formation of new focal adhesions and in conditions of cell migration, it would also be interesting to investigate complex formation of Rab proteins, such as Rab11 and Rab6, with the IGF-1R.

6.3.4 IGF-1R localisation in the Golgi as a potential biomarker

The lack of validated predictive biomarkers to select suitable patients has been cited as a reason for the failure of anti-IGF-1R agents in clinical trials. Despite much research in the area, no biomarker has yet been found to predict a positive outcome for the patient following IGF-1R inhibition (Simpson et al., 2017).

The IGF-1R is almost ubiquitously expressed in human tissues including cancer. However, mutations in the *igf-1r* are rarely reported in cancer (Arcaro, 2013), so the IGF-1R is not a main driver of cancer development (Vogelstein et al., 2013). Assessing IGF-1R levels alone shows no clear correlation between the expression level or its autophosphorylation/activity (Mukohara et al., 2009). In several breast cancer cell lines, the expression level

of the IGF-1R is relatively low, which could result in lack of sensitivity to IGF-1R targeted therapies.

IGF-1R in the nucleus has been proposed as a potential predictive biomarker in sarcoma (Asmane et al., 2012). In this study tumours from 16 patients treated with different anti-IGF-1R Abs were assessed by routine pathology to identify potential factors that modify the response. Nuclear staining was associated with enhanced progression-free survival and overall survival for all patients receiving IGF-1R-Ab therapy (Asmane et al., 2012). However, in prostate cancers, plasma membrane IGF-1R was predominantly found in benign glands, whereas in malignant epithelium IGF-1R was internalised and mainly localised to the cytoplasm and the nucleus. Furthermore, more advanced tumour stages were associated with nuclear IGF-1R (Aleksic et al., 2018).

Our data suggests that Golgi-localised IGF-1R is linked with an aggressive and migratory cancer cell phenotype and is regulated by the $Tyr^{1250/1251}$ phosphorylation. Moreover, Golgi-localised IGF-1R is active and can induce signalling (Figure 5.21, Figure 5.24). Therefore, IGF-1R targeting with monoclonal antibodies designed to prevent ligand binding or trigger receptor internalisation and degradation are unlikely to be effective in cells expressing Golgi-located IGF-1R. This problem is also proposed for the MET receptor, which can avoid inhibition by monoclonal antibodies by being localised and active in intracellular compartments, including the Golgi apparatus (Kim and Kim, 2017, Frazier et al., 2019).

Therefore, one of the most significant findings in this thesis work may be that Golgi-located IGF-1R is a potential biomarker to a) identify patients with

a higher risk of an aggressive phenotype and b) to select a subset where it is possible that anti-IGF-1R antibodies would not be effective. As a biomarker, Golgi-localised IGF-1R could be assessed in routine immunohistochemistry and pathology. However, the results presented in this thesis is limited to cell lines and to test this concept further it will be necessary to assess IGF-1R localisation in cohorts of benign tissue and malignant tumours from several cancer types. This would also establish whether location of the IGF-1R in the Golgi can be correlated with the patient's clinical outcome.

6.3.5 The insulin receptor and the Golgi apparatus

It is still of great interest to establish what distinguishes IGF-1R and IR signalling. A number of previous studies have also tried to address this (Tavare et al., 1992, Kaliman et al., 1992, Blakesley et al., 1996, Esposito et al., 1997, O'Connor et al., 1997, Chen et al., 1998, Hongo et al., 1998, Li et al., 1998, Liu et al., 1998, Kiely et al., 2002, Leahy et al., 2004, Kiely et al., 2005). The C-terminal tails of the IGF-1R and IR exhibit the greatest divergence in sequence of any domain in these receptors. It has been proposed as a regulatory domain and with potential to harbour key differences in function between these receptors (Miura et al., 1995b, Miura and Baserga, 1997, Leahy et al., 2004, Kiely et al., 2005, Kelly et al., 2012, Zheng et al., 2012). This study shows that phosphorylated $Tyr^{1250/1251}$ is linked to IGF-1R endocytosis and therefore activation of the SHC and MAPK pathways. Subsequently IGF-1R is translocated to the Golgi and can induce IGF-1 signalling. As $Tyr^{1250/1251}$ is not present in the IR C-terminal tail the question arises whether IR also has the capacity to translocate to the Golgi. Although not addressed in this study, this question retains considerable interest for future investigations.

6.4 CONCLUSION

The communication between plasma membrane signalling and the Golgi apparatus is essential for the regulation of multiple cellular processes including cell migration. Taken together, results from our study describe a novel trafficking route for the IGF-1R- from the plasma membrane to the Golgi apparatus. Golgi-localised IGF-1R is active and can signal, and therefore we present the Golgi-apparatus as a novel signalling compartment for the IGF-1R in migratory cells. This also provides a reasonable explanation for why targeting the IGF-1R on the cell surface showed poor efficacy in clinical trials and may help future approaches in targeting the IGF-1R. With IGF-1R and other oncogenic growth factor signalling occurring at the Golgi apparatus to promote an aggressive cancer phenotype, its targeting has great potential in cancer therapy.

7 REFERENCES

ACCONCIA, F., SIGISMUND, S. & POLO, S. 2009. Ubiquitin in trafficking: The network at work. *Experimental Cell Research,* 315**,** 1610-1618.

ADAMS, D. R., RON, D. & KIELY, P. A. 2011. RACK1, A multifaceted scaffolding protein: Structure and function. *Cell Commun Signal,* 9**,** 22.

ADAMS, T. E., EPA, V. C., GARRETT, T. P. J. & WARD*, C. W. 2000. Structure and function of the type 1 insulin-like growth factor receptor. *Cellular and Molecular Life Sciences CMLS,* 57**,** 1050-1093.

AFIFY, S. M. & SENO, M. 2019. Conversion of Stem Cells to Cancer Stem Cells: Undercurrent of Cancer Initiation. *Cancers (Basel),* 11.

AHMED, S. B. M. & PRIGENT, S. A. 2017. Insights into the Shc Family of Adaptor Proteins. *Journal of molecular signaling,* 12**,** 2-2.

AHN, J., TRUESDELL, P., MEENS, J., KADISH, C., YANG, X., BOAG, A. H. & CRAIG, A. W. B. 2013. Fer Protein-Tyrosine Kinase Promotes Lung Adenocarcinoma Cell Invasion and Tumor Metastasis. *Molecular Cancer Research,* 11**,** 952-963.

AIKEN, R., AXELSON, M., HARMENBERG, J., KLOCKARE, M., LARSSON, O. & WASSBERG, C. 2017. Phase I clinical trial of AXL1717 for treatment of relapsed malignant astrocytomas: analysis of dose and response. *Oncotarget,* 8**,** 81501-81510.

ALEKSIC, T., CHITNIS, M. M., PERESTENKO, O. V., GAO, S., THOMAS, P. H., TURNER, G. D., PROTHEROE, A. S., HOWARTH, M. & MACAULAY, V. M. 2010. Type 1 insulin-like growth factor receptor translocates to the nucleus of human tumor cells. *Cancer research,* 70**,** 6412-6419.

ALEKSIC, T., GRAY, N., WU, X., RIEUNIER, G., OSHER, E., MILLS, J., VERRILL, C., BRYANT, R. J., HAN, C., HUTCHINSON, K., LAMBERT, A. G., KUMAR, R., HAMDY, F. C., WEYER-CZERNILOFSKY, U., SANDERSON, M. P., BOGENRIEDER, T., TAYLOR, S. & MACAULAY, V. M. 2018. Nuclear IGF1R Interacts with Regulatory Regions of Chromatin to Promote RNA Polymerase II Recruitment and Gene Expression Associated with Advanced Tumor Stage. *Cancer Research,* 78**,** 3497-3509.

ALLARD, J. B. & DUAN, C. 2018. IGF-Binding Proteins: Why Do They Exist and Why Are There So Many? *Front Endocrinol (Lausanne),* 9**,** 117.

AMSELEM, S., DUQUESNOY, P., ATTREE, O., NOVELLI, G., BOUSNINA, S., POSTEL-VINAY, M.-C. & GOOSSENS, M. 1989. Laron Dwarfism and Mutations of the Growth Hormone–Receptor Gene. *New England Journal of Medicine,* 321**,** 989-995.

ANDERSSON, S., D'ARCY, P., LARSSON, O. & SEHAT, B. 2009. Focal adhesion kinase (FAK) activates and stabilizes IGF-1 receptor. *Biochemical and Biophysical Research Communications,* 387**,** 36-41.

ARAKI, E., LIPES, M. A., PATTI, M. E., BRÜNING, J. C., HAAG, B., 3RD, JOHNSON, R. S. & KAHN, C. R. 1994. Alternative pathway of insulin signalling in mice with targeted disruption of the IRS-1 gene. *Nature,* 372**,** 186-90.

ARCARO, A. 2013. Targeting the insulin-like growth factor-1 receptor in human cancer. *Frontiers in pharmacology,* 4**,** 30-30.

ARTEAGA, C. L., KITTEN, L. J., CORONADO, E. B., JACOBS, S., KULL, F. C., JR., ALLRED, D. C. & OSBORNE, C. K. 1989. Blockade of the type I somatomedin receptor inhibits growth of human breast cancer cells in athymic mice. *J Clin Invest,* 84**,** 1418-23.

ASLAM, M. I., HETTMER, S., ABRAHAM, J., LATOCHA, D., SOUNDARARAJAN, A., HUANG, E. T., GOROS, M. W., MICHALEK, J. E., WANG, S., MANSOOR, A., DRUKER, B. J., WAGERS, A. J., TYNER, J. W. & KELLER, C. 2013. Dynamic and nuclear expression of PDGFRα and IGF-1R in alveolar Rhabdomyosarcoma. *Mol Cancer Res,* 11**,** 1303-13.

ASMANE, I., WATKIN, E., ALBERTI, L., DUC, A., MAREC-BERARD, P., RAY-COQUARD, I., CASSIER, P., DECOUVELAERE, A. V., RANCHÈRE, D., KURTZ, J. E., BERGERAT, J. P. & BLAY, J. Y. 2012. Insulin-like growth factor type 1 receptor (IGF-1R) exclusive nuclear staining: a predictive biomarker for IGF-1R monoclonal antibody (Ab) therapy in sarcomas. *Eur J Cancer,* 48**,** 3027-35.

AVRUCH, J., KHOKHLATCHEV, A., KYRIAKIS, J. M., LUO, Z., TZIVION, G., VAVVAS, D. & ZHANG, X. F. 2001. Ras activation of the Raf kinase: tyrosine kinase recruitment of the MAP kinase cascade. *Recent Prog Horm Res,* 56**,** 127-55.

BACKER, J. M., SHOELSON, S. E., HARING, E. & WHITE, M. F. 1991. Insulin receptors internalize by a rapid, saturable pathway requiring receptor autophosphorylation and an intact juxtamembrane region. *J Cell Biol,* 115**,** 1535-45.

BAE, S., PARK, J. & KIM, J.-S. 2014. Cas-OFFinder: a fast and versatile algorithm that searches for potential off-target sites of Cas9 RNA-guided endonucleases. *Bioinformatics,* 30**,** 1473-1475.

BAILYES, E. M., NAVE, B. T., SOOS, M. A., ORR, S. R., HAYWARD, A. C. & SIDDLE, K. 1997. Insulin receptor/IGF-I receptor hybrids are widely distributed in mammalian tissues: quantification of individual receptor species by selective immunoprecipitation and immunoblotting. *Biochem J,* 327 (Pt 1)**,** 209-15.

BAJRAMI, I., MARLOW, R., VAN DE VEN, M., BROUGH, R., PEMBERTON, H. N., FRANKUM, J., SONG, F., RAFIQ, R., KONDE, A., KRASTEV, D. B., MENON, M., CAMPBELL, J., GULATI, A., KUMAR, R., PETTITT, S. J., GURDEN, M. D., CARDENOSA, M. L., CHONG, I., GAZINSKA, P., WALLBERG, F., SAWYER, E. J., MARTIN, L.-A., DOWSETT, M., LINARDOPOULOS, S., NATRAJAN, R., RYAN, C. J., DERKSEN, P. W. B., JONKERS, J., TUTT, A. N. J., ASHWORTH, A. & LORD, C. J. 2018. E-Cadherin/ROS1 Inhibitor Synthetic Lethality in Breast Cancer. *Cancer Discovery,* 8**,** 498-515.

BAKER, J., LIU, J.-P., ROBERTSON, E. J. & EFSTRATIADIS, A. 1993. Role of insulin-like growth factors in embryonic and postnatal growth. *Cell,* 75**,** 73-82.

BARATA, P., COONEY, M., TYLER, A., WRIGHT, J., DREICER, R. & GARCIA, J. A. 2018. A phase 2 study of OSI-906 (linsitinib, an insulin-like growth factor receptor-1 inhibitor) in patients with asymptomatic or mildly symptomatic (non-opioid requiring) metastatic castrate resistant prostate cancer (CRPC). *Investigational New Drugs,* 36**,** 451-457.

BARBIERI, M., BONAFÈ, M., FRANCESCHI, C. & PAOLISSO, G. 2003. Insulin/IGF-I-signaling pathway: an evolutionarily conserved mechanism of longevity from yeast to

humans. *American Journal of Physiology-Endocrinology and Metabolism,* 285**,** E1064-E1071.

BARD, F., MAZELIN, L., PÉCHOUX-LONGIN, C., MALHOTRA, V. & JURDIC, P. 2003. Src Regulates Golgi Structure and KDEL Receptor-dependent Retrograde Transport to the Endoplasmic Reticulum. *Journal of Biological Chemistry,* 278**,** 46601-46606.

BARRETT, J. P., MINOGUE, A. M., FALVEY, A. & LYNCH, M. A. 2015. Involvement of IGF-1 and Akt in M1/M2 activation state in bone marrow-derived macrophages. *Experimental Cell Research,* 335**,** 258-268.

BARTON-DAVIS, E. R., SHOTURMA, D. I., MUSARO, A., ROSENTHAL, N. & SWEENEY, H. L. 1998. Viral mediated expression of insulin-like growth factor I blocks the aging-related loss of skeletal muscle function. *Proc Natl Acad Sci U S A,* 95**,** 15603-7.

BASERGA, R., HONGO, A., RUBINI, M., PRISCO, M. & VALENTINIS, B. 1997. The IGF-I receptor in cell growth, transformation and apoptosis. *Biochimica et Biophysica Acta (BBA) - Reviews on Cancer,* 1332**,** F105-F126.

BAYNE, M. L., APPLEBAUM, J., UNDERWOOD, D., CHICCHI, G. G., GREEN, B. G., HAYES, N. S. & CASCIERI, M. A. 1989. The C region of human insulin-like growth factor (IGF) I is required for high affinity binding to the type 1 IGF receptor. *J Biol Chem,* 264**,** 11004-8.

BELFIORE, A., FRASCA, F., PANDINI, G., SCIACCA, L. & VIGNERI, R. 2009. Insulin receptor isoforms and insulin receptor/insulin-like growth factor receptor hybrids in physiology and disease. *Endocr Rev,* 30**,** 586-623.

BELFIORE, A., MALAGUARNERA, R., NICOLOSI, M. L., LAPPANO, R., RAGUSA, M., MORRIONE, A. & VELLA, V. 2018. A novel functional crosstalk between DDR1 and the IGF axis and its relevance for breast cancer. *Cell Adhesion & Migration,* 12**,** 305-314.

BENINI, S., MANARA, M. C., BALDINI, N., CERISANO, V., MASSIMO, S., MERCURI, M., LOLLINI, P. L., NANNI, P., PICCI, P. & SCOTLANDI, K. 2001. Inhibition of insulin-like growth factor I receptor increases the antitumor activity of doxorubicin and vincristine against Ewing's sarcoma cells. *Clin Cancer Res,* 7**,** 1790-7.

BERETTA, L., GINGRAS, A. C., SVITKIN, Y. V., HALL, M. N. & SONENBERG, N. 1996. Rapamycin blocks the phosphorylation of 4E-BP1 and inhibits cap-dependent initiation of translation. *Embo j,* 15**,** 658-64.

BID, H. K., ZHAN, J., PHELPS, D. A., KURMASHEVA, R. T. & HOUGHTON, P. J. 2012. Potent inhibition of angiogenesis by the IGF-1 receptor-targeting antibody SCH717454 is reversed by IGF-2. *Mol Cancer Ther,* 11**,** 649-59.

BIGGS, W. H., MEISENHELDER, J., HUNTER, T., CAVENEE, W. K. & ARDEN, K. C. 1999. Protein kinase B/Akt-mediated phosphorylation promotes nuclear exclusion of the winged helix transcription factor FKHR1. *Proceedings of the National Academy of Sciences,* 96**,** 7421-7426.

BISEL, B., WANG, Y., WEI, J.-H., XIANG, Y., TANG, D., MIRON-MENDOZA, M., YOSHIMURA, S.-I., NAKAMURA, N. & SEEMANN, J. 2008. ERK regulates Golgi and centrosome orientation towards the leading edge through GRASP65. *Journal of Cell Biology,* 182**,** 837-843.

BITAR, M. S. 1997. Insulin-like growth factor-1 reverses diabetes-induced wound healing impairment in rats. *Horm Metab Res,* 29**,** 383-6.

BLAKESLEY, V. A., KALEBIC, T., HELMAN, L. J., STANNARD, B., FARIA, T. N., ROBERTS, C. T., JR. & LEROITH, D. 1996. Tumorigenic and mitogenic capacities are reduced in transfected fibroblasts expressing mutant insulin-like growth factor (IGF)-I receptors. The role of tyrosine residues 1250, 1251, and 1316 in the carboxy-terminus of the IGF-I receptor. *Endocrinology,* 137**,** 410-7.

BLAKESLEY, V. A., KOVAL, A. P., STANNARD, B. S., SCRIMGEOUR, A. & LEROITH, D. 1998. Replacement of Tyrosine 1251 in the Carboxyl Terminus of the Insulin-like Growth Factor-I Receptor Disrupts the Actin Cytoskeleton and Inhibits Proliferation and Anchorage-independent Growth. *Journal of Biological Chemistry,* 273**,** 18411-18422.

BODZIN, A. S., WEI, Z., HURTT, R., GU, T. & DORIA, C. 2012. Gefitinib resistance in HCC mahlavu cells: upregulation of CD133 expression, activation of IGF-1R signaling pathway, and enhancement of IGF-1R nuclear translocation. *J Cell Physiol,* 227**,** 2947-52.

BOHULA, E. A., SALISBURY, A. J., SOHAIL, M., PLAYFORD, M. P., RIEDEMANN, J., SOUTHERN, E. M. & MACAULAY, V. M. 2003. The Efficacy of Small Interfering RNAs Targeted to the Type 1 Insulin-like Growth Factor Receptor (IGF1R) Is Influenced by Secondary Structure in the IGF1R Transcript. *Journal of Biological Chemistry,* 278**,** 15991-15997.

BOUCHER, J., SOFTIC, S., EL OUAAMARI, A., KRUMPOCH, M. T., KLEINRIDDERS, A., KULKARNI, R. N., O'NEILL, B. T. & KAHN, C. R. 2016. Differential Roles of Insulin and IGF-1 Receptors in Adipose Tissue Development and Function. *Diabetes,* 65**,** 2201-2213.

BOUGHERARA, H., SUBRA, F., CRÉPIN, R., TAUC, P., AUCLAIR, C. & POUL, M.-A. 2009. The Aberrant Localization of Oncogenic Kit Tyrosine Kinase Receptor Mutants Is Reversed on Specific Inhibitory Treatment. *Molecular Cancer Research,* 7**,** 1525-1533.

BOWE, R. A., COX, O. T., AYLLÓN, V., TRESSE, E., HEALY, N. C., EDMUNDS, S. J., HUIGSLOOT, M. & O'CONNOR, R. 2014. PDLIM2 regulates transcription factor activity in epithelial-to-mesenchymal transition via the COP9 signalosome. *Molecular Biology of the Cell,* 25**,** 184-195.

BRAHMKHATRI, V. P., PRASANNA, C. & ATREYA, H. S. 2015. Insulin-like growth factor system in cancer: novel targeted therapies. *BioMed research international,* 2015**,** 538019-538019.

BRODT, P., FALLAVOLLITA, L., KHATIB, A.-M., SAMANI, A. A. & ZHANG, D. 2001. Cooperative Regulation of the Invasive and Metastatic Phenotypes by Different Domains of the Type I Insulin-like Growth Factor Receptor β Subunit. *Journal of Biological Chemistry,* 276**,** 33608-33615.

BROWN-BORG, H. M., BORG, K. E., MELISKA, C. J. & BARTKE, A. 1996. Dwarf mice and the ageing process. *Nature,* 384**,** 33.

BRYWE, K. G., MALLARD, C., GUSTAVSSON, M., HEDTJÄRN, M., LEVERIN, A. L., WANG, X., BLOMGREN, K., ISGAARD, J. & HAGBERG, H. 2005. IGF-I neuroprotection in

the immature brain after hypoxia-ischemia, involvement of Akt and GSK3beta? *Eur J Neurosci,* 21**,** 1489-502.

BUCK, E., GOKHALE, P. C., KOUJAK, S., BROWN, E., EYZAGUIRRE, A., TAO, N., ROSENFELD-FRANKLIN, M., LERNER, L., CHIU, M. I., WILD, R., EPSTEIN, D., PACHTER, J. A. & MIGLARESE, M. R. 2010. Compensatory Insulin Receptor (IR) Activation on Inhibition of Insulin-Like Growth Factor-1 Receptor (IGF-1R): Rationale for Cotargeting IGF-1R and IR in Cancer. *Molecular Cancer Therapeutics,* 9**,** 2652-2664.

BUCKLEY, D. A., CHENG, A., KIELY, P. A., TREMBLAY, M. L. & O'CONNOR, R. 2002. Regulation of Insulin-Like Growth Factor Type I (IGF-I) Receptor Kinase Activity by Protein Tyrosine Phosphatase 1B (PTP-1B) and Enhanced IGF-I-Mediated Suppression of Apoptosis and Motility in PTP-1B-Deficient Fibroblasts. *Molecular and Cellular Biology,* 22**,** 1998-2010.

CARBONI, J. M., WITTMAN, M., YANG, Z., LEE, F., GREER, A., HURLBURT, W., HILLERMAN, S., CAO, C., CANTOR, G. H., DELL-JOHN, J., CHEN, C., DISCENZA, L., MENARD, K., LI, A., TRAINOR, G., VYAS, D., KRAMER, R., ATTAR, R. M. & GOTTARDIS, M. M. 2009. BMS-754807, a small molecule inhibitor of insulin-like growth factor-1R/IR. *Molecular Cancer Therapeutics,* 8**,** 3341-3349.

CARTER, S., BISCHOF, O., DEJEAN, A. & VOUSDEN, K. H. 2007. C-terminal modifications regulate MDM2 dissociation and nuclear export of p53. *Nature Cell Biology,* 9**,** 428-435.

CARVER, K. C., PIAZZA, T. M. & SCHULER, L. A. 2010. Prolactin enhances insulin-like growth factor I receptor phosphorylation by decreasing its association with the tyrosine phosphatase SHP-2 in MCF-7 breast cancer cells. *J Biol Chem,* 285**,** 8003-12.

CASWELL, P. T., CHAN, M., LINDSAY, A. J., MCCAFFREY, M. W., BOETTIGER, D. & NORMAN, J. C. 2008. Rab-coupling protein coordinates recycling of alpha5beta1 integrin and EGFR1 to promote cell migration in 3D microenvironments. *The Journal of cell biology,* 183**,** 143-155.

CASWELL, P. T. & NORMAN, J. C. 2006. Integrin trafficking and the control of cell migration. *Traffic,* 7**,** 14-21.

CHAKRAVARTI, A., LOEFFLER, J. S. & DYSON, N. J. 2002. Insulin-like growth factor receptor I mediates resistance to anti-epidermal growth factor receptor therapy in primary human glioblastoma cells through continued activation of phosphoinositide 3-kinase signaling. *Cancer Res,* 62**,** 200-7.

CHAN, J. M., STAMPFER, M. J., GIOVANNUCCI, E., GANN, P. H., MA, J., WILKINSON, P., HENNEKENS, C. H. & POLLAK, M. 1998. Plasma insulin-like growth factor-I and prostate cancer risk: a prospective study. *Science,* 279**,** 563-6.

CHAN, T. O., RITTENHOUSE, S. E. & TSICHLIS, P. N. 1999. AKT/PKB and other D3 phosphoinositide-regulated kinases: kinase activation by phosphoinositide-dependent phosphorylation. *Annu Rev Biochem,* 68**,** 965-1014.

CHAND, H. S., WOLDEGIORGIS, Z., SCHWALM, K., MCDONALD, J. & TESFAIGZI, Y. 2012. Acute inflammation induces insulin-like growth factor-1 to mediate Bcl-2 and Muc5ac expression in airway epithelial cells. *American journal of respiratory cell and molecular biology,* 47**,** 784-791.

CHANG, L. & KARIN, M. 2001. Mammalian MAP kinase signalling cascades. *Nature,* 410**,** 37-40.

CHAPUIS, N., TAMBURINI, J., CORNILLET-LEFEBVRE, P., GILLOT, L., BARDET, V., WILLEMS, L., PARK, S., GREEN, A. S., IFRAH, N., DREYFUS, F., MAYEUX, P., LACOMBE, C. & BOUSCARY, D. 2010. Autocrine IGF-1/IGF-1R signaling is responsible for constitutive PI3K/Akt activation in acute myeloid leukemia: therapeutic value of neutralizing anti-IGF-1R antibody. *Haematologica,* 95**,** 415-423.

CHARDIN, P., CAMONIS, J. H., GALE, N. W., VAN AELST, L., SCHLESSINGER, J., WIGLER, M. H. & BAR-SAGI, D. 1993. Human Sos1: a guanine nucleotide exchange factor for Ras that binds to GRB2. *Science,* 260**,** 1338-43.

CHEN, H.-N., YUAN, K., XIE, N., WANG, K., HUANG, Z., CHEN, Y., DOU, Q., WU, M., NICE, E. C., ZHOU, Z.-G. & HUANG, C. 2016. PDLIM1 Stabilizes the E-Cadherin/β-Catenin Complex to Prevent Epithelial–Mesenchymal Transition and Metastatic Potential of Colorectal Cancer Cells. *Cancer Research,* 76**,** 1122-1134.

CHEN, H., PARADIES, N. E., FEDOR-CHAIKEN, M. & BRACKENBURY, R. 1997. E-cadherin mediates adhesion and suppresses cell motility via distinct mechanisms. *Journal of Cell Science,* 110**,** 345-356.

CHEN, H., YAN, G. C. & GISHIZKY, M. L. 1998. Identification of structural characteristics that contribute to a difference in antiapoptotic function between human insulin and insulin-like growth factor 1 receptors. *Cell Growth Differ,* 9**,** 939-47.

CHEN, M., CHEN, S. C. & PALLEN, C. J. 2006. Integrin-induced tyrosine phosphorylation of protein-tyrosine phosphatase-alpha is required for cytoskeletal reorganization and cell migration. *J Biol Chem,* 281**,** 11972-80.

CHEN, W. C. & OBRINK, B. 1991. Cell-cell contacts mediated by E-cadherin (uvomorulin) restrict invasive behavior of L-cells. *J Cell Biol,* 114**,** 319-27.

CHIA, J., GOH, G., RACINE, V., NG, S., KUMAR, P. & BARD, F. 2012. RNAi screening reveals a large signaling network controlling the Golgi apparatus in human cells. *Molecular Systems Biology,* 8**,** 629.

CHIU, V. K., BIVONA, T., HACH, A., SAJOUS, J. B., SILLETTI, J., WIENER, H., JOHNSON, R. L., COX, A. D. & PHILIPS, M. R. 2002. Ras signalling on the endoplasmic reticulum and the Golgi. *Nature Cell Biology,* 4**,** 343-350.

CHOW, J. C., CONDORELLI, G. & SMITH, R. J. 1998. Insulin-like Growth Factor-I Receptor Internalization Regulates Signaling via the Shc/Mitogen-activated Protein Kinase Pathway, but Not the Insulin Receptor Substrate-1 Pathway. *Journal of Biological Chemistry,* 273**,** 4672-4680.

CHRISTOFFERSEN, C. T., BORNFELDT, K. E., ROTELLA, C. M., GONZALES, N., VISSING, H., SHYMKO, R. M., TEN HOEVE, J., GROFFEN, J., HEISTERKAMP, N. & DE MEYTS, P. 1994. Negative cooperativity in the insulin-like growth factor-I receptor and a chimeric IGF-I/insulin receptor. *Endocrinology,* 135**,** 472-475.

CHRISTOPOULOS, P. F., MSAOUEL, P. & KOUTSILIERIS, M. 2015. The role of the insulin-like growth factor-1 system in breast cancer. *Molecular cancer,* 14**,** 43-43.

CITORES, L., BAI, L., SØRENSEN, V. & OLSNES, S. 2007. Fibroblast growth factor receptor-induced phosphorylation of STAT1 at the golgi apparatus without translocation to the nucleus. *Journal of Cellular Physiology,* 212**,** 148-156.

CLARK, G. J., DRUGAN, J. K., ROSSMAN, K. L., CARPENTER, J. W., ROGERS-GRAHAM, K., FU, H., DER, C. J. & CAMPBELL, S. L. 1997. 14-3-3 zeta negatively regulates raf-1 activity by interactions with the Raf-1 cysteine-rich domain. *J Biol Chem,* 272**,** 20990-3.

CLEMMONS, D. R. 2012. Metabolic actions of insulin-like growth factor-I in normal physiology and diabetes. *Endocrinol Metab Clin North Am,* 41**,** 425-43, vii-viii.

CODONY-SERVAT, J., CUATRECASAS, M., ASENSIO, E., MONTIRONI, C., MARTÍNEZ-CARDÚS, A., MARÍN-AGUILERA, M., HORNDLER, C., MARTÍNEZ-BALIBREA, E., RUBINI, M., JARES, P., REIG, O., VICTORIA, I., GABA, L., MARTÍN-RICHARD, M., ALONSO, V., ESCUDERO, P., FERNÁNDEZ-MARTOS, C., FELIU, J., MÉNDEZ, J. C., MÉNDEZ, M., GALLEGO, J., SALUD, A., ROJO, F., CASTELLS, A., PRAT, A., ROSELL, R., GARCÍA-ALBÉNIZ, X., CAMPS, J. & MAUREL, J. 2017. Nuclear IGF-1R predicts chemotherapy and targeted therapy resistance in metastatic colorectal cancer. *British Journal of Cancer,* 117**,** 1777-1786.

COHEN, P., PEEHL, D. M., STAMEY, T. A., WILSON, K. F., CLEMMONS, D. R. & ROSENFELD, R. G. 1993. Elevated levels of insulin-like growth factor-binding protein-2 in the serum of prostate cancer patients. *J Clin Endocrinol Metab,* 76**,** 1031-5.

COLE, L. A., ZIRNGIBL, R., CRAIG, A. W. B., JIA, Z. & GREER, P. 1999. Mutation of a highly conserved aspartate residue in subdomain IX abolishes Fer protein-tyrosine kinase activity. *Protein Engineering, Design and Selection,* 12**,** 155-162.

CONG, L., RAN, F. A., COX, D., LIN, S., BARRETTO, R., HABIB, N., HSU, P. D., WU, X., JIANG, W., MARRAFFINI, L. A. & ZHANG, F. 2013. Multiplex genome engineering using CRISPR/Cas systems. *Science,* 339**,** 819-23.

CONOVER, C. A. & BALE, L. K. 2007. Loss of pregnancy-associated plasma protein A extends lifespan in mice. *Aging Cell,* 6**,** 727-9.

COPPOLA, D., FERBER, A., MIURA, M., SELL, C., D'AMBROSIO, C., RUBIN, R. & BASERGA, R. 1994. A functional insulin-like growth factor I receptor is required for the mitogenic and transforming activities of the epidermal growth factor receptor. *Mol Cell Biol,* 14**,** 4588-95.

CORTES, J., PAQUETTE, R., TALPAZ, M., PINILLA, J., ASATIANI, E., WETZLER, M., LIPTON, J. H., KASAP, C., BUI, L. A., CLARY, D. O. & SHAH, N. 2008. Preliminary Clinical Activity in a Phase I Trial of the BCR-ABL/IGF- 1R/Aurora Kinase Inhibitor XL228 in Patients with Ph++ Leukemias with Either Failure to Multiple TKI Therapies or with T315I Mutation. *Blood,* 112**,** 3232-3232.

COSTALES, J. & KOLEVZON, A. 2016. The therapeutic potential of insulin-like growth factor-1 in central nervous system disorders. *Neurosci Biobehav Rev,* 63**,** 207-22.

COX, M. E., GLEAVE, M. E., ZAKIKHANI, M., BELL, R. H., PIURA, E., VICKERS, E., CUNNINGHAM, M., LARSSON, O., FAZLI, L. & POLLAK, M. 2009. Insulin receptor expression by human prostate cancers. *The Prostate,* 69**,** 33-40.

COX, O. T., O'SHEA, S., TRESSE, E., BUSTAMANTE-GARRIDO, M., KIRAN-DEEVI, R. & O'CONNOR, R. 2015. IGF-1 Receptor and Adhesion Signaling: An Important Axis in Determining Cancer Cell Phenotype and Therapy Resistance. *Frontiers in Endocrinology,* 6.

CRUDDEN, C., SONG, D., CISMAS, S., TROCMÉ, E., PASCA, S., CALIN, G. A., GIRNITA, A. & GIRNITA, L. 2019. Below the Surface: IGF-1R Therapeutic Targeting and Its Endocytic Journey. *Cells,* 8**,** 1223.

D'AMBROSIO, C., FERBER, A., RESNICOFF, M. & BASERGA, R. 1996. A soluble insulin-like growth factor I receptor that induces apoptosis of tumor cells in vivo and inhibits tumorigenesis. *Cancer Res,* 56**,** 4013-20.

DATTA, S. R., DUDEK, H., TAO, X., MASTERS, S., FU, H., GOTOH, Y. & GREENBERG, M. E. 1997. Akt phosphorylation of BAD couples survival signals to the cell-intrinsic death machinery. *Cell,* 91**,** 231-41.

DE MATTEIS, M. A., MIRONOV, A. A. & BEZNOUSSENKO, G. V. 2008. The Golgi ribbon and the function of the Golgins. *In:* MIRONOV, A. A. & PAVELKA, M. (eds.) *The Golgi Apparatus: State of the art 110 years after Camillo Golgi's discovery.* Vienna: Springer Vienna.

DE MEYTS, P. 1994. The structural basis of insulin and insulin-like growth factor-I receptor binding and negative co-operativity, and its relevance to mitogenic versus metabolic signalling. *Diabetologia,* 37 Suppl 2**,** S135-48.

DE MEYTS, P. 2004. Insulin and its receptor: structure, function and evolution. *Bioessays,* 26**,** 1351-62.

DEANGELIS, T., FERBER, A. & BASERGA, R. 1995. Insulin-like growth factor I receptor is required for the mitogenic and transforming activities of the platelet-derived growth factor receptor. *J Cell Physiol,* 164**,** 214-21.

DEARTH, R. K., CUI, X., KIM, H. J., KUIATSE, I., LAWRENCE, N. A., ZHANG, X., DIVISOVA, J., BRITTON, O. L., MOHSIN, S., ALLRED, D. C., HADSELL, D. L. & LEE, A. V. 2006. Mammary tumorigenesis and metastasis caused by overexpression of insulin receptor substrate 1 (IRS-1) or IRS-2. *Mol Cell Biol,* 26**,** 9302-14.

DEKKERS, O. M., BIERMASZ, N. R., PEREIRA, A. M., ROMIJN, J. A. & VANDENBROUCKE, J. P. 2008. Mortality in Acromegaly: A Metaanalysis. *The Journal of Clinical Endocrinology & Metabolism,* 93**,** 61-67.

DENG, H., LIN, Y., BADIN, M., VASILCANU, D., STRÖMBERG, T., JERNBERG-WIKLUND, H., SEHAT, B. & LARSSON, O. 2011. Over-accumulation of nuclear IGF-1 receptor in tumor cells requires elevated expression of the receptor and the SUMO-conjugating enzyme Ubc9. *Biochemical and Biophysical Research Communications,* 404**,** 667-671.

DENLEY, A., COSGROVE, L. J., BOOKER, G. W., WALLACE, J. C. & FORBES, B. E. 2005. Molecular interactions of the IGF system. *Cytokine Growth Factor Rev,* 16**,** 421-39.

DEVOL, D. L., ROTWEIN, P., SADOW, J. L., NOVAKOFSKI, J. & BECHTEL, P. J. 1990. Activation of insulin-like growth factor gene expression during work-induced skeletal muscle growth. *American Journal of Physiology-Endocrinology and Metabolism,* 259**,** E89-E95.

DHILLON, A. S., MEIKLE, S., YAZICI, Z., EULITZ, M. & KOLCH, W. 2002. Regulation of Raf-1 activation and signalling by dephosphorylation. *The EMBO journal,* 21**,** 64-71.

DI GUGLIELMO, G. M., BAASS, P. C., OU, W. J., POSNER, B. I. & BERGERON, J. J. 1994. Compartmentalization of SHC, GRB2 and mSOS, and hyperphosphorylation of Raf-1 by EGF but not insulin in liver parenchyma. *The EMBO journal,* 13**,** 4269-4277.

DISANZA, A., FRITTOLI, E., PALAMIDESSI, A. & SCITA, G. 2009. Endocytosis and spatial restriction of cell signaling. *Molecular Oncology,* 3**,** 280-296.

DUNN, S. E., EHRLICH, M., SHARP, N. J., REISS, K., SOLOMON, G., HAWKINS, R., BASERGA, R. & BARRETT, J. C. 1998. A dominant negative mutant of the insulin-like growth factor-I receptor inhibits the adhesion, invasion, and metastasis of breast cancer. *Cancer Res,* 58**,** 3353-61.

DYER, A. H., VAHDATPOUR, C., SANFELIU, A. & TROPEA, D. 2016. The role of Insulin-Like Growth Factor 1 (IGF-1) in brain development, maturation and neuroplasticity. *Neuroscience,* 325**,** 89-99.

EIVERS, E., MCCARTHY, K., GLYNN, C., NOLAN, C. M. & BYRNES, L. 2004. Insulin-like growth factor (IGF) signalling is required for early dorso-anterior development of the zebrafish embryo. *Int J Dev Biol,* 48**,** 1131-40.

EMMERSON, E., CAMPBELL, L., DAVIES, F. C., ROSS, N. L., ASHCROFT, G. S., KRUST, A., CHAMBON, P. & HARDMAN, M. J. 2012. Insulin-like growth factor-1 promotes wound healing in estrogen-deprived mice: new insights into cutaneous IGF-1R/ERα cross talk. *J Invest Dermatol,* 132**,** 2838-48.

ESPOSITO, D. L., BLAKESLEY, V. A., KOVAL, A. P., SCRIMGEOUR, A. G. & LEROITH, D. 1997. Tyrosine residues in the C-terminal domain of the insulin-like growth factor-I receptor mediate mitogenic and tumorigenic signals. *Endocrinology,* 138**,** 2979-88.

FAN, G., ZHANG, S., GAO, Y., GREER, P. A. & TONKS, N. K. 2016. HGF-independent regulation of MET and GAB1 by nonreceptor tyrosine kinase FER potentiates metastasis in ovarian cancer. *Genes & Development,* 30**,** 1542-1557.

FARBER-KATZ, SUZETTE E., DIPPOLD, HOLLY C., BUSCHMAN, MATTHEW D., PETERMAN, MARSHALL C., XING, M., NOAKES, CHRISTOPHER J., TAT, J., NG, MICHELLE M., RAHAJENG, J., COWAN, DAVID M., FUCHS, GREG J., ZHOU, H. & FIELD, SETH J. 2014. DNA Damage Triggers Golgi Dispersal via DNA-PK and GOLPH3. *Cell,* 156**,** 413-427.

FARHAN, H. & RABOUILLE, C. 2011. Signalling to and from the secretory pathway. *Journal of Cell Science,* 124**,** 171-180.

FARHAN, H., WENDELER, M. W., MITROVIC, S., FAVA, E., SILBERBERG, Y., SHARAN, R., ZERIAL, M. & HAURI, H.-P. 2010. MAPK signaling to the early secretory pathway revealed by kinase/phosphatase functional screening. *The Journal of Cell Biology,* 189**,** 997-1011.

FAVELYUKIS, S., TILL, J. H., HUBBARD, S. R. & MILLER, W. T. 2001. Structure and autoregulation of the insulin-like growth factor 1 receptor kinase. *Nature Structural Biology,* 8**,** 1058-1063.

FAVRE, C., ZHDANOV, A., LEAHY, M., PAPKOVSKY, D. & O'CONNOR, R. 2010. Mitochondrial pyrimidine nucleotide carrier (PNC1) regulates mitochondrial biogenesis and the invasive phenotype of cancer cells. *Oncogene,* 29**,** 3964-3976.

FENG, Y. & DIMITROV, D. S. 2012. Antibody-based therapeutics against components of the IGF system. *OncoImmunology,* 1**,** 1390-1391.

FENG, Y., VENEMA, V. J., VENEMA, R. C., TSAI, N. & CALDWELL, R. B. 1999. VEGF Induces Nuclear Translocation of Flk-1/KDR, Endothelial Nitric Oxide Synthase, and Caveolin-1 in Vascular Endothelial Cells. *Biochemical and Biophysical Research Communications,* 256**,** 192-197.

FERBER, A., CHANG, C., SELL, C., PTASZNIK, A., CRISTOFALO, V. J., HUBBARD, K., OZER, H. L., ADAMO, M., ROBERTS, C. T., JR., LEROITH, D. & ET AL. 1993. Failure of senescent human fibroblasts to express the insulin-like growth factor-1 gene. *J Biol Chem,* 268**,** 17883-8.

FLORINI, J. R., EWTON, D. Z. & COOLICAN, S. A. 1996. Growth hormone and the insulin-like growth factor system in myogenesis. *Endocr Rev,* 17**,** 481-517.

FLOSSMANN-KAST, B. B. M., JEHLE, P. M., HOEFLICH, A., ADLER, G. & LUTZ, M. P. 1998. Src Stimulates Insulin-like Growth Factor I (IGF-I)-dependent Cell Proliferation by Increasing IGF-I Receptor Number in Human Pancreatic Carcinoma Cells. *Cancer Research,* 58**,** 3551-3554.

FLOYD, S., FAVRE, C., LASORSA, F. M., LEAHY, M., TRIGIANTE, G., STROEBEL, P., MARX, A., LOUGHRAN, G., O'CALLAGHAN, K., MAROBBIO, C. M., SLOTBOOM, D. J., KUNJI, E. R., PALMIERI, F. & O'CONNOR, R. 2007. The insulin-like growth factor-I-mTOR signaling pathway induces the mitochondrial pyrimidine nucleotide carrier to promote cell growth. *Mol Biol Cell,* 18**,** 3545-55.

FLURKEY, K., PAPACONSTANTINOU, J. & HARRISON, D. E. 2002. The Snell dwarf mutation Pit1(dw) can increase life span in mice. *Mech Ageing Dev,* 123**,** 121-30.

FOREST, A., AMATULLI, M., LUDWIG, D. L., DAMOCI, C. B., WANG, Y., BURNS, C. A., DONOHO, G. P., ZANELLA, N., FIEBIG, H. H., PREWETT, M. C., SURGULADZE, D., DELIGIO, J. T., HOUGHTON, P. J., SMITH, M. A. & NOVOSIADLY, R. 2015. Intrinsic Resistance to Cixutumumab Is Conferred by Distinct Isoforms of the Insulin Receptor. *Molecular cancer research : MCR,* 13**,** 1615-1626.

FOURRIERE, L., KASRI, A., GAREIL, N., BARDIN, S., BOUSQUET, H., PEREIRA, D., PEREZ, F., GOUD, B., BONCOMPAIN, G. & MISEREY-LENKEI, S. 2019. RAB6 and microtubules restrict protein secretion to focal adhesions. *The Journal of Cell Biology,* 218**,** 2215-2231.

FOX, E. M., KUBA, M. G., MILLER, T. W., DAVIES, B. R. & ARTEAGA, C. L. 2013. Autocrine IGF-I/insulin receptor axis compensates for inhibition of AKT in ER-positive breast cancer cells with resistance to estrogen deprivation. *Breast cancer research : BCR,* 15**,** R55-R55.

FRANKE, T. F., HORNIK, C. P., SEGEV, L., SHOSTAK, G. A. & SUGIMOTO, C. 2003. PI3K/Akt and apoptosis: size matters. *Oncogene,* 22**,** 8983-8998.

FRAZIER, N. M., BRAND, T., GORDAN, J. D., GRANDIS, J. & JURA, N. 2019. Overexpression-mediated activation of MET in the Golgi promotes HER3/ERBB3 phosphorylation. *Oncogene,* 38**,** 1936-1950.

FRIEDLANDER, T. W., WEINBERG, V. K., HUANG, Y., MI, J. T., FORMAKER, C. G., SMALL, E. J., HARZSTARK, A. L., LIN, A. M., FONG, L. & RYAN, C. J. 2012. A phase II study of insulin-like growth factor receptor inhibition with nordihydroguaiaretic acid in men with non-metastatic hormone-sensitive prostate cancer. *Oncol Rep,* 27**,** 3-9.

FRUMAN, D. A., CHIU, H., HOPKINS, B. D., BAGRODIA, S., CANTLEY, L. C. & ABRAHAM, R. T. 2017. The PI3K Pathway in Human Disease. *Cell,* 170**,** 605-635.

FU, Y., FODEN, J. A., KHAYTER, C., MAEDER, M. L., REYON, D., JOUNG, J. K. & SANDER, J. D. 2013. High-frequency off-target mutagenesis induced by CRISPR-Cas nucleases in human cells. *Nature Biotechnology,* 31**,** 822.

FUKUSHIMA, T., NAKAMURA, Y., YAMANAKA, D., SHIBANO, T., CHIDA, K., MINAMI, S., ASANO, T., HAKUNO, F. & TAKAHASHI, S.-I. 2012. Phosphatidylinositol 3-Kinase (PI3K) Activity Bound to Insulin-like Growth Factor-I (IGF-I) Receptor, which Is Continuously Sustained by IGF-I Stimulation, Is Required for IGF-I-induced Cell Proliferation. *Journal of Biological Chemistry,* 287**,** 29713-29721.

FURUKAWA, J., WRAIGHT, C. J., FREIER, S. M., PERALTA, E., ATLEY, L. M., MONIA, B. P., GLEAVE, M. E. & COX, M. E. 2010. Antisense oligonucleotide targeting of insulin-like growth factor-1 receptor (IGF-1R) in prostate cancer. *The Prostate,* 70**,** 206-218.

GIBSON, S. L., MA, Z. & SHAW, L. M. 2007. Divergent Roles for IRS-1 and IRS-2 in Breast Cancer Metastasis. *Cell Cycle,* 6**,** 631-637.

GINGRAS, A. C., RAUGHT, B., GYGI, S. P., NIEDZWIECKA, A., MIRON, M., BURLEY, S. K., POLAKIEWICZ, R. D., WYSLOUCH-CIESZYNSKA, A., AEBERSOLD, R. & SONENBERG, N. 2001. Hierarchical phosphorylation of the translation inhibitor 4E-BP1. *Genes Dev,* 15**,** 2852-64.

GIRNITA, A., GIRNITA, L., PRETE, F. D., BARTOLAZZI, A., LARSSON, O. & AXELSON, M. 2004. Cyclolignans as Inhibitors of the Insulin-Like Growth Factor-1 Receptor and Malignant Cell Growth. *Cancer Research,* 64**,** 236-242.

GIRNITA, L., GIRNITA, A. & LARSSON, O. 2003. Mdm2-dependent ubiquitination and degradation of the insulin-like growth factor 1 receptor. *Proceedings of the National Academy of Sciences,* 100**,** 8247-8252.

GIRNITA, L., SHENOY, S. K., SEHAT, B., VASILCANU, R., VASILCANU, D., GIRNITA, A., LEFKOWITZ, R. J. & LARSSON, O. 2007. β-Arrestin and Mdm2 Mediate IGF-1 Receptor-stimulated ERK Activation and Cell Cycle Progression. *Journal of Biological Chemistry,* 282**,** 11329-11338.

GOH, L. K. & SORKIN, A. 2013. Endocytosis of Receptor Tyrosine Kinases. *Cold Spring Harbor Perspectives in Biology,* 5.

GOPALAPPA, R., SURESH, B., RAMAKRISHNA, S. & KIM, H. 2018. Paired D10A Cas9 nickases are sometimes more efficient than individual nucleases for gene disruption. *Nucleic Acids Research,* 46**,** e71-e71.

GOTOH, N., TOYODA, M. & SHIBUYA, M. 1997. Tyrosine phosphorylation sites at amino acids 239 and 240 of Shc are involved in epidermal growth factor-induced mitogenic signaling that is distinct from Ras/mitogen-activated protein kinase activation. *Molecular and Cellular Biology,* 17**,** 1824-1831.

GOURMELEN, M., BOUC, Y. L., GIRARD, F. & BINOUX, M. 1984. Serum Levels of Insulin-Like Growth Factor (IGF) and IGF Binding Protein in Constitutionally Tall Children and Adolescents*. *The Journal of Clinical Endocrinology & Metabolism,* 59**,** 1197-1203.

GRAHAM, T. R., ZHAU, H. E., ODERO-MARAH, V. A., OSUNKOYA, A. O., KIMBRO, K. S., TIGHIOUART, M., LIU, T., SIMONS, J. W. & O'REGAN, R. M. 2008. Insulin-like growth factor-I-dependent up-regulation of ZEB1 drives epithelial-to-mesenchymal transition in human prostate cancer cells. *Cancer Res,* 68**,** 2479-88.

GREER, P. 2002. Closing in on the biological functions of Fps/Fes and Fer. *Nat Rev Mol Cell Biol,* 3**,** 278-89.

GRIMBERG, A. & COHEN, P. 2000. Role of insulin-like growth factors and their binding proteins in growth control and carcinogenesis. *J Cell Physiol,* 183**,** 1-9.

GU, H., MAEDA, H., MOON, J. J., LORD, J. D., YOAKIM, M., NELSON, B. H. & NEEL, B. G. 2000. New role for Shc in activation of the phosphatidylinositol 3-kinase/Akt pathway. *Mol Cell Biol,* 20**,** 7109-20.

GUAN, J., BENNET, L., GLUCKMAN, P. D. & GUNN, A. J. 2003. Insulin-like growth factor-1 and post-ischemic brain injury. *Prog Neurobiol,* 70**,** 443-62.

GUEVARA-AGUIRRE, J., BALASUBRAMANIAN, P., GUEVARA-AGUIRRE, M., WEI, M., MADIA, F., CHENG, C. W., HWANG, D., MARTIN-MONTALVO, A., SAAVEDRA, J., INGLES, S., DE CABO, R., COHEN, P. & LONGO, V. D. 2011. Growth hormone receptor deficiency is associated with a major reduction in pro-aging signaling, cancer, and diabetes in humans. *Sci Transl Med,* 3**,** 70ra13.

GULER, H. P., ZAPF, J., BINZ, K. & FROESCH, E. R. 1989. GROWTH PROMOTION USING RECOMBINANT INSULIN-LIKE GROWTH FACTOR-I. *In:* HEAP, R. B., PROSSER, C. G. & LAMMING, G. E. (eds.) *Biotechnology in Growth Regulation.* Butterworth-Heinemann.

GUO, C. & STARK, G. R. 2011. FER tyrosine kinase (FER) overexpression mediates resistance to quinacrine through EGF-dependent activation of NF-κB. *Proceedings of the National Academy of Sciences,* 108**,** 7968-7973.

GUSTAFSON, T. & RUTTER, W. 1990. The cysteine-rich domains of the insulin and insulin-like growth factor I receptors are primary determinants of hormone binding specificity. Evidence from receptor chimeras. *The Journal of biological chemistry,* 265**,** 18663-7.

GUSTAFSON, T. A., HE, W., CRAPARO, A., SCHAUB, C. D. & O'NEILL, T. J. 1995. Phosphotyrosine-dependent interaction of SHC and insulin receptor substrate 1 with the NPEY motif of the insulin receptor via a novel non-SH2 domain. *Mol Cell Biol,* 15**,** 2500-8.

HAIGLER, H. T., MCKANNA, J. A. & COHEN, S. 1979. Rapid stimulation of pinocytosis in human carcinoma cells A-431 by epidermal growth factor. *J Cell Biol,* 83**,** 82-90.

HAKUNO, F. & TAKAHASHI, S. I. 2018. IGF1 receptor signaling pathways. *J Mol Endocrinol,* 61**,** T69-t86.

HALUSKA, P., DHAR, A., HOU, X., HUANG, F., NUYTEN, D. S. A., PARK, J., BRODIE, A. H., INGLE, J. N., CARBONI, J. M., GOTTARDIS, M. M., WOLFF, A. C. & FINCKENSTEIN, F. G. 2011. Phase II trial of the dual IGF-1R/IR inhibitor BMS-754807 with or without letrozole in aromatase inhibitor-resistant breast cancer. *Journal of Clinical Oncology,* 29**,** TPS111-TPS111.

HAMIDI, H. & IVASKA, J. 2018. Every step of the way: integrins in cancer progression and metastasis. *Nature Reviews Cancer,* 18**,** 533-548.

HANAHAN, D. & WEINBERG, ROBERT A. 2011. Hallmarks of Cancer: The Next Generation. *Cell,* 144**,** 646-674.

HANKINSON, S. E., WILLETT, W. C., COLDITZ, G. A., HUNTER, D. J., MICHAUD, D. S., DEROO, B., ROSNER, B., SPEIZER, F. E. & POLLAK, M. 1998. Circulating concentrations of insulin-like growth factor-I and risk of breast cancer. *Lancet,* 351**,** 1393-6.

HARADA, H., ANDERSEN, J. S., MANN, M., TERADA, N. & KORSMEYER, S. J. 2001. p70S6 kinase signals cell survival as well as growth, inactivating the pro-apoptotic molecule BAD. *Proc Natl Acad Sci U S A,* 98**,** 9666-70.

HARRINGTON, E. A., BENNETT, M. R., FANIDI, A. & EVAN, G. I. 1994. c-Myc-induced apoptosis in fibroblasts is inhibited by specific cytokines. *The EMBO journal,* 13**,** 3286-3295.

HAUGH, J. M. & MEYER, T. 2002. Active EGF receptors have limited access to PtdIns(4,5)P₂ in endosomes: implications for phospholipase C and PI 3-kinase signaling. *Journal of Cell Science,* 115**,** 303-310.

HELLWIG, S., MIDUTURU, C. V., KANDA, S., ZHANG, J., FILIPPAKOPOULOS, P., SALAH, E., DENG, X., CHOI, H. G., ZHOU, W., HUR, W., KNAPP, S., GRAY, N. S. & SMITHGALL, T. E. 2012. Small-molecule inhibitors of the c-Fes protein-tyrosine kinase. *Chem Biol,* 19**,** 529-40.

HEMMINGS, B. A. & RESTUCCIA, D. F. 2012. PI3K-PKB/Akt pathway. *Cold Spring Harbor perspectives in biology,* 4**,** a011189-a011189.

HERMANTO, U., ZONG, C. S., LI, W. & WANG, L.-H. 2002. RACK1, an Insulin-Like Growth Factor I (IGF-I) Receptor-Interacting Protein, Modulates IGF-I-Dependent Integrin Signaling and Promotes Cell Spreading and Contact with Extracellular Matrix. *Molecular and Cellular Biology,* 22**,** 2345-2365.

HERNÁNDEZ-SÁNCHEZ, C., MANSILLA, A., DE PABLO, F. & ZARDOYA, R. 2008. Evolution of the Insulin Receptor Family and Receptor Isoform Expression in Vertebrates. *Molecular Biology and Evolution,* 25**,** 1043-1053.

HOEGE, C., PFANDER, B., MOLDOVAN, G.-L., PYROWOLAKIS, G. & JENTSCH, S. 2002. RAD6-dependent DNA repair is linked to modification of PCNA by ubiquitin and SUMO. *Nature,* 419**,** 135-141.

HOLDAWAY, I. M., BOLLAND, M. J. & GAMBLE, G. D. 2008. A meta-analysis of the effect of lowering serum levels of GH and IGF-I on mortality in acromegaly. *Eur J Endocrinol,* 159**,** 89-95.

HOLZENBERGER, M., DUPONT, J., DUCOS, B., LENEUVE, P., GÉLOËN, A., EVEN, P. C., CERVERA, P. & LE BOUC, Y. 2003. IGF-1 receptor regulates lifespan and resistance to oxidative stress in mice. *Nature,* 421**,** 182-7.

HONGO, A., YUMET, G., RESNICOFF, M., ROMANO, G., O'CONNOR, R. & BASERGA, R. 1998. Inhibition of Tumorigenesis and Induction of Apoptosis in Human Tumor Cells by the Stable Expression of a Myristylated COOH Terminus of the Insulin-like Growth Factor I Receptor. *Cancer Research,* 58**,** 2477-2484.

HSIEH, J., AIMONE, J. B., KASPAR, B. K., KUWABARA, T., NAKASHIMA, K. & GAGE, F. H. 2004. IGF-I instructs multipotent adult neural progenitor cells to become oligodendrocytes. *J Cell Biol,* 164**,** 111-22.

HUANG, F. & SORKIN, A. 2005. Growth Factor Receptor Binding Protein 2-mediated Recruitment of the RING Domain of Cbl to the Epidermal Growth Factor Receptor Is Essential and Sufficient to Support Receptor Endocytosis. *Molecular Biology of the Cell,* 16**,** 1268-1281.

HUBBARD, S. R. 1997. Crystal structure of the activated insulin receptor tyrosine kinase in complex with peptide substrate and ATP analog. *Embo j,* 16**,** 5572-81.

HUBBARD, S. R., WEI, L., ELLIS, L. & HENDRICKSON, W. A. 1994. Crystal structure of the tyrosine kinase domain of the human insulin receptor. *Nature,* 372**,** 746-54.

HUSAIN, S. R., HAN, J., AU, P., SHANNON, K. & PURI, R. K. 2015. Gene therapy for cancer: regulatory considerations for approval. *Cancer gene therapy,* 22**,** 554-563.

HUTTENLOCHER, A. & HORWITZ, A. R. 2011. Integrins in cell migration. *Cold Spring Harb Perspect Biol,* 3**,** a005074.

HUTTENLOCHER, A., LAKONISHOK, M., KINDER, M., WU, S., TRUONG, T., KNUDSEN, K. A. & HORWITZ, A. F. 1998. Integrin and Cadherin Synergy Regulates Contact Inhibition of Migration and Motile Activity. *Journal of Cell Biology,* 141**,** 515-526.

HYNES, R. O. 2002. Integrins: bidirectional, allosteric signaling machines. *Cell,* 110**,** 673-87.

HYNES, R. O. & LANDER, A. D. 1992. Contact and adhesive specificities in the associations, migrations, and targeting of cells and axons. *Cell,* 68**,** 303-22.

INSALL, R. H. & MACHESKY, L. M. 2009. Actin Dynamics at the Leading Edge: From Simple Machinery to Complex Networks. *Developmental Cell,* 17**,** 310-322.

IRELAND, L., SANTOS, A., AHMED, M. S., RAINER, C., NIELSEN, S. R., QUARANTA, V., WEYER-CZERNILOFSKY, U., ENGLE, D. D., PEREZ-MANCERA, P. A., COUPLAND, S. E., TAKTAK, A., BOGENRIEDER, T., TUVESON, D. A., CAMPBELL, F., SCHMID, M. C. & MIELGO, A. 2016. Chemoresistance in Pancreatic Cancer Is Driven by Stroma-Derived Insulin-Like Growth Factors. *Cancer Res,* 76**,** 6851-6863.

ISGAARD, J., ABERG, D. & NILSSON, M. 2007. Protective and regenerative effects of the GH/IGF-I axis on the brain. *Minerva Endocrinol,* 32**,** 103-13.

ITOH, T., ERDMANN, K. S., ROUX, A., HABERMANN, B., WERNER, H. & DE CAMILLI, P. 2005. Dynamin and the actin cytoskeleton cooperatively regulate plasma membrane invagination by BAR and F-BAR proteins. *Dev Cell,* 9**,** 791-804.

ITOH, T., HASEGAWA, J., TSUJITA, K., KANAHO, Y. & TAKENAWA, T. 2009. The Tyrosine Kinase Fer Is a Downstream Target of the PLD-PA Pathway that Regulates Cell Migration. *Science Signaling,* 2**,** ra52-ra52.

IVANOVA, I. A., VERMEULEN, J. F., ERCAN, C., HOUTHUIJZEN, J. M., SAIG, F. A., VLUG, E. J., VAN DER WALL, E., VAN DIEST, P. J., VOOIJS, M. & DERKSEN, P. W. B. 2013. FER kinase promotes breast cancer metastasis by regulating α6- and β1-integrin-dependent cell adhesion and anoikis resistance. *Oncogene,* 32**,** 5582-5592.

IVASKA, J. & HEINO, J. 2011. Cooperation Between Integrins and Growth Factor Receptors in Signaling and Endocytosis. *Annual Review of Cell and Developmental Biology,* 27**,** 291-320.

IVINS ZITO, C., KONTARIDIS, M. I., FORNARO, M., FENG, G.-S. & BENNETT, A. M. 2004. SHP-2 regulates the phosphatidylinositide 3′-kinase/Akt pathway and suppresses caspase 3-mediated apoptosis. *Journal of Cellular Physiology,* 199**,** 227-236.

JACINTO, E., LOEWITH, R., SCHMIDT, A., LIN, S., RÜEGG, M. A., HALL, A. & HALL, M. N. 2004. Mammalian TOR complex 2 controls the actin cytoskeleton and is rapamycin insensitive. *Nature Cell Biology,* 6**,** 1122-1128.

JEFFERIES, H. B., REINHARD, C., KOZMA, S. C. & THOMAS, G. 1994. Rapamycin selectively represses translation of the "polypyrimidine tract" mRNA family. *Proc Natl Acad Sci U S A,* 91**,** 4441-5.

JIANG, L., ZHU, W., STREICHER, K., MOREHOUSE, C., BROHAWN, P., GE, X., DONG, Z., YIN, X., ZHU, G., GU, Y., RANADE, K., HIGGS, B. W., YAO, Y. & HUANG, J. 2014. Increased IR-A/IR-B ratio in non-small cell lung cancers associates with lower epithelial-mesenchymal transition signature and longer survival in squamous cell lung carcinoma. *BMC Cancer,* 14**,** 131.

JIN, S. & LEVINE, A. J. 2001. The p53 functional circuit. *J Cell Sci,* 114**,** 4139-40.

JOFFRE, C., BARROW, R., MÉNARD, L., CALLEJA, V., HART, I. R. & KERMORGANT, S. 2011. A direct role for Met endocytosis in tumorigenesis. *Nature Cell Biology,* 13**,** 827.

JOHANNES, L. & POPOFF, V. 2008. Tracing the Retrograde Route in Protein Trafficking. *Cell,* 135**,** 1175-1187.

JOHNSTON, C. L., COX, H. C., GOMM, J. J. & COOMBES, R. C. 1995. Fibroblast Growth Factor Receptors (FGFRs) Localize in Different Cellular Compartments: A SPLICE VARIANT OF FGFR-3 LOCALIZES TO THE NUCLEUS. *Journal of Biological Chemistry,* 270**,** 30643-30650.

JONES, H. E., GODDARD, L., GEE, J. M., HISCOX, S., RUBINI, M., BARROW, D., KNOWLDEN, J. M., WILLIAMS, S., WAKELING, A. E. & NICHOLSON, R. I. 2004. Insulin-like growth factor-I receptor signalling and acquired resistance to gefitinib (ZD1839; Iressa) in human breast and prostate cancer cells. *Endocr Relat Cancer,* 11**,** 793-814.

JONES, J. I. & CLEMMONS, D. R. 1995. Insulin-Like Growth Factors and Their Binding Proteins: Biological Actions*. *Endocrine Reviews,* 16**,** 3-34.

JONES, M. C., CASWELL, P. T. & NORMAN, J. C. 2006. Endocytic recycling pathways: emerging regulators of cell migration. *Current Opinion in Cell Biology,* 18**,** 549-557.

KAAKS, R., JOHNSON, T., TIKK, K., SOOKTHAI, D., TJØNNELAND, A., ROSWALL, N., OVERVAD, K., CLAVEL-CHAPELON, F., BOUTRON-RUAULT, M. C., DOSSUS, L., RINALDI, S., ROMIEU, I., BOEING, H., SCHÜTZE, M., TRICHOPOULOU, A., LAGIOU, P., TRICHOPOULOS, D., PALLI, D., GRIONI, S., TUMINO, R., SACERDOTE, C., PANICO, S., BUCKLAND, G., ARGÜELLES, M., SÁNCHEZ, M. J., AMIANO, P., CHIRLAQUE, M. D., ARDANAZ, E., BUENO-DE-MESQUITA, H. B., VAN GILS, C. H., PEETERS, P. H., ANDERSSON, A., SUND, M., WEIDERPASS, E., GRAM, I. T., LUND, E., KHAW, K. T., WAREHAM, N., KEY, T. J., TRAVIS, R. C., MERRITT, M. A., GUNTER, M. J., RIBOLI, E. & LUKANOVA, A. 2014. Insulin-like growth factor I and risk of breast cancer by age and hormone receptor status-A prospective study within the EPIC cohort. *Int J Cancer,* 134**,** 2683-90.

KALEKO, M., RUTTER, W. J. & MILLER, A. D. 1990. Overexpression of the human insulinlike growth factor I receptor promotes ligand-dependent neoplastic transformation. *Molecular and Cellular Biology,* 10**,** 464-473.

KALIMAN, P., BARON, V., GAUTIER, N. & VAN OBBERGHEN, E. 1992. Antipeptide antibody to the insulin-like growth factor-I receptor sequence 1232-1246 inhibits the receptor kinase activity. *Journal of Biological Chemistry,* 267**,** 10645-10651.

KAMIOKA, Y., FUKUHARA, S., SAWA, H., NAGASHIMA, K., MASUDA, M., MATSUDA, M. & MOCHIZUKI, N. 2004. A novel dynamin-associating molecule, formin-binding protein 17, induces tubular membrane invaginations and participates in endocytosis. *J Biol Chem,* 279**,** 40091-9.

KANETY, H., MADJAR, Y., DAGAN, Y., LEVI, J., PAPA, M. Z., PARIENTE, C., GOLDWASSER, B. & KARASIK, A. 1993. Serum insulin-like growth factor-binding protein-2 (IGFBP-2) is increased and IGFBP-3 is decreased in patients with prostate cancer: correlation with serum prostate-specific antigen. *J Clin Endocrinol Metab,* 77**,** 229-33.

KAULFUSS, S., BURFEIND, P., GAEDCKE, J. & SCHARF, J. G. 2009. Dual silencing of insulin-like growth factor-I receptor and epidermal growth factor receptor in colorectal cancer cells is associated with decreased proliferation and enhanced apoptosis. *Mol Cancer Ther,* 8**,** 821-33.

KAVRAN, J. M., MCCABE, J. M., BYRNE, P. O., CONNACHER, M. K., WANG, Z., RAMEK, A., SARABIPOUR, S., SHAN, Y., SHAW, D. E., HRISTOVA, K., COLE, P. A. & LEAHY, D. J. 2014. How IGF-1 activates its receptor. *eLife,* 3**,** e03772.

KELLY, G. M., BUCKLEY, D. A., KIELY, P. A., ADAMS, D. R. & O'CONNOR, R. 2012. Serine Phosphorylation of the Insulin-like Growth Factor I (IGF-1) Receptor C-terminal Tail Restrains Kinase Activity and Cell Growth. *Journal of Biological Chemistry,* 287**,** 28180-28194.

KENYON, C., CHANG, J., GENSCH, E., RUDNER, A. & TABTIANG, R. 1993. A C. elegans mutant that lives twice as long as wild type. *Nature,* 366**,** 461-4.

KEY, T. J., APPLEBY, P. N., REEVES, G. K. & RODDAM, A. W. 2010. Insulin-like growth factor 1 (IGF1), IGF binding protein 3 (IGFBP3), and breast cancer risk: pooled individual data analysis of 17 prospective studies. *Lancet Oncol,* 11**,** 530-42.

KEYHANFAR, M., BOOKER, G. W., WHITTAKER, J., WALLACE, J. C. & FORBES, B. E. 2007. Precise mapping of an IGF-I-binding site on the IGF-1R. *The Biochemical journal,* 401**,** 269-277.

KHANNA, R. S., LE, H. T., WANG, J., FUNG, T. C. H. & PALLEN, C. J. 2015. The Interaction of Protein-tyrosine Phosphatase α (PTPα) and RACK1 Protein Enables Insulin-like Growth Factor 1 (IGF-1)-stimulated Abl-dependent and -independent Tyrosine Phosphorylation of PTPα. *Journal of Biological Chemistry,* 290**,** 9886-9895.

KHOLODENKO, B. N., HANCOCK, J. F. & KOLCH, W. 2010. Signalling ballet in space and time. *Nature reviews. Molecular cell biology,* 11**,** 414-426.

KHOURY, H., DANKORT, D. L., SADEKOVA, S., NAUJOKAS, M. A., MULLER, W. J. & PARK, M. 2001. Distinct tyrosine autophosphorylation sites mediate induction of epithelial mesenchymal like transition by an activated ErbB-2/Neu receptor. *Oncogene,* 20**,** 788-799.

KIELY, P. A., BAILLIE, G. S., BARRETT, R., BUCKLEY, D. A., ADAMS, D. R., HOUSLAY, M. D. & O'CONNOR, R. 2009. Phosphorylation of RACK1 on Tyrosine 52 by c-Abl Is Required for Insulin-like Growth Factor I-mediated Regulation of Focal Adhesion Kinase. *Journal of Biological Chemistry,* 284**,** 20263-20274.

KIELY, P. A., BAILLIE, G. S., LYNCH, M. J., HOUSLAY, M. D. & O'CONNOR, R. 2008. Tyrosine 302 in RACK1 Is Essential for Insulin-like Growth Factor-I-mediated Competitive Binding of PP2A and β1 Integrin and for Tumor Cell Proliferation and Migration. *Journal of Biological Chemistry,* 283**,** 22952-22961.

KIELY, P. A., LEAHY, M., O'GORMAN, D. & O'CONNOR, R. 2005. RACK1-mediated Integration of Adhesion and Insulin-like Growth Factor I (IGF-I) Signaling and Cell Migration Are Defective in Cells Expressing an IGF-I Receptor Mutated at Tyrosines 1250 and 1251. *Journal of Biological Chemistry,* 280**,** 7624-7633.

KIELY, P. A., O'GORMAN, D., LUONG, K., RON, D. & O'CONNOR, R. 2006. Insulin-Like Growth Factor I Controls a Mutually Exclusive Association of RACK1 with Protein Phosphatase 2A and β1 Integrin To Promote Cell Migration. *Molecular and Cellular Biology,* 26**,** 4041-4051.

KIELY, P. A., SANT, A. & O'CONNOR, R. 2002. RACK1 Is an Insulin-like Growth Factor 1 (IGF-1) Receptor-interacting Protein That Can Regulate IGF-1-mediated Akt Activation and Protection from Cell Death. *Journal of Biological Chemistry,* 277**,** 22581-22589.

KIM, H. J., LITZENBURGER, B. C., CUI, X., DELGADO, D. A., GRABINER, B. C., LIN, X., LEWIS, M. T., GOTTARDIS, M. M., WONG, T. W., ATTAR, R. M., CARBONI, J. M. & LEE, A. V. 2007. Constitutively active type I insulin-like growth factor receptor causes transformation and xenograft growth of immortalized mammary epithelial cells and is accompanied by an epithelial-to-mesenchymal transition mediated by NF-kappaB and snail. *Mol Cell Biol,* 27**,** 3165-75.

KIM, K.-H. & KIM, H. 2017. Progress of antibody-based inhibitors of the HGF–cMET axis in cancer therapy. *Experimental &Amp; Molecular Medicine,* 49**,** e307.

KIM, L. & WONG, T. W. 1995. The cytoplasmic tyrosine kinase FER is associated with the catenin-like substrate pp120 and is activated by growth factors. *Mol Cell Biol,* 15**,** 4553-61.

KIM, L. & WONG, T. W. 1998. Growth factor-dependent phosphorylation of the actin-binding protein cortactin is mediated by the cytoplasmic tyrosine kinase FER. *J Biol Chem,* 273**,** 23542-8.

KIM, S.-J. & KAHN, C. R. 1993. Insulin induces rapid accumulation of insulin receptors and increases tyrosine kinase activity in the nucleus of cultured adipocytes. *Journal of Cellular Physiology,* 157**,** 217-228.

KIMURA, K. D., TISSENBAUM, H. A., LIU, Y. & RUVKUN, G. 1997. daf-2, an insulin receptor-like gene that regulates longevity and diapause in Caenorhabditis elegans. *Science,* 277**,** 942-6.

KON, S., KOBAYASHI, N. & SATAKE, M. 2014. Altered trafficking of mutated growth factor receptors and their associated molecules. *Cellular Logistics,* 4**,** e28461.

KUPFER, A., DENNERT, G. & SINGER, S. J. 1983. Polarization of the Golgi apparatus and the microtubule-organizing center within cloned natural killer cells bound to their targets. *Proc Natl Acad Sci U S A,* 80**,** 7224-8.

LACY, M. Q., ALSINA, M., FONSECA, R., PACCAGNELLA, M. L., MELVIN, C. L., YIN, D., SHARMA, A., ENRIQUEZ SARANO, M., POLLAK, M., JAGANNATH, S., RICHARDSON, P. & GUALBERTO, A. 2008. Phase I, pharmacokinetic and pharmacodynamic study of the anti-insulinlike growth factor type 1 Receptor monoclonal antibody CP-751,871 in patients with multiple myeloma. *J Clin Oncol,* 26**,** 3196-203.

LAMBERT, A. W., PATTABIRAMAN, D. R. & WEINBERG, R. A. 2017. Emerging Biological Principles of Metastasis. *Cell,* 168**,** 670-691.

LAU, L., HANSFORD, L. M., CHENG, L. S., HANG, M., BARUCHEL, S., KAPLAN, D. R. & IRWIN, M. S. 2007. Cyclooxygenase inhibitors modulate the p53/HDM2 pathway and enhance chemotherapy-induced apoptosis in neuroblastoma. *Oncogene,* 26**,** 1920-1931.

LAW, J. H., HABIBI, G., HU, K., MASOUDI, H., WANG, M. Y. C., STRATFORD, A. L., PARK, E., GEE, J. M. W., FINLAY, P., JONES, H. E., NICHOLSON, R. I., CARBONI, J., GOTTARDIS, M., POLLAK, M. & DUNN, S. E. 2008. Phosphorylated Insulin-Like Growth Factor-I/Insulin Receptor Is Present in All Breast Cancer Subtypes and Is Related to Poor Survival. *Cancer Research,* 68**,** 10238-10246.

LAWRENCE, J. B., OXVIG, C., OVERGAARD, M. T., SOTTRUP-JENSEN, L., GLEICH, G. J., HAYS, L. G., YATES, J. R., 3RD & CONOVER, C. A. 1999. The insulin-like growth factor (IGF)-dependent IGF binding protein-4 protease secreted by human fibroblasts is pregnancy-associated plasma protein-A. *Proceedings of the National Academy of Sciences of the United States of America,* 96**,** 3149-3153.

LEAHY, M., LYONS, A., KRAUSE, D. & O'CONNOR, R. 2004. Impaired Shc, Ras, and MAPK Activation but Normal Akt Activation in FL5.12 Cells Expressing an Insulin-like Growth Factor I Receptor Mutated at Tyrosines 1250 and 1251. *Journal of Biological Chemistry,* 279**,** 18306-18313.

LEE, P. S., WANG, Y., DOMINGUEZ, M. G., YEUNG, Y. G., MURPHY, M. A., BOWTELL, D. D. & STANLEY, E. R. 1999. The Cbl protooncoprotein stimulates CSF-1 receptor multiubiquitination and endocytosis, and attenuates macrophage proliferation. *The EMBO journal,* 18**,** 3616-3628.

LEFKOWITZ, R. J. & SHENOY, S. K. 2005. Transduction of Receptor Signals by ß-Arrestins. *Science,* 308**,** 512-517.

LEIGHL, N. B., RIZVI, N. A., DE LIMA, L. G., JR., ARPORNWIRAT, W., RUDIN, C. M., CHIAPPORI, A. A., AHN, M.-J., CHOW, L. Q. M., BAZHENOVA, L., DECHAPHUNKUL, A., SUNPAWERAVONG, P., EATON, K., CHEN, J., MEDLEY, S., POONDRU, S., SINGH, M., STEINBERG, J., JUERGENS, R. A. & GADGEEL, S. M. 2017. Phase 2 Study of Erlotinib in Combination With Linsitinib (OSI-906) or Placebo in Chemotherapy-Naive Patients With Non–Small-Cell Lung Cancer and Activating Epidermal Growth Factor Receptor Mutations. *Clinical Lung Cancer,* 18**,** 34-42.e2.

LENNARTSSON, J., MA, H., WARDEGA, P., PELKA, K., ENGSTRÖM, U., HELLBERG, C. & HELDIN, C.-H. 2013. The Fer Tyrosine Kinase Is Important for Platelet-derived Growth Factor-BB-induced Signal Transducer and Activator of Transcription 3 (STAT3) Protein Phosphorylation, Colony Formation in Soft Agar, and Tumor Growth in Vivo. *Journal of Biological Chemistry,* 288**,** 15736-15744.

LEROITH, D., ADAMO, M., WERNER, H. & ROBERTS, C. T. 1991. Insulinlike growth factors and their receptors as growth regulators in normal physiology and pathologic states. *Trends in Endocrinology & Metabolism,* 2**,** 134-139.

LEVKOWITZ, G., WATERMAN, H., ETTENBERG, S. A., KATZ, M., TSYGANKOV, A. Y., ALROY, I., LAVI, S., IWAI, K., REISS, Y., CIECHANOVER, A., LIPKOWITZ, S. & YARDEN, Y. 1999. Ubiquitin ligase activity and tyrosine phosphorylation underlie suppression of growth factor signaling by c-Cbl/Sli-1. *Mol Cell,* 4**,** 1029-40.

LI, H., BATTH, I. S., QU, X., XU, L., SONG, N., WANG, R. & LIU, Y. 2017a. IGF-IR signaling in epithelial to mesenchymal transition and targeting IGF-IR therapy: overview and new insights. *Molecular cancer,* 16**,** 6-6.

LI, H., XU, L., LI, C., ZHAO, L., MA, Y., ZHENG, H., LI, Z., ZHANG, Y., WANG, R., LIU, Y. & QU, X. 2014. Ubiquitin ligase Cbl-b represses IGF-I-induced epithelial mesenchymal transition via ZEB2 and microRNA-200c regulation in gastric cancer cells. *Molecular Cancer,* 13**,** 136.

LI, J., CHOI, E., YU, H. & BAI, X.-C. 2019. Structural basis of the activation of type 1 insulin-like growth factor receptor. *Nature Communications,* 10**,** 4567.

LI, Q., HUTCHINS, A. P., CHEN, Y., LI, S., SHAN, Y., LIAO, B., ZHENG, D., SHI, X., LI, Y., CHAN, W.-Y., PAN, G., WEI, S., SHU, X. & PEI, D. 2017b. A sequential EMT-MET mechanism drives the differentiation of human embryonic stem cells towards hepatocytes. *Nature Communications,* 8**,** 15166.

LI, S., TERMINI, J., HAYWARD, A., SIDDLE, K., ZICK, Y., KOVAL, A., LEROITH, D. & FUJITA-YAMAGUCHI, Y. 1998. The carboxyl-terminal domain of insulin-like growth factor-I receptor interacts with the insulin receptor and activates its protein tyrosine kinase. *FEBS Lett,* 421**,** 45-9.

LIN, F.-T., DAAKA, Y. & LEFKOWITZ, R. J. 1998. β-Arrestins Regulate Mitogenic Signaling and Clathrin-mediated Endocytosis of the Insulin-like Growth Factor I Receptor. *Journal of Biological Chemistry,* 273**,** 31640-31643.

LIN, S.-Y., MAKINO, K., XIA, W., MATIN, A., WEN, Y., KWONG, K. Y., BOURGUIGNON, L. & HUNG, M.-C. 2001. Nuclear localization of EGF receptor and its potential new role as a transcription factor. *Nature Cell Biology,* 3**,** 802-808.

LIPPINCOTT-SCHWARTZ, J., YUAN, L. C., BONIFACINO, J. S. & KLAUSNER, R. D. 1989. Rapid redistribution of Golgi proteins into the ER in cells treated with brefeldin A: Evidence for membrane cycling from Golgi to ER. *Cell,* 56**,** 801-813.

LIU, B. A., ENGELMANN, B. W., JABLONOWSKI, K., HIGGINBOTHAM, K., STERGACHIS, A. B. & NASH, P. D. 2012. SRC Homology 2 Domain Binding Sites in Insulin, IGF-1 and FGF receptor mediated signaling networks reveal an extensive potential interactome. *Cell Communication and Signaling,* 10**,** 27.

LIU, C., ZHANG, Z., TANG, H., JIANG, Z., YOU, L. & LIAO, Y. 2014. Crosstalk between IGF-1R and other tumor promoting pathways. *Curr Pharm Des,* 20**,** 2912-21.

LIU, J. P., BAKER, J., PERKINS, A. S., ROBERTSON, E. J. & EFSTRATIADIS, A. 1993. Mice carrying null mutations of the genes encoding insulin-like growth factor I (Igf-1) and type 1 IGF receptor (Igf1r). *Cell,* 75**,** 59-72.

LIU, L., DAMEN, J. E., HUGHES, M. R., BABIC, I., JIRIK, F. R. & KRYSTAL, G. 1997. The Src homology 2 (SH2) domain of SH2-containing inositol phosphatase (SHIP) is essential for tyrosine phosphorylation of SHIP, its association with Shc, and its induction of apoptosis. *J Biol Chem,* 272**,** 8983-8.

LIU, L., WANG, X., LI, X., WU, X., TANG, M. & WANG, X. 2018a. Upregulation of IGF1 by tumor-associated macrophages promotes the proliferation and migration of epithelial ovarian cancer cells. *Oncol Rep,* 39**,** 818-826.

LIU, R., TANG, W., HAN, X., GENG, R., WANG, C. & ZHANG, Z. 2018b. Hepatocyte growth factor-induced mesenchymal-epithelial transition factor activation leads to insulin-like growth factor 1 receptor inhibitor unresponsiveness in gastric cancer cells. *Oncology letters,* 16**,** 5983-5991.

LIU, T. J., LAFORTUNE, T., HONDA, T., OHMORI, O., HATAKEYAMA, S., MEYER, T., JACKSON, D., DE GROOT, J. & YUNG, W. K. 2007. Inhibition of both focal adhesion kinase and insulin-like growth factor-I receptor kinase suppresses glioma proliferation in vitro and in vivo. *Mol Cancer Ther,* 6**,** 1357-67.

LIU, Y., LEHAR, S., CORVI, C., PAYNE, G. & O'CONNOR, R. 1998. Expression of the Insulin-like Growth Factor I Receptor C Terminus as a Myristylated Protein Leads to Induction of Apoptosis in Tumor Cells. *Cancer Research,* 58**,** 570-576.

LIVAK, K. J. & SCHMITTGEN, T. D. 2001. Analysis of relative gene expression data using real-time quantitative PCR and the 2(-Delta Delta C(T)) Method. *Methods,* 25**,** 402-8.

LOTTI, L. V., LANFRANCONE, L., MIGLIACCIO, E., ZOMPETTA, C., PELICCI, G., SALCINI, A. E., FALINI, B., PELICCI, P. G. & TORRISI, M. R. 1996. Sch proteins are localized on endoplasmic reticulum membranes and are redistributed after tyrosine kinase receptor activation. *Mol Cell Biol,* 16**,** 1946-54.

LU, Y., ZI, X. & POLLAK, M. 2004. Molecular mechanisms underlying IGF-I-induced attenuation of the growth-inhibitory activity of trastuzumab (Herceptin) on SKBR3 breast cancer cells. *Int J Cancer,* 108**,** 334-41.

LU, Y., ZI, X., ZHAO, Y., MASCARENHAS, D. & POLLAK, M. 2001. Insulin-like growth factor-I receptor signaling and resistance to trastuzumab (Herceptin). *J Natl Cancer Inst,* 93**,** 1852-7.

LUZI, L., CONFALONIERI, S., DI FIORE, P. P. & PELICCI, P. G. 2000. Evolution of Shc functions from nematode to human. *Curr Opin Genet Dev,* 10**,** 668-74.

LYONS, A., COLEMAN, M., RIIS, S., FAVRE, C., O'FLANAGAN, C. H., ZHDANOV, A. V., PAPKOVSKY, D. B., HURSTING, S. D. & O'CONNOR, R. 2017. Insulin-like growth factor 1 signaling is essential for mitochondrial biogenesis and mitophagy in cancer cells. *Journal of Biological Chemistry,* 292**,** 16983-16998.

MA, J., GIOVANNUCCI, E., POLLAK, M. & STAMPFER, M. 1999. R esponse : Re: Prospective Study of Colorectal Cancer Risk in Men and Plasma Levels of Insulin-Like Growth Factor (IGF)-I and IGF-Binding Protein-3. *JNCI: Journal of the National Cancer Institute,* 91**,** 2052-2052.

MA, Z., GIBSON, S. L., BYRNE, M. A., ZHANG, J., WHITE, M. F. & SHAW, L. M. 2006. Suppression of insulin receptor substrate 1 (IRS-1) promotes mammary tumor metastasis. *Mol Cell Biol,* 26**,** 9338-51.

MACAULAY, V. M. 1992. Insulin-like growth factors and cancer. *British journal of cancer,* 65**,** 311-320.

MACAULAY, V. M., MIDDLETON, M. R., ECKHARDT, S. G., RUDIN, C. M., JUERGENS, R. A., GEDRICH, R., GOGOV, S., MCCARTHY, S., POONDRU, S., STEPHENS, A. W. & GADGEEL, S. M. 2016. Phase I Dose-Escalation Study of Linsitinib (OSI-906) and Erlotinib in Patients with Advanced Solid Tumors. *Clinical Cancer Research,* 22**,** 2897-2907.

MACLEOD, K. F. 2020. Mitophagy and Mitochondrial Dysfunction in Cancer. *Annual Review of Cancer Biology,* 4**,** 41-60.

MADER, S., LEE, H., PAUSE, A. & SONENBERG, N. 1995. The translation initiation factor eIF-4E binds to a common motif shared by the translation factor eIF-4 gamma and the translational repressors 4E-binding proteins. *Mol Cell Biol,* 15**,** 4990-7.

MAHAUAD-FERNANDEZ, W. D. & OKEOMA, C. M. 2017. Cysteine-linked dimerization of BST-2 confers anoikis resistance to breast cancer cells by negating proapoptotic activities to promote tumor cell survival and growth. *Cell Death & Disease,* 8**,** e2687-e2687.

MAI, A., MUHARRAM, G., BARROW-MCGEE, R., BAGHIROV, H., RANTALA, J., KERMORGANT, S. & IVASKA, J. 2014. Distinct c-Met activation mechanisms induce cell rounding or invasion through pathways involving integrins, RhoA and HIP1. *J Cell Sci,* 127**,** 1938-52.

MAILLOUX, R. J. 2015. Teaching the fundamentals of electron transfer reactions in mitochondria and the production and detection of reactive oxygen species. *Redox Biol,* 4**,** 381-98.

MAKHOUL, C., GOSAVI, P. & GLEESON, P. A. 2018. The Golgi architecture and cell sensing. *Biochemical Society Transactions,* 46**,** 1063-1072.

MALAGUARNERA, R. & BELFIORE, A. 2014. The emerging role of insulin and insulin-like growth factor signaling in cancer stem cells. *Front Endocrinol (Lausanne),* 5**,** 10.

MALAGUARNERA, R., FRASCA, F., GAROZZO, A., GIANÌ, F., PANDINI, G., VELLA, V., VIGNERI, R. & BELFIORE, A. 2011. Insulin receptor isoforms and insulin-like growth factor receptor in human follicular cell precursors from papillary thyroid cancer and normal thyroid. *J Clin Endocrinol Metab,* 96**,** 766-74.

MALUMBRES, M. & BARBACID, M. 2003. RAS oncogenes: the first 30 years. *Nat Rev Cancer,* 3**,** 459-65.

MANES, S., MIRA, E., GOMEZ-MOUTON, C., ZHAO, Z. J., LACALLE, R. A. & MARTINEZ, A. C. 1999. Concerted activity of tyrosine phosphatase SHP-2 and focal adhesion kinase in regulation of cell motility. *Mol Cell Biol,* 19**,** 3125-35.

MANGIOLA, A., VIGO, V., ANILE, C., DE BONIS, P., MARZIALI, G. & LOFRESE, G. 2015. Role and Importance of IGF-1 in Traumatic Brain Injuries. *Biomed Res Int,* 2015**,** 736104.

MAO, Y., SHANG, Y., PHAM, V. C., ERNST, J. A., LILL, J. R., SCALES, S. J. & ZHA, J. 2011. Polyubiquitination of Insulin-like Growth Factor I Receptor (IGF-IR) Activation Loop Promotes Antibody-induced Receptor Internalization and Down-regulation. *Journal of Biological Chemistry,* 286**,** 41852-41861.

MARCOTTE, R., SAYAD, A., BROWN, K. R., SANCHEZ-GARCIA, F., REIMAND, J., HAIDER, M., VIRTANEN, C., BRADNER, J. E., BADER, G. D., MILLS, G. B., PE'ER, D., MOFFAT, J. & NEEL, B. G. 2016. Functional Genomic Landscape of Human Breast Cancer Drivers, Vulnerabilities, and Resistance. *Cell,* 164**,** 293-309.

MARINO-BUSLJE, C., MARTIN-MARTINEZ, M., MIZUGUCHI, K., SIDDLE, K. & BLUNDELL, T. L. 1999. The insulin receptor: from protein sequence to structure. *Biochem Soc Trans,* 27**,** 715-26.

MARSHALL, S. 1985. Kinetics of insulin receptor internalization and recycling in adipocytes. Shunting of receptors to a degradative pathway by inhibitors of recycling. *J Biol Chem,* 260**,** 4136-44.

MAURO, L., SISCI, D., BARTUCCI, M., SALERNO, M., KIM, J., TAM, T., GUVAKOVA, M. A., ANDO, S. & SURMACZ, E. 1999. SHC–α5β1 Integrin Interactions Regulate Breast Cancer Cell Adhesion and Motility. *Experimental Cell Research,* 252**,** 439-448.

MAYO, L. D., KESSLER, K. M., PINCHEIRA, R., WARREN, R. S. & DONNER, D. B. 2001. Vascular Endothelial Cell Growth Factor Activates CRE-binding Protein by Signaling through the KDR Receptor Tyrosine Kinase. *Journal of Biological Chemistry,* 276**,** 25184-25189.

MCKAY, M. M. & MORRISON, D. K. 2007. Integrating signals from RTKs to ERK/MAPK. *Oncogene,* 26**,** 3113-21.

MCMAHON, M., AYLLON, V., PANOV, K. I. & O'CONNOR, R. 2010. Ribosomal 18 S RNA processing by the IGF-I-responsive WDR3 protein is integrated with p53 function in cancer cell proliferation. *J Biol Chem,* 285**,** 18309-18.

MELMED, S. 2006. Medical progress: Acromegaly. *N Engl J Med,* 355**,** 2558-73.

MENDOZA, M. C., ER, E. E. & BLENIS, J. 2011. The Ras-ERK and PI3K-mTOR pathways: cross-talk and compensation. *Trends Biochem Sci,* 36**,** 320-8.

METZ, H. E. & HOUGHTON, A. M. 2011. Insulin receptor substrate regulation of phosphoinositide 3-kinase. *Clin Cancer Res,* 17**,** 206-11.

MIGLIACCIO, E., GIORGIO, M., MELE, S., PELICCI, G., REBOLDI, P., PANDOLFI, P. P., LANFRANCONE, L. & PELICCI, P. G. 1999. The p66shc adaptor protein controls oxidative stress response and life span in mammals. *Nature,* 402**,** 309-313.

MILLARTE, V. & FARHAN, H. 2012. The Golgi in Cell Migration: Regulation by Signal Transduction and Its Implications for Cancer Cell Metastasis. *The Scientific World Journal,* 2012**,** 11.

MILMAN, S., ATZMON, G., HUFFMAN, D. M., WAN, J., CRANDALL, J. P., COHEN, P. & BARZILAI, N. 2014. Low insulin-like growth factor-1 level predicts survival in humans with exceptional longevity. *Aging Cell,* 13**,** 769-71.

MIN, Y., ADACHI, Y., YAMAMOTO, H., IMSUMRAN, A., ARIMURA, Y., ENDO, T., HINODA, Y., LEE, C. T., NADAF, S., CARBONE, D. P. & IMAI, K. 2005. Insulin-like growth factor I receptor blockade enhances chemotherapy and radiation responses and inhibits tumour growth in human gastric cancer xenografts. *Gut,* 54**,** 591-600.

MIURA, M. & BASERGA, R. 1997. The Tyrosine Residue at 1250 of the Insulin-like Growth Factor I Receptor Is Required for Ligand-Mediated Internalization. *Biochemical and Biophysical Research Communications,* 239**,** 182-185.

MIURA, M., LI, S. & BASERGA, R. 1995a. Effect of a mutation at tyrosine 950 of the insulin-like growth factor I receptor on the growth and transformation of cells. *Cancer Res,* 55**,** 663-7.

MIURA, M., SURMACZ, E., BURGAUD, J.-L. & BASERGA, R. 1995b. Different Effects on Mitogenesis and Transformation of a Mutation at Tyrosine 1251 of the Insulin-like Growth Factor I Receptor. *Journal of Biological Chemistry,* 270**,** 22639-22644.

MOHAN, S., THOMPSON, G. R., AMAAR, Y. G., HATHAWAY, G., TSCHESCHE, H. & BAYLINK, D. J. 2002. ADAM-9 Is an Insulin-like Growth Factor Binding Protein-5 Protease Produced and Secreted by Human Osteoblasts. *Biochemistry,* 41**,** 15394-15403.

MONAMI, G., EMILIOZZI, V. & MORRIONE, A. 2008. Grb10/Nedd4-mediated multiubiquitination of the insulin-like growth factor receptor regulates receptor internalization. *Journal of Cellular Physiology,* 216**,** 426-437.

MONGET, P. & OXVIG, C. 2016. PAPP-A and the IGF system. *Ann Endocrinol (Paris),* 77**,** 90-6.

MONTAGUT, C. & SETTLEMAN, J. 2009. Targeting the RAF–MEK–ERK pathway in cancer therapy. *Cancer Letters,* 283**,** 125-134.

MOR, A. & PHILIPS, M. R. 2006. Compartmentalized Ras/MAPK signaling. *Annu Rev Immunol,* 24**,** 771-800.

MORGILLO, F., WOO, J. K., KIM, E. S., HONG, W. K. & LEE, H. Y. 2006. Heterodimerization of insulin-like growth factor receptor/epidermal growth factor receptor and induction of survivin expression counteract the antitumor action of erlotinib. *Cancer Res,* 66**,** 10100-11.

MORRIONE, A., DEANGELIS, T. & BASERGA, R. 1995. Failure of the bovine papillomavirus to transform mouse embryo fibroblasts with a targeted disruption of the insulin-like growth factor I receptor genes. *J Virol,* 69**,** 5300-3.

MOUSTAKAS, A. & DE HERREROS, A. G. 2017. Epithelial-mesenchymal transition in cancer. *Mol Oncol,* 11**,** 715-717.

MUKOHARA, T., SHIMADA, H., OGASAWARA, N., WANIKAWA, R., SHIMOMURA, M., NAKATSURA, T., ISHII, G., PARK, J. O., JANNE, P. A., SAIJO, N. & MINAMI, H. 2009. Sensitivity of breast cancer cell lines to the novel insulin-like growth factor-1 receptor (IGF-1R) inhibitor NVP-AEW541 is dependent on the level of IRS-1 expression. *Cancer Lett,* 282**,** 14-24.

MULLER, P. A. J., TRINIDAD, A. G., TIMPSON, P., MORTON, J. P., ZANIVAN, S., VAN DEN BERGHE, P. V. E., NIXON, C., KARIM, S. A., CASWELL, P. T., NOLL, J. E., COFFILL, C. R., LANE, D. P., SANSOM, O. J., NEILSEN, P. M., NORMAN, J. C. & VOUSDEN, K. H. 2013. Mutant p53 enhances MET trafficking and signalling to drive cell scattering and invasion. *Oncogene,* 32**,** 1252-1265.

MYERS, M. G., JR., GRAMMER, T. C., WANG, L. M., SUN, X. J., PIERCE, J. H., BLENIS, J. & WHITE, M. F. 1994. Insulin receptor substrate-1 mediates phosphatidylinositol 3'-kinase and p70S6k signaling during insulin, insulin-like growth factor-1, and interleukin-4 stimulation. *J Biol Chem,* 269**,** 28783-9.

MYNARCIK, D. C., YU, G. Q. & WHITTAKER, J. 1996. Alanine-scanning mutagenesis of a C-terminal ligand binding domain of the insulin receptor alpha subunit. *J Biol Chem,* 271**,** 2439-42.

NAGLE, A. M., LEVINE, K. M., TASDEMIR, N., SCOTT, J. A., BURLBAUGH, K., KEHM, J., KATZ, T. A., BOONE, D. N., JACOBSEN, B. M., ATKINSON, J. M., OESTERREICH, S. & LEE, A. V. 2018. Loss of E-cadherin Enhances IGF1–IGF1R Pathway Activation and Sensitizes Breast Cancers to Anti-IGF1R/InsR Inhibitors. *Clinical Cancer Research,* 024**,** 5165-5177.

NAGLE, J. A., MA, Z., BYRNE, M. A., WHITE, M. F. & SHAW, L. M. 2004. Involvement of Insulin Receptor Substrate 2 in Mammary Tumor Metastasis. *Molecular and Cellular Biology,* 24**,** 9726-9735.

NAHTA, R., YUAN, L. X., ZHANG, B., KOBAYASHI, R. & ESTEVA, F. J. 2005. Insulin-like growth factor-I receptor/human epidermal growth factor receptor 2 heterodimerization contributes to trastuzumab resistance of breast cancer cells. *Cancer Res,* 65**,** 11118-28.

NEMOTO, S., COMBS, C. A., FRENCH, S., AHN, B. H., FERGUSSON, M. M., BALABAN, R. S. & FINKEL, T. 2006. The mammalian longevity-associated gene product p66shc regulates mitochondrial metabolism. *J Biol Chem,* 281**,** 10555-60.

NEUMANN, S. & SCHMID, S. L. 2013. Dual Role of BAR Domain-containing Proteins in Regulating Vesicle Release Catalyzed by the GTPase, Dynamin-2. *Journal of Biological Chemistry,* 288**,** 25119-25128.

NIEPEL, M., HAFNER, M., PACE, E. A., CHUNG, M., CHAI, D. H., ZHOU, L., SCHOEBERL, B. & SORGER, P. K. 2013. Profiles of Basal and stimulated receptor signaling networks predict drug response in breast cancer lines. *Sci Signal,* 6**,** ra84.

NIETO, M. A., HUANG, R. Y., JACKSON, R. A. & THIERY, J. P. 2016. EMT: 2016. *Cell,* 166**,** 21-45.

NING, Y., SCHULLER, A. G. P., CONOVER, C. A. & PINTAR, J. E. 2008. Insulin-like growth factor (IGF) binding protein-4 is both a positive and negative regulator of IGF activity in vivo. *Molecular endocrinology (Baltimore, Md.),* 22**,** 1213-1225.

NIU, J., XU, Z., LI, X.-N. & HAN, Z. 2007. siRNA-mediated type 1 insulin-like growth factor receptor silencing induces chemosensitization of a human liver cancer cell line with mutant P53. *Cell Biology International,* 31**,** 156-164.

NORTHEY, J. J., CHMIELECKI, J., NGAN, E., RUSSO, C., ANNIS, M. G., MULLER, W. J. & SIEGEL, P. M. 2008. Signaling through ShcA Is Required for Transforming Growth Factor β- and Neu/ErbB-2-Induced Breast Cancer Cell Motility and Invasion. *Molecular and Cellular Biology,* 28**,** 3162-3176.

O'CONNOR, R. 2003. Regulation of IGF-I Receptor Signaling in Tumor Cells. *Horm Metab Res,* 35**,** 771-777.

O'CONNOR, R., KAUFFMANN-ZEH, A., LIU, Y., LEHAR, S., EVAN, G. I., BASERGA, R. & BLÄTTLER, W. A. 1997. Identification of domains of the insulin-like growth factor I receptor that are required for protection from apoptosis. *Molecular and cellular biology,* 17**,** 427-435.

O'FLANAGAN, C. H., O'SHEA, S., LYONS, A., FOGARTY, F. M., MCCABE, N., KENNEDY, R. D. & O'CONNOR, R. 2016. IGF-1R inhibition sensitizes breast cancer cells to ATM-related kinase (ATR) inhibitor and cisplatin. *Oncotarget,* 7**,** 56826-56841.

O'SULLIVAN, J. F., LEBLOND, A. L., KELLY, G., KUMAR, A. H., METHAROM, P., BUNEKER, C. K., ALIZADEH-VIKALI, N., HRISTOVA, I., HYNES, B. G., O'CONNOR, R. & CAPLICE, N. M. 2011. Potent long-term cardioprotective effects of single low-dose insulin-like growth factor-1 treatment postmyocardial infarction. *Circ Cardiovasc Interv,* 4**,** 327-35.

OBATA, Y., HORIKAWA, K., SHIINA, I., TAKAHASHI, T., MURATA, T., TASAKI, Y., SUZUKI, K., YONEKURA, K., ESUMI, H., NISHIDA, T. & ABE, R. 2018. Oncogenic Kit signalling on the Golgi is suppressed by blocking secretory trafficking with M-COPA in gastrointestinal stromal tumours. *Cancer Letters,* 415**,** 1-10.

OBATA, Y., HORIKAWA, K., TAKAHASHI, T., AKIEDA, Y., TSUJIMOTO, M., FLETCHER, J. A., ESUMI, H., NISHIDA, T. & ABE, R. 2017. Oncogenic signaling by Kit tyrosine kinase occurs selectively on the Golgi apparatus in gastrointestinal stromal tumors. *Oncogene,* 36**,** 3661-3672.

OFFTERDINGER , M., SCH¥ FER , C., WEIPOLTSHAMMER , K. & GRUNT , T. W. 2002. c-erbB-3 : a nuclear protein in mammary epithelial cells. *The Journal of Cell Biology,* 157**,** 929-940.

OSHER, E. & MACAULAY, V. M. 2019. Therapeutic Targeting of the IGF Axis. *Cells,* 8**,** 895.

OSORIO, F. G., SORIA-VALLES, C., SANTIAGO-FERNÁNDEZ, O., BERNAL, T., MITTELBRUNN, M., COLADO, E., RODRÍGUEZ, F., BONZON-KULICHENKO, E., VÁZQUEZ, J., PORTA-DE-LA-RIVA, M., CERÓN, J., FUEYO, A., LI, J., GREEN, A. R., FREIJE, J. M. & LÓPEZ-OTÍN, C. 2016. Loss of the proteostasis factor AIRAPL causes myeloid transformation by deregulating IGF-1 signaling. *Nat Med,* 22**,** 91-6.

OZA, A., KAYE, S., VAN TORNOUT, J., SESSA, C., GORE, M., NAUMANN, R. W., HIRTE, H., COLOMBO, N., CHEN, J., GORLA, S., POONDRU, S., SINGH, M., STEINBERG, J., YUEN, G. & BANERJEE, S. 2018. Phase 2 study evaluating intermittent and continuous linsitinib and weekly paclitaxel in patients with recurrent platinum resistant ovarian epithelial cancer. *Gynecologic Oncology,* 149**,** 275-282.

PACKHAM, S., WARSITO, D., LIN, Y., SADI, S., KARLSSON, R., SEHAT, B. & LARSSON, O. 2015. Nuclear translocation of IGF-1R via p150Glued and an importin-β/RanBP2-dependent pathway in cancer cells. *Oncogene,* 34**,** 2227-2238.

PALMITER, R. D., BRINSTER, R. L., HAMMER, R. E., TRUMBAUER, M. E., ROSENFELD, M. G., BIRNBERG, N. C. & EVANS, R. M. 1982. Dramatic growth of mice that develop from eggs microinjected with metallothionein-growth hormone fusion genes. *Nature,* 300**,** 611-5.

PANDINI, G., MEDICO, E., CONTE, E., SCIACCA, L., VIGNERI, R. & BELFIORE, A. 2003. Differential gene expression induced by insulin and insulin-like growth factor-II through the insulin receptor isoform A. *J Biol Chem,* 278**,** 42178-89.

PANDINI, G., WURCH, T., AKLA, B., CORVAIA, N., BELFIORE, A. & GOETSCH, L. 2007. Functional responses and in vivo anti-tumour activity of h7C10: a humanised monoclonal antibody with neutralising activity against the insulin-like growth factor-1 (IGF-1) receptor and insulin/IGF-1 hybrid receptors. *Eur J Cancer,* 43**,** 1318-27.

PASDER, O., SHPUNGIN, S., SALEM, Y., MAKOVSKY, A., VILCHICK, S., MICHAELI, S., MALOVANI, H. & NIR, U. 2006. Downregulation of Fer induces PP1 activation and cell-cycle arrest in malignant cells. *Oncogene,* 25**,** 4194-206.

PELICCI, G., LANFRANCONE, L., GRIGNANI, F., MCGLADE, J., CAVALLO, F., FORNI, G., NICOLETTI, I., GRIGNANI, F., PAWSON, T. & GIUSEPPE PELICCI, P. 1992. A novel transforming protein (SHC) with an SH2 domain is implicated in mitogenic signal transduction. *Cell,* 70**,** 93-104.

PELLEGRINI, M., PACINI, S. & BALDARI, C. T. 2005. p66SHC: the apoptotic side of Shc proteins. *Apoptosis,* 10**,** 13-8.

PEREIRA-LEAL, J. B. & SEABRA, M. C. 2001. Evolution of the Rab family of small GTP-binding proteins. *J Mol Biol,* 313**,** 889-901.

PETERSON, J. E., KULIK, G., JELINEK, T., REUTER, C. W. M., SHANNON, J. A. & WEBER, M. J. 1996. Src Phosphorylates the Insulin-like Growth Factor Type I Receptor on the Autophosphorylation Sites: REQUIREMENT FOR TRANSFORMATION BY src. *Journal of Biological Chemistry,* 271**,** 31562-31571.

PETLEY, T., GRAFF, K., JIANG, W., YANG, H. & FLORINI, J. 1999. Variation among cell types in the signaling pathways by which IGF-I stimulates specific cellular responses. *Horm Metab Res,* 31**,** 70-6.

PEYRAT, J. P., BONNETERRE, J., HECQUET, B., VENNIN, P., LOUCHEZ, M. M., FOURNIER, C., LEFEBVRE, J. & DEMAILLE, A. 1993. Plasma insulin-like growth factor-1 (IGF-1) concentrations in human breast cancer. *Eur J Cancer,* 29a**,** 492-7.

PICKAR-OLIVER, A. & GERSBACH, C. A. 2019. The next generation of CRISPR–Cas technologies and applications. *Nature Reviews Molecular Cell Biology,* 20**,** 490-507.

PIECZENIK, S. R. & NEUSTADT, J. 2007. Mitochondrial dysfunction and molecular pathways of disease. *Experimental and Molecular Pathology,* 83**,** 84-92.

POLLAK, M. 2008. Insulin and insulin-like growth factor signalling in neoplasia. *Nat Rev Cancer,* 8**,** 915-28.

POLLAK, M. 2012. The insulin and insulin-like growth factor receptor family in neoplasia: an update. *Nature Reviews Cancer,* 12**,** 159.

POLLAK, M. N. 1998. Endocrine effects of IGF-I on normal and transformed breast epithelial cells: potential relevance to strategies for breast cancer treatment and prevention. *Breast Cancer Research and Treatment,* 47**,** 209-217.

POLLAK, M. N., SCHERNHAMMER, E. S. & HANKINSON, S. E. 2004. Insulin-like growth factors and neoplasia. *Nat Rev Cancer,* 4**,** 505-18.

PRAGER, D., LI, H. L., YAMASAKI, H. & MELMED, S. 1994. Human insulin-like growth factor I receptor internalization. Role of the juxtamembrane domain. *Journal of Biological Chemistry,* 269**,** 11934-11937.

PREISINGER, C., SHORT, B., DE CORTE, V., BRUYNEEL, E., HAAS, A., KOPAJTICH, R., GETTEMANS, J. & BARR, F. A. 2004. YSK1 is activated by the Golgi matrix protein GM130 and plays a role in cell migration through its substrate 14-3-3zeta. *J Cell Biol,* 164**,** 1009-20.

PRISCO, M., HONGO, A., RIZZO, M. G., SACCHI, A. & BASERGA, R. 1997. The insulin-like growth factor I receptor as a physiologically relevant target of p53 in apoptosis caused by interleukin-3 withdrawal. *Molecular and Cellular Biology,* 17**,** 1084-1092.

PRISCO, M., SANTINI, F., BAFFA, R., LIU, M., DRAKAS, R., WU, A. & BASERGA, R. 2002. Nuclear translocation of insulin receptor substrate-1 by the simian virus 40 T antigen and the activated type 1 insulin-like growth factor receptor. *J Biol Chem,* 277**,** 32078-85.

PROCACCIA, S., ORDAN, M., COHEN, I., BENDETZ-NEZER, S. & SEGER, R. 2017. Direct binding of MEK1 and MEK2 to AKT induces Foxo1 phosphorylation, cellular migration and metastasis. *Scientific Reports,* 7**,** 43078.

PRONK, G. J., DE VRIES-SMITS, A. M., BUDAY, L., DOWNWARD, J., MAASSEN, J. A., MEDEMA, R. H. & BOS, J. L. 1994. Involvement of Shc in insulin- and epidermal growth factor-induced activation of p21ras. *Molecular and cellular biology,* 14**,** 1575-1581.

QU, X., WU, Z., DONG, W., ZHANG, T., WANG, L., PANG, Z., MA, W. & DU, J. 2017. Update of IGF-1 receptor inhibitor (ganitumab, dalotuzumab, cixutumumab, teprotumumab and figitumumab) effects on cancer therapy. *Oncotarget,* 8**,** 29501-29518.

QUAIL, D. F., BOWMAN, R. L., AKKARI, L., QUICK, M. L., SCHUHMACHER, A. J., HUSE, J. T., HOLLAND, E. C., SUTTON, J. C. & JOYCE, J. A. 2016. The tumor microenvironment underlies acquired resistance to CSF-1R inhibition in gliomas. *Science,* 352**,** aad3018.

RAJARAM, S., BAYLINK, D. J. & MOHAN, S. 1997. Insulin-like growth factor-binding proteins in serum and other biological fluids: regulation and functions. *Endocr Rev,* 18**,** 801-31.

RAMAKRISHNAN, V., KIMLINGER, T., HAUG, J., PAINULY, U., WELLIK, L., HALLING, T., RAJKUMAR, S. V. & KUMAR, S. 2012. Anti-myeloma activity of Akt inhibition is linked to the activation status of PI3K/Akt and MEK/ERK pathway. *PloS one,* 7**,** e50005-e50005.

RAMBOLD, A. S. & LIPPINCOTT-SCHWARTZ, J. 2011. Mechanisms of mitochondria and autophagy crosstalk. *Cell Cycle,* 10**,** 4032-4038.

REN, J., PULAKAT, L., WHALEY-CONNELL, A. & SOWERS, J. R. 2010. Mitochondrial biogenesis in the metabolic syndrome and cardiovascular disease. *Journal of Molecular Medicine,* 88**,** 993-1001.

RENEHAN, A. G., ZWAHLEN, M., MINDER, C., O'DWYER, S. T., SHALET, S. M. & EGGER, M. 2004. Insulin-like growth factor (IGF)-I, IGF binding protein-3, and cancer risk: systematic review and meta-regression analysis. *Lancet,* 363**,** 1346-53.

RESNICOFF, M., ABRAHAM, D., YUTANAWIBOONCHAI, W., ROTMAN, H. L., KAJSTURA, J., RUBIN, R., ZOLTICK, P. & BASERGA, R. 1995. The Insulin-like Growth Factor I Receptor Protects Tumor Cells from Apoptosis in Vivo. *Cancer Research,* 55**,** 2463-2469.

RESNICOFF, M., SELL, C., RUBINI, M., COPPOLA, D., AMBROSE, D., BASERGA, R. & RUBIN, R. 1994. Rat glioblastoma cells expressing an antisense RNA to the insulin-like growth factor-1 (IGF-1) receptor are nontumorigenic and induce regression of wild-type tumors. *Cancer Res,* 54**,** 2218-22.

RINALDI, S., CLEVELAND, R., NORAT, T., BIESSY, C., ROHRMANN, S., LINSEISEN, J., BOEING, H., PISCHON, T., PANICO, S., AGNOLI, C., PALLI, D., TUMINO, R., VINEIS, P., PEETERS, P. H., VAN GILS, C. H., BUENO-DE-MESQUITA, B. H., VRIELING, A., ALLEN, N. E., RODDAM, A., BINGHAM, S., KHAW, K. T., MANJER, J., BORGQUIST, S., DUMEAUX, V., TORHILD GRAM, I., LUND, E., TRICHOPOULOU, A., MAKRYGIANNIS, G., BENETOU, V., MOLINA, E., DONATE SUÁREZ, I., BARRICARTE GURREA, A., GONZALEZ, C. A., TORMO, M. J., ALTZIBAR, J. M., OLSEN, A., TJONNELAND, A., GRØNBAEK, H., OVERVAD, K., CLAVEL-CHAPELON, F., BOUTRON-RUAULT, M. C., MOROIS, S., SLIMANI, N., BOFFETTA, P., JENAB, M., RIBOLI, E. & KAAKS, R. 2010. Serum levels of IGF-I, IGFBP-3 and colorectal cancer risk: results from the EPIC cohort, plus a meta-analysis of prospective studies. *Int J Cancer,* 126**,** 1702-15.

RITOV, V. B., MENSHIKOVA, E. V., HE, J., FERRELL, R. E., GOODPASTER, B. H. & KELLEY, D. E. 2005. Deficiency of Subsarcolemmal Mitochondria in Obesity and Type 2 Diabetes. *Diabetes,* 54**,** 8-14.

ROBERTS, M., BARRY, S., WOODS, A., VAN DER SLUIJS, P. & NORMAN, J. 2001. PDGF-regulated rab4-dependent recycling of alphavbeta3 integrin from early endosomes is necessary for cell adhesion and spreading. *Curr Biol,* 11**,** 1392-402.

ROBERTS, P. J. & DER, C. J. 2007. Targeting the Raf-MEK-ERK mitogen-activated protein kinase cascade for the treatment of cancer. *Oncogene,* 26**,** 3291-310.

ROCHE, J. 2018. The Epithelial-to-Mesenchymal Transition in Cancer. *Cancers,* 10**,** 52.

ROMANELLI, R. J., LEBEAU, A. P., FULMER, C. G., LAZZARINO, D. A., HOCHBERG, A. & WOOD, T. L. 2007. Insulin-like Growth Factor Type-I Receptor Internalization and Recycling Mediate the Sustained Phosphorylation of Akt. *Journal of Biological Chemistry,* 282**,** 22513-22524.

ROSATO, R., VELTMAAT, J. M., GROFFEN, J. & HEISTERKAMP, N. 1998. Involvement of the tyrosine kinase fer in cell adhesion. *Molecular and cellular biology,* 18**,** 5762-5770.

ROSTOKER, R., ABELSON, S., BITTON-WORMS, K., GENKIN, I., BEN-SHMUEL, S., DAKWAR, M., ORR, Z. S., CASPI, A., TZUKERMAN, M. & LEROITH, D. 2015. Highly specific role of the insulin receptor in breast cancer progression. *Endocrine-related cancer,* 22**,** 145-157.

ROUDNICKY, F., DIETERICH, L. C., POYET, C., BUSER, L., WILD, P., TANG, D., CAMENZIND, P., HO, C. H., OTTO, V. I. & DETMAR, M. 2017. High expression of insulin receptor on tumour-associated blood vessels in invasive bladder cancer predicts poor overall and progression-free survival. *J Pathol,* 242**,** 193-205.

RUKSTALIS, J. M. & HABENER, J. F. 2007. Snail2, a mediator of epithelial-mesenchymal transitions, expressed in progenitor cells of the developing endocrine pancreas. *Gene Expr Patterns,* 7**,** 471-9.

RYAN, C. J., HARZSTARK, A. H., ROSENBERG, J., LIN, A., CLAROS, C., GOLDFINE, I. D., KERNER, J. F., SMALL, E. J. & YOUNGREN, J. F. 2008. A pilot dose-escalation study of the effects of nordihydroguareacetic acid on hormone and prostate specific antigen levels in patients with relapsed prostate cancer. *BJU Int,* 101**,** 436-9.

SACHDEV, D., HARTELL, J. S., LEE, A. V., ZHANG, X. & YEE, D. 2004. A dominant negative type I insulin-like growth factor receptor inhibits metastasis of human cancer cells. *J Biol Chem,* 279**,** 5017-24.

SACHDEV, D., LI, S. L., HARTELL, J. S., FUJITA-YAMAGUCHI, Y., MILLER, J. S. & YEE, D. 2003. A chimeric humanized single-chain antibody against the type I insulin-like growth factor (IGF) receptor renders breast cancer cells refractory to the mitogenic effects of IGF-I. *Cancer Res,* 63**,** 627-35.

SACHDEV, D., SINGH, R., FUJITA-YAMAGUCHI, Y. & YEE, D. 2006. Down-regulation of insulin receptor by antibodies against the type I insulin-like growth factor receptor: implications for anti-insulin-like growth factor therapy in breast cancer. *Cancer Res,* 66**,** 2391-402.

SÁDABA, M. C., MARTÍN-ESTAL, I., PUCHE, J. E. & CASTILLA-CORTÁZAR, I. 2016. Insulin-like growth factor 1 (IGF-1) therapy: Mitochondrial dysfunction and diseases. *Biochimica et Biophysica Acta (BBA) - Molecular Basis of Disease,* 1862**,** 1267-1278.

SAIKALI, Z., SETYA, H., SINGH, G. & PERSAD, S. 2008. Role of IGF-1/IGF-1R in regulation of invasion in DU145 prostate cancer cells. *Cancer Cell Int,* 8**,** 10.

SAMANI, A. A., CHEVET, E., FALLAVOLLITA, L., GALIPEAU, J. & BRODT, P. 2004. Loss of tumorigenicity and metastatic potential in carcinoma cells expressing the extracellular domain of the type 1 insulin-like growth factor receptor. *Cancer Res,* 64**,** 3380-5.

SAMANI, A. A., YAKAR, S., LEROITH, D. & BRODT, P. 2007. The Role of the IGF System in Cancer Growth and Metastasis: Overview and Recent Insights. *Endocrine Reviews,* 28**,** 20-47.

SANGRAR, W., SHI, C., MULLINS, G., LEBRUN, D., INGALLS, B. & GREER, P. A. 2015. Amplified Ras-MAPK signal states correlate with accelerated EGFR internalization, cytostasis and delayed HER2 tumor onset in Fer-deficient model systems. *Oncogene,* 34**,** 4109-4117.

SARASTE, J. & PRYDZ, K. 2019. A New Look at the Functional Organization of the Golgi Ribbon. *Frontiers in Cell and Developmental Biology,* 7.

SARBASSOV, D. D., GUERTIN, D. A., ALI, S. M. & SABATINI, D. M. 2005. Phosphorylation and regulation of Akt/PKB by the rictor-mTOR complex. *Science,* 307**,** 1098-101.

SARFSTEIN, R., PASMANIK-CHOR, M., YEHESKEL, A., EDRY, L., SHOMRON, N., WARMAN, N., WERTHEIMER, E., MAOR, S., SHOCHAT, L. & WERNER, H. 2012. Insulin-like growth factor-I receptor (IGF-IR) translocates to nucleus and autoregulates IGF-IR gene expression in breast cancer cells. *J Biol Chem,* 287**,** 2766-76.

SASAKI, K. & YOSHIDA, H. 2015. Organelle autoregulation—stress responses in the ER, Golgi, mitochondria and lysosome. *The Journal of Biochemistry,* 157**,** 185-195.

SASAOKA, T., ISHIKI, M., SAWA, T., ISHIHARA, H., TAKATA, Y., IMAMURA, T., USUI, I., OLEFSKY, J. M. & KOBAYASHI, M. 1996. Comparison of the insulin and insulin-like growth factor 1 mitogenic intracellular signaling pathways. *Endocrinology,* 137**,** 4427-34.

SCIACCA, L., COSTANTINO, A., PANDINI, G., MINEO, R., FRASCA, F., SCALIA, P., SBRACCIA, P., GOLDFINE, I. D., VIGNERI, R. & BELFIORE, A. 1999. Insulin receptor activation by IGF-II in breast cancers: evidence for a new autocrine/paracrine mechanism. *Oncogene,* 18**,** 2471-9.

SCIACCA, L., PRISCO, M., WU, A., BELFIORE, A., VIGNERI, R. & BASERGA, R. 2003. Signaling differences from the A and B isoforms of the insulin receptor (IR) in 32D cells in the presence or absence of IR substrate-1. *Endocrinology,* 144**,** 2650-8.

SCOTLANDI, K., AVNET, S., BENINI, S., MANARA, M. C., SERRA, M., CERISANO, V., PERDICHIZZI, S., LOLLINI, P.-L., DE GIOVANNI, C., LANDUZZI, L. & PICCI, P. 2002. Expression of an IGF-I receptor dominant negative mutant induces apoptosis, inhibits tumorigenesis and enhances chemosensitivity in Ewing's sarcoma cells. *International Journal of Cancer,* 101**,** 11-16.

SEGUIN, L., DESGROSELLIER, J. S., WEIS, S. M. & CHERESH, D. A. 2015. Integrins and cancer: regulators of cancer stemness, metastasis, and drug resistance. *Trends in cell biology,* 25**,** 234-240.

SEHAT, B., ANDERSSON, S., GIRNITA, L. & LARSSON, O. 2008. Identification of c-Cbl as a New Ligase for Insulin-like Growth Factor-I Receptor with Distinct Roles from Mdm2 in Receptor Ubiquitination and Endocytosis. *Cancer Research,* 68**,** 5669-5677.

SEHAT, B., ANDERSSON, S., VASILCANU, R., GIRNITA, L. & LARSSON, O. 2007. Role of Ubiquitination in IGF-1 Receptor Signaling and Degradation. *PLOS ONE,* 2**,** e340.

SEHAT, B., TOFIGH, A., LIN, Y., TROCMÉ, E., LILJEDAHL, U., LAGERGREN, J. & LARSSON, O. 2010. SUMOylation Mediates the Nuclear Translocation and Signaling of the IGF-1 Receptor. *Science Signaling,* 3**,** ra10-ra10.

SELL, C., BASERGA, R. & RUBIN, R. 1995. Insulin-like growth factor I (IGF-I) and the IGF-I receptor prevent etoposide-induced apoptosis. *Cancer Res,* 55**,** 303-6.

SELL, C., DUMENIL, G., DEVEAUD, C., MIURA, M., COPPOLA, D., DEANGELIS, T., RUBIN, R., EFSTRATIADIS, A. & BASERGA, R. 1994. Effect of a null mutation of the insulin-like growth factor I receptor gene on growth and transformation of mouse embryo fibroblasts. *Mol Cell Biol,* 14**,** 3604-12.

SELL, C., RUBINI, M., RUBIN, R., LIU, J. P., EFSTRATIADIS, A. & BASERGA, R. 1993. Simian virus 40 large tumor antigen is unable to transform mouse embryonic fibroblasts lacking type 1 insulin-like growth factor receptor. *Proceedings of the National Academy of Sciences of the United States of America,* 90**,** 11217-11221.

SENGUPTA, S., PETERSON, T. R. & SABATINI, D. M. 2010. Regulation of the mTOR complex 1 pathway by nutrients, growth factors, and stress. *Mol Cell,* 40**,** 310-22.

SEOL, K. C. & KIM, S. J. 2003. Nuclear matrix association of insulin receptor and IRS-1 by insulin in osteoblast-like UMR-106 cells. *Biochem Biophys Res Commun,* 306**,** 898-904.

SEPP-LORENZINO, L. 1998. Structure and function of the insulin-like growth factor I receptor. *Breast Cancer Research and Treatment,* 47**,** 235-253.

SHAW, L. M. 2011. The insulin receptor substrate (IRS) proteins: at the intersection of metabolism and cancer. *Cell cycle (Georgetown, Tex.),* 10**,** 1750-1756.

SHENG, B., WANG, X., SU, B., LEE, H.-G., CASADESUS, G., PERRY, G. & ZHU, X. 2012. Impaired mitochondrial biogenesis contributes to mitochondrial dysfunction in Alzheimer's disease. *Journal of Neurochemistry,* 120**,** 419-429.

SHI, Z., XU, W., LOECHEL, F., WEWER, U. M. & MURPHY, L. J. 2000. ADAM 12, a Disintegrin Metalloprotease, Interacts with Insulin-like Growth Factor-binding Protein-3. *Journal of Biological Chemistry,* 275**,** 18574-18580.

SIGISMUND, S., WOELK, T., PURI, C., MASPERO, E., TACCHETTI, C., TRANSIDICO, P., DI FIORE, P. P. & POLO, S. 2005. Clathrin-independent endocytosis of ubiquitinated cargos. *Proc Natl Acad Sci U S A,* 102**,** 2760-5.

SIMPSON, A., PETNGA, W., MACAULAY, V. M., WEYER-CZERNILOFSKY, U. & BOGENRIEDER, T. 2017. Insulin-Like Growth Factor (IGF) Pathway Targeting in Cancer: Role of the IGF Axis and Opportunities for Future Combination Studies. *Targeted oncology,* 12**,** 571-597.

SINGH, R. K., GAIKWAD, S. M., JINAGER, A., CHAUDHURY, S., MAHESHWARI, A. & RAY, P. 2014. IGF-1R inhibition potentiates cytotoxic effects of chemotherapeutic agents in early stages of chemoresistant ovarian cancer cells. *Cancer Lett,* 354**,** 254-62.

SIVAKUMAR, R., KOGA, H., SELVENDIRAN, K., MAEYAMA, M., UENO, T. & SATA, M. 2009. Autocrine loop for IGF-I receptor signaling in SLUG-mediated epithelial-mesenchymal transition. *Int J Oncol,* 34**,** 329-38.

SMITH, B. J., HUANG, K., KONG, G., CHAN, S. J., NAKAGAWA, S., MENTING, J. G., HU, S. Q., WHITTAKER, J., STEINER, D. F., KATSOYANNIS, P. G., WARD, C. W., WEISS, M. A. & LAWRENCE, M. C. 2010. Structural resolution of a tandem hormone-binding element in the insulin receptor and its implications for design of peptide agonists. *Proc Natl Acad Sci U S A,* 107**,** 6771-6.

SOOS, M. A., FIELD, C. E. & SIDDLE, K. 1993. Purified hybrid insulin/insulin-like growth factor-I receptors bind insulin-like growth factor-I, but not insulin, with high affinity. *Biochemical Journal,* 290**,** 419-426.

SORKIN, A. & GOH, L. K. 2008. Endocytosis and intracellular trafficking of ErbBs. *Experimental cell research,* 314**,** 3093-3106.

SOUTSCHEK, J., AKINC, A., BRAMLAGE, B., CHARISSE, K., CONSTIEN, R., DONOGHUE, M., ELBASHIR, S., GEICK, A., HADWIGER, P., HARBORTH, J., JOHN, M., KESAVAN, V., LAVINE, G., PANDEY, R. K., RACIE, T., RAJEEV, K. G., RÖHL, I., TOUDJARSKA, I., WANG, G., WUSCHKO, S., BUMCROT, D., KOTELIANSKY, V., LIMMER, S., MANOHARAN, M. & VORNLOCHER, H.-P. 2004. Therapeutic silencing of an endogenous gene by systemic administration of modified siRNAs. *Nature,* 432**,** 173-178.

SPENCE, J., SADIS, S., HAAS, A. L. & FINLEY, D. 1995. A ubiquitin mutant with specific defects in DNA repair and multiubiquitination. *Molecular and cellular biology,* 15**,** 1265-1273.

STACHOWIAK, E. K., FANG, X., MYERS, J., DUNHAM, S. & STACHOWIAK, M. K. 2003. cAMP-induced differentiation of human neuronal progenitor cells is mediated by nuclear fibroblast growth factor receptor-1 (FGFR1). *Journal of Neurochemistry,* 84**,** 1296-1312.

STANICKA, J., RIEGER, L., O'SHEA, S., COX, O., COLEMAN, M., O'FLANAGAN, C., ADDARIO, B., MCCABE, N., KENNEDY, R. & O'CONNOR, R. 2018. FES-related tyrosine kinase activates the insulin-like growth factor-1 receptor at sites of cell adhesion. *Oncogene,* 37**,** 3131-3150.

STEELE-PERKINS, G., TURNER, J., EDMAN, J. C., HARI, J., PIERCE, S. B., STOVER, C., RUTTER, W. J. & ROTH, R. A. 1988. Expression and characterization of a functional human insulin-like growth factor I receptor. *Journal of Biological Chemistry,* 263**,** 11486-11492.

STEVENSON, L. E., RAVICHANDRAN, K. S. & FRACKELTON, A. R., JR. 1999. Shc dominant negative disrupts cell cycle progression in both G0-G1 and G2-M of ErbB2-positive breast cancer cells. *Cell Growth Differ,* 10**,** 61-71.

STOELTZING, O., LIU, W., REINMUTH, N., FAN, F., PARIKH, A. A., BUCANA, C. D., EVANS, D. B., SEMENZA, G. L. & ELLIS, L. M. 2003. Regulation of hypoxia-inducible factor-1alpha, vascular endothelial growth factor, and angiogenesis by an insulin-like growth

factor-I receptor autocrine loop in human pancreatic cancer. *Am J Pathol,* 163**,** 1001-11.

SU, J., YANG, L.-T. & SAP, J. 1996. Association between Receptor Protein-tyrosine Phosphatase RPTPα and the Grb2 Adaptor: DUAL Src HOMOLOGY (SH) 2/SH3 DOMAIN REQUIREMENT AND FUNCTIONAL CONSEQUENCES. *Journal of Biological Chemistry,* 271**,** 28086-28096.

SUN, X. J., CRIMMINS, D. L., MYERS, M. G., JR., MIRALPEIX, M. & WHITE, M. F. 1993. Pleiotropic insulin signals are engaged by multisite phosphorylation of IRS-1. *Mol Cell Biol,* 13**,** 7418-28.

SUN, X. J., ROTHENBERG, P., KAHN, C. R., BACKER, J. M., ARAKI, E., WILDEN, P. A., CAHILL, D. A., GOLDSTEIN, B. J. & WHITE, M. F. 1991. Structure of the insulin receptor substrate IRS-1 defines a unique signal transduction protein. *Nature,* 352**,** 73-77.

SURINYA, K. H., FORBES, B. E., OCCHIODORO, F., BOOKER, G. W., FRANCIS, G. L., SIDDLE, K., WALLACE, J. C. & COSGROVE, L. J. 2008. An Investigation of the Ligand Binding Properties and Negative Cooperativity of Soluble Insulin-like Growth Factor Receptors. *Journal of Biological Chemistry,* 283**,** 5355-5363.

SUSSENBACH, J. S., STEENBERGH, P. H. & HOLTHUIZEN, P. 1992. Structure and expression of the human insulin-like growth factor genes. *Growth Regul,* 2**,** 1-9.

TABONE-EGLINGER, S., SUBRA, F., EL SAYADI, H., ALBERTI, L., TABONE, E., MICHOT, J.-P., THÉOU-ANTON, N., LEMOINE, A., BLAY, J.-Y. & EMILE, J.-F. 2008. KIT Mutations Induce Intracellular Retention and Activation of an Immature Form of the KIT Protein in Gastrointestinal Stromal Tumors. *Clinical Cancer Research,* 14**,** 2285-2294.

TALIAFERRO-SMITH, L., OBERLICK, E., LIU, T., MCGLOTHEN, T., ALCAIDE, T., TOBIN, R., DONNELLY, S., COMMANDER, R., KLINE, E., NAGARAJU, G. P., HAVEL, L., MARCUS, A., NAHTA, R. & O'REGAN, R. 2015. FAK activation is required for IGF1R-mediated regulation of EMT, migration, and invasion in mesenchymal triple negative breast cancer cells. *Oncotarget,* 6**,** 4757-72.

TANAKA, T., GRUSBY, M. J. & KAISHO, T. 2007. PDLIM2-mediated termination of transcription factor NF-kappaB activation by intranuclear sequestration and degradation of the p65 subunit. *Nat Immunol,* 8**,** 584-91.

TATAR, M., KOPELMAN, A., EPSTEIN, D., TU, M. P., YIN, C. M. & GAROFALO, R. S. 2001. A mutant Drosophila insulin receptor homolog that extends life-span and impairs neuroendocrine function. *Science,* 292**,** 107-10.

TAVARE, J. M., RAMOS, P. & ELLIS, L. 1992. An assessment of human insulin receptor phosphorylation and exogenous kinase activity following deletion of 69 residues from the carboxyl-terminus of the receptor beta-subunit. *Biochem Biophys Res Commun,* 188**,** 86-93.

TAZEARSLAN, C., HUANG, J., BARZILAI, N. & SUH, Y. 2011. Impaired IGF1R signaling in cells expressing longevity-associated human IGF1R alleles. *Aging Cell,* 10**,** 551-4.

TENNAGELS, N., HUBE-MAGG, C., WIRTH, A., NOELLE, V. & KLEIN, H. W. 1999. Expression, Purification, and Characterization of the Cytoplasmic Domain of the

Human IGF-1 Receptor Using a Baculovirus Expression System. *Biochemical and Biophysical Research Communications,* 260**,** 724-728.

THIERY, J. P. 2002. Epithelial-mesenchymal transitions in tumour progression. *Nat Rev Cancer,* 2**,** 442-54.

THORSON, J. A., YU, L. W., HSU, A. L., SHIH, N. Y., GRAVES, P. R., TANNER, J. W., ALLEN, P. M., PIWNICA-WORMS, H. & SHAW, A. S. 1998. 14-3-3 proteins are required for maintenance of Raf-1 phosphorylation and kinase activity. *Molecular and cellular biology,* 18**,** 5229-5238.

TOLCHER, A. W., SARANTOPOULOS, J., PATNAIK, A., PAPADOPOULOS, K., LIN, C.-C., RODON, J., MURPHY, B., ROTH, B., MCCAFFERY, I., GORSKI, K. S., KAISER, B., ZHU, M., DENG, H., FRIBERG, G. & PUZANOV, I. 2009. Phase I, Pharmacokinetic, and Pharmacodynamic Study of AMG 479, a Fully Human Monoclonal Antibody to Insulin-Like Growth Factor Receptor 1. *Journal of Clinical Oncology,* 27**,** 5800-5807.

TONKIN, J., TEMMERMAN, L., SAMPSON, R. D., GALLEGO-COLON, E., BARBERI, L., BILBAO, D., SCHNEIDER, M. D., MUSARÒ, A. & ROSENTHAL, N. 2015. Monocyte/Macrophage-derived IGF-1 Orchestrates Murine Skeletal Muscle Regeneration and Modulates Autocrine Polarization. *Molecular Therapy,* 23**,** 1189-1200.

TORETSKY, J. A., STEINBERG, S. M., THAKAR, M., COUNTS, D., PIRONIS, B., PARENTE, C., ESKENAZI, A., HELMAN, L. & WEXLER, L. H. 2001. Insulin-like growth factor type 1 (IGF-1) and IGF binding protein-3 in patients with Ewing sarcoma family of tumors. *Cancer,* 92**,** 2941-7.

TRAVIS, R. C., APPLEBY, P. N., MARTIN, R. M., HOLLY, J. M. P., ALBANES, D., BLACK, A., BUENO-DE-MESQUITA, H. B., CHAN, J. M., CHEN, C., CHIRLAQUE, M.-D., COOK, M. B., DESCHASAUX, M., DONOVAN, J. L., FERRUCCI, L., GALAN, P., GILES, G. G., GIOVANNUCCI, E. L., GUNTER, M. J., HABEL, L. A., HAMDY, F. C., HELZLSOUER, K. J., HERCBERG, S., HOOVER, R. N., JANSSEN, J. A. M. J. L., KAAKS, R., KUBO, T., LE MARCHAND, L., METTER, E. J., MIKAMI, K., MORRIS, J. K., NEAL, D. E., NEUHOUSER, M. L., OZASA, K., PALLI, D., PLATZ, E. A., POLLAK, M. N., PRICE, A. J., ROOBOL, M. J., SCHAEFER, C., SCHENK, J. M., SEVERI, G., STAMPFER, M. J., STATTIN, P., TAMAKOSHI, A., TANGEN, C. M., TOUVIER, M., WALD, N. J., WEISS, N. S., ZIEGLER, R. G., KEY, T. J. & ALLEN, N. E. 2016. A Meta-analysis of Individual Participant Data Reveals an Association between Circulating Levels of IGF-I and Prostate Cancer Risk. *Cancer Research,* 76**,** 2288-2300.

TROJAN, J., JOHNSON, T. R., RUDIN, S. D., ILAN, J., TYKOCINSKI, M. L. & ILAN, J. 1993. Treatment and prevention of rat glioblastoma by immunogenic C6 cells expressing antisense insulin-like growth factor I RNA. *Science,* 259**,** 94-7.

TURNEY, B. W., KERR, M., CHITNIS, M. M., LODHIA, K., WANG, Y., RIEDEMANN, J., ROCHESTER, M., PROTHEROE, A. S., BREWSTER, S. F. & MACAULAY, V. M. 2012. Depletion of the type 1 IGF receptor delays repair of radiation-induced DNA double strand breaks. *Radiotherapy and Oncology,* 103**,** 402-409.

UCAR, D. A., KURENOVA, E., GARRETT, T. J., CANCE, W. G., NYBERG, C., COX, A., MASSOLL, N., OSTROV, D. A., LAWRENCE, N., SEBTI, S. M., ZAJAC-KAYE, M. & HOCHWALD, S. N. 2012. Disruption of the protein interaction between FAK and IGF-1R inhibits melanoma tumor growth. *Cell Cycle,* 11**,** 3250-3259.

UGI, S., IMAMURA, T., RICKETTS, W. & OLEFSKY, J. M. 2002. Protein Phosphatase 2A Forms a Molecular Complex with Shc and Regulates Shc Tyrosine Phosphorylation and Downstream Mitogenic Signaling. *Molecular and Cellular Biology,* 22**,** 2375-2387.

ULANET, D. B., LUDWIG, D. L., KAHN, C. R. & HANAHAN, D. 2010. Insulin receptor functionally enhances multistage tumor progression and conveys intrinsic resistance to IGF-1R targeted therapy. *Proc Natl Acad Sci U S A,* 107**,** 10791-8.

ULLRICH, A., GRAY, A., TAM, A. W., YANG-FENG, T., TSUBOKAWA, M., COLLINS, C., HENZEL, W., LE BON, T., KATHURIA, S., CHEN, E. & ET AL. 1986. Insulin-like growth factor I receptor primary structure: comparison with insulin receptor suggests structural determinants that define functional specificity. *Embo j,* 5**,** 2503-12.

VALENTINIS, B., ROMANO, G., PERUZZI, F., MORRIONE, A., PRISCO, M., SODDU, S., CRISTOFANELLI, B., SACCHI, A. & BASERGA, R. 1999. Growth and differentiation signals by the insulin-like growth factor 1 receptor in hemopoietic cells are mediated through different pathways. *J Biol Chem,* 274**,** 12423-30.

VAN DER VEEKEN, J., OLIVEIRA, S., SCHIFFELERS, R. M., STORM, G., VAN BERGEN EN HENEGOUWEN, P. M. & ROOVERS, R. C. 2009. Crosstalk between epidermal growth factor receptor- and insulin-like growth factor-1 receptor signaling: implications for cancer therapy. *Curr Cancer Drug Targets,* 9**,** 748-60.

VAN GAAL, J. C., ROEFFEN, M. H., FLUCKE, U. E., VAN DER LAAK, J. A., VAN DER HEIJDEN, G., DE BONT, E. S., SUURMEIJER, A. J., VERSLEIJEN-JONKERS, Y. M. & VAN DER GRAAF, W. T. 2013. Simultaneous targeting of insulin-like growth factor-1 receptor and anaplastic lymphoma kinase in embryonal and alveolar rhabdomyosarcoma: a rational choice. *Eur J Cancer,* 49**,** 3462-70.

VAN MALDEGEM, A. M., BOVÉE, J. V. M. G., PETERSE, E. F. P., HOGENDOORN, P. C. W. & GELDERBLOM, H. 2016. Ewing sarcoma: The clinical relevance of the insulin-like growth factor 1 and the poly-ADP-ribose-polymerase pathway. *European Journal of Cancer,* 53**,** 171-180.

VECCHIONE, A., MARCHESE, A., HENRY, P., ROTIN, D. & MORRIONE, A. 2003. The Grb10/Nedd4 Complex Regulates Ligand-Induced Ubiquitination and Stability of the Insulin-Like Growth Factor I Receptor. *Molecular and Cellular Biology,* 23**,** 3363-3372.

VELLA, V., MILLUZZO, A., SCALISI, N. M., VIGNERI, P. & SCIACCA, L. 2018. Insulin Receptor Isoforms in Cancer. *Int J Mol Sci,* 19.

VIGNERI, R., GOLDFINE, I. D. & FRITTITTA, L. 2016. Insulin, insulin receptors, and cancer. *J Endocrinol Invest,* 39**,** 1365-1376.

VIVANCO, I. & SAWYERS, C. L. 2002. The phosphatidylinositol 3-Kinase AKT pathway in human cancer. *Nat Rev Cancer,* 2**,** 489-501.

VOGELSTEIN, B., PAPADOPOULOS, N., VELCULESCU, V. E., ZHOU, S., DIAZ, L. A., JR. & KINZLER, K. W. 2013. Cancer genome landscapes. *Science,* 339**,** 1546-58.

VOISSET, E., LOPEZ, S., CHAIX, A., GEORGES, C., HANSSENS, K., PRÉBET, T., DUBREUIL, P. & DE SEPULVEDA, P. 2010. FES kinases are required for oncogenic FLT3 signaling. *Leukemia,* 24**,** 721-728.

VOLIOVITCH, H., SCHINDLER, D. G., HADARI, Y. R., TAYLOR, S. I., ACCILI, D. & ZICK, Y. 1995. Tyrosine Phosphorylation of Insulin Receptor Substrate-1 in Vivo Depends upon the Presence of Its Pleckstrin Homology Region. *Journal of Biological Chemistry,* 270**,** 18083-18087.

VON ZASTROW, M. & SORKIN, A. 2007. Signaling on the endocytic pathway. *Current opinion in cell biology,* 19**,** 436-445.

WÄLCHLI, S., CURCHOD, M.-L., GOBERT, R. P., ARKINSTALL, S. & VAN HUIJSDUIJNEN, R. H. 2000. Identification of Tyrosine Phosphatases That Dephosphorylate the Insulin Receptor: A BRUTE FORCE APPROACH BASED ON "SUBSTRATE-TRAPPING" MUTANTS. *Journal of Biological Chemistry,* 275**,** 9792-9796.

WANG, C., WANG, X., GONG, G., BEN, Q., QIU, W., CHEN, Y., LI, G. & WANG, L. 2012. Increased risk of hepatocellular carcinoma in patients with diabetes mellitus: a systematic review and meta-analysis of cohort studies. *Int J Cancer,* 130**,** 1639-48.

WANG, S.-C., LIEN, H.-C., XIA, W., CHEN, I. F., LO, H.-W., WANG, Z., ALI-SEYED, M., LEE, D.-F., BARTHOLOMEUSZ, G., OU-YANG, F., GIRI, D. K. & HUNG, M.-C. 2004. Binding at and transactivation of the COX-2 promoter by nuclear tyrosine kinase receptor ErbB-2. *Cancer Cell,* 6**,** 251-261.

WANG, T., WANG, Y., MENENDEZ, A., FONG, C., BABEY, M., TAHIMIC, C. G. T., CHENG, Z., LI, A., CHANG, W. & BIKLE, D. D. 2015. Osteoblast-Specific Loss of IGF1R Signaling Results in Impaired Endochondral Bone Formation During Fracture Healing. *Journal of bone and mineral research : the official journal of the American Society for Bone and Mineral Research,* 30**,** 1572-1584.

WARAKY, A., AKOPYAN, K., PARROW, V., STROMBERG, T., AXELSON, M., ABRAHMSEN, L., LINDQVIST, A., LARSSON, O. & ALEEM, E. 2014. Picropodophyllin causes mitotic arrest and catastrophe by depolymerizing microtubules via insulin-like growth factor-1 receptor-independent mechanism. *Oncotarget,* 5**,** 8379-92.

WARREN, C. M., ZIYAD, S., BRIOT, A., DER, A. & IRUELA-ARISPE, M. L. 2014. A Ligand-Independent VEGFR2 Signaling Pathway Limits Angiogenic Responses in Diabetes. *Science Signaling,* 7**,** ra1-ra1.

WARSITO, D., LIN, Y., GNIRCK, A.-C., SEHAT, B. & LARSSON, O. 2016. Nuclearly translocated insulin-like growth factor 1 receptor phosphorylates histone H3 at tyrosine 41 and induces SNAI2 expression via Brg1 chromatin remodeling protein. *Oncotarget,* 7**,** 42288-42302.

WARSITO, D., SJÖSTRÖM, S., ANDERSSON, S., LARSSON, O. & SEHAT, B. 2012. Nuclear IGF1R is a transcriptional co-activator of LEF1/TCF. *EMBO reports,* 13**,** 244-250.

WARY, K. K., MAINIERO, F., ISAKOFF, S. J., MARCANTONIO, E. E. & GIANCOTTI, F. G. 1996. The Adaptor Protein Shc Couples a Class of Integrins to the Control of Cell Cycle Progression. *Cell,* 87**,** 733-743.

WATANABE, N., TAKAOKA, M., SAKURAMA, K., TOMONO, Y., HATAKEYAMA, S., OHMORI, O., MOTOKI, T., SHIRAKAWA, Y., YAMATSUJI, T., HAISA, M., MATSUOKA, J., BEER, D. G., NAGATSUKA, H., TANAKA, N. & NAOMOTO, Y. 2008. Dual tyrosine kinase inhibitor for focal adhesion kinase and insulin-like growth factor-

I receptor exhibits anticancer effect in esophageal adenocarcinoma in vitro and in vivo. *Clin Cancer Res,* 14**,** 4631-9.

WEI, C., WU, S., LI, X., WANG, Y., REN, R., LAI, Y. & YE, J. 2013. High expression of FER tyrosine kinase predicts poor prognosis in clear cell renal cell carcinoma. *Oncology letters,* 5**,** 473-478.

WEINSTEIN, D., SARFSTEIN, R., LARON, Z. & WERNER, H. 2014. Insulin receptor compensates for IGF1R inhibition and directly induces mitogenic activity in prostate cancer cells. *Endocr Connect,* 3**,** 24-35.

WENNERBERG, K., ROSSMAN, K. L. & DER, C. J. 2005. The Ras superfamily at a glance. *J Cell Sci,* 118**,** 843-6.

WEROHA, S. J. & HALUSKA, P. 2008. IGF-1 Receptor Inhibitors in Clinical Trials—Early Lessons. *Journal of Mammary Gland Biology and Neoplasia,* 13**,** 471-483.

WHITE, M. F. 2002. IRS proteins and the common path to diabetes. *American Journal of Physiology-Endocrinology and Metabolism,* 283**,** E413-E422.

WHITTAKER, J., GROTH, A. V., MYNARCIK, D. C., PLUZEK, L., GADSBØLL, V. L. & WHITTAKER, L. J. 2001. Alanine scanning mutagenesis of a type 1 insulin-like growth factor receptor ligand binding site. *J Biol Chem,* 276**,** 43980-6.

WHITTAKER, L., HAO, C., FU, W. & WHITTAKER, J. 2008. High-affinity insulin binding: insulin interacts with two receptor ligand binding sites. *Biochemistry,* 47**,** 12900-9.

WILLIAMS, P. F., MYNARCIK, D. C., YU, G. Q. & WHITTAKER, J. 1995. Mapping of an NH2-terminal ligand binding site of the insulin receptor by alanine scanning mutagenesis. *J Biol Chem,* 270**,** 3012-6.

WITHERS, D. J., GUTIERREZ, J. S., TOWERY, H., BURKS, D. J., REN, J. M., PREVIS, S., ZHANG, Y., BERNAL, D., PONS, S., SHULMAN, G. I., BONNER-WEIR, S. & WHITE, M. F. 1998. Disruption of IRS-2 causes type 2 diabetes in mice. *Nature,* 391**,** 900-4.

WORRALL, C., SULEYMANOVA, N., CRUDDEN, C., TROCOLI DRAKENSJÖ, I., CANDREA, E., NEDELCU, D., TAKAHASHI, S. I., GIRNITA, L. & GIRNITA, A. 2017. Unbalancing p53/Mdm2/IGF-1R axis by Mdm2 activation restrains the IGF-1-dependent invasive phenotype of skin melanoma. *Oncogene,* 36**,** 3274-3286.

WU, Y., TEWARI, M., CUI, S. & RUBIN, R. 1996. Activation of the insulin-like growth factor-I receptor inhibits tumor necrosis factor-induced cell death. *Journal of Cellular Physiology,* 168**,** 499-509.

XIANG, Z., KREISEL, F., CAIN, J., COLSON, A. & TOMASSON, M. H. 2007. Neoplasia Driven by Mutant c-KIT Is Mediated by Intracellular, Not Plasma Membrane, Receptor Signaling. *Molecular and Cellular Biology,* 27**,** 267-282.

XU, Y.-M., WANG, H.-J., CHEN, F., GUO, W.-H., WANG, Y.-Y., LI, H.-Y., TANG, J.-H., DING, Y., SHEN, Y.-C., LI, M., XUAN, W.-Y., LIU, L.-H., WANG, J., WANG, X.-R., GAO, Z.-J., LIANG, X.-B. & SU, D.-M. 2015. HRD1 suppresses the growth and metastasis of breast cancer cells by promoting IGF-1R degradation. *Oncotarget,* 6**,** 42854-42867.

XU, Y., KONG, G. K. W., MENTING, J. G., MARGETTS, M. B., DELAINE, C. A., JENKIN, L. M., KISELYOV, V. V., DE MEYTS, P., FORBES, B. E. & LAWRENCE, M. C. 2018. How ligand binds to the type 1 insulin-like growth factor receptor. *Nature Communications,* 9**,** 821.

YADAV, S., PURI, S. & LINSTEDT, A. D. 2009. A Primary Role for Golgi Positioning in Directed Secretion, Cell Polarity, and Wound Healing. *Molecular Biology of the Cell,* 20**,** 1728-1736.

YAKAR, S., LIU, J.-L., STANNARD, B., BUTLER, A., ACCILI, D., SAUER, B. & LEROITH, D. 1999. Normal growth and development in the absence of hepatic insulin-like growth factor I. *Proceedings of the National Academy of Sciences,* 96**,** 7324-7329.

YAMAZAKI, T., ZAAL, K., HAILEY, D., PRESLEY, J., LIPPINCOTT-SCHWARTZ, J. & SAMELSON, L. E. 2002. Role of Grb2 in EGF-stimulated EGFR internalization. *J Cell Sci,* 115**,** 1791-802.

YAN, C., XU, W., HUANG, Y., LI, M., SHEN, Y., YOU, H. & LIANG, X. 2016. HRD1-Mediated IGF-1R Ubiquitination Contributes to Renal Protection of Resveratrol in db/db Mice. *Molecular Endocrinology,* 30**,** 600-613.

YE, Q.-H., ZHU, W.-W., ZHANG, J.-B., QIN, Y., LU, M., LIN, G.-L., GUO, L., ZHANG, B., LIN, Z.-H., ROESSLER, S., FORGUES, M., JIA, H.-L., LU, L., ZHANG, X.-F., LIAN, B.-F., XIE, L., DONG, Q.-Z., TANG, Z.-Y., WANG, XIN W. & QIN, L.-X. 2016. GOLM1 Modulates EGFR/RTK Cell-Surface Recycling to Drive Hepatocellular Carcinoma Metastasis. *Cancer Cell,* 30**,** 444-458.

YENUSH, L., MAKATI, K. J., SMITH-HALL, J., ISHIBASHI, O., MYERS, M. G., JR. & WHITE, M. F. 1996. The pleckstrin homology domain is the principal link between the insulin receptor and IRS-1. *J Biol Chem,* 271**,** 24300-6.

YONEYAMA, T., ANGATA, K., BAO, X., COURTNEIDGE, S., CHANDA, S. K. & FUKUDA, M. 2012. Fer kinase regulates cell migration through alpha-dystroglycan glycosylation. *Mol Biol Cell,* 23**,** 771-80.

YONEYAMA, Y., LANZERSTORFER, P., NIWA, H., UMEHARA, T., SHIBANO, T., YOKOYAMA, S., CHIDA, K., WEGHUBER, J., HAKUNO, F. & TAKAHASHI, S.-I. 2018. IRS-1 acts as an endocytic regulator of IGF-I receptor to facilitate sustained IGF signaling. *eLife,* 7**,** e32893.

YOON, Y. S., KEUM, N., ZHANG, X., CHO, E. & GIOVANNUCCI, E. L. 2015. Circulating levels of IGF-1, IGFBP-3, and IGF-1/IGFBP-3 molar ratio and colorectal adenomas: A meta-analysis. *Cancer Epidemiol,* 39**,** 1026-35.

YOUNGREN, J. F., GABLE, K., PENARANDA, C., MADDUX, B. A., ZAVODOVSKAYA, M., LOBO, M., CAMPBELL, M., KERNER, J. & GOLDFINE, I. D. 2005. Nordihydroguaiaretic Acid (NDGA) Inhibits the IGF-1 and c-erbB2/HER2/neu Receptors and Suppresses Growth in Breast Cancer Cells. *Breast Cancer Research and Treatment,* 94**,** 37.

YU, D., WATANABE, H., SHIBUYA, H. & MIURA, M. 2003. Redundancy of Radioresistant Signaling Pathways Originating from Insulin-like Growth Factor I Receptor. *Journal of Biological Chemistry,* 278**,** 6702-6709.

YU, M., WANG, H., XU, Y., YU, D., LI, D., LIU, X. & DU, W. 2015. Insulin-like growth factor-1 (IGF-1) promotes myoblast proliferation and skeletal muscle growth of embryonic chickens via the PI3K/Akt signalling pathway. *Cell Biol Int,* 39**,** 910-22.

YU, W., YANG, L., LI, T. & ZHANG, Y. 2019. Cadherin Signaling in Cancer: Its Functions and Role as a Therapeutic Target. *Frontiers in Oncology,* 9.

YUEN, J. S. P., AKKAYA, E., WANG, Y., TAKIGUCHI, M., PEAK, S., SULLIVAN, M., PROTHEROE, A. S. & MACAULAY, V. M. 2009. Validation of the type 1 insulin-like growth factor receptor as a therapeutic target in renal cancer. *Molecular Cancer Therapeutics,* 8**,** 1448-1459.

YUKIMASA, S., MASAKI, T., YOSHIDA, S., UCHIDA, N., WATANABE, S., USUKI, H., YOSHIJI, H., MAETA, T., EBARA, K., NAKATSU, T., KUROKOHCHI, K. & KURIYAMA, S. 2005. Enhanced expression of p46 Shc in the nucleus and p52 Shc in the cytoplasm of human gastric cancer. *Int J Oncol,* 26**,** 905-11.

ZENG, L., SI, X., YU, W. P., LE, H. T., NG, K. P., TENG, R. M., RYAN, K., WANG, D. Z., PONNIAH, S. & PALLEN, C. J. 2003. PTP alpha regulates integrin-stimulated FAK autophosphorylation and cytoskeletal rearrangement in cell spreading and migration. *J Cell Biol,* 160**,** 137-46.

ZENG, S., XU, Z., LIPKOWITZ, S. & LONGLEY, J. B. 2005. Regulation of stem cell factor receptor signaling by Cbl family proteins (Cbl-b/c-Cbl). *Blood,* 105**,** 226-32.

ZERIAL, M. & MCBRIDE, H. 2001. Rab proteins as membrane organizers. *Nat Rev Mol Cell Biol,* 2**,** 107-17.

ZHANG, J., WANG, Z., ZHANG, S., CHEN, Y., XIONG, X., LI, X., TONKS, N. K. & FAN, G. 2018. Spatial regulation of signaling by the coordinated action of the protein tyrosine kinases MET and FER. *Cell Signal,* 50**,** 100-110.

ZHANG, S., ANJUM, R., SQUILLACE, R., NADWORNY, S., ZHOU, T., KEATS, J., NING, Y., WARDWELL, S. D., MILLER, D., SONG, Y., EICHINGER, L., MORAN, L., HUANG, W. S., LIU, S., ZOU, D., WANG, Y., MOHEMMAD, Q., JANG, H. G., YE, E., NARASIMHAN, N., WANG, F., MIRET, J., ZHU, X., CLACKSON, T., DALGARNO, D., SHAKESPEARE, W. C. & RIVERA, V. M. 2016. The Potent ALK Inhibitor Brigatinib (AP26113) Overcomes Mechanisms of Resistance to First- and Second-Generation ALK Inhibitors in Preclinical Models. *Clin Cancer Res,* 22**,** 5527-5538.

ZHAO, H. & GU, X. 2014. Silencing of insulin-like growth factor-1 receptor enhances the radiation sensitivity of human esophageal squamous cell carcinoma in vitro and in vivo. *World Journal of Surgical Oncology,* 12**,** 325.

ZHAO, T. & XU, Y. 2010. p53 and stem cells: new developments and new concerns. *Trends Cell Biol,* 20**,** 170-5.

ZHENG, H., WORRALL, C., SHEN, H., ISSAD, T., SEREGARD, S., GIRNITA, A. & GIRNITA, L. 2012. Selective recruitment of G protein-coupled receptor kinases (GRKs) controls signaling of the insulin-like growth factor 1 receptor. *Proceedings of the National Academy of Sciences,* 109**,** 7055-7060.

ZHENG, Y., SETHI, R., MANGALA, L. S., TAYLOR, C., GOLDSMITH, J., WANG, M., MASUDA, K., KARAMINEJADRANJBAR, M., MANNION, D., MIRANDA, F., HERRERO-GONZALEZ, S., HELLNER, K., CHEN, F., ALSAADI, A., ALBUKHARI, A.,

FOTSO, D. C., YAU, C., JIANG, D., PRADEEP, S., RODRIGUEZ-AGUAYO, C., LOPEZ-BERESTEIN, G., KNAPP, S., GRAY, N. S., CAMPO, L., MYERS, K. A., DHAR, S., FERGUSON, D., BAST, R. C., SOOD, A. K., VON DELFT, F. & AHMED, A. A. 2018. Tuning microtubule dynamics to enhance cancer therapy by modulating FER-mediated CRMP2 phosphorylation. *Nature Communications,* 9**,** 476.

ZHOU, B. P., DENG, J., XIA, W., XU, J., LI, Y. M., GUNDUZ, M. & HUNG, M. C. 2004. Dual regulation of Snail by GSK-3beta-mediated phosphorylation in control of epithelial-mesenchymal transition. *Nat Cell Biol,* 6**,** 931-40.

ZIEGLER, A. N., CHIDAMBARAM, S., FORBES, B. E., WOOD, T. L. & LEVISON, S. W. 2014. Insulin-like growth factor-II (IGF-II) and IGF-II analogs with enhanced insulin receptor-a binding affinity promote neural stem cell expansion. *J Biol Chem,* 289**,** 4626-33.

ZIEGLER, A. N., LEVISON, S. W. & WOOD, T. L. 2015. Insulin and IGF receptor signalling in neural-stem-cell homeostasis. *Nature reviews. Endocrinology,* 11**,** 161-170.

ZIMMERMANN, S. & MOELLING, K. 1999. Phosphorylation and regulation of Raf by Akt (protein kinase B). *Science,* 286**,** 1741-4.

ZIRNGIBL, R., SCHULZE, D., MIRSKI, S. E., COLE, S. P. & GREER, P. A. 2001. Subcellular localization analysis of the closely related Fps/Fes and Fer protein-tyrosine kinases suggests a distinct role for Fps/Fes in vesicular trafficking. *Exp Cell Res,* 266**,** 87-94.

ZOROV, D. B., JUHASZOVA, M. & SOLLOTT, S. J. 2014. Mitochondrial reactive oxygen species (ROS) and ROS-induced ROS release. *Physiol Rev,* 94**,** 909-50.

ZOUBEIDI, A., ROCHA, J., ZOUANAT, F. Z., HAMEL, L., SCARLATA, E., APRIKIAN, A. G. & CHEVALIER, S. 2009. The Fer tyrosine kinase cooperates with interleukin-6 to activate signal transducer and activator of transcription 3 and promote human prostate cancer cell growth. *Mol Cancer Res,* 7**,** 142-55.

8 APPENDIX

8.1 FES-RELATED TYROSINE KINASE ACTIVATES THE INSULIN-LIKE GROWTH FACTOR-1 RECEPTOR AT SITES OF CELL ADHESION

Oncogene
https://doi.org/10.1038/s41388-017-0113-z

ARTICLE

FES-related tyrosine kinase activates the insulin-like growth factor-1 receptor at sites of cell adhesion

Joanna Stanicka[1] · Leonie Rieger[1] · Sandra O'Shea[1] · Orla Cox[1] · Michael Coleman[1] · Ciara O'Flanagan[1] · Barbara Addario[1] · Nuala McCabe[2] · Richard Kennedy[2] · Rosemary O'Connor[1]

Received: 16 June 2017 / Revised: 8 November 2017 / Accepted: 6 December 2017
© Macmillan Publishers Limited, part of Springer Nature 2018

Abstract

IGF-1 receptor (IGF-1R) and integrin cooperative signaling promotes cancer cell survival, proliferation, and motility, but whether this influences cancer progression and therapy responses is largely unknown. Here we investigated the non-receptor tyrosine adhesion kinase FES-related (FER), following its identification as a potential mediator of sensitivity to IGF-1R kinase inhibition in a functional siRNA screen. We found that FER and the IGF-1R co-locate in cells and can be co-immunoprecipitated. Ectopic FER expression strongly enhanced IGF-1R expression and phosphorylation on tyrosines 950 and 1131. FER phosphorylated these sites in an IGF-1R kinase-independent manner and also enhanced IGF-1-mediated phosphorylation of SHC, and activation of either AKT or MAPK-signaling pathways in different cells. The IGF-1R, β1 Integrin, FER, and its substrate cortactin were all observed to co-locate in cell adhesion complexes, the disruption of which reduced IGF-1R expression and activity. High FER expression correlates with phosphorylation of SHC in breast cancer cell lines and with a poor prognosis in patient cohorts. FER and SHC phosphorylation and IGF-1R expression could be suppressed with a known anaplastic lymphoma kinase inhibitor (AP26113) that shows high specificity for FER kinase. Overall, we conclude that FER enhances IGF-1R expression, phosphorylation, and signaling to promote cooperative growth and adhesion signaling that may facilitate cancer progression.

Introduction

The insulin-like growth factor-1 receptor (IGF-1R) and its signaling pathway have a well-described function in sustaining a transformed phenotype [1–4]. *Igf-1r* knockout (*Igf-1r*$^{-/-}$) mouse derived fibroblasts are refractory to transformation by oncogenes [3]. The phosphorylated receptor recruits IRS-1, IRS-2, or SHC to activate signaling pathways that promote cell survival, proliferation, or motility [1, 5]. However, despite compelling evidence for IGF-1R activity in facilitating cancer progression, efforts to target the IGF-1R in cancer have resulted in poor efficacy and clinical response [2, 6, 7]. Many reasons have been proposed for this, including observations that expression of IGF ligands and IGF-1R may not always correlate with signaling activity [7–10]. This has confounded the identification of useful biomarkers for IGF-1R activity inhibition in cancer cells.

Others and we have previously established that IGF-1R kinase activity and signaling output are modulated by adhesion-associated protein complexes [2, 5, 11]. This cross-talk contributes to the mitogenic, migratory, and invasive phenotype of breast, lung, cervical, and prostate cancer [11–14]. Indeed, β1 Integrin ligation enhances IGF-1R surface expression and localization to sites of focal adhesion in prostate cancer cells [11]. A complex of IGF-1R with β1 Integrin that includes the scaffolding protein RACK1 and focal adhesion kinase, promotes MAPK pathway activity [5, 15]. Furthermore, adhesion-activated kinases SRC and FAK can directly phosphorylate IGF-1R in vitro and enhance IGF-1R-induced invasiveness of breast

Sandra O'Shea and Orla Cox Joint authorship.

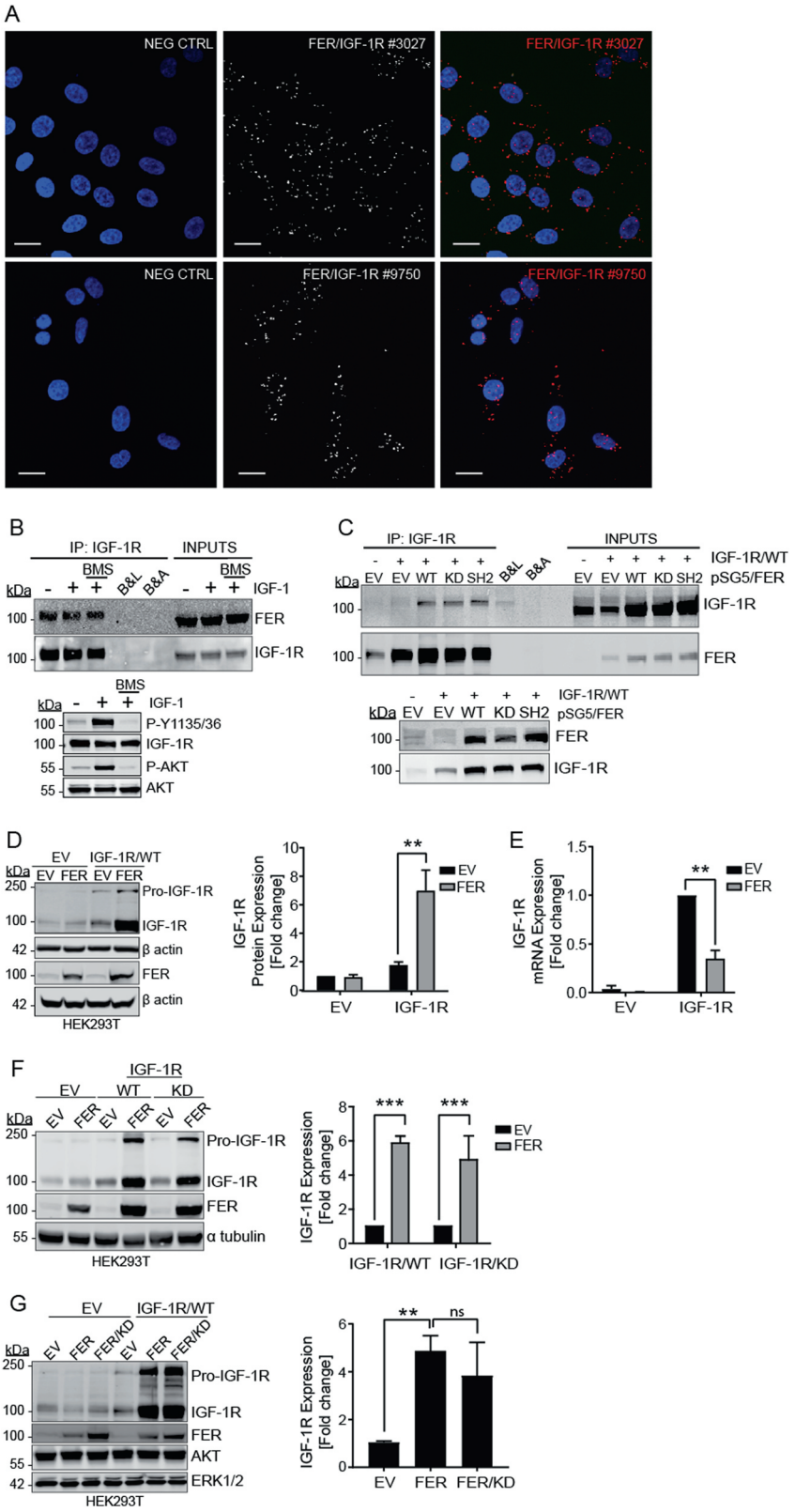
Electronic supplementary material The online version of this article (https://doi.org/10.1038/s41388-017-0113-z) contains supplementary material, which is available to authorized users.

✉ Rosemary O'Connor
r.oconnor@ucc.ie

[1] Cell Biology Laboratory, School of Biochemistry and Cell Biology, University College Cork, Cork, Ireland

[2] Centre for Cancer Research and Cell Biology and Almac Diagnostics, Queens University Belfast, Belfast, Northern Ireland

Published online: 15 March 2018


A
NEG CTRL
FER/IGF-1R #3027
FER/IGF-1R #3027
NEG CTRL
FER/IGF-1R #9750
FER/IGF-1R #9750
B
IP: IGF-1R
INPUTS
BMS
B&L
B&A
kDa
IGF-1
FER
IGF-1R
P-Y1135/36
P-AKT
AKT
C
IP: IGF-1R
INPUTS
IGF-1R/WT
EV EV WT KD SH2
pSG5/FER
IGF-1R
FER
D
EV
IGF-1R/WT
EV FER EV FER
Pro-IGF-1R
β actin
HEK293T
IGF-1R Protein Expression [Fold change]
**
E
IGF-1R mRNA Expression [Fold change]
F
IGF-1R
EV WT KD
α tubulin
IGF-1R Expression [Fold change]
***
IGF-1R/WT IGF-1R/KD
G
FER/KD
AKT
ERK1/2
ns

◀ **Fig. 1** FER associates with IGF-1R and enhances expression levels. **a** Proximity ligation assay (PLA) showing protein interaction between FER and IGF-1R in MCF-7 cells. Cells were cultured on coverslips, fixed, and probed with one of two rabbit anti-IGF-1R antibodies (#3027, top panels or #9750, bottom panels) and mouse anti-FER antibody (#4268), and then subjected to PLA as described in the methods section. Negative controls are cells without primary antibody subjected to PLA. Slides were examined by confocal microscopy using a Zeiss LSM700 inverted confocal microscope equipped with a × 60 oil-immersion objective, numerical aperture 1.4. Z-projected images of the collected Z-stack were performed and analyzed using the Olympus Fluoview software. Each white spot (red in merged images) represents a single interaction. The presented images are maximum intensity projections of Z-stacks acquired from a representative of three independent experiments. **b** Western blot analysis of co-immunoprecipitated IGF-1R and FER. The IGF-1R was immunoprecipitated from R + cells that were serum-starved (−), stimulated with IGF-1 (10 min; 10 ng/ml; +), or stimulated with IGF-1 in the presence of BMS-754807 (BMS). Beads-and-lysates (B&L) and beads-and-antibody (B&A) controls were included as well as cell lysates from the immunoprecipitation inputs. Blots were probed with anti-IGF-1R and anti-FER antibodies. The panel underneath shows the levels of P-1135/1136 IGF-1R and P-AKT in total lysates used for immunoprecipitation (as controls for BMS-754807 inhibition of IGF-1R kinase activity). **c** Western blot analysis of IGF-1R and FER co-immunoprecipitated from HEK293T cells. The IGF-1R was immunoprecipitated from cells that were transfected with plasmids encoding IGF-1R wild type (IGF-1R/WT (pcDNA3)), FER (WT (pSG5-FER)), FER/Kinase Dead (FER/KD; D743R mutant), an SH2-domain mutant of FER (R483Q; SH2), or corresponding empty vector plasmids (EV), 48 h post transfection. Beads-and-lysates (B&L) and beads-and-antibody (B&A) controls were included as well as the immunoprecipitation inputs. The panel below shows the levels of FER and IGF-1R in cell lysates used for immunoprecipitation. **d**, **e** FER enhances IGF-1R protein expression levels. HEK293T cells were co-transfected with empty vector (pcDNA3-EV; EV, *x*-axis on graph) or IGF-1R/WT (IGF-1R, x-axis on graph) plus either empty vector (pSG5-EV; EV, black bars on graph) or FER/WT (FER, gray bars on graph). Cells were lysed and immunoblotted for determination of IGF-1R and FER protein expression with β actin as a loading control **d**. mRNA expression of *igf-1r* was assessed by RT-qPCR using *igf-1r*-specific primers with *Ubiquitin C (UBC)* as a control to normalize mRNA levels **e**. The graphs show densitometry measurements of the average fold difference ± SEM in IGF-1R protein expression: **d**, or average fold change difference ± SEM in *igf-1r* mRNA expression: **e**, in FER-overexpressing cells compared with EV controls. Data are from $n \geq 3$ independent experiments, a two-way ANOVA with Bonferroni test was applied. **f** Expression of IGF-1R WT and KD are both enhanced by FER. Western blots were prepared with cell lysates from HEK293T cells (40 h post transfection) expressing either Empty Vector (pcDNA3; EV), IGF-1R/WT or Vector encoding IGF-1R/Kinase Dead (KD; K1003R mutant), as well as either empty vector (pSG5; EV) or FER. The blots were probed with anti-IGF-1R or anti-FER antibodies with β actin as a loading control. The graph represents densitometry measurements of average fold difference in IGF-1R protein expression ± SEM in cells expressing EV, IGF-1R/WT, or KD, together with EV or FER from four independent experiments. Two-way ANOVA with Bonferroni test was applied. **g** FER kinase activity is not required for FER-mediated increased expression of IGF-1R. After 40 h of transfection, HEK293T cells expressing empty vector (pcDNA3; EV), IGF-1R/WT, or IGF-1R/KD and/or empty vector control for FER (pSG5; EV), FER, or FER/KD, were lysed and immunoblotted IGF-1R and FER expression. Densitometry measurements of mean ± SEM fold-difference in IGF-1R protein expression from three independent experiments. A one-way ANOVA with Bonferroni test was applied

cancer cells [12, 14, 16, 17]. All of these observations indicate that the recruitment of the IGF-1R to adhesion complexes can significantly modify IGF-1R activation and signaling. However, it is not known whether adhesion signals are essential for IGF-1R activity in cancer progression or therapy responses.

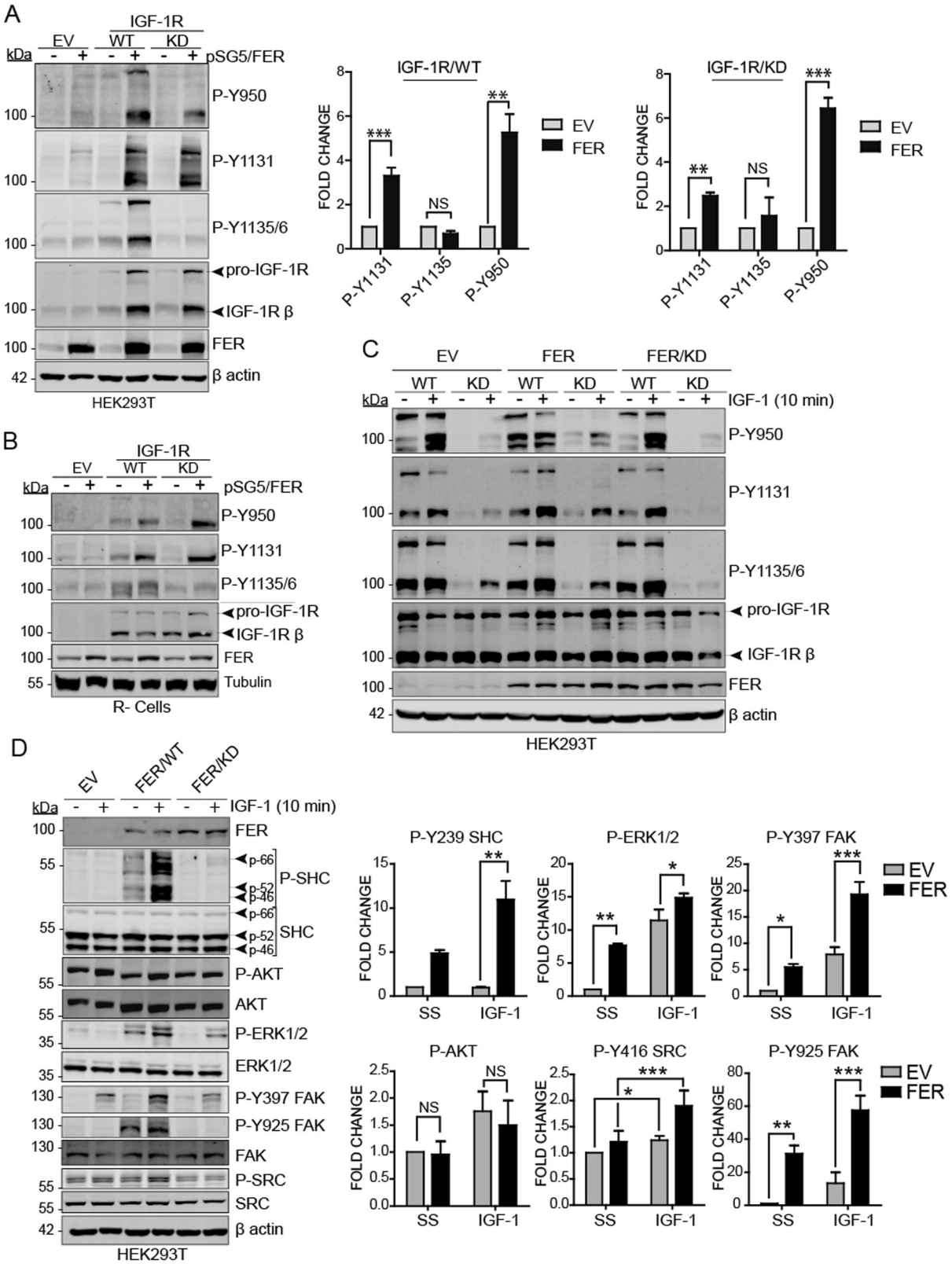
We addressed this question by screening for proteins that modulate the cytotoxic response to IGF-1R tyrosine kinase inhibition using a functional siRNA screen [18]. We identified the non-receptor tyrosine FES-related (FER) kinase as a mediator of sensitivity to the IGF-1R tyrosine kinase inhibitor, BMS-754807, in MCF-7 cells. FER, along with FES, belongs to a distinct subfamily of receptor tyrosine kinases that possess FES/CIP4 homology Bin-Amphiphysin-Rvs (F-BAR) domains [19]. FER activity has been described in several cancers, including lung, hepatic, prostate, and breast and is reported to facilitate tumorigenesis and chemoresistance by enhancing cell migration, invasion and proliferation [20–23]. FER has been shown to interact with the EGFR, PDGFR, FLT3, and c-MET [21, 24–26] and proposed to facilitate cross-talk between growth factor receptors and cell–cell or cell–matrix adhesion complexes [19].

In this study, we investigated whether FER modulates IGF-1R signaling in different cell lines. We found that FER associates with and enhances IGF-1R expression and activity at the plasma membrane and sites of cell adhesion. FER significantly increases IGF-1R phosphorylation on key tyrosines to enhance IGF-1-mediated activation of SHC and MAPK pathways in an adhesion-dependent manner. We conclude that FER kinase is an important modulator of IGF-1R activity in cancer cells. This may be particularly important in mesenchymal or migratory cancer cells where cooperative growth factor and adhesion signaling could facilitate cancer progression.

Results

FER associates with and enhances IGF-1R expression levels

We identified FER as a modifier of responses to IGF-1R kinase inhibition in an siRNA screen [18], which suggested that FER may modulate IGF-1R activity. A previous study using peptide libraries identified FER as a kinase that could phosphorylate specific tyrosines in the Insulin and IGF-1 Receptors [27]. Both of these observations suggested that FER could modulate IGF-1R activity. To investigate this we first tested whether FER and the IGF-1R interact. Using proximity ligation assays (PLA) with anti-FER and anti-IGF-1R antibodies, we observed that FER and IGF-1R are clearly found in proximity in MCF-7 cells (Fig. 1a). FER could also



be co-immunoprecipitated with the IGF-1R from R + cells (mouse embryonic fibroblasts derived from *igf-1r*$^{-/-}$ mouse with IGF-1R re-expressed) (Fig. 1b). This was evident in cells that were serum deprived or stimulated with IGF-1, and in the presence of an IGF-1R kinase inhibitor BMS-754807 that suppressed IGF-1R autophosphorylation and IGF-

◀ **Fig. 2** FER promotes phosphorylation of WT and kinase-inactive IGF-1R and enhances signaling output. **a**, **b** Western blotting analysis of IGF-1R phosphorylation in HEK293T **a** or R− **b** cells co-overexpressing: EV (−) or FER (+) with EV, IGF-1R/WT (WT), or IGF-1R/KD (KD). Cells were lysed 48 h after transfection and western blots were prepared to assess levels of P-Y950, P-Y1131, P-Y1135/1136, and total IGF-1R. The levels of total FER were assessed as a control for transfection efficiency. Densitometry measurements of mean ± SEM fold-difference in specific P-Y site as indicated on the x-axis based on at $n = 3$ independent experiments; Two-way ANOVA with Bonferroni test. **c** Western blotting analysis of IGF-1R phosphorylation in HEK293T cells co-overexpressing: EV, FER, or FER/KD with IGF-1R/WT (WT) or IGF-1R/KD (KD). At 48 h post transfection, cells were serum starved for 4 h, IGF-1 stimulated (10 min; 10 ng/ml; +) and subsequently lysed for western blots to assess levels of P-Y950, P-Y1131, P-Y1135/1136, and total IGF-1R. FER levels were assessed as a control for transfection efficiency. **d** Western blotting analysis of IGF-1-mediated downstream signaling pathways in HEK293T cells co-overexpressing: EV, FER, or FER/KD with IGF-1R/WT (WT) or IGF-1R/KD (KD). At 48 h post transfection, cells were serum starved for 4 h prior to IGF-1 stimulation (10 min; 10 ng/ml; +). Western blots were prepared to assess levels of P-SHC (Y239/Y240), P-FAK (Y397, Y925), P-SRC (Y416), and P-AKT (S473). The levels of total FER were assessed as a control for transfection efficiency. Densitometry measurements of mean ± SEM average fold difference in specific P–Y proteins/total protein levels as indicated above the graph, based on $n \geq 3$ independent experiments. Statistical analysis was performed using two-way ANOVA with Bonferroni test

induced activation of AKT (Fig. 1b bottom panel). The IGF-1R and FER could also be co-immunoprecipitated from HEK293T cells that were co-transfected with IGF-1R and either wild type FER (WT), kinase-inactive FER (KD), or a SH2-domain mutant of FER (R483Q) (Fig. 1c). Interestingly, in these experiments it was noted that levels of IGF-1R expression were apparently higher in cells transfected with FER than in vector-expressing controls.

We further tested the effects of FER on IGF-1R expression in HEK293T cells. Co-transfection of plasmids encoding FER and the IGF-1R resulted in a sixfold increase in IGF-1R protein levels compared with levels in cells transfected with IGF-1R and vector controls (Fig. 1d). This increase in protein was not owing to enhanced transcription because *Igf-1r* mRNA expression levels were lower in cells expressing FER than in controls (Fig. 1e).

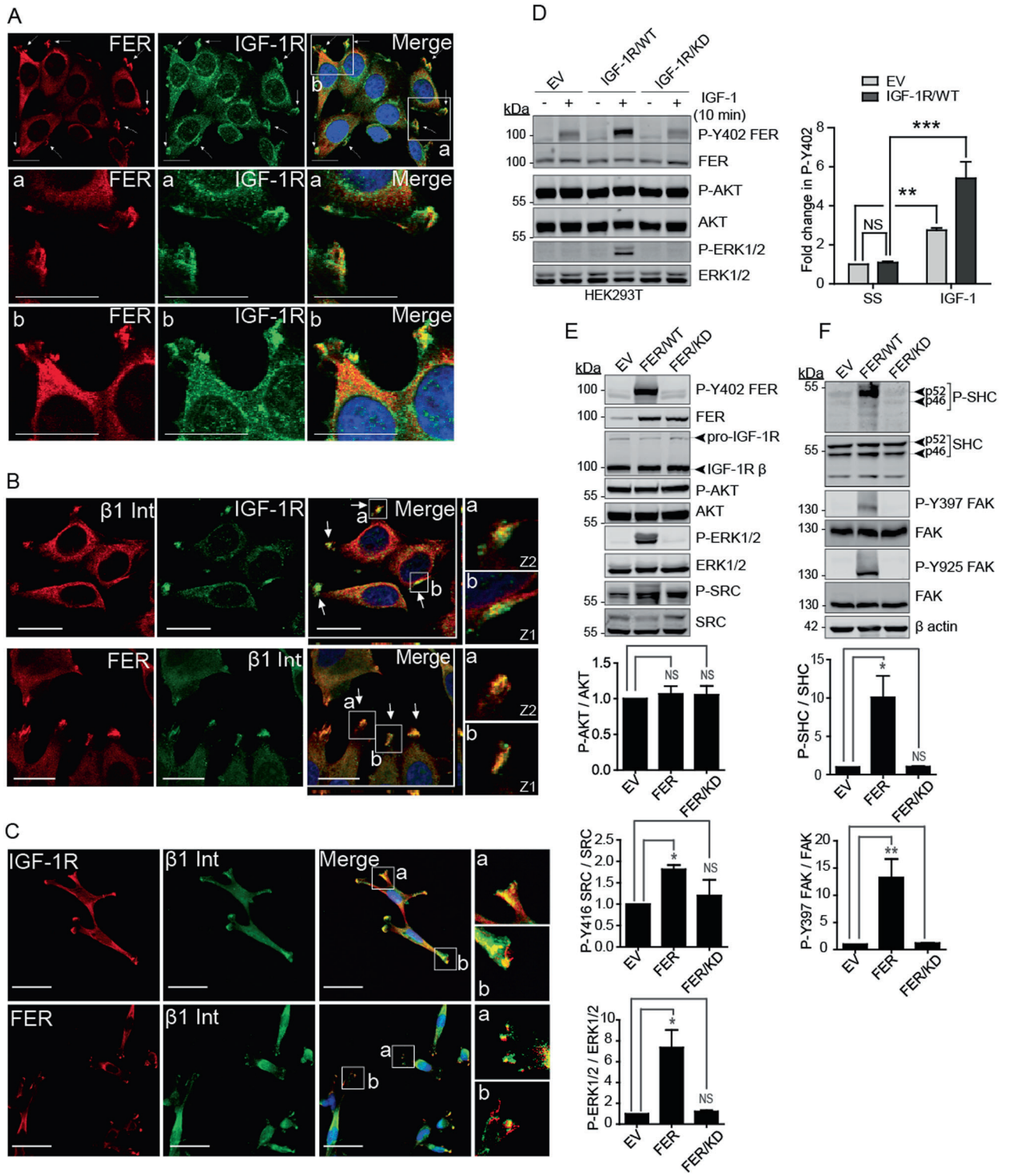
To test whether FER kinase activity was required to enhance IGF-1R protein levels, we transiently expressed IGF-1R in the presence of either FER/WT or FER/KD in HEK293T cells. Both FER/WT and FER/KD enhanced IGF-1R protein levels (Fig. 1f). Furthermore, levels of both IGF-1R/WT and kinase-dead IGF-1R (IGF-1R/KD) could be increased by co-transfection with FER (Fig. 1g). Taken together, these data indicate that FER and IGF-1R associate in different cells, and that FER enhances IGF-1R protein expression and steady state levels in a manner that is not dependent on either IGF-1R or FER kinase activity.

FER enhances phosphorylation of the IGF-1R and its signaling output

We next investigated whether FER influences IGF-1R phosphorylation and kinase activity by co-expressing FER with either IGF-1R/WT or IGF-1R/KD in HEK23T cells. We observed that FER expression specifically enhanced phosphorylation on Y950 (in the juxtamembrane region) and on Y1131 (in the kinase activation loop) on both IGF-1R/WT and IGF-1R/KD (Fig. 2a). Thus, IGF-1R kinase activity is not necessary for FER-enhanced phosphorylation of the Y950 and Y1131 sites. Phosphorylation of Y1135/1136 site in the kinase activation loop was evident with IGF-1R/WT, in the presence of FER, but not with kinase-inactive IGF-1R/KD (Fig. 2a), indicating that phosphorylation on this site by FER is dependent on IGF-1R activity.

To exclude the possibility that the effects of FER on phosphorylation of IGF-1R/KD were due to endogenous, albeit low, levels of IGF-1R expression in HEK293T cells, we carried out similar experiments in R− cells. We observed that co-expression of FER with IGF-1R WT or KD also enhanced phosphorylation on Y950 and Y1131. Again, FER did not enhance phosphorylation on the Y1135/1136 site in IGF-1R/KD (Fig. 2b). To test whether enhanced phosphorylation of the IGF-1R by FER required FER kinase activity, we co-expressed the IGF-1R/WT or IGF-1R/KD with either FER or FER/KD. These experiments demonstrated that enhanced phosphorylation of IGF-1R (WT or KD) on Y950 and Y1131 was observed in both serum-starved and IGF-1-stimulated cells. This was entirely dependent on an active FER kinase because the kinase-inactive FER/KD did not enhance IGF-1R phosphorylation (Fig. 2c).

As FER enhances phosphorylation of the IGF-1R independently of IGF-1R kinase activity, we next asked whether this phosphorylation enhances IGF-1 signaling responses. Ectopic FER expression in HEK293T cells did not alter IGF-1-stimulated activation of the PI3-K pathway, as measured by phosphorylation of AKT on S473 (Fig. 2d). This is likely resulting from the high basal levels of AKT phosphorylation present in HEK293T cells that are not reduced by serum starvation, with no further response to IGF-1 stimulation. However, basal levels of SHC and FAK phosphorylation are low in these cells, which is consistent with their relatively weak adhesion to the substratum. Overexpression of FER/WT, but not FER/KD, significantly increased both basal and IGF-1-stimulated phosphorylation of SHC and ERK1/2 (Fig. 2d). Importantly, in vector control cells, IGF-1 did not induce detectable phosphorylation of Y239/240 on SHC, but IGF-1-induced phosphorylation on these sites was evident in the presence of FER. Phosphorylation of FAK (Y397 and Y925) and SRC (Y416)



were also significantly enhanced by IGF-1 in FER/WT– but not in FER/KD-expressing cells (Fig. 2d).

Overall these data demonstrate that FER enhances phosphorylation of specific autophosphorylation sites on the IGF-1R in a FER kinase-dependent but IGF-1R kinase-independent manner. This is associated with enhanced IGF-1-signaling responses.

◀ **Fig. 3** FER, IGF-1R, and β1 integrin associate in adhesion complexes that enhance FER activity. **a–b** Co-localization of IGF1R with β1 integrin and FER with β1 integrin. Confocal images of MCF-7 cells grown for 24 h on coverslips and co-stained for FER (red) and IGF-1R (rabbit antibody, green; **a**) β1 integrin (red) and IGF-1R (mouse antibody, green; upper panels, **b**) and FER (red) and β1 integrin (green; lower panels, **b**) using antibodies described in methods. Co-localization is shown by the overlap of the fluorescent labels appearing in yellow. Cells were photographed using an Olympus Fluoview FV1000 confocal laser scanning microscope, and Z-stacks were acquired and analyzed using Fluoview Olympus software. At least two slices were acquired at different Z positions (Z1-Z2). Zoomed images (a, b) are presented in their respective Z-planes. Individual slices were 0.5-µm. Scale represents 20 µm. **c** MDA-MB-231 were grown on coverslips coated with 5 µg/cm^2 collagen I for 24 h and immunofluorescence staining was performed. IGF-1R (mouse, Millipore) and β1-Integrin (rabbit, green) are shown in the upper panels and FER (mouse) and β1-Integrin (rabbit, green) shown in the lower panels. A yellow signal depicts areas of co-localization of the red and green fluorescent labels. The nuclei were stained with Hoechst (blue). Original 40 × magnification, scale bars represent 200 µm. **d** FER phosphorylation is enhanced by cell adhesion. At 40 h post-plasmid DNA transfection, HEK293T cells expressing EV, IGF-1R/WT or IGF-1R/KD were serum-starved for 4 h and stimulated with IGF-1 (10 min; 10 ng/ml; +), lysed and immunoblotted for P-Y402 FER/ FER. P-AKT and P-ERK1/2 were used as IGF-1 signaling controls. Densitometry measurements of mean ± SEM average fold difference in P-Y402 FER in the above conditions based on three independent experiments; two-way ANOVA with Bonferroni test. **e**, **f** Western blotting analysis of EV, FER/WT, or FER/KD overexpressing HEK293T cells. 48 h post DNA transfection, cells were lysed and immunoblotted for the indicated phospho- and total protein levels. Densitometry measurements of mean ± SEM average fold difference in specific P-Y proteins/total protein levels as indicated on the *y*-axis in the described above conditions based on n ≥ 3 independent experiments. One-way ANOVA with Bonferroni test was applied

FER, IGF-1R, and β1 integrin associate in adhesion complexes that enhance FER activity

The IGF-1R has previously been demonstrated to participate in a signaling complex with β1 Integrin to promote cell proliferation and motility [5, 15]. FER has also been reported to regulate β1 integrin signaling [28], so we hypothesized that FER is a component of a signaling complex containing Integrin and IGF-1R. In agreement with our observations in Fig. 1 from PLA and immunoprecipitation, we observed that FER and IGF-1R strongly co-localize by co-immunofluorescence in MCF-7 cells (Fig. 3a). Furthermore, as shown by confocal microscopy the majority of surface IGF-1R in these cells is present at large complexes that also contain FER and β1 Integrin (Fig. 3b) and vinculin (Fig. S1). These complexes represent sites of focal cell adhesion. In MDA-MB-231 cells FER and the IGF-1R were also both observed to co-localize with β1 integrin at distinct sites of cell protrusion and adhesion (Fig. 3c).

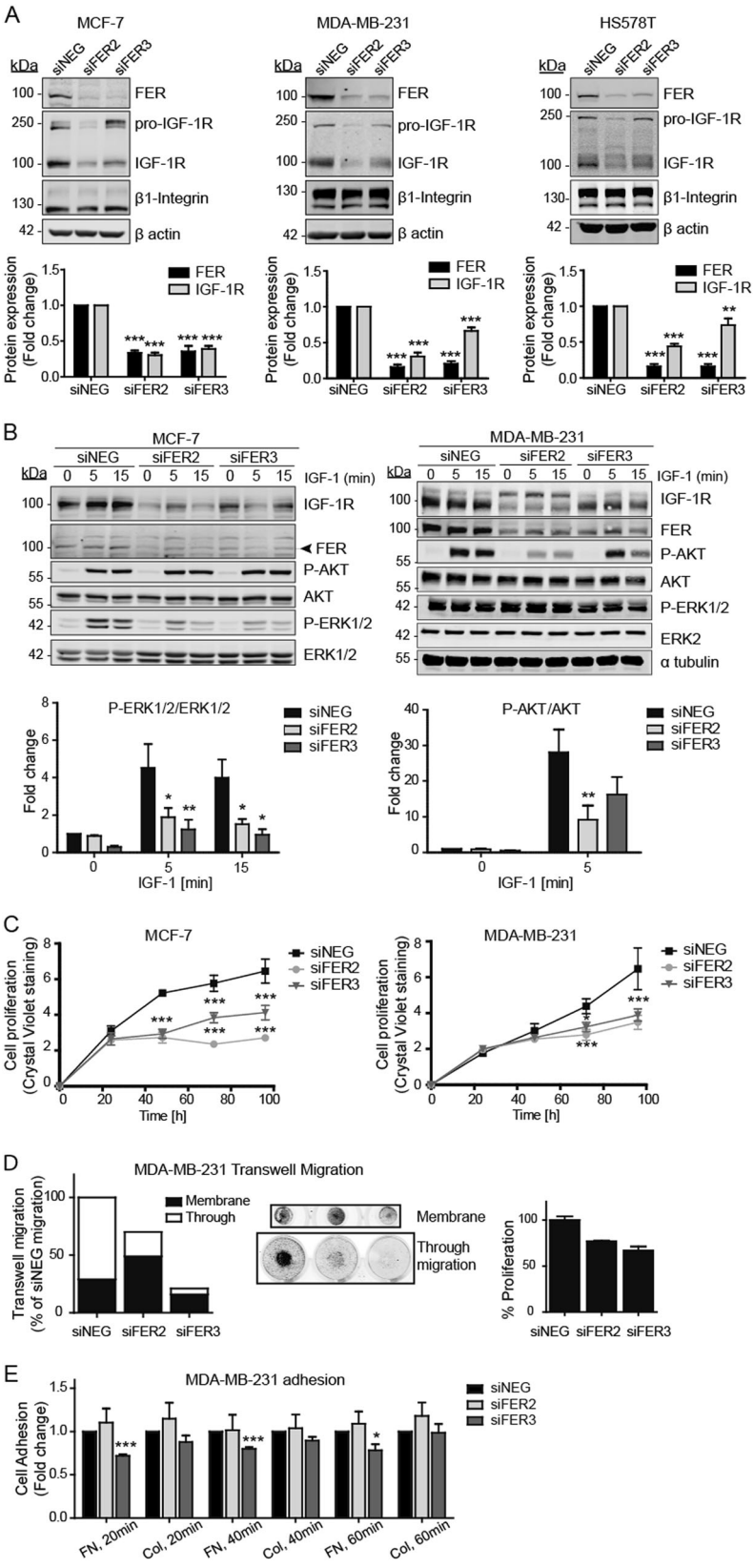
We next asked whether an activated IGF-1R affects FER kinase activity, by measuring FER autophosphorylation on Y402 in HEK293T cells transfected with empty vector, IGF-1R/WT or IGF-1R/KD. IGF-1 strongly promoted FER autophosphorylation in vector-expressing cells, which indicates that activation of endogenous IGF-1R is sufficient to enhance FER activity. FER autophosphorylation was further increased in cells expressing IGF-1R/WT but not in cells expressing IGF-1R/KD (Fig. 3d), thus confirming a requirement for activated IGF-1R in FER activation. Overexpression of FER/WT but not KD in HEK293T cells increased the phosphorylation of SHC (P-Y239/240) and ERK1/2 (P-T202/Y204) without any evident effect on phosphorylation of AKT (Fig. 3e). FER/WT also promoted a significant increase in phosphorylation of the focal adhesion-associated kinases SRC (Y416) and FAK (on both Y397 and Y925) (Fig. 3f).

Taken together, these results demonstrate that FER and the IGF-1R are components of β1 Integrin-anchored adhesion complexes that enhance activation and autophosphorylation of FER in an adhesion- and IGF-1-dependent manner. This suggests that the association of the IGF-1R with FER enhances cooperative IGF and adhesion signaling via the SHC, FAK and MAPK pathways and that these receptors may reciprocally activate each other.

FER suppression reduces IGF-1R expression and proliferation, and differentially affects cell migration

Having observed clear effects of FER on enhancing IGF-1R expression, phosphorylation, and signaling we next asked whether suppression of FER would alter IGF-1R expression and activity. To do this, we first screened a panel of siRNAs that specifically target FER in different breast cell lines (Fig. S2A). We observed a consistent suppression of FER with all siRNAs tested (except siFER4). IGF-1R expression levels were clearly reduced by most of these siRNAs in MCF-7, MDA-MB-231 cells, and HS578T cells and MCF10A cells (Fig. S2A). To investigate this further we focused on two siRNAs (siFER2 which suppressed IGF-1R significantly and siFER3 which suppressed IGF-1R to a lesser extent) to further examine the effects of FER suppression on IGF-1R expression in all four cell lines. Both siFER2 and 3 substantially decreased IGF-1R protein levels at 48 h post transfection in MCF-7, MDA-MB-231 and HS578T cells (Fig. 4a), whereas β1 Integrin levels were largely unaffected (Fig. 4a and Fig. S2B). Similar effects were observed with MCF10A cells at 48 h (Fig. S2D) and for all cell lines at 72 h post siRNA transfection (Fig. S2C and D).

We next investigated the effects of siFER2 and 3 on IGF-1 signaling in MCF-7 and MDA-MB-231 cells. In MCF-7 cells FER suppression had no effect on IGF-1-induced AKT phosphorylation, but both siRNAs clearly reduced IGF-1-


A
MCF-7
MDA-MB-231
HS578T
kDa
siNEG
siFER2
siFER3
FER
pro-IGF-1R
IGF-1R
β1-Integrin
β actin
Protein expression (Fold change)
B
IGF-1 (min)
P-AKT
AKT
P-ERK1/2
ERK1/2
ERK2
α tubulin
P-ERK1/2/ERK1/2
P-AKT/AKT
Fold change
IGF-1 [min]
C
Cell proliferation (Crystal Violet staining)
Time [h]
D
MDA-MB-231 Transwell Migration
Transwell migration (% of siNEG migration)
Membrane
Through
Through migration
% Proliferation
E
MDA-MB-231 adhesion
Cell Adhesion (Fold change)
FN, 20min
Col, 20min
FN, 40min
Col, 40min
FN, 60min
Col, 60min

◀ **Fig. 4** Suppression of FER with siRNA suppresses IGF-1R activity and cell proliferation, but variably affects migratory potential. **a** Suppression of FER with siRNAs affects IGF-1R levels: Protein expression of the indicated proteins was analyzed by immunoblotting in control (siNEG) cells and cells transfected with two different FER siRNAs (siFER2 or 3), 48 h post transfection. Graphs show densitometry measurements of mean fold difference ± SEM of IGF-1R expression in siFER-transfected cells compared with siNEG controls, from at least $n = 3$ independent experiments; Statistical analysis was performed using two-way ANOVA with Bonferroni test. **b** Western blot analysis of IGF-1R downstream signaling in cells with FER suppressed: At 48 h post transfection with siNEG or siFER, MCF-7, and MDA-MB-231 cells were serum starved for 4 h prior to stimulation with IGF-1 (10 ng/ml), for indicated times. Cell lysates were assessed by SDS-PAGE and immunoblotting for expression of FER, IGF-1R, P-AKT, P-ERK and non-phospho controls. Graphs of mean fold difference ± SEM of P-ERK and P-AKT expression are shown, quantified by densitometry from three independent experiments. Statistical significance was analyzed by two-way ANOVA with Bonferroni test. **c** FER suppression causes decreased cell proliferation: At 24 h post transfection with siNEG or siFER, cells were plated in triplicate at the same cell number and fixed and stained with crystal violet every 24 h for a further 96 h. Staining intensity at each timepoint was analyzed using an Odyssey scanner and densitometric measurements from three separate experiments ± SEM are shown. Statistical significance was determined using a two-way ANOVA with Bonferroni test. **d** FER siRNA 2 and 3 have variable effects on migration: At 24 h post transfection, siNEG, siFER2, and siFER3-transfected MDA-MB-231 cells were seeded onto the upper part of a transwell chamber in serum-free medium, and allowed to migrate towards serum for 24 h. Cells that had migrated to the underside of the transwell membrane ('Membrane'), and cells that had migrated through the membrane entirely and attached to the bottom of the well ('Through migration') were fixed and stained with crystal violet and quantified using an Odyssey scanner. Quantification of migration was first normalized to cell proliferation (shown in graph on right), for each cell type. Data are shown as percentage migration, of membrane or 'through' migration, with siNEG total cell migration set as 100%. Images of the transwell membrane- and 'through'- migrated cells are shown, $n = 1$ of three experiments with similar results. **e** siRNA3-transfected cells have decreased cell adhesion to fibronectin, whereas FER siRNA 2 does not affect adhesion: MDA-MB-231 cells were seeded onto fibronectin (FN; 5 µg/ml) or collagen I (Col; 10 µg/ml)-coated wells, 48 h post transfection with siNEG or siFER2 or 3. Cells were fixed and stained with crystal violet 20, 40, or 60 min later. Quantification of adherent cells was measured using Odyssey scanning and densitometry. Data are presented as fold-change of adhesion of siNEG cells, from three independent experiments, statistical analysis was performed using the Student's *t*-test

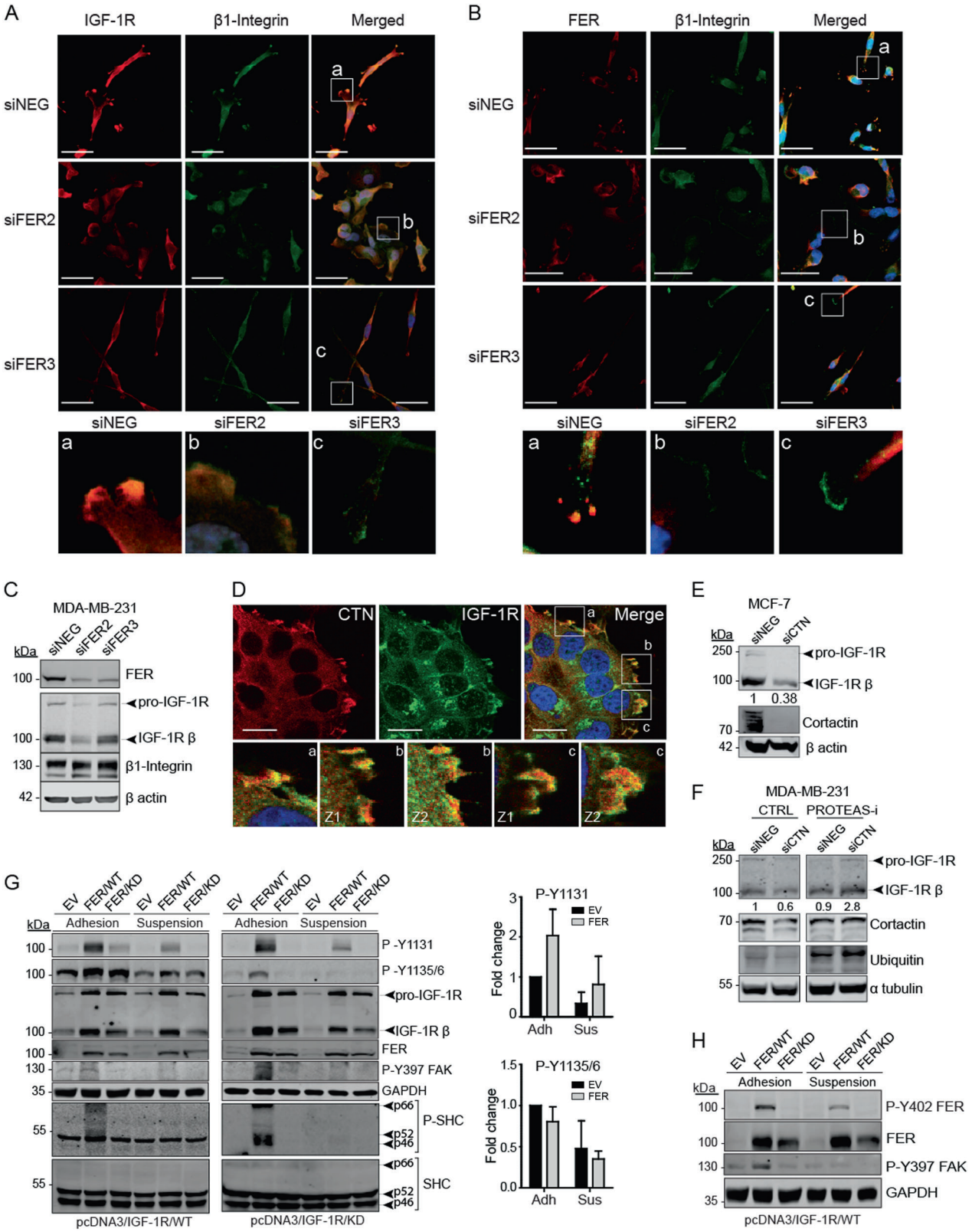
stimulated phosphorylation of ERK1/2 (Fig. 4b). In MDA-MB-231 cells phosphorylation of ERK1/2 is generally not responsive to serum withdrawal or IGF-1, but IGF-1 induces strong phosphorylation of AKT. Here FER suppression with both siRNAs reduced IGF-1-induced phosphorylation of AKT (Fig. 4b). These data indicate that FER suppression can suppress IGF-1 signaling responses. In line with this we observed that cell proliferation rates in MCF-7 and MDA-MB-231 cell lines were suppressed by both siFER2 and siFER3 (Fig. 4c).

We next investigated the migratory potential of MDA-MB-231 cells in Transwells with FER suppressed by siFER2 and siFER3. Surprisingly, we observed that siFER2 partially suppressed directional migration towards serum (approximately 30%) while siFER3 greatly impaired cell migration (by ~80%) (Fig. 4d). Interestingly, we noted that the morphology of cells transfected with either siFER2 or siFER3 was quite different (siFER2 caused cells to become more spread while siFER3 caused cells to become more spindle-like). These differences in morphology elicited by siFER2 and 3 were consistently and reproducibly observed in all cell lines transfected with these siRNAs (MCF-7, MDA-MB-231, HS578T, and MCF10A cells) (Fig. S2E). MDA-MB-231 cell adhesion to fibronectin was impaired by siFER3, but not by siFER2 (Fig. 4e). Thus, our data show that similar levels of FER suppression can result in different effects on cell morphology and migratory potential. Although we cannot explain these consistently different siRNA effects, the data suggest they may be related to suppressing essential FER function in the formation of dynamic cell adhesion structures, such as lamellipodia, which are necessary for cell migration.

Overall, we conclude that suppression of FER can reduce IGF-1R levels, IGF-1 signaling and cell proliferation. The data also indicate that similar suppression of FER does not correlate with similar effects on IGF-1R expression or cell phenotype, and FER suppression may result in different effects on cell morphology and migratory potential.

Co-location of IGF-1R with FER in adhesion complexes enhances IGF-1R activity

Next, we sought to investigate whether FER is required for IGF-1R activity in adhesion complexes. First, we investigated the effects of FER suppression with siFER2 and siFER3 on the association of IGF-1R and FER with β1 Integrin in MDA-MB-231 cells. In agreement with our observations on cell morphology (Fig. S2E), we observed that cells transfected with siFER2 were more spread with fewer directional lamellipodia, while cells transfected with siFER3 were elongated and spindle-like (Fig. 5a, b). Although IGF-1R could be observed to co-localize with β1 integrin in adhesion complexes in control siNEG cells (Fig. 5a top panels), as described for Fig 3a, b, these structures and IGF-1R/β1 Integrin co-localization were less evident in cells with FER suppressed (Fig 5a, b, c). As expected FER levels were suppressed by siFER2 and 3, and less association with β1 Integrin was also observed (Fig. 5b). In MCF-7 cells transfected with siFER2, cell adhesion sites appeared to be smaller and less mature with considerably less vinculin, β1 integrin and IGF-1R present (Fig. S2A-C). These immature adhesion sites were especially evident upon confocal imaging of siFER2-transfected cells that were stained for paxillin (Fig. S3B). Taken together, these data indicate that suppression of FER with either siFER2 or


A
IGF-1R
β1-Integrin
Merged
siNEG
siFER2
siFER3
B
FER
C
MDA-MB-231
kDa
FER
pro-IGF-1R
IGF-1R β
β1-Integrin
β actin
D
CTN
IGF-1R
Merge
Z1
Z2
E
MCF-7
pro-IGF-1R
IGF-1R β
Cortactin
β actin
F
MDA-MB-231
CTRL
PROTEAS-i
Ubiquitin
α tubulin
G
EV
FER/WT
FER/KD
Adhesion
Suspension
P -Y1131
P -Y1135/6
P-Y397 FAK
GAPDH
P-SHC
SHC
pcDNA3/IGF-1R/WT
pcDNA3/IGF-1R/KD
Fold change
Adh
Sus
H
P-Y402 FER

◀ **Fig. 5** Cell adhesion is required for FER-enhanced IGF-1R activity. **a**, **b** Immunofluorescence of MDA-MB-231 with suppressed FER. MDA-MB-231 were seeded onto coverslips coated with 5 μg/cm^2 collagen, 24 h post transfection with siNEG or siFER2 or 3. Cells were allowed to attach for 24 h, fixed, and stained with IGF-1R or β1-Integrin and FER. **a** MDA-MB-231 with suppressed FER showing less co-localization of IGF-1R (red) with β1-Integrin (green) in adhesion complexes indicated by a reduced yellow signal illustrated in siNEG merged image compared with merged images of siFER2 and siFER3-transfected cells. **b** MDA-MB-231 cells transfected with siFER2 or 3 show reduced FER staining (red), whereas β1-integrin (green) levels are similar. Images in **a** and **b** also illustrate differences in cell morphology between cells trasfected with siFER2 (more spread) and siFER3 (elongated). Images are 40 × and the scale bars represent 200 μm. **c** Representative western blots of MDA-MB-231 cells transfected with siNeg and siFer2 or 3 used for immunofluorescence staining. **d** Immunofluorescence showing cortactin and IGF-1R co-localization in MCF-7 cells. MCF-7 cells grown on coverslips for 24 h, fixed and stained with anti-IGF-R (rabbit/mouse; green) and anti-cortactin (mouse; red) antibodies. Slides were photographed using a confocal laser scanning microscope Z-stacks were acquired and analyzed using Fluoview Olympus software. At least two slices were acquired at different Z positions (Z1–Z2). Zoomed images (a, b, c) are presented in their respective Z-planes. Individual slices were 0.5 μm. Scale represents 20 μm. **e** Suppression of cortactin in MCF-7 cells reduces IGF-1R levels. MCF-7 transfected with negative control siRNA (siNEG) or cortactin siRNA (siCTN) were analyzed for IGF-1R and cortactin expression by western blotting. **f** MDA-MB-231 cells were transfected with negative control siRNA (siNEG) or cortactin siRNA (siCTN) and asessed for IGF-1R and cortactin expression. Cells were immediately either cultured in the presence of DMSO (CTRL) or Bortezomib (PROTEAS-i; 30 nM) for 24 h. Expression of IGF-1R, FER, and ubiquitin as a control for proteasome inhibition, were analyzed by western blotting. **g** Cell adhesion is required for FER-mediated IGF-1R phosphorylation. IGF-1R phosphorylation and FER signaling in HEK293T cells co-overexpressing: EV, FER/WT, or FER/KD with IGF-1R/WT (left panels) or IGF-1R/KD (right panels) as indicated. At 48 h post transfection, cells were transferred into suspension culture for 2 h, lysed and immunoblotted to assess levels of P-IGF-1R (Y1131, Y1135/6), IGF-1R, P-SHC (Y239/Y240), and P-FAK (Y397) as a control for loss of adhesion signaling. The levels of total FER were assessed as a control for transfection efficiency. The experiments were performed three times with similar results, and the graph represents quantification of Y1131 and Y1135/1136 (an average of two of these experiments in cell over-expressing FER/WT (black bars) or Empty Vector (grey bars)). **h** Loss of adhesion signaling decreases autophosphorylation on FER. IGF-1R/WT-expressing HEK293T cells were cultured as described in **g** above. A reduced level of P-Y402 FER was observed when cells were in suspension. P-Y397 FAK was used as a control for the loss of adhesion signals

siFER3 disrupts the formation of mature cell adhesions and functional lamellipodia necessary for directional cell migration.

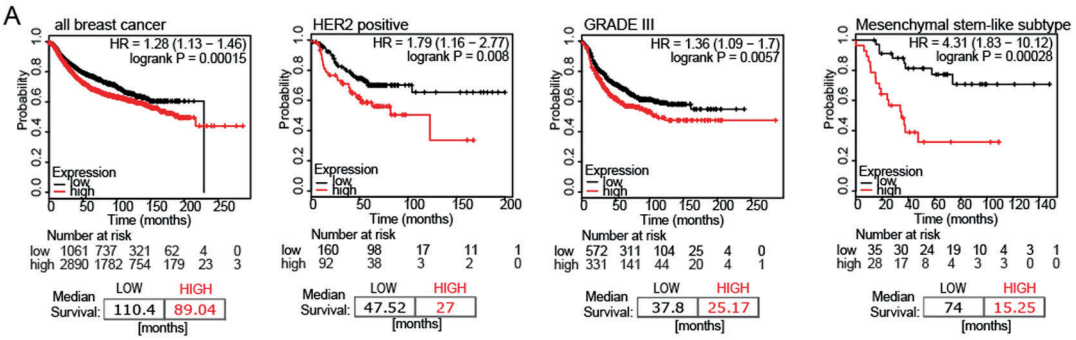
As siRNAs targeting FER apparently have different effects on cell morphology we also tested whether suppressing a well-described substrate of FER; cortical actin (cortactin, which has a role in both biosynthetic and recycling trafficking pathways [29–31]) had any effect on IGF-1R expression levels. We observed that the IGF-1R co-localizes with cortactin at sites of cell adhesion in MCF-7 cells (Fig. 5d). SiRNA-mediated suppression of cortactin reduced IGF-1R levels in both MCF-7 and MDA-MB-231 cells (Fig. 5e, f). This could be prevented by proteasome inhibition (shown for MDA-MB-231 cells in Fig. 5f).

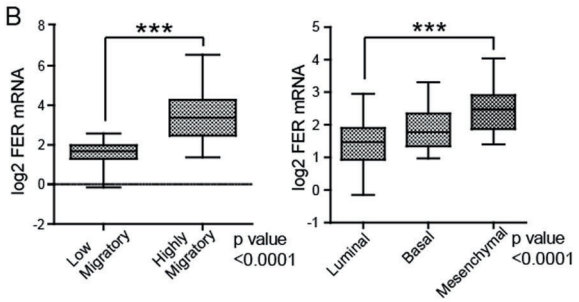
To further test whether cell adhesion is required for FER-enhanced IGF-1R activity we compared the effects of FER on IGF-1R autophosphorylation and signaling in HEK293T cells that were adherent or maintained in suspension. We observed that the FER-enhanced phosphorylation of IGF-1R/WT and IGF-1R/KD on Y1131 was completely abolished when cells were not allowed to adhere (Fig. 5g). As expected, the phosphorylation of SHC and FAK, evident in adherent cells expressing IGF-1R/WT and FER/WT, was absent in non-adherent cells (Fig. 5g). Phosphorylation on the Y1135/1136 site was reduced by lack of adhesion, but in agreement with results in Fig. 2, was not affected by FER. Interestingly, the effects of lack of cell adhesion on IGF-1R were accompanied by a reduction in FER autophosphorylation (Fig. 5h). This demonstrates that adhesion signals enhance FER activity and its potentiation of IGF-1R and SHC/ERK1/2 phosphorylation.

These observations suggest that FER promotes the assembly of mature cell adhesions, which enhances the phosphorylation and activity of the IGF-1R.

FER expression strongly correlates with EMT markers in mesenchymal-like breast cancer, and its activity can be suppressed by an ALK kinase inhibitor

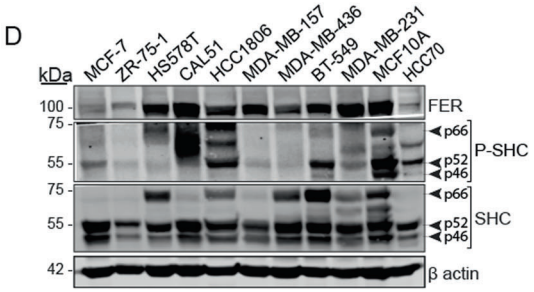
FER expression was previously associated with a poor outcome in triple-negative breast cancer [28]. We explored whether this may be related to FER function in enhancing IGF-1R and adhesion signaling in breast cancer by first analyzing available data sets from breast tumors and cell lines. Kaplan–Meier (KM) survival plots derived from The Cancer Genome Atlas (TCGA) data [32] demonstrated that high expression of FER is associated with poor relapse-free survival among breast cancer patients ($P = 0.00015$; $n = 3951$; Fig. 6a, Fig. S4A). Following exclusion of systemically untreated patients, the hazard ratio (HR) rose to 1.63, whereas the median survival almost halved with high FER expression (65.1–34.82 months; $P = 0.91 \times 10^{-9}$; Fig. S4A). FER expression influences the survival of patients of Grade III, estrogen receptor-negative and HER2-positive types of breast cancer (HR: 1.79; $P = 0.008$; median survival decrease from 47.52 to 27 months). Further analysis demonstrated that mesenchymal and mesenchymal stem-like (MSL) were the subtypes most linked to high FER expression, with decreased median survival of MSL patients from 74 to 15.25 months (HR: 4.31; $P = 0.00028$; Fig. 6a).

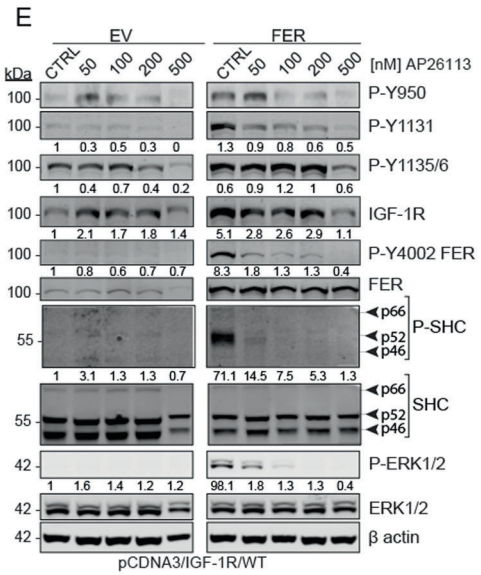


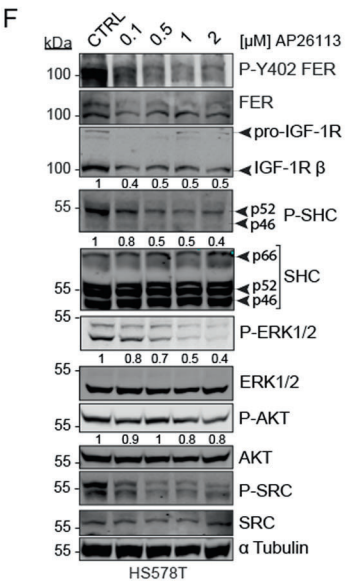


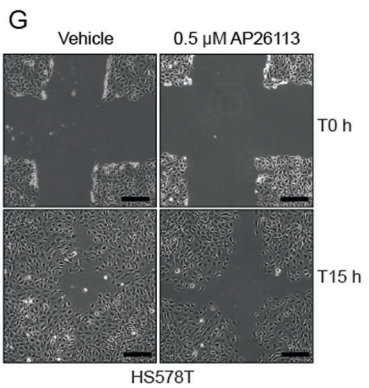
C

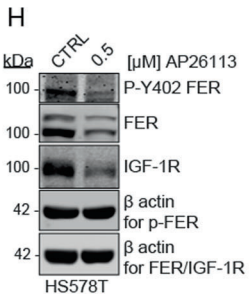
Gene	Pearson r	P value (two-tailed)	P value summary	R square
ZEB2	0.4213	< 0.0001	****	0.1775
ZEB1	0.3911	0.0003	***	0.1529
TWIST1	0.424	< 0.0001	****	0.1798
TWIST2	0.361	0.0009	***	0.1303
SNAI2	0.4526	< 0.0001	****	0.2048
VIM	0.4246	< 0.0001	****	0.1802
CDH1	-0.1676	0.1323	ns	0.0281











◀ **Fig. 6** High FER expression in mesenchymal breast cancer negatively correlates with relapse-free survival. Pharmacological inhibition of FER kinase abolishes its signaling. **a** Kaplan–Meier plots were drawn using data accessed through KM plotter, a publicly accessible interface for TGCA survival data. All data sets were assayed using probe ID: 206412. *P*-value, hazard ratio (HR) and median survival were calculated and are displayed. **b** RNA-Seq analysis of FER mRNA expression compared in low and highly migratory or luminal, basal A, and mesenchymal (basal B) breast cancer cell lines ($n = 78$), extracted from Marcotte et al. (2016). FER mRNA expression is plotted on a log2 scale. **c** table representing *in situ* analysis of correlation of FER and expression of several mesenchymal genes in breast cancer cell lines ($n = 82$), extracted from Marcotte et al. 2016. **d** Western blotting analysis of FER protein expression and phosphorylation of SHC in a panel of breast cancer cell lines. **e** Western blotting analysis of effects of FER-i (AP26113) on IGF-1R/WT and EV or FER-co-expressing HEK293T cells. At 48 h post transfection cells were cultured with AP26113 (0–500 nM) for 2 h, subsequently lyzed and immunoblotted for the indicated phospho- and total protein levels. FER immunoblot was included as an overexpression control. **f** Western blotting analysis of effects of FER-i (AP26113) on endogenous FER and signaling in HS578T cells. Cells were treated for 2 h with 0–2 μM, subsequently lyzed and immunoblotted for the indicated phospho- and total protein levels. **g**, **h** Effects of FER-i on HS578T cell migration were assessed by wound-healing assays as described in methods. Cell were pretreated with AP26113 prior to wounding and maintained in medium containing 0.5 μM inhibitor for 15 h post-wounding. Cells were photographed with at 10 × magnification and the images represents one of three independent experiments with similar results. After 15 h of exposure to AP26113 cells were lyzed and western blots prepared to assess levels of Y402 FER, total FER and IGF-1R **h**

Cells of these subtypes have been described as less-differentiated and to manifest a highly migratory/invasive phenotype [33]. Interestingly, IGF-1R activity in tumors has also been associated with a mesenchymal and stem-like phenotype of cancer cells [7, 33].

In line with these observations, analysis of RNA-Seq expression profiles of 82 breast cancer cell lines extracted from the study of Marcotte et al. [34] demonstrated that migratory and mesenchymal breast cancer cell lines express FER at significantly higher levels than luminal cell lines ($P < 0.0001$; Fig. 6b, Fig. S4C). Expression of FER was also strongly correlated with expression of EMT markers, including *ZEB1/2*, *TWIST1/2*, *SNAI2* (*SLUG*) and *VIM* (Pearson $R \sim 0.4$, $P < 0.0003$; Fig. 6c, S9). We also investigated whether FER expression correlates with these markers in patient samples using TCGA) RNA-Seq data from 1215 breast cancer patients. We found that FER expression strongly correlated with *ZEB1/2* (Pearson R: 0.6), *TWIST1* and *SNAI2* and other EMT markers (Fig. S4 B–E).

We also determined that FER expression in a panel of breast cancer cell lines could be positively correlated with phosphorylation of SHC (P-Y239/Y240) (Fig. 6d; S4F), noting that several of these cell lines expressed the p66 isoform of SHC that is associated with REDOX stress and more recently with coupling mechanical signals to activation of RhoA [35]. (The analysis of RNA sequencing (RNA-Seq) and reverse phase protein array (RPPA) data from 95 breast cancer patients, available from TCGA, further demonstrated a positive correlation in phosphorylation of SHC (P-Y317; Pearson *R*: 0.34; $P = 0.0008$) and SRC (P-Y416; Pearson *R*: 0.27; $P = 0.007$) and expression of FER (Fig. S4G).

All of the in silico analyses suggested an important function for FER in breast cancer aggressiveness. Therefore, we next sought to test the consequences of pharmacological inhibition of FER in breast cancer cells. As there is no specific FER kinase inhibitor available, we opted to test an inhibitor of the two anaplastic lymphoma kinase (ALK), AP26113 (Brigatinib). This compound potently inhibits FER in in vitro kinase assays and was described to have FER as its next most selective target following ALK [36]. A similar ALK inhibitor has been reported to inhibit FES kinase, which is structurally similar to FER [37] (Fig. S4H).

First, we tested AP26113 over a range of concentrations (50–500 nM) in HEK293T cells overexpressing FER (Fig. 6e). Concentrations as low as 50 nM, decreased FER autophosphorylation on Y402 by ~ 80% and also reduced FER-mediated phosphorylation of Y1131 in the IGF-1R. Consistent with our findings (Fig. 2) the inhibitor did not alter phosphorylation of Y1135/1136 in the IGF-1R (Fig. 6e). Moreover, this kinase inhibitor suppressed phosphorylation of SHC and ERK1/2. This indicates that AP26113 inhibits FER kinase activity and FER-induced signaling.

We also tested AP26113 on breast cancers cells that express endogenous levels of FER. HS578T cells were chosen for these studies as a mesenchymal-like/highly migratory breast cancer cell line with relatively high FER levels [38] (Fig. 6d). Exposure of HS578T cells to AP26113 (100–500 nM) resulted in inhibition of FER kinase autophosphorylation (Fig. 6f). Interestingly, FER levels were also suppressed. This may be due to destabilization of inactive FER as was previously reported [30]. AP26113 also reduced phosphorylation of SHC, SRC, and ERK1/2, without affecting AKT phosphorylation. Phosphorylation of the IGF-1R on Y950 and 1131 could not be detected in these cells probably because of the reduction in IGF-1R levels. We also asked whether AP26113 (0.5 μM) altered the motility of HS578T cells over 15 h in wound healing assays. We observed consistently impaired ability to fill the wound in the presence of AP26113 (Fig. 6g), and again, the drug reduced FER expression levels and phosphorylation, as well IGF-1R expression (Fig. 6h). Taken together, these data indicate that FER kinase activity and its actions in enhancing signaling pathways can be pharmacologically inhibited by the AP26113 inhibitor. This inhibitor is currently being tested in phase 2 clinical trials as a therapy for non-small cell lung cancer (ID:NCT02706626).

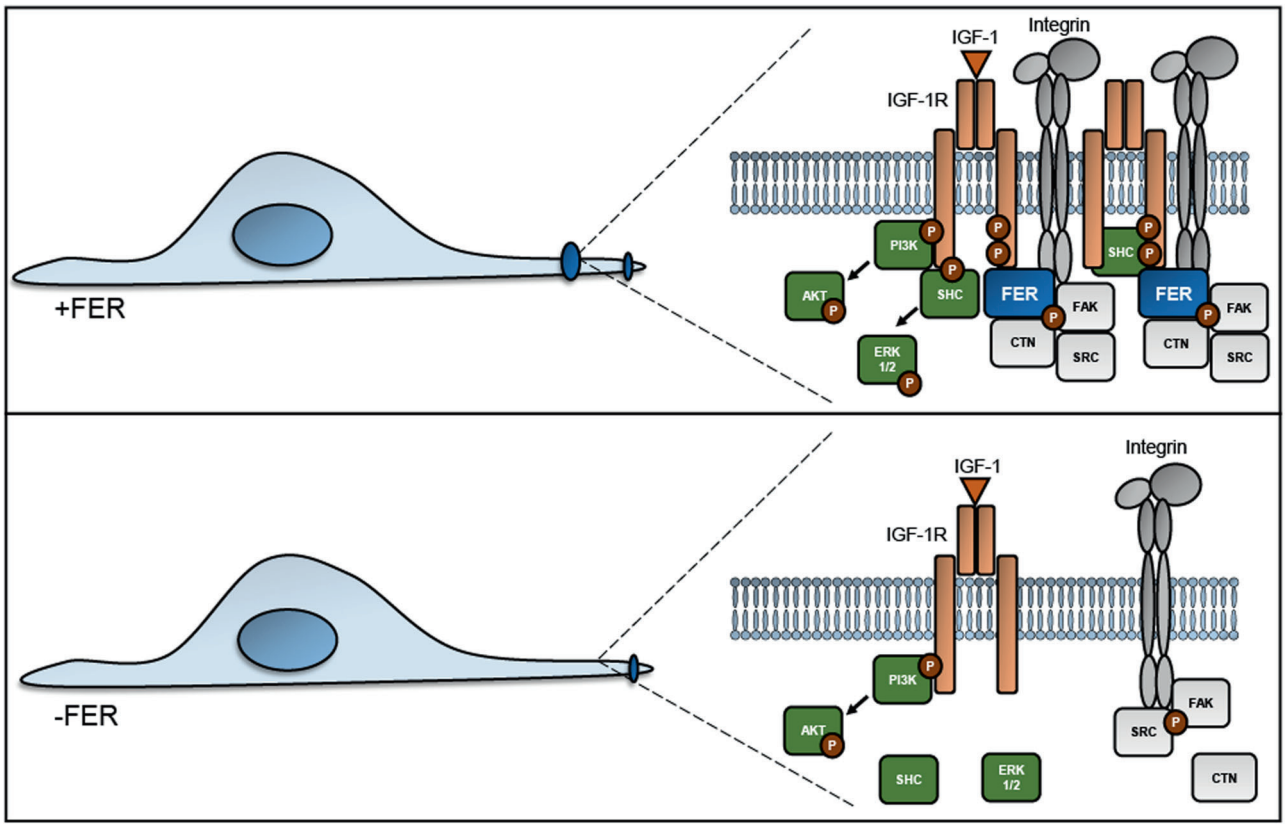


Fig. 7 Schematic representing the role of FER in potentiation of cooperative signaling between IGF-1R/β1 Integrin at sites of cell adhesion. We propose that the non-receptor tyrosine kinase FER is an important signaling node in cooperative signaling between the IGF-1R and cell adhesion signaling. FER-IGF-1R axis has a direct effect on IGF-1R steady state levels, its phosphorylation and signaling output. (CTN – cortactin)

Discussion

Cooperative IGF-1R and adhesion signaling has been proposed to facilitate cancer progression [2, 5, 39]. Here, we demonstrate that the non-receptor tyrosine kinase FER can regulate IGF-1R expression levels, activity, and adhesion-dependent signaling. FER has been reported to play a role in cross-talk between different receptor systems including cell–cell and cell-matrix complexes [19, 20]. Our findings (summarized in the model in Fig. 7) indicate that FER acts as an important node in such cross-talk between Integrin and IGF-1R signaling and that FER can be reciprocally activated by both IGF-1 and adhesion signaling.

Here, we show that FER and the IGF-1R strongly co-localize in cells, an interaction that does not require either FER or IGF-1R kinase activity. However, this interaction is essential for FER-enhanced IGF-1R phosphorylation and signaling. FER-induced phosphorylation of IGF-1R requires cell adhesion signals. It has been reported that FER regulates cellular distribution of Integrins by down-regulating surface expression of α6 and β1 Integrins [20]. Cooperation of growth factor receptors with different integrin heterodimers may positively or negatively impact growth factor activation and signaling [40]. Hence, the modulation of surface expression of different Integrin subunits can alter the growth factor signal. FER could facilitate IGF-1R association with Integrin-adhesion complexes, thus enhancing its phosphorylation and signaling output. We observed that FER generally promotes autophosphorylation of adhesion-associated kinases, SRC and FAK, and these can, in turn, directly phosphorylate IGF-1R, when activated by Integrin-mediated cell adhesion.

Although the role of FER in growth factor signaling has been previously documented [21, 22, 24], this is the first report of FER enhancing the expression levels and activity of the IGF-1R. FAK suppression has also been reported to decrease IGF-1R steady state levels [12, 16], again indicating that adhesion complexes support IGF-1R expression. The stability of other growth factor receptors can also be enhanced by adhesion complexes. For example, c-MET stability has been demonstrated to be dependent on Tensin-4, an adapter that links Integrins to β actin [41]. Therefore, we propose that the recruitment or localization of the IGF-1R to sites of cell adhesions results in enhanced IGF-1R stability. This could be mediated by the F-BAR domain of FER, because its oligomerization facilitates the formation of

lamellipodia [42, 43]. We observed that suppression of cortactin, a substrate of FER, reduced IGF-1R steady state levels. Cortactin has been previously documented to prevent ligand-induced EGFR degradation and to enhance β2 adrenergic receptor (β2AR) recycling [29, 44]. On the other hand, FER suppression was reported to accelerate EGFR internalization [23]. Therefore, FER and adhesion-mediated stability of IGF-1R could be achieved by either decreased internalization, cortactin-mediated recycling, or decreased IGF-1R proteostasis during biosynthesis. It is possible that the effects of FER on enhancing IGF-1R expression by regulating proteostasis could be mediated by FER altering the glycosylation of the IGF-1R receptor, because FER has been demonstrated to regulate laminin-binding glycan [45]. Indeed, impaired regulation of IGF-1R proteostasis associated with loss of the tumor suppressor protein AIRAPL has recently been associated with myeloid cell transformation and leukemia [46]. The FES protein, which is closely related to FER, has also been associated with acute myeloid leukemia where it can be activated by FLT3 [18] to promote cell survival. It is interesting to speculate that FES may mediate some of its survival functions in myeloid leukemia by enhancing the expression or activity of the IGF-1R. This however remains to be tested.

An unexpected finding of our study was that siRNA-mediated suppression of FER using different oligonucleotides consistently reduced FER expression to apparently similar levels while causing consistently different effects on cell morphology and migratory potential. Our study and that of Ivanova et al. [20] analyzed FER suppression in the MDA-MB-231 breast cancer cell line, which displays a mesenchymal phenotype. We noted that FER suppression with siFER2 in our study produced a similar phenotype to that described by Ivanova et al., with cells becoming more spread and less migratory. However, other siRNAs, in particular siFER3, which we also studied in detail, produced different effects on cell morphology and migration. Interestingly, the different siRNAs produced consistently similar effects on cell morphology in different cell lines, which suggests they selectively target certain isoforms or complexes of FER. We could not establish whether different isoforms were implicated because we only observed changes in one protein with the available antibody. However, our data and previous reports on FER function in cell adhesion complexes indicate that the alterations in cell morphology elicited by siFER2 and siFER3 are both consistent with disrupting the formation of lammelipodia. One predicted outcome is that cells would become more spread with weak adhesions and lack of directional lamellipodia (observed with siFER2) and a second is that cells may not properly form lamellipodia (observed with siFER3). An additional possibility, suggested by the high levels of p66SHC observed in breast cancer cell lines that also express FER highly, is that p66SHC-mediated activation of the RhoA pathway in fillopodia [35] may be affected by FER suppression. Overall, our observations illustrate that the use of selective siRNAs or shRNAs to investigate the physiological responses to FER suppression is not entirely straightforward.

A previous report demonstrated that that FER expression is associated with aggressive breast cancer in patients ($n = 485$) and inversely correlates with progression-free survival of ovarian cancer patients [24] [20]. Here, we analyzed a large subset of TCGA clinical survival data, which also shows that high FER expression (by RNA-Seq) correlates with poor relapse-free survival in breast cancer patients ($n = 3951$). High expression of FER particularly increases the HR in the mesenchymal-subtype cohort of breast cancer patients (HR: 4.31). In support of this, we observed that mesenchymal/highly migratory breast cancer cells express FER at significantly higher level than their counterparts. Considering the strong effects of ectopic FER expression on IGF-1R phosphorylation, we propose that FER could mediate potentiation of IGF-1 signaling, particularly in cancers with an EMT or stem-like phenotype. This is consistent with the observation that IGF-1R expression and activation may be elevated in breast cancer stem cells [33]. IGF-1R activity has also been implicated in the self-renewal of lung adenocarcinoma and chemoresistant colon cancer stem cells [33], and may also facilitate the EMT transition of breast, colon, prostate and lung cancer cells [2, 12, 47, 48].

As described here and elsewhere, the role of FER in supporting an invasive phenotype highlights the need to develop specific FER kinase inhibitors. Our results lead us to propose that AP26113, which inhibits FER kinase and signaling at nanomolar concentration, is an excellent candidate. AP26113 was developed as an ALK inhibitor and is in clinical trials phase 2 for non-small cell lung cancer (Brigatinib; ID: NCT02706626). TAE684, a similar ALK inhibitor has been reported recently to target FES that possesses a kinase domain highly homologous to FER [37]. Importantly, we observed that the residues required for interaction between TAE684 and FES kinase, that were identified by X-ray crystallography [37], are conserved in FER kinase. Inhibition of FER using AP26113 may present a useful therapeutic approach for mesenchymal-type breast cancers. In support of this concept, a tyrosine kinase inhibitor, PKC412 that was shown to specifically target a panel of post-EMT breast cancer cells mainly acts through inhibition of SYK and FER [49].

The ability of FER to mediate adhesion-enhanced phosphorylation of catalytically active or inactive IGF-1R in the presence of IGF-1R TKI (data not shown) could also

provide a mechanistic explanation for the lack of efficacy of IGF-1R TKIs in the clinic. This conclusion is supported by reports that co-targeting the IGF-1R with SRC and FAK in breast, lung, and pancreatic cancer models can synergistically decrease tumor growth [12, 14, 50]. Thus, co-targeting IGF-1R and adhesion signaling could improve the efficacy of IGF-1R inhibitors. We also propose that FER is a potential biomarker for adhesion-enhanced IGF-1R activity and its inhibition by AP26113 could effectively target tumor cells that are addicted to cooperative IGF-1R and adhesion signaling.

Materials and methods

Cell culture and IGF-1 stimulation

MCF-7, MDA-MB-231, MDA-MB-157, HEK293T, R−/IGF-1R/WT (+ 1.5 μg/ml puromycin), Hs578T, R− and R + cells were maintained in Dulbecco's Modified Eagles Medium (DMEM). MDA-MB-436 cells were cultured in a 50/50 mix of Leibovitz L15/RPMI media, and CAL51 cells in a 50/50 mix of DMEM/Hams Nutrient F12 media. HCC1806, ZR-75−1 and HCC70 cells were maintained in RPMI 1640. BT-549 cells were grown in RPMI 1640 with 0.023IU/ml Insulin. All media were supplemented with 10% (v/v) heat inactivated fetal bovine serum, 10 mM L-Glutamine, and 5 mg/ml penicillin/streptomycin. MCF10A cells were cultured as previously described [51]. Cells were cultured at 37 °C in a humidified atmosphere at 5% CO_2. All cells were determined to be free of mycoplasma.

For analysis of non-adherent (suspension) cells, cells were plated in duplicate on 10 cm plates and cultured overnight in complete medium. Cells from one plate of each cell type enzymatically detached for 5 min, and cells recovered by centrifugation (1000 RPM) for 5 min. Cells were then washed with PBS and re-suspended in complete medium (10 ml) in a 50 ml tube with occasional rotation for a total of 4 h prior to harvesting for lysis.

For analysis of IGF-1 stimulation responses, cells were cultured at seeding densities that allowed for an ~ 70% confluency after 20 h. Cells were incubated in serum-free medium for 4 h prior to stimulation with 10 ng/ml IGF-1 where appropriate. To terminate stimulation, cells were placed on ice and washed immediately with ice-cold PBS.

Immunofluorescence and PLA and microscopy

Cells were seeded on serum-coated 10 mm glass coverslips, washed with phosphate-buffered saline, fixed with 4% paraformaldehyde in PHEM buffer for 30 min at 37 °C, quenched with 50 mM Ammonium Chloride for 15 min, and permeabilized using 0.1% Triton/PHEM for 5 min. Cells were then blocked for 30 min using 5% donkey serum/PHEM, incubated for 1 h with the indicated primary antibodies diluted 1:100 (unless specifically stated otherwise in figure legends) in the blocking buffer and washed with PHEM buffer. This was followed by incubation with Alexa488- (1:200) or Cy3- (1:1000) conjugated secondary antibodies with Hoechst.

For Duolink PLA (Sigma Aldrich) experiments, cells were fixed, quenched, and permeabilized exactly in the same manner as for the standard immunofluorescence. Following this, cells were incubated with Duolink-blocking buffer in a pre-heated humidity chamber for 30 min at + 37 °C. Primary antibodies anti-IGF-1R (#3027 (1:200) or #9750 (1:100); Cell Signalling) and anti-FER (#4268 (1:200); Cell Signalling), were diluted in the Duolink-blocking buffer and incubated on the cells in a humidity chamber overnight. PLA anti-rabbit plus and anti-mouse minus probes were used to label primary antibodies. The probes were diluted 1:5 in a blocking buffer and slides were incubated in a pre-heated humidity chamber for 1 h at + 37 °C. The ligation stock (1:5) with ligase (1:40) was added to the coverslips for 30 min at + 37 °C. The amplification stock (1:5) with polymerase (1:80) was added to coverslips for 100 min. The solution was removed and coverslips dried at room temperature in the dark before mounting on slides using a minimal volume of Duolink In Situ Mounting Medium with DAPI.

Images were acquired using a SPOT charge-coupled device camera mounted on a Nikon T600 fluorescent microscope (Kingston Upon Thames, UK). For confocal microscopy, images were acquired using a Flouview FV1000 confocal laser scanning microscope (numerical aperture:1.4) with a × 60 oil or × 100 oil-immersion objective. Maximum intensity projections and *z*-stacks were processed and analyzed in Olympus Fluoview (FV10-ASW 4.0 Viewer) where brightness and contrast were adjusted.

SDS–PAGE and western blotting

Cellular protein extracts were prepared with a lysis buffer (NP-40 as described previously [5]) for 30 min on ice. Protein concentrations were determined via Bradford Assay, and samples were then either denatured by boiling for 5 min in 5 × loading buffer (2% w/v SDS, 8% v/v glycerol, 60 mM Tris-HCL, pH 6.8, 1.2% β-mercaptoethanol, and 0.2–0.4% Bromophenol Blue), or carried through to immunoprecipitation studies. Proteins were resolved by 4–20% sodium dodecyl sulfate–polyacrylamide gel electrophoresis (SDS–PAGE). Proteins were transferred to nitrocellulose membrane and blocked for 1 h at room temperature in 5% milk in Tris-buffered saline-T (20 mM Tris, 150 mM NaCl and 0.05% Tween 20, pH 7.6). Primary

antibodies were diluted in 5% milk in Tris-buffered saline-T and incubated with membranes at 4 °C overnight. IRDYE-conjugated secondary antibodies were used for detection with the Odyssey Image Scanner System (LI-COR Biosciences) and the Odyssey quantification software. Where re-probes were necessary, membranes were incubated with stripping buffer (200 mM NaOH, 1 % SDS) for 20 min at room temperature. Membranes were then washed, blocked, and incubated with appropriate antibodies.

Immunoprecipitation

Cell lysates were pre-cleared using Protein G-Agarose beads with lysis buffer and inhibitors for 1 hat 4 °C at a rotor speed of 5 RPM, and were then recovered by centrifugation at 3000 RPM for 3 min at 4 °C. Primary antibodies were incubated at 4 °C for 1 h. Immune complexes were obtained by adding 25 µl of pre-washed Protein G-Agarose beads for 1 h at 4 °C, and then recovered by centrifugation at 1000 RPM for 3 min at 4 °C. Immunoprecipitates were washed three times with ice-cold lysis buffer followed by centrifugation. In total, 2 × loading buffer was added to each sample prior to boiling for 5 min. Samples were separated by SDS-PAGE as described above.

DNA transfection and mutagenesis

Cells were transiently transfected with pcDNA3 plasmids encoding WT or mutant IGF-1R (IGF-1R/KD: K1003R) and pSG5 plasmids encoding FER kinase or kinase-dead FER Kinase (D743R; KD) or SH2-domain mutant (R483Q; SH2). The corresponding empty vector was transfected for each plasmid as control. Mutagenesis of pSG5 plasmid to introduce D743R (FER/KD and R483Q (FER/SH2) was carried out using the QuikChange Lightning site-directed mutagenesis kit (Agilent, #210518).

For transfection of R− cells, cells were seeded at a density of 1.5×10^6 cells/10 cm tissue culture dish, in antibiotic-free medium. Eighteen hours later, cells were transfected with relevant DNA (10 µg) and Lipofectamine 2000 (diluted in OptiMem) per 10 cm tissue culture dish and then incubated at 37 °C overnight. Transfected R− cells were subsequently split in preparation for experiments to be carried out 48 h after transfection. MCF-7 and MDA-MB-231 cells were transfected in a similar manner to R− cells, except for: seeding at 1.2×10^6 cells/10 cm and the use of Lipofectamine; For co-transfection of IGF-1R and FER in HEK 293-T cells; cells were transfected using Calcium Phosphate. In brief, cells were seeded 5 h prior to transfection at a confluency of 70%. The pSG5 vector encoding FER (3 µg) together with 1 µg of pcDNA3 IGF-1R expressing plasmids was added to CaCl2. The DNA/$CaCl_2$ mixture was then added dropwise to 2 × HBSS at a ratio of 1:1. Samples were allowed to stand for 1–2 min after which the solution was distributed to the pre-seeded cells. Cells were then cultured overnight and then re-seeded for experiments and lysed 24 h later.

siRNA transfection

A non-targeting oligonucleotide, Silencer Negative siRNA Control #2 (AM4311) from Ambion (Cambridgeshire, UK) was used as a Negative Control. Individual oligos targeting human FER kinase: siFER2 (S100287756; CAGATA-GATCCTAGTACAGAA) and siFER3 (S102622067; 5′-CAGAACAACTTAGTAGGATAA-3′ were obtained from Qiagen. Sequences for the other FER siRNAs from Qiagen tested are listed in Supplementary Table 1, as well as those of the SMARTpool ON-TARGETplus FER siRNA (L-003129-00-0005), which was purchased from Dharmacon. Transfections were performed using a final concentration of 20 nM siRNA, except where otherwise noted, using RNAiMAX, according to the manufacturer's recommendations. In brief, cells were trypsinized and re-suspended in antibiotic-free culture media with serum. siRNA oligonucleotides were diluted in OptiMem media. RNAiMAX transfection reagent was added to the siRNA solutions. siRNA/RNAiMAX complex was pipetted to six-well plate and $6.5–8.5 \times 10^5$ cells per well were then added. Cells were allowed to adhere overnight to the tissue culture plate. 24 h post transfection, the siRNA/RNAiMAX complex was removed and cells were re-seeded for experiments.

Cell proliferation, migration, and adhesion assays

Proliferation

Cells were transfected as described above and re-seeded in triplicate at 24 h post transfection (3.0×10^4 cells/well) in 24-well plates. Cells were collected every 24 h up to 96 h. Media was removed, cells were washed once with PBS and fixed with 96% Ethanol for 10 mins, followed by staining with 0.05% crystal violet in 20% Ethanol for 30 min. Staining was assessed using an Odyssey Scanner and quantified using Licor Image studio Lite software (LI-COR Biosciences).

Migration; wound-healing assay

HS578T cells were seeded in six-well plates at a concentration of 3.5×10^5 cells/ml 24 h prior to wounding. The monolayer was scratched using a sterile P10 tip (Time 0 h). Cells were allowed to migrate for 15 h and photographed using a 10 × objective at Time 0 h and 15 h.

Migration; transwell assay

Migration assays were performed using 6.5 mm transwell inserts with 8.0 µm membrane (costar#3422; Cambridge, MA), according to the manufacturer's recommendations. In brief, 24 h post transfection with siNEG, siFER2, or siFER3 siRNAs, 2×10^5 MDA-MB-231 cells were seeded onto the upper part of the transwell chamber in serum-free medium, and allowed to migrate toward 10% serum in the lower well of the chamber for 24 h. Cells were also added to two additional wells without transwells to serve as cell proliferation controls. These controls, cells that had migrated to the underside of the transwell membrane ("Membrane"), and cells that had migrated through the membrane entirely and attached to the bottom of the well ("Through migration") were fixed and stained with 0.05% crystal violet and scanned using the Odyssey scanner.

Adhesion assay

The wells of a 96-well plate were coated with 100 µl of fibronectin (Sigma, UK; 5 µg/ml) or collagen I (Gibco, Lifetechnologies, Grand Island, NY; 10 µg/ml) for 2 h at 37°C, The plates were washed and blocked with 100 µl of 2.5% bovine serum albumin/well for 1 h before further washing with PBS. Cells (100 µl containing 5×10^4 cells) were added to each coated well in triplicate and allowed to attach for the indicated times. The medium was removed, and attached cells were fixed with Methanol and stained with 0.05% Crystal Violet, scanned and quantified as described above.

RNA isolation and quantitative RT–PCR

Total RNA was isolated using the Trizol method and cDNA synthesis was carried out by reverse transcription with equal amounts of RNA (2 µg) using a cDNA synthesis kit (Invitrogen). Quantitative PCR was carried out using the LightCycler instrument; Roche Molecular Biochemicals (East Sussex, UK) with QuantiTect SYBR Green technology (Qiagen, Crawley, West Sussex, UK) using the following primers: (1) IGF-1R: Forward: 5′-ATGTCCAGGCCAAAACAGGAT-3′; Reverse: 5′-CCTCCCACTCATCAGGAACG-3′ (2) FER: Forward: 5′-GCTTCAGAAACGGCCATCAC-3′; Reverse: 5′-AGCGTCTCCATGATGAGGTG-3′. The delta–delta CT method was used to analyze data and determine relative mRNA expression levels.

Bioinformatics analysis

TCGA RNA-Seq data ($n = 1215$) was accessed from the MD-Anderson Standardized data browser (bioinformatics.mdanderson.org/cancer/databrowser/). Correlation of gene expression was calculated using Pearson's product moment correlation coefficient (r), statistical significance was determined using a modified t-test (P).

To determine correlation between protein levels and RNA levels in breast cancer, an RPPA dataset was downloaded, TCGA patient sample ID's were then aligned to the RNA-Seq matrix to ensure each pair corresponded to two different assays conducted on the same primary sample. Correlation was then calculated as for RNA-Seq analysis ($n = 95$).RNA-Seq data for an extended panel of breast cancer cell lines was obtained from the supplementary material of Marcotte et al. [34].

KM plotter analysis

The KM Plotter online survival analysis was used to generate KM plots [32]. Gene expression data and relapse-free and overall survival information are downloaded from GEO (Gene Expression Omnibus; Affymetrix microarrays only), EGA, and TCGA. Patient samples were split into two groups according to median expression of FER (ID: 206412). The two patient cohorts are compared by a KM survival plot, and the HR with 95% confidence intervals, median survival and log-rank P-value are calculated.

Statistical analysis and densitometry

Densitometry of western blots was carried out by measuring the intensity of immunolabelled protein bands using Odyssey/Image Studio Light Software. Results were expressed as ratio of phospho:total protein, or where relevant as ratios to total loading controls. In order to simultaneously investigate several IGF-1R phosphorylation sites, and FER/phospho-FER levels, technical replicates of lysates were run in parallel on the same or separate blots. To ensure consistent protein loading, each blot was probed with a loading control (e.g., actin, tubulin, GAPDH or pan-signaling proteins such as AKT, ERK1/2, or SHC), one of which was included in each figure dataset as a representative of protein loading for those samples. For data analysis of protein expression however, the respective protein loading control for each sample on a particular blot was used for normalization of protein expression. Changes in ratio of phospho/pan-protein levels were expressed as fold changes relative to the untreated control. Statistical significance was determined using Student's t-test using Microsoft Excel or GraphPad Prism. Significance was classified as a P-value of * < 0.05, ** < 0.01, *** < 0.001. Where specified, one- or two-way analysis of variance (GraphPad Prism) was used to determine significance, were a P-value of < 0.05 was deemed significant. All graphs were

produced using GraphPad Prism and are graphed using standard error of the mean.

Acknowledgements We would like to acknowledge Dr. Janina Berghoff for assistance with site-directed mutagenesis and Dr. Fionola Fogarty for assistance with the original siRNA screen. We also thank colleagues in the Cell Biology Laboratory and the Center for Cell Biology and Cancer Research for helpful discussions.

Funding This work was funded by a Science Foundation Ireland Principal Investigator award 11/PI/1139, and the European Union FP7 Marie Curie Industry-Academia Partnerships and Pathways (IAPP) Program 251480 BiomarkerIGF.

Author contributions JS, LR, OTC, SO'S, MC, CO'F, BA contributed to conception and design of experiments, acquisition and interpretation of data, and drafting the manuscript. NMcC and RK contributed to conception of study and reviewing the manuscript. RO'C contributed to conception design, interpretation of data and drafting the article.

Compliance with ethical standards

Conflict of interest The authors declare that they have no conflict of interest.

References

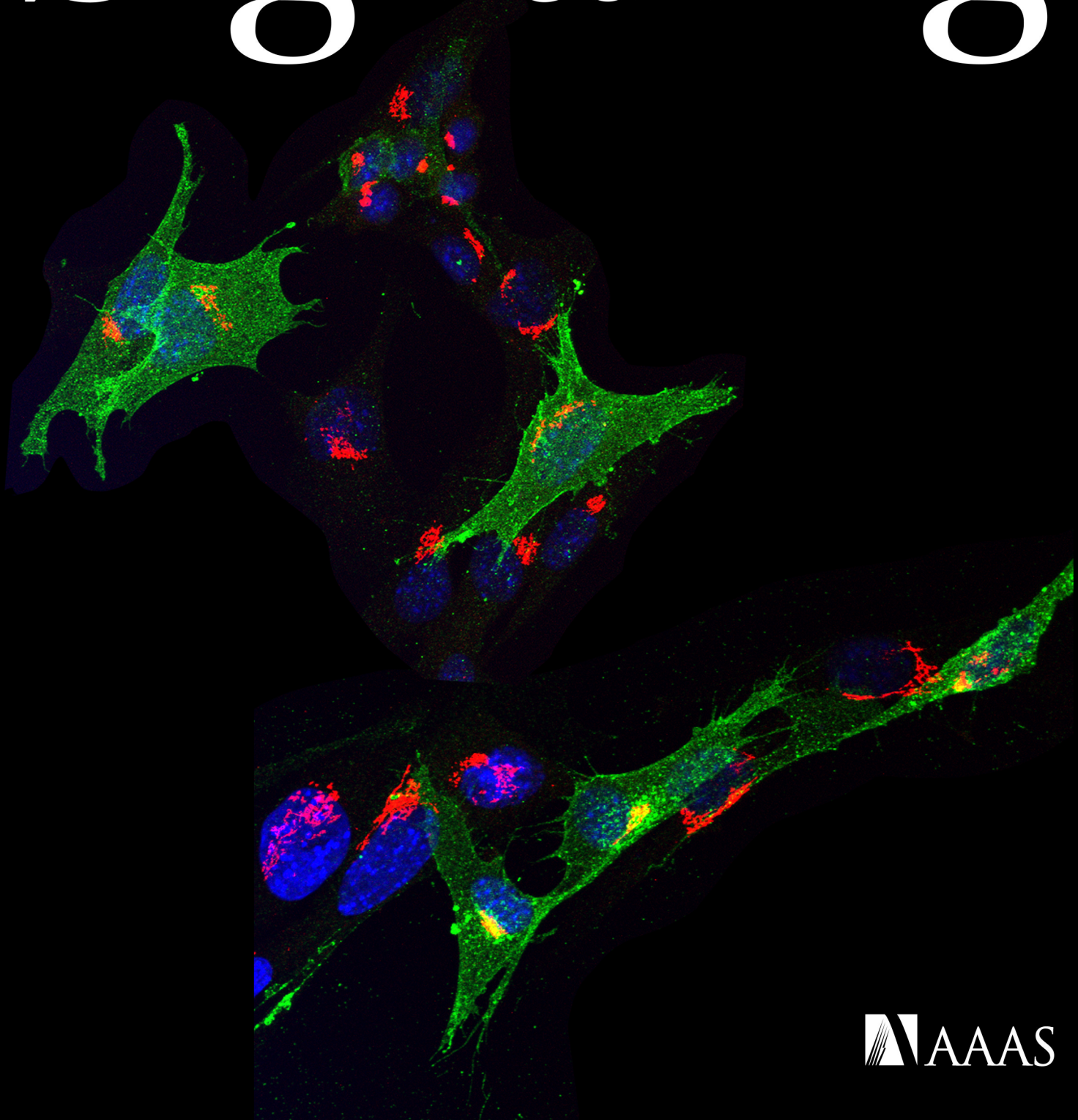
1. Samani AA, Yakar S, LeRoith D, Brodt P. The role of the IGF system in cancer growth and metastasis: overview and recent insights. Endocr Rev. 2007;28:20–47.
2. Cox OT, O'Shea S, Tresse E, Bustamante-Garrido M, Kiran-Deevi R, O'Connor R. IGF-1 receptor and adhesion signaling: an important axis in determining cancer cell phenotype and therapy resistance. Front Endocrinol. 2015;6:106.
3. Baserga R, Peruzzi F, Reiss K. The IGF-1 receptor in cancer biology. Int J Cancer. 2003;107:873–7.
4. Pollak M. The insulin and insulin-like growth factor receptor family in neoplasia: an update. Nat Rev Cancer. 2012;12:159–69.
5. Kiely PA, Leahy M, O'Gorman D, O'Connor R. RACK1-mediated integration of adhesion and insulin-like growth factor I (IGF-I) signaling and cell migration are defective in cells expressing an IGF-I receptor mutated at tyrosines 1250 and 1251. J Biol Chem. 2005;280:7624–33.
6. King H, Aleksic T, Haluska P, Macaulay VM. Can we unlock the potential of IGF-1R inhibition in cancer therapy? Cancer Treat Rev. 2014;40:1096–105.
7. Farabaugh SM, Boone DN, Lee AV. Role of IGF1R in breast cancer subtypes, stemness, and lineage differentiation. Front Endocrinol. 2015;6:59.
8. Niepel M, Hafner M, Pace EA, Chung M, Chai DH, Zhou L, et al. Profiles of basal and stimulated receptor signaling networks predict drug response in breast cancer lines. Sci Signal. 2013;6:ra84.
9. Kostler WJ, Hudelist G, Rabitsch W, Czerwenka K, Muller R, Singer CF, et al. Insulin-like growth factor-1 receptor (IGF-1R) expression does not predict for resistance to trastuzumab-based treatment in patients with Her-2/neu overexpressing metastatic breast cancer. J Cancer Res Clin Oncol. 2006;132:9–18.
10. Law JH, Habibi G, Hu K, Masoudi H, Wang MYC, Stratford AL, et al. Phosphorylated insulin-like growth factor-i/insulin receptor is present in all breast cancer subtypes and is related to poor survival. Cancer Res. 2008;68:10238–46.
11. Goel HL, Breen M, Zhang J, Das I, Aznavoorian-Cheshire S, Greenberg NM, et al. beta1A integrin expression is required for type 1 insulin-like growth factor receptor mitogenic and transforming activities and localization to focal contacts. Cancer Res. 2005;65:6692–700.
12. Taliaferro-Smith L, Oberlick E, Liu T, McGlothen T, Alcaide T, Tobin R, et al. FAK activation is required for IGF1R-mediated regulation of EMT, migration, and invasion in mesenchymal triple negative breast cancer cells. Oncotarget. 2015;6:4757–72.
13. Shen MR, Hsu YM, Hsu KF, Chen YF, Tang MJ, Chou CY. Insulin-like growth factor 1 is a potent stimulator of cervical cancer cell invasiveness and proliferation that is modulated by alphavbeta3 integrin signaling. Carcinogenesis. 2006;27:962–71.
14. Min HY, Yun HJ, Lee JS, Lee HJ, Cho J, Jang HJ, et al. Targeting the insulin-like growth factor receptor and Src signaling network for the treatment of non-small cell lung cancer. Mol Cancer. 2015;14:113.
15. Hermanto U, Zong CS, Li W, Wang L-H. RACK1, an insulin-like growth factor I (IGF-I) receptor-interacting protein, modulates IGF-I-dependent integrin signaling and promotes cell spreading and contact with extracellular matrix. Mol Cell Biol. 2002;22:2345–65.
16. Andersson S, D'Arcy P, Larsson O, Sehat B. Focal adhesion kinase (FAK) activates and stabilizes IGF-1 receptor. Biochem Biophys Res Commun. 2009;387:36–41.
17. Peterson JE, Kulik G, Jelinek T, Reuter CW, Shannon JA, Weber MJ. Src phosphorylates the insulin-like growth factor type I receptor on the autophosphorylation sites. Requirement for transformation by src. J Biol Chem. 1996;271:31562–71.
18. O'Flanagan CH, O'Shea S, Lyons A, Fogarty FM, McCabe N, Kennedy RD, et al. IGF-1R inhibition sensitizes breast cancer cells to ATM-related kinase (ATR) inhibitor and cisplatin. Oncotarget. 2016;7:56826–41.
19. Greer P. Closing in on the biological functions of fps/fes and fer. Nat Rev Mol Cell Biol. 2002;3:278–89.
20. Ivanova IA, Vermeulen JF, Ercan C, Houthuijzen JM, Saig FA, Vlug EJ, et al. FER kinase promotes breast cancer metastasis by regulating [alpha]6- and [beta]1-integrin-dependent cell adhesion and anoikis resistance. Oncogene. 2013;32:5582–92.
21. Guo C, Stark GR. FER tyrosine kinase (FER) overexpression mediates resistance to quinacrine through EGF-dependent activation of NF-kappaB. Proc Natl Acad Sci USA. 2011;108:7968–73.
22. Ahn J, Truesdell P, Meens J, Kadish C, Yang X, Boag AH, et al. Fer protein-tyrosine kinase promotes lung adenocarcinoma cell invasion and tumor metastasis. Mol Cancer Res. 2013;11:952–63.
23. Sangrar W, Shi C, Mullins G, LeBrun D, Ingalls B, Greer PA. Amplified Ras-MAPK signal states correlate with accelerated EGFR internalization, cytostasis and delayed HER2 tumor onset in Fer-deficient model systems. Oncogene. 2015;34:4109–17.
24. Fan G, Gao Y, Greer P, Tonks N. HGF-independent regulation of MET and Gab1 through non-receptor tyrosine kinase FER (609.4). FASEB J. 2014;28.
25. Lennartsson J, Ma H, Wardega P, Pelka K, Engstrom U, Hellberg C, et al. The Fer tyrosine kinase is important for platelet-derived growth factor-BB-induced signal transducer and activator of transcription 3 (STAT3) protein phosphorylation, colony formation in soft agar, and tumor growth in vivo. J Biol Chem. 2013;288:15736–44.
26. Voisset E, Lopez S, Chaix A, Georges C, Hanssens K, Prebet T, et al. FES kinases are required for oncogenic FLT3 signaling. Leukemia. 2010;24:721–728.
27. Liu BA, Engelmann BW, Jablonowski K, Higginbotham K, Stergachis AB, Nash PD. SRC homology 2 domain bbinding sites in insulin, IGF-1 and FGF receptor mediated signaling networks reveal an extensive potential interactome. Cell Commun Signal. 2012;10:27.
28. Ivanova IA, Vermeulen JF, Ercan C, Houthuijzen JM, Saig FA, Vlug EJ, et al. FER kinase promotes breast cancer metastasis by

regulating alpha6- and beta1-integrin-dependent cell adhesion and anoikis resistance. Oncogene. 2013;32:5582–92.
29. Vistein R, Puthenveedu MA. Src regulates sequence-dependent beta-2 adrenergic receptor recycling via cortactin phosphorylation. Traffic. 2014;15:1195–205.
30. Craig AWB, Zirngibl R, Williams K, Cole L-A, Greer PA. Mice devoid of Fer protein-tyrosine kinase activity are viable and fertile but display reduced cortactin phosphorylation. Mol Cell Biol. 2001;21:603–13.
31. Cao H, Weller S, Orth JD, Chen J, Huang B, Chen JL, et al. Actin and Arf1-dependent recruitment of a cortactin-dynamin complex to the Golgi regulates post-Golgi transport. Nat Cell Biol. 2005;7:483–92.
32. Szasz AM, Lanczky A, Nagy A, Forster S, Hark K, Green JE, et al. Cross-validation of survival associated biomarkers in gastric cancer using transcriptomic data of 1,065 patients. Oncotarget. 2016;7:49322–33.
33. Malaguarnera R, Belfiore A. The emerging role of insulin and insulin-like growth factor signaling in cancer stem cells. Front Endocrinol. 2014;5:10.
34. Marcotte R, Sayad A, Brown KR, Sanchez-Garcia F, Reimand J, Haider M, et al. Functional genomic landscape of human breast cancer drivers, vulnerabilities, and resistance. Cell. 2016;164:293–309.
35. Wu RF, Liao C, Fu G, Hayenga HN, Yang K, Ma Z, et al. p66Shc couples mechanical signals to RhoA through FAK-dependent recruitment of p115-RhoGEF and GEF-H1. Mol Cell Biol. 2016;36:2824–37.
36. Zhang S, Anjum R, Squillace R, Nadworny S, Zhou T, Keats J, et al. The potent ALK inhibitor brigatinib (AP26113) overcomes mechanisms of resistance to first- and second-generation ALK inhibitors in preclinical models. Clin Cancer Res. 2016;22:5527–38.
37. Hellwig S, Miduturu CV, Kanda S, Zhang J, Filippakopoulos P, Salah E, et al. Small molecule inhibitors of the c-Fes protein-tyrosine kinase. Chem Biol. 2012;19:529–40.
38. Charafe-Jauffret E, Ginestier C, Monville F, Finetti P, Adelaide J, Cervera N, et al. Gene expression profiling of breast cell lines identifies potential new basal markers. Oncogene. 2006;25:2273–84.
39. Zhang W, Zong CS, Hermanto U, Lopez-Bergami P, Ronai Ze, Wang L-H. RACK1 recruits STAT3 specifically to insulin and insulin-like growth factor 1 receptors for activation, which is important for regulating anchorage-independent growth. Mol Cell Biol. 2006;26:413–24.
40. Ivaska J, Heino J. Cooperation between integrins and growth factor receptors in signaling and endocytosis. Annu Rev Cell Dev Biol. 2011;27:291–320.
41. Muharram G, Sahgal P, Korpela T, De Franceschi N, Kaukonen R, Clark K, et al. Tensin-4-dependent MET stabilization Is essential for survival and proliferation in carcinoma cells. Dev Cell. 2014;29:421–36.
42. Oneyama C, Yoshikawa Y, Ninomiya Y, Iino T, Tsukita S, Okada M. Fer tyrosine kinase oligomer mediates and amplifies Src-induced tumor progression. Oncogene. 2016;35:501–12.
43. Itoh T, Hasegawa J, Tsujita K, Kanaho Y, Takenawa T. The tyrosine kinase Fer is a downstream target of the PLD-PA pathway that regulates cell migration. Sci Signal. 2009;2:ra52.
44. van Rossum A, Gibcus J, van der Wal J, Schuuring E. Cortactin overexpression results in sustained epidermal growth factor receptor signaling by preventing ligand-induced receptor degradation in human carcinoma cells. Breast Cancer Res. 2005;7:235–7.
45. Yoneyama T, Angata K, Bao X, Courtneidge S, Chanda SK, Fukuda M. Fer kinase regulates cell migration through α-dystroglycan glycosylation. Mol Biol Cell. 2012;23:771–80.
46. Osorio FG, Soria-Valles C, Santiago-Fernandez O, Bernal T, Mittelbrunn M, Colado E, et al. Loss of the proteostasis factor AIRAPL causes myeloid transformation by deregulating IGF-1 signaling. Nat Med. 2016;22:91–6.
47. Li H, Batth IS, Qu X, Xu L, Song N, Wang R, et al. IGF-IR signaling in epithelial to mesenchymal transition and targeting IGF-IR therapy: overview and new insights. Mol Cancer 2017;16:6.
48. Graham TR, Zhau HE, Odero-Marah VA, Osunkoya AO, Kimbro KS, Tighiouart M, et al. Insulin-like growth factor-I-dependent up-regulation of ZEB1 drives epithelial-to-mesenchymal transition in human prostate cancer cells. Cancer Res. 2008;68:2479–88.
49. Muellner MK, Mair B, Ibrahim Y, Kerzendorfer C, Lechtermann H, Trefzer C, et al. Targeting a cell state common to triple-negative breast cancers. Mol Syst Biol. 2015;11:789.
50. Zheng D, Golubovskaya V, Kurenova E, Wood C, Massoll NA, Ostrov D, et al. A novel strategy to inhibit FAK and IGF-1R decreases growth of pancreatic cancer xenografts. Mol Carcinog. 2010;49:200–9.
51. Deevi RK, Cox OT, O'Connor R. Essential function for PDLIM2 in cell polarization in three-dimensional cultures by feedback regulation of the beta1-integrin-RhoA signaling axis. Neoplasia. 2014;16:422–31.

8.2 IGF-1 RECEPTOR ACTIVITY IN THE GOLGI OF MIGRATORY CANCER CELLS DEPENDS ON ADHESION-DEPENDENT PHOSPHORYLATION OF TYR^{1250} AND TYR^{1251}

Science Signaling

26 MAY 2020



AAAS

CELL BIOLOGY

Copyright © 2020 The Authors, some rights reserved; exclusive licensee American Association for the Advancement of Science. No claim to original U.S. Government Works

IGF-1 receptor activity in the Golgi of migratory cancer cells depends on adhesion-dependent phosphorylation of Tyr^{1250} and Tyr^{1251}

Leonie Rieger, Sandra O'Shea, Grant Godsmark, Joanna Stanicka, Geraldine Kelly, Rosemary O'Connor*

Although insulin-like growth factor 1 (IGF-1) signaling promotes tumor growth and cancer progression, therapies that target the IGF-1 receptor (IGF-1R) have shown poor clinical efficacy. To address IGF-1R activity in cancer cells and how it differs from that of the closely related insulin receptor (IR), we focused on two tyrosines in the IGF-1R C-terminal tail that are not present in the IR and are essential for IGF-1–mediated cancer cell survival, migration, and tumorigenic growth. We found that Tyr^{1250} and Tyr^{1251} ($Tyr^{1250/1251}$) were autophosphorylated in a cell adhesion–dependent manner. To investigate the consequences of this phosphorylation, we generated phosphomimetic Y1250E/Y1251E (EE) and nonphosphorylatable Y1250F/Y1251F (FF) mutant forms of IGF-1R. Although fully competent in kinase activity and signaling, the EE mutant was more rapidly internalized and degraded than either the wild-type or FF receptor. IGF-1 promoted the accumulation of wild-type and EE IGF-1R within the Golgi apparatus, whereas the FF mutant remained at the plasma membrane. Golgi-associated IGF-1R signaling was a feature of migratory cancer cells, and Golgi disruption impaired IGF-1–induced signaling and cell migration. Upon the formation of new cell adhesions, IGF-1R transiently relocalized to the plasma membrane from the Golgi. Thus, phosphorylation at $Tyr^{1250/1251}$ promoted IGF-1R translocation to and signaling from the Golgi to support an aggressive cancer phenotype. This process distinguishes IGF-1R from IR signaling and could contribute to the poor clinical efficacy of antibodies that target IGF-1R on the cell surface.

INTRODUCTION

The receptor tyrosine kinase (RTK) insulin-like growth factor 1 receptor (IGF-1R) and its ligands (IGF-1 and IGF-2) are widely present throughout different cell and tissue types and play essential roles in cell, organ, and organismal growth (*1*, *2*). The IGF system is also linked to cancer risk, tumorigenesis, and tumor growth and survival and to promoting cell migration in both normal and transformed cells (*3*–*6*). Many preclinical studies have shown a clear effect of IGF-1R suppression or inhibition on limiting tumorigenesis, tumor growth, and metastatic potential (*3*, *4*, *6*). However, this has not been replicated in large-scale clinical trials, wherein IGF-1R–blocking antibodies and kinase inhibitors show an overall poor efficacy (*3*, *4*). There are no predictive biomarkers for IGF-1R activity, and there is limited understanding of the cellular signaling events that promote resistance to or evasion of IGF-1R inhibitors.

Although IGF-1 signaling in cancer cells has been extensively studied, it is still poorly understood how IGF-1R expression, abundance, and signaling output are influenced by oncogenic and adhesion signals in different cancers. Amounts of cell surface IGF-1R may not predict responses to ligand stimulation in terms of downstream signaling output, and this is apparently influenced by the cancer cell phenotype, such as migratory versus nonmigratory (*7*). We and others previously demonstrated that adhesion signals enhance IGF-1R activation and signaling and that integrin-mediated signaling is essential for IGF-1 to promote cancer cell proliferation and migration [reviewed in (*8*)]. Moreover, the association of IGF-1R with E-cadherin and with discoidin domain receptors, which are RTKs activated by binding to collagen, can control receptor stability and signaling output (*9*–*11*).

Cooperation between integrin β1 and IGF-1R signaling involves an adhesion-dependent signaling complex composed of scaffolding proteins, focal adhesion kinase (FAK), and phosphatases that ultimately leads to activation of mitogen-activated protein kinase (MAPK) pathways (*12*–*15*). Mutation of two tyrosines (Tyr^{1250} and Tyr^{1251}) in the C-terminal tail of IGF-1R is sufficient to abrogate the receptor's function in facilitating cellular transformation, cell survival, and migration (*16*–*18*). These tyrosine residues were also found to be essential for integrating IGF-1R and adhesion signaling (*14*). However, these tyrosines are not present in the human insulin receptor (IR), which has an almost identical kinase domain to the IGF-1R but shares less than 50% homology with the C-terminal tail. We previously hypothesized that the function of these tyrosines may distinguish IGF-1R and IR actions in cell growth and cancer (*14*, *17*, *19*). However, despite the clear loss of IGF-1R function observed upon mutation of Tyr^{1250} and Tyr^{1251} ($Tyr^{1250/1251}$) to phenylanines (Y1250F/Y1251F), and in silico predictions for phosphorylation in cells (*14*, *16*–*21*), evidence for actual phosphorylation in vivo has remained elusive, as has knowledge of how this phospho-site functions. This has hindered efforts to understand how these IGF-1R tyrosines facilitate tumorigenesis or how this site may distinguish IGF-1R and IR signaling.

In this study, using mass spectroscopy and phospho-specific antibodies, we established that the IGF-1R was basally autophosphorylated on $Tyr^{1250/1251}$ in cells, and this depended on IGF-1 and adhesion signaling. We determined the functions of $Tyr^{1250/1251}$ phosphorylation by using a phosphomimetic mutant (Y1250E/Y1251E, referred to as the EE mutant) form of IGF-1R, which was more rapidly internalized and less stable than the wild-type (WT) IGF-1R or the

Cell Biology Laboratory, School of Biochemistry and Cell Biology, BioSciences Institute, University College Cork, Cork, Ireland.
*Corresponding author. Email: r.oconnor@ucc.ie

Downloaded from http://stke.sciencemag.org/ on May 26, 2020

Y1250F/Y1251F (FF) mutant. Upon IGF-1 stimulation, both the WT and the EE mutant IGF-1R rapidly accumulated within the Golgi apparatus, whereas the FF mutant was retained on the plasma membrane. IGF-1R localization in the Golgi apparatus was associated with migratory potential, and an intact Golgi apparatus was required for IGF-1R signaling in migrating cells. Overall, the data indicate that $Tyr^{1250/1251}$ phosphorylation drives translocation of IGF-1R to the Golgi, where it contributes to a migratory phenotype. These results distinguish IGF-1R and IR function and may also explain the inefficacy of targeting cell surface IGF-1R with monoclonal antibodies in several cancers.

RESULTS

Phosphorylation of IGF-1R on $Tyr^{1250/1251}$ occurs in cells

First, to address the question whether the $Tyr^{1250/1251}$ site becomes phosphorylated in cells, we used mass spectroscopy and phosphopeptide analysis of IGF-1R immunoprecipitated from mouse embryonic fibroblasts derived from IGF-1R knockout (KO) mice (R- cells) transiently expressing the receptor and either serum-starved or stimulated with IGF-1. The isolation of IGF-1R phosphopeptides including $Tyr^{1250/1251}$ was less efficient than isolation of other phosphopeptides from the receptor, which we attributed to the fact that these tyrosines reside within a sequence (SFYYS) that also includes phosphorylated serines (*20*, *22*), and would thus be highly charged and difficult to capture. After peptide extraction and mass spectrometry analysis, a series of phosphopeptides was identified (ion score > 19) containing tyrosines that are known to be phosphorylated in response to IGF-1, including Tyr^{950} and the kinase activation site tyrosines Tyr^{1131}, Tyr^{1135}, and Tyr^{1136} (Fig. 1A). In addition, phosphopeptides were captured from both serum-starved and IGF-1–stimulated cells with phosphorylation on the Tyr^{1250} site, with a higher score indicating IGF-1–induced phosphorylation (Fig. 1A).

We next used an antibody specific for the phosphorylated $Tyr^{1250/1251}$ site to further assess $Tyr^{1250/1251}$ phosphorylation over time in response to either serum starvation or IGF-1. In phosphopeptide arrays, an antibody known to recognize phosphorylated Tyr^{1250} also detected peptides containing either the single phosphorylated site or the doubly phosphorylated site (fig. S1, A and B), and we therefore concluded that this antibody reacts with the $Tyr^{1250/1251}$ phosphosite. We next compared the profile of IGF-1–stimulated phosphorylation of the $Tyr^{1250/1251}$ phosphosite with the IGF-1R autophosphorylation sites Tyr^{950}, Tyr^{1131}, and $Tyr^{1135/1136}$. This analysis demonstrated that basal amounts of Tyr^{950}, Tyr^{1131}, and $Tyr^{1135/1136}$ phosphorylation were low and then rapidly induced by IGF-1 at 1 to 5 min. In contrast, basal phosphorylation of $Tyr^{1250/1251}$ was evident in serum-starved cells, and IGF-1–induced phosphorylation at this site accumulated more slowly than it did at the other sites (Fig. 1B). This result is consistent with the mass spectrometry analysis indicating phosphorylation in serum-starved cells (Fig. 1A).

Although IGF-1 displays greater affinity for IGF-1R than for IR, and insulin displays greater affinity for IR than for IGF-1R, each can activate the other receptor when the ligand concentration is high. Therefore, we investigated whether $Tyr^{1250/1251}$ phosphorylation was influenced by ligand concentration in serum-starved R- cells expressing WT IGF-1R stimulated with IGF-1 (either 1, 10, 50, or 100 ng/ml). From this, we observed that $Tyr^{1250/1251}$ phosphorylation was induced in a dose-responsive manner with the highest amounts of phosphorylation reached at 50 ng/ml (Fig. 1C). Insulin did not induce phosphorylation on $Tyr^{1250/1251}$ even at 100 ng/ml, although it modestly induced phosphorylation of the kinase AKT, which is known to mediate activation of the mammalian target of rapamycin pathway, metabolism, growth, and survival, but not phosphorylation of extracellular signal–regulated kinase (ERK), known to promote mitogenic, differentiation, and migratory signals, at this concentration (Fig. 1D). IGF-2 also induced $Tyr^{1250/1251}$ phosphorylation (Fig. 1D). We also observed phosphorylation on $Tyr^{1250/1251}$ of endogenous IGF-1R in the cancer cell lines MDA-MB-231, Cal-51, HS-578T, and DU-145 (Fig. 1E). Again, $Tyr^{1250/1251}$ phosphorylation was observed in serum-starved cells, and this increased upon IGF-1 stimulation (Fig. 1E). Together, these data demonstrate that $Tyr^{1250/1251}$ phosphorylation was present in cells at low basal amounts and was induced by IGF-1 in a concentration- and time-dependent manner.

Adhesion signals and IGF-1R kinase activity are required for $Tyr^{1250/1251}$ phosphorylation

Because IGF-1 enhanced phosphorylation of IGR-1R at $Tyr^{1250/1251}$ and this phosphorylation event had not previously been demonstrated in cells, we next investigated whether it was a bona fide autophosphorylation site in IGF-1R. The first approach was to determine whether $Tyr^{1250/1251}$ phosphorylation could be induced in the presence of an inhibitor of IGF-1R kinase activity. In serum-starved cells, $Tyr^{1250/1251}$ phosphorylation was not affected by the IGF-1R kinase inhibitor BMS-754807 (Fig. 2A). However, IGF-1–mediated enhancement of $Tyr^{1250/1251}$ phosphorylation was abolished by the kinase inhibitor, indicating that IGF-1–induced phosphorylation of $Tyr^{1250/1251}$ was likely a result of autophosphorylation. To further test autophosphorylation, we assessed autophosphorylation of WT IGF-1R and a kinase-inactive form of IGF-1R (K1003R, an adenosine triphosphate (ATP)–binding site mutant, referred to henceforth as KR), in the absence or presence of exogenously added ATP to stimulate kinase activity. Although phosphorylation on $Tyr^{1250/1251}$ was detectable on both the WT and KR receptors, this was increased by exogenous ATP on the WT but not on the KR receptor (Fig. 2B). This indicates that IGF-1R kinase activity was required for phosphorylation on $Tyr^{1250/1251}$. The observation that phosphorylation was evident with the KR mutant and with WT IGF-1R in serum-starved cells also suggests that other cellular kinases may phosphorylate $Tyr^{1250/1251}$.

Previous studies have shown that the $Tyr^{1250/1251}$ site is required for cooperative IGF-1R and adhesion signaling (*14*) and that IGF-1R kinase activity is influenced by adhesion signaling and adhesion-associated kinases (*23*, *24*). Therefore, we asked whether adhesion-activated kinases [feline sarcoma-related (FER), FAK, and Src] contributed to $Tyr^{1250/1251}$ phosphorylation. To test this, we used Cal-51 breast cancer cells, in which IGF-1 and adhesion signaling are active (*10*, *25*), and measured IGF-1–induced phosphorylation at the $Tyr^{1250/1251}$ site and at the $Tyr^{1135/1136}$ site, which is required for full kinase activation, in the presence of either the IGF-1R kinase inhibitor BMS-754807, a FER kinase inhibitor (AP-26113), a FAK kinase inhibitor (PF-573228), or a Src kinase inhibitor (PP2) (Fig. 2C). We observed that IGF-1–induced phosphorylation on both sites was decreased by BMS, AP-26113, and PF-573228 but not by PP2 (Fig. 2C). Thus, inhibition of IGF-1R, FER, or FAK kinase activity suppressed IGF-1R autophosphorylation and full kinase activation. A requirement for adhesion signaling in full IGF-1R autophosphorylation was also observed with cells that were detached from the

Downloaded from http://stke.sciencemag.org/ on May 26, 2020

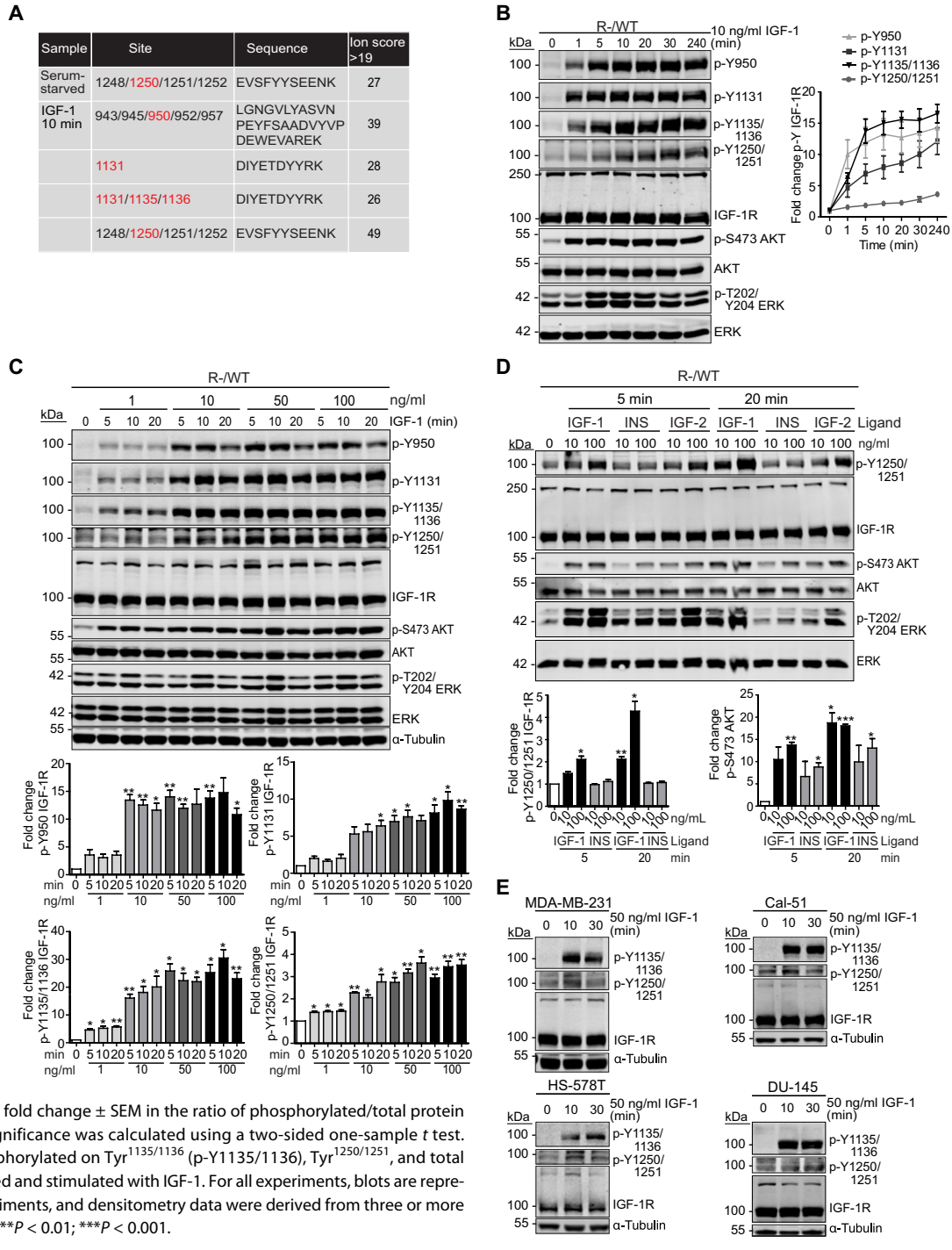


Fig. 1. Tyr$^{1250/1251}$ phosphorylation in cells. (**A**) Phophopeptides identified by mass spectroscopy from IGF-1R immunoprecipitated from R- cells stably expressing WT IGF-1R (R-/WT cells) after serum starvation or exposure to IGF-1. Phosphorylated (p-) IGF-1R tyrosines are indicated in red. (**B**) Immunoblotting for and quantification of the indicated phosphotyrosines (p-Y) in IGF-1R, the indicated phosphorylated forms of AKT and ERK, and total IGF-1R, AKT, and ERK from whole lysates of R-/WT cells. Total AKT and ERK are loading controls. Phosphotyrosine-containing proteins were quantified by densitometry, normalized to the protein loading control (total AKT, total ERK, and IGF-1R), and presented as average fold change ± SEM in the ratio of phosphorylated/total protein relative to the control condition (set to 1). (**C**) Immunoblotting for and quantification of the indicated phosphorylated forms of IGF-1R, total IGF-1R, ERK phosphorylated on Tyr^{202} and Tyr^{204} (p-T202/Y204), and total ERK from R-/WT cells stimulated with IGF-1 at the indicated concentrations and times after serum starvation. Quantification of phosphorylated/total IGF-1R is expressed as average fold change ± SEM relative to the control condition (set to 1). Significance was calculated using a two-sided one-sample *t* test. (**D**) Immunoblotting for and quantification of phosphorylated Tyr$^{1250/1251}$ in IGF-1R (p-Y1250/1251), total IGF-1R, AKT phosphorylated at Ser^{473}, total AKT, ERK phosphorylated at Thr^{202} and Tyr^{204}, and total ERK from R-/WT cells stimulated with IGF-1, IGF-2, or insulin (INS). Densitometry quantification is presented as the average fold change ± SEM in the ratio of phosphorylated/total protein relative to the control condition. Significance was calculated using a two-sided one-sample *t* test. (**E**) Immunoblotting for IGF-1R phosphorylated on Tyr$^{1135/1136}$ (p-Y1135/1136), Tyr$^{1250/1251}$, and total IGF-1R from cancer cells serum-starved and stimulated with IGF-1. For all experiments, blots are representative of $n \geq 3$ independent experiments, and densitometry data were derived from three or more independent experiments. *$P < 0.05$; **$P < 0.01$; ***$P < 0.001$.

substratum. IGF-1–stimulated phosphorylation of the Tyr^{950}, Tyr^{1131}, Tyr$^{1135/1136}$, and Tyr$^{1250/1251}$ sites was reduced by detachment of R- cells expressing WT IGF-1R, as well as by detachment of Cal-51 and DU-145 cancer cells (Fig. 2, D and E). IGF-1–induced activation of AKT and ERK was also reduced in detached cells compared to adherent cells (Fig. 2, D and E). We conclude that both IGF-1R and adhesion signaling were essential for maximal phosphorylation of the IGF-1R on Tyr$^{1250/1251}$ and that cell adhesion enhanced overall IGF-1R autophosphorylation and activation.

A Tyr$^{1250/1251}$ phosphomimetic mutant IGF-1R is fully active but rapidly turned over

The next question to be addressed was how phosphorylation on the Tyr$^{1250/1251}$ site contributed to IGF-1R function and signaling. To address this, we generated a phosphomimetic for this site, a mutant IGF-1R with tyrosines Tyr$^{1250/1251}$ substituted by negatively charged glutamic acids, the EE mutant. When transiently transfected into either R- cells or three different cancer cell lines (MCF-7, MDA-MB-231, and DU-145) in which the IGF-1R was knocked out by

Downloaded from http://stke.sciencemag.org/ on May 26, 2020

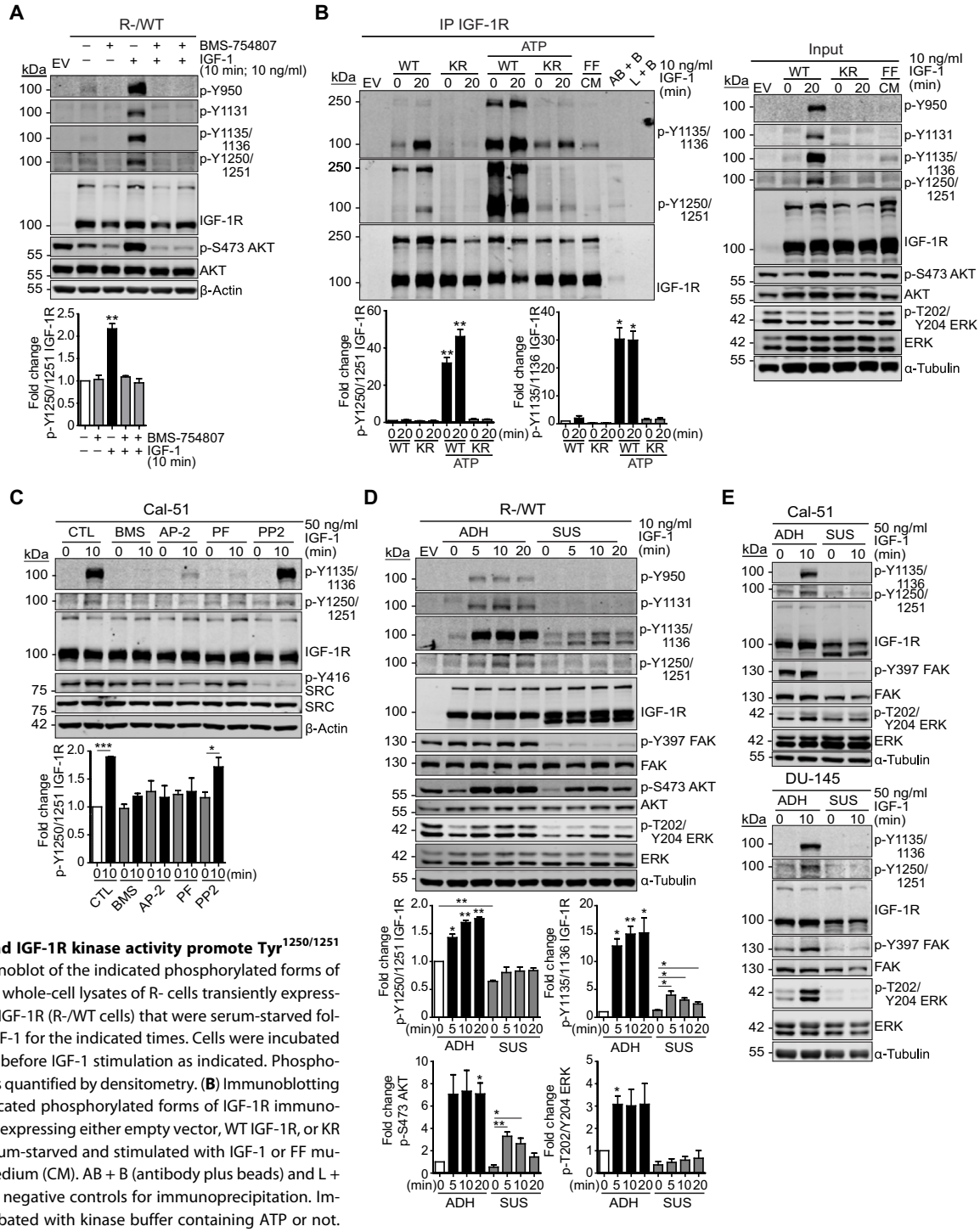


Fig. 2. Adhesion signals and IGF-1R kinase activity promote Tyr$^{1250/1251}$ phosphorylation. (**A**) Immunoblot of the indicated phosphorylated forms of IGF-1R and total IGF-1R from whole-cell lysates of R- cells transiently expressing empty vector (EV) or WT IGF-1R (R-/WT cells) that were serum-starved followed by stimulation with IGF-1 for the indicated times. Cells were incubated with BMS-754807 for 1 hour before IGF-1 stimulation as indicated. Phosphorylated Tyr$^{1250/1251}$ IGF-1R was quantified by densitometry. (**B**) Immunoblotting for the total IGF-1R and indicated phosphorylated forms of IGF-1R immunoprecipitated (IP) from R- cells expressing either empty vector, WT IGF-1R, or KR mutant IGF-1R that were serum-starved and stimulated with IGF-1 or FF mutant cultured in complete medium (CM). AB + B (antibody plus beads) and L + B (cell lysate plus beads) are negative controls for immunoprecipitation. Immunoprecipitates were incubated with kinase buffer containing ATP or not. IGF-1Rs phosphorylated on Tyr$^{1250/1251}$ and on Tyr$^{1135/1136}$ were quantified by densitometry. Protein input is shown in immunoblots for phosphorylated and total IGF-1R, AKT, and ERK. (**C**) Immunoblotting for and analysis of the indicated phosphorylated forms of IGF-1R and Src, total IGF-1R, and total Src from Cal-51 cells that were serum-starved, exposed to kinase inhibitors [BMS, BMS-754807 (IGF-1R inhibitor); AP-2, AP-26113 (FER inhibitor); PF, PF-573228 (FAK inhibitor); and PP2 (Src inhibitor)], and then stimulated with IGF-1. IGF-1R phosphorylated on Tyr$^{1250/1251}$ IGF-1R was quantified by densitometry. (**D**) Immunoblotting for the indicated phosphorylated forms of IGF-1R, FAK, AKT, and ERK and total IGF-1R, FAK, AKT, and ERK from adherent (ADH) and suspension-cultured (SUS) R-/WT cells stimulated with IGF-1 for the indicated times after serum starvation. The amounts of IGF-1R phosphorylated on Tyr$^{1250/1251}$ and on Tyr$^{1135/1136}$, AKT phosphorylated on Ser^{473}, and ERK phosphorylated on Thr^{202}/Tyr^{204} were quantified by densitometry. (**E**) Immunoblotting for the indicated phosphorylated forms of IGF-1R, FAK, and ERK and total IGF-1R, FAK, and ERK in adherent and suspension-cultured Cal-51 cells serum-starved and stimulated with IGF-1. For all experiments, densitometric quantification is presented as average fold change ± SEM in the ratio of phosphorylated/total protein relative to the control condition. Significance was calculated using a two-sided one-sample or two-sample *t* test. $n \geq 3$ independent experiments. *$P < 0.05$; **$P < 0.01$; ***$P < 0.001$.

Downloaded from http://stke.sciencemag.org/ on May 26, 2020

CRISPR technology, the EE mutant was consistently expressed at significantly lower levels than either the WT or FF IGF-1R (Fig. 3A). A similar pattern of lower receptor protein abundance was observed in R- cells stably expressing EE IGF-1R (fig. S2A), although mRNA expression across the transfected WT, FF, and EE constructs was similar (fig. S2B). Single mutation of either Tyr^{1250} or Tyr^{1251} to glutamic acid was also sufficient to impair receptor protein abundance compared to WT IGF-1R (fig. S2C).

Although present in lower amounts in cells, the EE mutant was observed to be functional and to mediate IGF-1–stimulated kinase activation and downstream signaling. Cells expressing either WT or EE IGF-1R exhibited similar IGF-1–stimulated AKT and ERK activation (Fig. 3B). The FF mutant exhibited lower IGF-1R and ERK activity than WT IGF-1R (Fig. 3B), which is consistent with previous studies (*19*). Transient overexpression of WT, FF, or EE IGF-1R in MDA-MB-231 IGF-1R KO cells (MDA-KO) also demonstrated that the activation of EE IGF-1R was comparable to that of WT IGF-1R, whereas it was higher than that of FF IGF-1R (Fig. 3C). In vitro kinase assays were used to compare the IGF-1R kinase activity of the EE mutant with WT IGF-1R and the FF mutant. In vitro EE IGF-1R kinase activity was similar to that of WT IGF-1R, whereas FF IGF-1R kinase activity was lower than that of WT IGF-1R (Fig. 3D), as also previously reported (*17*).

The lower cellular abundance of the EE mutant compared to WT IGF-1R and the FF mutant suggested that $Tyr^{1250/1251}$ phosphorylation influenced the translation or stability of the IGF-1R protein. We first ruled out the possibility that low EE protein was due to impaired protein synthesis by using cycloheximide (CHX) to transiently suppress protein synthesis and then assessing the amount of newly synthesized protein over time. In these experiments, it was clear that similar amounts of WT IGF-1R and mutant IGF-1Rs were restored after CHX exposure (Fig. 4A), thereby indicating similar amounts of synthesis. We next tested whether inhibition of proteasomal or lysosomal activity could restore EE IGF-1R protein in cells. The IGF-1R protein is synthesized as a proreceptor that is processed to yield an extracellular α chain and intracellular β chain. The functional receptor is a homodimer of two α chains and two β chains that are joined by disulfide bonds. Inhibition of proteasomal activity with MG-132 for 6 hours restored the EE β chain to protein abundances that were similar to those of WT IGF-1R and FF IGF-1R in control cells, and the abundance of the pro form of the receptor was also recovered (Fig. 4B). Lysosomal inhibition with E64D and leupeptin or chloroquine (CQ) did not affect EE protein abundance (Fig. 4C), indicating that the EE mutant was not more susceptible to lysosomal degradation than WT.

We also investigated whether stimulation of R- cells with high or low concentrations of IGF-1 influenced the degradation of the EE and WT IGF-1R compared to the FF IGF-1R. This demonstrated that IGF-1 stimulation at either high or low IGF-1 concentrations resulted in a similar reduction in amounts of the WT and EE receptors at 6 and 12 hours, whereas the abundance of the FF receptor was not significantly reduced after 6 hours and was comparable to its abundance in unstimulated cells (Fig. 4D). Thus, the FF mutant was protected from degradation. Together, these results demonstrate that the IGF-1R EE mutant was kinase active and responsive to IGF-1 but was less stable than WT IGF-1R. The data suggest that $Tyr^{1250/1251}$ phosphorylation accelerated IGF-1R protein turnover.

$Tyr^{1250/1251}$ phosphorylation promotes IGF-1R translocation to the Golgi apparatus

The EE IGF-1R mutant was highly active in signaling even with low amounts of protein in the cells, so we next investigated its subcellular location and compared IGF-1–stimulated internalization and trafficking of the EE receptor with that of the WT and FF receptors. Although, as expected, the WT receptor was mainly located on the cell membrane in serum-deprived cells, we observed that a pool of IGF-1R was located at the perinuclear region in these cells (Fig. 5A). In IGF-1–stimulated cells, both WT and EE receptors were visible in large intracellular vesicles. Over time, these vesicles appeared to accumulate at the perinuclear region and were less evident at the plasma membrane (Fig. 5A). These IGF-1R–containing vesicles were overall less evident in cells expressing the FF mutant receptor, in which the receptor was predominantly located at the plasma membrane (Fig. 5A). The relative translocation patterns of WT and EE IGF-1R in cells were illustrated by showing the intensity in IGF-1R fluorescence signal along a line that was drawn diagonally from cell membrane to cell membrane through the nucleus (Fig. 5B). Without IGF-1, cells expressing the EE mutant exhibited a clear peak in IGF-1R fluorescence signal close to the nucleus. This peak was less prominent in cells expressing WT IGF-1R and was not visible in cells expressing FF IGF-1R. Over time, cells expressing either WT or EE displayed a shift in IGF-1R fluorescence signal toward the nucleus and a reduction in signal intensity near the plasma membrane.

Receptor internalization was also assessed using in-cell Western assays to quantify the ratio of IGF-1R present at the plasma membrane relative to total amount of the receptor in cells that were stimulated with IGF-1. Whereas the amounts of the receptor at the cell surface declined in response to IGF-1 in cells expressing either the WT or EE receptors, the cell surface amounts of FF receptors were not altered (Fig. 5C). To test whether WT and EE IGF-1Rs were being actively internalized into vesicles, we used an antibody that recognizes the α chain of IGF-1R (IRα) and is known to induce IGF-1R internalization (*3*). R- cells expressing the WT, FF, or EE IGF-1R were serum-starved for 4 hours and cultured with the IRα antibody for 30 min either at 37°C (Fig. 5D) or on ice (fig. S3A) followed by staining with an antibody detecting the β chain of IGF-1R and immunofluorescence analysis for colocalization (Fig. 5D and fig. S3B). The IRα-specific antibody was internalized in vesicles after 30 min in cells expressing the WT or EE IGF-1R, whereas colocalization of IRα with the β chain was observed at the plasma membrane in cells expressing the FF mutant. We conclude that activated WT and EE IGF-1Rs were rapidly internalized into intracellular vesicles that accumulated at the perinuclear region over time. The observation that the FF mutant neither accumulated within vesicles nor underwent postendocytotic trafficking suggests that phosphorylation on $Tyr^{1250/1251}$ was required for internalization and accumulation of IGF-1R at the perinuclear region.

Postendocytic trafficking of surface receptors and proteins to the Golgi apparatus has been described as retrograde trafficking and a process that may be important for cell signaling (*26*, *27*). We therefore further investigated IGF-1R colocalization with the Golgi marker GM130 in cells expressing WT, FF, or EE IGF-1R. Over time, the WT and EE IGF-1Rs colocalized with GM130 at the cis-Golgi compartment (Fig. 6A). Colocalization of IGF-1R with a biotinylated form of the lectin *Vicia villosa* (VVA), which labels *N*-acetylgalactosamine and is a marker for both trans- and cis-Golgi, was also evident (Fig. 6B). The EE mutant was also observed at the Golgi apparatus in

Downloaded from http://stke.sciencemag.org/ on May 26, 2020

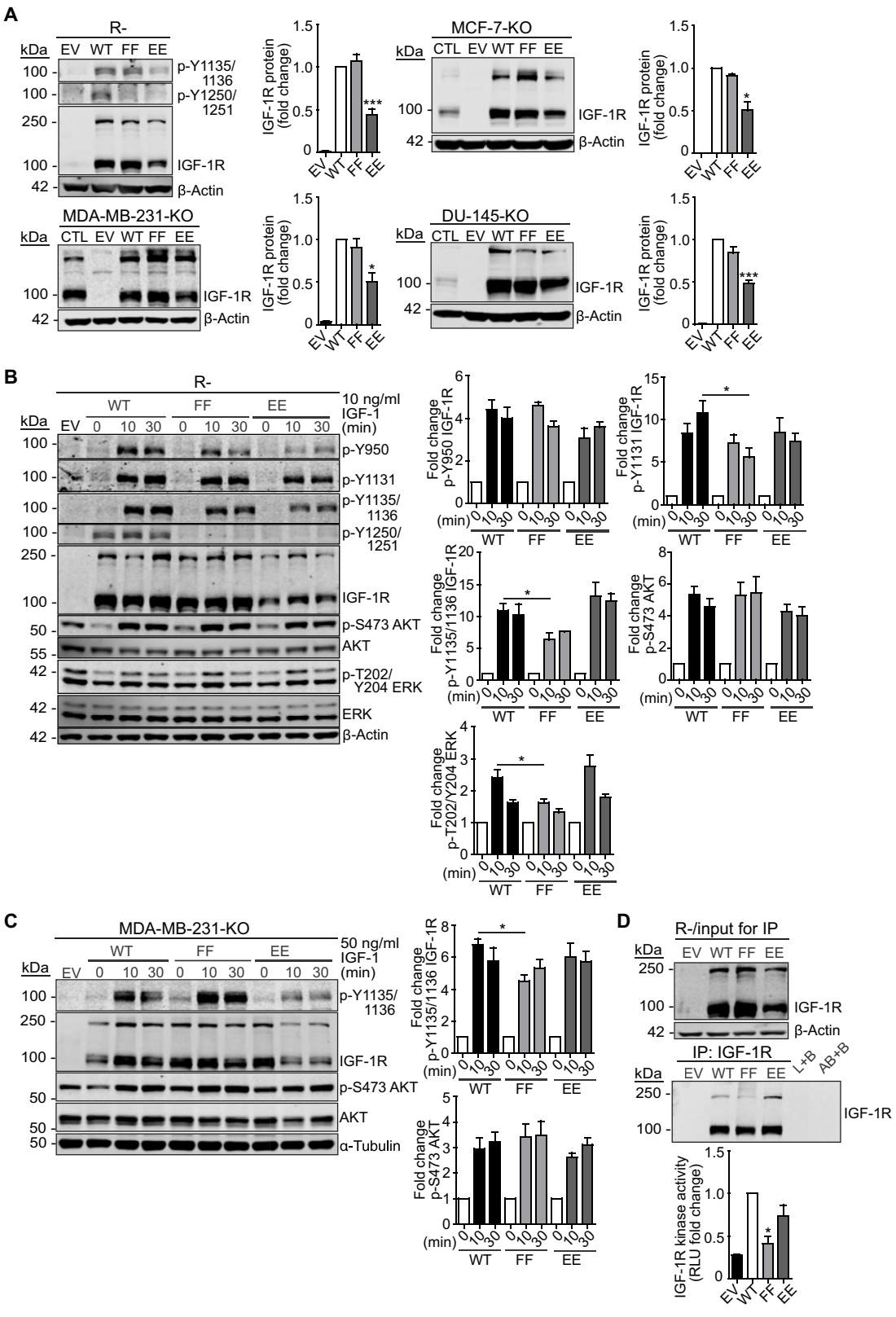


Fig. 3. Exogenously expressed Tyr$^{1250/1251}$ phosphomimetic (EE) IGF-1R is fully active. (**A**) Immunoblot of the indicated phosphorylated forms of IGF-1R and total IGF-R1 in R- cells and total IGF-1R in IGF-1R knockout (KO) MCF-7, MDA-MB-231, and DU-145 cells transiently expressing the WT, FF (Tyr$^{1250/1251}$ not phosphorylatable), or EE (Tyr$^{1250/1251}$ phosphomimetic) forms of IGF-1R. (**B**) Immunoblotting for the indicated phosphorylated forms of IGF-1R, AKT, and ERK and total IGF-1R, AKT, and ERK from R- cells transiently overexpressing the WT, FF, or EE form of IGF-1R and stimulated with IGF-1 for the indicated times after serum starvation. Significance was calculated using a two-sided two-sample *t* test. (**C**) Immunoblot of the indicated phosphorylated forms of IGF-1R and AKT and total IGF-1R and AKT in IGF-1R KO MDA-MB-231 cells transiently overexpressing IGF-1R WT, FF, or EE and stimulated with IGF-1 for the indicated times after serum starvation. For (A) to (C), densitometry quantification is presented as the average fold change ± SEM in ratio of phosphorylated/total protein relative to the control condition. $n \geq 3$ independent experiments. Significance was calculated using a two-sided two-sample *t* test. (**D**) Immunoblot of total IGF-1R from R- cells transiently overexpressing IGF-1R WT, FF, or EE used to determine protein input to immunoprecipitate for in vitro kinase assays followed by immunoblotting of immunoprecipitated IGF-1R (all adjusted to EE protein amounts). Kinase assay data are presented as average fold change ± SEM in kinase activity [measured in relative luciferase units (RLU)] relative to control condition (IGF-1R WT). $n = 3$ independent kinase preparations. Significance was calculated using two-sided one-sample *t* test. $^*P < 0.05$; $^{***}P < 0.001$.

serum-starved cells, suggesting that phosphorylation on Tyr$^{1250/1251}$ was sufficient for translocation to the Golgi. To further test whether WT and EE IGF-1Rs were present in the Golgi apparatus, we used brefeldin A (BFA) to induce cis-Golgi fragmentation (*28*) in R- cells expressing the WT, EE, or FF receptor. Fragmentation of the cis-Golgi resulted in lower amounts of WT and EE receptors (Fig. 6C),

Downloaded from http://stke.sciencemag.org/ on May 26, 2020

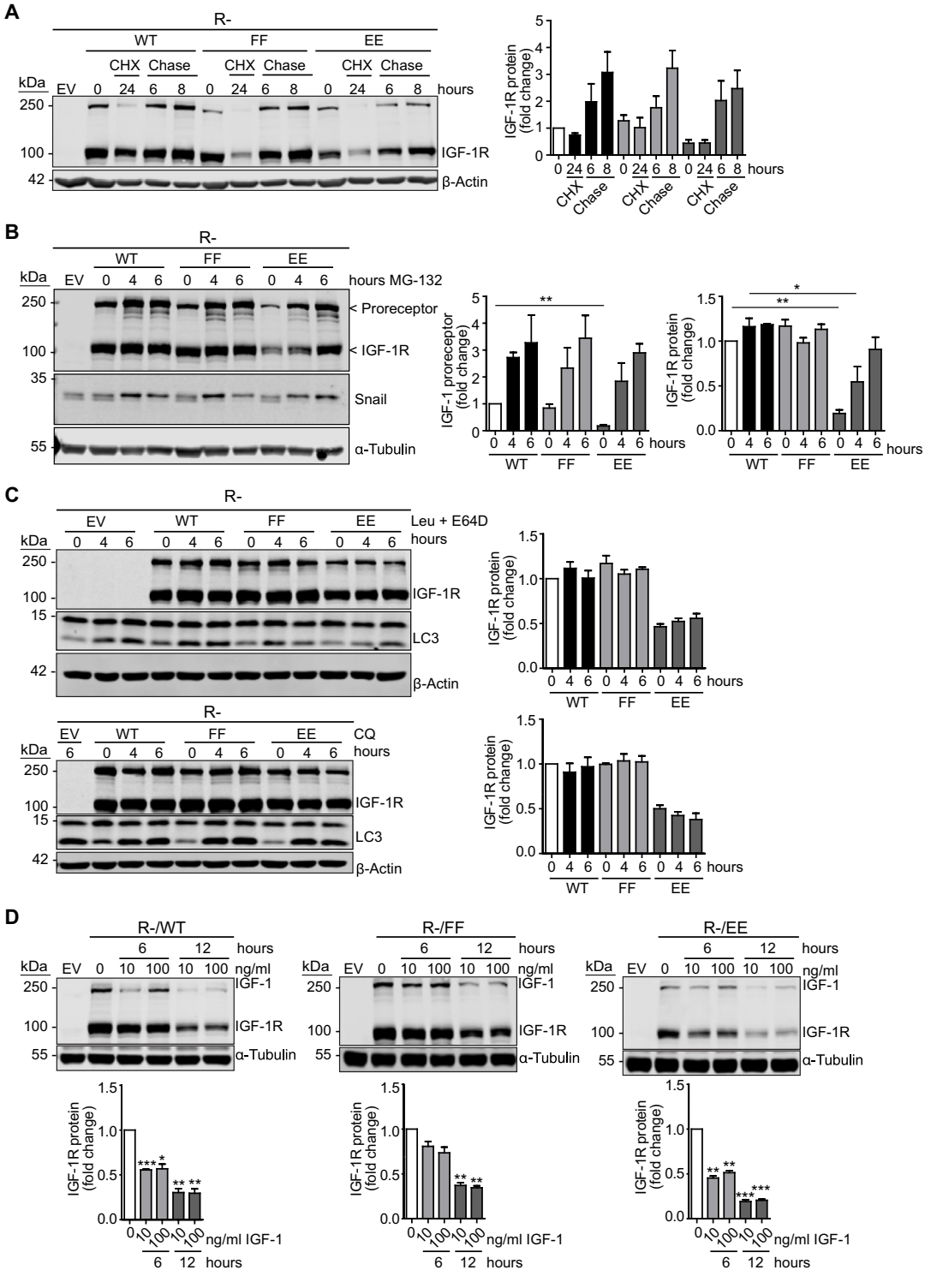


Fig. 4. The IGF-1R EE mutant is degraded more rapidly than WT IGF-1R. (**A**) Immunoblot for IGF-1R from R- cells transiently expressing IGF-1R WT, FF, or EE cultured in control medium (0 hours) or medium with cycloheximide (CHX) for 24 hours followed by culture in complete medium (chase). Densitometry quantification is presented as the average fold change ± SEM in IGF-1R protein relative to the control condition. $n = 3$ independent experiments. Significance was calculated using one-way ANOVA. (**B**) Immunoblot for total IGF-1R and Snail (Zinc finger protein SNAI1) from R- cells transiently expressing IGF-1R WT, FF, or EE cultured in control medium (0 hours) or medium containing the proteasome inhibitor MG-132. (**C**) Immunoblots for total IGF-1R and LC3 from cells transiently expressing IGF-1R WT, FF, or EE cultured in control medium (0 hours) or medium containing the lysosome inhibitors leupeptin and E64D (Leu + E64D) or chloroquine (CQ). (**D**) Immunoblots for IGF-1R from R- cells transiently expressing IGF-1R WT, FF, or EE stimulated with the indicated concentrations of IGF-1 for the indicated times. For (B) to (D), densitometry quantification is presented as average fold change ± SEM in IGF-1R protein relative to control condition. $n = 3$ independent experiments. Significance was calculated using a two-sided one-sample or two-sample *t* test. $^{*}P < 0.05$; $^{**}P < 0.01$; $^{***}P < 0.001$.

whereas BFA did not affect the FF mutant receptor. Together, these results indicate that IGF-1–induced internalization and accumulation of the IGF-1R in the Golgi apparatus required phosphorylation on $Tyr^{1250/1251}$.

$Tyr^{1250/1251}$ phosphorylation and adhesion signals promote IGF-1R presence in and signaling from the Golgi

The $Tyr^{1250/1251}$ site is required to support a transformed phenotype, cancer cell survival, cell migration, tumor growth, and metastasis in vivo (*3*, *18*, *29*). Because Golgi-derived signaling is implicated in cell migration (*30*), we hypothesized that $Tyr^{1250/1251}$ phosphorylation and IGF-1R Golgi localization may be a feature of migratory cancer cells. To test this, we compared IGF-1R localization in nonmigratory MCF-7 cancer cells to that in migratory MDA-MB-231 and HS-578T cells, both of which also exhibited relatively high IGF-1R $Tyr^{1250/1251}$ phosphorylation (Fig. 1E). Whereas the IGF-1R was evident at sites of focal adhesion (FA) in MCF-7 cells, it was also clearly located within the Golgi apparatus in MDA-MB-231 and HS-578T cells (Fig. 7A). IGF-1R abundance was reduced by the Golgi disruptor

Downloaded from http://stke.sciencemag.org/ on May 26, 2020

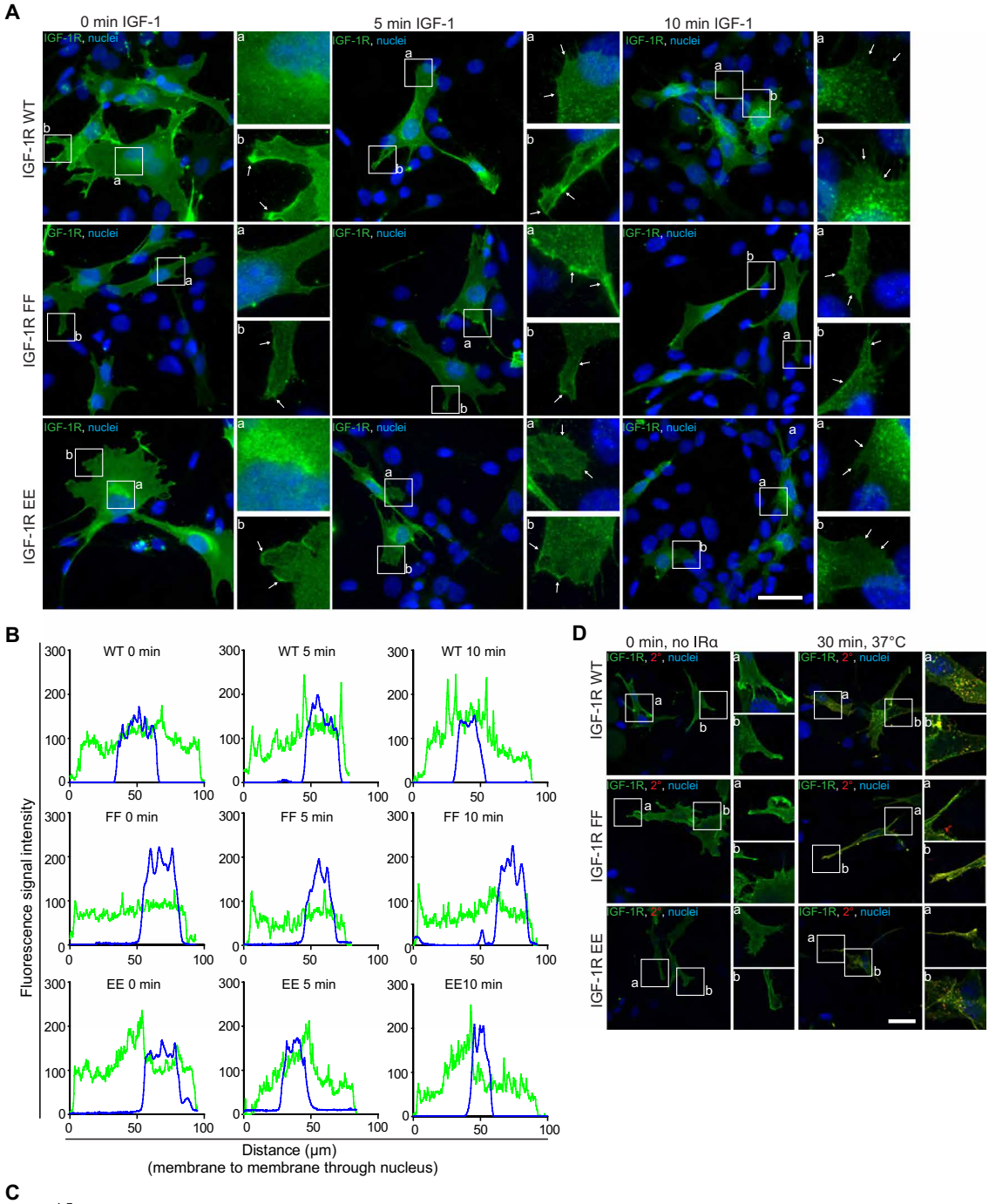


Fig. 5. Tyr$^{1250/1251}$ phosphorylation promotes IGF-1R internalization and translocation to the perinuclear region. (**A**) Immunofluorescence of R- cells transiently expressing the IGF-1R WT, FF, or EE mutant showing IGF-1R (green) and nuclei (blue) after serum starvation (0 min) or IGF-1 stimulation (5 and 10 min). Images are representative of $n \geq 4$ experiments. (**B**) IGF-1R staining intensity (green) in relation to the nuclear area (blue) measured using the RGB profiler from ImageJ software along a line drawn through the cell passing through the nucleus. (**C**) Results of in-cell Western assay from R- cells transiently transfected with WT, FF, or EE IGF-1R probed for total (TR) and surface (SR) IGF-1R. Densitometry quantification is presented as average fold change ± SEM in IGF-1R surface protein relative to the control condition. $n = 3$ independent experiments. Significance was calculated using a two-sided one-sample or two-sample *t* test. (**D**) Confocal microscopy showing R- cells transiently expressing the WT, FF, or EE IGF-1R that were serum-starved for 4 hours or incubated with an antibody binding to the IGF-1R α chain (IRα). Colocalization of IGF-1R IRα antibody [detected with secondary (2°) antibody, in red] and IGF-1Rβ (green) is indicated as a yellow signal. Images are representative of $n = 2$ independent experiments, each with $n \geq 3$ cells. *$P < 0.05$; **$P < 0.01$. Scale bars, 50 μm.

Downloaded from http://stke.sciencemag.org/ on May 26, 2020

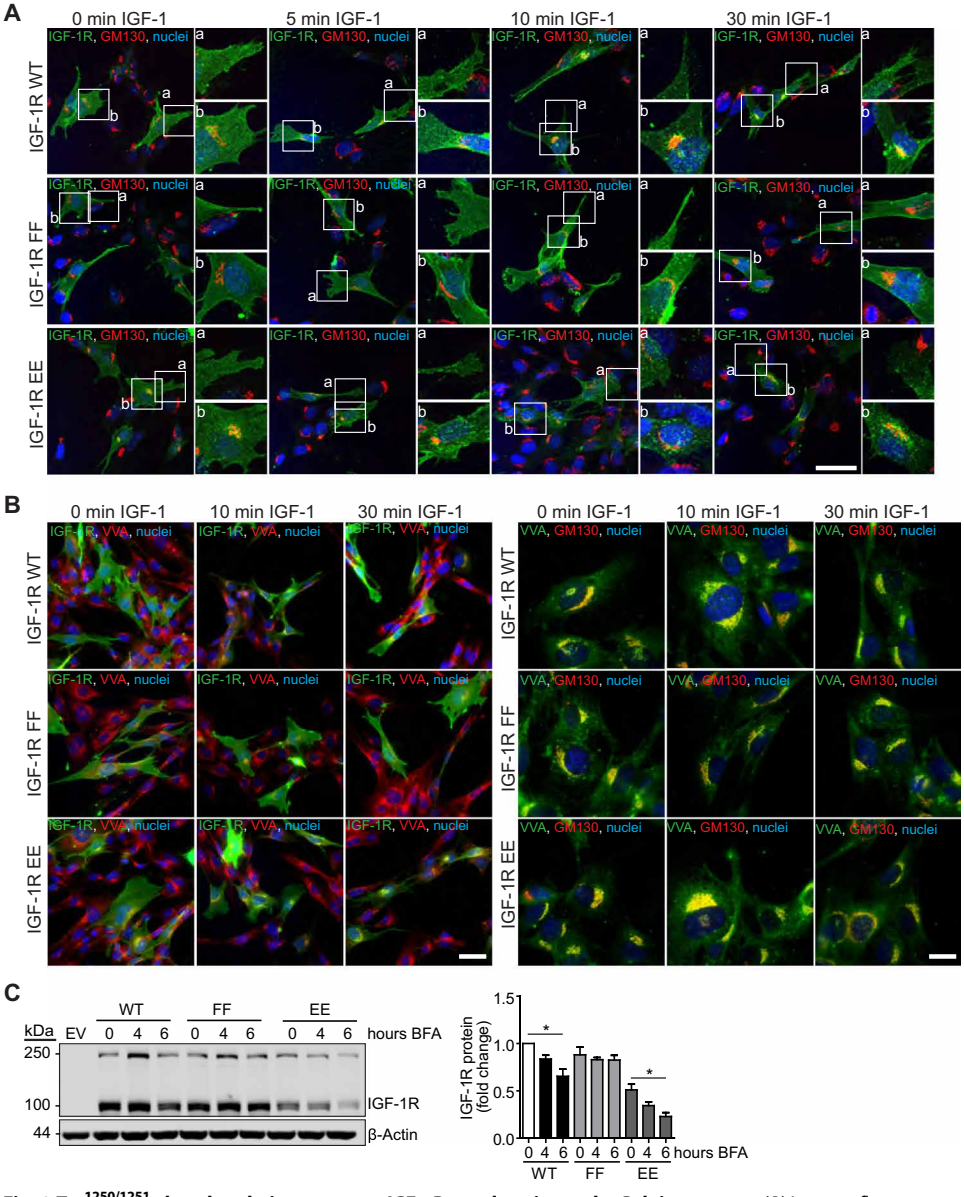


Fig. 6. Tyr$^{1250/1251}$ phosphorylation promotes IGF-1R translocation to the Golgi apparatus. (**A**) Immunofluorescence of R- cells expressing WT, FF, or EE IGF-1R that were either serum-starved (0 min) or stimulated with IGF-1 (5, 10, and 30 min) showing IGF-1R (green), the cis-Golgi marker GM130 (red), and nuclei (blue). Scale bar, 50 μm. Images are representatives of $n \geq 3$ independent experiments. (**B**) Immunofluorescence of R- cells expressing WT, FF, or EE IGF-1R after IGF-1 stimulation for the indicated times showing IGF-1R (green), the Golgi marker VVA (red or green) or GM130 (red), and nuclei (blue). Representative images of $n = 2$ independent experiments, with $n \geq 3$ images acquired for each experiment, are shown. Scale bars, 50 μm (IGF-1R and VVA) and 20 μm (VVA/GM130). (**C**) Immunoblot for total IGF-1R from R- cells transiently expressing WT, FF, or EE IGF-1R cultured in control medium (0 hours) or medium containing the Golgi disruptor brefeldin A (BFA). Densitometry quantification is presented as average fold change ± SEM in IGF-1R protein relative to the control condition. $n = 3$ independent experiments. Significance was calculated using a two-sided one-sample or two-sample *t* test. *$P < 0.05$.

BFA in MDA-MB-231 and HS-578T cells, but not in MCF-7 cells (Fig. 7B). Furthermore, although disruption of the Golgi with BFA did not alter the distribution of the IGF-1R at the plasma membrane in MCF-7 cells, BFA caused dispersal of the IGF-1R from the Golgi apparatus in MDA-MB-231 and HS-578T cells (Fig. 7C). In these cells, IGF-1R staining remained visible at the leading edge within lamellipodia. IGF-1–induced phosphorylation on Tyr$^{1250/1251}$ was detectable in both MCF-7 and HS-578T cells, but basal amounts of SHC [Src homology 2 (SH2) domain–containing] phosphorylation and IGF-1–induced SHC phosphorylation were impaired by BFA in HS-578T cells, but not in MCF-7 cells (Fig. 7D).

Because IGF-1R was observed at the lamellipodia of cells even when the Golgi was disrupted (Fig. 7C) and Tyr$^{1250/1251}$ phosphorylation required adhesion signaling (Fig. 2, C to E), we next investigated whether cell adhesion controlled IGF-1R localization at the plasma membrane or Golgi in MCF-7 and HS-578T cells. IGF-1R location and phosphorylation on Tyr$^{1250/1251}$ was monitored over time in response to the formation of nascent FA contacts in cells that were allowed to attach to fibronectin-coated plates and coverslips. Immunofluorescence showed that the IGF-1R was present at the plasma membrane in both cell types at 15 min after cell seeding (Fig. 8A). At this time, phosphorylation on Tyr$^{1250/1251}$ was low (Fig. 8B). In MCF-7 cells, the IGF-1R was observed in FAs at 30 min after cell seeding, and it remained there for up to 60 min (Fig. 8A). In HS-578T cells, most of the IGF-1R had moved from the plasma membrane to the Golgi at 30 min and was exclusively Golgi-localized by 60 min (Fig. 8A). In MCF-7 cells, phosphorylation on Tyr$^{1250/1251}$ remained low over time after cell adhesion, whereas in HS-578T cells, Tyr$^{1250/1251}$ phosphorylation increased over time after adhesion (Fig. 8B). These observations indicate that the IGF-1R was rapidly recruited to nascent FAs in HS-578T cells and that IGF-1R and adhesion-dependent Tyr$^{1250/1251}$ phosphorylation promoted subsequent translocation of the receptor to the Golgi.

Directed migration of epithelial cells requires the formation of leading edge protrusion and adhesion to the extracellular matrix (ECM), which involves the formation of new FAs (*30*). We therefore investigated whether the IGF-1R was recruited to FAs in migrating cells. At 6 hours after wounding a HS-578T cell monolayer, large FAs were visible at the leading edge of the migrating cells (Fig. 8C). In agreement with our earlier observations of IGF-1R at sites of adhesion in both migratory and nonmigratory cells (Fig. 7A), immunofluorescence analysis showed that the IGF-1R was clearly located within the protrusions of moving cells (Fig. 8C). In these cell cultures, it was also clear that the IGF-1R was predominantly located in the Golgi apparatus within cells that were part of the high-confluency

Downloaded from http://stke.sciencemag.org/ on May 26, 2020

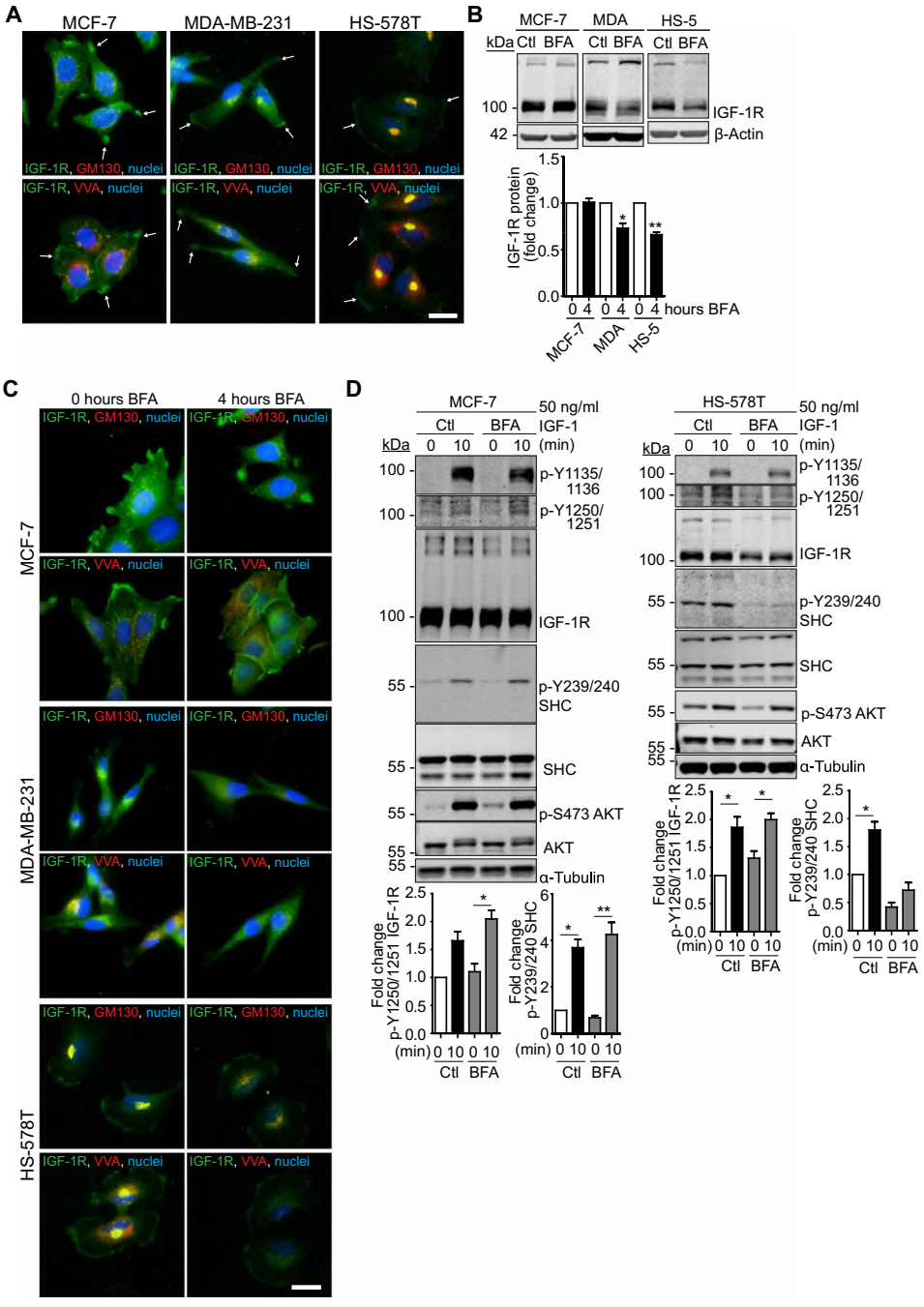


Fig. 7. Tyr$^{1250/1251}$ is phosphorylated in Golgi-localized IGF-1R in migratory cancer cells. (**A**) Immunofluorescence of MCF-7, MDA-MB-231, and HS578T cells stained to show IGF-1R (green) and either the cis-Golgi marker GM130 or the cis/trans-Golgi marker VVA (red). Images are representative of $n \geq 3$ independent experiments. (**B**) Immunoblot for IGF-1R from MCF-7, MDA-MB-231, and HS-578T cells cultured in control medium (0 hours) or medium containing the Golgi disruptor BFA for 4 hours. Densitometry quantification is presented as average fold change ± SEM in IGF-1R protein relative to the control condition. $n \geq 3$ independent experiments. Significance was calculated using a two-sided one-sample *t* test. (**C**) Immunofluorescence of MCF-7, MDA-MB-231, and HS-578T cells cultured in control medium (0 hours) or medium containing BFA for 4 hours and stained for IGF-1R (green) and either GM130 or VVA (red). Images are representatives of $n \geq 3$ independent experiments. (**D**) Immunoblot of the indicated phosphorylated forms of IGF-1R, SHC, and AKT and total IGR-1R, AKT, and SHC in lysates from MCF-7 and HS-578T cells stimulated with IGF-1 for the indicated time after 4-hour serum starvation in the presence or absence (Ctl) of BFA. Densitometry quantification is presented as the average fold change ± SEM in ratio of phosphorylated/total protein relative to the control condition. $n \geq 3$ independent experiments. Significance was calculated using a two-sided one-sample or two-sample *t* test. *$P < 0.05$; **$P < 0.01$. All scale bars, 20 μm.

monolayer. BFA abolished IGF-1–stimulated HS-578T cell migration (Fig. 8D), indicating that the Golgi apparatus is essential for IGF-1–promoted cell migration.

To better understand what promoted IGF-1R localization to the Golgi, we further assessed IGF-1R localization in MCF-7 and HS-578T cells that were cultured to either subconfluence, which allows for cell migration and cell-matrix contacts, or high confluence, which favors cell-cell adhesion. We observed that when cell-cell adherence was high in MCF-7 cells, the IGF-1R was located at the plasma membrane sites of cell-cell adhesion as previously described (*9*), whereas it was located at sites of focal cell adhesion in subconfluent cultures (Fig. 8E). In these MCF-7 cultures, basal phosphorylation on Tyr$^{1250/1251}$ was present, and IGF-1–induced phosphorylation of SHC was evident (Fig. 8F). In contrast, in subconfluent HS-578T cells, the IGF-1R was located at the leading edge and in the Golgi with significant IGF-1–induced phosphorylation of Tyr$^{1250/1251}$ evident, whereas in confluent cells, the IGF-1R was predominantly located in the Golgi (Fig. 8E), where constitutive Tyr$^{1250/1251}$ phosphorylation was evident (Fig. 8, E and F). HS-578T cells growing under high-confluency conditions exhibited little IGF-1–stimulated SHC phosphorylation (Fig. 8F). However, induction of phosphorylation on Tyr$^{1135/1136}$ and activation of AKT and ERK were present, confirming that the IGF-1R was active within the Golgi in these cells. Together, these data indicate that phosphorylation on Tyr$^{1250/1251}$ promoted the accumulation of IGF-1R in the Golgi. Within the Golgi, the IGF-1R was active and induced downstream signaling. On the other hand, cell-ECM adhesion signals during cell migration enhanced IGF-1–induced phosphorylation on Tyr$^{1250/1251}$, resulting in the IGF-1R being located both in the Golgi and at the leading edge of migrating cells.

DISCUSSION

Although IGF-1 signaling has a well-described function in facilitating tumorigenesis and promoting tumor growth, it is unresolved why the abundance of IGF-1R does not correlate with its activity in cancer cells and why IGF-1R–targeting

Downloaded from http://stke.sciencemag.org/ on May 26, 2020

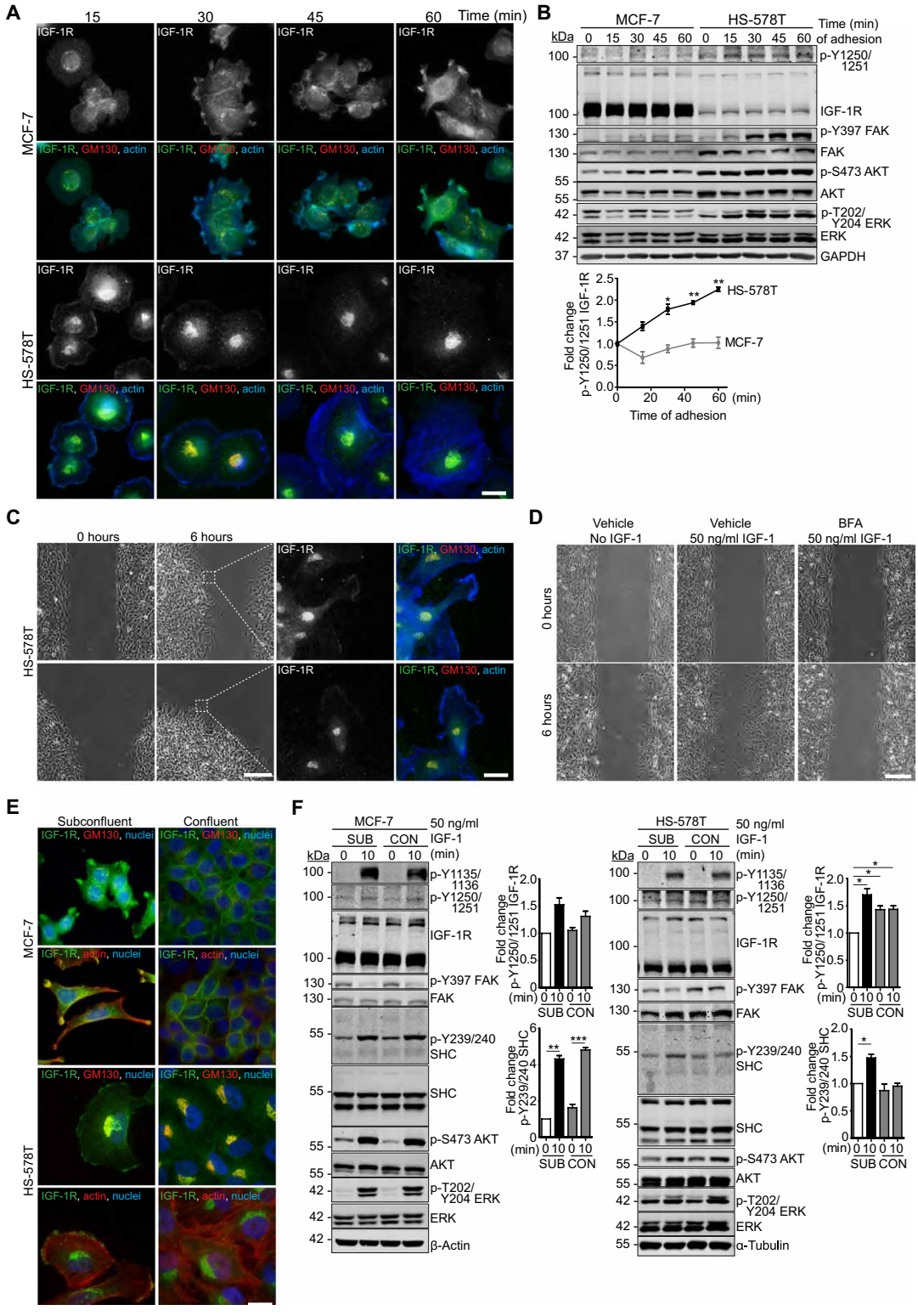


Fig. 8. Tyr$^{1250/1251}$ phosphorylation correlates with IGF-1R presence in the Golgi in migrating cancer cells. (**A**) Immunofluorescence of MCF-7 and HS-578T cells stained for IGF-1R (green), the cis-Golgi marker GM130 (red), and actin (blue) at the indicated times after being cultured on fibronectin-coated coverslips. Images are representative of $n \geq 3$ independent experiments. (**B**) Immunoblotting for the indicated phosphorylated forms of IGF-1R, FAK, AKT, and ERK and total IGF-1R, FAK, AKT, and ERK from MCF-7 and HS-578T cells cultured on fibronectin-coated plates for the indicated times. Densitometry quantification is presented as the average fold change ± SEM in ratio of phosphorylated/total IGF-1R relative to the control condition over time. $n \geq 3$ independent experiments. Significance was calculated using a two-sided one-sample *t* test. (**C**) Phase-contrast images of HS-578T cells in a scratch wound assay at the indicated time points, and these cells were fixed and stained for IGF-1R (green), GM130 (red), and actin (blue). Images are representative of $n = 3$ independent experiments. (**D**) Phase-contrast images of HS-578T cells in a wounding assay in serum-free control medium (no IGF-1) or in the presence of IGF-1, with vehicle or BFA added at 0 and 6 hours after wounding. Images are representative of $n = 3$ independent experiments. (**E**) Immunofluorescence of subconfluent and confluent MCF-7 and HS-578T cells stained for IGF-1R (green) and either GM130 or actin (red). Images are representative of $n = 3$ independent experiments. (**F**) Immunoblotting for the indicated phosphorylated forms of IGF-1R, FAK, SHC, AKT, and ERK and total IGF-1R, FAK, SHC, AKT, and ERK from subconfluent (SUB) and confluent (CON) MCF-7 and HS-578T cells stimulated with IGF-1 after serum starvation. Densitometry quantification is presented as the average fold change ± SEM in ratio of phosphorylated/total protein relative to the control condition. $n = 3$ independent experiments. Significance was calculated using a two-sided one-sample or two sample *t* test. $^*P < 0.05$; $^{**}P < 0.01$; $^{***}P < 0.001$. Scale bars, 250 μm (phase) and 20 μm (fluorescence). GAPDH, glyceraldehyde-3-phosphate dehydrogenase.

drugs have been largely ineffective. Our findings here (summarized in the model in Fig. 9) explain a previously hidden activity of the IGF-1R in promoting an aggressive cancer phenotype and evading therapy. Adhesion-dependent phosphorylation of the IGF-1R on Tyr$^{1250/1251}$ promoted receptor translocation from the plasma membrane to the Golgi, whence it elicited signaling and was available for

Downloaded from http://stke.sciencemag.org/ on May 26, 2020

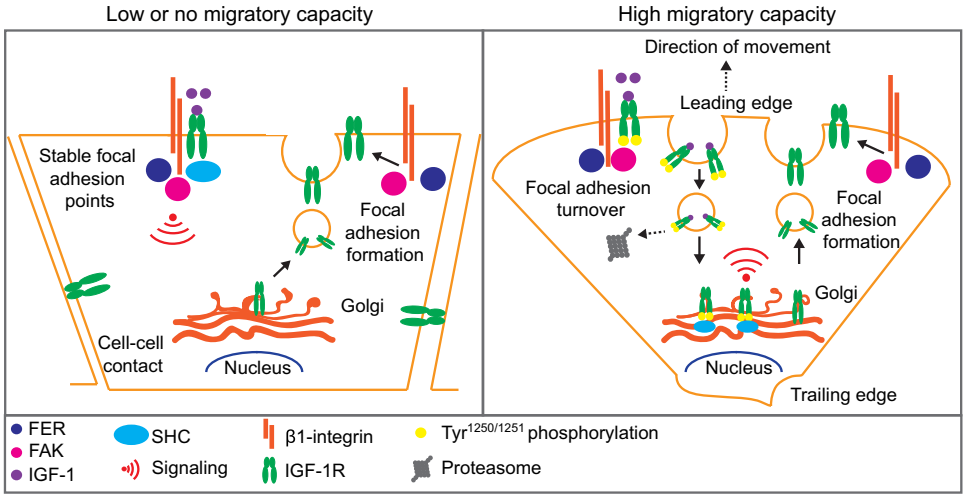


Fig. 9. Model for function of Tyr$^{1250/1251}$ phosphorylation in determining IGF-1R location and signaling in the Golgi apparatus. IGF-1 and adhesion signals promote the phosphorylation of IGF-1R at Tyr$^{1250/1251}$ in both nonmigratory and migratory cells. In nonmigratory cells, the IGF-1R is predominantly located at the plasma membrane or at stable FA points. In migratory cells, the IGF-1R is predominantly located in the Golgi apparatus. Upon induction of cell migration, IGF-1R translocates from the Golgi to the leading edge of the cell, subsequently becomes phosphorylated, and returns to the Golgi, where it mediates signaling to downstream effectors, including SHC and ERK.

transport to and from new FA sites in migrating cells. Ligand- and adhesion-stimulated Tyr$^{1250/1251}$ phosphorylation and receptor internalization also accelerated the turnover of the receptor.

Previous studies have reported that IGF-1R activity and signaling can be modulated by cell adhesion signals [reviewed in (*8*)] and directly by adhesion-associated kinases including FAK, Src, and FER (*23*, *24*, *31*–*33*). The presence of Tyr$^{1250/1251}$ is necessary for the integration of IGF-1R and integrin β1 signaling mediated by their corecruitment into a scaffolding complex containing receptor for activated C kinase 1(RACK-1), SHC, and other mediators that stimulate MAPK signaling (*12*, *14*). Loss of this interaction with mutation of the tyrosines to phenylalanine results in impaired IGF-1–induced cell migration and tumor growth in vivo (*14*, *18*). Our observations here, specifically that the phosphomimetic EE mutant (for Tyr$^{1250/1251}$ phosphorylation) was more rapidly internalized and trafficked from the Golgi apparatus to the leading edge of migrating cells, indicate that phosphorylation on this site is necessary for cooperation with adhesion signaling. IGF-1 also stimulates the internalization of WT IGF-1R to the Golgi, demonstrating that this is an intrinsic component of IGF-1R signaling when it is phosphorylated on these residues. In migrating cells, the removal of IGF-1R from FA points induced by phosphorylation on Tyr$^{1250/1251}$ may facilitate the disassembly of FAs to promote the migration of cells and may also explain the impaired migratory capacity of cells expressing the FF mutant, wherein the IGF-1R is retained at the plasma membrane.

It is well documented that the outcome of RTK activation and signaling can vary depending on receptor location (*34*–*36*). Compartmentalization of RTK signaling may facilitate the recruitment of different effector proteins that might be dictated by a specific cell phenotype. Emerging evidence suggests an important role for the Golgi in oncogenic RTK signaling (*37*–*39*). Overexpressed or mutated forms of the RTK MET cause ligand-independent activation and signaling from MET, including the phosphorylation of the RTK human epidermal growth factor receptor 3 (HER3; also known as ERBB3), in the Golgi (*37*). Similarly, mutated forms of the RTK KIT are retained in the Golgi where they are active and induce downstream signaling (*38*, *40*–*42*). The RTKs vascular endothelial growth factor receptor 2, fibroblast growth factor receptor, and epidermal growth factor receptor (EGFR; also called HER1 and ERBB1) are also reported to be located at and induce signaling from the Golgi (*27*, *35*, *43*). Our findings with the IGF-1R add important knowledge to the understanding of Golgi-derived RTK signaling, because we demonstrate that trafficking of this RTK to the Golgi apparatus is promoted by a specific adhesion- and ligand-dependent phosphorylation on Tyr$^{1250/1251}$. In migrating cells, the IGF-1R was located at the leading edge of nascent FAs and was subsequently rapidly trafficked back to the Golgi. This suggests that a pool of IGF-1R phosphorylated at Tyr$^{1250/1251}$ is stored in the Golgi for signaling and fast trafficking back to the membrane in migrating cells. A similar trafficking route is proposed for Golgi membrane protein 1–mediated trafficking of ligand-activated EGFR in hepatocellular carcinoma (*27*).

We have not, however, established whether the IGF-1R is a cargo protein, whether it might participate in regulating the secretion of proteins from the Golgi, or what controls its trafficking out of the Golgi. Phosphorylation on Tyr$^{1250/1251}$ was low when the IGF-1R was recruited to the membrane, which suggests that phosphatases may facilitate the dephosphorylation of Tyr$^{1250/1251}$, leading to the release of IGF-1R from its Golgi location. Once located at points of nascent FAs, the IGF-1R may promote the recruitment of other interaction partners and proteins, leading to the stabilization of FAs. It is likely that the IGF-1R is subsequently removed from FAs after phosphorylation on Tyr$^{1250/1251}$. An alternative possibility is that the IGF-1R traffics to the Golgi compartment as part of a multiprotein complex that is stored there for signaling.

Golgi-derived oncogenic signaling may be especially active in cell migration (*30*). Here, we observed that fragmentation of the Golgi impaired cell migration in the presence of IGF-1. This was associated with impaired SHC phosphorylation in migratory HS-578T cells but not in nonmigratory MCF-7 cells. This is consistent with a previously described requirement for an intact Golgi apparatus in activating the RAS pathway and ERK signaling to establish cell polarity in migrating cells (*30*). The observation that impaired SHC phosphorylation was not observed in nonmigratory cells suggests that different signaling outcomes can be dictated by the same receptor depending on its location and on the cell phenotype as previously suggested (*7*). Our data suggest that distinct cell adhesion signals have an essential function in determining IGF-1R autophosphorylation and location. Mesenchymal cancer cells exhibiting high migratory capacity and aggressiveness are often deficient in E-cadherin, which interacts with the IGF-1R and may retain it at cell-cell junctions in, for example, MCF-7 cells (*9*). Loss of E-cadherin would therefore be likely to alter IGF-1R localization and potentially facilitate interactions with integrins.

Downloaded from http://stke.sciencemag.org/ on May 26, 2020

Activated intracellular and nuclear IGF-1R have previously been linked to an aggressive cancer phenotype. Intracellular IGF-1R is more abundant in malignant than in benign epithelium in samples from patients with prostate cancer (*44*), and nuclear IGF-1R has been proposed to facilitate breast and prostate cancer (*45*, *46*). Moreover, although abundance of the IGF-1R itself is not associated with survival in patients with breast cancer, high amounts of IGF-1R phosphorylation are linked to poor outcomes (*47*). Our finding of Golgi-derived IGF-1R signaling offers a mechanistic explanation for these effects, because although the EE IGF-1R was present in lower amounts in cells, it retained high activity.

In summary, phosphorylation-specific trafficking of the IGF-1R to the Golgi and the association of this with aggressive cancer phenotype has important consequences for IGF-1 signaling. Phosphorylated $Tyr^{1250/1251}$ could be a biomarker for identifying subsets of cancer that may not be targetable with antibodies targeting the receptor but may be amenable to other therapies that would target an IGF-1R signaling hub within the Golgi. Moreover, this phosphorylation site may distinguish IGF-1R and IR signaling in cells.

MATERIALS AND METHODS

Cell culture, ligand stimulation, and pharmacological inhibitors

R- cells, MDA-MB-231, and HS578T cells were maintained in Dulbecco's modified Eagle's medium (DMEM). Cal-51 were cultured in 50/50 mix of DMEM/Ham's Nutrient F12 media. Prostate cancer DU-145 cells were cultured in RPMI 1640. Media were supplemented with 10% (v/v) heat-inactivated fetal bovine serum, 10 mM L-glutamine, with penicillin/streptomycin (5 mg/ml) added. Cells were cultured at 37°C in a humidified atmosphere at 5% CO_2. All cells were determined to be free of mycoplasma by specific DNA staining and routinely maintained in culture for up to 6 to 8 weeks for use in experiments.

For the analysis of IGF-1 stimulation in Western blotting, cells were seeded 20 hours before starvation and allowed to reach about 70% confluency. Cells were serum-starved for 4 hours followed by stimulation with the indicated concentrations of IGF-1, IGF-2, or insulin. Generally, R- cells transiently expressing the IGF-1R were stimulated with IGF-1 (10 ng/ml), and cell lines with endogenous IGF-1R were stimulated with IGF-1 (50 ng/ml).

For the analysis of detached cells (suspension), cells seeded on 10-cm plates were cultured overnight in complete medium and then starved from serum for 4 hours in total. After 3 hours, cells were enzymatically detached and left in suspension for 1 hour. Cells were then stimulated with IGF-1, centrifuged at 1000 rpm for 5 min, washed with phosphate-buffered saline (PBS), and lysed. Kinase inhibitors BMS-754807 (300 and 1000 nM; Stratech/Selleckchem, catalog no. S1124-SEL), AP-26113 (500 nM; Stratech/Selleckchem, catalog no. S7000-SEL), PF-573228 (9 μM; Tocris Bioscience, catalog no. 3239-10), and PP2 (35 μM; Sigma/Merck, catalog no. 529573-5mg) were added to cells for the last hour of 4-hour serum starvation.

The proteosomal or lysosomal inhibitors MG-132 (10 μM; Calbiochem, catalog no. 474790), leupeptin (2 μM; Sigma/Merck, catalog no. L2884-25mg), E64 (2.6 μM; Sigma/Merck, catalog no. E3132-5mg), and CQ (50 μM; Cell Signaling, catalog no. 14774) were added to cell cultures for 4 or 6 hours, and the appropriate vehicle was added to controls (0 hours). The Golgi disruptor BFA (10 μg/ml; Sigma/Merck, catalog no. B7651-5mg) was added to cells in complete medium.

Generation and transfection of IGF-1R mutants

Cells were transiently transfected with pcDNA4 plasmid encoding the WT IGF-1R or kinase-dead (K1003R) mutant and pcDNA4 plasmid encoding IGF-1R WT, FF, or EE mutants. R- cells were seeded 24 hours before transfection at a density of about 1.0×10^6 cells per 10-cm plate. Lipofectamine 2000 (Invitrogen, catalog no. 11668-019) diluted in Opti-MEM was used to transfect cells with relevant DNA plasmid (12 to 16 μg). After 24 hours, cells were reseeded for experiments at 48 hours after transfection.

MDA-MB-231, MCF-7, and DU-145 cells were seeded 24 hours before transfection to about 70% confluency in six-well or 10-cm plates for transfection with Lipofectamine 2000. All cell lines were transfected with 2 μg per six-well plate and 12 μg per 10-cm plate of pcDNA4 plasmid. Cells were reseeded in new plates at 24 hours after transfection for subsequent experiments.

IGF-1R mutants were generated using the QuikChange Lightning Site-Directed Mutagenesis Kit (Agilent, #210518). The pcDNA4 plasmid encoding WT IGF-1R was used to generate the K1003R, Y1250/Y1251 to phenylalanine (FF) and glutamic acid (EE) mutants.

IGF-1R KO cells were generated using CRISPR technology. The IGF-1R Double Nickase Plasmid (h) (sc-400084-NIC) was obtained from Santa Cruz Biotechnology Inc., and transfection was carried out as described by the supplier protocol. Selection of transfected cells was achieved using puromycin (0.5 μg/ml for MDA-MB-231 and MCF-7 cells and 0.4 μg/ml for DU-145 cells). IGF-1R KO cell pools were selected by immunoblotting for IGF-1R and then cloned by serial dilution. IGF-1R KO clones were also subsequently pooled to ensure that they represented the original cell cultures. These pools were used for stable transfection of pcDNA4 plasmids encoding the WT, FF, or EE IGF-1R followed by selection in medium supplemented with zeocin (400 μg/ml) over 4 weeks.

SDS–polyacrylamide gel electrophoresis and Western blotting

Cells were washed with ice-cold PBS twice and lysed immediately with cold lysis buffer [20 mM tris (pH 8), 50 mM NaCl, 50 mM NaF, and 1% NP-40] containing protease and phosphatase inhibitors for 30 min on ice followed by centrifugation at 14,000 rpm for 15 min at 4°C. Samples were denatured by boiling for 5 min with 5X SDS–polyacrylamide gel electrophoresis (PAGE) loading buffer. Technical replicates of the same denatured samples (30 μg of protein) were separated on 8 to 10% gels to enable analysis of distinct IGF-1R phospho-sites. Proteins were then transferred to nitrocellulose membranes that were blocked for 1 hour at room temperature in 5% bovine serum albumin (BSA) in tris-buffered saline-T [20 mM tris, 150 mM NaCl, and 0.05% Tween 20 (pH 7.6)] (TBS-T). Primary antibodies were diluted at 1:1000 or 1:10,000 dilution for β-actin in TBS-T containing 5% milk or BSA and incubated with membranes at 4°C overnight. To detect distinct IGF-1R phospho-sites, each blot was incubated with rabbit phospho–IGF-1R or mouse/rabbit total IGF-1R antibodies and a mouse antibody detecting a protein input control (tubulin). For detection of p-Thr^{202}/Tyr^{204}/ERK, p-Ser^{473}/AKT and p-$Tyr^{239/240}$ blots were probed with a combination of rabbit antibody detecting the phosphorylated protein, a mouse antibody detecting the total protein, followed by mouse antibodies to detect the input control. IRDye-conjugated secondary antibodies (1:10,000) were used for detection with the Odyssey Image Scanner System (LI-COR Biosciences). Image studio quantification software was used for densitometry. Each phospho–IGF-1R protein was normalized

Downloaded from http://stke.sciencemag.org/ on May 26, 2020

to total IGF-1R or first to the input control and then to total IGF-1R. Other phosphoproteins were normalized to their respective total protein.

Phospho-Tyr$^{1250/1251}$ antibody adsorption and IGF-1R phosphopeptide array

The phospho-Tyr^{1250} IGF-1R (Santa Cruz Biotechnology Inc., catalog no. SC-293102 and Biorbyt, catalog no. orb43345) was adsorbed to nitrocellulose membranes that were coated with nonphosphorylated SFYYS peptide. Membranes dotted with peptide were allowed to dry completely and blocked with PBS containing 1% BSA for 1 hour at room temperature. These membranes were then incubated with the phospho-Tyr^{1250} antibody for 1 hour rotating at room temperature and the antibody recovered for subsequent use in Western blotting.

Custom-made Intavis CelluSpots peptide arrays (catalog no. 32.100) containing 18–amino acid peptide sequences of the IGF-1R and the IR encompassing specific tyrosines and serines phosphorylated or nonphosphorylated immobilized on glass arrays were used to analyze the specificity of the commercial p-Tyr^{1250} IGF-1R antibody. The phospho-Tyr^{1250} antibody (1/500) was incubated with slides that were subsequently processed in the same way as Western blots.

Immunoprecipitation and in vitro kinase assays

Cells were lysed, and 0.5 to 1 mg of protein lysate was incubated with antibodies detecting IGF-IR [IGF-IRβ Antibody (C-20), catalog no. sc-713, Santa Cruz Biotechnology Inc.; IGF-1Rα Antibody (αIR3), catalog no. GR11L, Merck; IGF-IRβ Antibody, catalog no. 3027, Cell Signaling] at 1/100 dilution overnight rotating at 4°C. Immune complexes were obtained by adding 50 μl of prewashed protein G agarose beads to the antibody-lysate mix for 2 hours at 4°C. Beads were washed three times using lysis buffer, and loading dye was added to the washed beads (2×) before samples were boiled for 5 min at 95°C and centrifuged at 14,000 rpm for 2 min followed by SDS-PAGE and Western blotting. To investigate multiple IGF-1R phospho-sites, denatured samples were split for two sets of gels. The antibody detecting the phospho-site was then removed using stripping buffer (200 mM NaOH with 1% SDS) and incubated with total IGF-1R (1:1000).

The ADP-Glo Kinase Assay kit (Promega) was used for in vitro kinase assays. For kinase assay, protein inputs to immunoprecipitations of IGF-1R WT and FF were adjusted to be equivalent to EE. Beads with immunoprecipitated IGF-1R were washed twice with kinase buffer [40 mM tris (pH 7.5), 20 mM $MgCl_2$, 2 mM $MnCl_2$, BSA (0.1 mg/ml), 2 mM dithiothreitol, and 100 μM sodium vanadate] and then incubated with kinase buffer containing 150 μM ATP (ADP-Glo Kinase Assay) and poly(Glu, Tyr) (2 mg/ml) (4:1) (P0275, Sigma) as an exogenous substrate for 30 min, with samples mixed every 10 min. Beads were centrifuged for 30 s at 14,000 rpm, and triplicates (5 μl) of supernatant were added to a white 384-well plate for incubation with ADP-Glo (5 μl per sample) for 60 min at room temperature. The ADP-Glo Kinase detection reagent (10 μl) was added to each reaction for 30 min at room temperature, and kinase activity was measured with a luminometer (BioTek).

Mass spectrometry

Mass spectrometry for phospho-peptide mapping of the IGF-1R was carried out at the FingerPrints Proteomics Facility at the University of Dundee. IGF-1R was immunoprecipitated from R- cells transfected with pcDNA3 IGF-1R WT and that were either serum-starved or stimulated with IGF-1 were transferred as protein G agarose–bound protein precipitates to the Dundee facility, where they were subjected to trypsin/AspN digestion and enrichment of phosphorpeptides by titanium dioxide. Mass spectrometry was performed using an Orbitrap Velos system.

Quantitative polymerase chain reaction

R- cells transiently expressing WT, FF, or EE IGF-1R were prepared for RNA extraction 48 hours after transfection. RNA was extracted using the PureLink RNA Mini Kit (Thermo Fisher Scientific) according to the manufacturer's protocol. To synthesize complementary DNA, 1 μg of RNA and the QuantiTect reverse transcription kit (Qiagen) were used. Quantitative polymerase chain reaction was performed using the Roche FastStart essential DNA Green Master Kit and the LightCycler 96 Instrument (Roche Diagnostics). Actin was used as housekeeping control. The 2 CT method was used to analyze data and to determine relative mRNA expression levels. IGF-1R mRNA expression values were normalized to actin and expressed as fold change relative to the WT IGF-1R (set to 1). The following primer set was used to detect IGF-1R: 5′ATGTCCAGGCCAAACAGGAT′3 (forward) and 5′CCTCCCACTCATCAGGAACG′3 (reverse).

Immunofluorescence

Cells were cultured on 12-mm glass coverslips, washed with PBS, fixed with 4% paraformaldehyde in PHEM (60 mM PIPES, 25 mM HEPES, 10 mM EGTA, 2 mM $MgCl_2$; pH 6.9) buffer for 60 min at room temperature, quenched with 50 mM ammonium chloride for 20 min, and permeabilized using 0.1% Triton/PHEM for 5 min. PHEM buffer containing donkey serum (10%) was used for blocking and dilution of antibodies. Coverslips were incubated with primary antibodies at 4°C, washed with PHEM three times followed by secondary antibodies and Hoechst dye to stain nuclei. The following reagents were used: IGF-1R in mouse cells (1/200), Cell Signaling, antibody catalog no. 9750; for human cells, catalog no. 3027 (1/200 for MCF-7 cells and 1/100 for other cell lines); the cis-Golgi apparatus: GM130 (1/200; D catalog no. 610822); cis- and trans-Golgi network: biotinylated VVA (1/400; Lectin Vector Laboratories, catalog no. B-1235-2). The following fluorophore-conjugated secondary antibodies, Cy3-conjugated AffiniPure donkey anti-mouse antibody (1:1000), Alexa Fluor 488–conjucated AffiniPure donkey (1/200), Alexa Fluor 594–conjucated streptavidin (1:1000), and Alexa Fluor 488–conjucated streptavidin (1/200) were used for detection of primary antibodies. Phalloidin (tetramethyl rhodamine isothiocyanate, Sigma, catalog no. P1951 or Alexa Fluor 405, Thermo Fisher Scientific, catalog no. A30104) was used to detect actin, and Hoechst was used to stain nuclei.

To assess internalization of activated IGF-1R, cells were serum-starved for 4 hours and incubated with the IGF-1R α chain (IRα) antibody for 30 min either on ice or at 37°C. Cells were then fixed and stained with an antibody detecting the IGF-1R β chain (green). Cells were then incubated with secondary antibodies detecting either the IRα (red) or IGF-1R (green). IRα antibody bound or internalized with surface-located IGF-1R appeared yellow.

Images were acquired using a SPOT charge-coupled device camera mounted on a Nikon T600 fluorescent microscope or a Nikon DSFi1c camera attached to the Leica DM LB2 microscope. For confocal microscopy, images were acquired using an Olympus Fluoview FV1000 confocal laser scanning microscope (numerical aperture, 1.4) with a 60× immersion objective. Maximum intensity projections and *z*-stacks were processed in ImageJ. Brightness and contrast were

Downloaded from http://stke.sciencemag.org/ on May 26, 2020

adjusted in Adobe Photoshop if needed. To determine fluorescence intensity within the cells, ImageJ software was used to determine fluorescence signal intensity within the cells.

In-cell Western assays for IGF-1R

Cells were seeded at 5×10^4 cells per well in 96-well tissue culture plates in complete medium for 24 hours, washed three times with PBS, and serum-starved for 4 hours followed by stimulation with IGF-1 (10 ng/ml) for 10 min or left in serum-free medium or complete medium. Cells were immediately fixed with 100 µl of a freshly prepared fixing solution (4% formaldehyde/PHEM) and incubated at room temperature for 30 min followed by quenching with 50 mM ammonium chloride for 20 min and washing with PHEM. Cells in wells with complete medium or incubated with p-AKT/AKT and one 3X set of the secondary control antibody were permeabilized using 0.1% Triton/PHEM for 5 min and washed with PHEM. All wells were then blocked for 1 hour with 50 µl of blocking buffer (5% goat serum/PHEM). Primary antibody (IGF-1R IR3 for surface and Cell Signaling IGF-1Rβ catalog no. 3027 or p- Ser^{473}/AKT) was added for 2 hours with gentle rocking followed by washing and incubation with secondary antibody. Goat anti-mouse IRDye 680 (1:1000) (Odyssey infrared imaging system, catalog no. 926-32220) or Goat anti-rabbit IRDye 800 (1:1000) (Odyssey infrared imaging system, catalog no. 926-32211) were used to detect primary antibodies. Syto60 (Invitrogen) was also included (1:10,000) as a cell-permeable nucleic acid stain that fluoresces at 680 nm and was detected using the Odyssey infrared scanner. Cells were washed five times with PHEM. Plates were dried, and IGF-1R (surface and total levels) intensity was quantified using the Image studio quantification software with normalization to Syto60 levels.

Cell migration assays

HS578T cells were seeded in Culture-Insert 2 Well 35-mm plates (ibidi GmbH, catalog no. 81176) (4.0×10^5 cells/ml, 70 µl per well). Cells were allowed to attach for 24 hours in serum-free medium containing either dimethyl sulfoxide (vehicle) or the Golgi disruptor BFA (10 µg/ml) for 4 hours. The wound was generated by removal of the insert, and the medium in respective dishes was then supplemented with IGF-1 (50 ng/ml). Wounds were photographed with a Nikon charge-coupled device camera connected with the Nikon Eclipse TE 300 microscope (×10 magnification) after 0 and 6 hours of migration. For immunofluorescence, HS578T cells were seeded in Culture-Insert 2 Well inserts on coverslips (ibidi GmbH, catalog no. 80209) and allowed to attach for 24 hours The wound area was photographed with a Nikon charge-coupled device camera connected with the Nikon Eclipse TE 300 microscope at 0 and 6 hours of migration. Subsequently, coverslips were recovered for immunofluorescence.

Statistical analysis

Western blot densitometry results were expressed as fold change in the ratio of phospho/total protein relative to the control condition (set to 1), which is indicated as a white bar in each graph. For calculations comparing fold change of each group to the control, one-sample *t* tests were used to test the null hypothesis that the expected ratio was 1. For calculations comparing fold change of groups (≠ control condition), independent two-sample *t* tests were used. *P* values were adjusted using Benjamini-Hochberg correction for multiple testing. A 3 × 3 analysis of variance (ANOVA) was conducted to examine the main effects of group and condition and the interaction between group and condition in Fig. 4A. Statistical significance was determined using a P value of <0.05, and all tests were two tailed.

SUPPLEMENTARY MATERIALS

stke.sciencemag.org/cgi/content/full/13/633/eaba3176/DC1

Fig. S1. Immunoreactivity of phosphorylated Tyr^{1250} IGF-1R antibody.

Fig. S2. Protein abundance and mRNA expression for WT and mutant IGF-1Rs stably expressed in R- cells.

Fig. S3. WT and EE IGF-1Rs internalize in large vesicles upon IRα antibody stimulation.

View/request a protocol for this paper from *Bio-protocol*.

REFERENCES AND NOTES

1. J. P. Liu, J. Baker, A. S. Perkins, E. J. Robertson, A. Efstratiadis, Mice carrying null mutations of the genes encoding insulin-like growth factor I (Igf-1) and type 1 IGF receptor (Igf1r). *Cell* **75**, 59–72 (1993).
2. M. Pollak, The insulin and insulin-like growth factor receptor family in neoplasia: An update. *Nat. Rev. Cancer* **12**, 159–169 (2012).
3. E. Osher, V. M. Macaulay, Therapeutic targeting of the IGF axis. *Cell* **8**, E895 (2019).
4. V. P. Brahmkhatri, C. Prasanna, H. S. Atreya, Insulin-like growth factor system in cancer: Novel targeted therapies. *Biomed. Res. Int.* **2015**, 538019 (2015).
5. P. F. Christopoulos, P. Msaouel, M. Koutsilieris, The role of the insulin-like growth factor-1 system in breast cancer. *Mol. Cancer* **14**, 43 (2015).
6. A. Arcaro, Targeting the insulin-like growth factor-1 receptor in human cancer. *Front. Pharmacol.* **4**, 30–30 (2013).
7. M. Niepel, M. Hafner, E. A. Pace, M. Chung, D. H. Chai, L. Zhou, B. Schoeberl, P. K. Sorger, Profiles of Basal and stimulated receptor signaling networks predict drug response in breast cancer lines. *Sci. Signal.* **6**, ra84 (2013).
8. O. T. Cox, S. O'Shea, E. Tresse, M. Bustamante-Garrido, R. Kiran-Deevi, R. O'Connor, IGF-1 receptor and adhesion signaling: An important axis in determining cancer cell phenotype and therapy resistance. *Front. Endocrinol.* **6**, (2015).
9. A. M. Nagle, M. Levine, N. Tasdemir, J. A. Scott, K. Burlbaugh, J. Kehm, T. A. Katz, D. N. Boone, B. M. Jacobsen, J. M. Atkinson, S. Oesterreich, A. V. Lee, Loss of E-cadherin enhances IGF1–IGF1R pathway activation and sensitizes breast cancers to anti-IGF1R/InsR inhibitors. *Clin. Cancer Res.* **24**, 5165–5177 (2018).
10. I. Bajrami, R. Marlow, M. van de Ven, R. Brough, H. N. Pemberton, J. Frankum, F. Song, R. Rafiq, A. Konde, D. B. Krastev, M. Menon, J. Campbell, A. Gulati, R. Kumar, S. J. Pettitt, M. D. Gurden, M. L. Cardenosa, I. Chong, P. Gazinska, F. Wallberg, E. J. Sawyer, L. A. Martin, M. Dowsett, S. Linardopoulos, R. Natrajan, C. J. Ryan, P. W. B. Derksen, J. Jonkers, A. N. J. Tutt, A. Ashworth, C. J. Lord, E-Cadherin/ROS1 inhibitor synthetic lethality in breast cancer. *Cancer Discov.* **8**, 498–515 (2018).
11. A. Belfiore, R. Malaguarnera, M. L. Nicolosi, R. Lappano, M. Ragusa, A. Morrione, V. Vella, A novel functional crosstalk between DDR1 and the IGF axis and its relevance for breast cancer. *Cell Adh. Migr.* **12**, 305–314 (2018).
12. U. Hermanto, C. S. Zong, W. Li, L.-H. Wang, RACK1, an insulin-like growth factor I (IGF-I) receptor-interacting protein, modulates IGF-I-dependent integrin signaling and promotes cell spreading and contact with extracellular matrix. *Mol. Cell. Biol.* **22**, 2345–2365 (2002).
13. P. A. Kiely, G. S. Baillie, M. J. Lynch, M. D. Houslay, R. O'Connor, Tyrosine 302 in RACK1 is essential for insulin-like growth factor-I-mediated competitive binding of PP2A and β1 integrin and for tumor cell proliferation and migration. *J. Biol. Chem.* **283**, 22952–22961 (2008).
14. P. A. Kiely, M. Leahy, D. O'Gorman, R. O'Connor, RACK1-mediated integration of adhesion and insulin-like growth factor I (IGF-I) signaling and cell migration are defective in cells expressing an IGF-I receptor mutated at tyrosines 1250 and 1251. *J. Biol. Chem.* **280**, 7624–7633 (2005).
15. V. A. Blakesley, A. P. Koval, B. S. Stannard, A. Scrimgeour, D. LeRoith, Replacement of tyrosine 1251 in the carboxyl terminus of the insulin-like growth factor-I receptor disrupts the actin cytoskeleton and inhibits proliferation and anchorage-independent growth. *J. Biol. Chem.* **273**, 18411–18422 (1998).
16. M. Miura, E. Surmacz, J.-L. Burgaud, R. Baserga, Different effects on mitogenesis and transformation of a mutation at tyrosine 1251 of the insulin-like growth factor I receptor. *J. Biol. Chem.* **270**, 22639–22644 (1995).
17. R. O'Connor, A. Kauffmann-Zeh, Y. Liu, S. Lehar, G. I. Evan, R. Baserga, W. A. Blättler, Identification of domains of the insulin-like growth factor I receptor that are required for protection from apoptosis. *Mol. Cell. Biol.* **17**, 427–435 (1997).
18. P. Brodt, L. Fallavollita, A.-M. Khatib, A. A. Samani, D. Zhang, Cooperative regulation of the invasive and metastatic phenotypes by different domains of the type I insulin-like growth factor receptor β subunit. *J. Biol. Chem.* **276**, 33608–33615 (2001).

Downloaded from http://stke.sciencemag.org/ on May 26, 2020

19. M. Leahy, A. Lyons, D. Krause, R. O'Connor, Impaired Shc, Ras, and MAPK activation but normal Akt activation in FL5.12 cells expressing an insulin-like growth factor I receptor mutated at tyrosines 1250 and 1251. *J. Biol. Chem.* **279**, 18306–18313 (2004).
20. G. M. Kelly, D. A. Buckley, P. A. Kiely, D. R. Adams, R. O'Connor, Serine phosphorylation of the insulin-like growth factor I (IGF-1) receptor C-terminal tail restrains kinase activity and cell growth. *J. Biol. Chem.* **287**, 28180–28194 (2012).
21. V. A. Blakesley, T. Kalebic, L. J. Helman, B. Stannard, T. N. Faria, C. T. Roberts Jr., D. LeRoith, Tumorigenic and mitogenic capacities are reduced in transfected fibroblasts expressing mutant insulin-like growth factor (IGF)-I receptors. The role of tyrosine residues 1250, 1251, and 1316 in the carboxy-terminus of the IGF-I receptor. *Endocrinology* **137**, 410–417 (1996).
22. H. Zheng, C. Worrall, H. Shen, T. Issad, S. Seregard, A. Girnita, L. Girnita, Selective recruitment of G protein-coupled receptor kinases (GRKs) controls signaling of the insulin-like growth factor 1 receptor. *Proc. Natl. Acad. Sci. U.S.A.* **109**, 7055–7060 (2012).
23. J. Stanicka, L. Rieger, S. O'Shea, O. Cox, M. Coleman, C. O'Flanagan, B. Addario, N. McCabe, R. Kennedy, R. O'Connor, FES-related tyrosine kinase activates the insulin-like growth factor-1 receptor at sites of cell adhesion. *Oncogene* **37**, 3131–3150 (2018).
24. L. Taliaferro-Smith, E. Oberlick, T. Liu, T. McGlothen, T. Alcaide, R. Tobin, S. Donnelly, R. Commander, E. Kline, G. P. Nagaraju, L. Havel, A. Marcus, R. Nahta, R. O'Regan, FAK activation is required for IGF1R-mediated regulation of EMT, migration, and invasion in mesenchymal triple negative breast cancer cells. *Oncotarget* **6**, 4757–4772 (2015).
25. W. D. Mahauad-Fernandez, C. M. Okeoma, Cysteine-linked dimerization of BST-2 confers anoikis resistance to breast cancer cells by negating proapoptotic activities to promote tumor cell survival and growth. *Cell Death Dis.* **8**, e2687–e2687 (2017).
26. L. Johannes, V. Popoff, Tracing the retrograde route in protein trafficking. *Cell* **135**, 1175–1187 (2008).
27. Q.-H. Ye, W. W. Zhu, J. B. Zhang, Y. Qin, M. Lu, G. L. Lin, L. Guo, B. Zhang, Z. H. Lin, S. Roessler, M. Forgues, H. L. Jia, L. Lu, X. F. Zhang, B. F. Lian, L. Xie, Q. Z. Dong, Z. Y. Tang, X. W. Wang, L. X. Qin, GOLM1 modulates EGFR/RTK cell-surface recycling to drive hepatocellular carcinoma metastasis. *Cancer Cell* **30**, 444–458 (2016).
28. J. Lippincott-Schwartz, L. C. Yuan, J. S. Bonifacino, R. D. Klausner, Rapid redistribution of Golgi proteins into the ER in cells treated with brefeldin A: Evidence for membrane cycling from Golgi to ER. *Cell* **56**, 801–813 (1989).
29. A. A. Samani, S. Yakar, D. LeRoith, P. Brodt, The role of the IGF system in cancer growth and metastasis: Overview and recent insights. *Endocr. Rev.* **28**, 20–47 (2007).
30. V. Millarte, H. Farhan, The Golgi in cell migration: Regulation by signal transduction and its implications for cancer cell metastasis. *Scientific World Journal* **2012**, 48278 (2012).
31. D. A. Ucar, Disruption of the protein interaction between FAK and IGF-1R inhibits melanoma tumor growth. *Cell Cycle* **11**, 3250–3259 (2012).
32. J. E. Peterson, G. Kulik, T. Jelinek, C. W. M. Reuter, J. A. Shannon, M. J. Weber, Src phosphorylates the insulin-like growth factor type I receptor on the autophosphorylation sites: Requirement for transformation by src. *J. Biol. Chem.* **271**, 31562–31571 (1996).
33. B. B. M. Flossmann-Kast, P. M. Jehle, A. Hoeflich, G. Adler, M. P. Lutz, Src stimulates insulin-like growth factor I (IGF-I)-dependent cell proliferation by increasing IGF-I receptor number in human pancreatic carcinoma cells. *Cancer Res.* **58**, 3551–3554 (1998).
34. Y. Yoneyama, P. Lanzerstorfer, H. Niwa, T. Umehara, T. Shibano, S. Yokoyama, K. Chida, J. Weghuber, F. Hakuno, S. I. Takahashi, IRS-1 acts as an endocytic regulator of IGF-I receptor to facilitate sustained IGF signaling. *eLife* **7**, e32893 (2018).
35. C. M. Warren, S. Ziyad, A. Briot, A. Der, M. L. Iruela-Arispe, A ligand-independent VEGFR2 signaling pathway limits angiogenic responses in diabetes. *Sci. Signal.* **7**, ra1 (2014).
36. A. Disanza, E. Frittoli, A. Palamidessi, G. Scita, Endocytosis and spatial restriction of cell signaling. *Mol. Oncol.* **3**, 280–296 (2009).
37. N. M. Frazier, T. Brand, J. D. Gordan, J. Grandis, N. Jura, Overexpression-mediated activation of MET in the Golgi promotes HER3/ERBB3 phosphorylation. *Oncogene* **38**, 1936–1950 (2019).
38. Y. Obata, K. Horikawa, I. Shiina, T. Takahashi, T. Murata, Y. Tasaki, K. Suzuki, K. Yonekura, H. Esumi, T. Nishida, R. Abe, Oncogenic Kit signalling on the Golgi is suppressed by blocking secretory trafficking with M-COPA in gastrointestinal stromal tumours. *Cancer Lett.* **415**, 1–10 (2018).
39. Y. Obata, K. Horikawa, T. Takahashi, Y. Akieda, M. Tsujimoto, J. A. Fletcher, H. Esumi, T. Nishida, R. Abe, Oncogenic signaling by Kit tyrosine kinase occurs selectively on the Golgi apparatus in gastrointestinal stromal tumors. *Oncogene* **36**, 3661–3672 (2017).
40. Z. Xiang, F. Kreisel, J. Cain, A. Colson, M. H. Tomasson, Neoplasia driven by mutant c-KIT is mediated by intracellular, not plasma membrane, receptor signaling. *Mol. Cell. Biol.* **27**, 267–282 (2007).
41. S. Tabone-Eglinger, F. Subra, H. el Sayadi, L. Alberti, E. Tabone, J. P. Michot, N. Theou-Anton, A. Lemoine, J. Y. Blay, J. F. Emile, KIT mutations induce intracellular retention and activation of an immature form of the KIT protein in gastrointestinal stromal tumors. *Clin. Cancer Res.* **14**, 2285–2294 (2008).
42. H. Bougherara, F. Subra, R. Crépin, P. Tauc, C. Auclair, M. A. Poul, The aberrant localization of oncogenic kit tyrosine kinase receptor mutants is reversed on specific inhibitory treatment. *Mol. Cancer Res.* **7**, 1525–1533 (2009).
43. L. Citores, L. Bai, V. Sørensen, S. Olsnes, Fibroblast growth factor receptor-induced phosphorylation of STAT1 at the golgi apparatus without translocation to the nucleus. *J. Cell. Physiol.* **212**, 148–156 (2007).
44. T. Aleksic, N. Gray, X. Wu, G. Rieunier, E. Osher, J. Mills, C. Verrill, R. J. Bryant, C. Han, K. Hutchinson, A. G. Lambert, R. Kumar, F. C. Hamdy, U. Weyer-Czernilofsky, M. P. Sanderson, T. Bogenrieder, S. Taylor, V. M. Macaulay, Nuclear IGF1R interacts with regulatory regions of chromatin to promote RNA polymerase II recruitment and gene expression associated with advanced tumor stage. *Cancer Res.* **78**, 3497–3509 (2018).
45. T. Aleksic, M. M. Chitnis, O. V. Perestenko, S. Gao, P. H. Thomas, G. D. Turner, A. S. Protheroe, M. Howarth, V. M. Macaulay, Type 1 insulin-like growth factor receptor translocates to the nucleus of human tumor cells. *Cancer Res.* **70**, 6412–6419 (2010).
46. H. Deng, Y. Lin, M. Badin, D. Vasilcanu, T. Strömberg, H. Jernberg-Wiklund, B. Sehat, O. Larsson, Over-accumulation of nuclear IGF-1 receptor in tumor cells requires elevated expression of the receptor and the SUMO-conjugating enzyme Ubc9. *Biochem. Biophys. Res. Commun.* **404**, 667–671 (2011).
47. J. H. Law, G. Habibi, K. Hu, H. Masoudi, M. Y. C. Wang, A. L. Stratford, E. Park, J. M. W. Gee, P. Finlay, H. E. Jones, R. I. Nicholson, J. Carboni, M. Gottardis, M. Pollak, S. E. Dunn, Phosphorylated insulin-like growth factor-i/insulin receptor is present in all breast cancer subtypes and is related to poor survival. *Cancer Res.* **68**, 10238–10246 (2008).
48. Y. Perez-Riverol, A. Csordas, J. Bai, M. Bernal-Llinares, S. Hewapathirana, D. J. Kundu, A. Inuganti, J. Griss, G. Mayer, M. Eisenacher, E. Pérez, J. Uszkoreit, J. Pfeuffer, T. Sachsenberg, S. Yilmaz, S. Tiwary, J. Cox, E. Audain, M. Walzer, A. F. Jarnuczak, T. Ternent, A. Brazma, J. A. Vizcaíno, The PRIDE database and related tools and resources in 2019: Improving support for quantification data. *Nucleic Acids Res.* **47**, D442–D450 (2018).

Acknowledgments: We would like to acknowledge J. Berghoff, M. Coleman, D. Buckley, A. O'Connell, and M. Hirsch for assistance with site-directed mutagenesis, peptides, and transfections. We also acknowledge O. Cox and N. Kedersha for assistance with immunofluorescence. We thank K. O'Sullivan from the School of Mathematical Sciences for advice on statistical analyses and colleagues in the Department of Biochemistry and Cell Biology for helpful suggestions. We also thank D. Lamont of the FingerPrints Proteomics Facility at the University of Dundee, which is supported by the "Wellcome Trust Technology Platform" award [097945/B/11/Z]. In addition, we thank colleagues in the Department of Biochemistry and Cell Biology for helpful suggestions. **Funding:** This work was funded by Science Foundation Ireland Principal Investigator Awards 16/A/4505 and 11/PI/1139. **Author contributions:** L.R., S.O'S., G.G., J.S., and G.K. contributed to conception and design of experiments, acquisition and interpretation of data, and drafting of the manuscript. R.O'C. contributed to conception design, interpretation of data, and drafting of the article. **Competing interests:** The authors declare that they have no competing interests. **Data and materials availability:** The mass spectrometry proteomics data have been deposited to the ProteomeXchange Consortium via the PRIDE partner repository (*48*) with the dataset identifier PXD017644. All other data needed to evaluate the conclusions in the paper are present in the paper or the Supplementary Materials.

Submitted 26 November 2019
Accepted 16 April 2020
Published 26 May 2020
10.1126/scisignal.aba3176

Citation: L. Rieger, S. O'Shea, G. Godsmark, J. Stanicka, G. Kelly, R. O'Connor, IGF-1 receptor activity in the Golgi of migratory cancer cells depends on adhesion-dependent phosphorylation of Tyr^{1250} and Tyr^{1251}. *Sci. Signal.* **13**, eaba3176 (2020).

Downloaded from http://stke.sciencemag.org/ on May 26, 2020

Science Signaling

IGF-1 receptor activity in the Golgi of migratory cancer cells depends on adhesion-dependent phosphorylation of Tyr ^{1250} and Tyr^{1251}

Leonie Rieger, Sandra O'Shea, Grant Godsmark, Joanna Stanicka, Geraldine Kelly and Rosemary O'Connor

Sci. Signal. **13** (633), eaba3176.
DOI: 10.1126/scisignal.aba3176

How IGF-1R promotes cell migration

Signaling through the insulin-like growth factor 1 receptor (IGF-1R) promotes cancer progression, but therapies that limit IGF-1R signaling have performed poorly. Rieger *et al.* found that the residues Tyr^{1250} and Tyr^{1251}, which are required for IGF-1R to support cancer cell growth (see the Focus by Crudden and Girnita), underwent autophosphorylation when cells were adherent. Experiments with IGF-1Rs containing phosphomimetic or nonphosphorylatable substitutions at these sites demonstrated that IGF-1 induced IGF-1R translocation to the Golgi, where it enhanced cell migration before being degraded or recycled to the plasma membrane. These findings show that phosphorylation-dependent trafficking of IGF-1R promotes aggressive cancer cell behaviors and may explain why targeting plasma membrane–localized IGF-1R is not effective.

ARTICLE TOOLS http://stke.sciencemag.org/content/13/633/eaba3176

SUPPLEMENTARY MATERIALS http://stke.sciencemag.org/content/suppl/2020/05/21/13.633.eaba3176.DC1

RELATED CONTENT
http://stke.sciencemag.org/content/sigtrans/11/541/eaat0114.full
http://stke.sciencemag.org/content/sigtrans/11/515/eaaq1060.full
http://stke.sciencemag.org/content/sigtrans/13/633/eabb7887.full

REFERENCES This article cites 47 articles, 22 of which you can access for free
http://stke.sciencemag.org/content/13/633/eaba3176#BIBL

PERMISSIONS http://www.sciencemag.org/help/reprints-and-permissions

Use of this article is subject to the Terms of Service

Science Signaling (ISSN 1937-9145) is published by the American Association for the Advancement of Science, 1200 New York Avenue NW, Washington, DC 20005. The title *Science Signaling* is a registered trademark of AAAS.

Copyright © 2020 The Authors, some rights reserved; exclusive licensee American Association for the Advancement of Science. No claim to original U.S. Government Works

Downloaded from http://stke.sciencemag.org/ on May 26, 2020